

NANOTECH FRANCE 2016

International Nanotechnology Conference
1 - 3 June 2016

Pôle Universitaire Léonard de Vinci, La Défense
Paris - France

Organizer



SETCOR
Conferences & Events

www.sector.org

In Collaboration with



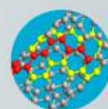
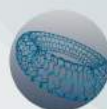
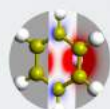
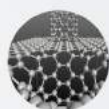
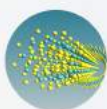
Joint Conference



ATOMISTIX TOOLKIT

Atomic-Scale Modeling Software for Nanotechnology

Atomistix ToolKit (ATK) offers unique capabilities for simulating electrical transport properties of nanodevices on the atomic scale. Based on an open architecture which integrates a powerful scripting language with a graphical user interface, ATK is a comprehensive platform for studies in nanoelectronics, using both accurate first-principles (DFT) and fast semi-empirical methods and classical potentials. Moreover, ATK includes a very advanced electrostatic model to allow realistic simulations of nanoscale transistor structures.



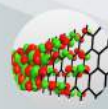
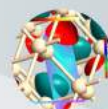
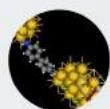
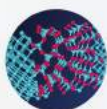
Study

graphene & nanotubes
nanowires
magnetic tunnel junctions
molecular electronics
complex interfaces
high-K dielectrics
spintronics
single-electron transistor
phonons and phonon transport
transistor DOS
Nudged Elastic Band
stress and strain
topological insulators



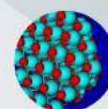
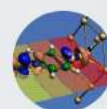
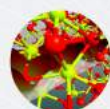
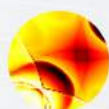
Calculate

I-V curve
transistor characteristics
spin current
Schottky barrier
leakage current
contact resistance
tunnel magneto-resistance
charge stability diagram
classical potential
Molecular Dynamics nanotube
complex bandstructure
transition states
thermal transport
spin transfer torque



ATK is also an ideal tool for educational courses in various subjects, from basic quantum mechanics to graduate courses in nanoelectronics. Special discounts are available for teaching licenses.

Since 2006, over 800 scientific articles have been published using ATK. The software is used by over 300 research groups at leading universities, government labs, and electronics companies around the world, in a wide range of application areas (see other side).



Quantum
Wise
When every atom matters



Download a free trial:

www.quantumwise.com

Application areas

The unique capabilities of Atomistix ToolKit are currently being applied in a wide variety of areas, such as carbon and molecular electronics, nanowires, and spintronics devices, as well as for assessing the structural and electrical properties of new electronic materials like high-k dielectrics or organic electronic materials.

Molecular Electronics

- Current-voltage (I-V) characteristics of rectifying molecular junctions (single molecules between metal electrodes), i.e. molecular diodes and switches. The active component can be an organic or organometallic molecule, a metallic nanocluster, etc.
- Resistivity of insulating or conducting molecular wires, free or attached to surfaces.
- Investigation of optical switches
- Inelastic spectroscopy.



Bulk and nanoscale semiconductors

- Surface states in semiconducting nanowires.
- Leakage currents in ultra-shallow junctions with high/low-k dielectrics.
- Schottky barriers of complex interfaces.
- Activation energies of defect diffusion.
- Work function of nanostructured surfaces (nanoclusters, wires).
- Binding energies of defects in bulk semiconductors, nanowires, or nanotubes.
- Nonparabolicity parameters.
- Phonon limited mobility.



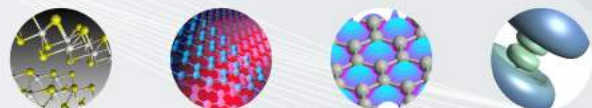
Carbon-based Electronics

- Transport properties (conductance, I-V) of carbon or boron-nitride nanotubes, with or without defects and impurities.
- Graphene nanoribbons, e.g. for field-effect transistor applications; also bilayer structures.
- Multiwall nanotubes, for applications as nanoscale variable resistors or capacitors.
- Contact resistance and capacitance of metal, nanotube and graphene interfaces and junctions.
- I-V characteristics of functionalized nanotubes or graphene for sensor applications.



3-Terminal devices

- Advanced electrostatic model with dielectric and biased metallic region.
- Calculation of transistor characteristics.
- Charge stability diagrams of weakly coupled single-electron transistors in Coulomb blockade regime (sequential tunneling).



Nanowires

- I-V characteristics of metallic nanowires and atomic point contacts.
- Electromigration and non-equilibrium current-induced forces in atomic wires.
- Mobility limited by random scattering.



Magnetic systems and spintronics

- Spin tunneling mechanisms in magnetotunnel junction (MTJ) for MRAM/read applications.
- Spin torque transfer in MTJs.
- I-V characteristics of molecular spintronics structures.
- Non-collinear, including spin spin-orbit.
- Transport properties of magnetic metallic nanowires.



Computational science has become critical to scientific leadership, economic competitiveness, and national security. Breakthroughs and innovations will be won by those most skilled with advanced computing systems and computational science applications.

US President's Information Technology Advisory Committee

QuantumWise, Virtual NanoLab, Atomistix ToolKit, and NanoLanguage are registered trademarks used under licence.

© QuantumWise 2015

QuantumWise A/S

Fruebjergvej 3, Box 4
DK-2100 Copenhagen
DENMARK

Quantum
Wise
When every atom matters

www.quantumwise.com

info@quantumwise.com

+45 699 01 888

+45 698 02 801



Registration Opening for all conferences Nanotech France 2016, EGF 2016, NanoMatEn 2016 and NanoMetrology 2016

May 31 st , 2016		
15:00-18:00	Registration / Welcoming Cocktail Reception	Registration Area

Nanotech France 2016 Sessions Program

June 1 st , 2016		
08:30-12:00	Registration	Registration Area
09:00-12:45	Nanotech Plenary Session I	Amphitheatre H
09:00-12:45	Joint Symposium on Functional Hybrids and Clay Nanomaterials	Room 261
12:00-14:00	Lunch Break / Exhibition / Poster Session I	Restaurant / Main Hall
14:00-16:00	Session I: Nanomaterials Fabrication / Synthesis	Room 211
	Session II - Nanomaterials synthesis and properties	Room 212
	Joint Symposium on Functional Hybrids and Clay Nanomaterials	Room 261
16:00-16:30	Coffee Break / Exhibition / Poster Session I	Main Hall
16:30-19:00	Session I: Nanomaterials Fabrication / Synthesis	Room 211
	Session II - Nanomaterials synthesis and properties	Room 212
	Joint Symposium on Functional Hybrids and Clay Nanomaterials	Room 261
June 2 nd , 2016		
09:15-12:45	Nanotech Plenary session II	Amphitheatre H
10:00-10:30	Coffee Break / Exhibition / Poster Session II	Main Hall
10:30-12:45	Session III: NanoBioMedecine /Nanosafety	Room 508
12:00-14:00	Lunch break / Exhibition / Poster session II	Restaurant / Main Hall
14:00-16:00	Session III: NanoBioMedecine /Nanosafety	Room 508
16:00-16:30	Coffee break / Exhibition / Poster session II	Main Hall
16:30 -19:00	Session III: NanoBioMedecine /Nanosafety	Room 508
18:30-20:30	Networking Cocktail – Meet Elsevier Team	Main Hall
June 3 rd , 2016		
09:00-10:00	Session IV: NanoElectronics/NanoPhotonics	Room 211
	Industrial session: InnovNano France 2016	Room 508
10:00-10:30	Coffee Break + Exhibition	Main Hall
10:30-13:00	Session IV: NanoElectronics/NanoPhotonics	Room 211
	Industrial session:InnovNano France 2016	Room 508

NanoMetrology France 2016 Sessions Program

June 1 st , 2016		
08:30-12:00	Registration	Registration Area
09:00-12:45	Nanotech Plenary Session I	Amphitheatre H
10:30-11:00	Coffee Break / Exhibition / Poster Session II	Main Hall
11:00-12:45	Session I: Nanomaterials characterization	Room 508
	Symposium on Nanospectroscopy	Room 561
12:00 - 14:00	Lunch Break / Exhibition / Poster Session I	Restaurant / Main Hall
14:00 16:00	Session I: Nanomaterials characterization	Room 508
	Symposium on Nanospectroscopy	Room 561
16:00 -16:30	Coffee Break / Exhibition / Poster Session I	Main Hall
16:30 19:00	Session I: Nanomaterials characterization	Room 508
	Symposium on Nanospectroscopy	Room 561

June 2 nd , 2016		
09:15-12:45	Nanotech Plenary session II	Amphitheatre H
09:00-10:00	Symposium on Detection, location & quantification Nano	Room 511
10:00 - 10:30	Coffee Break / Exhibition / Poster Session II	Main Hall
10:30 -12:45	Symposium on Detection, location & quantification Nano	Room 511
12:00 -14:00	Lunch break / Exhibition / Poster session II	Restaurant / Main Hall
14:00 -16:00	Symposium on Detection, location & quantification Nano	Room 511
16:00 - 16:30	Coffee break / Exhibition / Poster session II	Main Hall
16:30 -19:00	Symposium on Detection, location & quantification Nano	Room 511
18:30 -20:30	Networking Cocktail – Meet Elsevier Team	Main Hall

NanMaterials for Energy and Environment - NanoMatEn 2016

Sessions Program

June 1 st , 2016		
08:30-12:00	Registration / Welcome Coffee	Registration Area
09:00-12:45	Nanotech Plenary Session I	Amphitheatre H
12:00-14:00	Lunch Break / Exhibition / Poster Session I	Restaurant / Main Hall
June 2 nd , 2016		
08:30-12:45	Nanotech Plenary session II	Amphitheatre H
10:30-11:00	Coffee Break / Exhibition / Poster Session II	Main Hall
10:30-12:45	NanoMatEn 2016 Session I: NanoEnergy	Room 211
	NanoMatEn 2016 Session II: Nanotechnology for Environmental	Room 212
12:00-14:00	Lunch break / Exhibition / Poster session II	Restaurant / Main Hall
14:00-16:00	NanoMatEn 2016 Session I: NanoEnergy	Room 211
	NanoMatEn 2016 Session II: Nanotechnology for Environmental	Room 212
	Symposium on Nanotechnology for Photovoltaics	Room 260
16:00-16:30	Coffee break / Exhibition / Poster session II	Main Hall
16:30-19:00	NanoMatEn 2016 Session I: NanoEnergy	Room 211
	NanoMatEn 2016 Session II: Nanotechnology for Environmental	Room 212
	Symposium on Nanotechnology for Photovoltaics	Room 260
18:30-20:30	Networking Cocktail – Meet Elsevier Team	Main Hall
June 3 rd , 2016		
08:30-10:30	NanoMatEn 2016 Session III: Nanotechnology for water treatment	Room 561
10:30-11:00	Coffee Break / Exhibition	Main Hall
11:00-13:00	NanoMatEn 2016 Session III: Nanotechnology for water treatment	Room 561

European Graphene Forum - EGF 2016 Sessions Program

June 1 st , 2016		
08:30-12:00	Registration / Welcome Coffee	Registration Area
09:00-10:30	EGF2016 Plenary Session I	Amphitheatre G
10:30-11:00	Coffee Break / Exhibition / Poster Session II	Main Hall
11:00-12:45	EGF2016 Plenary Session I	Amphitheatre G
12:45-14:00	Lunch Break / Exhibition / Poster Session I	Restaurant / Main Hall
14:00-16:00	EGF 2016- Session I: Graphene and 2D Materials Synthesis, characterization and properties	Amphitheatre G
16:00-16:30	Coffee Break / Exhibition / Poster Session I	Main Hall
16:30-19:00	EGF 2016- Session I: Graphene and 2D Materials Synthesis, characterization and properties	Amphitheatre G

June 2 nd , 2016		
09:15-12:45	EGF 2016 Plenary Session II	Amphitheatre G
10:30-11:00	Coffee Break / Exhibition / Poster Session II	Main Hall
10:30-12:45	EGF 2016 Plenary Session II	Amphitheatre G
12:00-14:00	Lunch break / Exhibition / Poster session II	Restaurant / Main Hall
14:00-16:00	EGF 2016- Session II: Graphene and 2D Materials characterization and properties	Amphitheatre G
	EGF 2016- Session III: Graphene and 2D Materials properties and applications	Room 561
16:00-16:30	Coffee break / Exhibition / Poster session II	Main Hall
16:30-19:00	EGF 2016- Session II: Graphene and 2D Materials characterization and properties	Amphitheatre G
	EGF 2016- Session III: Graphene and 2D Materials properties and applications	Room 561
18:30-20:30	Networking Cocktail – Meet Elsevier Team	Main Hall

June 3 rd , 2016		
08:30-10:00	EGF 2016- Session IV: Graphene and 2D Materials applications	Room 511
10:00-10:30	Coffee Break / Exhibition	Main Hall
10:30-13:00	EGF 2016- Session IV: Graphene and 2D Materials applications	Room 511

Nanotech France 2016 Conference Preliminary Program

June 1st, 2016 Nanotech Plenary session I		
Amphitheatre H		
Session's Chairs: Prof. Jupille Jacques, Institut des Nanosciences de Paris - France. Prof. James M Hill, University of South Australia – Australia		
08:30-12:00	Conferences Registration	
09:00-09:30	Club nanoMetrology: a French Initiative to improve the Reliability of Measurements at the Nanoscale. A review after 4 years. G. Favre , K. Aguir, D. Bernard, O. Bezencenet, J. Carimalo, N. Feltin, B. Gautier, A. Levenson, T. Macé, P. Maillot and J.-M. Moschetta	Dr. Georges Favre , Laboratoire national de métrologie et d'essais (LNE) – France
09:30-10:00	European standardization in nanotechnologies and relation with International work. How standardization can help industry and regulators in developing safe products? P. Conner	Mr. Patrice Conner , AFNOR Standardization, Management and Consumer Services Dep- France
10:00-10:30	Mathematical modelling in nanotechnology J. Hill	Prof. James M Hill , University of South Australia – Australia
10:30-11:00	Coffee Break / Exhibition/ Posters Session I	
11:00-11:30	Water collection/Repellency of Bioinspired Micro/Nano-structured Surfaces Y. Zheng	Prof. Yongmei Zheng , Beihang University – China
11:30-12:00	Ultrasonic Spray Coating as a versatile technique for the large area deposition of functional nanoparticles J. Stryckers and W. Deferme	Prof. Wim Deferme , Hasselt University - Belgium
12:45-14:00	Lunch Break / Exhibition / Posters session I	

June 1st, 2016 Session I: Nanomaterials Fabrication / Synthesis		
Conference Room 211		
Session's Chairs: Prof. Jacques Jupille, Institut des Nanosciences de Paris – France/ Prof. Nicolas Fressengeas, Lorraine University – France/ Dr. Valentina Beghetto, Ca' Foscary, University of Venice – Italy / Prof. Valentin Rodionov, King Abdullah University of Science and Technology - Saudi Arabia		
14:00-14:15	Rational Synthesis of Chirality-Pure Single Walled Carbon Nanotube K.Yu. Amsharov	Dr. Konstantin Amsharov , University of Erlangen-Nürnberg – Germany
14:15-14:30	New frontiers and technologies for advanced materials V. Beghetto , L. Agostinis, R. Taffarello and R. Samiolo	Dr. Valentina Beghetto , Ca' Foscary, University of Venice - Italy
14:30-14:45	Weak interactions for strong complexation between DNA nano-rods and lipids L. Navailles , K. Bougis, R. Leite Rubim, N. Ziane, J. Peyencet, A. Bentaleb, A. Février, B.B. Gerbelli, C.L.P. Oliveira, A. de Oliveira, . Schoentgen, G. Tonelli, P. Barthélémy and F. Nallet	Dr. Laurence Navailles , CNRS/ Bordeaux University, France

14:45-15:00	Repeat proteins as template to organize photoactive molecules S. Hernández Mejías , J. López-Andarias, K. Erazo, C. Atienza, N. Martín and A.L. Cortajarena	Ms. Sara Hernández , IMDEA-Nanociencia, Madrid - Spain
15:00-15:15	Chemical Reactions Directed Evolution of Complex Peptide Nanostructures A.K. Das	Dr Apurba K. Das , Indian Institute of Technology Indore- India
15:15-15:30	Metal nanoparticles for optical limiting prepared via citrate reduction C. S. Hege , S. Dengler and B. Eberle	Ms. Cordula Hege , Fraunhofer IOSB – Germany
15:30-15:45	Shape and Pore Size Controlled Scalable Synthesis of Functional Oxide Nanostructures through Exothermic Chemical Reactions A. Voskanyan and K.Y. Chan	Mr. Albert Voskanyan , The University of Hong Kong - Hong Kong
15:45-16:00	Ultrasonic Spray Coating as a scale-up technique for the deposition of hybrid magnetic-plasmonic nanocomposites J. Stryckers , T. Swusten, W. Brullot, J. D'Haen, T. Verbiest and W. Deferme	Mr. Jeroen Stryckers , Hasselt University - Belgium
16:00-16:30	Coffee Break / Exhibition/ Posters Session I	
16:30-16:45	The Development and Application of Vacuum-interconnected Technology for Nanofabrications S. A. Ding and H. Yang	Dr. Sunan Ding , SuZhou Institute of Nano-Tech and Nano-Bionics / Chinese Academy of Sciences - China
16:45-17:00	Functionalization of single wall carbon nanotube for cesium sorption H. Draouil , L. Alvarez, J. Cambedouzou, M. A. Zaibi and J.-L. Bantignies	Ms. Hajer Draouil , Tunis University - Tunisia
17:00-17:15	Development of a new direct liquid injection system for nanoparticle deposition by chemical vapor deposition using nanoparticle solutions M.Vervaele , B. De Roo, M.Rajala, H.Guillon, J.W.Seo and J.P.Locquet	Mr. Mattias Vervaele , KU Leuven - Belgium
17:15-17:30	Composite production for Cold Gas Spray and photocatalytic behavior of the multifunctional coatings S. Dosta , M. Robotti, I. G. Cano, N. Cinca, A. Concustell, J. M. Guilemany	Dr. Sergi Dosta , University of Barcelona - Spain
17:30-17:45	Application of Spark discharge method for in situ synthesis of copper nano particles on cotton fabrics S. Shahidi , A.Jamali 2, S.D. Sharifi and H. Ghomi	Dr. Sheila Shahidi , Islamic Azad University- Iran
17:45-18:00	Controlled resonance energy transfer under one- and two-photon excitations in a hybrid material engineered from quantum dots and the photosensitive protein bacteriorhodopsin V. Krivenkov , P. Samokhvalov, R. Bilan, D. Solovyeva, A. Chistyakov and I. Nabiev	Mr. Victor Krivenkov , National Research Nuclear University - Russian Federation
18:00-18:15	Microwave Assisted Synthesized ZnO nanorods arrays on Tetrapak Substrate A.Pimental , B. Coelho, S. Ferreira, A. Araújo, D. Nunes, M. Oliveira, R.Franco, H. Águas, R. Martins and E. Fortunato	Dr. Ana Pimentel , Universidade NOVA de Lisboa - Portugal
18:15-18:30	Fabrication of Metal Nanotubes via Short-Circuit Diffusion Process and The Diffusion Model S. Baylan , E. Rabkin and G. Richter	Mrs. Semanur Baylan , Max Planck Institute for Intelligent Systems- Germany
18:30-18:45	Design and characterization of nanowired microwave devices in substrate integrated waveguide technology V. Van Kerckhoven , L. Piraux and I. Huynen	Mr. Vivien Van Kerckhoven , Université catholique de Louvain - Belgium
18:45-19:00	G-doping in Thin Si Nano-grating Layers A. Tavkhelidze, L. Jangidze, M. Mebonia , G. Skhiladze, D. Ursutiu, C. Samoilă, Z. Taliashvili, and L. Nadaraia	Mr. Mikheil Mebonia , Ilia State University- Germany

June 1st, 2016
Session II - Nanomaterials synthesis and properties

Conference Room 212

Session's Chairs:

Prof. Wim Deferme, Hasselt University – Belgium/ Prof. Yongmei Zheng, Beihang University – China/ Dr. Karine Bonnot, French German Research Institute of Saint-Louis – France/ Prof. Tahar Laoui, King Fahd University of Petroleum and Minerals- Saudi Arabia

14:00-14:30	Surface-Engineered Mechanically Hard Tungsten Disulfide (WS ₂) Inorganic Nanotubes (INTs-WS ₂)– Novel Chemically Tailored Nanoscale CNT-Replacement Inorganic “Nanofillers” J.-P. Lellouche, D. Raichman and J. Laloy	Prof. Jean-Paul Lellouche, Bar-Ilan University - Israel
14:30-14:45	Reinforcing Acrylonitrile Rubber With Graphene: Inspection of Mechanical, Thermal and Cure Kinetics Properties B. Mensah and C. Nah	Mr. Bismark Mensah, Chonbuk National University - Rep. of Korea
14:45-15:00	Development of Flexural Properties in Woven-fabric/Epoxy Resin CFRP Panels with Additional Nano Rubber Particle Reinforcement J. Sirichantra, T. Pullawan, P. Lamo and S. Kumwongwian	Dr. Jariyavadee Sirichantra, Ministry of Science and Technology - Thailand
15:00-15:15	The effect of dispersion method and processing condition on the structure properties of polystyrene/graphene oxide nanocomposites Z. Mohammadsalih, B.J. Inkson and B. Chen	Mr. Zaid Mohammadsalih, University of Sheffield - UK
15:15-15:30	Hollow Nanoparticles for Applications in Lightweight Nano-composites V. Rodionov and T. Sainsbury	Prof. Valentin Rodionov, King Abdullah University of Science and Technology - Saudi Arabia
15:30-15:45	Functionalization and optical properties of inorganic liquid crystals M. Thiriet, K. Lahlil, J.P. Boilot, J. Peretti and T. Gacoin	Ms. Maud Thiriet, Ecole Polytechnique, CNRS – France
15:45-16:00	Chip Calorimetry for Investigating the Co-detection of Hexogen and Pentrite Vapors by Nanostructured Porous Materials K. Bonnot, L. Schlur and D. Spitzer	Dr. Karine Bonnot, French German Research Institute of Saint-Louis - France
16:00-16:30	Coffee Break / Exhibition/ Posters Session I	
16:30-16:45	Development of fire retardant treatment with silica nanoparticles to apply onto bio-based composite materials M. Bourebrab, G. Durand, A. Taylor, R. Hadden and L. Bisby	Ms. Marion Bourebrab, University of Edinburgh - UK
16:45-17:00	Resistive sensors from nanoparticle assemblies L. Baklouti and F. Favier	Ms Linda Baklouti, University of Montpellier – France
17:00-17:15	Effect of nano Zinc oxide particles on weathering properties of epoxy coatings D. Shalini and A.S.Khanna	Mrs. Dolai Shalini, IIT Bombay – India
17:15-17:30	Facile Synthesis of Scalable Hierarchical Surfaced Titanium Di-oxide Hollow Sphere for Hydrogen Generation Application K.K. Jeremy Ang, B.Y.Liang Tan, J.Juay and D. Sun	Mr. Koon Keong Jeremy Ang, Nanyang Technological University – Singapore
17:30-17:45	Solid Cation-exchange Resin catalysed Esterification of Lactic Acid with Ethanol: A Novel Kinetic Study. E. Okon and G. Edward	Mrs. Edidiong Okon, The Robert Gordon University Aberdeen – UK
17:45-18:00	Resistive Switching in Self-ordered TiO ₂ Nanocolumn Arrays M. Marik, M. Bendova, J. Hubalek and A. Mozalev	Mr. Marian Marik, Brno University of Technology - Czech Republic

18:00-18:15	Formulation and Characterization of Garlic oil nanoparticles with enhanced Anti-Microbial Activities S. Fahmy and W. Mamdouh	Mr. Sherif Fahmy , The American University in Cairo – Egypt
18:15-18:30	Neutron radiation resistance of ferroelectric copolymer filled with Al ₂ O ₃ and ZnO nanoparticles S.Rouabah , B. Vincent, D.Rouxel, A.Chaabi, S.Girard, P. Paillet and M. Gaillardin	Ms. Sawsen Rouabah , Jean Lamour Institute – France
18:30-18:45	The Synthesis of Blue Colored Zirconia and Its Application on Automotive Industry A.Yurdakul and H. Gocmez	Dr. Arife Yurdakul , Dumlupinar University- Turkey
18:45-19:00	Effect of nanoclay on short term water absorption and swelling of composites made by wood poplar flour and recycled polystyrene A. Tavasoli , A. Samariha, M. Nemati and Z. Masoomi	Dr. Afshin Tavasoli , Islamic Azad University- Iran

June 1st, 2016

Nanotech France 2016: Joint Symposium on Functional Hybrids and Clay Nanomaterials

Conference Room 261

Session's Chairs:

Prof. Eduardo Ruiz-Hitzky and Dr. Pilar Aranda, Materials Science Institute of Madrid (ICMM-CSIC) - Spain

Prof. Alicia de Andrés, Materials Science Institute of Madrid (CSIC) - Spain

Dr Mercedes Vila, Ctechnano-coating technologies S.L - Spain

Dr. Vanessa Prevot, Blaise Pascal University - France

09:00-09:05	Welcome from the symposium chairs	Chairs
09:05-09:40	Clay-graphene nanocomposites E. Ruiz-Hitzky	Prof. Eduardo Ruiz-Hitzky , Materials Science Institute of Madrid (ICMM-CSIC) – Spain
09:40-09:55	Graphene / Ru nanostructure transparent hybrid systems for sensing applications L. Álvarez-Fraga, F. Jiménez-Villacorta , E. Climent-Pascual, R. Ramirez-Jiménez, C. Prieto and A. de Andrés	Dr. Felix Jimenez-Villacorta , Materials Science Institute of Madrid (CSIC) – Spain
09:55-10:10	Thermal properties of LDPE Graphene filled nanocomposites designed for HVDC cable accessories. K. Gaska , R. Hafiizh Azhari, R. Kadar, M. Andersson and S. Gubanski	Dr. Karolina Gaska , Chalmers University of Technology – Sweden
10:10-10:30	Coffee Break / Exhibition/ Posters session I	
10:30-11:05	Multi-parameter monitoring of in vitro tissue models using organic electronics R.M Owens	Dr. Roisin Owens , Ecole des Mines de. St. Etienne – France
11:05-11:30	DNA-based bionanocomposites for gene transfer and biotechnological applications. F.A.Castro-Smirnov , O. Piétrement, P. Aranda, J. Ayache, E. Le Cam, J-R. Bertrand, B.S. Lopez and E.Ruiz-Hitzky	Prof Fidel A. Castro-Smirnov , University of Informatic Sciences – Cuba
11:30-11:55	In Vivo Multimodal Deep Tissue Imaging with Hybrid Nanostructures D. H. Ortgies , L. de la Cueva, B. del Rosal, F. Sanz-Rodríguez, N. Fernández, M. C. Iglesias-de la Cruz, G. Salas, D. Cabrera, F. J. Teran, D. Jaque and E. Martín Rodríguez	Dr. Dirk Ortgies , Autonomous University of Madrid – Spain
11:55-12:10	Magneto-photo-thermal Nanomaterials as Efficient Nanoheaters for Tumor Therapy A. Espinosa , R. Di Corato, J. Kolosnjaj-Tabi, M. Bugnet, G. Radtke, S. Neveu, G. A. Botton, P. Flaud, A. Abou-Hassan, T. Pellegrino and C. Wilhelm	Dr Ana Espinosa , Paris Diderot University - France

12:10-12:25	Adsorption of diclofenac pharmaceutical product onto clay mineral and organoclay derivatives T. De Oliveira and R.Guégan	Mr. Tiago De Oliveira , Institut des Sciences de la Terre d'Orléans – France
12:45-14:00	Lunch Break / Exhibition / Posters session I	
14:00-14:25	Sepiolite-Nanocellulose Assembly as new Nanofibrous Hybrid Materials M. M. González del Campo, M. Darder, P. Aranda and E. Ruiz-Hitzky	Dr. Margarita Darder , Materials Science Institute of Madrid, CSIC-Madrid - Spain
14:25-14:40	Multi-enzyme/layered double hydroxide-based biohybrids for the synthesis of chiral polyols in cascade reaction F. Bruna Gonzalez , M. De Sousa, M. Lorillière, G. Ali, T. Gefflaut, V. de Berardinis, L. Pollegioni, W.-D. Fessner, C. Forano, V. Prévot, C. Mousty, F.Charmantay and L. Hecquet	Dr. Felipe Bruna Gonzalez , Blaise Pascal University - France
14:40-14:55	Biohybrids based on zein and montmorillonite: preparation and use as nanofiller in clay-based bionanocomposites A.C.S. Alcântara, M. Darder, P. Aranda and E. Ruiz-Hitzky	Dr. Pilar Aranda , Materials Science Institute of Madrid, CSIC-Madrid - Spain
14:55-15:30	Hybrid Photonics for Energy Efficiency P.G. Lagoudakis	Prof. Pavlos G. Lagoudakis , University of Southampton - UK
15:30-15:55	Plasmon assisted Nd ³⁺ -based solid-state nanolaser P. Molina, E. Yraola, M.O. Ramírez, C. Tserkezis, J.L. Plaza, J.Aizpurua, J.Bravo-Abad and L.E. Bausá	Prof. Luisa Bausá , Autonomous University of Madrid – Spain
15:55-16:15	Coffee Break /Exhibition/ Posters Session I	
16:15-16:40	MoSi ₂ -Si ₃ N ₄ Composite Absorber for Concentrated Solar Power (CSP) A. Rodríguez-Palomo, D. Hernández-Pinilla, E. Céspedes, L. Álvarez-Fraga, F. Jiménez-Villacorta, R. Jiménez-Riobóo and C. Prieto	Prof. Carlo Prieto , Materials Science Institute of Madrid (CSIC) – Spain
16:40-16:55	Hybrid photonic crystal LED renders 123% color conversion effective quantum yield M. Brossard , C. Krishnan, K.-Y. Lee, J.-K. Huang, C.-H. Lin, H.-C. Kuo, M. D. B. Charlton and P. G. Lagoudakis	Dr. Mael Brossard , University of Southampton – UK
16:55-17:10	ZnO-clay nanoarchitectures: preparation and uses as photocatalyst M. Akkari, P. Aranda, H. Ben Rhaïem, A. Ben Haj Amara and E. Ruiz-Hitzky	Dr. Pilar Aranda , Materials Science Institute of Madrid, CSIC-Madrid - Spain
17:10-17:40	Atomic and Molecular Layer Deposition of Hybrid Nanostructured Materials M.Vila	Dr. Mercedes Vila Juárez , CTECH Nano-Coating Technologies S.L – Spain
17:45-17:55	Maya Blue-Based Nanostructured Clay Materials for Colouring Geopolymers C.M. Ouellet-Plamondon , P. Aranda, A. Favier, G. Habert, H. Van Damme and E. Ruiz-Hitzky	Prof. Claudiane Ouellet-Plamondon , École de Technologie Supérieure – Canada
17:55-18:10	Multifunctional Metallic Janus MOF Particles Synthesized by the Desymmetrization at Interfaces Approach A. Ayala , I. Imaz and D. Maspoch	Mr. Abraham Ayala Hernández , Autonomous University of Barcelona - Spain
18:10-18:25	Nanoclays for adsorption of tartrazine: A sustainable application C. del Hoyo Martínez , M. S. Lozano García and V. Sánchez Escribano	Prof. Carmen del Hoyo Martínez , University of Salamanca – Spain
18:25-18:40	Study of synthetic talc growth by EXAFS: basic research to support technology transfer A. Dumas , M. Mizrahi, F. Martin, F. Requejo, M. Claverie, C. Aymonier	Dr Angela Dumas , Institut de Chimie de la Matière Condensée de Bordeaux (ICMCB) – France

June 2nd, 2016
Nanotech Plenary session II

Amphitheatre H

Session's Chairs:
Prof. Jupille Jacques, Institut des Nanosciences de Paris – France/ Prof. Alejandro Pérez-Rodríguez, Catalonia Institute for Energy Research, IREC – Spain

09:15-10:00	DNA-controlled fusion of liposomes O.Ries, P.Löffler and S.Vogel	Prof Stefan Vogel , University of Southern Denmark - Denmark
10:00-10:30	Coffee Break / exhPosters Session	
10:30-11:15	Meeting the needs for aged and released nanomaterials required for further testing B. Nowack	Prof. Bernd Nowack , Empa, Swiss Federal Laboratories for Materials Science and Technology - Switzerland
11:15-12:00	Resonant Raman scattering methodologies for assessment of nanometric layers in high efficiency chalcogenide solar cells M. Guc, D. Hariskos, W. Hempel, F. Oliva, L. Calvo-Barrio, T. Jawhari, V. Izquierdo-Roca and A. Pérez-Rodríguez	Prof. Alejandro Pérez-Rodríguez , Catalonia Institute for Energy Research, IREC - Spain
12:00-12:30	Publish books chapters with SETCOR, in collaboration with Elsevier.	Mr Simon Holt/ Mr Matthew Deans , Elsevier Publishing- UK
12:45-14:00	Lunch Break/ Exhibition/ Posters session II	

June 2nd, 2016
Session III: NanoBioMedecine/Nanosafety

Conference Room 508

Session's Chairs:
Prof. Danail Hristozov, University Ca' Foscari Venice – Italy/ Dr. Nicklas Raun Jacobsen, National Research Centre for the Working Environment, Copenhagen – Denmark/ Prof. Kevin Braeckmans, Ghent University - Belgium

10:30-11:00	Engineered cell wall binding domains of lysins for the multiplexed detection and rapid separation of food-borne pathogens M. Kong and S. Ryu	Prof. Sangryeol Ryu , Seoul National University - Republic of Korea
11:00-11:15	Room-temperature aqueous synthesis of ultra-small Cu ₂ -xSe nanoparticles for highly efficient photoacoustic imaging-guided photothermal cancer therapy S. Zhang , J. Xiong, L. Zhang, Z. Li and S. Dou	Mr. Shaohua Zhang , University of Wollongong - Australia .
11:15-11:30	Selective cancer cell toxicity and radiosensitization using mixed-oxide high atomic number nanoparticles S.Grellet , S. Kaas, E. Crabb, S. Allman and J.Golding	Ms Sophie Grellet The Open University - UK
11:30-11:45	Doxorubicin-loaded BN Nanoparticles for Cancer Therapy I.V. Sukhorukova , I.Yu. Zhitnyak, A.M. Kovalskii, N.A. Gloushankova, D.V. Golberg and D.V. Shtansky	Mrs. Irina Sukhorukova , National University of Science and Technology- Russia
11:45-12:00	Antimicrobial electrospun nanofibrous scaffolds for gingival fibroblast growth A. Baranowska-Korczync , M. Jasiurkowska-Delaporte, B. Grześkowiak, M. Jarek, A. Warowicka, B. M. Maciejewska, J. Jurga-Stopa and S. Jurga	Dr. Anna Baranowska-Korczync , Adam Mickiewicz University - Poland
12:00-12:15	Development of new biocompatible □-Ti coatings on Ti6Al4V for medical applications E. Frutos and T. Polcar	Dr. Emilio Torres , Czech Technical University in Prague - Czech Republic

12:15-12:30	Wound healing evaluation of collagen-laminin dermal matrix E.H. Gokce , S. Tuncay-Tanriverdi, İ. Eroglu, N. Tsapis, I. Tekmen, E. Fattal and O. Ozer	Dr. Evren Homan Gökçe , University of Ege- Turkey
12:30-12:45	Nanostructured Copper Hydroxide on Graphene Pore Structure for Non-enzymatic Electrochemical Glucose Sensor I. Shackery and S. C. Jun	Mr. Iman Shackery , Yonsei University, Seoul - Rep. of Korea
12:45-13:00	An innovative detection platform to support nanomedicine characterisation and development C. Desmet , A. Valsesia, R. La Spina, P. Urban, F. Rossi and P. Colpo	Dr. Cloe Desmet , European Commission Joint Research Centre – Italy
12:45-14:00 Lunch Break / Exhibition / Posters session II		
14:00-14:30	Highly controlled delivery of macromolecules and contrast agents in living cells by laser-induced vapour nanobubbles R. Xiong, F. Joris, L. Wayteck, K. Raemdonck, K. Peynshaert, I. Lentacker, A. G. Skirtach and K. Braeckmans	Prof. Kevin Braeckmans , Ghent University - Belgium
14:30-14:45	Imidazolium-derived nanostructures for drug delivery M. Rodrigues , E. Amirthalingam, D. Limón, A. Calpena, D. B. Amabilino and L. Pérez-García	Dr. Mafalda Rodrigues , Barcelona University – Spain
14:45-15:00	The development and evaluation of a novel hybrid PLGA nanoparticle-Pheroid® system with the potential to improve tuberculosis therapy M.P. Chelopo , L. Kalombo, J. Wesley-Smith, B. Naicker, M. Glyn, A. Grobler and R. Hayeshi	Ms. Madichaba P Chelopo , North-West University and CSIR - South Africa
15:00-15:15	A novel SPION-eicosane coating material for on-demand drug release triggered by magnetic hyperthermia L. Che Rose , A.G. Mayes and H. Suhaimi	Dr Laili Che Rose , Malaysia Terengganu University – Malaysia
15:15-15:30	Morphology effect of mesoporous silica nanoparticles on drug delivery S. Rahmani , L. Lichon, M. Maynadier, M. Garcia, M. Gary-Bobo, M. Ferid, C. Charnay and J.O. Durand	Ms. Saher Rahmani , Institut Charles Gerhardt Montpellier University - France
15:30-15:45	Application of samarium oxide to evaluate the in vivo bio-distribution of PLGA nanoparticles V. Mandiwana , L. Kalombo, J.R. Zeevaart and A. Grobler	Ms. Vusani Mandiwana , CSIR, North West University - South Africa
15:45-16:00	Efficient drug delivery with synthesized mitoxantrone-gold nanoparticle conjugates for in vitro breast cancer therapy A. Jafarizad , S. gharibian, G. Pavon-Djavid and D. Ekinici	Dr. Abbas Jafarizad , Sahand University of Technolog- Iran .
16:00-16:30 Coffee Break / Exhibition / Posters Session II		
16:30-17:00	Toxicology: Pulmonary and systemic toxicity caused by nanoparticles NR. Jacobsen	Dr. Nicklas Raun Jacobsen , National Research Centre for the Working Environment- Copenhagen - Denmark
17:00-17:15	Measurement of airborne engineered nanoparticles M. Levin	Dr. Markus Levin , National Research Center for the Working Environment - Denmark
17:15-17:30	Evaluation of Dithizone-Based Colorimetric Sensors for Silver Nanoparticles in Aqueous Media N. Wasukan , S. Srisung, M. Kuno, K. Kulthong and R. Maniratanachote	Dr. Nootcharin Wasukan , Srinakharinwirot University - Bangkok-Thailand
17:30-17:45	Drosophila melanogaster as a suitable in vivo model to determine potential side effects of nanomaterials M. Alaraby , A. Hernández and R. Marcos	Mr. Mohamed Alaraby , Autonomous University of Barcelona – Spain
17:45-18:00	Determination for Stability Constant of Silver-DMSA Nanoparticles S. Srisung , N. Wasukan, K. Kulthong and R. Maniratanachote	Dr. Sujittra Srisung , Srinakharinwirot University- Thailand
18:00-18:15	Legal Metrology Framework for Nanotechnology in Australia S. Devasahayam	Dr. Sheila Devasahayam , Federation University Australia, Victoria – Australia

18:15-18:30	Effects of Different Printing Ink Binders on Printability and Biodegradability of Polylactic Acid Film S. Netpradit , S. Binraman and C. Ladmai	Dr. Suchapa Netpradit , King Mongkut's University of Technology Thonburi - Thailand
18:30-18:45	Effect of the supply air supporting the shaping of the exhaust air flow during the processing of nanomaterials T. Jankowski	Mr. Tomasz Jankowski , Central Institute for Labour Protection – National Research Institute – Poland
18:45-19:00	High stability metal nanoparticles for healthcare applications E. El-Meliegy	Prof. Emad El-Meliegy , National Research Centre, Ceramics – Egypt
19:00-19:15	Overview of available data of occupational exposure to manufactured nanomaterials, approaches and needs S. Bau and O. Witschger	Dr. Sébastien Bau , Institut National de Recherche et de Sécurité- France

June 3rd, 2016

Session IV: NanoElectronics/NanoPhotonics

Conference Room 211

Session's Chairs:

Prof. Philippe Godignon, CNM-CSIC Barcelona-Spain – France/ Prof. Aurica Farcas, "Petru Poni" Institute of Macromolecular Chemistry – Romania

09:00-09:45	Nanoscale Magnetic Skyrmions- A New twist for Spintronics R. Wiesendanger	Prof. Roland Wiesendanger , University of Hamburg – Germany
09:45-10:00	Density of states and electrical properties of nanocrystalline Co ²⁺ and Ta ⁵⁺ substituted barium bismuth niobate P. Dhak , A.Kundu, M.K. Adak, D. Dhak and A.O. Sjøstad	Dr. Prasanta Dhak , University of Oslo – Norway
10:00-10:30	Coffee Break / Exhibition	
10:30-10:45	Self-powered high photoresponse ultraviolet photodetector based on dual ion beam sputtered Ga doped ZnO P. Sharma, R.Singh, R. Bhardwaj, and S. Mukherjee	Prof. Shaibal Mukherjee , Indian Institute of Technology, Indore – India
10:45-11:00	Perovskite Oxide Spin Filters B. Prasad and M.G. Blamire	Dr. Bhagwati Prasad , Max Planck Institute for Solid State Research- Stuttgart - Germany
11:00-11:15	New fundamental effects in single molecular circuitry A.C. Aragonès , N. Darwish, F. Sanz, E. Ruiz and I.Díez-Pérez	Mr. Albert Aragonès , University of Barcelona - Spain
11:15-11:30	Synaptic Weight Modulation and Logic Function Learning with Electro-grafted Nano Organic Memristors Y-P. Lin , C.H. Bennett, D. Chabi, D. Vodenicarevic, D. Querlioz, T. Cabaret, A. Balan, B. Jousset, C. Gamrat, J-O. Klein and V. Derycke	Dr. Yu-Pu Lin , CEA Saclay - France
11:30-11:45	Quantum Interference Effect In Anthraquinone Solid State Junctions M. L. Della Rocca , C. Bessis, C. Barraud, P. Martin, J.-C. Lacroix, T. Markussen and P. Lafarge	Dr. Maria Luisa Della Rocca , Paris Diderot University - France
11:45-12:00	Impact of Surface Modification of ITO Bottom Electrode on Switching Characteristics of ZnO-based Transparent Resistive Memory Devices Fabricated on Polymer Substrate F. M. Simanjuntak and T. Y. Tseng	Mr. Firman Mangasa Simanjuntak , National Chiao Tung University – Taiwan
12:00-12:15	Synthesis of ZrO ₂ films by spray pyrolysis ultrasonic presenting the up conversion phenomenon P. E. Ortiz-Ortega and M García-Hipólito	Mr. Pedro Enrique Ortiz Ortega , National Autonomous University of Mexico - Mexico .

12:15-12:30	Conjugated Polyrotaxanes: A Critical Assessment of Photo-physical Properties in Correlation with the Effect of the Nature of Host Molecules Encapsulation A. Farcas , A.-M. Resmerita and P.-H. Aubert	Prof. Aurica Farcas , "Petru Poni" Institute of Macromolecular Chemistry – Romania
12:30-12:45	Designing High Performance Digital Logic NOT Gate Using Single Electron Box (SEB) Nano-Devices D. Bahrepour	Dr. Davoud Bahrepour , Islamic Azad University- Iran
12:45-13:00	Use of Nanobiomechanics robots to tackle HIV virus A. Vohra	Mr. Amit Vohra , Bharat Electronics Limited- India

June 3rd, 2016 InnovNanoFrance 2016 : Industrial Session		
Conference Room 508		
Session's Chairs: Dr. Julio Gomez, CEO, Avanzare Innovacion Tecnologica S.L.- Spain		
09:00-9:30	Graphene based supercapacitors: results and perspectives P. Bondavalli and G. Pognon	Dr. Paolo Bondavalli , Head of Nanomaterial topic team, Thales Research and Technology – France
09:30-09:00	Graphene Roadmap: Wafer Scale Integration Mr Iñigo Charola	Mr. Iñigo Charola , Business Development Director- Graphenea - Spain
10:00-10:30	Coffee Break / Exhibition	
10:30-11:00	Static Multiple Light Scattering to monitor protein aggregation and pigments dispersibility C. Tisserand , G. Brambilla, P. Bru and G. Meunier	Dr. Christelle Tisserand , Formulation Company – France
11:00-11:30	Bulk graphene production and application in composites, energy and coatings J. Gomez , J. Perez and E. Villaro	Dr. Julio Gomez , CEO- Avanzare Innovacion Tecnologica S.L.- Spain
11:30-12:00	Graphene: the early commercialisation prospects R. Gibbs	Mr. Ray Gibbs , CEO- Hatydale Graphene Industries Plc- UK
12:00-12:30	3D Printing Sets New Standards in Microfabrication A. Legant	Mr. Alexander Legant , Nanoscribe GmbH, Eggenstein, Leopoldshafen – Germany
12:30-13:00	Graphene grown on SiC substrates for applications in electronics L. Serrano , A. García-García, A. Ballestar, J. M. de Teresa, M. R. Ibarra and P. Godignon	Dr. Luis Serrano , Graphene Nanotech (GPNT) - Spain

Posters Session I: June 1st 2016 Nanotech France 2016: Nanomaterials synthesis, characterization/Nanometrology and properties		
Exhibition and Poster Hall		
N.	Title	Author/Affiliation/Country
1	Organic solvent resistant polyelectrolyte multilayers : effect of the sulfonic to carboxylic content P. Argkarawanitnan and S. T. Dubas	Ms. Patsarat Argkarawanitnan , Chulalongkorn University, Bangkok – Thailand
2	Solvothermal hot injection synthesis of AgNi nanoalloy V. Vykoukal , J. Bursik, P. Roupčová and J. Pinkas	Mr. Vit Vykoukal , Masaryk University - Czech Republic
3	Layer-by-Layer Deposition of Photocatalysts on PU foam C. Wechwithayakhlung and S. Dubas	Ms. Chayanit Wechwithayakhlung , Chulalongkorn University, Bangkok – Thailand

4	Thickness dependent optical properties of the large area synthesized few layers MoSe ₂ on SiO ₂ and Al ₂ O ₃ substrates by Molecular Beam Epitaxy Y. H. Choi , D. H. Lim, J. H. Jung, K. -H. Yoo, B. -Y. Yoo and M. -H. Cho	Mr. Yoonho Choi , Yonsei University, Seoul - Republic of Korea
5	Influence of superficial morphology in the growth of zinc oxide nanowires Arana J A , Monroy B M and Santana G	Mr. Julio Alejandro Arana Trenado , National Autonomous University of Mexico - Mexico .
6	Plasma functionalized POSS / PDMS nano-composite membranes for solvent separation by pervaporation X. Chen , Z. Chen, R. d'Agostino, L. F. Dumée, X. J. Dai and K. Magniez	Mr Xiao. Chen , Deakin University - Australia
7	New molecular precursors for AgCu nanoalloy preparation V.Vykoukal, J. Bursik, P.Roupcova, V. Halasta and J. Pinkas	Prof. Jiri Pinkas , Masaryk University - Czech Republic
8	Influence of nano-particles on the surface morphology and properties of fouling release coatings based on polydimethylsiloxane Z. Zhang , H. Zhou and Y. Qi	Prof. Zhanping Zhang , Dalian Maritime University – China
9	Effect of operating conditions on adhesion strength of Cu/AlN laminate fabricated by High Vacuum Surface Controlled Direct Bonding S-C. Lim and K.B. Jang	Dr. Sung-Chul Lim , Korea Institute of Industrial Technology, Songdo-dong – Rep. of Korea
10	Enhancement of the TFT's performance by slight phosphorus doping: Lower density of states within the grain boundaries and higher stability M. Zaghdoudi , R.Rogel, T.Mohammed-Brahim and H. Ezzaouia	Mrs. Mariem Zaghdoudi , Institute of Environmental Science and Technology – Tunisia
11	The Green Synthesis, Characterization, and Antioxidant Activities of Silver Nanoparticles Synthesized from Asphodelus aestivus Aqueous Extract B. Kivçak , T. Erdoğan, P. Taştan, B. Sümer Tüzün and M. Özyazıcı	Prof. Bijen Kivçak , Ege University, Izmir – Turkey
12	Synthesis of Monodisperse Gold Nanoparticles for Plasmonics S. Marguet , J. Caron, A. Habert and M. Khaywah	Dr. Sylvie Marguet , CNRS/CEA Saclay – France
13	Enhanced Mass Activity of Pt as Au@Pt Nanoparticles on reduced Graphene Oxide Support for Methanol and Ethanol Oxidation P. Gnanaprakasam , S. E. Jeena and T. Selvaraju	Mr. P. Gnanaprakasam , Karunya University- India
14	Formation of Germanium Analog of The Tubular Aluminosilicate imogolite Containing Fe M. Ookawa , E. Kato, M. Watanabe, K. Osada, M. Yoshikawa and S. Yamane	Dr. Masashi Ookawa , National Institute of Technology, Numazu College – Japan
15	Dispersion Characteristics of Layered Double Hydroxides in the presence of amphipathic macroRAFT agents M. Pavlovic , V. Prevot, E. Bourgeat-Lami and I. Szilagyí	Mr. Marko Pavlovic , University of Geneva - Switzerland
16	Tuning the structure and the mechanical properties of epoxy-silica sol-gel hybrid materials B. Domènech, I. Mata and E. Molins	Dr. Ignasi Mata , Materials Science Institute -Barcelona (ICMAB-CSIC) - Spain .
17	High performance Transparent Electrode Consisting of Silver and Graphene Hybrid Structure Fabricated by Near-Field Electro-Spinning D. H. Youn , Y. J. Yu, S. J. Yun, H. K. Choi, J. S. Choi, G. H. Kim and C. G. Choi	Dr. Doo-Hyeb Youn , Electronics and Telecommunications Research Institute- Republic of Korea
18	Plasmonic Ag ultrafine nanoparticle-graphene substrates for Raman enhancement E.Climent-Pascual , F. Jimenez-Villacorta, L. Álvarez-Fraga, R. Ramírez-Jiménez, C. Prieto and A. De Andrés	Dr. Esteban Climent-Pascual , ICMM-CSIC - Spain
19	Self-cleaning Properties of Nanostructured Polypropylene Foils Fabricated by Roll-to-Roll Extrusion Coating A. Telecka and R. Taboryski	Ms. Agnieszka Telecka , Danish Technical University Nanotech DTU – Denmark

20	Chemical and electronic structure profiling in the top few nanometers of hydrothermally prepared and plasma hydrogenated ZnO nanorods M. Al-Saadi	Mr. Mubarak Al-Saadi , Sultan Qaboos University (SQU) - Oman
21	Fluorescent Photosensitive Vitroceramics with Silver and Samarium Additives: Improvement of Writing Accuracy and Efficiency for 3D Optical Storage Media C. Busuioc , S. Jinga and E. Pavel	Dr. Cristina Busuioc , Polytechnic University of Bucharest - Romania
22	Transparent and Hard PTFE-like Coatings by RF magnetron Sputtering of PTFE Polymer Target Y. S. Song and J. Kim	Dr. Young Sik Song , KITECH-Surface Technology R&BD Group-Incheon - Republic of Korea
23	Mathematical Modeling Process of Sedimentation Magnetic Nanoparticles on the Walls of Blood Vessels M.A. Shumova , D.V. Korolev, O.A. Smolyanskaya and S.A. Chivilikhin	Mrs. Maria Shumova , ITMO University, Saint-Petersburg - Russian Federation
24	Grown of silicon nanowires for possible solar cell applications J. Salazar , G. Santana and B. M. Monroy	Ms. Jenifer Salazar , National Autonomous University of Mexico – Mexico
25	Applications of Positron Probe in polymer nanocomposites G.B.Xie, J.Zhong, S.Gao and B. Wang	Prof. Bo Wang , Wuhan University – China
26	Modeling and Simulation of P-Type Cu ₂ O Thin-Film Transistors Using COMSOL Multiphysics S. Alsharif , H. Farhan and H. Aljawhari	Mrs. Sarah Alsharif , King Abdulaziz University - Saudi Arabia
27	MoN-decorated Nitrogen Doped Carbon Nanotubes Anode With High Lithium Storage Performance S.M. Abbas , Z. Rehman, A. Rehman and N. Ahmad	Mr. Syed Mustansar Abbas , National Centre for Physics, Islamabad - Pakistan
28	Low Frequency Noise Spectroscopy in n-channel UTBOX de-vices with 20 nm Si film B. Nafaa , B. Cretu, N. Ismail, O. Touayar, E. Simoen, J.-M. Routoure, R. Carin, M. Aoulaiche and C. Claeys	Ms. Beya Nafaa , Institut National de Sciences Appliquées et de Technologie- Tunisia
29	Aluminum oxide nanopores and nanowires F. Flores-Gracia , J. Martínez-Juárez, J.A. Luna-López, R.R. González-Jiménez	Dr. Francisco Flores , Autonomous University of Puebla- Mexico

Posters Session II: June 2nd, 2016

Nanotech France 2016: NanoBioMedecine/Nanosafety

Exhibition and Poster Hall

1	Investigation of Biomolecule Release Behaviours From Titanium Surfaces with Controllable Porosity C. Bayram	Mr. Cem Bayram , Hacettepe University - Turkey
2	UV Crosslinkable PLGA-b-PEG Nanoparticle Integrated Gel Networks for Topical Drug Delivery M. Gultekinoglu , I. Eroglu, C. Bayram, E.A. Aksoy and K. Ulubayram	Mrs. Merve Gultekinoglu , Hacettepe University - Turkey
3	New Outlook on Parkinson's Treatment: A Dual Targeting Nanoparticle Complex for More Efficient Delivery of Curcumin Improves Neuroprotection N. Beals , P. Kharel, W. Geldenhuys and S. Basu	Mr. Nathan Beals , Kent State University- USA
4	Biodegradable mesoporous silica nanoparticles from synthesis to anti-cancer application S. Seré , J. Belmans, B. De Roo, M. Vervaele, S. Van Gool and J. P. Locquet	Ms. Stephanie Seré , KU Leuven- Belgium
5	Formulation and Characterization of Liposomes Loaded with Resveratrol using Plackett-Burman Experimental Design S. Al-Edresi , S. Freeman, H. Aojula and J. Penny	Mr. Sarmad Al-Edresi , University of Manchester- United Kingdom
6	Biological interactions monitoring of B-16 Melanoma cells using electrochemical impedance spectroscopy C. Marculescu , B. Tincu, A. Avram, T. Burinaru, C. Voitincu and M. Avram	Dr. Catalin Marculescu , National Institute for Research and Development in Microtechnologies – Bucharest- Romania

7	Formulation and In Vitro Evaluation of Simvastatin Loaded Nanostructured Lipid Carriers D. Örgül , H. Eroğlu and S. Hekimoğlu	Mrs. Dilara Örgül , Hacettepe University- Turkey
8	Kinetics of mRNA Onset Time in Single Cell Arrays N. Mehrotra , A.Reiser, R. Krzyszton and J.O. Rädler	Ms. Neha Mehrotra , Ludwig-Maximilians-University-Munich- Germany
9	Magnetocloric effect for inducing hypothermia as new therapeutic strategy for stroke R. Iglesias , A. Vieites-Prado, B. Argibay, F. Campos, M. Bañobre-López, T. Sobrino, J. Rivas and J. Castillo	Dr.Ramón Iglesias , University of Santiago de Compostela- Spain .
10	Lipid membrane anchors in Lipid-Nucleic acid (LiNA) conjugates for liposome fusion O. Ries , P.M. G. Löffler and S.Vogel	Dr. Oliver Ries , University of Southern Denmark- Denmark
11	One-pot Solventless Preparation of PEGylated Black Phosphorus Nanoparticles for Photoacoustic Imaging and Photo-thermal Therapy of Cancer C. Sun , C. Zhao and Z. Li	Ms. Caixia Sun , East China University of Science and Technology Shanghai- China
12	The ultra-structural analysis of antibody conjugated gold nanoparticles on fiber optic particles plasmon resonance (FOPPR) enabled bio-sensor C-Y. Hsieh , Y-N. Wu, S-R. Wu, C-Y. Chiang and L-K. Chau	Ms. Ching-Yi Hsieh , National Cheng Kung University- Taiwan
13	In situ Synthesis of Nano-copper on Denim Garment for Antibacterial Purposes D. Zarbaf , M. Montazer and A. Sadeghian Maryan	Mr. Dara Zarbaf , Islamic Azad University- Tehran- Iran
14	Filtering Pigments from honey by nanofiber membrane F.Azizzadeh and F. Altay	Mrs. Farzaneh Azizzadeh , Istanbul Technical University - Turkey
15	Physicochemical and mechanical characterization of electrospun poly-ε-caprolactone nanofibers loaded with cilostazol M. Rychter , A. Baranowska-Korczyn, M. Jarek, B.M. Maciejewska, L. Emerson Coy and J. Lulek	Mr. Marek Rychter , Poznań University of Medical Sciences- Poland

Posters Session II: June 2nd, 2016

Nanotech France 2016: Nanoelectronics/ NanoPhotonics

Exhibition and Poster Hall

N.	Title	Author/Affiliation/Country
1	Green Emissive Perovskite Light-Emitting Diodes Via Morphological Control of Perovskite Films M. H. Song and J. C. Yu	Prof. Myoung Hoon Song , Ulsan National Institute of Science and Technology (UNIST)- Republic of Korea
2	Influence of electrical pulses on lithium cobalt oxide thin films : memristive behaviour and potential applications V. S. Nguyen , V. H. Mai, A. Moradpour,..P.Chrétien and O. Schneegans	Mr. Van Son Nguyen , Paris Sud University - France
3	Al ₂ O ₃ passivation effect in HfO ₂ -Al ₂ O ₃ laminate structures grown on InP substrates H-K. Kang , Y-S. Kang, D-K. Kim, M. Back, Y-S. An, J-D. Song, H. Kim and M-H. Cho	Mr. Hang-Kyu Kang , Yonsei University-Seoul - Republic of Korea
4	Flexible Microelectrode Patterning with Thin Polymer Stencils Prepared using PEGDA/Silicate Nanocomposites Y.H. Kim , Y.K. Lee, T.Kim, S.Goel, H.J. Kim and S-J. Choi	Dr. Young Ho Kim , Daegu-Gyeongbuk Medical Innovation Foundation, Daegu - Republic of Korea
5	Molecular switches - from STM-induced single molecule chemistry to switching of entire layers T.Leoni , T.Lelaidier, A.Thomas, O.Siri and C.Becker	Dr. Thomas Leoni , Aix Marseille University - France

NanoMetrology France 2016 Preliminary Program

June 1st, 2016

Session I: Methodologies for nanomaterials characterization

Conference Room 508

Session Chairs:

Dr. Georges Favre, Laboratoire national de métrologie et d'essais(LNE) - France
Prof. James M. Hill, University of South Australia - Australia

11:00-11:30	Exact solutions for the axial pressure profiles in channels with Maxwell slip flow A. C. Hoffmann , S. Karakitsiou and B. Holst	Prof. Alex Christian Hoffmann , University of Bergen - Norway
11:30-12:00	Dynamic identification of perforated MEMS devices by the continuous wavelet transform J. Lardiès and T.P. Le	Prof. Joseph Lardies , FEMTO-ST Institute- Bourgogne Franche-Comté University - France
12:00-12:30	General atomistic approach for modeling metal-semiconductor interfaces using density functional theory and non-equilibrium Green's function D. Stradi , U. Martinez, A. Blom, M. Brandbyge and K. Stokbro	Dr. Daniele Stradi , Quantumwise-Danemark
12:30-12:45	Sidewall Roughness of Nanoelectronic and Nanophotonic Structures: Metrological Challenges and their Critical Role in Applications V. Constantoudis , G. Patsis and E. Gogolides	Dr. Vassilios Constantoudis , NCSR Demokritos/ Nanometrisis-Greece
12:45-14:00	Lunch Break / Exhibition / Poster Session I	
14:00-14:30	Implementation of Process Analytical Technology for the multi-sectoral manufacturing of nanoparticles by wet milling C. Vairon , D. Bordeaux and A. Blasco	Ms. Celine Vairon , SDTech company - UK
14:30-14:45	A SAXS/WAXS Laboratory Instrument for Nanomaterials characterization O. Taché , A. Thill, D. Carrière, F. Testard and O. Spalla	Mr. Olivier Taché , LIONS, NIMBE, CEA Paris Saclay University- France
14:45-15:00	MEMS for in-situ TEM nanoscience on dry and wet samples L. Jalabert , T. Ishida, T. Sato, M. Egawa, G. Valet, S. Volz and H. Fujita	Dr. Laurent Jalabert , LAAS-CNRS-France
15:00-15:15	Characterization of nanomaterials by A4F-UV-MALLS-ICPMS, Sp-ICPMS and DLS: Application to foodstuff, consumer products, environmental and medicinal samples M. Menta , I. de La Calle and M. Klein	Dr. Mathieu Menta , Ultra-Traces Analyses Aquitaine (UT2A)- Pau - France
15:15-15:30	Design of experiment for uncertainty evaluation of nanoparticle diameter measurements with AFM B. De Boeck , J. Pétry, N. Sebaihi and M. Dobre	Dr. Bert De Boeck , FPS Economy (NMI Belgium)- Belgium
15:30-15:45	Local resistance imaging on soft materials by conducting probe atomic force microscopy in intermittent contact mode A. Vecchiola , P. Chrétien, K. Bouzehouane, O. Schneegans, P. Seneor, S. Tatay and F. Houzé	Dr. Aymeric Vecchiola , Unité Mixte de Physique CNRS/Thales - France
15:45-16:00	Continuous monitoring of tip radius during atomic force microscopy imaging using higher harmonics E. Rull Trinidad, F. Gramazio, M. Lorenzoni, F. Pérez Murano, U. Staufer and J. Fraxedas ²	Dr. Jordi Fraxedas , Catalan Institute of Nanoscience and Nanotechnology (ICN2) - Spain
16:00-16:30	Coffee Break / Exhibition/ Posters Session I	

16:30-16:45	Measurement uncertainty evaluation of a metrological AFM by modeling its position measurement system P. Ceria , S. Ducourtieux, Y. Boukellal and A. Allard	Mr. Paul Ceria , LNE- Laboratoire National de metrologie et d'Essais- France
16:45-17:00	Quantitative X-ray Resolution of the Atomic Structure of Metal Oxide Nanotubes: the Imogolite Case M.-S. Amara, S. Rouzière, E. Paineau, E. Poli, J. D. Elliott, G. Teobaldi and P. Launois	Dr. Pascale Launois , Paris Sud University- France
17:00-17:15	Water in Single-Walled Carbon Nanotubes: structural and dynamical analyses E. Paineau , S. Dalla-Bernardina, J.B. Brubach, S. Rouzière, P. Judeinstein, S. Rols, P. Roy and P. Launois	Dr. Erwan Paineau , Paris Sud University - France
17:15-17:30	An Accurate Reconvergent Fanout Aware Algorithm for nano-Circuits Reliability Ranking W. Ibrahim and H. Amer	Prof. Walid Ibrahim , UAE University - UAE
17:30-17:45	Modeling and Analysis of scatterometry with high-harmonic-generation EUV source Y-S. Ku , Y-C. Chen, C-L. Yeh, Y-C. Hsieh, C-H. Cho and C-W. Lo	Dr. Yi-sha Ku , Industrial Technology Research Institute - Taiwan
17:45-18:00	Influence of the probe-surface contact area on AFM tribological investigation of nanopatterned Si surfaces A. Rota , E. Serpini, G. C. Gazzadi and S. Valeri	Dr. Alberto Rota , CNR Nanoscience Institute-Modena - Italy
18:00-18:15	Simultaneous Topographical, Spectroscopic and Electrical Map-ping at the Nanoscale A. Zoladek-Lemanczyk , N. Kumar, A.A. Y, Guilbert, S.M. Tuladhar, T. Kirchartz, B.C. Schroeder, I. McCulloch, J. Nelson, D. Roy and F. A. Castro	Dr. Alina Zoladek-Lemanczyk , National Physical Laboratory- UK
18:15-18:30	Interaction between Hybrid Inclusions mediated by surfactant membranes E. Azar and D. Constantin	Mrs. Elise Azar , Paris Sud University-France
18:30-18:45	Micro to Atomic Scale Observations on Nano-sized Y-TZP Powder Produced by One-Step Hydrothermal Route A. Yurdakul, H. Gocmez and H. Yurdakul	Dr. Hilmi Yurdakul , Dumlupinar University- Turkey
18:45-19:00	First steps towards instantaneous positioning of Nanorobots equipped with graphene antenna in large scaled nano-systems D. Moffo and P. Canalda	Mr. Dernas Moffo , University of Bourgogne-Franche-Comté- France

June 1st, 2016 Nanometrology France 2016: Symposium on Nanospectroscopy		
Conference Room 561		
Chairs: Prof. Pierre-Michel Adam University of technology of Troyes- France		
11:00-11:30	Nanospectroscopy of optical antennas and coupled hybrid antenna-nanoemitter-structures M. Fleischer	Prof. Monika Fleischer , Institute for Applied Physics-Eberhard Karls University, Tübingen - Germany
11:30-12:00	Nanospectroscopy with Silver Nanowires S. Mackowski	Prof. Sebastian Mackowski , Nicolaus Copernicus University- Poland
12:00-12:30	Addressing Challenges in Fabrication of Nanoscale Interstices at Molecular resolutions for Nanospectroscopies S. Krishnamoorthy	Dr. Sivashankar Krishnamoorthy , Luxembourg Institute of Science and Technology- Luxembourg
12:30-12:45	Real-time sensing of chemical and biological species into individual cells with single-molecule resolution P. Actis	Dr. Paolo Actis , BioNano Consulting /School of Electronic and Electrical Engineering, University of Leeds- United Kingdom

12:45-14:00 Lunch Break / Exhibition / Poster Session I		
14:00-14:30	Resonant Surface-enhanced Raman Scattering by Optical Phonons in CdSe Nanocrystals on Metal Nanocluster Arrays A.G. Milekhin, V.M. Dzhagan and D.R.T. Zahn	Prof. Dietrich R.T. Zahn , Chemnitz University of Technology- Germany
14:30-14:45	Approaching single molecule detection using plasmonic nanogaps A.R. L. Marshall, J. Stokes, J-S. Bouillard and A.M. Adawi	Dr. Jean-Sebastien Bouillard , University of Hull - United Kingdom
14:45-15:00	Colloidal Gold Nanostructures for Plasmonics M. Y. Khaywah and S. Marguet	Dr. Mohammad Yehia Khaywah , CNRS/CEA Saclay - France
15:00-15:15	Intermixing length measurement with up to sub-nm accuracy by XEDS spectrum imaging E Carbo-Argibay, C. Afonso, M. S. Claro and D. G. Stroppa	Dr. Daniel Stroppa , International Iberian Nanotechnology Laboratory - Portugal .
15:15-15:30	High resolution solid state NMR spectroscopy in surface organometallic chemistry: access to molecular understanding of active sites of well-defined heterogeneous catalysts. E.Abou-Hamad and J-M. Basset	Dr. Edy Abou Hamad , King Abdullah University of Science and Technology (KAUST) - Saudi Arabia
15:30-16:00	Aluminum plasmonics for UV nanooptics J. Martin , D. Khlopin, F. F. Zhang, Silvère Schuermans, D. Gérard, J. Proust and J. Plain	Dr. Jérôme Martin , de Technologie University of Troyes - France
16:00-16:30 Coffee Break / Posters Session I		
16:30-16:45	Scanning Tunneling Spectroscopy approaches for Nano-structures characterization B. Naydenov , J.Li, P. Barimar, and J.J. Boland	Dr. Borislav Naydenov , Trinity College Dublin - Ireland
16:45-17:00	Material optical properties by spectroscopic ellipsometry of thin particulate films O. Zhuromskyy, S. Golkar, I. Spies, R. Klupp-Taylor, U. Peschel,	Dr Oleksandr Zhuromskyy , Erlangen-Nürnberg University- Germany
17:00-17:15	Investigations and Conclusions regarding Metrological Fundamentals for 'true' Nanovolume Spectroscopy. N. MacMillan	Mr. Norman McMillan , Institute of Technology Carlow - Ireland
17:15-17:30	Emerging Applications of Nanoscale Zinc Oxide D. Rogers , V. E. Sandana, F. H. Teherani and P. Bove.	Dr. David Rogers , Nanovation Company - France
17:30-17:45	Investigation of Diamond-Like Carbon Films Physical Properties Using Multifractal Analysis N. Margaryan , Zh. Panosyan, A. Mailyan and S. Voskanyan	Mr. Narek Margaryan , National Polytechnic University of Armenia – Armenia

<p style="text-align: center;">June 2nd, 2016 Nanometrology France 2016: Symposium on Detection, location & quantification of nanomaterials and by-product released from nano-enable products</p>		
Conference Room 511		
<p style="text-align: center;">Session Chairs: Prof. Jean-Yves Bottero, CNRS-CEREGE-France and Duke University - USA</p>		
09:00-09:30	Towards a Better Understanding of Interaction Mechanisms and Thermodynamic Properties of Nanomaterials Interacting with BioMacromolecules. S. Stoll , F. Loosli, O. Oriekhova, F. Carnal and A. Clavier	Dr. Serge Stoll , Institute F.-A. Forel, University of Geneva - Switzerland

09:30-10:00	Silver Nanoparticles in managed waste facilities: From metallic to sulfidic and back again. R. Kaegi , C. Meier, A. Voegelin, A. Pradas del Real, G. Sarret, and C.R. Mueller	Dr. Ralf Kaegi , Eawag, Swiss Federal Institute of Aquatic Science and Technology - Switzerland
10:00-10:30 Coffee Break / Posters Session II		
10:30-11:00	Rules and rates of release from nano-enabled products N. Neubauer	Dr. Nicole Neuabuer , BASF SE, Company – Germany
11:00-11:30	Response of microbial communities and plant to metal oxide- and carbon-based nanomaterials in a plant-soil-based system C. Santaella , B. Collin, M. Hamidat, M. Barakat, P. Ortet and W. Achouak	Dr. Catherine Santaella , CNRS Marseille/ CEA Cadarache- France
11:30-11:50	Effect of chemical transformations of silver in nanoAg-enabled textiles on their antimicrobial efficacy and release G. Lowry and T. Dankovich	Prof. Gregory Lowry , Carnegie Mellon University - USA
11:50-12:10	Multi-scale X-ray computed-tomography for the 3D detection and location of nanomaterials in manufactured materials and complex media P. Chaurand , D. Borschneck, V. Vidal, C. Levard, L. Scifo, J. Perrin and J. Rose	Mrs. Perrine Chaurand , CEREGE-Aix-Marseille University- France
12:10-12:30	Indoor mesocosms: an integrated approach to assess the environmental risks of nanomaterials M. Auffan , M. Tella, L. Brousset, C. Santaella, J. Rose, A. Thiéry, J.Y. Bottero	Dr. Melanie Auffan , CEREGE/CNRS-Aix-Marseille University- France
12:30-12:45	Effect of nanoceria biotransformation in activated sludge on the microbiota associated to canola roots B. Collin , E. Doelsch, M. Auffan, N. Roche, M. Barakat, P. Ortet, W. Achouak and C. Santaella	Dr. Blanche Collin , Aix-Marseille University- France
12:45-14:00 Lunch Break / Exhibition / Posters session II		
14:00-14:30	Some challenges and solutions for detecting engineered nanoparticles in environmental samples M. Hadioui, K. Proulx, L. Frechette-Viens, T. Theoret and K.J. Wilkinson	Prof. Kevin Wilkinson , University of Montreal – Canada
14:30-14:45	Behavior of Engineered CeO ₂ Nanoparticles Released in Aquatic Systems O. Oriekhova and S. Stoll	Ms. Olena Oriekhova , Institute F.-A. Forel, University of Geneva - Switzerland
14:45-15:00	Elucidation of standard specimen preparation techniques of nano-enabled products for characterization using field-emission scanning electron microscope A. Sohrabi	Dr. Abouzar Sohrabi , Sharif University of Technology, Tehran – Iran
15:00-15:15	Influence of nano-TiO ₂ with Different Crystalline Phases on Bioaccumulation of Perfluorooctanesulfonate by Fishes Living in Different Water Layers L.Y. Zhu and L.W. Qiang	Prof. Lingyan Zhu , Nankai University - China
15:15-15:30	Assessing the heteroaggregation of manufactured nanoparticles with naturally occurring colloids in a typical surface water D. Slomberg, J. Labille , A. Praetorius, C. Harns, J-Y. Bottero, P. Ollivier, M. Scheringe ² , N. Sani-Kast, S. Ilina and J. Brant	Dr. Jerome Labille , CEREGE, Aix-Marseille University- France
15:30-15:45	Behavior of engineered nanomaterials from marketed tiles under standardized abrasion conditions. C. Bressot , O. Aguerre-Chariol, C., Pagnoux and M., Morgeneyer	Mr. Christophe Bressot , Institut National de l'Environnement Industriel et des Risques (INERIS), Limoges - France
15:45-16:00	Marine plastic litters: the unanalyzed nano-fraction J. Gigault, B. Pedrono , B. Maxit and A. Ter Halle	Mr. Boris Pedrono , Cordouan Technologies, Pessac - France

16:00-16:30	Coffee Break / Exhibition/ Posters Session II	
16:30-16:45	Challenges on fate, behavior and effects of nanomaterials in the marine environment C. Mouneyrac	Prof. Catherine Mouneyrac , Université Catholique de l'Ouest- France
16:45-17:00	Sulfidation pathways of Silver Nanoparticles in the presence of Humic Acid B. Thalmann , A. Voegelin, E. Morgenroth and R. Kaegi	Dr. Basilius Thalmann , Eawag, Swiss Federal Institute of Aquatic Science and Technology - Switzerland
17:00-17:15	Mechanism of CuO/ZnO nanoparticle sulfidation: Insights from electron microscopy A. Gogos , B. Thalmann and R. Kaegi	Dr. Alexander Gogos , Eawag, Swiss Federal Institute of Aquatic Science and Technology - Switzerland
17:15-17:30	Development of the first generation of hybrid metrology algorithms dedicated to nanoparticles measurement with AFM and SEM techniques A.Dervillé, A.Delvallée, S.Martinez,...,L.Devoille, Y.Zimmermann, J.Foucher and G.Favre	Dr. Johann Foucher , POLLEN Metrology Company - France
17:30-17:45	Toward the direct quantification of dissolution and aggregation of AgNPs using AF4-UVD-MALLS-ICP-MS and Cryo-TEM analysis I.A.M Worms , A. Arnould, R. Soulas, J-F. Damlencourt, S. Motellier, E. Mintz, I. Michaud-Soret and D. Truffier-Boutry	Dr. Isabelle Worms , CEA, Grenoble,DRF/BIG/LCBM/BioMet - France
17:45-18:00	Particle Size Distribution Analysis of Complex Fe ₂ O ₃ Nano-particle Aggregates Embedded in High Density Polyethylene Matrix T. Uusimäki , T. Wagner, E. Verleysen, J. Mielke, P. Müller and R.Kägi	Dr. Toni Uusimäki , ETH- Eawag- Switzerland
18:00-18:15	Combination of micro- and nano- computed X-ray tomography for the characterization of nanomaterial-plant interactions C. Levard, A.E. P. del Real, A. Avellan, F. Schwab , P. Chaurand, D. Borschneck, V. Vidal, M. Auffan, G. Sarret and J. Rose	Dr. Fabienne Schwab , Aix-Marseille University-CNRS- France
18:15-18:30	Piezo-Resistive Sensing Active (PRSA) Probes integrated into a Nanomeasuring Machine (NMM-1) A. El Melegy , T. Hausotte, M. A. Younes and M. Amer	Dr. Ahmed El Melegy , FAU Erlangen-Nürnberg University - Germany
18:30-18:45	One pot Green synthesis of fluorescent Zinc oxide nanoparticles and its biological effects A. Mallick , P. Kumari, S.K.Verma	Dr. Muhammad Anwar Mallick , Vinoba Bhawe University- India
18:45-19:00	Adsorption properties of DOX antibiotic from aqueous solutions onto pristine and magnetized carbon nanotubes. A. Terechshenko , K.Korzhybayeva, M.R.Babaa, Jorge O. Oña-Ruales and Z. Bakenov	Ms. Alina Terechshenko , Nazarbayev University- Kazakhstan

NanoMaterials for Energy and Environment - NanMatEn 2016

Preliminary Program

June 2nd, 2016 NanoMatEn 2016 Session I: NanoEnergy		
Conference Room 211		
Session Chairs: Prof. Je-Lueng Shie, National I-Lan University – Taiwan Prof. Nicolas Fressengeas, Lorraine University – France		
10:30-11:00	Multi-functional Thin Films for Solar Energy Utilization J. He	Prof. Junhui He , Technical Institute of Physics and Chemistry, Chinese Academy of Sciences - China .
11:00-11:30	Comparative study of PN, PIN and new Schottky based InGaN thin films solar cells A. Adaine, S. Ould Saad Hamady and N. Fressengeas	Prof. Nicolas Fressengeas , Lorraine University - France
11:30-12:00	Hybrid Heterojunction PEDOT:PSS/GaAs Thin Film Solar Cells Via Wafer-Bonding Technique K.W. Sun	Prof. Kien Wen Sun , National Chiao Tung University - Taiwan
12:00-12:15	Role of methylammonium molecules on the electronic transport properties of organometallic perovskite CH ₃ NH ₃ PbI ₃ G. R. Berdiyorov , F. El-Mellouhi, M. E. Madjet, F. H. Alharbi, and S. N. Rashkeev	Dr. Golibjon Berdiyorov , Qatar Environment and Energy Research Institute - Qatar
12:15-12:30	Surface Modification for Enhancing Perovskite Solar Cell Performance W. Yu , Tom Wu and Aram Amassian	Dr. Weili Yu , King Abdullah University of Science and Technology - Saudi Arabia .
12:30-12:45	The TiO ₂ -dye interface in DSSCs: comparing single crystals and thin films and deposition methods, sensitized in UHV and liquid solution Z. Besharat , R. Alvarez Asencio, M. Götelid, M. Johnson and M. W. Rutland	Ms. Zahra Besharat , KTH Royal Institute of Technology - Sweden
12:45-14:00	Lunch Break / Exhibition / Posters session II	
14:00-14:15	Photoelectric and Photothermoelectric Material of SBA-15/K-OMS-2 on Photoelectrochemical Solar Cell Application C-H. Lee, J-L. Shie , Y. Li and C-Y. Chang	Prof. Je-Lueng Shie , National I-Lan University - Taiwan
14:15-14:30	Aluminum-Carbon Nanotube Nanocomposite for Silicon Solar Cell Back Metallization K. El-Rafei, A. Esawi , O. Tobail and A. Klingner	Dr. Amal Esawi , The American University in Cairo - Egypt
14:30-14:45	Co-based mesoporous spinels for oxygen evolution reaction in alkaline medium A. Habrioux , I. Abidat, C. Canaff, D. Dambournet, C. Comminges, T. Napporn and K.B. Kokoh	Dr. Aurélien Habrioux , University of Poitiers - France
14:45-15:00	Coupled surface-plasmon/thermoelectric power generators based on TCO nanowires A. Catellani, A. Ruini, M. Buongiorno Nardelli and A. Calzolari	Dr. Arrigo Calzolari , CNR-NANO Istituto Nanoscienze, Centro S3 - Italy
15:00-15:15	Core-shell Ni-NiF ₂ as cathode materials for secondary lithium batteries L. Doubtsof , L. Jouffret, P. Bonnet and K. Guerin	Mrs. Lea Doubtsof , Institut de Chimie de Clermont-Ferrand. Clermont University - France
15:15-15:30	Ultra-Thin copper oxide nanowires grown by atmospheric pressure afterglow for water splitting application A. Imam , T. Gries, K. Hussein and T. Belmonte	Mr. Abdallah Imam , Lorraine University - France

15:30-15:45	Energy transfer between up-converting nanocrystals and organic polymer J. Grzelak , K. Ciszak, M. Nyk, D. Piatkowski and S. Mackowski	Ms. Justyna Grzelak , Nicolaus Copernicus University - Poland
15:45-16:00	Energy Harvesting with Decorative Colour Specific Windows B. Fisher , E. New, D. Kutsarov, V. Stolojan and S. R. P. Silva	Mr. Brett Fisher , University of Surrey - UK
16:00-16:30 Coffee Break / Exhibition / Posters Session II		
16:30-16:45	Enhanced Thermal Conductivity of Nanofluids Containing Two-Dimensional Materials D. Lee , G. Lee, J-J. Park and M. Lee	Dr. Dongju Lee , Korea Atomic Energy Research Institute – Republic. of Korea
16:45-17:00	Nanofluids with enhanced thermal properties: an experimental and theoretical analysis J. Navas , A. Sánchez-Coronilla, E.I. Martín, R. Gómez-Villarejo, ..., C. Fernández-Lorenzo and J. Martín-Calleja	Dr. Javier Navas , Cádiz University - Spain
17:00-17:15	New Composites “LiCl/vermiculite” for Sorptive Heat Storage A.D. Grekova , L.G. Gordeeva and Y.I. Aristov	Dr. Alexandra Grekova , Novosibirsk State University - Russian Federation
17:15-17:30	Pseudocapacitive Study of Nickel Oxide Nanomaterials for Electrochemical Energy storage L. Meda , J. Adkins and C. Arnold	Dr. Lamartine Meda , Xavier Univresity of Louisiana- USA

June 2nd, 2016		
NanoMatEn 2016 Session II: Nanotechnology for Environmental applications		
Conference Room 212		
Session Chairs: Prof. Joydeep Dutta, KTH Royal Institute of Technology – Sweden/ Prof. M. Carmen Hermosin, IRNAS-CSIC-Sevilla- Spain/ Prof. Tahar Laoui, King Fahd University of Petroleum and Minerals- Saudi Arabia		
10:30-11:00	Effect of Sb segregation on conductance and catalytic activity at Pt/Sb-doped SnO ₂ interface: a synergetic computational and experimental study Q.Fu, L.C. Colmenares Rausseo†, U.Martinez , P.I.Dahl, J.M.García Lastra, P.E. Vullum, I-H. Svenum and T.Vegge	Dr. Umberto Martinez , Quantumwise - Danemark
11:00-11:15	Au@Pt Core-shell Mesoporous Nanoballs and Nanoparticles as Efficient Electrocatalysts for formic acid and glucose oxidation T.W. Napporn , Y. Holade, A. Lehoux, H. Remita and K. B. Kokoh	Dr. Teko W. Napporn , Poitiers University- France
11:15-11:30	First insight into fluorinated Pt/carbon aerogels as more corrosion-resistant electrocatalysts for Proton Exchange Membrane Fuel Cells Cathodes Y. Ahmad , S. Berthon-Fabry, L. Dubau, K.Guerin and M. Chatenet	Dr. Yasser Ahmad , Blaise Pascal University- France
11:30-11:45	Label-Free Surface Plasmon Resonance Biosensing with Titanium Nitride Thin film S.P. Ng, G. Qiu, Z. Deng and C.M.L. Wu	Prof. Chi-Man Wu , City University of Hong Kong - China
11:45-12:00	Effect of calcination temperature on photocatalytic activity of TiO ₂ /Bi ₂ O ₃ Nanofibers in the photodegradation of Acid Orange 7 (AO7) under visible light irradiation J.Jermyn , S.SiangLee, Benny Y.Liang Tan, H.Bai and D. Delai Sun	Mr. Jermyn Juay , Nanyang Technological University - Singapore
12:00-12:15	Facile Synthesis of Highly Efficient One-Dimensional Plasmonic Photo-catalysts J. Xiong and Z. Li	Ms. Jinyan Xiong , The University of Wollongong- Australia .

12:15-12:30	Analytical TEM study on the behavior of CeO ₂ nanoparticles in Sb-V-CeO ₂ /TiO ₂ catalysts for NH ₃ -SCR Y.E. Jeong , P.A.Kumar, K-Y. Lee and H.P. Ha	Ms. Young Eun Jeong , Korea Institute of Science and Technology- Seoul- Republic of Korea
12:30-12:45	Photodegradation of Ofloxacin with nano-go/m Composite and it's reuse P. Alicanoğlu and D. T. Sponza	Mrs. Pelin Alicanoglu , Pamukkale University-Turkey
12:45-14:00 Lunch Break / Exhibition / Posters session II		
14:00-14:15	Nanostructures as Catalysts for H ₂ O ₂ Electrogeneration and Degradation of Organic Pollutants M. C. Santos	Prof. Mauro Santos , ABC Federal University - Brazil
14:15-14:30	Designing efficient bimetallic photocatalysts for hydrogen production E. Aronovitch , P.Kalisman, L. Houben, L. Amirav and M.Bar-Sadan	Mr. Eran Aronovitch , Ben-Gurion University of the Negev- Israel
14:30-14:45	Enhancing Cuprous Oxide Stability for Hydrogen Evolution J. Azevedo , S.D. Tilley, M. Schreier, M. Stefik, L. Steier, P. Dias, C.T. Sousa, J.P. Araújo, M.T. Mayer, M. Graetzel and A. Mendes	Mr. João Azevedo , LEPABE-Porto University - Portugal
14:45-15:00	Preparation of Basic Type of Activated Alumina Supports for using in Production and Separation of Hydrogen M. Duran and F.N. Tüzün	Dr. Fatma Nihal Tuzun , Hitit University - Turkey
15:00-15:15	On the applicability of Johnson-Mehl-Avrami-Kolmogorov (JMAK) approach in explaining the hydrogen sorption kinetics in nanocrystalline magnesium hydride S. Shrinivasan , A. Gangrade, N.K. Gor, H.-Y. Tien, M. Tanniru, F. Ebrahimi and S.S.V. Tatiparti	Prof. Sankara Sarma Tatipari , Indian Institute of Technology Bombay - India .
15:15-15:30	Improving the Adhesion Capacity of Foliar Nitrogen Fertilizer through Nano networks D. Cai , N. Zhong, P. Zhao and Z. Wu	Dr. Dongqing Cai , Hefei Institutes of Physical Science, Chinese Academy of Sciences - China
15:30-15:45	Development of an "anti-bug" Bicomponent Fibre M. Bischoff , G. Seide and T. Gries	Mrs. Merle Bischoff , Institut für Textiltechnik, RWTH Aachen University- Germany
15:45-16:00	Molecularly Imprinted Polymer Nano layers for the electrochemical detection of pesticides S. Bouden , V. Bertagna, B. Cagnon and C. Vautrin-UI	Dr. Sarra Bouden , Orléans University- France
16:00-16:30 Coffee Break / Exhibition/ Posters Session II		
16:30-16:45	Carbon Nanofibers-Ionic Liquid Composite Sensors For Detection of Trace Heavy Metals L. Oularbi , M. El Rhazi and M. Turmine	Mr. Larbi. Oularbi , University Hassan II Casablanca, Morocco/ Sorbonne University, UPMC University- France
16:45-17:00	Zero valent iron nanoparticles for remediation of soils contaminated with heavy metals O. Cortes, S.Machado, N.Vital, H.Gouveia , V.Correia,T. Albergaria and C. Delerue Matos	Dr. Helena Gouveia , ISQ, Taguspark –Oeiras- Portugal
17:00-17:15	Development of nano-porous geopolymer for passive cooling systems M. Alshaaer , J. Alkafawein, Y. Al-Fayez, T. Fahmy, M. Zamorano Toro and M. Martín Morales	Prof. Mazen Alshaaer , Prince Sattam Bin Abdulaziz University- Saudi Arabia
17:15-17:30	Novel Zeolite-Polyurethane Membrane for Environmental Applications H.Shehu and E.Gobina	Ms. Habiba Shehu , Robert Gordon University-Aberdeen- United Kingdom
17:30-17:45	Flue Gases Capturing Capacity of Nano-porous organic Materials R. Ullah , M. Atilhan and C.T. Yavuz	Dr. Ruh Ullah , , Qatar University- Qatar

June 2nd, 2016
NanoMatEn 2016- Symposium on Nanotechnology for Photovoltaics

Conference Room 260

Session Chairs:
Prof. Alejandro Perez-Rodriguez, IREC- Catalonia Institute for Energy Research - Spain

14:00-14:45	High efficiency thin film photovoltaic cells in novel light confinement architectures	Prof. Jordi Martorell - ICFO - Barcelona- Spain
14:45-15:30	Nano-architectures and organic-inorganic hybrid material combinations for novel photovoltaic device concepts S. Christiansen , S. Schmitt, S. Jäckle, G. Sarau, M. Göbelt, R. Keding, M. Mattiza, B. Hoffmann and M. Latzel	Prof. Silke Christiansen , Helmholtz Zentrum für Materialien und Energie, HZB (Berlin), Germany- Germany
15:30-15:45	Metal Oxide Nanorod Arrays Fabricated by Solution Processes for Applications in Hybrid Photovoltaic Cells S. Chuangchote , W.Arparate, N.Laosiripojana and T. Sagawa	Dr. Surawut Chuangchote , King Mongkut's University of Technology Thonburi- Thailand
15:45-16:00	Boosting impact of nanometric Ge layers on the synthesis and performance in Cu ₂ ZnSnSe ₄ solar cells P.Pistor , S.Giraldo, M.Neuschitzer, M. Placidi A.Pérez-Rodriguez and E.Saucedo	Dr. Paul Pistor , Catalonia Institute for Energy Research- (IREC) - Spain
16:00-16:30 Coffee Break / Exhibition / Posters session II		
16:30-16:45	Thin Epitaxial Silicon Foils Using Porous-Silicon-Based Lift-Off for Photovoltaic Application I. Gordon	Dr. Ivan Gordon , Photovoltaics Department IMEC-Leuven- Belgium
16:45-17:15	Photon managements by employing one- and two-dimensional structures for optoelectronic devices J-H. He, and J.R.D.Retamal	Dr. Jose Ramon Duran Retamal , King Abdullah University of Science & Technology, Saudi Arabia
17:15-17:30	Electric and Photovoltaic Behavior of Novel Few Layer α -MoTe ₂ / MoS ₂ Dichalcogenide Heterojunction A.Pezeshki and S. Im	Mrs. Atiye Pezeshki , Yonsei University- Seoul - Republic of Korea
17:30-17:45	Zinc selenide as a potential Cd-free buffer nanolayer for CZTSe solar cells M.Placidi , M. Espindola-Rodriguez, H. Xie, F. Oliva, Y. Sanchez, M. Neuschitzer, S. Giraldo, I. Becerril-Romero, P. Pistor, V. Izquierdo-Roca, E. Saucedo and A. Pérez-Rodríguez	Dr. Marcel Placidi , Catalonia Institute for Energy Research (IREC) - Spain
17:45-18:00	SURMOFs and CNCs as novel tuneable Materials for Optical, Photonic as well as for Solar Energy Materials E. Redel	Dr. Engelbert Redel , Karlsruhe Institute of Technology (KIT) - Germany

June 3rd, 2016
NanoMatEn 2016- Session III: Nanotechnology for water treatment

Conference Room 561

Session Chairs:
Prof. Joydeep Dutta, KTH Royal Institute of Technology - Sweden
Dr. Alberto Figoli, Institute on Membrane Technology (CNR-ITM) - Italy

08:30-09:15	Nanotechnology for cleaning water: redox reactions the way out?	Prof. Joydeep Dutta , KTH Royal Institute of Technology - Sweden
09:15-09:30	Nanostructured membranes for water desalination: an overview M.Faccini and M. Boerrigter	Dr. Mirko Faccini , LEITAT Technological Center- Spain

09:30-09:45	Decontamination of wastewater using nanocarbon compounds insert in diatomite mesoporous structure E. Flores, O. Enriquez, J. De la Cruz, A. López, G.Poma and M.Quintana	Dr. Maria Quintana , Engineering and Technological University, Lima - Peru
09:45-10:00	Functionalization of glassy carbon electrode by amines electrochemical oxidation for micro-pollutants detection in water D. Pally, M. Alaaeddine, B. Cagnon, V. Bertagna , R. Benoit, F. Podvorica and C. Vautrin	Dr. Valerie Bertagna , University of Orleans - France
10:00-10:30 Coffee Break / Exhibition		
10:30-11:00	PVDF UF hollow-fiber membrane production as pre-treatment system in Water Desalination Reverse Osmosis Unit A. Figoli , O. Saoncella, S. Xue, S. Simone, F.Galiano, M. Boerrigter, C. Chaumette, M. Faccini and E. Drioli	Dr. Alberto Figoli , Institute on Membrane Technology (CNR-ITM) - Italy
11:00-11:15	Development of Alumina-Carbon Nanotubes Porous Membranes Using Spark Plasma Sintering Process for Water Purification T. Laoui , H. K. Shahzad, M. A. Hussein, F. Patel, N. Al Aqeeli and M. A. Atieh	Prof. Tahar Laoui , King Fahd University of Petroleum and Minerals- Saudi Arabia
11:15-11:30	The efficient separation of oil-water emulsions with a flexible, superhydrophilic and self-cleaning TiO ₂ /Fe ₂ O ₃ membrane B.Y.L. Tana , J. Juaya, J.K.K. Anga, Z.Liub and D. Suna	Mr. Benny Tan , Nanyang Technological University - Singapore
11:30-11:45	Nanostructure formation, characterization and application of ba-nana peels nanosorbent in mine water treatment O. Atiba-Oyewo , M.S. Onyango and C. Wolkersdorfer	Ms. Opeyemi Atiba-Oyewo , Tshwane University of Technology - South Africa
11:45-12:00	Fabrication of hematite photoanode for solar water splitting by using pulsed laser deposition C-P.Yen , Y-J. Li, S-J. Luo, J.Wang, C-J.Tseng and S-Y Chen	Mr. Chih-ping Yen , National Taiwan University - Taiwan
12:00-12:15	Molecular Dynamics-Continuum Hybrid Simulation of Water Transport through Carbon Nanotube Membranes A. Kudaikulov , A. Kaltayev and C. Josserand	Mr. Aziz Kudaikulov , Al-Farabi Kazakh National University - Kazakhstan
12:15-12:30	Titanium Dioxide-Based Nanocatalysts Constructed from Natural Sources for Photocatalytic Wastewater Treatment P. Kemacheevakul and S.Chuangchote	Dr. Patiya Kemacheevakul , King Mongkut's University of Technology - Thailand
12:30-12:45	Magnetic Nanoparticles Stabilized by Lignocellulosic Waste as Green Adsorbent For Cr(VI) Removal from Waste Water I.L.A. Ouma , A.E. Ofomaja and E.B. Naidoo,	Ms. Linda Ouma , Vaal University of Technology- South Africa

Posters Session II: June 2nd, 2016

NanoMatEn 2016

Exhibition and Poster Hall

N.	Title	Author/Affiliation/Country
1	Solar charged redox flow battery K. Wedege , J. Azevedo, A. Khataee, A. Mendes and A. Bentien	Ms. Kristina Wedege , Aarhus University - Denmark
2	Novel Methods for the Deposition of Solution-Processed CdTe Inks for Photovoltaic Applications J.C. Russell , J.M. Kurley, H. Zhang and D. Talapin	Mr Jake Russell , University of Chicago - USA
3	Enhancement of power conversion efficiency of dye-sensitized solar cells via incorporation of GaN semiconductor materials synthesized in hot-wall CVD furnace. M. Baisariyev , R.Iskakov, G. Sugurbekova	Mr. Murat Baisariyev , Nazarbayev University - Kazakhstan

4	Fabrication of Hierarchical Nanostructures for Perfect Anti-reflection Coating S.J. Cho and T. An	Prof. Taechang An , Andong National University - Republic of Korea.
5	Modeling infrared radiation transport in insulating dielectric nanocomposites to minimize radiative thermal losses J.Tang , V.Thakore and T.Ala-Nissilä	Ms. Janika Tang , Aalto University - Finland
6	Numerical Investigations of Heat Transfer in Rectangular Micro-Channels during Single Phase Fluid Flow using Cooling Nanoliquids L. Snoussi , N. Ouerfelli, F.B.M. Belgacem and A. Guizani	Dr. Lotfi Snoussi , Research and Technologies Centre of Energy – Tunisia
7	The performance fo Zn/Ni battery using NixZn(1-x)O as anodic material to suppress Zn dendrite Y. Im , K;Su Park, T.W. Cho, J-S. Lee and M.Kang	Mr. Younghwan Im , Yeungnam University - Republic of Korea
8	Kinetic mechanisms of hydrogen sorption in nanocrystalline magnesium (hydride) S. Shrinivasan , A. Gangrade, N.K. Gor, H.-Y. Tien, M. Tanniru, F. Ebrahimi and S.S.V. Tatiparti	Ms. Sweta Shrinivasan , Indian Institute of Technology Bombay – India
9	Hydrogen production from propane steam reforming over 30NiFe1-xO/70Al2O3 catalysts Kang Min Kim ¹ , Byeong Sub Kwak ¹ , No-Kuk Park ² , Tae Jin Lee ² , Misook Kang ^{*1}	Mr. Kang Min Kim , Yeungnam University - Republic of Korea
10	Hydrogen production by propane steam reforming over transition metal (A = Fe, Co, Ni, Cu) in Mn-based metal oxide structure J. Yeon Do and M. Kang	Ms. Jeong Yeon Do , Yeungnam University - Republic of Korea
11	Three-metallic Mn-based Ni1-XCoXMnO4/γ-Al2O3 (X=0.2, 0.3, 0.4, 0.5) catalysts for hydrogen production via steam reforming of propane gas S.W. Jo and M. Kang	Mr. SeungWon Jo , Yeungnam University - Republic of Korea
12	Effective hydrogen production from propane stream reforming on Co/Cex/γ-Al2O3 M.Park and M.Kang	Mr. Minkyu Park , Yeungnam University - Republic of Korea.
13	Oxygen Reduction Reaction Catalyzed by Manganese Dioxide Nanoflowers L.R. Aveiro , V.S. Antonin, A.G.M. da Silva, E. G. Candido, P.H.C.Camargo and M.C. dos Santos	Mrs. Luci Aveiro , ABC Federal University - Brazil
14	W@Au nanostructures as catalysts for H2O2 electrogeneration V. S. Antonin , L.S. Parreira, F.L. Silva, R.B. Valim, P. Hammer, M.R.V. Lanza and M. C. Santos	Ms. Vanessa Antonin , ABC Federal University - Brazil
15	Selective removal of lead using a nanocompound basedon diatomite and graphene oxide E. Flores , O. Enriquez, J. De la Cruz, A. López, G. Poma and M. Quintana	Ms. Elena Flores , Universidad de Ingenieria y Tecnologia - Peru
16	Hybrid Nanocomposite of Nanocellulose-Silver Nanoparticles-Graphene Oxide for Environmental Remediation Purposes S.W. Chook ,C.H. Chia and S. Zakaria	Dr. Soon Wei Chook , National University of Malaysia (UKM) – Malaysia
17	Study of degradability of starch-based films mixing with nano-Titanium dioxide J. Komatitaya , S. Mataweechotikul and A. Simprasert	Dr. Juntira Komatitaya , King Mongkut University of Technology Thonburi-Bangkok- Thailand
18	Synthesis and Characterization of Superparamagnetic Magnetite/Modified Magnetite Nano-Particles (Fe3O4@SiO2@L) H. Çiftci, B. Ersoy and A. Evcin	Prof. Bahri Ersoy , Afyon Kocatepe University- Turkey
19	Determination of the equilibrium constant of 1,3,5-nickel bencenotricarboxylate, Ni-HKUST-1 J. Vargas , J. Balmaseda and R. Salcedo	Ms. Jaquebet Vargas Bustamante , Universidad Nacional Autónoma de México- Mexico
20	Nanocomposite films as a gas sensor for organic compounds S.Ali , B. Horrocks and A. Houlton	Mrs. Shams Ali , Newcastle University- United Kigndom
21	Synthesis and characterization of ZnO-Ag nanoparticles supported on MCM-41 as a photocatalyst for degradation Congo Red E. M. Barrera-Rendón , G. García-Rosales and J. Jiménez-Becerril	Ms. Eva M. Barrera Rendón , Toluca Technology Institute- Mexico

22	Synthesis and Evaluation of a Carbon-TiO ₂ -CeO ₂ composite for the degradation of phenol Y. Lara-Lopez , G. García-Rosales and J. Jiménez-Becerril	Ms. Yoselin Lara-Lopez , Toluca Technology Institute- Mexico
23	Low Cost and Free TCO Porous Coal as a Counter Electrode (CE) for Dye Sensitized Solar Cell (DSSC) M.Y. Feteiha , S. Ebrahim and L. Saad	Dr. Mohamed Feteiha , Alexandria University- Egypt
24	Facile formation of fullerene nanostructures and their application to polymer solar cells S. Woo , W.-H. Kim and S.-J. Sung	Dr. Sungho Woo , Daegu Gyeongbuk Institute of Science & Technology- Republic of Korea
25	Comparison of the systemic nanoherbicide Imazamox-LDH obtained by direct synthesis and reconstruction: preliminary results R. Khatem, A. Bakthi and M.C. Hermosin	Prof. M. Carmen Hermosin , IRNAS-CSIC-Sevilla- Spain
26	Polymer optimised dewatering of sludge using Geotubes, a systematic approach H. Haase , W. Lieske, T. Schanz and H. Dehn	Mr. Wolfgang Lieske , Ruhr-University- Germany

European Graphene Forum – EGF 2016

Preliminary Program

June 1st, 2016 EGF 2016- Plenary session I		
Amphitheatre G		
Session's Chairs: Dr Cinzia Casiraghi, University of Manchester- UK Prof. Giancarlo Faini, Laboratoire de Photonique et de Nanostructures, CNRS - France		
09:00-9:40	Supramolecular approaches to 2-D materials: from complex structures to sophisticated functions P.Samori	Prof. Paolo Samori , Stasbourg University - France
09:40-10:20	Water-based 2D-crystal Inks: from Production to Devices C. Casiraghi	Dr. Cinzia Casiraghi , University of Manchester- U K
10:30-11:00 Lunch Break / Exhibition / Posters Session I		
11:00-11:30	PN Junction Based Devices in Ultra-Clean Graphene P. Rickhaus, M-H. Liu, P. Makk, M. Jung, C. Handschin, S. Zihlmann, E. Tovari, R. Maurand, M. Weiss, K. Richter and C. Schönenberger	Prof. Christian Schönenberger , University of Basel - Switzerland
11:30-12:00	2-D Nanocarbons: Attraction, Reality and Future Z. Liu	Prof Zhongfan Liu , Peking University- Beijing - China
12:00- 12:30	Effects of morphology and surface chemistry of graphite nanoplates on dispersion and network formation in polypropylene melts R. M. Santos and J. A. Covas	Prof. José Covas , University of Minho - Portugal
12:30-12:45	Exploring Graphene Plasmonics for Novel Applications: From Tunable Absorption Enhancement to Strong Optical Forces J. Zhang , W. Liu, Z. Zhu, C. Guo, K. Liu, X. Yuan and S. Qin	Dr. Jianfa Zhang , National University of Defense Technology- China
12:45-13:00	Scalable Few Layer Graphene Production by Graphite Exfoliation in Liquids C. Damm , T. J. Nacken, H. Xing, Y. Hambal and W. Peukert	Dr. Cornelia Damm , University Erlangen-Nürnberg- Germany
12:45-14:00 Lunch Break / Exhibition / Posters Session I		
EGF 2016- Session I: Graphene and 2D Materials Synthesis, characterization and properties		
Session's Chairs: Prof Zhongfan Liu, Peking University, Beijing – China/ Prof. Andrey Chuvilin, CIC nanoGUNE – Spain		
14:00-14:15	CVD-grown large-area monolayer MoS ₂ using H ₂ S D. Dumcenco , D. Ovchinnikov, O. Lopez-Sanchez, P. Gillet, D. T. L. Alexander, S. Lazar, A. Radenovic and A. Kis	Dr. Dumitru Dumcenco , EPFL - Switzerland
14:15-14:30	Centimeter-scale synthesis of ultrathin layered MoO ₃ by van der Waals epitaxy A.J. Molina-Mendoza , J.L. Lado, J. Island, M. Angel Niño, L. Aballe, M. Foerster, F.Y. Bruno, H.S. J. van der Zant, G. Rubio-Bollinger, N. Agraït, E.M. Perez, J. Fernández-Rossier and A. Castellanos-Gomez	Mr. Aday J Molina-Mendoza , Universidad Autonoma de Madrid - Spain
14:30-14:45	Plasma-assisted CVD graphene synthesis and characterization on nickel substrates P. Pop-Ghe , L. Krückemeier, N. Wöhrle and V. Buck	Ms. Patricia Pop-Ghe , University of Duisburg - Essen- Germany
14:45-15:00	A Record-Breaking mobility for CVD Graphene by suppressing the effect of charged impurities R. Nashed , K. Brenner and A. Naeemi	Mr. Ramy Nashed , Georgia Institute of Technology – USA
15:00-15:15	Chemical Kinetics during CVD Growth of Graphene S. Farhat , I. Hinkov, H-A. Mehedi and A. Gicque	Dr. Farhat Samir , CNRS LSPM-Paris 13 University- France

15:15-15:30	Optimized Synthesis of Graphene by Cobalt-Catalyzed Decomposition of Methane with Plasma-Enhanced CVD H.-A. Mehedi , B. Baudrillart, D. Alloyeau, C. Ricolleau, J. Lagoutte, A. Gicquel and S. Farhat	Dr. Hasan Al Mehedi , CNRS LSPM-Paris 13 University- France
15:30-15:45	Tuning the nature of nitrogen atoms in N-containing RGO: Enhanced thermal oxidation stability by nitrogen doping S. Sandoval , N. Kumar, A. Sundaresan, C. N. R. Rao, A. Fuertes and G. Tobias	Ms. Stefania Sandoval Rojano , Institute of Materials Science of Barcelona - Spain
15:45-16:00	Towards High Quality Graphene Flakes by Electrochemical Exfoliation of Graphite With Multifunctional Electrolytes J.M. Munuera , J.I. Paredes, S. Villar-Rodil, M. Ayán-Varela, A. Martínez-Alonso and J.M.D. Tascón	Mr. Jose Munuera , Instituto Nacional del Carbón, INCAR-CSIC - Spain
16:00-16:15	Deoxygenation of Graphene Oxide by Metalorganic Compounds N. Jalagonia , T. Kuchukhidze, N. Jalabadze, V. Tsitsishvili and R.Chedia	Mrs. Natia Jalagonia , Ilia Vekua Sukhumi Institute of Physics and Technology, Tbilisi - Georgia
16:15-16:30 Coffee Break / Exhibition / Posters Session I		
16:30-16:45	Functionalization of Graphene by [2+1] Cycloaddition Reaction at Ambient Conditions A. Faghani, R. Haag and M. Adeli	Prof. Mohsen Adeli , Free University of Berlin - Germany
16:45-17:00	A facile and scalable way to produce reduced graphene oxide/epoxy nanocomposites G.B. Olowojoba , S. Kopsidas, S.Eslava, E.S. Gutierrez, A.J. Kinloch, C.Mattevi, V.G. Rocha and A.C. Taylor	Dr. Ganiu B. Olowojoba , Imperial College London, London - UK
17:00-17:15	Benzoxazine-functionalized graphene oxide for synthesis of new nanocomposites I. Biru , C. Damian, S. A. Garea and H. Iovu	Mrs. Luliana Biru , University Politehnica of Bucharest - Romania
17:15-17:30	Electrodeposition process of graphene nano-plates on open-cells aluminum foams – a critical review A. Simoncini , V. Tagliaferri and N. Ucciardello	Mr. Alessandro Simoncini , University of Rome “Tor Vergata” - Italy
17:30-17:45	Optimization of In-Situ Polymerization Process of Graphene Nano-Platelet Composites B. Yang , J. Doucette and P. Mertiny	Mr. Bo Yang , University of Alberta - Canada
17:45-18:00	Multilayered Membranes based on Graphene and Natural Polymers for Biomedical Applications M. C. Paiva , E. Cunha, D. Moura, C. Silva, M. F. Proença and N. Alves	Dr. Maria Paiva , University of Minho- Portugal
18:00-18:15	Antimicrobial properties of RGO modified with Polysulfone Brushes and their nanocomposites J.Peña-Bahamonde , H.Nguyen, V.San Miguel, J.C.Cabanelas and D. Rodrigues	Mrs. Janire Pena Bahamonde , University Carlos III Madrid- Spain
18:15-18:30	Room-temperature positive magnetoresistance in functionalized graphene grown by CVD O.V. Kononenko , V. N. Matveev, V.I. Levashov and V.T. Volkov	Dr. Oleg Kononenko , Institute of Microelectronics Technology and High Purity Materials- Russian Federation
18:30-18:45	Defects in irradiated graphene on metallic substrates I. Shchedrina , C. Corbel, N. Ollier, O. Cavani, T. Wade, M. Konczykowski, J-P. Renault, J. Ghilan, H. Randriamahazaka, C.S. Cojocar, I. Florea and B. Geffroy	Dr. Irina Shchedrina , Ecole polytechnique - France
18:45-19:00	High porosity Graphene/Fe3O4 scaffolds for Electromagnetic Interference Shielding M. González , J. Pozuelo and J. Baselga	Mrs. Marta González , University Carlos III of Madrid- Spain
19:00-19:15	Effect of Post-Exfoliation Annealing and Ultrasonic Treatments on Mechanically Exfoliated MoS2 P. Budania , N. Mitchell and D. McNeill	Ms. Prachi Budania , Queen's University, Belfast – UK

June 2nd , 2016

EGF 2016- Plenary session II

Amphitheatre G

Session's Chairs:

**Prof. Giancarlo Faini, Laboratoire de Photonique et de Nanostructures, CNRS – France
Dr. Konstantin Amsharov, University of Erlangen-Nürnberg – Germany/ Prof. Alberto Fina,
Polytechnic University of Turin – Italy**

08:30-9:15	2D Materials: technology, standards and science A.H. Castro Neto	Prof. Antonio H. Castro Neto , National University of Singapore - Singapore
09:15-10:00	Graphene-based Platforms for Biosensing Applications A. Merkoçi	Prof. Arben Merkoçi , ICN2/ CSIC/The Barcelona Institute of Science and Technology - Spain
10:00-10:30 Coffee Break / Exhibition / Posters Session II		
10:30-11:00	Carbon Based Nano-Materials/Devices K.S. Kim	Prof Kwang S. Kim , Ulsan National Institute of Science and Technology - Korea
11:00-11:30	Reaction kinetics of Stone - Wales rotation in graphene A. Chuvilin , S. T. Skowron, V. O. Koroteev, M. Baldoni, S. Lopatin, A. Zurutuza and E. Bichoutskaia	Prof. Andrey Chuvilin , CIC nanoGUNE – Spain
11:30-12:00	Ultrafast Generation of Plasmon Polaritons in High Mobility Graphene D.N. Basov	Prof. Dmitri Basov , University of California and Columbia University - USA
12:00-12:30	Design and fabrication of Graphene based platforms for Raman sensing L. Álvarez-Fraga, F. Jimenez-Villacorta, E. Climent-Pascual, R. Ramírez-Jiménez, C. Prieto and A. de Andrés	Prof. Alicia de Andrés , Materials Science Institute of Madrid (CSIC) – Spain
12:30-12:45	Imaging and spectroscopy on the 10-nm length scale M. Eisele	Mr. Max Eisele , Neaspec GmbH- Germany
12:45-14:00 Lunch Break / Exhibition / Posters session II		
EGF 2016- Session II: Graphene and 2D Materials characterization and properties		
Chairs: Giancarlo Faini, Laboratoire de Photonique et de Nanostructures, CNRS – France/ Dr. Konstantin Amsharov, University of Erlangen-Nürnberg – Germany/ Prof. Alberto Fina, Polytechnic University of Turin – Italy		
14:00-14:40	Graphene nanoplatelets for thermally conductive polymer nano-composites via melt reactive extrusion A. Fina , S. Colonna, O. Monticelli, M. Tortello, R.S. Gonnelli, J. Gomez, M. Pavese, F. Giorgis and G. Saracco	Prof. Alberto Fina , Polytechnic University of Turin - Italy
14:40-15:00	Reduced Graphene Oxide Enhances Horseradish Peroxidase Stability by Serving as Radical Scavenger and Redox Mediator C. Zhang , S. Chen, P.J. J. Alvarez and W. Chen	Prof. Chengdong Zhang , Nankai University- China
15:00-15:30	Ab-initio calculations and simple models of electronic excitations in 2D materials and heterostructures K.S. Thygesen	Prof. Kristian S. Thygesen , Technical University of Denmark- Denmark
15:30-15:45	Mechanical Property Enhancement of In-Situ Synthesized Three-Dimensional Network Graphene Reinforced Copper Nanocomposites X. Zhang , C.N. He and N.Q. Zhao	Mr. Xiang Zhang , Tianjin University- China
15:45-16:00	Next-Generation of Graphene Composites: Surface-Modified GO with Tunable Flake Orientation M. Wåhländer , F. Nilsson, A. Carlmark, S. Edmondson and E. Malmström	Mr. Martin Wåhländer , KTH Royal Institute of Technology - Sweden

16:00-16:30 Coffee Break / Exhibition / Posters session II		
16:30-16:45	Tunable Magnetism of Adatoms adsorbed on Bilayer Graphene D. Nafday , M. Kabir and T. Saha Dasgupta	Ms. Dhani Nafday , S.N. Bose National Center for Basic Sciences- Kolkata-India
16:45-17:00	Ultrafast optics in graphene K. Liu , J.F. Zhang, Z.H. Zhu, C.C. Guo, X.D. Yuan, W.M. Ye and S.Q. Qin	Prof. Ken Liu , National University of Defense Technology- China
17:00-17:15	Graphynes: from Competitors to Graphene to Atomic Sieves and Scatter F. Viñes , M. Manadé, S. Kim, P. Gamallo, J.Y. Lee and F. Il-Ias	Dr. Francesc Viñes , Barcelona University- Spain
17:15-17:30	Combination of the PDCs Route with the SPS Process to Easily Obtain Large and Pure h-BN Nanosheets Y. Li, S. Yuan, P. Steyer , B. Toury, V. Garnier, A. Brioude and C. Journet	Dr. Philippe Steyer , INSA Lyon- France.
17:30-17:45	Graphene based Electrically Tunable Hybrid Plasmonic-photonic Waveguide with Low-loss and Nano-scale Optical Confinement L.Singh ,Sulabh and M. Kumar	Dr Mukesh Kumar , Indian Institute of Technology- Indore- India
17:45-18:00	Electrochemically exfoliated graphite for solution-processed transparent conductive electrodes. A.Ly , P. Viville and R. Lazzaroni	Mr. Ahmadou Ly , Mons University- Belgium
18:00-18:15	Discontinuous bilayer graphene chemiresistors P. Krauss and J. J. Schneider	Mr Peter Krauss , Technische Universität Darmstadt -Germany
18:15-18:30	Spin noise in graphene detected via cross-correlation S. Omar , I.J. Vera-Marun, M.H.D. Guimarães, A. Kaverzin and B.J. van Wees	Mr. Siddhartha Omar , University of Groningen- The Netherlands
18:30-18:45	Graphene oxide framework membranes: Control the 2D interspacing toward strict molecular sieving G. Zeng , G. Li, B. Qi, X. He, Y. Zhang and Y. Sun	Dr. Gaofeng Zeng , Shanghai Advanced Research Institute, Chinese Academy of Sciences - China
18:45-19:00	Hydrogen-decorated stabilization and thermal conductivity of penta-silicene: A first principles calculation H. K. Liu , Y. Lin and M. Hu	Mr. Huake Liu , RWTH Aachen University- Germany
19:00-19:15	Enhancing the performance of dye-sensitized solar cells by incorporating various ratios of platinum and reduced graphene oxide thin film as a counter electrode N. Ahmad-Ludin , A. Bolhan, M. Y. Sulaiman, M. S. Suait, M. A. Mat-Teridi, M. A. Ibrahim, S. Sepeai, K. Sopian and H. Arakawa	Dr. Norasikin Ahmad Ludin , Kebangsaan University – Malaysia

<p style="text-align: center;">June 2nd, 2016</p> <p style="text-align: center;">EGF 2016- Session III: Graphene and 2D Materials properties and applications</p> <p style="text-align: center;">Conference Room 561</p>		
<p style="text-align: center;">Session's Chairs: Dr Cinzia Casiraghi, University of Manchester- UK Prof. Alicia de Andrés, Materials Science Institute of Madrid (CSIC), Spain</p>		
14:00-14:30	Platinum-Gold Alloy Nanoparticles Decorated Crumpled Graphene for Electrocatalyst H.D. Jang , S.K. Kim, J-H. Choi and H.Chang	Prof. Hee Dong Jang , Korea Institute of Geoscience and Mineral Resources - Republic of Korea
14:30-15:00	Graphene Transistor Monitoring Properties of Functional Oxides D.Suh	Prof. Dongseok Suh , Sungkyunkwan University - Republic of Korea

15:00-15:15	Infrared spectroscopy of closely aligned heterostructures of graphene and hexagonal boron nitride D.S.L. Abergel and M. Mucha-Kruczyński	Dr. David Abergel , Nordita, KTH Royal Institute of Technology and Stockholm University- Sweden
15:15-15:30	Anisotropy of Unstrained Pristine Graphene G. Shpenkov	Dr. Georgi Shpenkov , Academy of Computer Science and Management- Poland
15:30-15:45	Temperature dependent fracture of defected graphene sheets: a Molecular Dynamics study S. Nasiri and M. Zaiser	Mrs. Samaneh Nasiri , Friedrich-alexander University- Germany
15:45-16:00	Graphene: A Tunable Kerr Nonlinear Medium B. Semnani , A.H. Majedi and S. Safavi-Naeini	Mr. Behrooz Semnani , University of Waterloo- Canada
16:00-16:30 Coffee Break / Exhibition / Posters session II		
16:30-16:45	Substantial improvement of graphene-enhanced raman scattering through strain engineering of graphene G. Dobrik, P. Nemes-Incze, L.P. Biró and L. Tapasztó	Dr. Levente Tapasztó , Centre For Energy Research Hungarian Academy of Sciences- Hungary
16:45-17:00	Evaluation of Graphene Suspensions T.J. Nacken , C. E. Halbig, C. Damm, J. Walter, S. Eigler and W. Peukert	Mr. Thomas Nacken , University Erlangen-Nürnberg - Germany .
17:00-17:15	Pt nanoparticles supported on rGO/SiC hybrid material as a cathode catalyst in DMFC B. Ozdincer , K. K. Maniam and S. M. Holmes	Mr. Baki Ozdincer , The University of Manchester – UK
17:15-17:30	Graphene based coatings against corrosion K.S. Aneja , S. Bohm, A.S. Khanna and M. Thompson	Mr. Karanveer. S. Aneja , Indian Institute of Technology Bombay - India
17:30-17:45	Impact of reduction degree of graphene oxide on the photocatalytic activity of graphene oxide/TiO ₂ nanotubes M. Hamandi , G. Berhault, C. Guillard and H. Kochkar	Mrs. Marwa Hamandi , Claude Bernard University Lyon – France
17:45-18:00	Fabrication of Graphene oxides (GO) based rGO-TiO ₂ /Fe ₃ O ₄ nanocomposites for the removal of Methylene Blue and Arsenic(III) from Wastewater P. Benjwal , M. Kumar, P. Chamoli and K.K. Kar	Ms. Poonam Benjwal , Indian Institute of Technology Kanpur- India
18:00-18:15	Graphene nanoplatelets biocompatibility is improved by surface adsorption of polymers A. Pinto, A. Moreira, F. Magalhães and I. Gonçalves	Dr. Inês C. Gonçalves , University of Porto- Portugal
18:15-18:30	Functionalization of graphene field-effect transistor channel for ischemic stroke biomarker detection P. D. Cabral , E. Fernandes, F. Cerqueira, G. Machado Jr., J. Borme and P. Alpuim	Ms. Patricia Cabral da Silva , International Iberian Nanotechnology Laboratory- Portugal
18:30-18:45	A Novel SPR biosensor chip with Graphene Oxide Linking Layer Yu.V. Stebunov , O.A. Aftenieva, A.V. Arsenin and V.S. Volkov	Mr. Yury Stebunov , Moscow Institute of Physics and Technology- Russian Federation
18:45-19:00	Heartbeat resistive sensor based on graphene nanobelt thin films A. Alaferdov, R. Savu, S. Rackauskas, T. Rackauskas, E. Joanni and S A. Moshkalev	Dr. Stanislav Moshkalev , UNICAMP, Center for Semiconductor Components- Brazil
19:00-19:15	The potential of graphene based active components in silicon photonic systems D. Schall , and D. Neumaier	Mr. Daniel Schall , AMO GmbH-Aachen- Germany
19:15-19:30	Few-Layer Graphene Langmuir Nanofilm Decorated by Palladium Nanoparticles for NO ₂ and H ₂ Gas Sensing D. Kostiuk , S. Luby, M. Demydenko, Y. Halahovets, P. Siffalovic, K. Vegso, J. Ivanco, M. Jergel, M. Kotlar, R. Redhammer and E. Majkova*	Dr. Dmytro Kostiuk , Slovak Academy of Sciences- Slovakia

June 3rd, 2016
EGF 2016- Session IV: Graphene and 2D Materials applications

Conference Room 511

Session's Chairs:
Prof Valerio Pruneri, ICFO-The Institute of Photonic Sciences and ICREA- Spain
Prof. Thomas Mueller, Institute of Photonics, Vienna University of Technology – Austria

08:30-09:00	Radionuclide Therapy with Neutron-Activated Graphen Oxide Nanoplatelets J Kim and M. Jay	Prof. Michael Jay , University of North Carolina- USA
09:00-09:30	Thixotropic Properties of Graphene Oxide/Hydrogel for 3D Bioprinting H. Li and L. Li	Prof. Lin Li , Nanyang Technological University- Singapore
09:30-10:00	Graphene for transparent electrodes and sensing applications V.Pruneri	Prof. Valerio Pruneri , ICFO-The Institute of Photonic Sciences and ICREA- Spain
10:00-10:30 Coffee Break / Exhibition		
10:30-11:00	Ballistic transport regimes in hBN-encapsulated graphene devices J.Wallbank and V. Falko	Dr. John Wallbank , National Graphene Institute, University of Manchester - UK
11:00-11:30	Optoelectronics with atomically thin materials T.Mueller	Prof. Thomas Mueller , Institute of Photonics, Vienna University of Technology - Austria
11:30-12:00	Nonlinear Electrodynamics and Optics of Graphene S.A. Mikhailov	Dr. Sergey Mikhailov , University of Augsburg - Germany
12:00-12:30	Graphene membranes and their use as pressure sensors H.S.J. van der Zant	Prof. Herre S.J. van der Zant , Delft University of Technology - The Netherlands
12:30-13:00	Functionalized graphene for flexible light-emitting devices E;T;Alonso, G;Karkera, G;F. Jones, S;Russo, M.F. Craciun	Prof. Monica F. Craciun , University of Exeter - UK

Posters Session II: June 2nd, 2016
European Graphene Forum - EGF 2016

Exhibition and Poster Hall

N.	Title	Author/Affiliation/Country
1	Formation of Continuous Few-layer MoS ₂ Nanosheet Filmfor Sensing and Detection Applications M.Demydenko , M.Jergel, D.Kostiuk, Y.Halahovets, M.Kotlar, P.Siffalovic, K.Vegso and E.Majkova	Dr. Maksym Demydenko , Slovak Academy of Sciences - Slovakia
2	Grain Boundary Structures and Electronic Properties of Hexagonal Boron Nitride on Cu (111) Q. Li , Y. Zhang and Z. Liu	Ms. Qiucheng Li , Peking University, Beijing - Republic of China
3	Large-scale Synthesis of Defects-selective Graphene Quantum Dots for Cell Imaging by Ultrasonic-assisted Liquid-Phase Exfoliation L. Lu and Y.T. Pei	Mr. Liqiang Lu , University of Groningen - Netherlands
4	CVD growth of large single crystal graphene L. Lin , H. Ren, J. Li, N. Kang, H. Q. Xu, H. Peng and Z. Liu	Mr. Li Lin , Peking University- China.
5	Fabrication and Characterizaiton of Near Infrared Detectors based on MoS ₂ Few-layers Grown with Chemical Vapor Deposition X. Wang, L.L. Shiau and B.K. Tay	Prof. Beng Kang Tay , Nanyang Technological University- Singapore

6	Silver/nitrogen-doped reduced graphene oxide as an electrocatalyst for oxygen reduction in alkaline medium L.T. Soo, K.S. Loh , A.B. Mohamad, W.R.W. Daud and W.Y. Wong	Dr. Kee Shyuan Loh , Kebangsaan Malaysia University- Malaysia
7	Adsorption Abilities of TiO ₂ -R-OH-rGO Nanocomposites E. Kusiak-Nejman , A. Wanag, J. Kapica-Kozar, Ł. Kowalczyk, A.W. Morawski, L. Lipińska and M. Aksienionek	Dr. Ewelina Kusiak-Nejman , West Pomeranian University of Technology- Poland
8	Preparation and Tribological Performance of Nickel-Graphene Oxide Composite Coatings S. Qi , X. Li and H. Dong	Mr Shaojun Qi , University of Birmingham- United Kingdom
9	One - pot preparation of SERS nanocomposites of silver and graphene oxide with tunable properties M.O. Volodina , A.V. Sidorov, E.A. Eremina and E.A. Goodilin	Mrs. Mariia Volodina , Lomonosov Moscow State University- Russian Federation
10	Reduced graphene oxide on/in metallic substrates: coating and composite M.A.Rodríguez-Escudero, A.Argumanez, I. Llorente, O. Caballero-Calero, M.S. MartínGonzález, R. Fernandez and M.C.García-Alonso	Mrs. M Cristina Garcia-Alonso , The Spanish National Research Council (CSIC)- Spain
11	High orientation degree of graphene nanoplatelets in spark plasma sintered silicon nitride composites O. Tapasztó , L. Tapasztó, V. Puchy, J. Dusza, C. Balázs and K. Balázs	Dr. Orsolya Tapasztó , Center for Energy Research, Institute of Technical Physics and Materials Sciences- Hungary
12	Observation of Alkali Metal Adsorption on Freestanding Graphene by Means of LEEPS Microscopy M. Lorenzo , J. Vergés, C. Escher, J.-N.Longchamp and H.-W. Fink	Ms. Marianna Lorenzo , University of Zurich- Switzerland
13	3D nanodendrites consisting of Pd and N-doped carbon nanoparticles as bifunctional catalyst H. K. Sadhanala , R. Nandan, and K. K. Nanda	Mr. Hari Krishna Sadhanala , Indian Institute of Science- Bangalore- India .
14	Graphene growth and transfer towards flexible substrates for microwave applications J. Njeim , A. Madouri, A. Cavanna, P. Chrétien, A. Jaffré, Z. Ren and D. Brunel	Ms. Joanna Njeim , Pierre et Marie Curie University- France
15	Multi-layered graphene interface for enhancing the stretchability of brittle conductive layers S. Won, Y. Hwangbo , K-S. Kim, H-J. Lee and J-H. Kim	Dr. Yun Hwangbo , Korea Institute of Machinery & Materials (KIMM)- Republic of Korea
16	Experimental study of the electrical properties of multilayer graphene-fullerene C60-multilayer graphene junctions E. Benítez and D. Mendoza.	Mr. Erick Benitez , National Autonomous University of Mexico - Mexico .
17	Spin transport in fully hexagonal boron nitride encapsulated graphene M. Gurram , S. Omar, S. Zihlmann, P. Makk, C. Schönenberger and B.J. van Wees	Mr. Mallikarjuna Gurram , University of Groningen- The Netherlands
18	Ultra-Broadband Strong Absorption Enhancement in Graphene with Plasmonic Light Trapping F. Xiong and J. Zhang	Mr. Xiong Feng , National University of Defense Technology- China
19	Novel Aerosol Synthesis of Pt Nanoparticles-Laden Graphene via Microwave Plasma Spray Pyrolysis and Their Enhanced Methanol Oxidation Reaction H. Chang , E.H. Jo, S.K. Kim and H.D. Jang	Dr. Hankwon Chang , Korea Institute of Geoscience & Mineral Resources- Republic of Korea
20	Diverse anisotropy of phonon transport in two-dimensional group IV-VI compounds: A comparative study G. Qin and M. Hu	Mr. Guangzhao Qin , RWTH Aachen University- Germany
21	Effect of modified Graphene and Montmorillonites and their mixtures on the properties of biodegradable PLA/PCL blend A. Habi , B.S.Bouakaz, Y. Grohens and I. Pillin	Dr. Abderrahmane Habi , A. Mira de Béjaia University - Algeria .
22	Magneto-optical characterization of super-lattices in graphene T. Wolf , I. P. Levkivskyi, O. Zilberberg and G. Blatter	Mr. Tobias Wolf , ETH Zurich- Switzerland
23	Conference topic: applications of graphene in biomedical area Graphene Oxide Based Sensing of Small Molecules O.A. Aftenieva , Yu.V. Stebunov and A.V. Arsenin	Ms. Olha Aftenieva , Moscow Institute of Physics and Technology- Russian Federation
24	Development of Graphene-based Barriers for Solar Cells G. Rossi , M.Sarno, C.Cirillo and L. Incarnato	Dr. Gabriella Rossi , University of Salerno - Italy

Nanotech Plenary Session I

Club nanoMetrology : a French Initiative to improve the Reliability of Measurements at the Nanoscale. A review after 4 years

G. Favre¹, K. Aguir², D. Bernard³, O. Bezencenet⁴, J. Carimalo⁵, N. Feltin¹, B. Gautier⁶, A. Levenson⁷, T. Macé⁸, P. Maillot⁹, J.-M. Moschetta⁸

¹ LNE, 29 avenue Roger Hennequin, 78197 Trappes / France, ² Aix-Marseille Université – IM2NP, St. Jérôme, 13397 Marseille / France, ³ CEA, 17 rue des Martyrs 38000 Grenoble / France, ⁴ Thales Research & Technology, 1 avenue Augustin Fresnel, 91767 Palaiseau / France, ⁵ CNRS – Institut de Physique, 3, rue Michel Ange, 75794 PARIS / France, ⁶ INL/INSA Lyon, 7 avenue Capelle, 69621 Villeurbanne / France, ⁷ NanoSciences France (C’Nano), CNRS/LPN, Route de Nozay 91460 Marcoussis / France, ⁸ LNE, 1 rue Gaston Boissier, 75724 Paris / France, ⁹ STMicroelectronics, ZI de Rousset Avenue Coq, 13106 Rousset / France

Abstract:

Nanotechnologies offer ever-increasing number of applications in all sectors of industry. However most of the measurement capabilities dedicated to nanomaterials properties are still in their infancy, while industrial processes involve quality insurance management which relies on demonstrated reliable tools. Therefore the lack of suitable metrology slows down the technological integration of certain nano-objects or nanostructures. In parallel, the development of nanomaterials raises the question of their regulation and possible risks for health, safety and environment, while all reports published by government agencies and standardization bodies point out the lack of tools, reference materials and methodologies that would establish the metrological traceability of measurements and thus allow the comparability of data.

Support to industry in nanotechnologies and analysis of risk / benefit ratio of nanomaterials demand therefore the development of a new metrology: the nanometrology. In order to bring some answers to this wide and complex area, LNE (the French National Metrology Institute) and CNRS created in 2011 the Club nanoMetrology (CnM) with the support of French Ministry of Industry.

At present, more than 340 members have joined the CnM, one third coming from SMEs, start-ups and large industrial groups (producers, companies in processing and integration, instrument manufacturers ...).



Figure 1: Figure showing the periodic structure provided by the CNRS/LPN & LNE to be used in the frame of the interlaboratory comparison organized by the CnM in 2014. Main highlights of the CnM actions (in particular the first inter-comparison on nanomaterial characterization at the French national scale) and present outlook will be presented.

Keywords: network, nanometrology, metrological traceability, reliability, inter-comparison, standards, working groups, dissemination.

References:

1. Nanofutures, “Integrated Research and Industrial Roadmap for European Nanotechnology”, 2012, <http://www.nanofutures.info/>
2. Co-nanomet project outputs, www.co-nanomet.eu
3. French Decree n 2012-232 (2012), <https://www.r-nano.fr/>
4. www.club-nanometrologie.fr

European standardization in nanotechnologies and relation with International work. How standardization can help industry and regulators in developing safe products?

P. Conner,¹

¹ AFNOR Standardization, Management and Consumer Services Department, La Plaine Saint-Denis, FRANCE

Abstract:

Nanotechnologies have enormous potential to contribute to human flourishing in responsible and sustainable ways. They are rapidly developing field of science, technology and innovation. As enabling technologies, their full scope of applications is potentially very wide. Major implications are expected in many areas, e.g. healthcare, information and communication technologies, energy production and storage, materials science/chemical engineering, manufacturing, environmental protection, consumer products, etc. However, nanotechnologies are unlikely to realize their full potential unless their associated societal and ethical issues are adequately attended. Namely nanotechnologies and nanoparticles may expose humans and the environment to new health risks, possibly involving quite different mechanisms of interference with the physiology of human and environmental species.

One of the building blocks of the “safe, integrated and responsible” approach is standardization. Both the Economic and Social Committee and the European Parliament have highlighted the importance to be attached to standardization as a means to accompany the introduction on the market of nanotechnologies and nanomaterials, and a means to facilitate the implementation of regulation. ISO and CEN have respectively started in 2005 and 2006 to deal with selected topics related to this emerging and enabling technology.

In the beginning of 2010, EC DG “Enterprise and Industry” addressed the mandate M/461 to CEN, CENELEC and ETSI for standardization activities regarding nanotechnologies and nanomaterials. Thus CEN/TC 352 “Nanotechnologies” has been asked to take the leadership for the coordination in the execution of M/461 (46 topics to be standardized) and to contact relevant European and International Technical committees and interested stakeholders as appropriate (56 structures have been identified). Prior

requests from M/461 deal with characterization and exposure of nanomaterials and any matters related to Health, Safety and Environment. Answers will be given to: What are the structures and how they work? Where are we right now and how work is going from now onwards? How CEN’s work and targets deal with and interact with global matters in this field?

Keywords: nanotechnologies, responsible and sustainable ways, enabling technologies, healthcare, information, communication technologies, energy production, storage, materials science, chemical engineering, manufacturing, environmental protection, consumer products, nanoparticles, health risks, nanomaterials, regulation, ISO, CEN/TC 352 “Nanotechnologies”, characterization, exposure, health, safety.

Mathematical modelling in nanotechnology

Professor James M. Hill

School of Information Technology and Mathematical Sciences,

University of South Australia, Mawson Lakes Campus,

GPO Box 2471, Adelaide, SA 5001, Australia

Email: jim.hill@unisa.edu.au

Abstract

In this talk we present an overview of the mathematical modelling contributions of the Nanomechanics Groups at the Universities of South Australia, Adelaide and Wollongong. We assume that individual atomic interactions follow the Lennard-Jones potential, and that molecular interactions can be approximated by replacement of their actual atomic structure with either a continuous distribution of atoms having a constant atomic surface density, or with a continuous distribution of atoms throughout the volume with constant volume atomic density. Fullerenes and carbon nanotubes are well known to have many unique properties, such as low weight, high strength, flexibility, high thermal conductivity and chemical stability, and they have many potential applications in novel nano-devices. One concept that illustrates our progress in nanomechanics, and has attracted much attention, is the creation of nano-oscillators, to produce frequencies in the gigahertz range, for applications such as ultra-fast optical filters and nano-antennae. The sliding of an inner shell inside an outer shell of a multi-walled carbon nanotube can generate oscillatory frequencies up to several gigahertz, and the shorter the inner tube the higher the frequency. A C_{60} -nanotube oscillator generates high frequencies by oscillating a C_{60} fullerene inside a single-walled carbon nanotube. As a means of illustrating nanomechanical modelling we discuss the underlying mechanisms of nano-oscillators using the Lennard-Jones potential together with the continuous approach. This modelling approach applies to many problems, and three illustrative examples of recent work in hydrogen storage, nanocomputing and nanomedicine are briefly discussed. At the nano scale the geometric notions of well defined space and packing may have a

greater importance, and some results on the structure of nanotubes, including carbon, boron nitride, boron and silicon, and on related nanostructures arising from geometric considerations only are also presented.

Water collection/Repellency of Bioinspired Micro/Nano-structured Surfaces

Y. Zheng

Beihang University, School of Chemistry and Environment, Beijing, China

Abstract:

Inspired by the roles of micro- and nanostructures in the water collecting ability of spider silk, a series of functional fibers are designed by using nanotechnology-related methods. The “spindle-knot/joint” structures demonstrate the cooperation of multiple gradients in driving tiny water drops to collect water at micro- and nano-level. The geometrical-engineered thin fibers display a much higher water capturing ability than normal fibers in fog flows; the bead-on-string hetero-structured micro-fibers are capable of intelligently responding to environmental changes in humidity; the tiny water droplets can be controlled the transport in directions by designing the temperature, photo, rough-responded surfaces on fibers; the continuous size spindle-knots fiber can realize the droplet transport in a long distance for water collection in efficiency (**Figure 1**). By integrative gradient features of surfaces between spider silk and beetle back, a kind of wettable star-shape pattern surface also realizes the effect of water repellency rather than others. Otherwise, learning from butterfly wing and plant leaf display water repellency and low-temperature superhydrophobicity, bioinspired surfaces with optimal micro- and nanostructures display distinctly anti-icing, ice-phobic and de-ice abilities. It is also demonstrated further that the oriented or asymmetric features on geometries at micro- and nano-level can generate the driving of droplets that is resulted from the surface energy gradient,. Especially, the superhydrophilic oriented-nanohaired surface exhibits the directional transport of drop as the surface is at high temperature. These studies are greatly significant to help to design the novel functional engineering wettability-controlled surfaces

Keywords: bioinspired, micro-/nanostructure, gradient, wettability application..

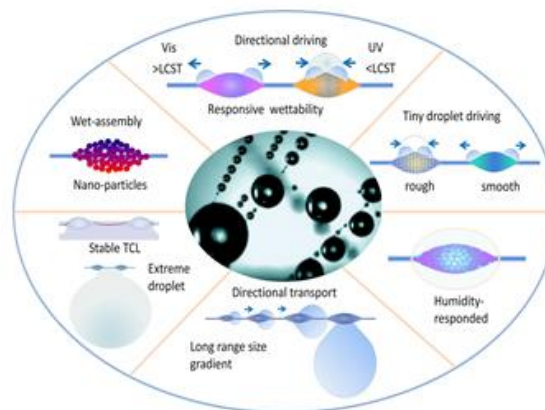


Figure 1:Figure 1 illustrates the bioinspired wettability surfaces with micro- and nanostructures to control the water collection and repellency.

References:

- Zheng, Y., Bai, H., Zhong, H., Tian, X., Nie, F., Zhai, J., Zhao, Y., Jiang L. (2010) Directional water collection on wetted spider silk. *Nature*, 463, 640–643.
- Chen, Y., Zheng, Y. (2014) Bioinspired micro-/nanostructure fibers with water-collecting properties. *Nanoscale* 6, 7703–7714.
- Zheng, Y. (2015) Bio-inspired wettability surfaces: Development in micro- and nanostructures. *Pan Stanford Publishing. USA*, 0–216.
- Zhang, M., Zheng, Y. (2016) Bioinspired structure materials to control water-collecting properties. *Materials Today: Proceedings*, 3, 696–702.

Ultrasonic Spray Coating as a versatile technique for the large area deposition of functional nanoparticles

J. Stryckers,^{1,2} W. Deferme,^{1,3,*}

¹Institute for Materials Research (IMO-IMOMECE), Hasselt University, Diepenbeek, Belgium

²IMEC vzw – Division IMOMECE, Wetenschapspark 1, B-3590 Diepenbeek, Belgium

³Flanders Make vzw, Oude Diestersebaan 133, B-3920 Lommel, Belgium

Abstract:

Solution deposition techniques allow the deposition of thin films at atmospheric pressure and ambient temperatures. A direct advantage of this is the absence of high temperatures and near vacuum pressures that allow the use of flexible substrates such as PET, textile or paper.

Spin coating is the laboratory standard when producing thin films of typically ~100 nm. Despite its ease-of-use, the spin coating process does not comply well with large-area production. Nor is the process compatible with high throughput roll-to-roll production and it does not allow patterning. Furthermore, spin coating is a wasteful process.

Ultrasonic spray coating on the other hand has virtually no limitation in substrate size and a low utilization of material. It is possible to apply a variety of particle mixtures to a wide range of substrates and it allows to engineer the thin film depositions by manipulating the tunable spray coating parameters.

The focus of our research was directed to deposit eco-friendly, water-based nanoparticle inks into layers with desired thickness and morphology, by optimising the ultrasonic spray coating parameters and the deposition temperature. It is shown in this work that nanoparticles with different diameters can be deposited in thin films. Gold and magnetite nanoparticles (<30nm) for magneto-optical, P3HT-PCBM nanoparticles (~100nm) for organic photovoltaic and molecular imprinted polymer particles (~1µm) for biosensing applications are the subject of the study. Due to the narrow distribution of the droplet size and the deagglomeration of the particles during ultrasonic spray coating, it is demonstrated that eco-friendly, water-based nanoparticle inks can be deposited into layers with desired thickness and morphology.

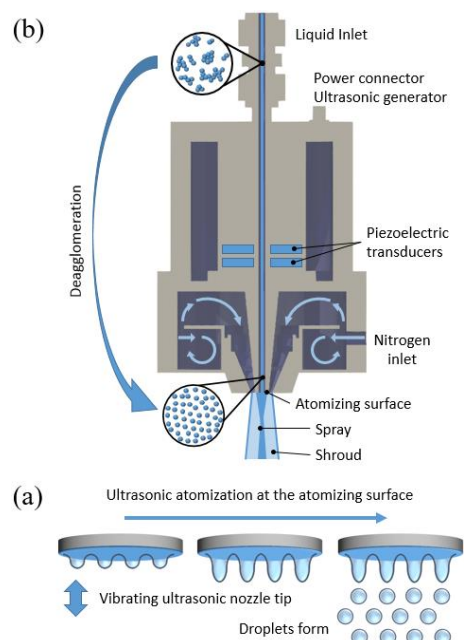


Figure 1: (a) Ultrasonic atomization principle at the atomizing surface (b) Cross-section of an ultrasonic spray nozzle and deagglomeration of nanoparticles

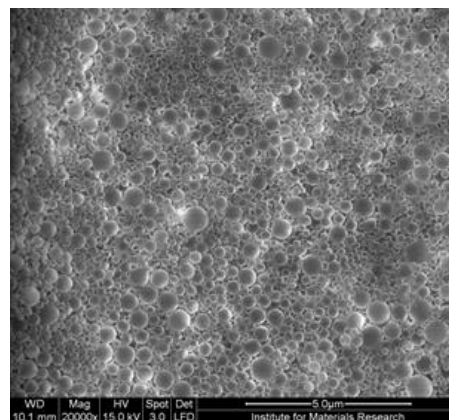


Figure 2: Optimized 10µm thick polystyrene nanoparticle layer

Keywords: ultrasonic spray coating, eco-friendly nanoparticle inks, magneto-optics, organic photovoltaics, biosensor applications

Nanotech France 2016 Session I

Nanomaterials Fabrication / Synthesis

Rational Synthesis of Chirality-Pure Single Walled Carbon Nanotube

K.Yu. Amsharov*

University of Erlangen-Nürnberg, Institute of Organic Chemistry, Erlangen, German

Abstract:

Over the last decade, Single-Walled Carbon Nanotubes (SWCNTs) have attracted tremendous attention from almost all areas of science because of their extraordinary chemical and physical properties. The diversity in electronic properties of SWCNTs which vary from semi-conducting to metallic strongly depends on the atomic structure or chirality which is uniquely determined the tube connectivity by the pair of chiral index (n,m) . The ability to tune the band gap over a rather wide range together with extra high chemical, mechanical and thermo- stability makes SWCNTs very promising candidates for many potential applications. However, the widespread use of SWCNTs has remained elusive due to a lack of efficient production techniques of chirality-pure samples. Although significant efforts have been made in selective SWCNT syntheses, no efficient pathway to truly single-chirality SWCNTs was found. Previously we have shown that specially designed polycyclic aromatic hydrocarbons (PAHs) can be quantitatively converted to the “preprogrammed” carbon nanostructure, such as buckybowls and fullerenes by surface assisted cyclodehydrogenation (SACDH),[1] and have further demonstrated that the approach can be extended to the fabrication of CNT end-caps and even ultra-short singly-capped nanotubes bearing several CNT segments.[2] The tubes obtained by this route are already bonded to the metal and can be used directly for the SWCNT fabrication on the same metal surface. Finally we have demonstrated that CNT seeds are active in tube growth initiation and can be indeed grown to isomerically pure SWCNTs exclusively by epitaxial elongation under Chemical Vapor Deposition (CVD) condition (Figure 1).[3] Our finding shows that the uncontrolled CNT nucleation can be avoided and an isomerically pure and defect free SWCNTs can be effectively fabricated in bulk.[3] Based on this discovery a one-pot synthesis strategy appears to be very attractive for the preparative synthesis of chirality pure SWCNTs. Since virtually all types of SWCNTs can be grown on

metal catalyst surfaces by common CVD approaches, it seems to be highly realistic to extend the pre-sented strategy for synthesis of SWCNTs with various possible chiralities.[4]

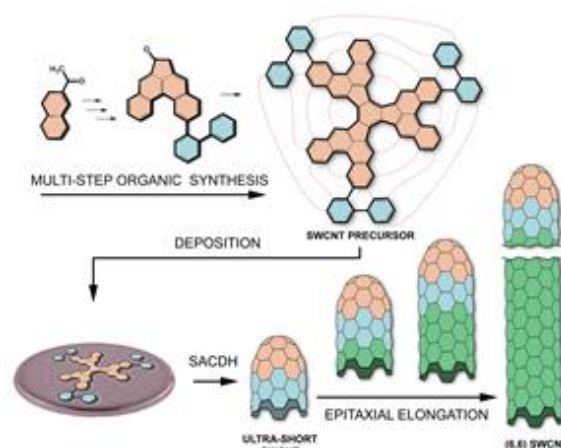


Figure 1: The general scheme for the chirality controlled SWCNT synthesis on the example of (6,6) SWCNT fabrication, showing four main steps: precursor synthesis, precursor deposition on the metal surface, surface assisted cyclodehydrogenation (SACDH) to the ultra-short SWCNT and the final growth to the isomerically pure nanotube.

Keywords: Single walled carbon nanotube, rational synthesis, isomer-pure SWCNTs, chirality-controlled synthesis.

References:

- 1) K. Amsharov, N. Adurakhmanova, S. Stepanow, S. Rauschenbach, M. Jansen and K. Kern, *Angew. Chem. Int. Ed.*, 49, 9392, (2010);
- 2) N. Abdurakhmanova, A. Mueller, S. Stepanow, S. Rauchenbach, M. Jansen, K. Kern and K. Amsharov, *Carbon*, 84, 444, (2015);
- 3) J. R. Sanchez-Valencia, T. Dienel, O. Gröning, I. Shorubalko, A. Mueller, M. Jansen, K. Amsharov, P. Ruffieux and R. Fasel, *Nature*, 512, 61, (2014);
- 4) K. Amsharov *Phys. Status Solidi B*, (2015), DOI:10.1002/pssb.201552189

New frontiers and technologies for advanced materials

V. Beghetto*^{1,2}, L. Agostinis¹, R. Taffarello², R. Samiolo²

¹Department of Molecular Sciences and Nanosystems, Università Ca' Foscari Venezia, Via Torinon 155, 30172 Mestre, Venezia.

²CROSSING S.r.l., Piazza delle Istituzioni 27/H, 31100 Treviso.

Abstract:

The project is concerned with the development of a new class of molecules used as activating agents for “cross-linking” (ACL) and their application for the preparation of innovative materials. Crossing, an Academic Spin off and innovative Start Up, is developing the know-how for the industrial production and use of new families of organic compounds such as ACLs.

The great potential of this class of molecules is embedded in their multiple applications. Today poor availability and high costs of cross-linking agents, drastically limits the use of similar compounds, except for pharmaceutical and biomedical engineering applications [1,2].

These activators are able to link together different molecules with a “lock and key” mechanism shown in Figure 1 in which the hands exemplify the function of the activators.

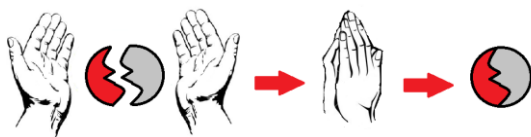


Figure 1. ACLx “lock and key” mechanism.

Another interesting characteristic, bound to the particular nature of the ACLs, relates to the modularity of the structure of these compounds. Indeed, the structure of the ACLs is such that it can be easily modified, providing the end user with a wide range of homologue compounds, which can vary in activity, performance, speed of action etc. ACLs may thus be specifically formulated and optimized as a function of the specific use.

The range of ACLs that Crossing intends to develop industrially are not currently available on the world market.

The main activities to be developed are:

1) Development of the synthesis procedure for the industrial production of the first activator head of the family (ACL11), with top-down ap-

proach and implementation of a pilot plant (patent pending regarding the industrial production of ACLx).

2) Outsourcing for the production of ACL11.

3) Development of further homologous activators (ACLx), related to ACL11, with top-down approach and implementation of a pilot plant.

4) Diversification of the sectors of employment of ACLx industrialized (patent pending regarding the industrial application of ACLx as leather tanning agents alternative to chrome salts).

5) Industrialization and commissioning of production plants for ACLx.

6) Development of a network of technical and industrial relations for the acceleration of the processes above.

Keywords: cross-linking, advanced materials, collagen, leather, packaging, antimicrobial, textile

References:

- [1] Albericio F., Chinchilla R., Dodsworth, D. J., Najera C., Organic Preparations and Procedures Int., 33, 203-313, 2001.
- [2] El-faham A., Albericio F., Chem. Rev., 111, 6557–6602, 2011.

Weak interactions for strong complexation between DNA nano-rods and lipids

L. Navailles,^{1,*} K. Bougis,¹ R. Leite Rubim,^{1,2} N. Ziane,¹ J. Peyencet,¹ A. Bentaleb,¹ A. Février,¹
B. B. Gerbelli,² C.L.P. Oliveira,² Andreoli de Oliveira,² . Schoentgen,¹
G. Tonelli,¹ P. Barthélémy,³ F. Nallet,¹

¹Centre de Recherche Paul Pascal, UPR CNRS 8641, Bordeaux University, France

²Universidade de São Paulo, Instituto de Física-GFCx, P.O.B. 66318, São Paulo, Brazil

³ChemBioPharm, ARNA, INSERM U1212 / UMR CNRS 5320, Bordeaux University, France

Abstract:

Various weak interactions can be used to improve the complex formation between DNA and lipids. Using two different examples, we propose using the hydrophobic effect, confinement, entropy, interfacial interactions and specific interactions as tools for building new supramolecular assemblies that could be used as a versatile carriers of both hydrophobic and hydrophilic therapeutic molecules.

First approach: surfactant lamellar phases are particularly attractive for preparing layered composite structures because colloidal particles can be intercalated within or between surfactant bilayers. The effect of soft confinement on DNA ordering was investigated by varying the water content of a **neutral** lipid lamellar host. A rich polymorphism was found, ranging from weakly correlated DNA-DNA in-plane organizations to highly ordered structures. Structural transitions were observed. The bilayer structural changes are discussed in analogy with the so-called “brush-to-mushroom” transition induced by lateral confinement, relevant for long linear polymers grafted onto rigid surfaces, taking also into account the role of vertical confinement. We suggest that the alteration of membrane steric interactions, together with the appearance of interfacial interactions between bilayers and DNA molecules may be a relevant mechanism for the emergence of highly ordered structures in the concentrated regime of the nanocomposite.

Second approach: hybrid constructions based on nucleosides and lipophilic components, known as nucleolipids, have become an extremely interesting class of molecules, especially for their potential biomedical applications. In this context, it seemed important to define the nature and estimate the strength of their interaction with polynucleotides. In a large number of systems, we

demonstrate the preferential formation by hydrogen bonding of complexes where complementary adenine and thymine moieties associate. Two different mechanisms for the formation of the complexes are proposed.

Keywords: soft matter, self-organisation, lamellar phase, nucleolipids, soft confinement, SAXS, vectorization, gene therapy.

References:

1. Bougis, K., Leite Rubim, R., Ziane, N., Peyencet, J., Bentaleb, A., Février, A., Oliveira, C.L.P., Andreoli de Oliveira, E., Navailles, L., Nallet, F., (2015), Stabilising lamellar stacks of lipid bilayers with soft confinement and steric effects, *Eur. Phys. J. E*, 38, 78, 1-10.
2. Bougis, K., Leite Rubim, R., Ziane, N., Peyencet, J., Bentaleb, A., Février, A., Oliveira, C.L.P., Andreoli de Oliveira, E., Nallet, F., Navailles, L., (2016), *unpublished results*
3. Tonelli, G., Oumzil, K., Nallet, F., Gaillard, C., Navailles, L., Barthélémy, P., (2013), Amino Acid–Nucleotide–Lipids: Effect of Amino Acid on the Self-Assembly Properties, *Langmuir*, 29, 5547–5555.
4. Schoentgen, E., Tonelli, G., Nallet, F., Gaillard, C., Barthélémy, P., Navailles, L., (2016), *unpublished results*

Repeat proteins as template to organize photoactive molecules

Sara Hernández Mejías,^{1,2,*} Javier López-Andarias,³ Kevin Erazo¹, Carmen Atienza³, Nazario Martín^{1,2} and Aitziber L. Cortajarena^{1,2}

¹Instituto Madrileño de Estudios Avanzados en Nanociencia (IMDEA-Nanociencia) 28049-Madrid, Spain.

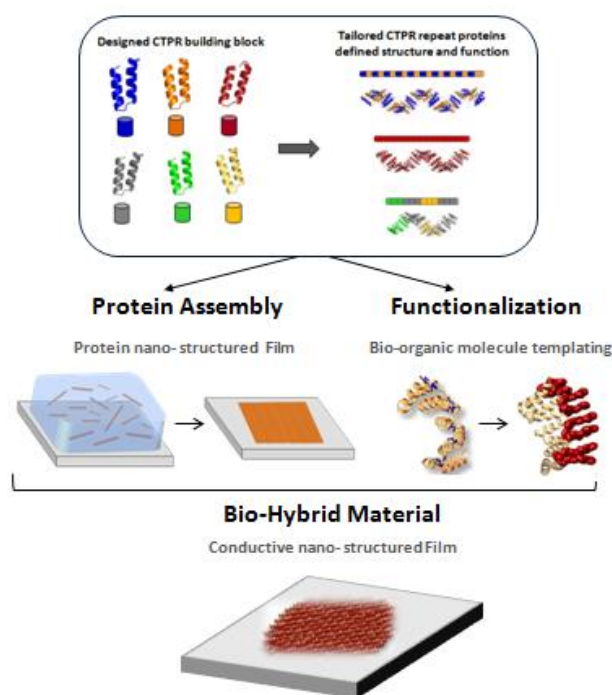
²CNB-CSIC-IMDEA Nanociencia Associated Unit “unidad de Nanobiotechnología” 28049-Madrid, Spain.

³Departamento de Química Orgánica, Facultad de C.C Químicas, Universidad Complutense de Madrid, Ciudad Universitaria sn, Madrid, Spain.

Abstract: The development of application-oriented innovative materials requires methods for control of structures along different size scales. Bottom-up self-assembly that relies on highly specific biomolecular interactions of small defined components, is an attractive approach for biomaterial design and nanostructure templating. In this work, we used modular designed consensus tetratricopeptide repeat proteins (CTPRs) for the generation of functional nanostructures and nanostructured materials. CTPR arrays contain multiple identical repeats that interact through a single inter-repeat interface to form elongated superhelical structures. We have characterized the self-assembly properties of long consensus repeat protein arrays in self-standing films to use them as templates for the creation of functional materials. We show the use of the proteins and generated structures as a template to organize photoactive organic molecules. We propose to use CTPR proteins in order to template donor-acceptor pairs for electro-active materials. In order to achieve an efficient electron transfer the arrays of molecules need to be ordered at defined distances. We show the data in which we explore the potential of CTPR protein scaffolds for nanometer-precise arrangement of the molecules. We are able to form photo-active films using the conjugates where we obtain photo-induced current transport.

Keywords: protein design, protein assembly, bio-conjugates, photo-active molecules, bio-hybrid materials,.

Figure 1. A) Generation of designed repeat proteins using modify modules, in different colors in the left, to form different repeat proteins depending on the application, in the right. B) In the left, protein film generation by the control in the protein self-assembly. In the right, controlled functionalization of the proteins to use as a template to organize photoactive molecules. C) Combining control in the assembly and in the functionalization, generation of conductive nano-structured film where the photoactive molecules are organized in solid state.



References:

1. Kajander, T.; Cortajarena, A. L.; Mochrie, S. G.; Regan, L. *Acta Crystallographica* **2007**, D63, 800.
2. Cortajarena, A. L. & Regan, L. (2006). Ligand binding by TPR domains. *Protein Science* **15**, 1193-1198.
3. Cortajarena, A. L., Mochrie, S. G. & Regan, L. (2011). Modulating repeat protein stability: The effect of individual helix stability on the collective behavior of the ensemble. *Protein Sci* **20**, 1042-7.
4. Grove, T. Z.; Regan, L.; Cortajarena, A. L. *Journal of the Royal Society, Interface* **2013**, 10, 20130051.
5. Lopez-Andarias, J.; Lopez, J.L.; Atienza, C.; Brunetti, F.G.; Romero-Nieto, C.; Guldi, D.M.; Martin, N. Controlling the crystalline three-dimensional order in bulk materials by single-wall carbon nanotubes. *Nature communications* **2014**, 5, 3763.

Chemical Reactions Directed Evolution of Complex Peptide Nanostructures

Apurba K. Das

Department of Chemistry, Indian Institute of Technology Indore, India, Email: apurba.das@iiti.ac.in

Abstract:

Self-assembly plays a vital role in constructing complex functional materials for the applications in biosensing, drug delivery and wound healing treatment. Peptide self-assembly leading to supramolecular hydrogels have been reported in response to external stimuli including sonication,¹ pH, ionic strength, temperature, light, chemical fuel² and enzyme-catalyzed reactions.³ Dynamic covalent chemistry exploits the reversibility of chemical reactions for the generation of library molecules under thermodynamic control.

We have developed oxo-ester and selenoester mediated native chemical ligation reactions of small peptides with N-terminus aromatic protecting group *i.e.* Naphthalene-2-methoxycarbonyl (Nmoc)⁴ that self-assemble to form self-supporting hydrogel and ultimately leads to a nanostructured predominating product. The peptide self-assembly is based on the formation of hydrogen bonding as well as π - π stacking interaction of highly conjugated aromatic moieties. In this procedure, the redox active NCL peptides lead to the formation of a N-capped single predominating product. Self-assembly via hydrogen bonding, oxidation and reduction of disulfide bonds and π -stacking interactions of Nmoc peptides is the driving force for the formation of single predominating product. Formation of nanofibers^{5,6} in self-supporting hydrogel was observed in time dependent manner by scanning electron microscopy. Product conversion was observed by HPLC and further properties were studied by fluorescence, time correlated single photon counting and rheology.

References

1. Maity, D. B. Rasale, A. K. Das, *Soft Matter*, **2012**, 8, 5301-5308.
2. I. Maity, D. B. Rasale, A. K. Das, *RSC Advances*, **2013**, 3, 6395-6400.
3. D. B. Rasale, I. Maity, M. Konda, A. K. Das, *Chem. Commun.*, **2013**, 49, 4815-4817.
4. D. B. Rasale, I. Maity, A. K. Das, *RSC Advances*, **2012**, 2, 9791-9794.
5. I. Maity, T. K. Mukherjee, A. K. Das, *New Journal of Chemistry*, 2014, 38, 376-385.
6. I. Maity, D. B. Rasale, A. K. Das, *RSC Advances*, **2014**, 4, 2984-2988.

Metal nanoparticles for optical limiting prepared via citrate reduction

C. S. Hege,^{1,*} S. Dengler,¹ B. Eberle,¹

¹ Fraunhofer IOSB, Department Optronics, Ettlingen, Germany

Abstract:

Metal nanoparticles as well as several organic and inorganic materials, dyes or macrocyclic rings with conjugated π -system act optically nonlinear [1]. They can be used to attenuate intense laser beams while showing high transmittance at low intensity levels. By utilizing them in so called optical limiting devices they can prevent sensors or the human eye from laser induced damage [2]. In this study we examined the influence of different reduction methods regarding the optical limiting properties of thus produced nanoparticles. Reduction with sodium citrate was compared to sodium borohydride.

In case of citrate reduction a seed-mediated growth approach was used. In the growth step the impact of different factors like pH was analysed.

The citrate seeds tend to have a wormlike structure. Addition of citrate acid to the growth solution leads to smaller nanoparticles. Sodium hydroxide addition induces cubic nanoparticles.

The silver citrate seeds hold better optical limiting ability than the sodium borohydride silver nanoparticles stabilized with PVP (see Figure 1).

Keywords: Optical limiting, nanoparticle synthesis, sodium citrate, sodium borohydride

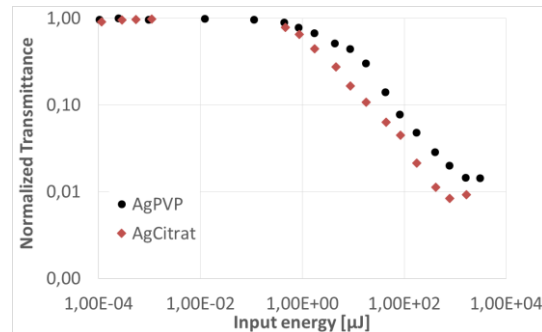


Figure 1: Measurement of the optical limiting behavior of silver nanoparticles at 532 nm. The nonlinear threshold is located around input energies of 1 μ J. The silver nanoparticles stabilized with citrate showed better optical limiting properties than the PVP-stabilized silver nanoparticles.

References:

1. Hollins, R. C., (1999), Materials for optical limiters, *Current Opinion in Solid State and Materials Science*, 4(2), 189–196.
2. Dengler S, Hege C, Eberle B., (2014) Preparation and characterization of novel nanosized hybrid materials and their nonlinear optical properties, *Proc. SPIE* 9253, p 925317

Shape and Pore Size Controlled Scalable Synthesis of Functional Oxide Nanostructures through Exothermic Chemical Reactions

A. Voskanyan,* K.Y. Chan

The University of Hong Kong, Department of Chemistry, Hong Kong

Abstract:

Mesoporous metal oxides with uniform shape and porosity are of considerable interest. Their economical production at a large scale in an efficient manner, however, still remains a challenging task for commercialization. We report for the first time a scalable, economic, energy and time efficient method for the synthesis of crystalline mesoporous oxide catalysts (Cr_2O_3 , CeO_2) with tailored shape and porosity, by utilizing exothermic chemical reactions (Figure 1). In contrast to wet methods, such as hydrothermal synthesis (e.g. soft or hard templates method) which takes hours to proceed in a constant temperature and constant volume reactor, exothermic reactions has rapid thermal and mass transfer processes. The high temperature required for crystal nucleation is achieved by the self-generated heat. Rapid cooling (typically few seconds) does not provide sufficient time for extended crystal growth, leading to nanoscale crystals. By carefully controlling the synthesis conditions metal oxides with uniform shape, uniform porosity, high specific surface area, high pore volume and high crystallinity can be fabricated. As-prepared mesoporous CeO_2 possesses uniform 22 nm pores, 0.6 ml/g pore volume, which is the highest pore volume for CeO_2 reported. The porosity estimated from pore volume of 0.6 ml/g and CeO_2 density (7.28 g/ml) is 81%, which is higher than the theoretical limit (74%) of closed packed spherical cavities. The additional porosity above the closed packed spheres limit may come from micropores between the CeO_2 nanocrystals since the measured micropore volume is 0.075 ml/g, which is equivalent to 12.5% porosity. The estimated porosity of 81% approaches the value (>90%) of common aerogels which are open frameworks formed by networked nanoparticles. We used combination of different characterization techniques to understand the mechanistic details of the process.

The obtained mesoporous CeO_2 catalyst exhibited excellent catalytic activity for soot and carbon monoxide oxidation. In principle this method can be applied to synthesize different high porosity

crystalline metal oxides (binary, ternary). Large scale production of CeO_2 has been demonstrated by 0.5 kg ceria-3 catalyst produced within five hours.

Keywords: exothermic reactions, nanoporous oxides, ceria, heat transfer, catalytic applications, oxidation,

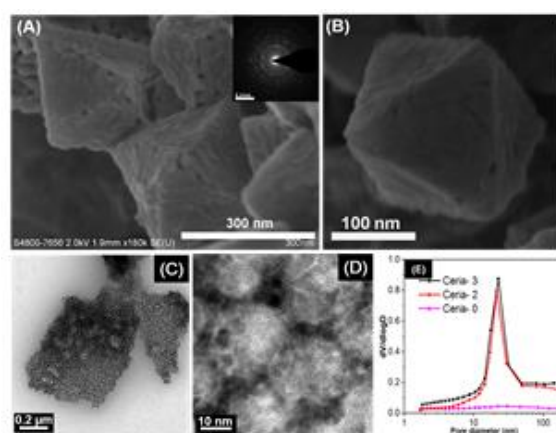


Figure 1: SEM images of Cr_2O_3 octahedra (A, B), TEM images of CeO_2 catalyst (C, D) and BJH pore size distribution plots of CeO_2 catalysts prepared through exothermic chemical reactions.

References:

1. Voskanyan, A. A., Li, C.Y.V., Chan, K.Y., Gao, L. (2015) Combustion synthesis of Cr_2O_3 octahedra with a chromium-containing metal-organic framework as a sacrificial template *CrystEngComm*, 17, 2620-2623.
2. Voskanyan, A. A., Chan, K.Y., Li, C.Y.V. (2016) Towards mass production of uniform crystalline mesoporous CeO_2 catalyst with tailored porosity *J. Am. Chem. Soc.* Submitted.

Ultrasonic Spray Coating as a scale-up technique for the deposition of hybrid magnetic-plasmonic nanocomposites

Jeroen Stryckers^{1,2}, Tom Swusten³, Ward Brulot³, Jan D'Haen^{1,2}, Thierry Verbiest³ and Wim. Deferme^{1,4}

¹ Institute for Materials Research (IMO-IMOMEC), Hasselt University, Diepenbeek, Belgium

² IMEC vzw – Division IMOMEC, Wetenschapspark 1, B-3590 Diepenbeek, Belgium

³ Laboratory for Molecular Electronics and Photonics, KU Leuven

⁴ Flanders Make vzw, Oude Diestersebaan 133, B-3920 Lommel, Belgium

Abstract:

Ultrasonic spray coating is presented as a stable and linear mass production compatible method to deposit gold and iron oxide nanoparticles towards magneto-optic applications. In a first step, gold nanoparticles, having a diameter around 10nm, were deposited from a water-based ink using the ultrasonic spray coating technique. Layer formation, covering rate (see figure 1) and absorbance are compared with state-of-the-art layer-by-layer deposition.

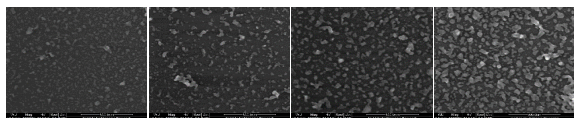


Figure 1: Covering rate of Au nanoparticles deposited by ultrasonic spray coating showing a growing covering rate as the amount of layers is augmented.

In a next step, superparamagnetic iron oxide nanoparticles, having also a diameter of 10nm, synthesized using a modified forced hydrolysis method were functionalized with six different molecules, precipitated and dried. Dispersed in a single solvent ink, dependent on their functionalization, they were ultrasonically spray coated in ambient conditions. These layers were deposited as a single layer or as part of a hybrid gold-magnetite nanocomposite stack. Optical and magneto-optical properties of single and hybrid layers with increasing thickness were studied and their properties are compared with identical layers deposited using layer-by-layer deposition, as seen in figure 2.

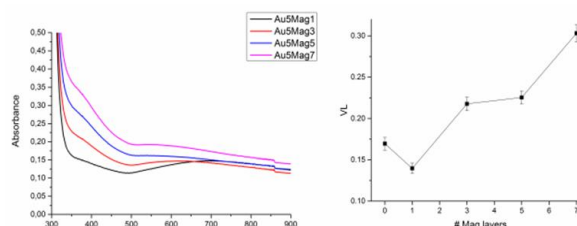


Figure 2: (left) UV-VIS spectra of respectively 1, 3, 5, 7 layers of Magnetite deposited on top of 5 layers of gold. (right) Faraday rotation of the layers, 0 corresponds with only 5 layers of gold nanoparticles

It is shown in this work that, in comparison with the layer-by-layer deposition, coverage of the substrates can be tuned extremely precise by the ultrasonic spray coating technique, which opens new and innovative applications with improved properties for these magnetic-plasmonic nanocomposites.

Keywords: ultrasonic spray coating, magnetic-plasmonic nanocomposites, Faraday rotation

The Development and Application of Vacuum-interconnected Technology for Nano-fabrications

S. A. Ding and H. Yang

SuZhou Institute of Nano-Tech and Nano-Bionics, Chinese Academy of Sciences, SuZhou, China

Abstract:

From microelectronics to nano-electronics, the surface and interface properties of materials and devices are more and more important, comparing to the bulk properties. Manufacturing under ultra-clean rooms eventually could not prevent contaminations from O_2 , C, and H_2O -vapor, during wafer transferring through air, which are very critical to improving the nano-devices performance and reliability. For example, the two major challenges of GaN-based HEMT power devices are off-current leaking and dynamic-current collapse, and the root causes are believe to be related to the interfacial defects or impurities. The best solution of eliminating these unfavorable issues is to process the wafers in a well-controlled environment, without exposure wafers to air during the whole process flow. At present, a vacuum-interconnected R&D facility is being built at Suzhou Institute of Nano-tech and Nano-bionics, CAS, which links more than 30 processing and characterization tools through UHV tubes with a diameter of 150 millimeters and total length of 100 meters. Therefore, it is possible to integrate critical processes together under a vacuum environment, and avoid any uncontrollable contaminations on wafer surfaces during wafer transfer between processing steps. This newly developed technology will not only largely reduce the process steps but also greatly enhance the device performance. In additional, there are also in-line characterization and analytical tools connected to the system, which are very necessary and useful to study the material intrinsic properties and processing mechanisms. This talk will focus on the advantages of vacuum-interconnected technology and its applications on researches, developing and fabrications of advanced III-V semiconductor nano-devices.

Keywords: Nano-electronics, Nano-devices, vacuum-interconnected-system, in-line processing and characterization, III-V semiconductors

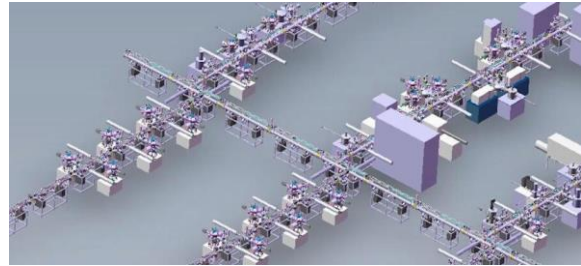


Figure 1: The effect drawing of the vacuum-interconnected R&D facility, which is under construction in Suzhou, China. There are three major functional platforms-material growth, characterization, and device processing-linked together through 100m UHV tubes for wafer transfer.



Figure 2: Picture of a corner of the vacuum-interconnected facility. Wafers could be transferred quickly by using automatically controlled cars in UHV tubes (pressure $< 5 \times 10^{-8}$ Pa) between processing tools, avoiding any uncontrollable contaminations in air.

Functionalization of single wall carbon nanotube for cesium sorption

H. Draouil^{1,2,3,4}, L. Alvarez², J. Cambedouzou³, M. A. Zaibi^{4,5}, J.-L. Bantignies²

¹Unité Nanomatériaux et Photonique - Faculté des Sciences de Tunis, Tunisie

²Laboratoire Charles Coulomb - Université de Montpellier, France

³Institut de Chimie Séparative de Marcoule, UMR 5257 CEA/CNRS/UM/ENSCM, F-30207 Bagnols sur Cèze, France.

⁴Ecole Nationale Supérieure d'Ingénieurs de Tunis-Université de Tunis-Tunisie

⁵Laboratoire LANSER Borj-Cédria Hamm-Lif, Tunisia

Abstract:

During nuclear accidents, several radioactive effluents are released in the environment. Therefore, effluents of low and medium activity are disseminated in the sea or the atmosphere, including amounts of cesium.

The major challenge of the radioactive decontamination is to achieve this process by generating a minimum quantity of waste and secondary effluents. The solid-liquid extraction can be an interesting option [1].

In this work, we used carbon nanostructures including carbon nanotube for the decontamination of effluents containing cesium. We operated surface modifications of these structures by functionalizing them with hexaferrocyanate nanoparticles. This functionalization is done in two steps. Firstly, an amine function is grafted onto the nanotube surface, and secondly hexaferrocyanure is grown from the supported amines.

Using different techniques of characterization, involving Raman spectroscopy, X-ray photoemission spectroscopy and thermogravimetric analysis, we discuss hexaferrocyanate grafting on the surface of carbon supports [2-4]. We are now working on the quantification of cesium extraction by these hybrid systems, and we compare their efficiency with regards to ungrafted nanotubes (see Figure 1).

Keywords: carbon nanostructure, single wall carbon nanotube, cesium, sorption, Raman spectroscopy, X-Ray Photoemission spectroscopy

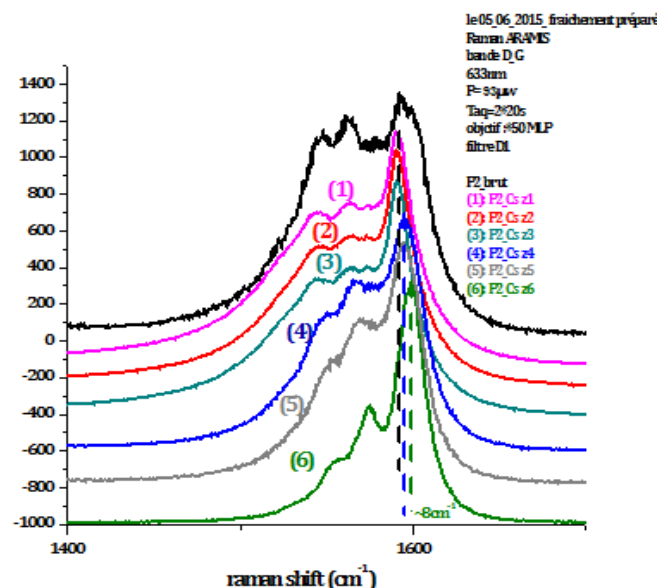


Figure 1: Figure illustrating Raman spectroscopy analyzes of longitudinal modes for raw nanotubes and nanotubes exposed to cesium.

References:

1. H. Kaper, J. Nicolle, J. Cambedouzou, A. Granjean, Mater. Chem. Phys., 147, 147-154 (2014)
2. Itzel J. Ramirez-Calera, Victor Meza-Laguna, Taras Yu. Gromovoy, Ma. Isabel. Chavez-Uribe, Vladimir Hanpei Yang, Sha Wu, Yunping Duan, Xiaofei Fu, Junming Wu, 258, 3012-3018 (2012)
3. Y. Yamada, H. Yasuda, K. Murota, M. Nakamura, T. Sodesawa, S. Sato, J Mater Sci, 48, 8171-8198, (2013)
4. Laurent Alvarez, Fallou Fall, Anouar Belhboub, Rozenn Le Parc, Yann Almadori, Raul Arenal, Raymond Aznar, Philippe Dieudonné-George, Patrick Hermet, Abdelali Rahmani, Bruno Jousselme, Stéphane Campidelli, Julien Cambedouzou, Takeshi Saito and Jean-Louis Bantignies, Phys. Chem. C, 119 (9), 5203-5210, (2015)

Development of a new direct liquid injection system for nanoparticle deposition by chemical vapor deposition using nanoparticle solutions

M.Vervaele^{1*}, B. De Roo¹, M.Rajala², H.Guillon³, J.W.Seo⁴ and J.P.Locquet¹

¹KU Leuven., Department of Physics and Astronomy, Heverlee, Belgium

²DCA Instruments, Turku, Finland

³Kemstream, Montpellier, France

⁴KU Leuven., Department of Materials Engineering, Heverlee, Belgium

Abstract:

Nanoparticles of different materials are already used in many applications. In some applications these nanoparticles need to be deposited on a substrate in a fast and reproducible way. We have developed a new direct liquid injection system for nanoparticle deposition by chemical vapor deposition using a liquid nanoparticle precursor. The system is designed to deposit nanoparticles in a controlled and reproducible way by using two direct liquid injectors to deliver nanoparticles to the system. To allow injection and evaporation of the liquid, a direct liquid injection and vaporization system is mounted on top of the process chamber. The nanoparticle solution is first evaporated after which the nanoparticles flow onto a substrate inside the vacuum chamber. The deposition of the nanoparticles is controlled by parameters such as deposition temperature, partial pressure of the gases and flow rate of the nanoparticle suspension. The concentration of the deposited nanoparticles can be varied simply by changing the flow rate and deposition time.

A big advantage of this technique is the wide range of films that can be produced by varying the precursors and nanoparticles used. Perhaps more important is the general applicability; chemical vapor deposition is already widely used in the glazing and microelectronics industries, hence this approach could be easily integrated into the design of useful products and devices.

Keywords: nanoparticle vapor deposition, direct liquid injection chemical vapor deposition, nanoparticle precursors

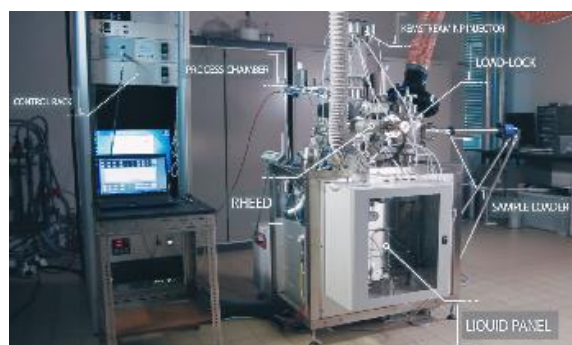


Figure 1: Illustration of the new direct liquid injection system for nanoparticle deposition by chemical vapor deposition using a liquid nanoparticle precursor.

References:

1. Vervaele *et al.* (2016), Development of a new direct liquid injection system for nanoparticle deposition by chemical vapor deposition using nanoparticle solutions, Review of scientific instruments, Accepted
2. De Roo *et al.* (2016), Development of a fluorescence based flux sensor for thin film growth and nanoparticle deposition, Submitted

Composite production for Cold Gas Spray and photocatalytic behavior of the multifunctional coatings

S. Dosta, M. Robotti, I. G. Cano, N. Cinca, A. Concustell, J. M. Guilemany

Thermal Spray Centre, CPT, University of Barcelona. Departament de Ciència dels Materials i Enginyeria Metal·lúrgica, Martí i Franquès 1, E-08028, Barcelona, Spain.

Contact details: sdosta@cptub.eu - (+34) 934034449

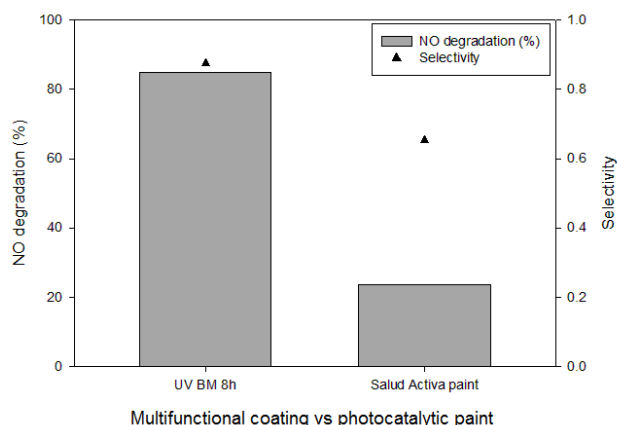
Abstract:

Cold Gas Spray (CGS) deposition of ceramic nano-particles represents nowadays a very innovative trend. In this work, titanium dioxide TiO_2 nanoparticles were mixed with a ductile material in order to obtain a tailor-made nanocomposite feedstock, using different mixing techniques. Mechanical union of TiO_2 nanoparticles around polymeric microparticles was investigated, as well as their influence on structure and morphology. The best mixtures were selected in order to be sprayed by CGS. Adequate spraying deposition parameters were chosen in order to develop well-bonded coatings onto various substrates and enhance the desired properties of the products. Feedstocks and coatings were characterized by Optical Microscopy (OM) and Scanning Electron Microscopy (SEM).

Multifunctional properties given by titanium dioxide nanoparticles, such as air purification, NO_x abatement, self-cleaning and photocatalysis were measured.

Furthermore, manufactured coatings were compared with a commercial photocatalytic paint, giving improved results such as higher NO_x degradation.

Keywords: Titanium dioxide, ceramic polymeric nanocomposite, Cold Gas Spray, multifunctional coatings, photocatalysis.



Application of Spark discharge method for in situ synthesis of copper nano particles on cotton fabrics

Sheila Shahidi^{1,*}, Amir Jamali², Sanaz Dalal Sharifi³ and Hamid Ghomi²

¹ Young Researchers and Elite Club, Arak Branch, Islamic Azad University, Arak, Iran,

sh-shahidi@iau-arak.ac.ir

² Laser and Plasma Research Institute, Shahid Beheshti University, 1983963113 Evin, Tehran, Iran

³ Department of Textile, Science and Research Branch, Islamic Azad University, Tehran, Iran

Abstract:

Nano particles with special properties such as copper nano particles have been widely surveyed in diverse scientific fields. The properties of nano particles are very widespread, for example, can be easily altered by varying their size, shape, and chemical environment. Also individuals' interests have increased in developing nanoparticles on fabrics to their potential in various applications such as medical clothes, wound dressings, healthcare (including disposable) appliances, protective garments, veterinary, and military among others. Recently there has been increased attention paid to the in situ synthesis of nano particles in textile fabrics. One of the methods for nano particles synthesis is spark-discharge method (SDM) in liquid that is a useful way for synthesis of nano particles. Unlike conventional methods for metal nano particles synthesis, SDM method does not require application of chemical surfactants and stabilizers. SDM is an attractive method to manufacture fine powder at low temperature and offers a simple, non toxic, and low-cost alternative to conventional techniques.

In this research, the SDM method was used for in situ synthesis of copper nano particles on cotton fabrics for producing antibacterial textile. The schematic of system is shown in Figure 1. A variety of analytical techniques were applied for the characterization of both Cu Nano particles and synthesized Cu NPs on cotton fabrics. The structural characterization of the particles was carried out by the X-ray powder diffraction (XRD) method. Also the morphological properties of treated cotton samples were investigated using Scanning electron microscope. Particle size and size distribution were measured by dynamic light scattering (DLS) apparatus. The results show that, concentration of 100 ppm is enough for killing 10^7 CFU/ml of bacteria. It is indicated that the synthesised Cu- NPs are very strong against S-Aureus. Also the durability of

antibacterial efficiency after 15 times of washing was tested. The results confirm that, the antibacterial fastness properties are significant and no colonies spread over agar plate after 15 cycles of washing.

It was concluded that, SDM for in situ synthesis of nano Cu on cotton fabrics in batch systems is very promising method.

Keywords: Antibacterial Textile, Spark Discharge Method, Cotton, Copper nano particles

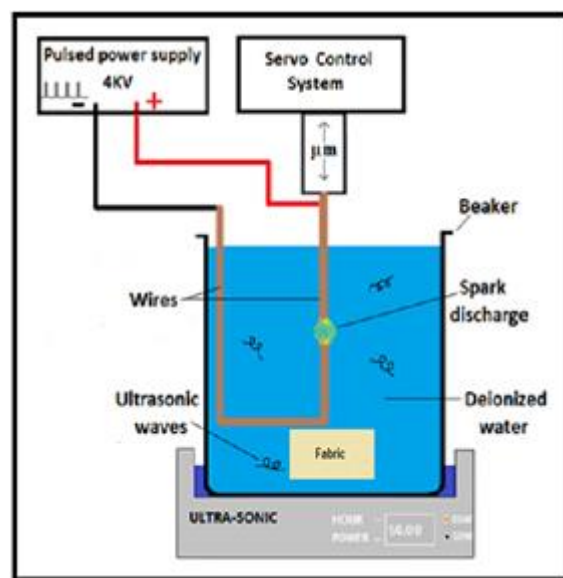


Figure 1: The schematic of Spark Discharge Method for insitu synthesise of copper nano particles on cotton fabrics

Microwave Assisted Synthesized ZnO nanorods arrays on Tetrapak Substrate

A. Pimentel^{1*}, B. Coelho¹, S. Ferreira¹, A. Araújo¹, D. Nunes¹, M. Oliveira², R. Franco², H. Águas¹, R. Martins¹, E. Fortunato^{1*}

¹ CENIMAT/I3N, Departamento de Ciência dos Materiais, Faculdade de Ciências e Tecnologia, Universidade Nova de Lisboa, 2829-516 Caparica, Portugal

² REQUIMTE/CQFB, Departamento de Química, Faculdade de Ciências e Tecnologia, Universidade Nova de Lisboa, 2829-516 Caparica, Portugal

Abstract: An intense effort has been made recently in scientific community for the use of cost-efficient substrates in several applications such as low-cost platform for medical paper diagnostics, analysis and/or quality control devices (Araújo *et al.*; 2014).

Zinc Oxide (ZnO) is an n-type semiconductor with a wide and direct band gap of about 3.37 eV and a large free exciton binding energy of 60 meV at room temperature which allows it to act as an efficient semiconductor material. The physical and chemical properties of ZnO nanomaterials vary as a function of size, shape, morphology and crystalline structures. Many efforts have been devoted to the development of the shape and size of nanostructures. Different techniques, precursors and solvents can be used to prepare a variety of nanostructures. Thus, new synthesis strategies are vital for the development of novel nanomaterials (Pimentel *et al.*, 2015).

Conventional heating is known to be inefficient and time and energy consuming. Microwave irradiation is relatively cheap due to its unique features such as short reaction time, enhanced reaction selectivity, energy saving, homogeneous volumetric heating and high reaction rate.

In the present work, a cardboard substrate (tetrapak) is used to grow ZnO nanostructures. This cardboard substrate is cost-efficient, highly sensitive and amiable to several different environments and target analytes. It is extremely robust when compared to common paper. Moreover, ZnO nanostructures with hexagonal structure were synthesized by hydrothermal method assisted by microwave radiation on tetrapak substrate. The effect of time and temperature on ZnO synthesis was compared. The ZnO synthesis time was varied from 5 min to 30 min and the synthesis temperature changed from 70 °C to 120 °C. We will present scanning electron microscopy (SEM) and X-Ray diffraction (XRD) measurements and optical characterization of samples

synthesized with different temperatures and growth time.

By using ZnO nanorods on cardboard substrate, we will demonstrate the feasibility of nanoplasmonic cardboard substrates for reproducible and stable SERS substrates with a tunable visible resonance.

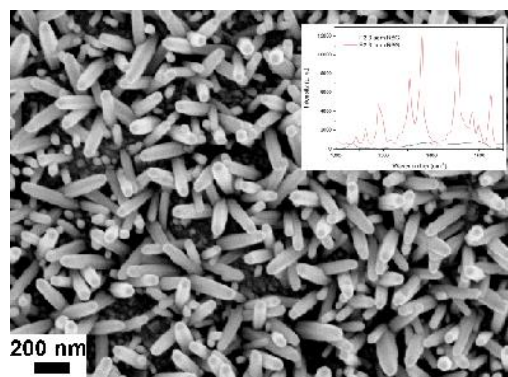


Figure 1: SEM image of ZnO nanorods synthesized by hydrothermal method assisted by microwave radiation on tetrapak substrate. The inset shows the SERS signal of the produced ZnO nanorods.

Keywords: Zinc Oxide, Tetrapak, Microwave synthesis, SERS

References:

1. Araújo, A., Caro, C., Mendes, M. Nunes, D., Fortunato, E., Franco, R., Águas, H., Martins, R. (2014) Highly efficient nanoplasmonic SERS on cardboard packing substrates, *Nanotechnology*, 25, 415202 - 415211.
2. Pimentel, A., Rodrigues, J., Duarte, P., Nunes, D. Costa, F.M., Monteiro, T., Martins, R., Fortunato, E. (2015) Effect of solvents on ZnO nanostructures synthesized by solvothermal method assisted by microwave radiation – a photocatalytic study, *J. Of Mater. Scienc.* 50, 5777-5787.

Fabrication of Metal Nanotubes via Short-Circuit Diffusion Process and The Diffusion Model

S. Baylan,^{1,*} E. Rabkin,² G. Richter¹

¹Max Planck Institute for Intelligent Systems, Stuttgart, Germany

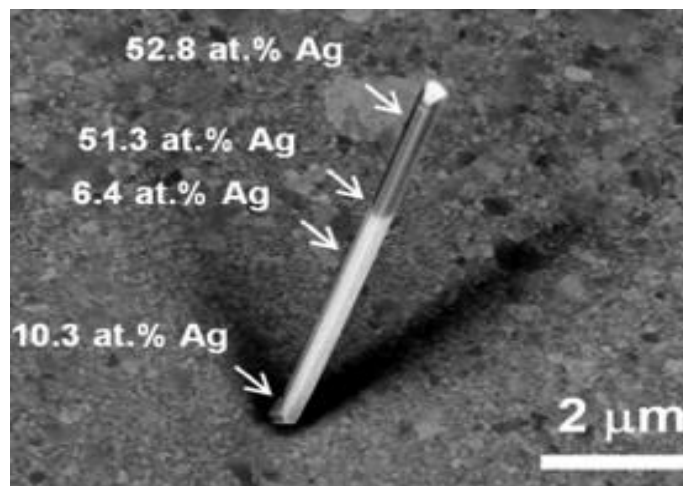
²Technion, Material Science and Engineering, Haifa, Israel

Abstract:

Hollow metal nanostructures are of great interest because of their unique plasmonic, catalytic and magnetic properties and their usage in the field of nanotechnology. Various methods have been applied to produce nanostructures mostly based on the template approach, which often result in polycrystalline nanostructures with a high concentration of impurities and defects. The process of pores nucleation and growth is difficult to control and their size and shape are limited since they are greatly dependent on the template. Thus, it becomes an important issue to produce these structures. Therefore, we introduce a new route to synthesis perfectly single crystalline, defect free and freestanding metal nanotubes (NTs) from a metal nanowhisker (NW) template by the dissolution of the core material by the grain boundary diffusion.

With this aim, single crystalline Ag nanowhiskers (diameter: 100-150 nm and length: 4-30 μm) were synthesized on a carbon-coated Si/SiO₂/Si₃N₄ substrate by molecular beam epitaxy. Different materials (Au, Pd, Co) were grown as shell on the Ag NWs to produce core-shell nanowhiskers. The metal nanotubes (Au, Pd and Co) were obtained via annealing of these core-shell structures. After the fabrication of the metal nanotubes, the kinetic study was done and a diffusion model was formulated. The kinetic study showed the relationship between the time for the formation of hollowing and the size of the nanowhisker. The diffusion model can be used for different material systems of similar micro-structure.

The method which was used to fabricate single crystalline free standing metal nanotubes (Au, Pd and Co) via short-circuit diffusion process can be used as an alternative new route and might help to find a new application areas in addition to the potential applications because of the micro-structure improvements.



Keywords: metal nanotubes, core-shell, diffusion, molecular beam epitaxy, Ag, Au, Pd, Co.

Figure 1: Typical SEM image of Au nanotube. Figure illustrates the hollowing process on the Ag-Au core shell structures.

References:

1. Baylan, S.; Richter, G.; Beregovsky, M.; Amram, D.; Rabkin, E., The kinetics of hollowing of Ag-Au core-shell nanowhiskers controlled by short-circuit diffusion. *Acta Materialia*. **2014**, 82, 145-154.

Design and characterization of nanowired microwave devices in substrate integrated waveguide technology

V. Van Kerckhoven,^{1,2,*} L. Piraux,¹ I. Huynen²

¹ Institute of Condensed Matter and Nanosciences (IMCN), Université catholique de Louvain
Louvain-La-Neuve, Belgium

² Institute of Information and Communication Technologies, Electronics and Applied Mathematics (ICTEAM), Université catholique de Louvain, Louvain-La-Neuve, Belgium

Abstract:

We propose a new way to design and fabricate microwave devices combining the technology of metallic nanowires aligned in a nanoporous medium and that of substrate integrated waveguides. Our approach paves the way for a new architecture of nanowired microwave devices offering immunity to radiation losses, excellent temperature stability and increased miniaturization compatible with high-frequency monolithic integrated circuits technology. The basic studied structure is a substrate integrated waveguide (SIW) in which the vertical walls consist of nanowires arrays (Figure 1). The electrodeposited nanowires are embedded in porous alumina template on silicon substrate to guarantee compatibility with electronic standards. Exploiting the specific permittivity and permeability of nanowires arrays, the waveguide can be modified to achieve different types of microwave devices. This is done by properly placing nanowires arrays in the SIW and exploiting effects like electromagnetic band-gap (Figure 2) or ferromagnetic resonance to control microwave propagation. A laser-assisted process was developed to produce patterned growth of vertically aligned nanowire arrays for monolithic microwave integrated devices. A precise control is achieved thanks to the versatility and selectivity of electro-deposition process and fine positioning of multiple nanowires arrays.

This new fabrication strategy has proven its efficiency for the realisation of compact planar integrated circuits such as filters, couplers, antennas, phase shifters, isolators, ...

Keywords: nanowires, microwave, devices, substrate integrated waveguide, laser, patterning, unreciprocity, ferromagnetic resonance, electromagnetic band-gap.

Figure 1: Schematic view of the studied substrate integrated waveguide and microstrip connections using nanoporous alumina template on

Si. A laser-assisted process is used to produce patterned growth of vertically aligned nanowire arrays in the porous structure.

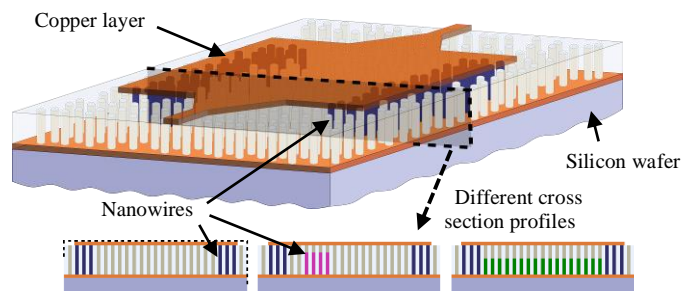
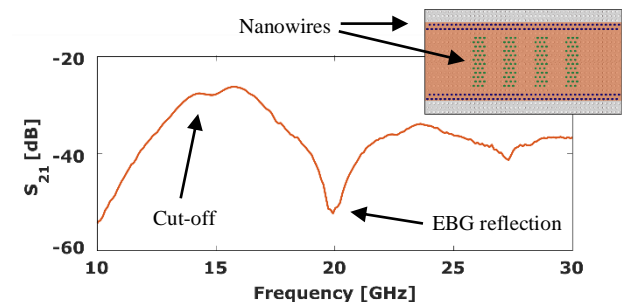


Figure 2: Microwave measurement on SIW electromagnetic band-gap (EBG) filter and schematic top view of the realized device. The four nanowired strips placed along the guide create filtering effect at 20 GHz and cut-off frequency is induced by effective nanowired walls of the SIW.



References:

- Van Kerckhoven, V., Piraux, L., Huynen, I. (2014) Substrate integrated waveguide isolator based on ferromagnetic nanowires in porous alumina template, *Applied Physics Letters*, 105, 183107
- Hamoir, G., Piraux, L., Huynen, I. (2013) Control of Microwave Circulation Using Unbiased Ferromagnetic Nanowires Arrays, *IEEE Transactions on Magnetics*, 49, 4261-4264
- Saib, A., Huynen, I. (2006) Periodic Metamaterials Combining Ferromagnetic Nanowires and Dielectric Structures for Planar Circuits Applications, *Electromagnetics*, 26, 261-2

G-doping in Thin Si Nano-grating Layers

A. Tavkhelidze¹, L. Jangidze², M. Mebonia^{1,3}, G. Skhiladze², D. Ursutiu⁴, C. Samoila⁴, Z. Taliashvili² and L. Nadaraia⁵

¹ Ilia State University, Cholokashvili Ave. 3-5, 0162 Tbilisi, Georgia

² Institute of Micro and Nano Electronics, Chavchavadze Ave. 13, 0179 Tbilisi, Georgia

³ Semiconductor Nanoelectronics, Peter Grünberg Institut PGI, Forschungszentrum Jülich GmbH, D-52425 Jülich, Germany

⁴ Transilvania University of Brasov, Faculty of Electrical Engineering and Computer Science, Electronics and Computer Department, 1 Politehnicii, 500024 Brasov, Romania

⁵ Georgian Technical University, 77 Kostava Str., Tbilisi 0175, Georgia

Abstract:

Recently, new quantum effects have been studied in thin nano-grating layers. Nano-grating (NG) dramatically changes electronic, thermoelectric and electron emission properties, when grating pitch size becomes comparable with the electron's de Broglie wavelength. This is due to the special boundary conditions imposed by NG on the electron wave function. Supplementary boundary conditions forbid some quantum states, and the density of quantum states is reduced (in all bands). Electrons rejected from the valence band occupy empty quantum states in the conduction band. Electron concentration n in the conduction band increases, which was termed as geometry-induced doping or G-doping.

Nanostructures were fabricated with laser interference lithography, using blue-violet semiconductor laser with 375 nm wavelength. Nanostructures were investigated on 70 nm thin device layer of Silicon on insulator (SOI) wafer. Both 4-wire Van der Pauw (4W) and 2-wire methods (2W) were used for I-V characteristics, as along (R_{\parallel}) as across (R_{\perp}) the grating direction with and without temperature gradient.

It was observed that nanograting reduces resistivity of Si layer from ≈ 10 Ohm cm (plain layer) to 5×10^{-2} - 8×10^{-3} Ohm cm. This reduction is in agreement with theoretical prediction of G-doping in nano-grating layers. Value 10^{-2} Ohm cm corresponds to "impurity" concentration of $3 \times 10^{-2} \text{ cm}^{-3}$ (Phosphorous in Si). Both I-V characteristics were linear indicating good quality of ohmic contacts. Most samples show resistivity anisotropy which varied in the range of 0.2–1. Resistivity temperature dependence matches G-doping theory. G-doping does not require ionized impurities. This allows high carrier mobility and temperature independent carrier concentration. This technology can be used for solar cells and other

photovoltaic devices, ultra-high frequency electronics, and power electronics.

Keywords: Nanostructuring, nano-grating, interference lithography, doping

References:

1. Tavkhelidze, Geometry-induced electron doping in periodic semiconductor nanostructures, *Physica E*, v. 60, pp. 4-10 (2014).
2. D. Kakulia, A. Tavkhelidze, V. Gogoberidze, M. Mebonia, Density of quantum states in quasi-1D layers, *Physica E: Low-dimensional Systems and Nanostructures*, 78, Pages 49-55 (2016).
3. A. Tavkhelidze, Large enhancement of the thermoelectric figure of merit in a ridged quantum well, *Nanotechnology*, 20, 405401 (2009).
4. A. N. Tavkhelidze, Nanostructured electrodes for thermionic and thermo-tunnel devices, *J. Appl. Phys.* 108, 044313 (2010).

Nanotech France 2016 Session II

Nanomaterials Synthesis and properties

Surface-Engineered Mechanically Hard Tungsten Disulfide (WS₂) Inorganic Nanotubes (INTs-WS₂)– Novel Chemically Taylored Nanoscale CNT-Replacement Inorganic “Nanofillers”

J.-P. Lellouche,^{1*} D. Raichman, & J. Laloy²

¹ Department of Chemistry & Institute of Nanotechnology & Advanced Materials (BINA), Bar-Ilan University, 5290002 Ramat-Gan, Israel

² Namur Nanosafety Centre, Dpt of Pharmacy, Namur University, Belgium

Abstract:

An innovative method of surface functionalization (*polycarboxylation* – *polyCOOH shell formation*) of hydrophobic tungsten disulfide (WS₂) multi-walled inorganic nanotubes (INTs-WS₂) has been successfully developed and optimized (DoE - Statistical Design Of Experiments methods) using *N*-based electrophilic species (*imminium salt chemistry*). This sidewall polyCOOH-enabling functionalization showed extreme COOH-based chemical versatility for innovative interfacial chemistries. Indeed and for example, it enabled the effective fabrication of a wide range of *covalent* WS₂-INTs surface modifications (**polyNH₂**, **polyOH**, **polySH** as 1st series examples) *via* (i) polyCOOH chemical activation (EDC, CDI) and (ii) 2nd step covalent nucleophilic substitutions by short ω -aminated ligands H₂N-linker-**X** (**X** outer surface functionality).

Resulting fully characterized functional WS₂ INTs (*f*-INTs-WS₂) have a quite wide potential for use as novel functional nanoscale fillers toward new mechanically strengthened and/or conductive composite polymeric matrices (case of hybrid polythiophene-decorated *f*-INTs-WS₂ nanocomposites, Figure 1). Corresponding novel functional nanomaterials/“nanoscale fillers” have been also shown to be non-toxic in preliminary toxicity studies, which opens a wide R&D route/progress for relating end-user applications.

Keywords: Transition metal dichalcogenide nanomaterials, surface engineering of nanomaterials, Vilsmeier-Haack complexes, DoE global optimization, functional inorganic tungsten disulfide nanotubes, hybrid conductive nanomaterials

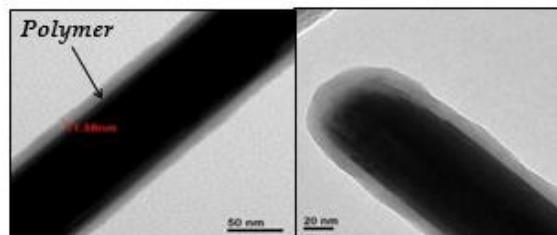


Figure 1: Highly conformal oxidative generation of a conductive functional (*polyCOOH*) polythiophene-based organic shell onto inorganic WS₂-INTs nanotubes

References:

1. Raichman, D., Strawser, D., Lellouche, J.-P. (2014), Design of Experiments: Optimizing the Polycarboxylation/functionalization of Tungsten Disulfide Nanotubes, *Inorganics*, 2(3), 455-467.
2. Raichman, D., Strawser, D., Lellouche, J.-P. (2015), Covalent Functionalization/Polycarboxylation of Tungsten Disulfide Inorganic Nanotubes (INTs-WS₂), *Nano Research*, 8(5), 1454-1463.
3. Lellouche, J.-P., Sade, H., Ben-Ishay, R., Ben Shabat Binyamini, R., Raichman, D., Harel, Y., (2015 registration), Metal Chalcogenide Nanostructures, US Provisional Patent Application n° 62/266,627.

Reinforcing Acrylonitrile Rubber With Graphene: Inspection of Mechanical, Thermal and Cure Kinetics Properties

B. Mensah¹ and C. Nah¹

¹BK21 Plus Haptic Polymer Composites Reserch Team and Department of Polymer-Nano Science and Technology, Chonbuk National University, South Korea

Abstract:

Since the discovery of graphene (G) by (Novoselov *et al.*; 2004), a great deal of interest has been focused on its incorporation into polymer materials aiming to the preparation of G-based polymer nanocomposites. Currently, there are few literatures on G or derivative G (GRD) based elastomeric nanocomposites because of the difficulties in attaining proper dispersion, by avoiding re-agglomeration tendency of the GRD sheets. Furthermore, the reinforcement behavior of GO and G in a typical polymeric matrix is still not well understood. We report here a comparative study of G and graphene oxide (GO) nanoparticles synthesized via modified Hummer's route (Hummers *et al.*;1985). We assess the quality of the nanoparticles (GO and G) by techniques such as; X-ray photoelectron spectroscopy, Raman spectroscopy, Fourier tranform infrared, and transmission electron microscopy etc. We prepare a nanocomposite of NBR-GO and NBR-G by solution mixing method and study their physical properties. Major properties considered include mechanical properties, thermal stability, and cure kinetics. We observe that the NBR-nanocomposites are generally found to show improved mechanical and thermal stability properties but exhibit inferior cure kinetics behavior by comparison. The observed enhancement are attributed to the better dispersion of fillers within NBR matrix, confirmed by SEM and TEM observations as well as the strong hydrogen bonds between the nitrile units of NBR molecules and the oxygenated functional groups (eg. OH-, and -COOH) on graphene sheets (see Figure 1). However, in view of cure kinetics, the poorer curing behavior may be attributed to absorption of cure ingredient and perhaps the numerous reaction mechanism ensued during vulcanization of the composites (Mathew *et al.*;2008). With proper modification techniques of GRD, and composites preparation, Elastomeric-GRD based nanocomposites could serve as

green material for various applications in rubber nanotechnology industry.

Keywords: graphene, graphene oxide, acrylonitrile-butadiene rubber, cure kinetics, dispersion, modulus.

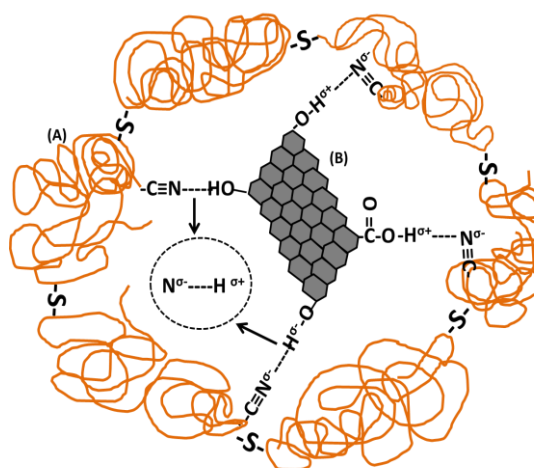


Figure 1: A schematic representation of the reaction between G(A) with a rubber molecule (B)

References:

- Novoselov, K. S., Geim, A. K., Morozov S. V., Jiang D, Zhang, Y., Dubonos, S. V., Grigorieva, IV., Firsov, A. A. (2004) Electric field effect in atomically thin carbon films. *Science*, 306, 666-669,.
- Hummers W.S., Offeman RE. (1958) PREPARATION OF GRAPHITIC OXIDE. *J Am Chem Soc*, 80, 1339-1339.
- Mathew, G., Rhee, J. M., Lee, Y. S., Park, D. H., Nah, C. (2008). Cure kinetics of ethylene acrylate rubber/clay nanocomposites. *J Ind Eng Chemistry*, 14, 60-65.

Development of Flexural Properties in Woven-fabric/Epoxy Resin CFRP Panels with Additional Nano Rubber Particle Reinforcement

J. Sirichantra,^{1,*} T. Pullawan,¹ P. Lamo,¹ S. Kumwongwian¹

¹Department of Science Service, Ministry of Science and Technology, Bangkok, Thailand

Abstract: Twill woven carbon fibre fabric have been impregnated with the modified epoxy resins with additional nano rubber particles (Narpow[®]UFPR VP-501) in the range of 0 to 1 wt%. The laminates were studied in flexural properties and sectioned subsequently for microstructural damage investigation. In addition, the TEM observation was used to investigate the nano-sized Narpow[®]UFPR VP-501 dispersed in the epoxy resin matrix. The results showed that the panels with modified epoxy resins by adding nano rubber particles up to 1 wt% were developed approximately 16% and 17% in the flexural strength and modulus of elasticity in bending, respectively. For microstructural damage investigation, the cross sections of the specimens with additional 0 and 1 wt% nano rubber particles were examined after the flexural test as shown in Figure 1. It can be seen that for the specimen without nano rubber particle (Figures 1(a)) that substantial delamination of the composite has occurred after the flexural test, whereas less damage is evident in the specimen containing a dispersion of 1 wt% nano rubber particles (Figure 1(b)). This is consistent with a higher resistance to delamination being shown by the specimens additionally reinforced with 1 wt% nano rubber particles after the bending flexural test of the specimen. The observation suggest that the enhanced flexural properties are a consequence of the nano rubber particles producing a reduction in the extent of delamination during bending fracture of the specimens. In addition, the TEM images gave representative shape distributions of the Narpow[®]UFPR VP-501 dispersed in the epoxy resin matrix (Figure 2). The diameter of nano rubber particles ranges from about 50 to 100 nm.

Keywords: carbon fibre fabric, CFRP, nano rubber particle, modified epoxy resin, flexural properties, delamination

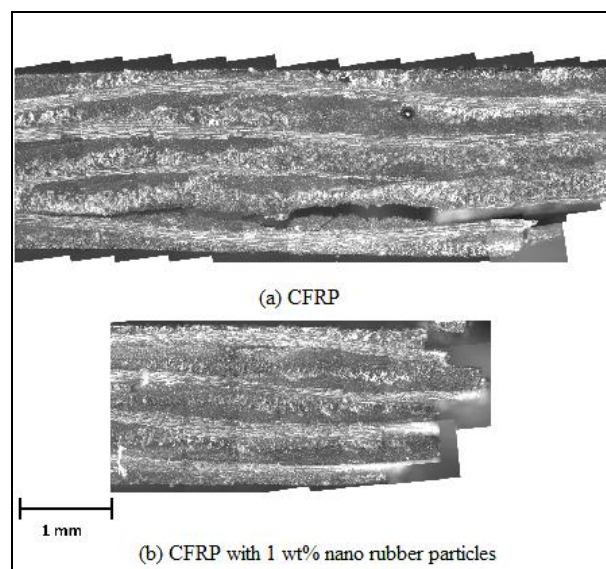


Figure 1: Cross sections of the specimens after the bending flexural test for Narpow[®]UFPR VP-501 additions (a) 0 wt%, (b) 1 wt%

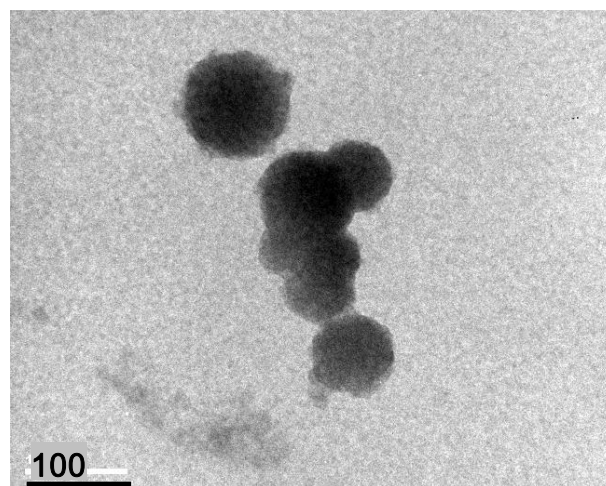


Figure 2: TEM images of the round shape distributions of the Narpow[®]UFPR VP-501 dispersed in the epoxy resin matrix

The effect of dispersion method and processing condition on the structure properties of polystyrene/graphene oxide nanocomposites

Z. Mohammadsalih, B.J. Inkson, B. Chen

Department of Materials Science and Engineering, University of Sheffield, Mappin Street, Sheffield, UK

Abstract:

The homogeneous dispersion of graphene sheets in the polymer matrix can be considered as one of the major challenges to prepare high performance polymer graphene nanocomposites (Pokharel et al. 2015). Several techniques have been used to ensure a good dispersion of the nanoparticles in the polymer matrix such as sonication and shear mixing (Prolongo et al. 2008). Using a suitable organic or aqueous medium represents another important factor to ensure a good dispersion of graphene nanosheets (Johnson et al. 2015). In this study, polystyrene (PS) was reinforced with 0.5 wt.% of graphene oxide (GO) and polymer nanocomposites (PNCs) of PS and GO were prepared using solution blending methods (Figure 1). Two different solvents were used to prepare the PNCs which were dimethylformamide (DMF) and tetrahydrofuran (THF). Magnetic stirring and water bath sonication were employed to prepare the first set of PS-GO nanocomposite samples using DMF. In the second set of samples THF was used as the solvent instead of DMF and magnetic stirring, water bath sonication and shear mixing were utilised to disperse the nanoparticles in the matrix. Different periods of mixing time were also examined in the last two methods to study their effect on the structure and properties on the resultant nanocomposites. Fourier transform infrared spectroscopy, scanning electron microscopy and atomic force microscopy were used to characterise the structure of GO and PS-GO nanocomposites. Tensile testing, dynamic mechanical analysis (DMA) and thermogravimetric analysis (TGA) were performed to investigate the mechanical and thermal properties of the nanocomposites. The results showed that the use of DMF as the dispersing medium led to the formation of

unstable suspensions and poorly dispersed samples. On the other hand the use of THF resulted in stable suspensions and well-dispersed samples which led to enhanced mechanical properties. The tensile Young's modulus and tensile strength for the PS-GO nanocomposite increased by 29% and 22% respectively as compared with neat PS (dispersed by water bath sonication for 1 h and shear mixing for 2 h). DMA results showed an increase in the storage modulus by 35% under the same mixing conditions. TGA results showed that thermal degradation temperature was increased slightly in the nanocomposite. In conclusion, using synergistic techniques of mixing with a suitable organic solvent led to a relatively good dispersion of graphene nanosheets in polystyrene matrix resulting in improved mechanical properties as compared with neat PS.

Keywords: Polystyrene, graphene oxide, nanocomposite, processing condition, dispersion technique.

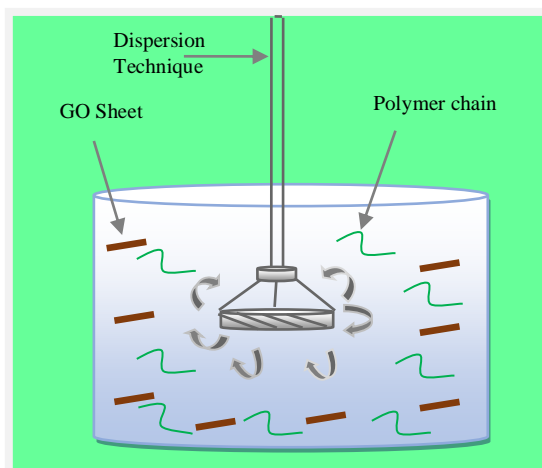


Figure 1: Schematic of GO sheets dispersing in a polymer solution.

Hollow Nanoparticles for Applications in Lightweight Nanocomposites

V. Rodionov,^{1*} T. Sainsbury²

¹KAUST Catalysis Center and Division of Physical Sciences and Engineering, King Abdullah University of Science and Technology, Thuwal, 23955-6900, Kingdom of Saudi Arabia

²National Physical Laboratory, Hampton Road, Teddington, Middlesex, United Kingdom TW11 0LW

Abstract: Materials that are tough, yet light are highly desirable for many defense applications, such as airframes, UAVs/drones, vehicle parts, and body armor. Composite materials, especially fiber-reinforced resins, are a privileged class of materials that combine light weight and extreme mechanical strength.

A variety of substances have been applied as interphase agents between reinforcing fibers and resins in composites (Ajayan *et al.*, 2003; Manias, 2005). SiO₂ nanoparticles are commonly used for improve the compressive properties and stability of composite materials, especially those based on epoxy resins (Bondioli *et al.*, 2005). However, a high weight loading of SiO₂ (> 10 wt.%) is commonly needed. This leads to an undesirable increase in the weight of the composite due to the high density of SiO₂.

A need exists for additives that could improve the mechanical properties of the resin and prevent fiber delamination without penalizing the weight of the composite. We propose to solve the problem by using suitably functionalized hollow silica or organo-silica nanoparticles as interphase agents. These particles are remarkably light, yet they have many of the same beneficial properties as the traditional SiO₂-based interphase agents. Blending in as little as 0.1 wt % of one of our nanoparticle formulations have increased the ultimate strength of common aerospace resins by up to 100%.

This technology offers a drop-in replacement for existing interphase agents in carbon fiber and similar composites. Materials prepared with the use of our hollow-particle interphase agent can be up to 20% lighter than the materials currently on the market. Furthermore, better dispersibility of our interphase agent allows easier curing procedures, and simplifies manufacturing of more complex parts and objects.

Keywords: nanoparticles, structural composites, lightweight materials, epoxy resin, polyurethane.

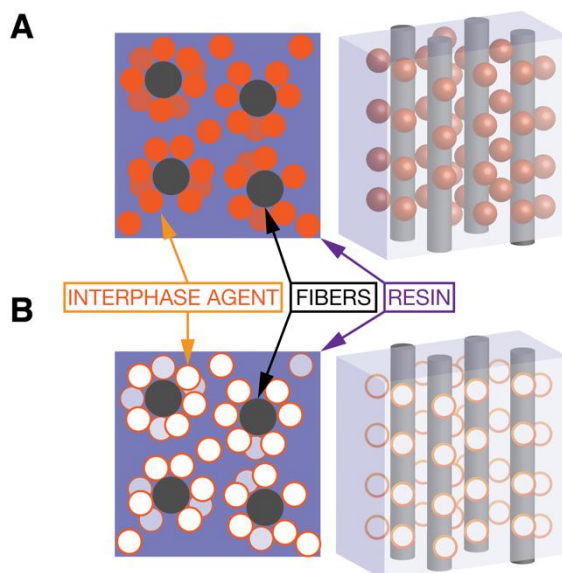


Figure 1: Nanocomposites utilizing a traditional solid-particle (A) and hollow-particle (B) interphase agents. A loading of as low as 0.01 wt % of hollow nanoparticles is sufficient to improve the ultimate strength of an epoxy resin by up to 100%.

References:

1. P.M. Ajayan, L.S. Schadler, P.V. Braun *Nanocomposite science and technology*. Wiley, 2003 (ISBN 3-527-30359-6).
2. F. Bondioli, V. Cannillo, E. Fabbri, M. Messori *J. Appl. Polym. Sci.*, 2005, **97**, 2382-2386.
3. E. Manias *Nature Mat.* 2005, **6** (1), 9–11.

Functionalization and optical properties of inorganic liquid crystals

M. Thiriet, K. Lahlil, J.P. Boilot, J. Peretti, T. Gacoin

Laboratoire de Physique de la Matière Condensée, Ecole Polytechnique-CNRS, 91128 Palaiseau, France

Abstract:

Mineral liquid crystals combine the athermal lyotropic phase behavior with the intrinsic properties of minerals such as large refractive index and dichroism. However, practical use of such systems has long been limited due to the difficulty in synthesis, stabilization, and control of colloidal behavior of anisotropic mineral nanoparticles. We here report on a new mineral liquid crystal system composed of sodium yttrium fluorides (NaYF_4) nanorods. $\text{NaYF}_4:\text{Yb}/\text{Er}$ nanorods with tuned size and aspect ratio were obtained through an optimized hydro-thermal route. Doping the particles with lanthanides like erbium or ytterbium offers a particularly interesting luminescence upconversion. The nanorods have been functionalized with different molecules including phosphonate or carboxylate functions, which react very efficiently to the nanoparticles surface. This grafting, which is very easy to implement, was characterized by NMR and IR. Functionalized nanoparticles allow to obtain very concentrated solutions, showing an outstanding colloidal stability. This stabilization opens a large field of research for studying physical properties coming from the anisotropic shape of the nanoparticles. We can mention the elaboration of thin films of particles aligned in the same direction or their alignment by an electric field. These last electro-optical properties have been investigated, especially the influence of the frequency and the amplitude of the applied electric field, as well as the particles functionalization.

Keywords: Inorganic liquid crystals, hydrothermal synthesis, stabilization by functionalization, electro-optical properties, up-conversion luminescence

References:

1. Kim, J., De la Cotte, A., Deloncle, R., Archambeau, S., Biver, C., Cano, J.-P., Lahlil, K., Boilot, J.-P., Grelet, E., Gacoin, T. (2012), LaPO_4 Mineral Liquid Crystalline Suspensions

with Outstanding Colloidal Stability for Electro-Optical Applications, *Adv. Funct. Mater*, 22, 4949-4956.

2. Thiriet, M., Lahlil, K., Boilot, J.-P., Peretti, J., Gacoin, T. Functionalization and optical properties of NaYF_4 nanorods suspensions, submitted.

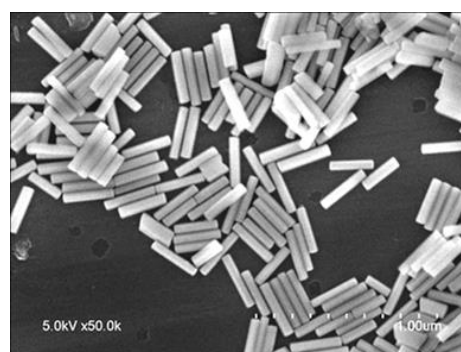


Figure 1: SEM picture of $\text{NaYF}_4:\text{Yb}/\text{Er}$ nanorods

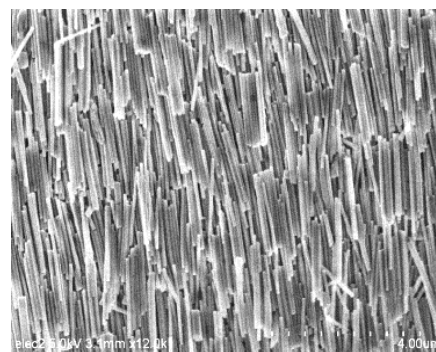


Figure 2: Assembly of nanorods aligned by an electric field



Figure 3: Luminescence by up-conversion for an IR excitation

Chip Calorimetry for Investigating the Co-Detection of Hexogen and Pentrite Vapors by Nanostructured Porous Materials

K. Bonnot,^{1,*} L. Schlur,¹ D. Spitzer¹

¹Nanomatériaux pour les Systèmes Sous Sollicitations Extrêmes (NS3E) UMR 3208
ISL/CNRS/UNISTRA, French German Research Institute of Saint-Louis, 68301 Saint-Louis, France

Abstract: Detecting explosives in air is challenging for homeland security applications due to threatening increased of terrorism explosive bombs against populations. However there is also a crucial need for (i) identifying the threat at the level of traces or sub-traces, and (ii) understanding the competition existing between various threats for their detection and between threats and interferents. We recently developed an innovative technology for identifying explosives at a solid state within few second on femtogramme mass and single microcrystal with nanocalorimetry. (Piazzon et al., 2010)

In a recent published work we have used nanocalorimetry to discriminate between hexogen (RDX) and pentrite (PETN) vapors once adsorbed on porous materials. (Bonnot et al., 2015) Once explosive vapor is trapped in a material, fast heating at 3000 K/s up to 360°C \pm 5°C lead to a thermal pattern which is specific to the explosive and its interaction with the porous material. The obtained signatures permit simultaneously detecting and identifying the vapors in just some few milliseconds. Further investigations on the use of nanocalorimetry for the identification of threats, show that the technique permits to accurately determine the presence or the absence of adsorbed explosive(s) on the porous material when two explosives are present simultaneously in the air. This allowed us to investigate the way PETN and RDX vapors interact with porous material used for their detection when they are both present in air at the same time. Up to now it is the first time that microthermal analysis is used to characterize explosive interactions with porous material, with the aim to detect and identify these explosives when they are present in the air.

Keywords: Explosive identification, nanoporous materials, competitive adsorption, chip-calorimetry, nanocalorimetry.

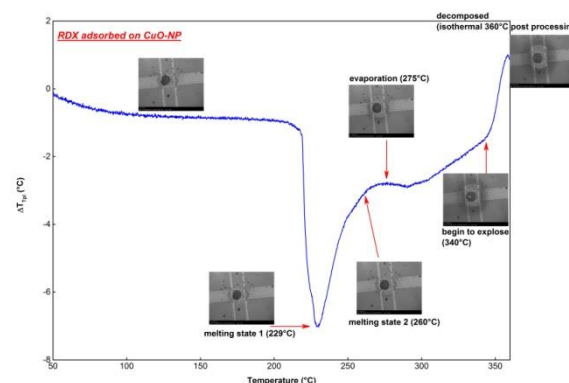


Figure 1: Figure illustrating the thermal pattern recorded when the copper oxide nanoparticles subjected to RDX are heated up to 360°C at a rate of 3000 K/s. at first the RDX desorbs at 229°C from the copper-oxide nanoparticles on which it was adsorbed before decomposing at 260°C inside the porous material.

References:

1. Piazzon, N., Rosenthal, M., Bondar, A., Spitzer, D. and Ivanov, D.A. (2010) Characterization of explosives traces by the nanocalorimetry, *J. Phys. Chem. of Solids*, 71, 114–118
2. Bonnot, K., Doblas, D., Schnell, F., Schlur, L., Spitzer, D. (2015) Chip calorimetry for the sensitive identification of hexogen and pentrite from their decomposition inside copper oxide nanoparticles, *Anal. Chem.*, 87, 9494-9499.

Development of fire retardant treatment with silica nanoparticles to apply onto bio-based composite materials

Marion Bourebrab^{1,2,3*}, Géraldine Durand³, Alan Taylor³, Rory Hadden¹, Luke Bisby¹

¹ BRE Centre for Fire Safety Engineering, Institute of Infrastructure and the Environment, School of Engineering, the University of Edinburgh, UK

² National Structure Integrity Research Centre (NSIRC), Cambridge, UK

³ TWI Ltd., Cambridge, UK * Corresponding author: marion.bourebrab@ed.ac.uk

Abstract: The work carried out is aligned with the European collaborative project ISOBIO, coordinated by TWI Ltd. (UK). This project aims at developing a new approach to fabricate low embodied energy insulating materials made from bio-derived aggregates (e.g. straw or hemp shivs) and binders. Good thermal insulation and humidity buffering are key properties for such materials. In addition, bio-based materials used for construction can be engineered to have desirable fire performance by modification of the materials' properties. However, to reduce the embedded energy in the material and to improve moisture and thermal buffering it is necessary for it to be permeable (breathable). This therefore introduces the need for alternative treatments to provide fire retardancy.

The approach adopted is to develop a halogen-free and phosphorus-free fire retardant to be applied as a surface treatment onto bio-aggregates for use within insulation panels. The materials need to repel liquid water and prevent condensation to minimise issues related to degradation, such as rotting. These target properties, namely hydrophobicity, condensation prevention, breathability, fire retardancy and durability will be achieved with a silica-based treatment.

In fact, silica has been identified in many studies [1] [2] to be good fire retardant when applied on polymers, due to an accumulation of silica at the surface that acts as an insulation barrier [3]. Such characteristics are being evaluated for the natural fibre composite to quantify the impact of silica on fire retardancy properties. The technology considered in this project is based on silica nanoparticles. These nanoparticles are synthesised,

analysed and then functionalised with silanes to confer hydrophobicity to the bio-aggregates and bonding between one another (figure 1). Various parameters are being evaluated in order to design the most appropriate silica nanoparticles for the application, such as the loading of nanoparticles, the functionalisation agents used, their respective ratios and the method of coating.

Keywords: silica nanoparticles, functionalised nanoparticles, surface treatment, bio-materials, insulation, fire retardancy, hydrophobicity.

References:

1. T. Kashiwagi, J.W. Gilman, K.M. Butler, R.H. Harris, J.R. Shields. Flame Retardant Mechanism of Silica Gel/Silica. *Fire and Materials*. 2000, Vol. 24, pp. 277-289.
2. Hshieh, F-Y. Shielding Effects of Silica-ash Layer on the Combustion of Silicones and Their Possible Applications on the Fire Retardancy of Organic Polymers. *Fire and Materials*. 1998, Vol. 22, pp. 69-76.
3. L.A. Lowden, T.R. Richard Hull. Flammability behaviour of wood and a review of the methods for its reduction. *Fire Science Reviews*. 2013, Vol. 2, 4.

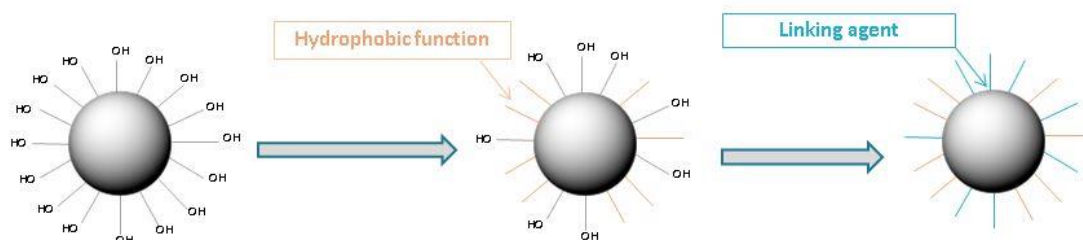


Figure 1: Schematic of the functionalisation process of silica nanoparticles

Resistive sensors from nanoparticle assemblies

L. BAKLOUTI¹, F. FAVIER¹

¹Institut Charles Gerhardt Montpellier, UMR 5253 CNRS, Université de Montpellier Campus Triolet, 34095 Montpellier cedex 05, France.

Abstract:

A gas sensor allows the detection thanks to the specific reactivity of its sensitive material towards the target gas.

The use of resistive sensors is based on measuring the variation of their electrical conductivity when the target gas is in contact with the sensitive material.

In our study, we chose to work with core-shell nanoparticles as sensing materials. The idea consists on decorating spherical gold nanoparticles, insensitive to the target gases, with a shell based on a different material. The latter provides the specific sensitivity to the sensor.

Previous work in our laboratory focused on Au@Pd and Au@Pt nanoparticles as H₂ sensors. The work was extended to other shell materials to examine their sensitivity towards H₂ as well as other target gases including NH₃.

Au@SnO₂ and Au@Ag nanoparticles were synthesized and then assembled by Langmuir Blodgett technique. The assembly resulted in close-packed core-shell nanoparticle layers. These layers were transferred, by simple dip-coating, to a glass slide supporting interdigitated electrodes. Sensing performances of the as fabricated sensors were evaluated.

Au@SnO₂ based sensors were tested under H₂ while Au@Ag based sensors were tested under NH₃. Both sensors showed responses towards the target gases.

Among the main sensor properties requested and studied we note : sensitivity, selectivity, response and recovery times

Langmuir-Blodgett organized assemblies of core-shell nanoparticles showed attractive sensing performances towards H₂ and NH₃ in extended concentration ranges.

Another important contribution concerns the elucidation of the sensing mechanisms

Keywords: resistive sensor, core-shell nanoparticles, Langmuir-Blodgett technique, sensitivity, selectivity.

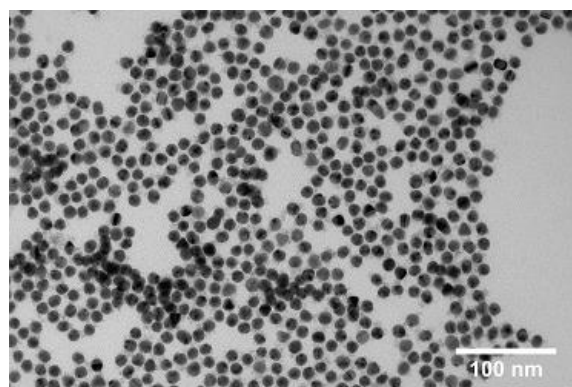


Figure1 TEM images of Au@SnO₂ nanoparticles.

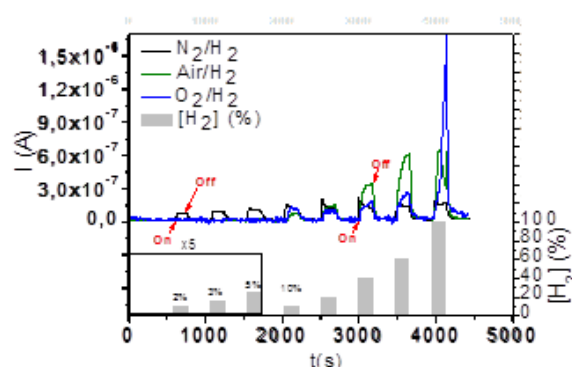


Figure 2 Responses of an Au@SnO₂ NPs based sensor $i=f(t)$ within H₂ concentration in N₂, synthetic air and O₂.

Effect of nano Zinc oxide particles on weathering properties of epoxy coatings

Dolai Shalini,^{1,2,*} A.S.Khanna,^{1,2}

^{1,2} IIT Bombay, Department of Metallurgical Engineering and Material Science, Mumbai, India

Abstract:

The exterior durability of epoxy coatings is poor as they tend to chalking and undergo weathering under sunlight. Even a micro defect in a coating, especially in steel structures, pipe lines, automobiles and airplane components can lead to localized corrosion of the substrate thus leading to catastrophic disasters. Current study involves studying the effect of Nano ZnO (used as a UV blocker) in the epoxy coatings as it is known to improve the weathering properties. In addition to this, Nano ZnO can also improve the mechanical properties and corrosion resistance without affecting the optical clarity of clear epoxy coats. Current study focuses on exploring the additional benefits associated with introducing Nano ZnO into epoxy coatings. Nano ZnO powder was incorporated into the clear epoxy resin and commercial epoxy coat at different loading levels to study its effect on performance, mechanical and optical properties of the coating. Ultra violet weathering tests were done to study their weatherability, an advanced non destructive technology called as Electro chemical impedance spectroscopy (EIS) was used for studying corrosion properties and mechanical tests like tensile testing to study the tensile strength of the coating, taber abrasion to study the wear resistance, pull off adhesion and hardness tests were carried to evaluate the mechanical properties.

Keywords: Epoxy coatings, nano zinc oxides, weathering properties, corrosion resistance, mechanical properties..



Figure 1: Epoxy coated sample undergone chalking after 72 hours of exposure to UV(B) radiation. Corrosion initiation in the effected area can be seen in the figure. The main aim of this work is to decrease the degradation due to weathering using nano Zinc oxide.

References:

1. A.S Khanna., High Performance Coatings, 1st edision, Woodhead, 2008. Print
2. A.S Khanna, Nanotechnology in High Performance Paint Coatings, Asian J. Exp. Sci., Vol. 21, No. 2, 2008; 25-32.

Synthesis of Scalable Hierarchical Surfaced Copper Oxide - Titanium Dioxide Sphere for Water Treatment

Jeremy Koon Keong Ang¹, Benny Yong Liang Tan¹, Jermyn, Juay¹, Yong Hao Kok¹, Hongwei Bai², Darren Delai Sun^{1*}

¹School of Civil and Environmental Engineering, Nanyang Technological University, Singapore

²Energy Research Institute @ NTU, Nanyang Technological University, Singapore

Abstract: The need for a scalable spherical hollow titanium dioxide (TiO₂) nanomaterials is in demand and researches has developed many methods to achieve the desired morphological structure to lower density and increase active area for adsorption and photocatalysis [1]. The advantages of hollow spheres however, is limited largely by the smooth surface of the hollow structures. Hence, research to further optimize surface morphology of spherical materials to further maximize the potential of the spherical morphology. However, the optimisation of the morphology typically requires multiple steps and applies the use of additives for the synthesis process. This report will focus on the facile and scalable synthesis of hierarchical surfaced titanium hollow spheres, through the adoption of a solvothermal method. The process will incorporate the use of hard template method for controllable size, using carbonaceous spheres synthesized through glucose as the sacrificial template, owing to its green and sustainable synthesis in addition to the distribution of functional groups which make surface modifications unnecessary [2]. The formation of a hierarchical surface was observed after solvothermal synthesis of the producing urchin like hierarchical TiO₂ spheres with a copper infused carbonaceous spheres as the inner template. The incorporation of copper oxide into the carbon spheres was obtained through diffusion [3]. Such direct approach to synthesize a hierarchical surface TiO₂ spheres comprising only of a solvent and precursor solution. The carbonaceous hard template not only provides ease of scalability and size controllability but also the incorporation of multiple elements. The report will then discuss on the morphological structure and factors which will affect the photocatalysis performance of the material by assessing the photocatalytic oxidation performance of the Cu-TiO₂ Hollow

Keywords: titanium dioxide, copper oxide, hollow structures, hierarchical structures, photocatalysis, solvothermal, calcination,.

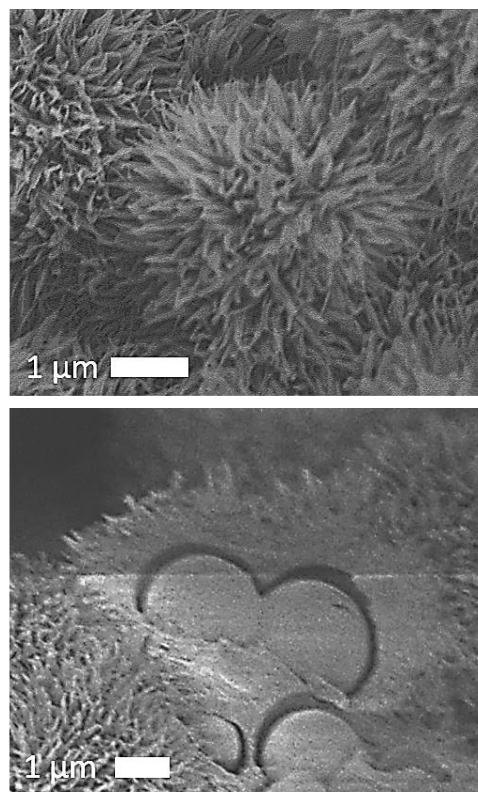


Figure 1: (a) depicts the formation of the hierarchical Cu-TiO₂ spheres after the solvothermal process. (b) the formation of the hierarchical surfaces atop the spherical carbonaceous spheres template with the incorporation of copper observable with the darker coloured surface.

References:

1. Hu, J., et al., *Fabrication and application of inorganic hollow spheres*. Chemical Society Reviews, 2011. **40**(11): p. 5472-5491.
2. Sun, X. and Y. Li, *Colloidal Carbon Spheres and Their Core/Shell Structures with Noble-Metal Nanoparticles*. Angewandte Chemie, 2004. **116**(5): p. 607-611.
3. Zhang, G. and X. Lou, *General synthesis of multi-shelled mixed metal oxide hollow spheres with superior lithium storage properties*. Angewandte Chemie (International ed. in English), 2014. **53**(34): p. 9041-9044.

Solid Cation-exchange Resin catalysed Esterification of Lactic Acid with Ethanol: A Novel Kinetic Study.

E. Okon,^{1,2,*} G. Edward,^{1,2}

^{1,2} Center for Process Integration and Membrane Technology (CPIMT), School of Engineering.
The Robert Gordon University Aberdeen, AB10 7GJ, United Kingdom

E-mail: e.p.okon@rgu.ac.uk, & *Corresponding Author email: e.gobina@rgu.ac.uk. Phone No.: +44(0)1224262348.

Abstract:

Cation-exchange resin catalysts have attracted a lot of attention in the esterification process involving carboxylic acid and alcohol to produce organic ester and water as the by-product. In this work, the esterification of lactic acid and ethanol to produce ethyl lactate using different cation-exchange resin catalysts was carried out at 100 °C. The cation-exchange resin used for the esterification process was amberlyst 36. The characterisation of the resin catalysts was determined using different methods including Fourier Transform Infrared - Attenuated Total Reflection (Nicolet iS10 FTIR-ATR) and liquid nitrogen adsorption/desorption (Quantachrome, 2013 Autosorption) at 77 K. methods The esterification product was tested using FTIR to determine the most adsorbed components on the surface of the resin catalysts. The absorption band at 2998 nm depicts C = O bond (carbonyl group) while the band at 1745 nm showed O-H bond (hydroxyl group), suggesting ethanol and water as the most adsorbed components on the surface of the resin catalysts. Two simplified mechanism based on Langmuir-Hinshelwood model were employed to describe the components that adsorbed most on the surface of the catalysts. The kinetic study of the retention time and the peak areas of the esterification product catalysed with the different catalysts were compared using an autosampler gas chromatography coupled with mass spectrometry (7890B autosampler GC-MS). The surface area and pore size of the cation-exchange resin was determined using the BET (Brunauer-Emmett-Teller) and BJH (Barrette – Joyner Halenda) methods respectively. The BET result of amberlyst 36 was found to be 33.883 m²/g. The BET isotherm of the cation-exchange resin exhibited a type IV isotherm which was in agreement with the IUPAC classification for mesoporous material.

Keywords: Kinetics, ethyl lactate, esterification, lactic acid, and characterisation and cation-exchange resin.

Figure 1: Figure describe the experimental setup of the question in which the paper is aiming to solve: To carried out the esterification of ethyl lactate using solid cation-exchange resin and kinetic study of the adsorption components on the surface of the catalysts using Langmuir model.

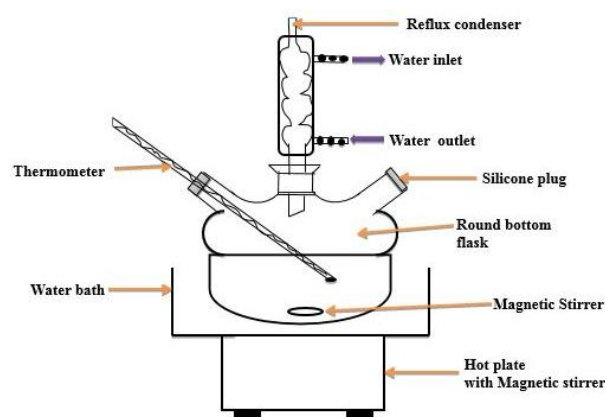


Figure 2: Figure describe the esterification experimental setup [1].

References:

1. Edidiong Okon, Habiba Shehu, Edward Gobina. Experimental Characterisation of Cation-exchange Resin for Biomass Green Solvent Production. *Journal of Scientific Engineering and Technology*. 2016; 5(4); Pp 173 – 179.

Resistive Switching in Self-ordered TiO₂ Nanocolumn Arrays

M. Marik,* M. Bendova, J. Hubalek, A. Mozalev

CEITEC - Central European Institute of Technology, Brno University of Technology, Brno, Czech Republic

Abstract:

Modulation of electrical resistance (resistance switching) by voltage applied to or by current flowing through a device is a growing research field nowadays with the potential of the devices to be utilized for memory applications. Switching phenomena have been observed in numerous materials, including some dielectric binary oxides, perovskites, and semiconductors. (Yang *et al.*; 2013) In the present study, we investigate resistive switching behavior of TiO₂ nanocolumn arrays prepared *via* the originally developed porous-anodic-alumina-assisted anodizing of sputter-deposited Ti layers. Fabrication of self-ordered TiO₂ nanocolumns consists of several steps. An Al(250 nm) / Ti(200 nm) bilayer sputter-deposited on a SiO₂-coated Si wafer is electrochemically anodized in oxalic acid at 40 V, this being followed by reanodizing to 100 V (Sjöström *et al.*; 2010). This leads to growth of ~150 nm long TiO₂ columns embedded in the alumina matrix (Figure 1). The length of the columns may be tuned by changing the final voltage value at the reanodization step. Thermal annealing may be applied to alter the film crystal structure.

In order to create an electrical contact to the TiO₂ columns inside the pores, gold is electrochemically deposited onto the column tops and over the alumina surface and an upper electrode is formed in this way. To confine the electrode area to approx. 100 μm x 100 μm, a photolithography followed by chemical etching of Au is performed. As the bottom electrode, the remaining Ti layer below the columns is used.

Electrical characterization of the films by means of *I*(*V*) measurements for estimating their switching behavior shows a substantial resistivity change in dependence of the applied voltage (Figure 2). The ratio of the OFF and ON resistivities is ranged between 10 and 1000, depending on the columns' properties. Thus, the TiO₂ nanocolumns developed here exhibit promising memristive properties. A thorough investigation is now in progress.

Research leading to these results was supported by GAČR grant no. 15-23005Y.

Keywords: resistive switching, memristor, self-ordered nanostructures, porous-anodic-alumina-assisted anodizing.

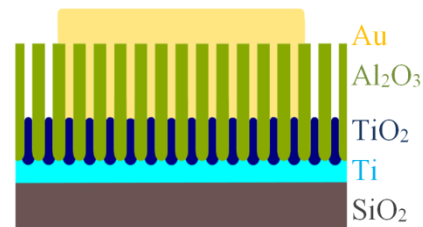


Figure 1: A scheme of the samples: TiO₂ columns embedded in alumina matrix and contacted by electrochemically deposited Au.

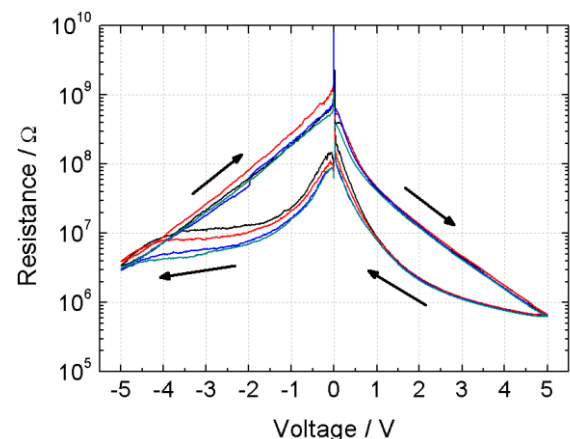


Figure 2: *R*(*V*) characteristics of a sample anodized at 100 V, as calculated from the measured *I*(*V*) cycles. The resistivity change clearly manifests the memristive behavior of the TiO₂ nanocolumns. Arrows show the sweep direction.

References:

1. SJÖSTRÖM, T., FOX, N., SU, B., A study on the formation of titania nanopillars during porous anodic alumina through-mask anodization of Ti substrates, *Electrochim. Acta*, 2010, 56, 203–210.
2. YANG, J. J. S.; STRUKOV, D. B.; STEWART, D. R., Memristive devices for computing. *Nat Nanotechnol* 2013, 8 (1), 13-24.

Formulation and Characterization of Garlic oil nanoparticles with enhanced Anti-Microbial Activities

Sherif Fahmy^{1,2}, Wael Mamdouh^{1,2*}

¹Department of Chemistry, School of Sciences and Engineering (SSE), The American University in Cairo (AUC), AUC Avenue, P.O. Box 74, New Cairo 11835, Egypt.

²Yousef Jameel Science and Technology Research Center (YJSTRC), School of Sciences and Engineering (SSE), The American University in Cairo (AUC), AUC Avenue, P.O. Box 74, New Cairo 11835, Egypt.

E-mails: Sheriffahmy@aucegypt.edu

*Corresponding author E-mail: wael_mamdouh@aucegypt.edu

Abstract

Bacterial infections are considered the second main cause of death worldwide and the third main cause of death in the developed countries [1] and as a result, many antibacterial coatings have been prepared in order to fight the different strains of bacteria and decrease the mortality rates.

In the present study, garlic oil (GO) colloidal nano-particles (NPs) were prepared by combining GO with poly lactic-co-glycolic acid (PLGA) polymer by Single emulsion/solvent evaporation (SE/SE) method.[2, 3] Different PLGA/GO NP formulations were prepared by high speed homogenizer at different homogenization time intervals. A number of preparation factors were carefully controlled in order to have stable and uniform size distribution of the different PLGA/GO-Colloidal NPs formulations. Complete characterization of the particle sizes, zeta potential, poly dispersity index (PDI), the GO% in each PLGA/GO-Colloidal NPs formulation, the morphology (by using Scanning Electron Microscope (SEM)), and the chemical structural characteristics (by using Fourier Transform-Infra-red spectroscopy (FT-IR) and Ultraviolet-Visible spectrophotometry (UV-vis), were carried out. In addition, antibacterial assessment has been carried out against *Eichercia Coli* (*E. coli*) and *Staphylococcus aureus* (*S. aureus*) bacteria using Colony Counting Method (CCM) (Figure 1).

Interestingly, the size of the PLGA/GO-Colloidal NPs was found to be in the range of 201 – 319 nm (which was reduced by more than 10 folds compared to the GO particles). In addition, the antibacterial activities of the different PLGA/GO formulations against both *E. coli* and *S. aureus* were enhanced by 70-78 % of bacterial inhibition compared with GO in the bulk form.

Keywords: PLGA, Garlic oil, Nanoparticles, *E. coli*, *S. aureus*.

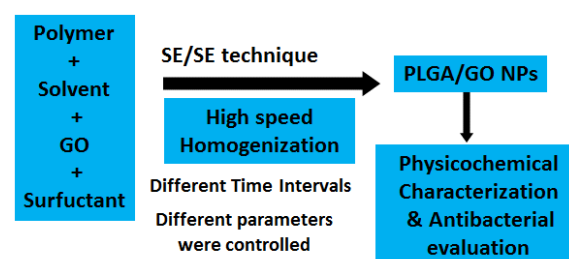


Figure 1. A schematic representation summarizing the preparation steps of each of PLGA/GO NPs.

These results shed more insights into the important factors that need to be considered when preparing NPs conjugates from natural materials, and open new avenues in exploring other extracts with promising antibacterial activities.

References:

- 1- Linscott A. Food-borne illness. Clinical Microbiology Newsletter. 2011;33:41-45.
- 2- Budhian A, Siegel S, Winey K. Haloperiddol- loaded PLGA nanoparticles: systematic study of particle size and drug content. Ijpharm. 2007;336:367-375.
- 3- Esfandyari-Manesh M, Ghaedi Z, Asemi M, Khvi M, Manayi A, Jamalifar H, Atyabi F, Dinarvand R. Study of antimicrobial activity of anethole and carvone loaded PLGA nanoparticles. Jopr. 2013;7:290-295.

Neutron radiation resistance of ferroelectric copolymer filled with Al_2O_3 and ZnO nanoparticles

S.Rouabah,^{1,2,*} B. Vincent,² D.Rouxel,² A.Chaabi,¹ S.Girard,³ P. Paillet,⁴ M. Gaillardin,⁴

¹ Université des frères Mentouri1, faculté des sciences de la technologie, Département d'Electronique, Laboratoire Hyperfréquences et Semi-conducteurs (LHS), 25000, Constantine, Algérie

² Institut Jean Lamour, UMR CNRS 7198, , 54506, Vandoeuvre lès Nancy, France

³ Laboratoire Hubert Curien, Université de Lyon, Université de Saint-Etienne, 42000 Saint-Etienne, France

⁴ CEA DAM DIF, 91297, Arpajon , Cedex France

Abstract: Hybrid nanocomposites[1-3] based on oxide nanoparticles incorporated in polymer matrix have been extensively studied the past few years. In this paper we study the ability of these materials to withstand radiation environments such as those encountered in nuclear power plants. Because the defects induced by irradiation can be generated through both ionization and atomic displacement damages in such environments, we have to consider their relative incidence on the physical properties by performing tests at different facilities (^{60}Co source or reactors). In this work, we focus on the mechanical and elasto-optic properties variations occurring after irradiation by neutron (0.8MeV), that are assumed to be the most impacting type of particles.

In this paper, two nanocomposites are studied. One was P(VDF-TrFE) matrix filled with ZnO nanoparticles and for the other one Al_2O_3 nanoparticles were incorporated to the matrix.

For such materials, Brillouin spectroscopy can provide information on both elastic and elasto-optic variation. We demonstrate here that this last one is as a good diagnostic of chemical and structural modifications. We will present in this paper some results about these specific measurements.

We can assume that, for both samples, heavy atoms (Zn and Al) are responsible for the increase of the interaction between matter and neutrons. However, results show that for high concentration of nanofillers the behaviours of our two different nanocomposites with neutron fluences 5.10^{14} n/cm^2 are in opposition. Alumina nanoparticles are known to increase the elastic constants and then act in our case as a protection against the physical consequences of atomic displacement damages induced by neutrons. On the contrary, for ZnO nanoparticles, elastic as well as elasto-optic properties are strongly influenced

by neutron fluence because the pristine samples are softer than pure P(VDF-TrFE) and also because Zn is a heavier atom than Al.

Keywords: Nanocomposites, neutron, Radiation, Brillouin spectroscopy, elasto-optic, P(VDF-TrFE)

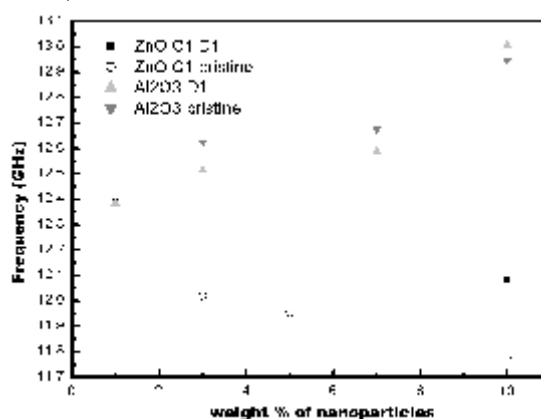


Figure 1: Figure illustrating phonon frequency for pristine P(VDF-TrFE) and nanocomposite with ZnO (increase of the effect with the increase of wt% and the opposite behavior for alumina)

References:

1. Borjanovic, V., Bisticic, L., Mikav, L., McGuire, G.E., Zamboni, I., Jaksic, M., Shenderova, O. (2012) Polymer nanocomposites with improved resistance to ionizing radiation, *Journal of Vacuum Science and technology*. Volume 30 Number 4.
2. Allayarov, S.R., Ol'khov, Y.A., Sheftan, I.N., Muntele, K.I., Ila, D., Dixon, D.A. (2012) Effect of accelerated protons on the molecular topological structure and thermal stability of Poly(vinylidene fluoride), *High energy chemistry*, Vol.46, No.2, 84-90.
3. Indoli, A.P., Gaur, M.S. (2012) Optical properties of solution grown PVDF-ZnO nanocomposite thin films, *Springer Science+ Business Media Dordrecht*.

The Synthesis of Blue Colored Zirconia and Its Application on Automotive Industry

A.Yurdakul^{1*} H. Gocmez¹

¹Dumlupinar University, Department of Material Science and Engineering, Kutahya, TURKEY

Abstract:

Ceramic based welding pins are used to automotive industry as a connecting element. The main function of welding pin provides to combine the nut on the metal surface. These materials are required to have high strength and fracture toughness because of operating under a heavy load. They are also subjected to temperature changes during process. Therefore, they must have a good thermal shock resistance. Indeed, ZrO₂ based ceramic is the one of best material for this kind of application. According to literature, Hydrothermal is convenient method to synthesis nanosized blue colored ZrO₂ powder. The production of Y-TZP powders with blue-colored and ≤ 5 nm grain size was successfully obtained from ZrO₂-Y₂O₃-Al₂O₃-CoO system by hydrothermal method in one-step. The blue-colored ZrO₂ ceramics with 16.85 MPa.m^{1/2} fracture toughness and 9.79 GPa hardness values were produced for 98.20% of theoretical density. The obtained sintered zirconia meets criteria for application required high wear resistance and excellent mechanical properties.

Keywords: automotive industry, ceramic welding pin, hydrothermal powder synthesis, Y-TZP.

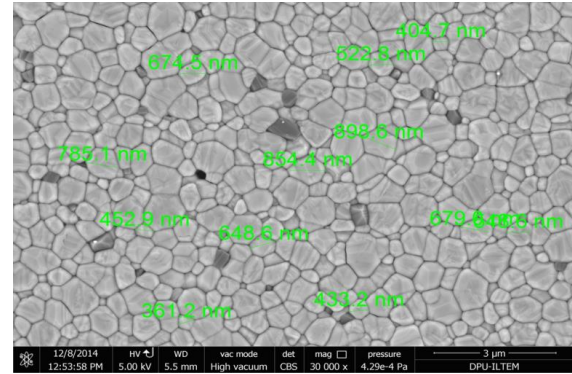


Figure 1: SEM image showing the sintered blue colored zirconia ceramic.

References:

1. McLaren, E.A., Giordano, R.A., (2005), Zirconia based ceramics: Material Properties, Esthetics, and Layering Techniques of a New Veneering Porcelain, VM9.
2. Radhika, S.P., Sreeram, K.J., Nair, B.U., (2012), Rare earth doped cobalt aluminate blue as an environmentally benign colorant, Journal of Advanced Ceramics, 1(4), 301-309.
3. Witek S.R., Butler E.P., (1986), Zirconia particles coarsening and the effect of zirconia additions on the mechanical properties of certain commercial aluminas, J. Am. Ceram. Soc., 69, 523-9.
4. Wang, W., Xie, Z., Liu, G. ve Yang, W., (2009), Fabrication Of Blue-Colored Zirconia Ceramics via Heterogeneous Nucleation Method, American Chemical Society, cilt 9, 4373-4377.

Effect of nanoclay on short term water absorption and swelling of composites made by wood poplar flour and recycled polystyrene

A. Tavasoli^{1*}, A. Samariha², M. Nemati², Z. Masoomi³

¹Department of Agriculture, Faculty of Landscape, Islamic Azad University, Mashhad Branch, Mashhad, Iran.

²Young Researchers and Elites Club, Science and Research Branch, Islamic Azad University, Tehran, Iran.

³Department of Industrial Design, Islamic Azad University, Mashhad Branch, Mashhad, Iran.

*Corresponding author: tavasoliaf@gmail.com

Abstract:

In this research effect of nanoclay content on short term water absorption and swelling of nano composites made by poplar flour and recycled polystyrene were investigated. Composite samples were produced by injection moulding method. 0,3 and 6 % nanoclay with 3 % MAPP were mixed to produce nanocomposites.

Nano composite samples were soaked at distilled water and 2 and 24 hours water absorption and swelling were measured according to DIN standard. Results showed that by increasing nanoclay content, water absorption and swelling of nanocomposites were decreased. Scanning electron microscopy pictures showed that by adding more nanoclay to composites, adhesion between fibers and polymer matrix has improved and voids and hollows decreased.

Keywords: nanoclay, water absorption, Composite

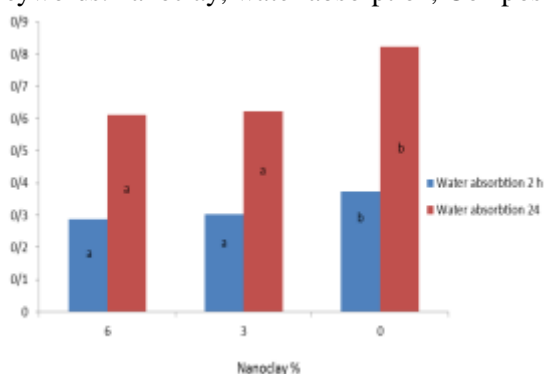
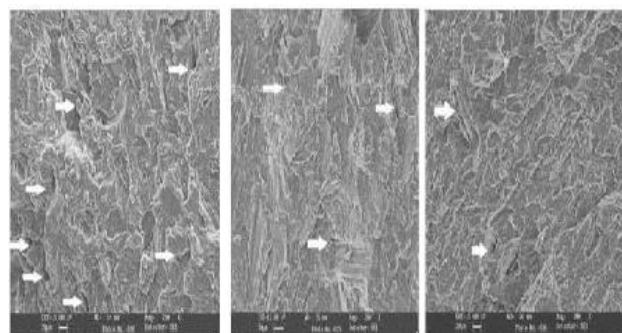


Figure 1: showed that water absorption has decreased by addition of nanoclay to composites. Higher addition of nanoclay has no effect on water absorption of composites.



a) 0% nanoclay b) 3% nanoclay c) 6% nanoclay

Figure 2: Morphological improvement of the polymer matrix and fibers shows in figure 2(a-c). It was cleared that by adding nanoclay to composite, voids and hollows decreased.

References:

1. Arbelaiz, A., Fernandez, B., Cantero, G., Liano-Ponte, R., Valea, A., and Mondragon, I., 2005. Mechanical properties of flax fibre/polypropylene composites influence of fibre/matrix modification and glass fibre hybridization, *Journal of Composites*, Vol.36, pp. 1637-1644.
2. Das, S., Sara, A. K., Choudhury, P. K., Basak, R. K., Mitra, B. C., Todd, T., Lang, S. 2000. Effect of steam pretreatment of jute fiber on dimensional stability of jute composite. *Journal of Applied Polymer Science* 76, 1652-1661.
3. Espert, A. Vilaplana, F. and Karlsson, S. 2004. Comparison of water absorption in natural cellulosic fibers from wood and one-year crops in polypropylene composites and its influence on their mechanical properties. *Composites, Part A*, 35: 1267-1276.

**Nanotech France 2016:
Joint Symposium on Functional
Hybrids and Clay Nanomaterials**

Clay-graphene nanocomposites

E. Ruiz-Hitzky

Instituto de Ciencia de Materiales de Madrid, CSIC, C/Sor Juana Inés de la Cruz 3, 28049 Madrid, Spain
eduardo@icmm.csic.es

Abstract:

An interesting meeting point between 2D materials can result from the assembly of clays and graphene. In fact, abundant deposits of clay minerals and graphite are spread out around our planet. Clay minerals exhibit a layered structural arrangement based on the stacking of silicate sheets that can be submitted to delamination processes. Similarly, graphite is composed of a piling of graphene arranged as monolayers of sp^2 bonded carbon atoms. As it is well known, delamination or exfoliation of graphite submitted to physical or chemical procedures give rise to graphene monolayers or few-layers graphene. Both types of delaminated 2D solids exhibit interesting surface properties, including porosity and intercalation ability, which can be used for preparation of hybrid, biohybrid and composite materials provided of potential interest in advanced applications. In this context, clays and graphene can be combined at the nanometer scale (Figure 1) giving composites of potential interest as materials for applications in energy storage, conductive polymer nanocomposites and electro-responsive elements for sensing devices. To achieve clay-graphene systems two approaches have been recently developed: i) sonomechanical direct assembling of both components from aqueous dispersions (1), and ii) thermal treatment, at relatively low temperature ($< 800^\circ\text{C}$) and in the absence on of oxygen of organic compounds adsorbed on clays (2,3). Layered clays like montmorillonite and fibrous clays like sepiolite are good components supports for the synthesis of diverse clay-graphene materials, which exhibit electrical conductivity that depends on the content ofn assembled carbon as well as on the adopted experimental conditions in the preparation procedure.

Keywords: Graphene, smectite clays, montmorillonite, fibrous clays, sepiolite, nanocomposites, conducting materials.

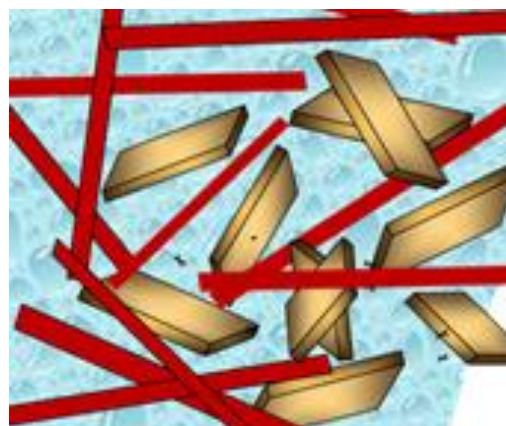


Figure 1: Schematic representation of a clay-graphene composite prepared by assembling of graphene nanoplatelets (in brown color) and nanofibrous clay sepiolite (in red color).

References:

1. E. Ruiz-Hitzky, M. Sobral, C. Nunes, A. Gomez-Avilés, C. Ruiz-García, M. Darder, P. Ferreira, P. Aranda, *in preparation*.
2. Ruiz-Hitzky E.; Darder, M.; Fernandes, F.M.; Zatile, E.; Palomares, F.J.; Aranda, P.; *Adv. Mater.*, 2011, 23, 5250-5255.
3. Ruiz-García C.; Darder, M.; Aranda, P.; Ruiz-Hitzky E.; *J. Mater. Chem. A*, 2014, 2, 2009-2017.

Acknowledgements:

Financial support from MINECO, Spain (MAT2012-31759 & MAT2015-71117-R) and the EU COST Action MP1202 is acknowledged. Contributions from P. Aranda, M. Darder, A. Gómez-Avilés, C. Ruiz-García (ICMM-CSIC) and C. Nunes, P. Ferreira, M. Sobral (University of Aveiro) are gratefully acknowledged.

Graphene / Ru nanostructure transparent hybrid systems for sensing applications

L. Álvarez-Fraga¹, F. Jiménez-Villacorta¹, E. Climent-Pascual¹, R. Ramirez-Jiménez^{1,2}, C. Prieto¹ and A. de Andrés¹

¹Instituto de Ciencia de Materiales de Madrid, Consejo Superior de Investigaciones Científicas. Cantoblanco 28049 Madrid, (Spain).

²Departamento de Física, Escuela Politécnica Superior, Universidad Carlos III de Madrid, Avenida Universidad 30, Leganés, 28911 Madrid, (Spain).

Abstract:

Graphene/plasmonic metal nanoparticle hybrid materials are emerging candidates for the development of a new generation of transparent (bio)sensors [1]. One of the current research strategies, named ultraviolet – surface enhanced Raman scattering (UV-SERS), consists of combining surface and resonance enhancements at UV wavelengths, is envisioned to increase the sensitivity of Raman signal in chemical and biological detection. To this purpose, graphene/nanoruthenium hybrid materials have been fabricated and studied. In this case, Ru nanostructures can act simultaneously as a catalyst for graphene formation, and as an intercalated UV plasmon resonance source to eventually enhance the detection performance [2].

A detailed characterization of the influence of preparation conditions on the crystallinity and morphology of the Ru nanostructured layers was carried out utilizing synchrotron x-ray diffraction, scanning electron microscopy and atomic force microscopy. Graphene formation on the Ru nanostructures and its characteristics (single layer, SLG, or multilayer graphene, MLG) are analyzed by force and Raman spectroscopies. The crystalline structure and morphology of the Ru nanostructured layers, tailored with deposition parameters, are observed to determine the quality of the obtained graphene. (Figure 1). The localized plasmon resonance associated with the Ru nanoparticles shifts with graphene growth ranging very close to the SLG interband transition at 4.6 eV, which indicates some coupling between graphene electronic structure and Ru free electrons, and is enhanced and shifted up to 5.3 eV when MLG is present.

Keywords: Graphene-based hybrid materials, Ultraviolet-surface enhanced Raman scattering (UV-SERS), scanning electron and force mi-

croscopies, Raman spectroscopy, biosensing applications.

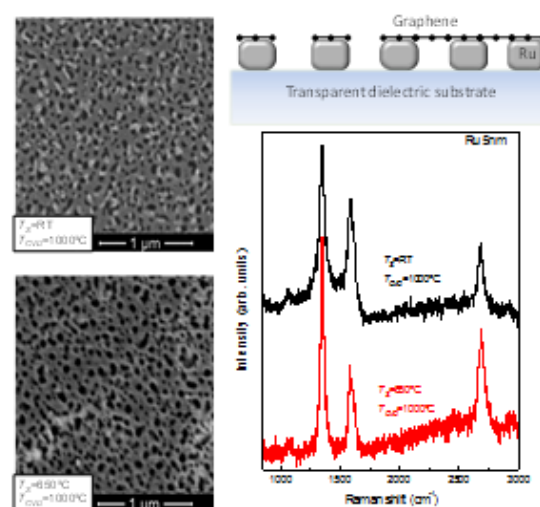


Figure 1: SEM images of two graphene/ruthenium nanoparticle samples, with their respective Raman spectra, confirming the formation of single-layer and multi-layer graphene on the Ru nanostructures.

References:

- [1] Jimenez-Villacorta F., Climent-Pascual E., Ramirez-Jimenez R., SanchezMarcos J., Prieto C., de Andrés A., (2016) Graphene – ultrasmall silver nanoparticle interactions and their effect on electronic transport and Raman enhancement, *Carbon*, doi: 10.1016/j.carbon.2016.02.006.
- [2] L. Álvarez-Fraga, F. Jiménez-Villacorta, E. Climent-Pascual, R. Ramirez-Jiménez, C. Prieto and A. de Andrés, In Preparation.

Thermal properties of LDPE Graphene filled nanocomposites designed for HVDC cable accessories.

K. Gaska,^{1*} R. Hafiizh Azhari¹, R. Kadar², M. Andersson³, S. Gubanski,¹

¹Department of Materials and Manufacturing Technology, High Voltage Engineering, Chalmers University of Technology, 41296 Göteborg, Sweden

²Department of Materials and Manufacturing Technology, Polymeric Materials and Composites, Chalmers University of Technology, 41296 Göteborg, Sweden

³Department of Chemistry and Chemical Engineering, Chalmers University of Technology, 41296 Göteborg, Sweden

Abstract:

The development of HVDC cable technology will result in increased electric stress on the insulation systems, where the weakest points appear in cable terminations and joints. Therefore controlling the field distribution in these components is a crucial issue. This function is fulfilled by field grading materials consisting of polymer composites filled with semi-conducting ceramic particles such as SiC, ZnO or carbon black. The nonlinear electrical conductivity is provided by the percolated structure of the filler particles. However relatively high filler loads need to be used (30% to 40%), which affect negatively the mechanical properties and can deteriorate manufacturing process due to increased viscosity. The alternative approach is to use conductive particles of graphene (GnP) for the sake of its unique electrical, thermal and mechanical properties. The main advantage is a possibility to obtain percolation threshold for low graphene loading contents.

The technique chosen to produce nanocomposites is a precoating technique proposed by Drzal group [1, 2], in which liquid phase exfoliation of graphene nanopowder is carried out by means of chemical wet dispersion in acetone, followed by sonication. GnP-LDPE masterbatches were extruded afterwards by means of single-screw extruder from Brabender, with a screw diameter $D=19$ mm and a screw length of $25 D$ equipped with conveyor belt. The screw rotational speeds applied were 5 and 45 rpm, which corresponds to shear rates of 118 and 1062 and draw ratios of 1 and 0.5. The two different rotation speed of the extruder screw was used to check if additional exfoliation process could possibly take place and what was its impact on the dispersion of the filler particles in LDPE matrix. Samples were prepared in form of tapes with graphene contents of 1%, 3%, 5% and 7.5%.

Investigations presented in this paper concentrate on elucidating the variations in the applied processing technique on the composite morphology. It was achieved by means of DSC and TGA analyses as well as microscopic observations. Results of measurements of composites' thermal conductivity are also reported.

Keywords: Graphene, nanocomposites, polyethylene, melt extrusion, processing, thermal conductivity

References:

1. Kalaitzidou K., Fukushima H., Drzal L.T (2007) A new compounding method for exfoliated graphite-polypropylene nanocomposites with enhanced flexural properties and lower percolation threshold, *Composites Science and Technology*, 67, 2045–2051.
2. Wu H., Rook B., Drzal L. T. (2013), *Dispersion Optimization of Exfoliated Graphene Nanoplatelet in Polyetherimide Nanocomposites: Extrusion, Precoating, and Solid State Ball Milling Polymer Composites*, 8, 471-491.

Multi-parameter monitoring of *in vitro* tissue models using organic electronics

R.M Owens,¹

¹Ecole des Mines de. St. Etienne, Dept. of Bioelectronics, Gardanne, France

Abstract:

Organic bioelectronics refers in part to the coupling of conducting polymer based devices with biological systems, proven repeatedly in the last decade to provide numerous advantages to a wide variety of biomedical applications in terms of sensitivity, specificity and most importantly, bridging of the biotic/abiotic interface. We focus on the unique properties of organic electronic materials that allow easy processing, and flexibility in design as well as chemical tunability, to develop state-of-the-art tools to (1) develop relevant *in vitro* models by creating more '*in vivo*' like environments and (2) monitor cells *i.e.* for diagnostic purposes following exposure to toxins or pathogens. We have successfully demonstrated the use of the organic electrochemical transistor (OECT) for monitoring *in vitro* models of the gastrointestinal tract, the kidney and the blood brain barrier.

For each application, we attempt to recreate the *in vivo* conditions through the use of microfluidics, biofunctionalised materials, and combinations of different cell types, while simultaneously designing the materials/devices in the most appropriate form factor to suit the model at hand. Our goal is to develop physiologically relevant *in vitro* models with integrated monitoring systems that obviate the need for animal experimentation in diagnostics, toxicology or drug development. In this presentation, I will focus on demonstrating how we adapt the OECT to generate a 'tool-box' of methods to continuously monitor live cells *in vitro*. The toolbox includes electronic impedance monitoring, metabolite sensing, high resolution imaging and an automated electrical wound healing assay.

Keywords: OECT, conducting polymer, *in vitro* toxicology, microfluidics, 3D tissues

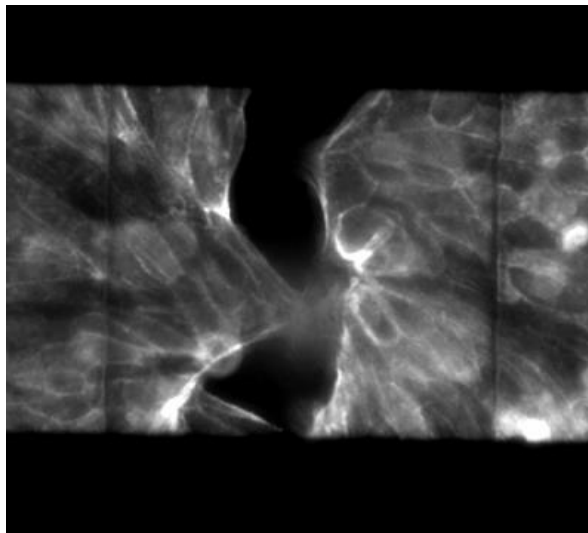


Figure 1: Image of the channel of an Organic Electrochemical transistor (50 x50 μ m) in the centre. The black borders top and bottom are the gold lines insulated by parylene. MDCK II cells (Madin Darby Canine Kidney) were transfected with Lifeact (red fluorescent protein) for live cell imaging, possible thanks to the optical transparency of the conducting polymer used in the channel (PEDOT:PSS). Cells were exposed to a DC (direct current) pulse which killed the cells on the active area. Approximately 2 hours post pulse (the time the image was taken), the cells begin to migrate across the channel as they 'heal'. Electrical and optical images are correlated to monitor cell behaviour during healing.

References:

1. V.C. Curto, A. Hama, **R.M. Owens.**, Integration of microfluidics with the OECT for a cell biology toolbox. *In preparation*.
2. X. Strakosas, M. Bongo, **R.M. Owens.** "The organic electrochemical transistor for biological applications". *Journal of applied polymer science* 132 (15) (2015)
3. M. Ramuz, A. Hama, M. Huerta, J. Rivnay, P. Leleux, **R.M. Owens.** "Combined optical/electronic monitoring of epithelial cells *in vitro*. *Advanced Materials* Early on line view DOI: 10.1002/adma.201401706 (2014)

DNA-based bionanocomposites for gene transfer and biotechnological applications.

Fidel Antonio Castro-Smirnov^{1,5}, Olivier Piétrement², Pilar Aranda⁴, Jeanne Ayache², Eric Le Cam², Jean-Remy Bertrand³, Bernard S. Lopez¹ and Eduardo Ruiz-Hitzky⁴

¹CNRS UMR 8200, Institut de Cancérologie Gustave-Roussy, Université Paris Sud, team labeled “Ligue 2014”, 114 rue Edouard Vaillant, 94805 Villejuif, France.

²Maintenance des Génomes, Microscopies Moléculaires, CNRS UMR 8126 and University of Paris Sud, Institut de Cancérologie Gustave-Roussy, 114 rue Edouard Vaillant, 94805 Villejuif, France.

³CNRS UMR 8121, Laboratoire de Vectorologie et Thérapeutiques Anticancéreuses, IGR.

⁴Instituto de Ciencia de Materiales de Madrid (ICMM-CSIC), c/Sor Juana Inés de la Cruz 3, 28049 Madrid, Spain.

⁵Universidad de las Ciencias Informáticas, Carretera a San Antonio de los Baños, km 2 1/2, 19370 Havana, Cuba.

Abstract:

Nanofibers of sepiolite, a natural silicate belonging to the clay minerals family, might constitute a potential promising nanocarrier for the non-viral transfer of bio-molecules. Sepiolite nanofibers efficiently binds different types of nucleic acids (genomic DNA, plasmid DNA, single strand and double strand oligonucleotides and RNA) through electrostatic interactions, hydrogen bonding, cation bridges, and van der Waals forces, resulting in bionanocomposites provided with the latent bioactivity characteristic of DNA and RNA species. By combining fluorescence microscopy, transmission electron microscopy (TEM), time-lapse video microscopy and flow cytometry analysis (FACS), we show that sepiolite can be spontaneously internalized into mammalian cells through both endocytic and non-endocytic pathways. Furthermore, we show that sepiolite is able to stably transfer plasmid DNA into mammalian cells and that the efficiency can be optimized. These results open the way to the use of sepiolite and DNA-based bionanocomposites as a novel class of nanoplatform for gene transfer with potential clinical applications, as well as for the development of novel biological models of interest for Academia and biotechnological applications.

Keywords: Sepiolite, DNA, clay minerals, bionanocomposites, mammalian cells, bacteria, endocytosis, DNA transfection, transformation, gene transfer, gene therapy.

References:

E. Ruiz-Hitzky, M. Darder, F.M. Fernandes, B. Wicklein, A.C.S. Alcântara, P. Aranda, “Bionanocomposites based on fibrous clays”, *Pogr. Polym. Sci.* 38, 1392-1414 (2013).

E. Ruiz-Hitzky, M. Darder, P. Aranda, M.A. Martín Del Burgo, G. Del Real, “Virus-bionanocomposite materials: application for flu vaccines”, *Adv. Mater.* 21, 4167–4171, (2009).

In Vivo Multimodal Deep Tissue Imaging with Hybrid Nanostructures

D. H. Ortgies,^{1,4} L. de la Cueva,⁵ B. del Rosal,¹ F. Sanz-Rodríguez,^{2,4} N. Fernández,³ M. C. Iglesias-de la Cruz,^{3,4} G. Salas,^{5,6} D. Cabrera,⁵ F. J. Teran,^{5,6} D. Jaque,^{1,4} and E. Martín Rodríguez,^{1,4}

¹ Fluorescence Imaging Group, Departamento de Física de Materiales, Facultad de Ciencias, Universidad Autónoma de Madrid, C/Francisco Tomás y Valiente 7, 28049 Madrid, Spain

² Fluorescence Imaging Group, Departamento de Biología, Facultad de Ciencias, Universidad Autónoma de Madrid, C/Darwin 2, 28049 Madrid, Spain

³ Fluorescence Imaging Group, Departamento de Fisiología, Facultad de Medicina, Universidad Autónoma de Madrid, Avda. Arzobispo Morcillo 2, 28029 Madrid, Spain

⁴ Instituto Ramón y Cajal de Investigación Sanitaria IRYCIS, Ctra. Colmenar km. 9.100, 28034 Madrid, Spain

⁵ iMdea-Nanociencia, Campus Universitario de Cantoblanco, 28049 Madrid, Spain

⁶ Nanobiotechnología (IMDEA-Nanociencia), Unidad Asociada al Centro Nacional de Biotecnología (CSIC), Madrid, Spain

Abstract:

Luminescent nanoparticles (LNPs) brought great advances to the areas of imaging and sensing but most of them use UV or visible light and are hence limited to cellular or topical applications. For in vivo bioimaging LNPs working in the infrared hold more promise because of their ability to penetrate biological tissue.^[1]

Combining our interest in LNPs that emit IR light between 1000 – 1350 nm, an area with minimal tissue absorption and scattering, which is defined as the 2nd biological window (II-BW), with the desire for multifunctional nanoparticles, we developed hybrid nanostructures (HNSs) through the encapsulation of superparamagnetic iron oxide and infrared emitting quantum dots, which absorb and emit in the II-BW, with PLGA, a biocompatible, FDA-approved polymer that is ideally suited for in vivo applications. We demonstrated the HNSs applicability for in vivo multimodal imaging (MRI and infrared fluorescence) in mice and their multifunctionality was studied through the assessment of their applicability as potential magnetic heating agents in hyperthermia treatments.^[2]

In summary, HNSs for in vivo multimodal imaging were synthesized and their features were studied in ex vivo and in vivo experiments. The capability of the magnetic-fluorescent HNSs for hyperthermia treatments was also demonstrated.

Keywords: infrared fluorescence, bioimaging, MRI, multimodal, multifunctional.

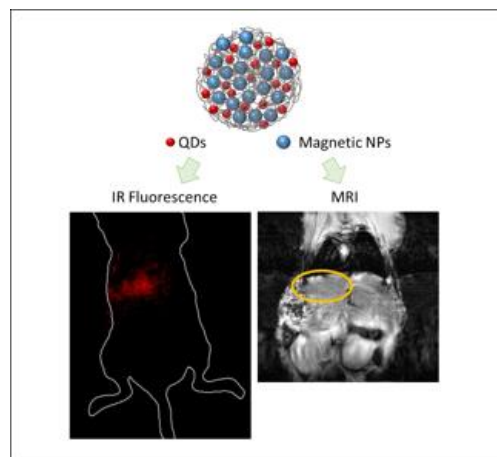


Figure 1: Above: Schematic representation of HNSs, Below: Multimodal imaging in a mouse (left: infrared fluorescence, right: MRI) employing the HNSs

References:

- [1] Navarro Cerón, E., Ortgies, D. H., del Rosal, B., Ren, F., Benayas, A., Vetrone, F., Ma, D., Sanz-Rodríguez, F., García Solé, J., Jaque, D., Martín Rodríguez, E. (2015). Hybrid Nanostructures for High-Sensitivity Luminescence Nanothermometry in the Second Biological Window. *Advanced Materials*, 27, 4781–4787.
- [2] Ortgies, D. H., de la Cueva, L., del Rosal, B., Sanz-Rodríguez, F., Fernández, N., Iglesias-de la Cruz, M. C., Salas, G., Cabrera, D. Teran, F. J., Jaque, D., Martín Rodríguez, E. (2016). In Vivo Deep Tissue Fluorescence and Magnetic Imaging Employing Hybrid Nanostructures. *ACS Applied Materials & Interfaces*, 8, 1406–1414.

Magneto-photo-thermal Nanomaterials as Efficient Nanoheaters for Tumor Therapy

A. Espinosa^{1*}, R. Di Corato¹, J. Kolosnjaj-Tabi¹, M. Bugnet², G. Radtke³, S. Neveu⁴, G. A. Botton², P. Flaud¹, A. Abou-Hassan⁴, T. Pellegrino⁵ and C. Wilhelm¹

¹Laboratoire Matière et Systèmes Complexes, UMR 7057, CNRS and University Paris Diderot, 75205 Paris cedex 13, France

²Department of Materials Science and Engineering and Canadian Centre for Electron Microscopy, McMaster University, 1280 Main street West, Hamilton, ON, L8S4M1 Canada

³Institut de Minéralogie, de Physique des Matériaux et de Cosmochimie (IMPMC), UMR 7590, CNRS, UPMC, 4 place Jussieu, 75005 Paris, France

⁴Sorbonne Universités, Physicochimie des Electrolytes et Nanosystèmes Interfaciaux (PHENIX), UMR 8234, Université Pierre et Marie Curie UPMC-CNRS, 75252 Paris cedex 05, France

⁵Istituto Italiano di Tecnologia, I-16163 Genoa, Italy

Abstract:

New multifunctional nanomaterials that combine different therapeutic capabilities in one-single object are attracting increasing attention in cancer battle.¹ Nanostructures which couple magnetic and plasmonic properties have demonstrated a synergistic therapeutic and diagnostic potential: iron oxide cores (magnetic) bring potential for magnetic resonance imaging (MRI), magnetic manipulation and targeting, while gold layers (plasmonic) were integrated to provide optical response of the hybrids for imaging or photo-thermal heating. However, nanomaterials that incorporate the simultaneous action of magnetism and light to efficiently deliver heating to induce tumour cell death (hyperthermia) are rare. Here, we explore two examples of nanostructures devoted to thermal-therapies under magneto-photo-thermal action: i) magnetic-plasmonic nanohybrids (composed of a core optimized for high efficiency in magnetic hyperthermia, and a gold shell with tunable plasmonic properties from the visible to the near infrared region (NIR)² and ii) iron oxide cube-shaped nanomaterials (Figure 1).³ Efficient and amplified heat conversion was achieved for both cases, either in suspension till *in vivo* conditions, becoming into a new dual hyperthermic-modality for tumor treatment with minimal collateral tissue damage.

Keywords: magnetic hyperthermia, photothermal, magneto-plasmonic nanohybrids, iron oxide nanoparticles, nanomedicine, bimodal hyperthermia

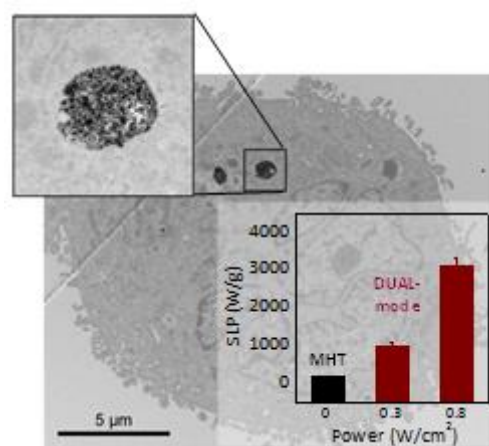


Figure1: Iron oxide nanocube-mediated heating in cancer cells. Inset: Heating efficiency (SLP, in W/g) under magnetic hyperthermia only and combined with photothermia (dual-mode).

References:

1. Di Corato R, et al. (2015), Combining magnetic hyperthermia and photodynamic therapy for tumor ablation with photoresponsive magnetic liposomes. *ACS Nano* 9, 2904-2916.
2. A. Espinosa, et al. (2015), Can magneto-plasmonic nanohybrids efficiently combine photothermia with magnetic hyperthermia?. *Nanoscale* 7, 18872-18877.
3. A. Espinosa, et al. (2016), The duality of iron oxide nanoparticles in cancer therapy: amplification of the heating efficiency by magnetic hyperthermia and photothermal bimodal treatment. *ACS Nano* 10, 2436-2446.

Adsorption of diclofenac pharmaceutical product onto clay mineral and organoclay derivatives

T. De Oliveira⁽¹⁾, R. Guégan⁽¹⁾

⁽¹⁾ Institut des Sciences de la Terre d'Orléans, UMR 7327, CNRS-Université d'Orléans, 1A Rue de la Férellerie, 45071 Orléans Cedex 2, France

Abstract: Pharmaceutical products (PPs) are non-biodegraded substances which are more and more commonly found in sewage and surface water (Thiebault et al., 2015). Although being present at low concentration, these substances have been recognized to drive to toxic effects on several ecosystems. Among recalcitrant PPs to water treatments, diclofenac, a nonsteroidal anti-inflammatory substance, shows a high toxicity (Ferrari et al., 2003) and remains at high concentration in the environment (Miege et al., 2009) due to its particular resistance to the current treatment (Verlicchi et al., 2014). For this purpose, new techniques including adsorbents have to be developed for the adsorption of PPs (Guégan et al., 2015).

In the present contribution, the adsorption of diclofenac onto a clay mineral and its organoclay derivatives has been studied with a particular understanding of the interactional mechanisms of this PP with the prepared adsorbents. The experimental data obtained by a set of complementary techniques (X-ray diffraction, infrared spectroscopy, gas chromatography coupled with mass spectroscopy) reveal that organoclays prepared with the use of two different cationic long-alkyl chains surfactants (BDTA and HDTMA) show a particular affinity to diclofenac which is enhanced as the density of surfactant is increased while the nature appears to play a minor role.

Keywords:

adsorption, composite layered materials, clay mineral, cationic surfactant, organoclay, pharmaceutical product, water

References:

Ferrari B., Paxéus N., Giudice R.L., Pollio A., Garric J., (2003) Ecotoxicological impact of pharmaceuticals found in treated wastewaters: study of carbamazepine, clofibric acid, and diclofenac. *Ecotoxicology and Environmental Safety*, Vol. 55, pp. 359-370

Guégan R., Giovanela M., Warmont F., Motelica-Heino M., (2015) Nonionic organoclay: A 'Swiss Army knife' for the adsorption of organic micro-pollutants? *Journal of Colloid and Interface Science*, Vol. 437, pp. 71-79

Miege C., Choubert J.-M., Ribeiro L., Eusèbe M., Coquery M., (2009) Fate of pharmaceuticals and personal care products in wastewater treatment plants-conception of a database and first results. *Environmental Pollution*, Vol. 157, pp. 1724-1726

Thiebault T., Guégan R., Boussafir M., (2015) Adsorption mechanisms of emerging micro-pollutants with a clay mineral: Case of tramadol and doxepine pharmaceutical products. *Journal of Colloid and Interface Science*, Vol. 453, pp. 1-8

Verlicchi P., Zambello E., (2014) How efficient are constructed wetlands in removing pharmaceuticals from untreated and treated urban wastewater? A review. *Science of the Total Environment*, Vol. 470-471, pp. 1281-1306

Sepiolite-Nanocellulose Assembly as new Nanofibrous Hybrid Materials

M. M. González del Campo, M. Darder*, P. Aranda, E. Ruiz-Hitzky

Instituto de Ciencia de Materiales de Madrid, CSIC, C/Sor Juana Inés de la Cruz 3, 28049 Madrid, Spain, *presenting author: darder@icmm.csic.es

Abstract:

Bionanocomposites are hybrid materials prepared from natural polymers and inorganic solids with particle size in the nanometer scale, such as clays (Darder et al., 2007). Different type of biopolymers can be employed in the preparation of bionanocomposites with special interest focusing on the use of polysaccharides. Cellulose is the most abundant, renewable and biodegradable natural polysaccharide in Earth and, thus, materials based on cellulose (wood, flax, cotton, hemp...) have been widely used for thousands of years by men.

The present work intends to explore the preparation and characterization of bionanocomposites consisting in the assembly of cellulosic materials and fibrous clays (sepiolite) as inorganic components. The cellulose nanofibers (CNF) were gently provided by Prof. P. Mutjé (Univ. of Girona, Spain), prepared following the methodology by Saito et al. (2007). The obtained CNF are around 4-20 nm in width and a few microns in length. As inorganic counterpart, a commercial sepiolite of rheological grade and dimensions close to those of CNF was employed.

The methodology used for the preparation of this hybrid material has consisted in the application of shear force and ultrasound energy to aqueous suspensions of CNF and sepiolite (Ruiz-Hitzky y col., 2014), getting stable gels which can be conformed as films. The subsequent characterization of these materials has corroborated the suitability of the employed methodology to obtain homogeneous hybrid materials showing good interaction between the organic and the inorganic fibers.

The stability of these films makes them good candidates for different applications either as absorbents or for more advanced application such as sensors, requiring in this case the incorporation of other nanoparticles or functional groups. In this way, multiwalled carbon nanotubes have been successfully incorporated into this hybrid system, giving rise to conducting materials which are currently being explored for uses as active phase in sensor devices.

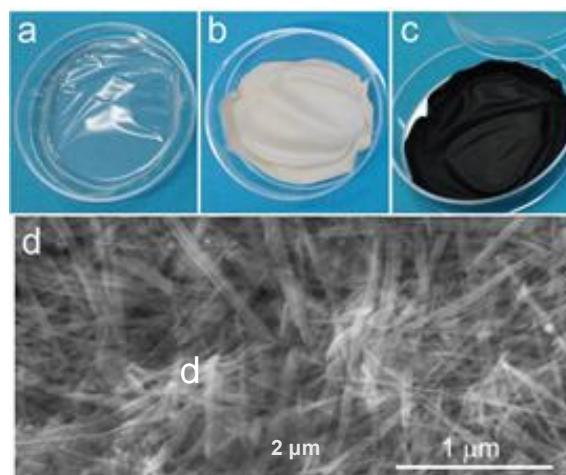


Figure 1: Films of (a) CNF (b) CNF-sepiolite, and (c) CNF-sepiolite-MWCNT, (d) FE-SEM imagen CNF-sepiolite.

Keywords: Bionanocomposites, fibrous clays, sepiolite, cellulose nanofibers, multiwalled carbon nanotubes.

References:

Darder, M., Aranda, P., Ruiz-Hitzky, E. (2007) Bionanocomposites: A new concept of ecological, bioinspired and functional hybrid materials, *Adv. Mater.* 19, 1309–1319.

Ruiz-Hitzky, E., Aranda P., Darder, González del Campo, M.M. (2014) Spanish patent P201431000.

Saito T, Kimura S, Nishivama Y, Isogai A. (2007) Cellulose Nanofibers prepared by TEMPO-Mediated Oxidation of Native Cellulose, *Biomacromolecules*, 8 2485-2491.

Acknowledgements:

MINECO, Spain (Projects: MAT2012-31759, BES-2013-064677 & MAT2015-71117-R) and the EU COST Action MP1202. We thank Dr. J. Bettini from LNNano-CNPq, Brazil, for FE-SEM characterization.

Multi-enzyme/layered double hydroxide-based biohybrids for the synthesis of chiral polyols in cascade reaction

F. Bruna Gonzalez¹, M. De Sousa¹, M. Lorillière¹, G. Ali¹, T. Gefflaut¹, V. de Berardinis³, L. Pollegioni⁴, W.-D. Fessner², C. Forano¹, V. Prévot¹, C. Mousty¹, F. Charmantray¹, L. Hecquet¹

¹ICCF- CNRS UMR 6296, BP 10448, F-63177 Aubière, France

²Technische Universität Darmstadt, Petersenstraße 22, D-64287 Darmstadt, Germany

³CEA, DSV, IG, Genoscope, 2 rue Gaston-Crémieux, F-91057 Evry, France

⁴Department of Biotechnology and Molecular Sciences, University of Insubria, Varese, Italy

Abstract:

Highly efficient functional materials can be developed thanks to the association of biological materials with inorganic components to generate the so-called biohybrid materials. In particular, layered double hydroxides (LDH), since their layers are positively charged, can favorably interact with biomolecules which often bear an overall negative charge at neutral pH values. Different strategies were developed for the design of LDH biohybrids containing enzymes. Transketolase (TK, EC 2.2.1.1.), a thiamine diphosphate-dependent enzyme, reveals an efficient biocatalyst to ensure the stereospecific transfer of a two-carbon ketol unit to the carbonyl of a variety of aldehydes leading to chiral polyols of biological interest. We have recently identified a thermostable and highly robust TK from *Geobacillus stearothermophilus* (TKgst) offering interesting opportunities.

In this presentation, we will describe the transketolase immobilization on LDH allowing easy use, storage and reuse of the supported enzyme and how it is possible to extend the immobilization strategy to the co-immobilization of D-amino oxidase / TKgst or α -transaminase / TKgst@LDH. These biohybrids are of special interest in cascade enzymatic reactions since they catalyze the *in situ* formation of β -hydroxypyruvate (HPA) from D- or L-serine respectively. The released HPA is readily converted upon TK-catalyzed reaction yielding the corresponding α -ketose product in the presence of an acceptor aldehyde. In resume, we will describe the synthesis and the characterization of biohybrids, and some applications in biocatalysis for the synthesis of chiral polyols.

Keywords: biohybrids, layered double hydroxides, biocatalysis, transketolase, D-amino acid oxidase, transaminase, co-immobilization of enzymes, chiral polyols.

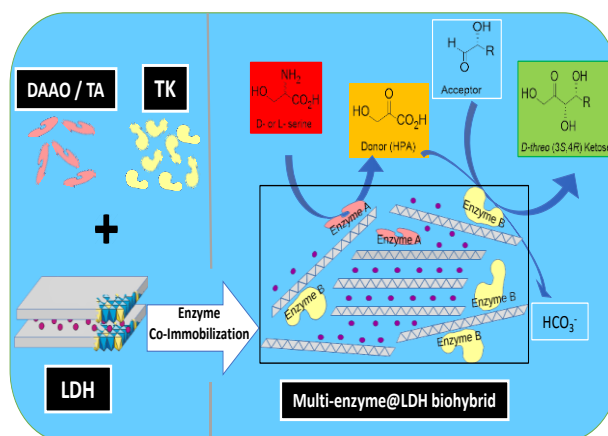


Figure 1: General scheme of a biocatalyst based on D-amino acid oxidase / TKgst@LDH or α -transaminase / TKgst@LDH nanohybrids for the synthesis of D-threo (3S, 4R) ketoses, using D- or L-serine for the *in situ* generation of HPA as donor for TKgst and yielding the ketose product.

References:

- Abdoul Zabar, J., Sorel, I., F. Charmantray, F., Hélaine, V., Devamani, T., Yi, D., de Berardinis, V., Louis, D., Marlière, P., Fessner, W.-D., Hecquet, L. (2013), Thermostable Transketolase from *Geobacillus stearothermophilus*: Characterization and Catalytic Properties, *Adv. Synth. Catal.*, 355,116-128.
- Ali, G., Moreau, T., Forano, C., Mousty, C., Prevot, V., Charmantray, F., Hecquet, L. (2015), Chiral polyol synthesis catalyzed by a thermostable Transketolase immobilized on Layered Double Hydroxides in Ionic liquids. *ChemCatChem*, 7, 3163–3170.

Biohybrids based on zein and montmorillonite: preparation and use as nanofiller in clay-based bionanocomposites

A.C.S. Alcântara^a, M. Darder, P. Aranda* and E. Ruiz-Hitzky

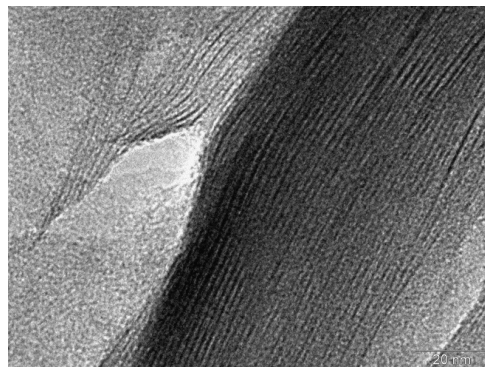
Materials Science Institute of Madrid, CSIC, c/ Sor Juana Inés de la Cruz 3, 28049 Madrid, Spain

^aPresent address: Universidade Federal do Maranhão, Departamento de Química, 65080-805- São Luís – MA, Brazil* presenting author: pilar.aranda@csic.es

Abstract: Amongst organic-inorganic hybrids those implying the use of biological species as organic counterpart represent a growing field of research centred in the development of advanced functional or structural materials (Ruiz-Hitzky et al., 2008). Bionanocomposites are biohybrid materials involving polymers from biological origin, being the most common ones based on poly(lactic acid) or polysaccharides, such as chitosan or starch, and clay minerals as inorganic nanofiller (Ruiz-Hitzky et al., 2015). Although less explored, polypeptides and proteins have been also intercalated in the interlamellar space of smectite clays such as montmorillonite, forming a protein-clay biohybrid material. Bionanocomposites based on the assembling of zein with montmorillonite have been prepared by the thermo-plasticization and blown extrusion techniques (Luecha et al., 2010; Nedi et al., 2012) as well as from protein solved in ethanol/water mixtures (Alcântara et al., 2011). using organoclays, but in this communication we will show that it is possible to prepare the bionanocomposites using sodium montmorillonite in which the process is controlled working with the solubility properties of zein. The mechanism of the biohybrid formation will be explained considering the complex structure of zein and the role of the amino acids in its composition, as well as the specific conformation of this protein. Aspects on the physicochemical characterization of the resulting biohybrids (Figure 1) and their application biofillers in the preparation of diverse ecofriendly nanocomposites based on zein and starch will be also discussed. In this sense, it will be shown that the incorporation of the biofiller improves the compatibility with the polymer matrix, while keeping the biocompatible character of the material, and additionally play a role for incorporating barrier properties as reported for other biorganoclays used in the preparation of reinforced bioplastics (Chivrac et al., 2010; Alcântara et al. 2016).

Keywords: zein, montmorillonite, bionanocomposites, biohybrids, biofillers

Figure 1: TEM image of one of the biohybrids prepared by intercalation of zein in Na-montmorillonite clay.



Reference:

- Ruiz-Hitzky, E., Darder, M., and Aranda, P. (2008). In *Bio-inorganic Hybrid Nanomaterials-Strategies, Syntheses, Characterization and Application*, Chap. 2, 1–40, Ruiz-Hitzky, E., Ariga, K., and Lvov, Y. M., eds., Wiley-VCH, Weinheim.
- Ruiz-Hitzky, E., Aranda, P., Darder, M. (2015) In *Tailored Organic-Inorganic Materials*, Chap. 6, 245–297, Brunet, E., Colón J.L., Clearfield, A. eds., John Wiley & Sons Inc., Hoboken.
- Luecha, J., Sozer, N., Kokini, J. L. (2010) Synthesis and properties of corn zein/montmorillonite nanocomposite films. *J. Mater. Sci.*, 45, 3529–3537.
- Nedi, I., Maio, E.D, Iannace, S. (2012) The role of protein– plasticizer-clay interactions on processing and properties of thermoplastic zein bionanocomposites. *J. Appl. Polym. Sci.*, 125, 314–323
- Alcântara, A.C.S., Aranda, P., Darder, M., Ruiz-Hitzky, E. (2011) Zein-clay biohybrids as nanofillers of alginate based bionanocomposites, *Proc. ACS 241st National Meeting and Exposition*, Anaheim, CA 2011, Vol. 241, 299-PMSE, 114-115.
- Chivrac, F., Pollet, E., Dole, P., and Avérous, L. (2010) Starch-based nanobiocomposites: Plasticizer impact on the montmorillonite exfoliation process. *Carbohydr. Polym.*, 79:941-947.
- Alcântara, A.C.S., Darder, M., Aranda, P., Ayral, A., Ruiz-Hitzky, E. (2016) Bionanocomposites based on polysaccharides and fibrous clays for packaging applications, *J. Appl. Polym. Sci.* DOI: 10.1002/app.42362, 1–14.
- Acknowledgements:** CICYT (Spain, projects MAT2012-31759 & MAT2015-71117-R) and the EU COST Action MP1202.

Hybrid Photonics for Energy Efficiency

Pavlos G. Lagoudakis,¹

¹ University of Southampton, Department of Physics & Astronomy, Southampton, UK

Abstract:

The brightness, large absorption cross-section and flexibility of colloidal nanocrystal quantum-dots (NQDs) and organic semiconductors render them promising new materials for light harvesting and light emitting applications. However, both classes of material are plagued by low-charge-transfer efficiency that limits the overall power conversion efficiency when compared to silicon-based or epitaxial p-n junction photovoltaics, and epitaxial light emitting diodes. A route to circumvent altogether issues associated to low charge transfer in NQDs and organic semiconductors is to engineer devices that utilize alternative energy transfer schemes to electrical injection and transport while still benefiting from their large oscillator strength.

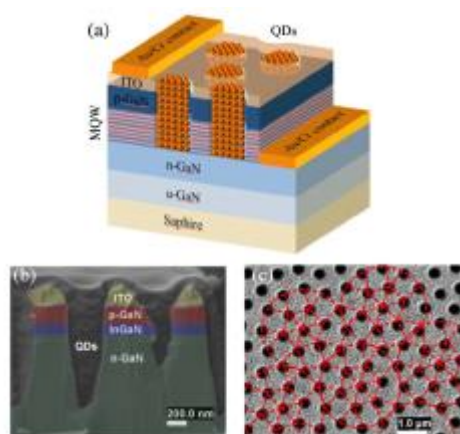


Figure 1: (a) Schematic representation, (b) cross-sectional, and (c) top scanning electron microscopy images of a photonic quasi-crystal LED hybridized with NQD color converters.

In nature, funnelling of energy between different chromophores predominantly occurs through a non-radiative dipole-dipole coupling mechanism, commonly referred to as resonance energy transfer. Non-radiative energy transfer does not involve charge transfer or emission and absorption of photons between donor and acceptor and can exceed the radiative energy transfer routinely used in phosphor light emitting devices. Theoretical calculations and recent experimental observations demonstrate that free quantum well excitons can undergo resonance energy transfer with an order of magnitude higher rate compared to

localized, point-like excitons exemplifying the potential of hybrid photonic devices utilising resonance energy transfer as a means to overcome charge transfer related limitations [1].

Here, I will present recent advances in the field of hybrid photonics in architectures where non-radiative energy transfer is used to combine the high carrier mobility of single crystal inorganic semiconductor heterostructures and the versatility offered by colloidal NQDs and organic semiconductors in light harvesting and light emitting configurations such as those depicted in Figures 1&2 [2-4].

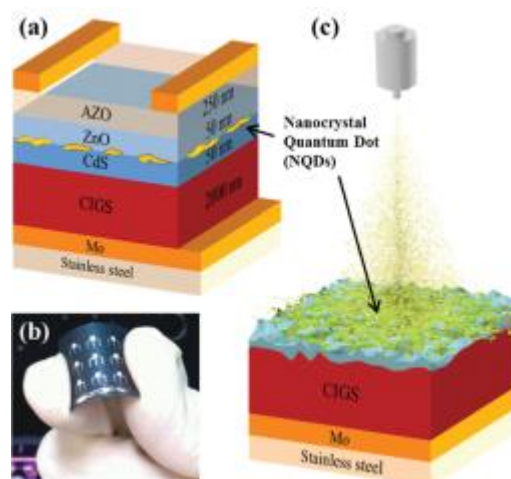


Figure 2: (a) Schematic illustration of a flexible inkjet-printed NQD/CIGS hybrid solar cell. (b) Photograph of a hybrid device. (c) Schematic of the pulsed-spray NQD deposition system.

Keywords: hybrid photonics, photovoltaics, solar cells, LEDs, energy, NRET, RET, resonance energy transfer, nanophotonics, .

References:

1. Rindermann J.J. et al Phys. Rev. Lett. **107**, 236805 (2011)
2. Liao Yu-Kuang et al Adv. Energy Mater. **5**, 1401280 (2015)
3. Brossard M. et al Adv. Optical Mater. **3**, 263 (2015)
4. Krishnan C. et al Optica **3**, *in-print* (2016)

Plasmon assisted Nd³⁺-based solid-state nanolaser

P. Molina,¹ E. Yraola,¹ M.O. Ramírez,¹ C. Tserkezis,² J.L. Plaza¹, J. Aizpurua,² J. Bravo-Abad³ and L.E. Bausá^{1,*}

¹Dept. Física de Materiales and Instituto Nicolás Cabrera Universidad Autónoma de Madrid, 28049-Madrid, Spain

²Center for Materials Physics (CSIC-UPV/EHU) and Donostia International Physics Center (DIPC), Paseo Manuel Lardizabal 4, 20018-Donostia-San Sebastián, Spain

³Dept. Física Teórica de la Materia Condensada and Condensed Matter Physics Center (IFIMAC), Universidad Autónoma de Madrid, 28049-Madrid, Spain

Abstract:

Today the field of solid state lasers (SSL) has evolved to a vast list of designs and configurations to cover applications in a wide range of scientific and technological fronts. However, the new challenges in nanoscience and nanotechnology require coherent light sources operating in the sub-micrometer range. Such sources are really promising since the manipulation of coherent light in nanometric spatial scales can generate a revolution in a variety of applications ranging from sensors to biomedicine and from imaging technologies to the information technology.

Here, we demonstrate threshold conditions for laser action at the nanoscale in a SSL due to the presence of plasmonic structures. The system operates at room temperature with a laser emission wavelength close to 1 μm . The solid state gain medium is constituted by a Nd³⁺ doped periodically poled LiNbO₃ (Nd³⁺:PPLN) laser crystal on which long chains of closely spaced silver interacting nanoparticles have been fabricated. The broad radiative plasmonic modes supported by the chains of metallic nanoparticles extend from the visible down to the NIR, matching the relevant transitions of the Nd³⁺ laser ions and being responsible for the sub-wavelength optical confinement of the laser mode. As a consequence, a dramatic reduction of the pump power at threshold (50%) and a remarkable improvement (up to 15-fold) of the slope efficiency compared to the case of the conventional bulk laser operation are obtained.

The results can open a systematic roadmap to implement the nanoscale confinement effect in many other ions and compounds of solid-state laser physics, by the right choice of plasmonic antenna morphology and configuration. The work opens the possibility to extend the results to the extremely vast list of solid state gain media constituted by hundreds of host-optically ion

combinations (for instance Nd³⁺, Er³⁺, Yb³⁺, Cr³⁺, Ti³⁺,...), which cover the spectral range from the ultraviolet to the mid-infrared with advantages of compactness, chemical and thermal frequency stability, and with the subsequent broad range of applications.

Keywords: plasmonic nanolaser, solid state laser, Nd³⁺, chains of Ag nanoparticles.

References:

Molina, P., Yraola, E., Ramírez, M.O., Tserkezis, C., Plaza, J.L., Aizpurua, J., Bravo-Abad, J., Bausá, L.E. (2016) Plasmon assisted Nd³⁺ based solid-state nanolaser” *Nano Letters*, In Press.

MoSi₂–Si₃N₄ Composite Absorber for Concentrated Solar Power (CSP)

A. Rodríguez-Palomo¹, D. Hernández-Pinilla^{1,2}, E. Céspedes^{1,3}, L. Álvarez-Fraga¹, F. Jiménez-Villacorta¹, R. Jiménez-Riobóo¹ and C. Prieto¹

¹Instituto de Ciencia de Materiales de Madrid, CSIC, Cantoblanco, 28049-Madrid, Spain

²Dept. Física de Materiales, Universidad Autónoma de Madrid, 28049-Madrid, Spain.

³IMDEA Nanociencia, 28049-Madrid, Spain

Abstract:

A novel absorbing composite based on MoSi₂–Si₃N₄ has been investigated to be used in high temperature solar selective coatings (SSC) for harvesting energy in concentrated solar power (CSP) collectors.

A good balance between performance and cost is obtained with SSCs based on a multilayer made of the following four layers: (i) an infrared reflective metallic layer (IR-mirror) placed close to the substrate, (ii) a high metal volume fraction (HMF) composite layer, (iii) a low metal volume fraction (LMVF) composite layer, and (iv) an anti-reflective (AR) layer.

Several informations are needed to optimize the optical properties of solar selective stacks arriving to the highest values in absorptivity and the lowest in thermal emissivity (Céspedes et al. 2014). For this purpose, the following issues have to be considered for the final application of such a coating:

(a) the study of the complex refractive index of each component, (b) simulation of the UV-Vis-IR reflectance of the whole stack based on the complex dielectric permittivity of the components, (c) optimization of the optical absorptivity and thermal emissivity by selecting the appropriate thickness and composition of each layer, (d) sputtering deposition of whole multilayer stacks, (e) optical characterization and comparison with calculated reflectance and, finally, (f) thermal annealing to study the chemical stability and ageing of the prepared materials.

In this communication, we report on SSCs based on silver as IR-mirror metallic layer, a double composite layer of MoSi₂ embedded in Si₃N₄ and Si₃N₄ as AR layer. The optical characterization shown in Fig. 1 evidences the suitability (Hernández-Pinilla et al. 2016) of this absorbing composite for high temperature CSP applications, as well as the thermal stability of the stacks after consecutive annealing treatments

above 600 °C without any hint of ageing degradation.

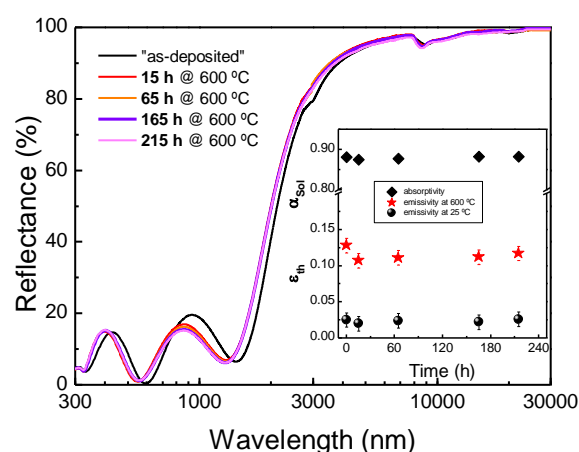


Figure 1: Reflectance spectra of representative SSC after long time periods of vacuum annealing at 600 °C. The inset shows the evolution of solar absorptivity and thermal emissivity.

Keywords: Solar Selective Coating, Concentrated Solar Power.

References:

- Céspedes E., et al. (2014) Novel Mo–Si₃N₄ based selective coating for high temperature concentrating solar power applications, *Sol. Energy Mater Sol. Cells* 122, 217-225.
- Hernández-Pinilla D. et al. (2016) MoSi₂–Si₃N₄ Absorber for High Temperature Solar Selective Coating, *Sol. Energy Mater Sol. Cells*, In Press.

Hybrid photonic crystal LED renders 123% color conversion effective quantum yield

M. Brossard,^{1,*} C. Krishnan,² K.-Y. Lee,³ J.-K. Huang,⁴ C.-H. Lin,^{3,4} H.-C. Kuo,⁴ M. D. B. Charlton,¹ P. G. Lagoudakis²

¹School of Physics and Astronomy, University of Southampton, Southampton, UK

²School of Electronics and Computer Science, University of Southampton, Southampton, UK

³Luxtaltek Corporation, Chunan Miaoli 350, Taiwan

⁴Department of Photonics & Institute of Electro-Optical Engineering, National Chiao Tung University, Hsinchu 300, Taiwan

Abstract:

Colloidal quantum dots (QDs) have emerged as promising color conversion light emitters for solid state lighting applications due to their emission tunability and near-unity photoluminescence quantum yields. In current commercial light emitting diodes (LEDs), QDs are dispersed into an encapsulation layer in a far field architecture, where the majority of the light emitted by the LED remains trapped within the epitaxy due to total internal reflection, drastically reducing out-coupling efficiency. Here, we demonstrate a photonic quasi-crystal (PQC) hybrid LED geometry that allows QD emitters to be placed in close proximity to the multiple quantum wells (MQWs) of the active area (Figure 1). This architecture greatly improves coupling between MQWs and QDs, simultaneously allowing non-radiative resonant energy transfer (RET) between the MQWs and the QDs and near-field radiative coupling of trapped (guided)-modes in the LED to the emitters. In this configuration, we demonstrate record-breaking effective quantum yields reaching 123% for single color conversion LEDs and 110% for white light emitting devices. We also use time-resolved spectroscopy to study RET between the MQWs and the QDs, and demonstrate transfer efficiencies in excess of 80%. We believe that these hybrid PQC LED structures, fabricated with low-cost nano-imprint lithography and using cheap colloidal QD emitters, could represent an important technological breakthrough for the solid state lighting industry.

Keywords: Quantum-well; Photonic quasi crystals; Light-emitting diodes; Quantum dots, Resonant energy transfer.

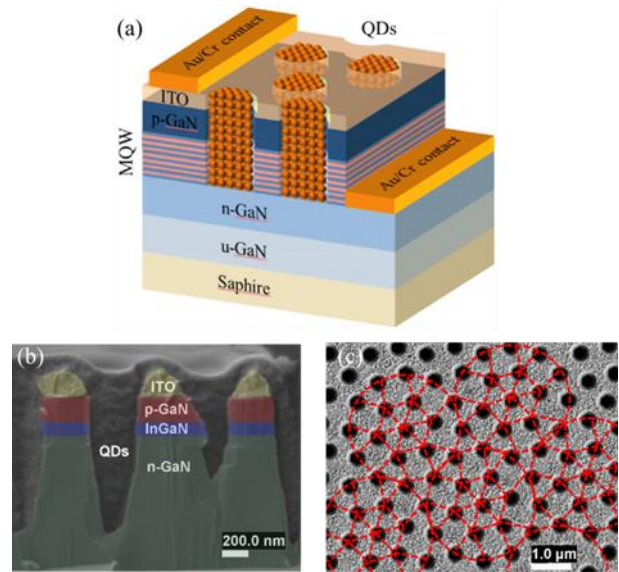


Figure 1: (a) Schematic representation, (b) cross-sectional and (c) top SEM images of a photonic quasi-crystal LED hybridized with QD color converters.

Reference:

Brossard, M., Krishnan, C., Lee, K.-Y., Huang, J.-K., Lin, C.-H., Kuo, H.-C., Charlton, M. D. B., Lagoudakis, P. G., Hybrid photonic crystal LED renders 123% color conversion effective quantum yield, *Optica*, in print (2016)

ZnO-clay nanoarchitectures: preparation and uses as photocatalyst

M. Akkari^{1,2}, P. Aranda¹, H. Ben Rhaïem², A. Ben Haj Amara², E. Ruiz-Hitzky¹

¹ Materials Science Institute of Madrid, CSIC, c/ Sor Juana Inés de la Cruz 3, 28049 Madrid, Spain

² Laboratory of Physics of Lamellar Materials and Hybrid Nano-Materials, Faculty of Sciences of Bizerte, University of Carthage, 7021 Zarzouna, Tunisia

Abstract: The development of porous nanostructured materials based on clay minerals is a topic of great importance being typically used in catalysis and adsorption applications (Ruiz-Hitzky et al., 2012; Aranda et al., 2014). Amongst other approaches it has been reported a colloidal route that involves the use of organoclays and metal alcoxides to develop new porous clay nanoarchitectures from both layered and fibrous clays (Ruiz-Hitzky and Aranda, 2014). In this communication it will be introduced new porous ZnO and ZnO/SiO₂-clay nanoarchitectures based on both layered and fibrous silicates by applying methodologies of synthesis characterized by the use of intermediate organoclays for favouring the assembly of the involved oxide nanoparticles.

On the one side, ZnO-clay porous materials were prepared following a new approach based on the assembly of previously prepared ZnO nanoparticles (NP) to organoclays prepared by treatment with cetyltrimethylammonium bromide of two montmorillonite layered silicates (Wyoming montmorillonite commercialized as Cloisite® by Southern Clay Products and, an iron-rich smectite from Gafsa, Tunisia described by Letaief et al., 2002) and a sepiolite fibrous clay (clay mineral from Vallecas, Spain, commercialized as Pangel® S9, by TOLSA SA). The assembly procedure implies the dispersion of the organophilic clays in 2-propanol together with and ZnO NPs, previously prepared from zinc acetate in presence of KOH in methanol at reflux, to achieve intermediate ZnO/clay organo-heterostructures (Akkari et al., 2016). After thermal treatment, the organic matter is removed and the ZnO NPs become finally assembled to the clay being consolidated the resulting ZnO/clay nanoarchitectures (Figure 1).

On the other side, ZnO NP were assembled to SiO₂-organoclay clay heterostructures prepared following a methodology developed at the ICMM-CSIC that uses a colloidal route to assemble SiO₂ and other type of NP to layered and fibrous clays (Ruiz-Hitzky and Aranda, 2014). This approach intends to procure larger surfac-

es for the assembly of the ZnO NP as for instance, in the case of layered clays it is possible to even reach the delamination of the clay during the formation of silica networks from alcoxysilanes previously associated with the clay. In the present case intermediatesilica-clay heterostructures were prepared from the organoclays using tetramethoxysilane (TMOS) as silica precursor but they were not submitted to the thermal treatment till treatment with a suspension of ZnO NP in 2-propanol under ultrasonication. Heating the resulting materials to eliminate the organic matter produces ZnO/SiO₂ nanoparticles homogeneously dispersed on delaminated layered clays or on the external surface of the fibrous clay.

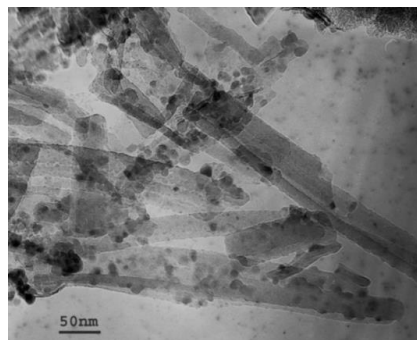


Figure 1: TEM image of one of the ZnO/SEP nanoarchitectures prepared in this case by combining dispersions of the organoclay and ZnO NPs.

Both types of ZnO-clay heterostructures have been characterized by diverse techniques (XRD, FTIR, chemical analysis, specific surface area and porosity determinations, TEM and SEM-EDX,...) and their activity in the photocatalytic decomposition of methylene blue dye in water was evaluated in view to establish their potential interest as photocatalyst for degradation of organic pollutants in water.

Keywords: smectites, sepiolite, ZnO nanoparticles, heterostructured materials, photocatalysis.

Acknowledgements: CICYT (Spain, projects MAT2012-31759 & MAT2015-71117-R), CSIC (Spain, project COOPA20077) and the EU COST Action MP1202.

Atomic and Molecular Layer Deposition of Hybrid Nanostructured Materials

M. Vila,^{1,*}

¹CTECHnano-Coating Technologies S.L. Tolosa Hiribidea, San Sebastián 20018. Spain

Abstract:

Different from chemical vapor deposition (CVD) and physical vapor deposition (PVD), atomic layer deposition (ALD) is based on saturated surface reactions. In this case, the thin films are grown in a layer-by-layer fashion allowing sub-nanometer thickness control, low temperature depositions, good uniformity and superior step coverage on high specific surface area components compared to CVD and PVD.

These advantages of ALD over other thin film deposition processes have been conventionally applied mainly in semiconductor electronic industry on the preparation of layers of outstanding High-K dielectric materials.

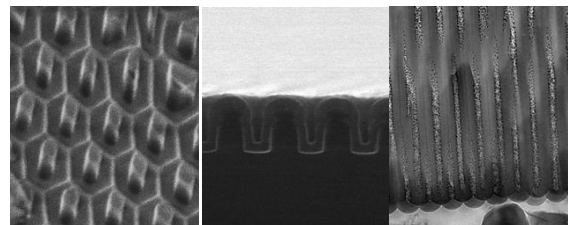
But, due to the advances in tool design and recipe development, the importance of ALD is rapidly expanding for producing innovative nanoscale materials.

ALD new applications are highly multidisciplinary. It has an emerging potential on photovoltaic cells, flexible electronics, enhanced performance glass, paper and textiles, new generation transistors, sensors, and advanced energy materials technology. Innovations brought by nanotechnology to biosciences and biosensors are also proving to be good candidates to benefit from these potentialities and its surface functionalization possibilities.

Some of these advanced applications require the deposition of hybrid materials that could combine the beneficial aspects of both inorganic and organic phases.

Molecular layer deposition (MLD) methods extend the ALD strategy to include organic and hybrid organic–inorganic polymeric materials, so a combination of both techniques opens the door to the creating of highly attractive nanostructural frameworks.

Keywords: Materials deposition, atomic layer deposition, hybrid nanomaterials, hybrid coatings.



Images courtesy of Mato Knez research group

Figure 1: Figure illustrating several structures that could be prepared by this technique, emphasising the high surface-area porous structures that could be deposited at low temperature, providing good uniformity and superior step coverage.

References:

Hybrid nanomaterials through molecular and atomic layer deposition: Top down, bottom up, and in-between approaches to new materials. K. Gregorczyk, M. Knez, *Progress in Materials Science*. 75, 2016, 1–37.

S. M. George. B. Yoon, A. A. Dameron. Surface Chemistry for Molecular Layer Deposition of Organic and Hybrid Organic–Inorganic Polymers. *Acc. Chem. Res.*, **2009**, 42 (4), 498–508

Maya Blue-Based Nanostructured Clay Materials for Colouring Geopolymers

C.M. Ouellet-Plamondon,^{1*} P. Aranda,² A. Favier,³ G. Habert,¹ H. Van Damme,⁴ E. Ruiz-Hitzky²

¹ Institute for Construction and Infrastructure Management, Chair of Sustainable Construction, ETH Zurich, Switzerland

² Materials Science Institute of Madrid, CSIC, c/ Sor Juana Inés de la Cruz 3, 28049 Madrid, Spain

³ Laboratory of Construction materials, EPFL Lausanne, Switzerland

⁴ Department of Civil & Environmental Engineering, MIT, and MSE2, the joint MIT-CNRS Unit, 77 Massachusetts Avenue, Room 1-278, Cambridge, MA, USA

* Present address: Department of Construction Engineering, École de Technologie Supérieure, 1100 Notre-Dame West, Montréal (Québec), H3C 1K3, Canada.

Abstract:

Maya Blue is an ancient nanostructured pigment synthesized by assembling indigo, a natural dye, with palygorskite, a microfibrinous clay mineral. The novelty of our approach is to mimic "pre-Columbian nanotechnology" and to functionalize geopolymers with a sepiolite-based organic-inorganic hybrid material inspired from the Maya Blue pigment. It is acid- and UV-resistant, as confirmed by the stability of Maya mural paintings over time. We synthesized analogous pigments, using methylene blue (MB) and methyl red (MR) as organic dyes and sepiolite as fibrous clay mineral, a parent clay to palygorskite. We used an aqueous (as) and a solid-state (ss) method, both leading to encapsulation of dye monomers into the clay micropores, as confirmed by UV-VIS spectroscopy. The clay dye hybrids were further characterized by specific surface area and dye content determinations. The solid state method allowed to encapsulate a larger quantity of dye and provided a stronger colour. This nanostructured pigment was then incorporated into a geopolymer matrix at room temperature. Calorimetry and X-ray diffraction support that the sepiolite clay does not participate to the geopolymerisation reaction. The stability of the new coloured geopolymer materials to hydrogen peroxide, UV and acid conditions were tested. It was confirmed that it is the prior encapsulation of the dye into sepiolite that leads to the stability of the pigment in the geopolymer matrix. The methylene blue hybrid is more stable to environmental conditions (UV and hydrogen peroxide) than the methyl red one. This first study opens the way to numerous possibilities for functionalizing inorganic binder materials with organic elements that would be otherwise sensitive to thermal treatment in conventional ceramic processing.

Keywords: Maya Blue, sepiolite, geopolymer, methylene blue, methyl red, UV stability

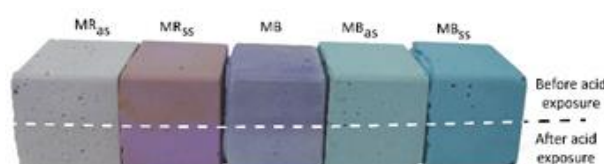


Figure 1: Change of colour of geopolymer with hydrogen peroxide, from left to right: sepiolite + MR_{as}, sepiolite + MR_{ss}, only MB, sepiolite + MB_{as}, sepiolite with MB_{ss}. Upper part, before H₂O₂ exposure and lower part after exposure

Reference:

Ouellet-Plamondon, C., Aranda, P., Favier, A., Habert, G., van Damme, H., Ruiz-Hitzky, E. (2015) The Maya blue nanostructured material concept applied to colouring geopolymers. *RSC Advances*, 5, 98834-98841.

Multifunctional Metallic Janus MOF Particles Synthesized by the Desymmetrization at Interfaces Approach

A. Ayala,¹ Dr. I. Imaz,¹ Prof. D. Maspoch,^{1,2}

¹ Supramolecular NanoChemistry and Materials Group, ICN2-Institut Catala de Nanociencia i Nanotecnologia, Campus UAB 08193 Bellaterra, Barcelona (Spain).

² Institució Catalana de Recerca i Estudis Avançats (ICREA) 08100 Barcelona (Spain)

Abstract:

Metal–Organic Frameworks (MOFs) are a new family of crystalline porous solids constructed by linking metal ions/clusters to organic ligands through coordination bonds. They are characterized by extremely large surface areas and high structural/compositional flexibility that confer them high potential for myriad applications, including gas storage, separation, catalysis, etc.^{1,2} However, beyond the improvements that an adequate design can induce in the MOF properties,^{3,4} the optimization and the presence of MOFs in future real applications must come also from their combination with other type of materials; thereby creating composites.

In this communication, we present a general strategy for the formation of discrete porous metallic Janus MOF nanocomposites, based on direct evaporation of metals on the surface of colloidal MOF crystals that have been pre-immobilized onto planar surfaces. The approach that we used is also known as *desymmetrization at interfaces*. We will explain the different steps of this novel methodology, the flexibility of the approach, and how the new nano composites combine the properties of both components (e.g. Co for introduce magnetism) to be used as advanced adsorbents for pollutant sequestration (e.g. Hg²⁺) in water.

Keywords: Metal Organic Frameworks, porous materials, sequestration of pollutants.

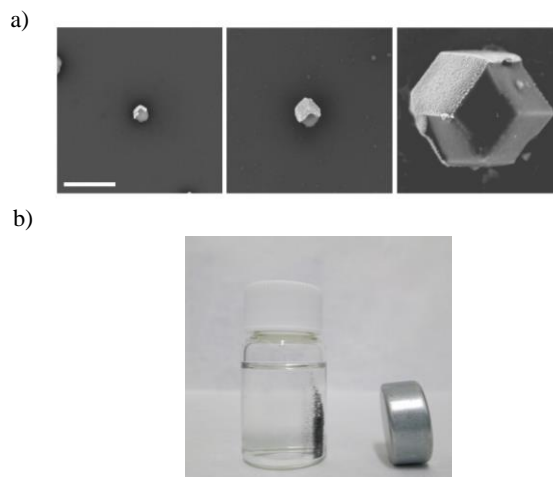


Figure 1: a) SEM images of Janus ZIF-8@Au particles with a size of around 100 nm, 200 nm and 1 μm. Scale bar: 500 nm (from left to right). b) Photography image showing that Janus UiO-66@Co nanocomposites can be guided with a magnet.

References:

- 1] F. Paolo, B. Dario, H. Anita J. and D. Cara M., Adv. Mater. 2012, 24, 3153-3168.
- [2] S. Melinda, Y. Nobuhiro, and G. Steve, Acc. Chem. Res. 2014, 2, 459-469.
- [3] Y. Nobuhiro, S. Melinda and G. Steve, J. Am. Chem. Soc. 2013, 135, 34-37.
- [4] L. Guang, C. Chenlong, Z. Weina, L. Yayuan, and H. Fengwei, Chem. Asian J. 2013, 8, 69–72

Nanoclays for adsorption of tartrazine: A sustainable application

C. del Hoyo Martínez, M. S. Lozano García and V. Sánchez Escribano
Departamento de Química Inorgánica.

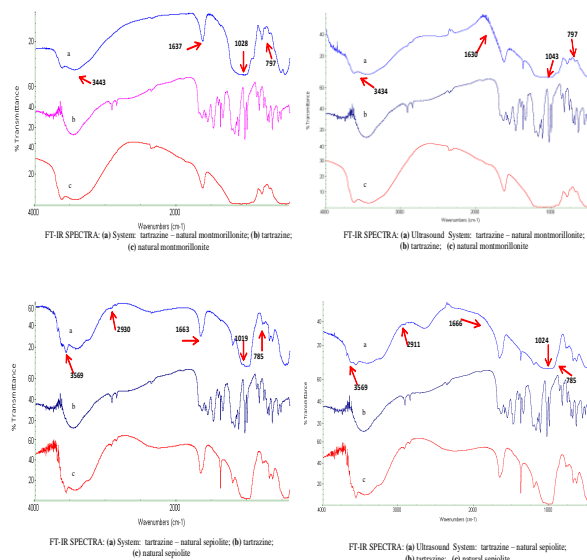
Abstract:

Drinking water is an increasingly scarce commodity, especially in the countries with the lowest human development index, where millions of people do not have any access to sources of clean water to meet their basic needs and often become vehicle diseases. That is why water pollution is an issue of vital importance to be solved. Removal of dyes effluent is one of the most significant and difficult to treat environmental problems since many of the dyes are of synthetic origin and a complex molecular structure, making them more stable and difficult to biodegrade. Sorption techniques produce high quality treated effluent and sorption processes have been investigated as a method of removing dyes wastewater. Tartrazine is a typical synthetic, watersoluble anionic dye. This substance appears to cause the most allergic and intolerances reactions of all the azo dyes, particularly among asthmatics and those with aspirins intolerance. Consequently, the wastewater containing tartrazine with various concentrations should be treated before.

The adsorption of tartrazine by montmorillonite and sepiolite is studied in this work. Results show a strong interaction between clays and the colorants because of the cationic exchange and the realignments of the organic molecule when the adsorption takes place. Ultrasound technique improves the colorant adsorption by the clays.

Keywords: Adsorption, clays, ultrasound technique, tartrazine

Figure 1: FT-IR Spectra: Systems Tartrazine-natural montmorillonite, natural sepiolite and ultrasounds systems



References:

- C. del Hoyo Martínez, J. Cuéllar Antequera, V. Sánchez Escribano, M. S. Lozano García, R. Cutillas Díez, "Clays and Clay minerals and their environmental application in Food Technology", Geophysical Research Abstract. EGU. Vol 15, 13726-13728. 2013.
- C. del Hoyo Martínez, M. S. Lozano García, V. Sánchez Escribano, J. Cuéllar Antequera, "Modified Nanoclays for an Environmental Application". Phantoms Foundation Imagenano Vol. 3, 8-10. 2015. M. S. Lozano García, C. del Hoyo Martínez, J. Cuéllar Antequera V. Sánchez Escribano, "Technique for adsorption of contaminants by nano clays". Phantoms Foundation Imagenano Vol. 3, 17-19. 2015.
- O. Korkut, E. Sayan, O. Lacin, B. Bayrak. "Investigation of adsorption and ultrasound assisted desorption of lead (II) and copper (II) on local bentonite: A modelling study" Desalination Vol. 259, pp 243-248. 2010.
- V.K. Gupta, Suhas. "Application of low-cost adsorbents for dyw removal. A review" Journal of Environmental Management Vol. 90, pp 2313-2342. 2009.

Study of synthetic talc growth by EXAFS: basic research to support technology transfer

Angela Dumas¹, Martin Mizrahi², François Martin³, Felix Requejo², Marie Claverie¹, Cyril Aymonier¹

¹ Institut de Chimie de la Matière Condensée de Bordeaux (ICMCB), 87 Avenue du Dr. Schweizer
33608 Pessac, France

² Instituto de Investigaciones Fisicoquímicas Teóricas y Aplicadas (INIFTA), CONICET-UNLP, diag.
113 y calle 64, 1900 La Plata, Argentina

³ Géosciences Environnement Toulouse (GET), UMR 5563 (UPS-CNRS-IRD-CNES), 14 Avenue
Edouard Belin, 31400 Toulouse, France

Abstract:

Synthetic talc ($\text{Mg}_3\text{Si}_4\text{O}_{10}(\text{OH})_2$) began to be developed at a laboratory scale ten years ago as a technical solution to perform new lubricant composite materials.¹ In collaboration with industrial partners, synthesis processes were recently revised and improved^{2,3} to obtain an economically viable process. Nowadays, synthetic talc appears in various industrial sectors as a competitive and original fillers.^{4,5} While synthetic talc is a well-documented product,^{6,7} very few information is available about the early stages of its formation. However, understanding talc crystallogenesi mechanisms is of primordial importance before developing this filler on a preindustrial scale.

Extended X-ray Absorption Fine Structure (EXAFS) was used to probe the immediate environment of the octahedral cation of the talc precursor sample (PT) and talc samples (T). EXAFS spectroscopy is particularly interesting because this technique is chemically selective and well suited for poorly crystalline and non-crystalline materials.⁸ To study the structural evolution of the octahedral sheet, synthetic Nitalcs were used because Ni atoms have more suitable energy absorption for the use of EXAFS measurements than Mg atoms.

This work aimed to understand the mechanisms of transformation from the amorphous talc precursor to crystalline synthetic talc synthesized at 100, 200 and 300 °C during 6 hours. EXAFS data evidenced a T-O-T (Tetrahedral-Octahedral-Tetrahedral) nano-entity as soon as the talc precursor precipitated. With the synthesis temperature, these talc units are interlocked through the octahedral sheet. Simultaneously with the synthesis temperature, the tetrahedral sheets are developed, and Si–O–Si chains are progressively formed. Based on this growth mechanism, intracrystalline distribution of Ni

and Mg in the octahedral sheet was also studied as a function of hydrothermal temperature

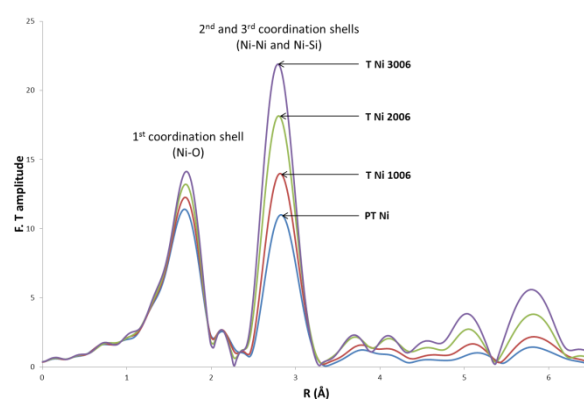


Figure 1: Fourier transforms of the talc precursor and the talc synthesized at 100, 200, and 300 °C.

Keywords: synthetic talc, EXAFS, talc precursor, crystallogenesi

References:

1. Martin et al. International patent: WO 2009081046 A9 2008
2. Dumas et al. International patent: WO 2013004979 A1 2013
3. Dumas et al. Applied Clay Science 2013; 85:8–18
4. Yousfi et al. Journal of Colloid and Interface Science 2013; 403:29–42
5. Yousfi et al. Journal of Applied Polymer Science 2014; 131.
6. Dumas et al. Physics and Chemistry of Minerals 2013; 40:361–73
7. Dumas A. PhD thesis UPS, 2013
8. Newville, M. Rev. Mineral. Geochem. 2014, 78, 33–74.

Nanotech Plenary Session II

DNA-controlled fusion of liposomes

Oliver Ries, Philipp Löffler and Stefan Vogel*

Biomolecular Nanoscale Engineering Center - BioNEC, Department of Physics, Chemistry and Pharmacy, University of Southern Denmark, Campusvej 55, 5230 Odense M, Denmark

Abstract:

Fusion of lipid bilayers is an ubiquitous process in nature. The merging of two biomembranes leading to release of encapsulated content in a controlled way is crucial, e.g. for cell signaling, exocytosis and intracellular trafficking. Pioneering attempts by Boxer and Höök et al. showed the feasibility of artificial liposome fusion controlled by supramolecular interactions of lipid-nucleic acid conjugates (LiNAs).[1] It could be shown that LiNAs are able to mimic the basic functional behaviour of the natural SNARE complex.

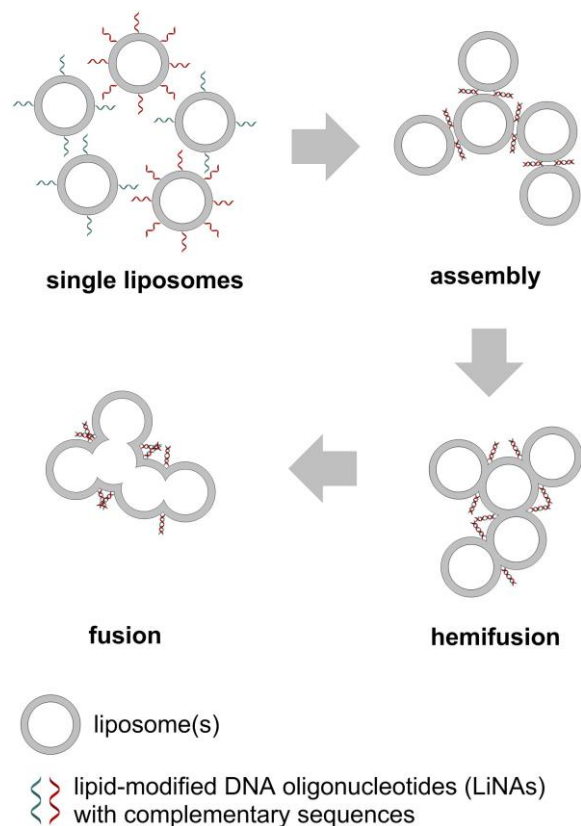


Figure 1: Schematic illustration of DNA-mediated and controlled assembly and hemifusion/fusion process.

Assembly as the first step towards fusion has been reported earlier [2-4] by us and is the initial process necessary for controlled fusion, a process followed by hemifusion and finally fusion of DNA-functionalized liposomes. Key parameters

such as oligonucleotide sequence and length, oligonucleotide design and membrane anchors structure are investigated. Content and lipid-mixing assays show key steps during hemifusion or fusion and open the path for reactant mixing and chemistry in nanoscale reaction containers (liposomes). Chemistry in very small volumes is relevant for the understanding of chemistry under “crowded” conditions (like in cells) and the effect of water “activity” on chemistry under non-bulk solvent conditions in very confined small spaces (cell biology).

Keywords: membrane fusion, oligonucleotides, DNA, supramolecular chemistry.

References:

1. a) G. Stengel, R. Zahn and F. Höök, (2007), DNA-Induced Programmable Fusion of Phospholipid Vesicles, *J. Am. Chem. Soc.*, 129, 9584. b) Y. M. Chan, B. van Lengerich and S. Boxer, (2009), Effects of linker sequences on vesicle fusion mediated by lipid-anchored DNA oligonucleotides, *Proc. Nat. Acad. Sci. U. S. A.*, 106, 979.
2. Ries, O.; Löffler, P. M. G.; Vogel, S., (2015), *Org. Biomol. Chem.*, 9673-9680979.
3. a) Jakobsen, U.; Simonsen A. C. and Vogel S., (2008), DNA-Controlled Assembly of Soft Nanoparticles, *J. Am. Chem. Soc.*, 130, 10462-10463. b) Jakobsen, U.; Vogel, S. (2013), Assembly of Liposomes Controlled by Triple Helix Formation, *Bioconjugate Chem.* 24, 1485. c) Jakobsen, U.; Vogel, S. (2009), DNA-Controlled Assembly of Liposomes in Diagnostics, *Methods Enzymol.* 464, 233.

Meeting the needs for aged and released nanomaterials required for further testing

B. Nowack,^{1*}

¹ Empa, Swiss Federal Laboratories for Materials Science and Technology, St. Gallen, Switzerland

Abstract:

The analysis of the potential risks of engineered nanomaterials (ENM) has so far been almost exclusively focused on the pristine, as-produced particles. However, when considering a life-cycle perspective, it is clear that ENM released from genuine products during manufacturing, use, and disposal is far more relevant. Research on release of materials from nano-products is growing and the next necessary step is to investigate the behavior and effects of these released materials in the environment and on humans. Therefore, sufficient amounts of released materials need to be available for further testing. In addition, ENM-free reference materials are needed since many processes not only release ENM but also nano-sized fragments from the ENM-containing matrix that may interfere with further tests. The SUN consortium (Project on “Sustainable Nanotechnologies”, EU 7th Framework funding) uses methods to characterize and quantify nanomaterials released from composite samples that are exposed to environmental stressors. Here we describe an approach to provide materials in hundreds of gram quantities mimicking actual released materials from coatings and polymer nanocomposites by producing what is called “Fragmented Products” (FP). These FP can further be exposed to environmental conditions (e.g. humidity, light) to produce “Weathered Fragmented Products” (WFP) or can be subjected to a further size fractionation to isolate “Sieved Fragmented Products” (SFP) that are representative for inhalation studies. In this perspective we describe the approach, and the used methods to obtain released materials in amounts large enough to be suitable for further fate and (eco)toxicity testing. We present a case study (nanoparticulate organic pigment in polypropylene) to show exemplarily the procedures used to produce the FP. We present some characterization data of the FP and discuss critically the further potential and the usefulness of the approach we developed.

Keywords: engineered nanomaterials, release, aging, weathering, fragmentation, products, polymers, coatings

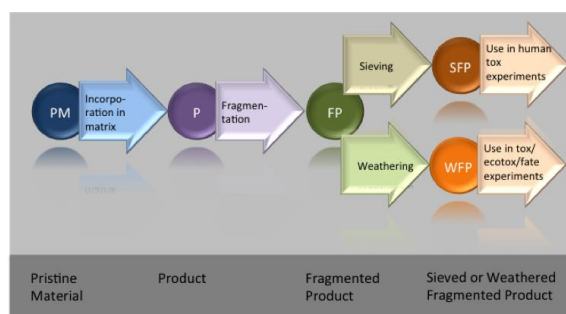


Figure 1: The SUN concept: Pristine nanomaterials are formulated into products that are then fragmented in “Fragmented product (FP)”. These FP can be sieved to produce a fine fraction or weathered to produce weathered fragments. These fragmented products can be used in tox, ecotox and fate studies in large quantities.

References:

1. Nowack, B.; Boldrin, A.; Caballero, A.; Foss Hansen, S.; Gottschalk, F.; Heggelund, L.; Hennig, M.; Mackevica, A.; Maes, H.; Navratilova, J.; Neubauer, N.; Peters, R.; Rose, J.; Schäffer, A.; Scifo, L.; van Leeuwen, S.; von der Kammer, F.; Wohlleben, W.; Hristozov, D. (2016) Meeting the needs for aged and released nanomaterials required for further testing – the SUN approach. *Environ. Sci. Technol.* **50**: 2747-2753.

Resonant Raman scattering methodologies for assessment of nanometric layers in high efficiency chalcogenide solar cells

M. Güç¹, D. Hariskos², W. Hempel², F. Oliva¹, L. Calvo-Barrio^{3,4}, T. Jawhari³, V. Izquierdo-Roca¹, A. Pérez-Rodríguez^{1,4,*}

¹Catalonia Institute for Energy Research (IREC), Sant Adrià del Besòs (Barcelona), Spain

²Zentrum für Sonnenenergie- und Wasserstoff-Forschung Baden-Württemberg, Stuttgart, Germany

³Centres Científics i Tecnològics CCiTUB, Universitat de Barcelona, Barcelona, Spain

⁴IN²UB, Departament d'Electrònica, Universitat de Barcelona, Barcelona, Spain

*E-mail: aperezr@irec.cat

Abstract:

High efficiency chalcogenide solar cell architectures involve the integration of buffer nanometric layers for the formation of the device heterojunction. This includes mainly CdS layers with thicknesses in the range of 30-60 nm, and alternative Cd-free layers based on Zn(O,S) and Zn(S,Se) alloys have more recently been developed. In all cases, control of the thickness and composition of the layers are relevant to achieve high performance devices. However, assessment of these parameters is currently compromised by their nanometric thickness. In this framework, this work reviews the development of resonant Raman scattering methodologies for the quantitative assessment of the thickness and composition of the buffer layers. The analysis of the data obtained from different kinds of layers confirms the potential of Raman scattering based techniques for the non-destructive monitoring of these nanometric layers in advanced high efficient devices.

Keywords: resonant Raman scattering, thin film solar cells, chalcogenide solar cells.

Thin film solar cells based on chalcogenide semiconductors have a strong interest because of their potential for the achievement of cost-effective devices. This includes more mature chalcopyrite Cu(In,Ga)(S,Se)₂ (CIGS) technologies that have recently achieved a record cell efficiency of 22.3% [1] and are already at the industrial stage, as well as emerging kesterite Cu₂ZnSn(S,Se)₄ (CZTS) based devices that avoid the use of scarce elements, being very well suited for their sustainable deployment at Terawatt levels. Main advantages of these technologies are related to

their high potential for reduction of production costs as well as their high technological flexibility, which allows the development of cost-effective devices with weight and shape well adapted to different customized applications, as building integration.

In these technologies, the device architecture includes a nanometric n-type (buffer) layer located between the p-type chalcogenide absorber and the transparent conductive oxide window layer. This buffer layer has typically a thickness in the range 20 – 40 nm. Currently, most of processes implemented at industrial scale use a CdS buffer layer. However, the relatively low bandgap of CdS limits the device performance in the UV region. This, together with concerns related to the high toxicity of Cd, have motivated the development of alternative Cd-free layers as those based in Zn(O,S) or Zn(S,Se) alloys. In all these cases, it is very important to control the presence of thickness and composition inhomogeneity in the grown layers. This is strongly relevant because layer and process inhomogeneity are responsible of the significant reduction of the efficiency of the solar modules in relation to those achieved at cell level. Control of these inhomogeneity implies the need for reliable and high sensitivity tools (if possible non-destructive) allowing their detection at early process stages. However, in the case of the buffer layers, this is compromised by their nanometric thickness.

In this framework, this work reports the development of resonant Raman scattering methodologies for the non-destructive assessment of these buffer nanometric layers. Raman scattering is a non-destructive technique well suited for these applications, being the Raman spectra sensitive to structural and chemico-physical

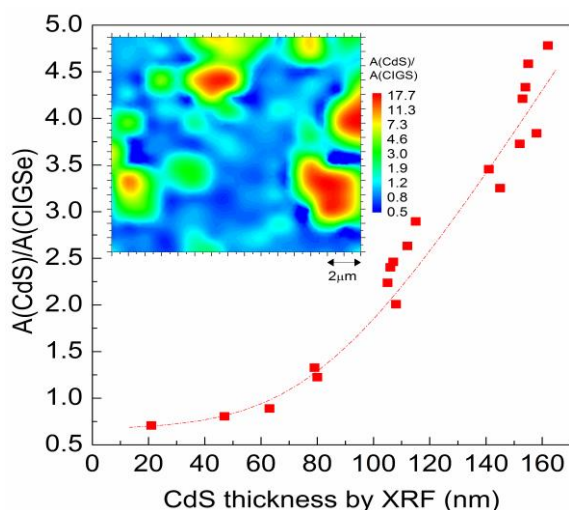


Figure 1: Dependence of CdS thickness on relative integrated intensity of CdS and CIGSe peaks. The inset shows the mapping of a CdS layer region $50 \times 50 \mu\text{m}^2$.

properties of the layers that have a direct impact in the device efficiency. In addition, the use of near resonant excitation conditions (where the excitation wavelength approaches a real energy level in the band structure) leads to a strong enhancement in the intensity of the Raman peaks, overcoming the problems related to the nanometric layer dimensions. This also allows a strong decrease of the measuring time, achieving times compatible with the implementation of the technique as in-situ/on-line process monitoring tool in industrial processes. The technique can also be easily coupled to mapping facilities at macroscopic and microscopic levels, for the detection of the layer inhomogeneity with different spatial resolutions.

Detection of thickness inhomogeneity is based on the strong dependence of the intensity of the Raman peaks on the layer thickness, as shown in Figure 1. This figure plots the relative integral intensity of the main CdS Raman peak in relation to that of the underlying absorber that has been measured on reference CIGS cells that were fabricated with CdS buffer layers with different thicknesses. This dependence has also been applied for the detection of microscopic thickness inhomogeneity as shown in the inset.

On the other hand, one of the main challenges for the alternative buffer layers based on Zn(O,S) or Zn(S,Se) solid solutions is related with the control of the alloy composition. In these systems, resonant excitation conditions show a dependence on the alloy composition. In

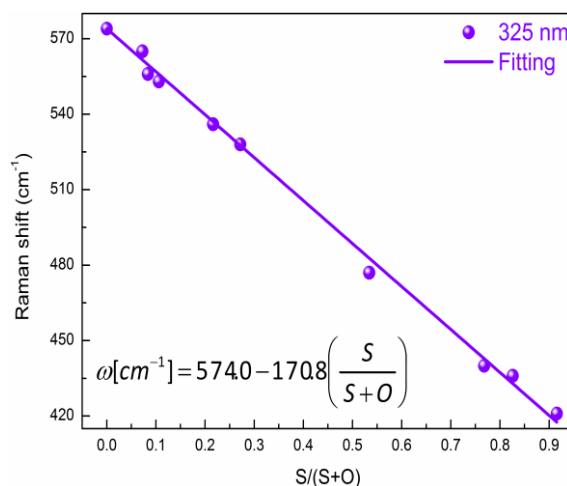


Figure 2: Frequency of ZnO-like Raman peak versus $S/(S+O)$ ratio measured from Zn(O,S) solid solutions. The solid line represents the linear fit to the experimental data.

these cases, different methodologies are developed for the quantitative assessment of the composition at the different layer composition regions, based in the analysis of both the frequency and the relative intensity of the main Raman peaks [2,3].

Figure 2 shows an example of this methodology, based on the existence of a simple linear dependence of the frequency of the ZnO-like Raman peak from Zn(O,S) on the alloy composition. Even if this linear behavior holds in almost all the composition region (from stoichiometric ZnO to very close to stoichiometric ZnS), the need to keep resonant excitation conditions for the measurement of nanometric layers conditions the applicability of this methodology for layers with composition close to $S/(S+O) = 0.5$. In this case, the analysis of the relative intensity of the ZnS like Raman peak gives an alternative procedure for the high sensitivity assessment of the layer composition. Detailed analysis of the intensity of the ZnS and ZnSe like peaks also provides with similar methodologies for the quantitative assessment of the buffer composition.

References:

1. Press release: “Solar Frontier Achieves World Record Thin-Film Solar Cell Efficiency 22.3% <http://www.solar-frontier.com/eng/news/2015/C051171.html>
2. M. Dimitrievska et al, *Phys. Chem. Chem. Phys.*, DOI: 10.1039/C5CP04498G
3. M. Guc et al, *RCS Advanced* (submitted).

Nanotech France 2016 Session III

NanoBioMedecine / Nanosafety

Engineered cell wall binding domains of lysins for the multiplexed detection and rapid separation of food-borne pathogens

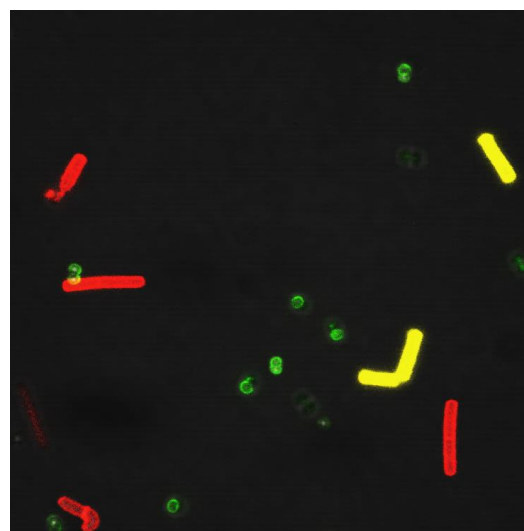
Minsuk Kong, Sangryeol Ryu

Department of Food and Animal Biotechnology, Department of Agricultural Biotechnology, Research Institute for Agriculture and Life Sciences, and Center for Food and Bioconvergence, Seoul National University, Seoul, 151-921, South Korea

Abstract:

Novel and specific bioprobes are an essential part in biosensors for detection of pathogenic bacteria. Although antibodies are the most commonly used biorecognition elements, they are suffered from cross-reactivity and high production cost. Recently, phages have gained increasing interest as alternatives to antibodies due to the host specificity and low-cost. However, lysis-mediated phage infection process remains a burden for the reliable detection methods. Here, we produced engineered cell wall binding domains (CBD) of several phage lysins in *E. coli* and tested their feasibility as new probes to detect multiple pathogens. Confocal laser scanning microscopy revealed that the three different pathogens (*Bacillus cereus*, *Staphylococcus aureus*, and *Clostridium perfringens*) were clearly identified by its colors and the presence of non-target bacteria did not interfere with the target-specific binding property of each CBD. The magnetic nanoclusters (MNCs) coated with CBD can be used to separate and concentrate the target bacteria from liquid sample. The CBD-coated MNCs achieved 70 to 90% capture of target bacteria with less than 10% non-specific recovery, showing better cell capture efficiency than a commercial antibody-based immunomagnetic separation. This CBD-based magnetic assay is useful for pre-analytical sample processing, especially for separating target bacteria from complex food matrices. In addition, CBDs-coated MNCs can be easily incorporated to other rapid biosensing platforms and thus offer a great potential in developing CBD-based biosensors.

Keywords: Bacteriophage, lysin, cell wall binding domain (CBD), magnetic nanoclusters (MNCs), detection, fluorescence, bioprobes, pathogenic bacteria



bacteria were labeled by three CBD fusion proteins with different fluorescent markers. EGFP-SA_CBD for *S. aureus* (green), mCherry-BC_CBD for *B. cereus* (red), and EYFP-CP_CBD for *C. perfringens* (yellow).

References:

- Kretzer et al., (2011) Use of high-affinity cell wall binding domains of bacteriophage endolysins for immobilization and separation of bacterial cells, *Appl. Environ. Microbiol.*, 73, 1992-2000.
- Kong et al., (2015) A novel and highly specific phage endolysin cell wall binding domain for detection of *Bacillus cereus*, *Eur. Biophys. J.*, 44, 437-446.
- Chen et al., (2015) Bacteriophage-based nanoprobe for rapid bacteria separation, *Nanoscale*, 7, 16230-16236.

Figure 1: Simultaneous detection of multiple pathogens in liquid sample. Multiple pathogenic

Selective cancer cell toxicity and radiosensitization using mixed-oxide high atomic number nanoparticles

Sophie Grellet¹, Søren Kaas¹, Eleanor Crabb¹, Sarah Allman¹, Jon Golding,¹

¹The Open University, Milton Keynes, UK

Abstract:

Radiotherapy is currently used in around 50% of cancer treatments. Although it is generally effective, it is damaging to surrounding healthy tissues. This damage can be reduced by better targeting to cancer cells. Improved radiotherapy outcomes can be achieved by targeting heavy elements to cancer cells, since these produce energetic electrons and free radicals upon irradiation that further increase the effectiveness of radiotherapy. Because of their biocompatibility and amenability to surface modification, gold nanoparticles (AuNPs) show significant promise in this area. We observe that acute 3hr exposure of cells to 2nm gold nanoparticles, bearing a 50:50 ratio of alpha-galactose and PEGamine ligands, results in selective chemotoxicity toward cancer cells at nanomolar concentrations, without affecting normal cells (Figure 1). Chemotoxicity is prevented by antioxidant co-administration and is partially prevented by a pan-caspase inhibitor (Z-VAD-fmk). Our initial results suggest that AuNP toxicity is additive with using X-ray radiotherapy. Cerium oxide NPs are one of the most studied metal oxides NPs due to their high redox and oxygen transport properties [1]. They are interesting for radiotherapy applications because they adsorb oxygen and may therefore favour the radiolytic production of oxygen-containing free radicals, especially under low-oxygen conditions, such as the environment of most solid tumours. The surface oxygen vacancy of ceria NPs therefore makes them an interesting tool for pro-oxidant properties [2,3].

Nevertheless, the potential of ceria as a radiosensitiser has not been investigated extensively as it has a relatively low atomic number. It will therefore produce a low flux of secondary electrons upon irradiation which could potentially displace the adsorbed oxygen.

We have been working on the fabrication of mixed ceria NPs, incorporating gold or bismuth, to increase the flux of secondary electrons (Figure 2). It is hoped these effects combined will further facilitate the localized generation of ROS and increase effectiveness of targeted radiotherapy. We predict that these new mixed-oxide ceria NPs will have better radiosensitisation potential than

pure ceria NPs, and could be used to effectively target hypoxic cancer cells.

Keywords: nanoparticles, chemotherapeutic, radiosensitizer, cancer cell targeting, reactive oxygen species production, ROS, uptake, toxicity

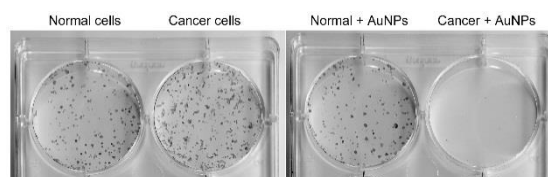


Figure 1. Six-day clonogenic assay of HSC-3 cancer cells and HaCaT normal cells, with or without acute exposure to at 10 µg/ml AuNPs

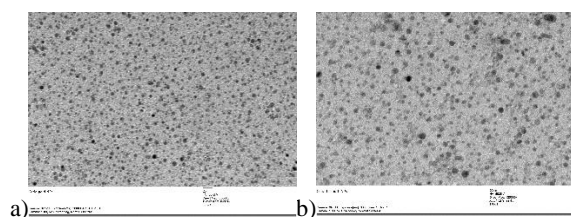


Figure 2: NPs observed by transmission electron microscopy (average size 3 nm). a) ceria-gold NPs ; b) ceria-bismuth NPs

References:

1. Sun, C., Li, H., Chen, L. (2012) Nanostructured ceria-based materials: synthesis, properties, and applications. *Energy & Environmental Science* 5: 8475-8505.
2. Celardo, I., Pedersen, J.Z., Traversa, E., Ghibelli, L. (2011) Pharmacological potential of cerium oxide nanoparticles. *Nanoscale* 3: 1411-1420.
3. Goharshadi, E.K., Samiee, S., Nancarrow, P. (2011) Fabrication of cerium oxide nanoparticles: Characterization and optical properties. *Journal of Colloid and Interface Science* 356: 473-480.

Doxorubicin-loaded BN Nanoparticles for Cancer Therapy

I.V. Sukhorukova¹, I.Yu. Zhitnyak², A.M. Kovalskii¹, N.A. Gloushankova², D.V. Golberg³, D.V. Shtansky¹

¹National University of Science and Technology "MISIS", Leninsky prospect 4, Moscow, 119049, Russia, irina_btnn@mail.ru

²N.N. Blokhin Russian Cancer Research Center, Kashirskoe shosse 24, Moscow 115478, Russia

³National Institute for Materials Science (NIMS), Namiki 1-1, Tsukuba, Ibaraki 3050044, Japan

Abstract:

Nanoparticles (NPs) have a great potential as nanosized drug delivery carriers. Such systems must safely deliver the drug to the site of tumor without drug leakage, effectively penetrate inside cancer cells, and provide intracellular drug release. However, although nanoparticles offer many advantages as drug carrier systems, there are still many limitations to be solved such as instability, inadequate tissue distribution, small drug loading and toxicity. The present work is focused on the fabrication of BN nanoparticles (BNNPs) with a petal-like surface structure, which are able to absorb a large amount of anti-tumor drug, and their utilization by neoplastic cells.

The BNNPs were prepared by chemical vapor deposition (CVD) method using boron oxide vapor and flowing ammonia in a vertical induction furnace. The temperature in the precursor location area was maintained at 1310°C. The powder mixture of pure FeO, MgO, and B was used as a precursor. In order to separate the agglomerates into individual nanoparticles, BNNPs were ultrasonically treated in a distilled water solution (BNNPs concentration 2 mg/ml). Thorough structural characterization revealed that the surface of hollow BNNPs had been made of numerous nanosheet petals (Fig.1). The chemical treatment in Earle's balanced salt solution for 14 days did not affect the average size and morphology of BNNPs. The BNNPs loaded with Doxorubicin (DOX) were stable at neutral pH but effectively released DOX at pH 4.5–5.5. MTT assay and cell growth tests showed that BNNPs-DOX had been toxic for neoplastic IAR-6-1 cells.

The cytotoxicity of BNNPs-DOX was comparable with free DOX at identical concentrations in the range of 0.26–1.04 µg/ml. The BNNPs-DOX nanocarriers were internalized into IAR-6-1 neoplastic cells using endocytic pathways, and then DOX was released from nanosized drug delivery carriers and accumulated both in nuclei and cytoplasm resulting in cell death.

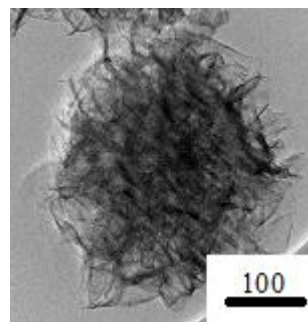


Figure 1. TEM image of BN nanoparticles

Compared with other known nanosystems for targeted drug delivery, BNNPs has a number of advantages: BNNPs is not toxic; has high chemical stability; particle spherical shape is optimal for uptake by tumor cells, BNNPs have an optimal size 100–150 nm both in terms of drug loading and uptake by the tumor cells; high specific surface area, the presence of the internal cavity and hexagonal structure with a high lattice parameter (high interplane distance between the basal planes) are beneficial in terms of sorption capacity and effective drug release. In addition, BN nanostructures with different morphologies can be obtained in a single process cycle that does not require further processing, for instance, creating mesoporous structures on their surface.

Future works will be focused on the additional functionalization of BNNPs to further improve their biological performance.

Keywords: BN nanoparticles, chemical vapor deposition, neoplastic cells, drug delivery nanocarriers, doxorubicin, drug release

Antimicrobial electrospun nanofibrous scaffolds for gingival fibroblast growth

A. Baranowska-Korczyn.^{1*} M. Jasiurkowska-Delaporte¹, B. Grześkowiak,¹
M. Jarek,¹ A. Warowicka,¹ B. M. Maciejewska,^{1,2} J. Jurga-Stopa,³ S. Jurga^{1,2}

¹NanoBioMedical Centre, Adam Mickiewicz University, Umultowska 85, PL-61614 Poznań, Poland

² Department of Macromolecular Physics, Faculty of Physics, Adam Mickiewicz University, Umultowska 85, PL-61614 Poznań, Poland

³Department of Biomaterials and Experimental Dentistry, Poznań University of Medical Sciences, Fredry 10, PL-61701 Poznań, Poland

*akorczyn@amu.edu.pl

Abstract:

In recent years, tissue engineering has focused on designing three-dimensional (3D), biocompatible, antimicrobial nanomaterials for regenerative medicine, drug delivery systems and wound dressing. A large range of nanostructures have been employed to give mechanical support for cell proliferation and differentiation, or have been combined into composite scaffolds to improve their physio-chemical properties. 3D structure, large surface to volume ratio, and similarity to the fibrous architecture of the extracellular matrix (ECM) make electrospun nanofibrous scaffolds one of the most attractive materials for tissue engineering applications.¹

In this study, the PCL (Fig. 1) and PVP electrospun nanofibers were applied as human gingival fibroblast (HGF-1) scaffold and antimicrobial membranes for potential dental purposes. The nuclei and cytoskeleton morphology of HGF-1 cells grown on both types of nanofibers was unchanged. The direction of cell growth was governed by nanofiber number and alignment. Hydrophilic PVP nanofibers demonstrated low stability in a biological environment in comparison to hydrophobic PCL nanofibers. In addition, antibiotics were incorporated within the nanofibers. PCL/ampicillin mats were successfully prepared using a drum collector. The composed nanofibers were studied by Raman spectroscopy and DSC analysis. Conductivity measurements of the soaking solution using Broad Band Dielectric methods found the mechanism of drug release to be based on Fickian diffusion, and the WST-1 test found the PCL and PCL/ampicillin nanofibers to have minimal cytotoxicity. The mats released antibiotics and showed antibacterial activity against a selected dental caries pathogen. The zone of growth inhibition for *Streptococcus*

sanguinis was directly proportional into the content of ampicillin incorporated to the mats.

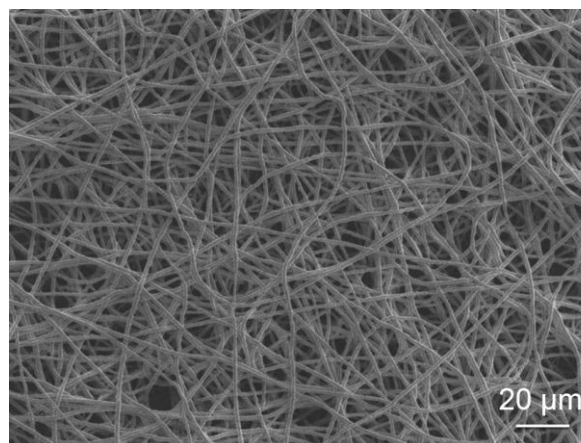


Figure 1: SEM image of PCL nanofibers.

Keywords: electrospinning, nanofibers, scaffolds, dental applications, gingival fibroblasts, HGF-1, antibacterial activity

Acknowledgments

The research was supported by the National Science Centre (Grant Sonata 6: UMO-2013/11/D/ST5/02900), the European Social Fund (POKL.04.03.00-00-015/12) and Nation Centre for Research and Development (Grant: PBS1/A9/13/2012).

References:

Agarwal, S., Wendorff, J.H., Greiner A. (2009), Recent Advances in Electrospun Nanofibrous Scaffolds for Cardiac Tissue Engineering, *Advanced Functional Materials*, 21, 3343–3351.

Development of new biocompatible β -Ti coatings on Ti6Al4V for medical applications

E. Frutos¹, T. Polcar^{1,2}

¹ Department of Control Engineering, Faculty of Electrical Engineering, Czech Technical University in Prague, Technická 2, Prague 6, Czech Republic

² National Centre for Advanced Tribology (nCATS), University of Southampton, University Road, Southampton SO17 1BJ UK.

Abstract: Around 70-80% of implants are still made of the traditional metallic materials (Stainless steel, Co-Cr alloys and Ti alloys). These materials are not free of interactions with the physiological environment, since its high chloride ions content together to the biological macromolecules and proteins activity are able to influence corrosion, increasing the ion release into surrounding tissue of alloying elements such as nickel (Ni), presents in stainless steel and Co-Cr alloys, which is widely recognized as a high risk element from the point of view of incompatibility problems [1]. Others elements such as vanadium (V) and aluminium (Al), usually used in development of Ti alloys for biomedical applications, have shown be a cause of Alzheimer's disease [2] and neurotoxic [3], respectively. On the other hand, Young's modulus of these materials are higher compared with bone. This produces negative effects as stress shielding, in prosthesis with a great load bearing, which may lead to bone atrophy and a poor bone remodelling.

Recently, low modulus Ti alloys, composed of non-toxic elements, have been developed for biomedical applications. Its values lie between around 40 and 80 GPa. Nevertheless, Young's modulus values can be lowered by processing control the texture, and therefore these may be similar to the top of the range for bone (30 GPa). However, these β -Ti alloys not show higher structural stiffness and therefore their use is quite limited. Thereby, the development of surface modifications or coatings with higher biocompatibility and better mechanical properties able to increase osseointegration of the implant, minimizing effects as stress shielding, is fundamental.

Sputtering techniques are extremely versatile with great potential to produce nanostructured, homogeneous, dense, compacts and free-cracks coatings. Therefore it could be a new route to produce β -Ti textured coatings on Ti or stainless steels alloys, free of toxic elements. The focus of

this work is to produce different ternary (Ti-Nb-Zr and Zr-Nb-Ti) coatings with dissimilar stoichiometry in order to get coatings with low Young's modulus (β -Ti phase) in order to get a better load transfer between bone and metallic surface. Research in this area is still in an embryonic state with no relevant studies published in the area of the coating materials referred to above.

Results regarding to grain size, texture and residual stress magnitude of Ti-20Nb-XZr (X=7, 13, 20, 25 w.%) and Zr-20-YTi (Y=7, 13, 20, 25 w.%), as a function of sputtering conditions, will be shown. Of particular interest will be the changes in the residual stress values along the thickness, manifested by Ti-20Nb-13Zr, as a function of bias voltage on the substrate. Furthermore we will correlate the magnitude of this residual stress with the higher or lower percentage of β -Ti phase (BCC phase) inside of the coating. Since higher BCC phase concentration is fundamental in order to get a lower Young's modulus, and therefore produces coatings with a lower stress shielding able to reduce the failure of the implant as a consequence of bone atrophy and a poor bone remodelling when there is a big difference in the Young's modulus values between metallic implant and surrounding bone tissue.

Keywords: β -Ti alloys, residual stresses, Young's modulus, X-ray diffraction biomedical applications.

References:

1. P.J. Uggowitzer, W-F. Bähre, MO Speidel. Adv Powder Metall Part Mater 1997;3:113-121.
2. D.P. Perl, A.R. Brody. Science. 1980;208:297-299.
3. B. Boyce, J. Byars, S. McWilliams, M. Mocan, H Elder, I boyle, et. al. Br Med J. 1992;45:502-508.

Wound healing evaluation of collagen-laminin dermal matrix

E.H. Gokce¹, S. Tuncay-Tanriverdi¹, İ. Eroglu², N. Tsapis³, I. Tekmen⁴, E. Fattal³, O. Ozer¹

¹University of Ege, Faculty of Pharmacy, Dept. of Pharmaceutical Technology, 35100, Izmir, TURKEY

²Hacettepe University, Faculty of Pharmacy, Dept. of Basic Pharmaceutical Sciences, 06100 Ankara, Turkey

³Univ Paris-Sud, Institut Galien Paris-Sud, CNRS UMR 8612, LabEx LERMIT, Faculté de Pharmacie, 5 rue J.B. Clément, 92296 Châtenay-Malabry, FRANCE

⁴Dokuz Eylul University, School of Medicine, Dept. of Histology and Embryology, 35340, Izmir, TURKEY

Abstract: Dermal matrices (DM) containing compounds that provide required mechanical support while speeding up the healing of wounds have been suggested as an alternative strategy, for chronic diabetic wounds (1). A three dimensional collagen-laminin porous DM was prepared for this aim. DM was fabricated by freeze-drying (Alpha 1-2 LO plus, UK) and cross-linked by UV-light (UVP-CL 1000, UK). The diameter:thickness ratio of DM-MP-RSV was determined as 2.24 ± 0.05 cm: 0.64 ± 0.04 cm. The distribution of laminin was checked by confocal laser scanning microscopy (Zeiss LSM/510/ 1mW Helium Neon). A confocal microscope was used to observe at a wavelength of $\lambda_{ex} = 543$ nm and $\lambda_{em} = 570$ nm/620 nm for Rhodamine B and Nile red; $\lambda_{ex} = 486$ nm and $\lambda_{em} = 515$ nm for FITC. As seen in Fig 1. laminin (in red) was homogenously distributed on the collagen fibers (in green).

Texture profile analysis (TPA) was performed on DM before and after UV cross-linking, using a software-controlled penetrometer (TA-TX Plus, Stable Micro Systems, Godalming, UK). Texture profile analysis determined that cross-linking was required for mechanical support. The results obtained after crosslinking were as the following: 21.2 ± 0.5 N for hardness, 18.3 ± 0.3 N.mm for compressibility, 1.01 ± 0.01 for cohesiveness and 0.963 ± 0.1 for elasticity. The water content of DM was determined by thermal gravimetric analyzer (TGA-4000, Perkin Elmer). TGA studies showed that water uptake capacity was 84.2%. Collagenase was dissolved in pH 7.4 PBS to give a concentration of 28 unit/mL. These mixtures were incubated at 37 °C for 10 min to keep enzymes active and mixed with a magnetic stirrer. DM was added to the enzyme solution and the degradation time was observed as 30 min.

Wistar albino rats received streptozotocin (60 mg/kg) intraperitoneally for induction of diabetes (2). After the treatment with DM at 17th day, histopathological evaluations were conducted for observation with light microscopy. Histopathological studies revealed that collagen fibers were intense and improved by the presence of formulation without any signs of inflammation. The remodeling phase of wound was completed.

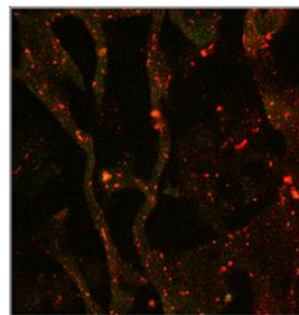


Figure 1: CLSM images of DM, collagen fibers of dermal matrix in green, laminin in red

Keywords: wound healing, dermal matrix, tissue, collagen, laminin, *in vivo* wound model

Acknowledgements

This study (No:111S183) was granted by TUBITAK 1001. Authors thank FABAL for TGA facilities.

References:

1. Huang, S., Fu, X., (2010) Naturally derived materials-based cell and drug delivery systems in skin regeneration, *J. Control. Release*, 142, 149-159.
2. Kant, V., Gopal, A., Pathak, N.N., Kumar, P., Tandan, S.K., Kumar, D., (2014) Antioxidant and anti-inflammatory potential of curcumin accelerated the cutaneous wound healing in streptozotocin-induced diabetic rats, *Int. Immunopharmacol.* 20, 322-330.

Nanostructured Copper Hydroxide on Graphene Pore Structure for Non-enzymatic Electrochemical Glucose Sensor

I. Shackery,¹ S. C. Jun,^{1,*}

¹ School of Mechanical Engineering, Yonsei University, Seoul 120-749, Republic of Korea

Abstract:

The glucose sensing has wide range of application with significant role in clinical diagnostics, food industry and biotechnology [1]. The crucial importance of glucose sensors make it necessary to develop fast, accurate and reliable methods for glucose determination. The commercial glucose sensors are based on the enzymes which provide good selectivity and high sensitivity. But they are suffer from thermal and chemical instability, sensitivity to temperature, pH and humidity which comes from the nature of enzymes. Thus, to overcome above-mentioned drawbacks of enzyme based glucose sensors, several attempts have been done in order to achieve a simple, cheap, accurate and fast enzyme-free glucose sensor.

We report the synthesis of the flower-like nanostructure of copper hydroxide ($\text{Cu}(\text{OH})_2$) on freestanding graphene pore structure (GPS) via a simple and cost-effective chemical bath deposition (CBD) method. The CBD is a facile method which provide relatively inexpensive, simple and convenient route for large area deposition. Meanwhile electrochemical sensors are simple, operative, sensitive, high time efficiency and reasonably inexpensive compare to other methods. The structural and morphological characterization of $\text{Cu}(\text{OH})_2$ reveals that, $\text{Cu}(\text{OH})_2$ nano structure, consists of nanorods (diameter ~ 100 nm), are well covered over the porous graphene framework (Figure 1). The electrocatalytic activity of the nanocomposite, investigated by cyclic voltammetry (CV) and amperometric methods. The nanostructure morphology leads to be a high specific surface area, which provides the structural foundation for the high sensitivity. Significantly, $\text{Cu}(\text{OH})_2/\text{GPS}$ electrode showed the excellent sensitivity (up to $3.36 \text{ mA mM}^{-1} \text{ cm}^{-2}$), low detection limit ($1.2 \text{ }\mu\text{M}$), wide linear range ($1.2 \text{ }\mu\text{M} \sim 6 \text{ mM}$). The $\text{Cu}(\text{OH})_2/\text{GPS}$ exhibited good reproducibility and excellent selectivity toward usual interfering materials such as lactose, fructose, Acetaminophen, ascorbic

acid, dopamine and urea in 1 M KOH aqueous electrolyte.

Keywords: Non-enzymatic glucose sensor, Graphene pore structure, Metal hydroxide, Bio sensing.

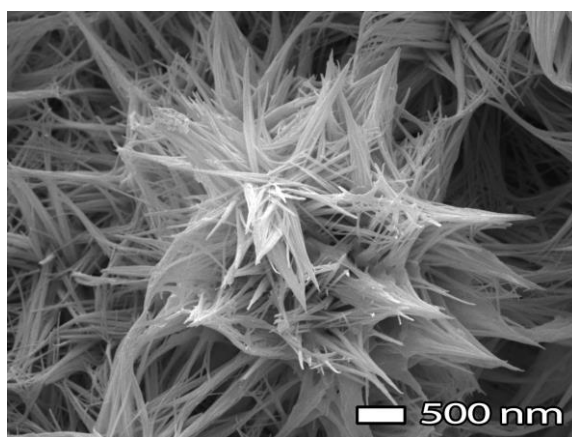


Figure 1: The SEM image of nanostructure copper hydroxide on graphene pore structure.

References:

1. Wang, J., Electrochemical glucose biosensors. *Chemical reviews*, 2008. 108(2): p. 814-825.
2. Shackery, I., Patil, U., Song, M. J., Sohn, J. S., Kulkarni, S., Some, S., ... & Jun, S. C. (2015). Sensitivity Enhancement in Nickel Hydroxide/3D-Graphene as Enzymeless Glucose Detection. *Electroanalysis*, 27(10), 2363-2370..

An innovative detection platform to support nanomedicine characterisation and development

C. Desmet*, A. Valsesia, R. La Spina, P. Urban, F. Rossi, P. Colpo

European Commission Joint Research Centre, Institute for Health and Consumer Protection, NanoBioScience Unit, Italy.

Abstract:

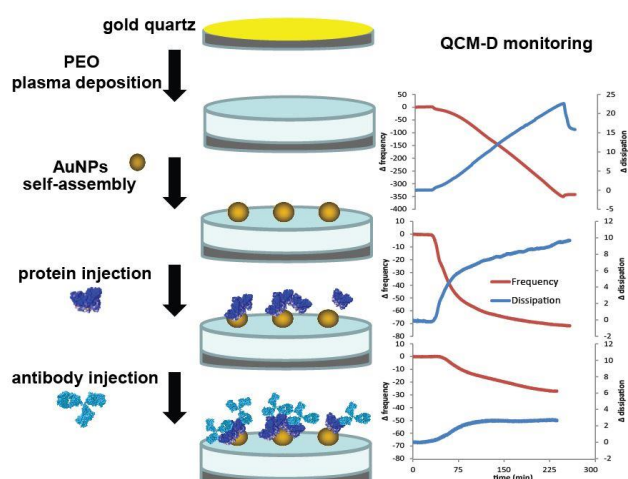
At the interface between nanotechnology and biology, nanomedicine unveils new challenges for the scientific community. While nanoparticles (NPs) represent an opportunity to achieve refined targeting for imaging and selective treatments, NPs modifications for targeting purposes and their interactions with biomolecules have to be well characterized. In particular, the determination of the structure morphology and stability of nanoparticle–protein complexes is important to understand the behaviour of nanoparticles in biological systems. Protein coverage, affinity and structures when interacting with NPs are fundamental parameters to be determined.

In the present study, we propose a straightforward method based on a quartz crystal microbalance with dissipation monitoring (QCM-D) to support the producers in the development and validation of nanomedicines. The platform is based on the surface modification of quartz crystal sensors with a plasma polymerized poly (ethylene oxide), which allows NPs binding while avoiding biomolecules adsorption¹. It enables the direct quantification and characterization of NPs and their interaction with biomolecules. First, the signal measured for NPs adsorption on the substrate was analyzed to quantify the material bound, which was then validated by Scanning Electron Microscopy. Moreover, the frequency and dissipation changes showed to be size-dependent. Those results demonstrated the suitability of the method for NPs size determination. Then, the NPs interaction with biomolecules, and more specifically the protein corona formation was investigated by flowing a serum albumin on the NPs-PEO quartz. The number of proteins per nanoparticle was assessed and validated by comparison with other methods based on size measurement². Finally, the ability of the NP-protein complex to be involved in biomolecular recognition with a specific antibody was evaluated, providing information on the tertiary structure

preservation and accessibility of the binding site. Those promising results demonstrated the potential of the method as a powerful tool for nanomedicine assessment applications.

Figure 1: QCM-D monitoring of the changes on the sensor surface, related to the NPs binding and interactions with biomolecules

Keywords: engineered nanomaterials, nanomedicine assessment, nanoparticles-proteins interactions



tions, quartz crystal microbalance.

References:

1. Muldur S. K. *et al.* (2015) Modulation of surface bio-functionality by using gold nanostructures on protein repellent surfaces, *RSC Advances*, 5, 83187-83196
2. Capomaccio R. *et al.* (2015) Determination of the structure and morphology of gold nanoparticle–HSA protein complexes, *Nanoscale*, 7, 17653-17657

Highly controlled delivery of macromolecules and contrast agents in living cells by laser-induced vapour nanobubbles

Ranhua Xiong^{1,2}, Freya Joris¹, Laura Wayteck¹, Koen Raemdonck¹, Karen Peynshaert¹, Ine Lentacker¹, Ine De Cock¹, Peter Verstraelen⁶, Winnok De Vos⁶, Jo Demeester¹, Stefaan C. De Smedt¹, Andre G. Skirtach^{2,3,4}, Kevin Braeckmans^{1,2,5}

¹Laboratory of General Biochemistry and Physical Pharmacy, Ghent University, Belgium

²Centre for Nano- and Biophotonics, Ghent University, Belgium

³Department of Molecular Biotechnology, Ghent University, Belgium

⁴Max-Planck Institute of Colloids and Interfaces, 14424 Potsdam, Germany

⁵Univ Lille 1, IEMN & PhLAM, F-59652 Villeneuve Dascq, France

⁶Laboratory of Cell Biology & Histology, University of Antwerp, Belgium

Abstract: There is great interest in delivering macromolecular agents like siRNA and contrast agents such as quantum dots into living cells for therapeutic and diagnostic purposes. Although substantial effort has gone into designing non-viral nanocarriers for intracellular delivery of these materials, entrapment in endosomes after endocytocytic uptake remains a major bottleneck. Laser-induced photoporation in combination with plasmonic (e.g. gold) nanoparticles, is an alternative physical method that is receiving increasing attention for delivering macromolecules in cells. By using appropriate pulsed laser light, gold nanoparticles can be quickly heated so that water vapour nanobubbles can emerge in hydrated tissue. When the gold nanoparticles are adsorbed to the cell membrane, these laser-induced vapour nanobubbles can create pores in the membrane. Macromolecules or nanoparticles in the surrounding cell medium can then diffuse through the pores directly into the cell's cytoplasm. Using this photoporation methodology, we have demonstrated that cells can be efficiently transfected with siRNA, including hard to transfect cytotoxic T-cells. In addition, we have shown that vapour nanobubble photoporation is ideally suited for efficient delivery of contrast agents like fluorescent dextrans and quantum dots into cells. Applications range from long-term cell tracking for *in vivo* cell therapies, to labelling of selected cells (e.g. primary neuronal cells) in culture for high-content screening. Combined with the fact that little or no cytotoxicity is induced, we conclude that laser-induced membrane poration by vapour nanobubbles is highly promising delivery method whose applications have only just begun to be explored.

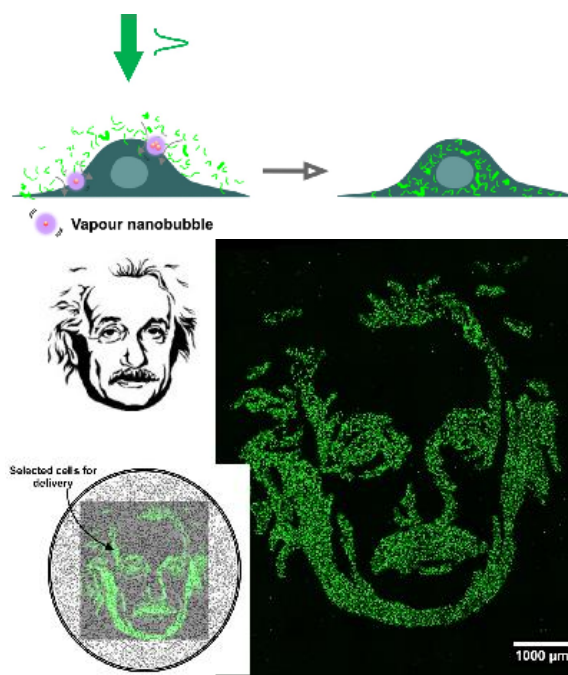


Figure 1: Laser-induced vapour nanobubbles can perforate the cell membrane, allowing therapeutic molecules or contrast agents to enter cells which are irradiated by suitable pulsed laser light.

Keywords: gold nanoparticles, laser therapy, drug delivery, diagnostics, theranostics, bio-imaging.

References:

Xiong R. et al. Comparison of gold nanoparticle mediated photoporation: vapor nanobubbles outperform direct heating for delivering macromolecules in live cells. *ACS Nano* 8, 6288-6296 (2014).

Acknowledgement: KB acknowledges financial support from the European Research Council (ERC) under the European Union's Horizon 2020 research and innovation program (grant agreement No 648124).

Imidazolium-derived nanostructures for drug delivery

M. Rodrigues,^{1,2,*} E. Amirthalingam,^{1,2} D. Limón,^{1,2} A. Calpena,^{2,3} D. B. Amabilino,⁴ L. Pérez-García^{1,2}

¹Universitat de Barcelona, Department of Pharmacology and Therapeutic Chemistry, Barcelona, Spain

²Institut de Nanociència i Nanotecnologia IN2UB, Barcelona, Spain ³Universitat de Barcelona, Department of Pharmacy and Pharmaceutical Technology, Barcelona, Spain ⁴Institut de Ciència de Materials de Barcelona (ICMAB-CSIC), Bellaterra, Spain

Abstract:

Supramolecular chemistry is a discipline that allows the synthesis and assembly of complex nanostructures by strong (covalent) or weak (van der Waals, hydrogen bonds, electrostatic) bonds.

We present here a family of imidazolium-derived gemini-type amphiphilic molecules that can be used to obtain different nanostructured materials.

The imidazolium moiety allows these molecules to interact and stabilize gold nanoparticles (GNP). The synthesis of GNP could be performed using two different methods, either biphasic system through a modification of the Brust-Schiffrin method, or in aqueous medium. The different methods allowed obtaining either organic-soluble or water-soluble monodisperse GNP with diameters between 8 and 10 nm.

On the other hand, the amphiphilic character of the molecules leads to the spontaneous self-assembly of supramolecular gels in an aqueous solution containing ethanol. The formed gels are composed of fibers with approximately 100 nm wide, which fuse and cross forming a network. Each fiber appears to be composed of thinner fibers that are flat, and arrange themselves in bigger structures.

These molecules also present the ability to recognize and complex anions, which allowed incorporating anionic model drugs on the different nanostructures, that could furthermore be released on a sustained manner. Additionally, their toxicity is similar to the one observed for other ionic liquids with similar characteristics, showing promising applications as delivery vehicles.

Finally, the gels could also be used as template for the synthesis of gold nanoparticles with improved monodispersion and defined geometry.

Keywords: gold nanoparticles, supramolecular gels, drug delivery

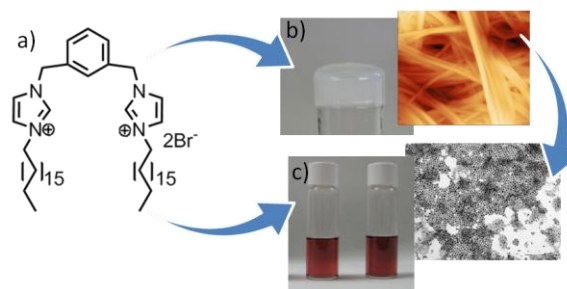


Figure 1: Imidazolium-based amphiphile (a) used to obtain supramolecular gels (b) and gold nanoparticles (c) that furthermore can be synthesized using the gel as template.

References:

Casal-Dujat, L. et al. (2012) Gemini imidazolium amphiphiles for the synthesis, stabilization, and drug delivery from gold nanoparticles, *Langmuir*, **28**, 2368-2381.

Rodrigues, M. et al. (2014) Supramolecular gels based on a gemini imidazolium amphiphile as molecular material for drug delivery, *J. Mat. Chem.*, **2**, 5419-5429.

Rodrigues, M. et al. (2015) In situ template synthesis of gold nanoparticles using a bis-imidazolium amphiphile-based hydrogel, *J. Colloid Interface Sci.*, **446**, 53-58.

Acknowledgements:

This work was supported by the EU ERDF (FEDER) funds and the Spanish Government grants TEC2011-29140-C03-01/02 and TEC2014-5194-C2-1/2.

The development and evaluation of a novel hybrid PLGA nanoparticle-Pheroid[®] system with the potential to improve tuberculosis therapy

Madichaba P Chelopo^{1,2*}, Lonji Kalombo¹, James Wesley-Smith³, Brendon Naicker¹, Matthew Glyn², Anne Grobler², Rose Hayeshi²

¹Polymer and Composites, CSIR Materials Science and Manufacturing, PO Box 395, Pretoria, 0001

²DST/NWU Preclinical Drug development Platform, North-West University, Potchefstroom, 2520

³DST/CSIR National Centre for Nanostructured Materials, , CSIR Materials Science and Manufacturing PO Box 395, Pretoria, 0001

Abstract:

Hybrid drug delivery systems, composed of a polymeric nanoparticles (NPs) core and liposomes have recently emerged in an effort to mitigate some limitations associated with the individual drug delivery systems (1) (2). This study explores the combination of two unique delivery systems namely polymeric poly lactic-co-glycolic acid (PLGA) nanoparticles (NPs) as well as and Pheroid[®] technology. The PLGA NPs with size ranging between 200 to 310 nm were obtained, while free Pheroid vesicles with a wide size range from 100 nm to 4500 nm were acquired. These solid NPs were combined with Pheroid[®] vesicles using two types of mixing approaches named, pre-mix and post-mix. The particle size for the hybrid system ranged from approximately 1990 nm to 2250 nm while the zeta potential ranged from -22 to -25 mV using laser scattering technique. There was an observed increase in the size population of the Pheroid[®] vesicles when combined with NPs depending on the surface charge of the NPs. More physicochemical properties of this novel hybrid were obtained through transmission electron microscopy (TEM) and confocal laser scanning microscopy (CLSM). CLSM images and some TEM images, showed possible localization of the NPs with the vesicles. Biological *in vitro* experiments were conducted to evaluate the effect of this hybrid system on cytotoxicity, permeability as well as uptake using caco-2 cell line. The *in vivo* evaluation of this novel hybrid system was done to investigate its potential application to address challenges in tuberculosis (TB) therapy and South Africa accounts for over 80% of all TB cases worldwide (3). Balb/c female mice were used to determine the pharmacokinetics of anti-TB drug (rifampicin or isoniazid)-loaded hybrid delivery system.

Keywords: PLGA nanoparticles, Pheroid[®] vesicles, Lipid-polymer hybrid nanoparticles, Drug delivery, Tuberculosis, Rifampicin, Isoniazid

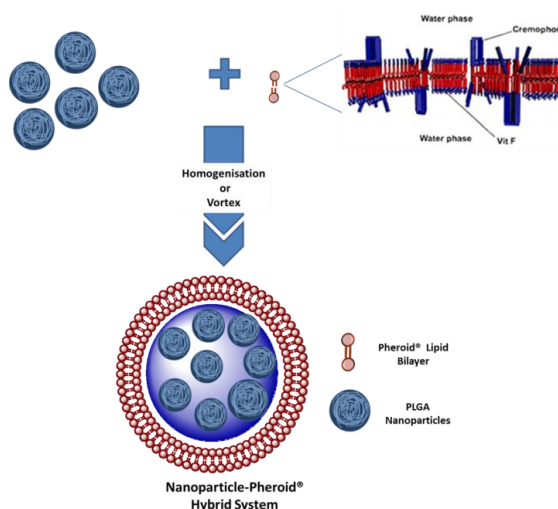


Figure 1: Illustration of the possible combination of Pheroid[®] and NPs to form a novel NP-Pheroid hybrid system.. The optimal combination of the two systems can be determined by a number of factors which include, the charge of the nanoparticle, mixing method and the amount of NPs.

References:

1. Mandal, B. t. c. M. f., Bhattacharjee, H., Mittal, N., Sah, H., Balabathula, P., Thoma, L. A., and Wood, G. C. (2013) *Nanomedicine: Nanotechnology, Biology and Medicine* **9**, 474-491
2. Zhang, L., Chan, J. M., Gu, F. X., Rhee, J.-W., Wang, A. Z., Radovic-Moreno, A. F., Alexis, F., Langer, R., and Farokhzad, O. C. (2008) *ACS Nano* **2**, 1696-1702
3. WHO. (2013) Global Tuberculosis Report. World Health Organization

A novel SPION-eicosane coating material for on-demand drug release triggered by magnetic hyperthermia

L. Che Rose,^{1*} A.G. Mayes², H. Suhaimi¹.

¹University Malaysia Terengganu, School of Fundamental Science, Universiti Malaysia Terengganu, 21030 Kuala Terengganu, Terengganu Darul Iman, Malaysia

²School of Chemistry, University of East Anglia, Norwich Research Park, Norwich, NR4 7TJ, UK

Abstract:

An orally-administered system for targeted, on-demand drug delivery to the gastrointestinal (GI) tract is highly desirable due to the high instances of diseases of that organ system and harsh mechanical and physical conditions any such system has to endure. To that end, we present an iron oxide nanoparticle/wax composite capsule coating using magnetic hyperthermia as a release trigger. The coating is synthesised using a simple dip-coating process from pharmaceutically approved materials using a gelatin drug capsule as a template. We show that the coating is impervious to chemical conditions within the GI tract and is completely melted within two minutes when exposed to an RF magnetic field under biologically-relevant conditions. The overall simplicity of action, durability and non-toxic and inexpensive nature of our system demonstrated herein are key for successful drug delivery systems. Selective targeting of such drug delivery systems has focused largely on the conjugation of cancer targeting tags (proteins, peptides, sugars) to nanoparticle surfaces and surface coatings or as part of micellar systems. These have proved of limited value due to size restrictions placed on such constructions by the reticuloendothelial system, which clears foreign bodies above 20 nm in [hydrodynamic] diameter. Many systems focus on the treatment of tumours via the vascular network, but as yet, “on-demand” drug delivery systems for exclusive use in the GI tract are underdeveloped. Current systems rely on simple pH switches or degradation through bacterial enzyme action, which can be somewhat unpredictable and offers limited control. To address this problem, we propose a drug delivery system for use in the GI tract, with potential for magnetic targeting and tracking, which can release its payload on demand using localised

magnetic hyperthermia to trigger release. The system we propose is shown in Fig. 1.

Keywords: gastrointestinal (GI) tract, iron oxide nanoparticle, drug deliver, hyperthermia

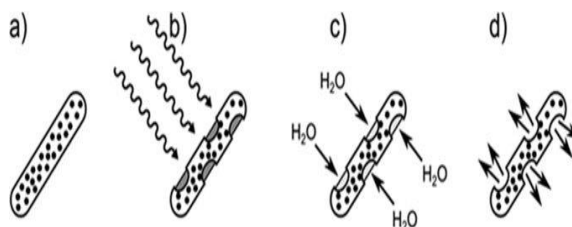


Figure 1: The process of capsule exposure and drug release: (a) An iron oxide and eicosane coated capsule, (b) upon exposure to radiowaves, heating occurs causing melting and formation of holes in the coating and exposure of the capsule to the surrounding environment, (c) fluid ingress cause capsule dissolution and (d) drug release

References:

1. Friend, D. R New Oral delivery systems for treatment of inflammatory bowel disease. *Adv. Drug Deliv. Rev.* 57, 247-265 (2005)
2. Lautenschlager. C., Schmidt, C., Fischer, D. & Stallmach. A Drug delivery startegies in the theraphy of inflammatory bowel disease . *Adv. Drug Deliv. Rev.* 71, 58-76 (2014)

Morphology effect of mesoporous silica nanoparticles on drug delivery

Saher Rahmani^{1,2}, Laure Lichon³, Marie Maynadier³, Marcel Garcia³, Magali Gary-Bobo³, Mokhtar Ferid², Clarence Charnay¹ and Jean Olivier Durand¹

¹ Institut Charles Gerhardt Montpellier, UMR-5253 CNRS-UM2-ENSCM-UM1cc 1701, Place Eugène Bataillon, F-34095 Montpellier cedex 05, France.

² Laboratoire de Physico-Chimie des Matériaux Minéraux et leurs Applications, Centre National de Recherches en Sciences des Matériaux, B.P. 95, Hammam-Lif 2050, Tunisia

³ Institut des Biomolécules Max Mousseron, UMR 5247 CNRS, UM-ENSCM, 15 Avenue Charles Flahault, 34093, Montpellier Cedex 05, France

Abstract: Mesoporous silica nanoparticles (MSNs) have recently attracted much attention in the biomedical field due to their unique characteristics, including high surface area, large pore volume, and uniform porosity, excellent biocompatibility and in vivo biodegradability [1] making them ideal candidates for drug delivery [2].

The interaction between MSNs and cells has been studied extensively, but the effect of nanoparticles shape on cell behavior has received little attention.

Recent observations in biological systems suggest that physical parameters of nanoparticles, like shape, size and surface charge, can effect their nonspecific uptake into cells [3]. Particle shape has been considered to play an important role in both the systemic distribution of nanoparticles and the cellular interactions with nanoparticles. Shape is an important physical characteristic that has an important role in modeling cellular responsiveness and associated application in biotechnology[4]. However only few reports described how nanospherical silica nanoparticles effect drug delivery.

In the current work the influence of MSN shape on the effectiveness of drug delivery was investigated with special emphasis on cancer therapy. In this study we designed a series of MSNs with controlled shape: sphere and rod exhibiting similar chemical composition, by controlling the ratio of reagents in sol gel reaction.

Owing to their high porosity and a high specific surface area ($930 \text{ m}^2\text{g}^{-1}$), the various shape of MSN were then applied as drug nano-carriers and loaded with doxorubicin. The loading capacities were calculated from the UV-visible analysis of the supernatant reaching up to 20 and 30 % of Dox loaded in MSNs.

We reported here that the interaction of nanoparticles with cells (MCF 7) and the drug delivery efficiency are enhanced by particle shape and

a very efficient cancer cell killing was observed with MSN-Rod.

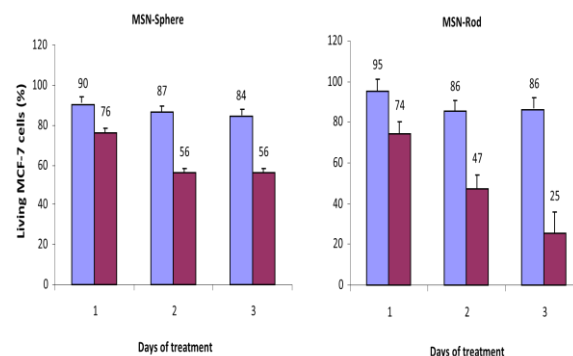


Figure : Cytotoxicity of the MSN-Sphere and MSN-Rod on MCF-7 cancer cells.

Keywords: Mesoporous silica nanoparticles, doxorubicin, drug delivery, biomedical applications.

References:

1. Tarn, D.; Ashley, C. E.; Xue, M.; Carnes, E. C.; Zink, J. I.; Brinker, C. J. Mesoporous Silica Nanoparticle Nanocarriers: Biofunctionality and Biocompatibility. *Acc. Chem. Res.* 2013, 46, 792–801.
2. C. Mauriello-Jimenez, J. Croissant, M. Maynadier, X. Cattoen, M. Wong Chi Man, J. Vergnaud, V. Chaleix, V. Sol, M. Garcia, M. Gary-Bobo, L. Raehm and J.-O. Durand, *J. Mater. Chem. B*, 2015, 3, 3681–3684
3. X. Huang, X. Teng, D. Chen, F. Tang, J. He, The effect of the shape of mesoporous silica nanoparticles on cellular uptake and cell function, *Biomaterials* 31, 2010, 3, 438–448.
4. Gratton, S. E. A.; Ropp, P. A.; Pohlhaus, P. D.; Luft, J. C.; Madden, V. J.; Napier, M. E.; DeSimone, J. M. The Effect of Particle Design on Cellular Internalization Pathways. *Proc. Natl. Acad. Sci. U.S.A.* 2008, 105, 11613–11618.

Application of samarium oxide to evaluate the *in vivo* bio-distribution of PLGA nanoparticles

V. Mandiwana^{1,2*}, L. Kalombo¹, J.R. Zeevaart^{2,3}, A. Grobler²

¹CSIR Materials Science and Manufacturing, Polymers and Composites, Pretoria, South Africa

²DST/NWU Preclinical Drug Development Platform, North-West University, Potchefstroom, South Africa

³Radiochemistry and Applied Chemistry, Nuclear Energy Corporation of South Africa, Pelindaba, South Africa

Abstract:

Developing nanoparticulate delivery systems that will allow easy movement and localisation of a drug to the target tissue and provide more controlled release of the drug *in vivo* is a challenge for researchers in nanomedicine. The aim of this study was to evaluate the biodistribution of nano-delivery systems poly(D,L-lactide-co-glycolide) (PLGA) nanoparticles containing samarium-153 oxide ($[^{153}\text{Sm}]\text{Sm}_2\text{O}_3$) as radiotracer after oral and intravenous administration to rats to prove that orally administered nanoparticles indeed alter the biodistribution of a drug as compared to the drug on its own.

Stable samarium-152 oxide ($[^{152}\text{Sm}]\text{Sm}_2\text{O}_3$) was encapsulated in polymeric PLGA nanoparticles. These were then activated in the SAFARI-1 nuclear research reactor to produce radioactive $[^{153}\text{Sm}]\text{Sm}_2\text{O}_3$ loaded-PLGA nanoparticles. Both the stable nanoparticles as well as the fully decayed activated nanoparticles were characterized for size, Zeta potential and morphology using dynamic light scattering and scanning electron microscopy (SEM). The nanoparticle compounds were orally and intravenously (IV) administered to rats in order to trace their uptake and biodistribution through imaging and *ex vivo* biodistribution studies.

The PLGA nanoparticles containing $[^{153}\text{Sm}]\text{Sm}_2\text{O}_3$ were spherical in morphology and smaller than 500 nm, therefore meeting the objective of producing radiolabelled nanoparticles smaller than 500 nm. Various parameters were optimized to obtain an average particle size ranging between 250 and 300 nm, with an average polydispersity index (PDI) ≤ 0.3 after spray drying. The particles had a Zeta potential ranging between 5 and 20 mV. The Sm_2O_3 -PLGA nanoparticles had an average size of 281 ± 6.3 nm and a PDI average of 0.22. The orally administered $[^{153}\text{Sm}]\text{Sm}_2\text{O}_3$ -PLGA nanoparticles were

deposited in various organs which includes bone with a total of 0.3% of the Injected Dose (ID) per gram vs the control of $[^{153}\text{Sm}]\text{Sm}_2\text{O}_3$ which showed no uptake in any organs except the gastrointestinal (GI) tract. The IV injected $[^{153}\text{Sm}]\text{Sm}_2\text{O}_3$ -PLGA nanoparticles exhibited the highest localisation of nanoparticles in the spleen (8.63%ID/g) and liver (3.07%ID/g) but low bone uptake was achieved, 0.09%ID/g.

Based on the imaging and the biodistribution studies, it can be concluded that there was a significant transfer of the orally administered radiolabelled nanoparticles from the stomach to other organs vs the controls. Furthermore, this biodistribution of the nano carriers warrants surface modification and optimisation of the nanoparticles to avoid higher particle localisation in the stomach.

Keywords: Biodistribution, *in vivo*, imaging, nanoparticles, PLGA, samarium oxide, drug delivery, nanomedicine

Efficient drug delivery with synthesized mitoxantrone-gold nanoparticle conjugates for in vitro breast cancer therapy

A. Jafarizad,^{1,2,*} S. gharibian,² G. Pavon-Djavid,³ D. ekinci,¹

¹Department of Chemistry, Faculty of Science, Atatürk University, 25240 Erzurum, Turkey

²Department of Chemical Engineering, Sahand University of Technology, 51335-1996, Tabriz, Iran.

³INSERM, U1148, Université Paris 13, Université Paris7, Sorbonne Paris Cité LVTS, 46, rue Henri Huchard, 75877 Paris, France

Abstract:

Breast cancer is the most common female cancer worldwide representing 23% of all cancers in women owing to limitations in existing therapeutic methods such as surgery, radiotherapy and chemotherapy. Nowadays nanoparticles have proven to be a promising help for increasing treatments rate and improving chemotherapy and radiotherapy methods. As an instance, drugs can be conjugated on nanoparticles like gold (Au) and thus can reduce the side effects by getting localized better on tumor sites. Enhanced permeability, retention effect, high biocompatibility and Surface Plasmon Resonance (SPR) in the visible region is some of the most interesting properties of AuNPs. Mitoxantrone (MTX) is one of the chemotherapeutic drugs, which can be applied for the treatment of breast and brain cancers. In this study, first the 3-mercapto succinimide-MTX (MSM) were synthesized using MPA. The 3-mercapto propionic acid (MPA) linker thiol moieties provide a direct connection to the nanoparticles surface. Then, the MSM was used for grafting of the AuNPs surface (AuSMTX) and synthesized compounds were characterized by several instrumental techniques such as Ft-IR, UV-vis, TEM and etc. Finally, the ability of AuSMTX nanocomposite as a smart drug and the other synthesized compounds to treat MCF-7 cells were compared using MTT assay.

Keywords: Gold nanoparticles, cancer, Mitoxantrone, Drug delivery.

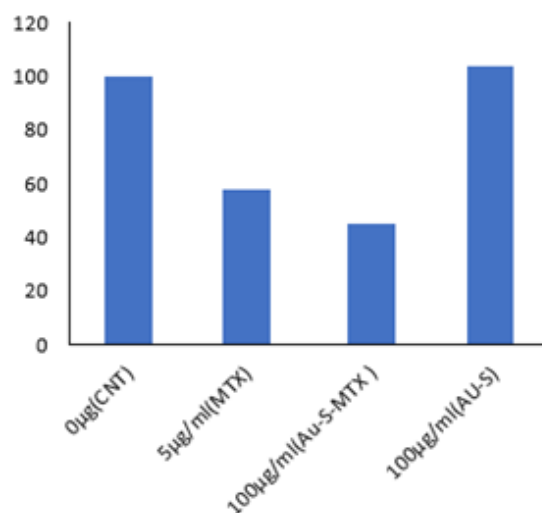


Figure1. Results of The MTT assay of nanoparticle in MCF7cell line

References:

Elstner, E., et al., Novel therapeutic approach: ligands for PPAR γ and retinoid receptors induce apoptosis in bcl-2-positive human breast cancer cells. Breast cancer research and treatment, 2002. 74(2): p. 155-165.

Dreaden, E.C., et al., Size matters: gold nanoparticles in targeted cancer drug delivery. Therapeutic delivery, 2012. 3(4): p. 457-478

Toxicology: Pulmonary and systemic toxicity caused by nanoparticles

NR. Jacobsen

National Research Center for the Working Environment, Copenhagen, Denmark

Abstract:

Nanomaterials possess unique physicochemical properties that make new technological advances possible. The vast possibilities for applications in medicine, industry and consumer products have led to a dramatic increase in number of nanoparticle containing products, and a consequent increased occupational, consumer and environmental exposure. This has raised strong concerns about possible health risks caused by exposure to engineered nanoparticles. Such concerns have propelled toxicology of nanomaterials to the forefront of toxicological research.

Inhalation may cause local inflammation, genotoxic and carcinogenic effects at the point of entry which have led to classification as possible human carcinogens of some particles. The importance of particle size and other physical chemical characteristics in relation to toxicity and possible mechanisms will be illustrated through examples.

Inhalation of particles is also associated with increased risk of cardiovascular disease in epidemiological studies. It has been shown that inhalation of nanomaterials induces a pulmonary inflammation that is proportional to the total surface area of the inhaled and pulmonary deposited dose of nanomaterials. Additionally, the pulmonary inflammation correlates closely with the acute phase response (a systemic alarm response) measured as Serum Amyloid A3 (*Saa3* mRNA). In humans the blood levels of SAA are associated with risk of cardiovascular disease in a prospective study. A correlation with acute phase response implies that inhalation of nanosized particles would induce a much stronger inflammation and acute phase response compared to larger similar particles.

The above underscores the importance for size specific occupational exposure limits (OEL) as the current limits may not provide adequate safety. Still, only few recommendations exist for

specific nanomaterials, and employers should minimize workers exposure.

Keywords: Toxicology, nanoparticles, physical chemical parameters, genotoxicity, carcinogenicity, translocation, cardiovascular disease.

Measurement of airborne engineered nanoparticles

M. Levin,^{1,2,*} B

¹National Research Center for the Working Environment, DK-2100, Copenhagen, Denmark

²Advance Cleantech ApS, Kajakvej 2, DK-2770, Copenhagen, Denmark

Abstract:

For exposure measurement of engineered nanomaterials (ENM), traditional gravimetric analysis alone is known to be insufficient due to the low total mass of the aerosol. Direct reading instruments for measurement of particle number, size and surface area are often used as replacement or complement to the gravimetric measurement. Proper aerosol measurements within industrial processes demand a high time resolution in order to properly capture fast transients in the particle concentrations and sizes. An analysis of workplace measurements suggest that short singular release events may generally be detected in number concentration measurements at a time-resolution lower than ca. 1 minute (Asbach et al., 2014). However, the high temporal resolution and the needed measurement procedure should not come at the cost of reliability of the measurement. Therefore thorough evaluation of the performances and data achieved by different candidates for aerosol monitoring should be completed.

A comparison between three different types of particle sizing instruments (Fast Mobility Particle Sizer (FMPS), Electrical Low Pressure Impactor (ELPI) and Scanning Mobility Particle Sizer (SMPS)) and one Condensation Particle Counter was done to compare instrument response in terms of size distributions and number concentration. Spherical oil droplets in 39 different sizes, with Geometric Mean Diameter (GMD) ranging from 50 to 820 nm were used as test particles. A spark discharge generator was used to generate Au particles either as agglomerates (20-200 nm) or sintered to spherical shape (20-80 nm). Further, complexly shaped ENM particles generated through the use of a rotating drum were used to assess the comparability of direct measurement of lung deposited surface area as compared to calculated values of the same, based on size, density and specific surface area.

Keywords: protein folding, nanoporous sol-gel glasses, silica-based biomaterials, circular dichroism spectroscopy, surface hydration, crowding effects, micropatterning, biomedical applications.

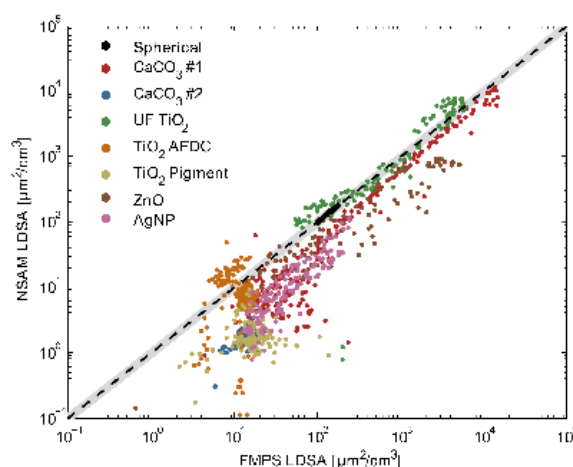


Figure 1: Figure showing the comparison of alveolar deposited surface area measured by Nanoparticle Surface Area Monitor with calculated values based on measurement with Fast Mobility Particle Sizer for eight different materials. Grey area denotes $\pm 20\%$ uncertainty.

This work was funded by the 'Danish Centre for Nanosafety' (20110092173/3) from the Danish Working environment Research Foundation and the EU Framework 7 Programme NANOREG (310584).

References:

Asbach, C et al., 2014. Chapter 7 Examples and Case Studies. In HANDBOOK OF NANOSAFETY

Evaluation of Dithizone-Based Colorimetric Sensors for Silver Nanoparticles in Aqueous Media

N. Wasukan,^{1,2,*} S. Srisung¹, M. Kuno¹, K. Kulthong², R. Maniratanachote²

¹Srinakharinwirot University, Department of Chemistry, Bangkok, Thailand

²Natinal Nanotechnology Center, National Science and Technology Development Agency, Pathumthani, Thailand

Abstract:

Recently, a simplicity, rapidity, high sensitivity and selectivity colorimetric sensors are widely investigating for heavy metal ions on aquatic environment. Silver nanoparticles (AgNPs) are increasing utilization in consumer products due to its antibacterial effect causing the industrial concern has raised to environment. Dithizone is one of the most considered effective chelating reagents for metal ions with the stable complexes and intensity color. In this study, the selective colorimetric sensor of dithizone was selected for AgNPs detection in aqueous media. Spectrum of the ligand is characterized by two peaks at about 445 nm and 620 nm, which are responsible for green color of the solution. The selectivity towards AgNPs compared with the other metal ions (Na^+ , K^+ , Cu^{2+} , Mg^{2+} , Ba^{2+} , Mn^{2+} , Fe^{3+} , Co^{2+} , Ni^{2+} , Cu^{2+} , Ag^+ , Zn^{2+} , Cd^{2+} , Hg^{2+} and Pb^{2+}) were investigated with the concentration of 1.0×10^{-5} M metal ions. It was found that a distinct color change from green to orange was noticed only in the case of AgNPs-dithizone complexes. In pH dependence, the complexes demonstrated an obviously change of color at $\text{pH} > 6$ at room temperature, having a maximum wavelength at 477 nm. This result has been confirmed by UV-Vis spectroscopy technique. Moreover, the interaction of AgNPs-dithizone complexes was supported by UV-Vis spectroscopy, FT-IR spectrum and ^1H NMR spectra that were simulated by using B3LYP/6-31G(d,p) method compared with the experimental data. Therefore, a remarkable feature of this method can be applied to the determination of AgNPs in the environment water samples.

Keywords: silver nanoparticles (AgNPs), dithizone, Colorimetric sensors, DFT, Aquatic environment

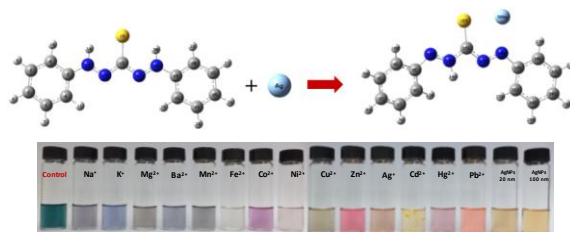


Figure 1: The interaction of silver–dithizone complexes and color of dithizone changes upon the addition of metal ions.

References:

1. Eschwege, K.G., Conradie, J., Kuhn, A. (2011), Dithizone and its oxidation products: a DFT, spectroscopic, and X-ray structural study, *J. Phys. Chem. A*, 115, 14637-14646.
2. Tavallali, H., Deilamy-Rad, G., Parhami, A., Mousavi, S.Z. (2014), Dithizone as novel and efficient chromogenic probe for cyanide detection in aqueous media through nucleophilic addition into diazenylthione moiety. *Spectrochim. Acta. Mol. Biomol. Spectros.*, 121, 139-146.

Drosophila melanogaster as a suitable in vivo model to determine potential side effects of nanomaterials

Mohamed Alaraby^{1,2}, Alba Hernández^{1,3}, Ricard Marcos^{1,3,*}

¹Grup de Mutagènesi, Departament de Genètica i de Microbiologia, Facultat de Biociències, Universitat Autònoma de Barcelona, Campus de Bellaterra, 08193 Cerdanyola del Vallès, Spain.

²Zoology Department, Faculty of Sciences, Sohag University (82524), Sohag, Egypt.

³CIBER Epidemiología y Salud Pública, ISCIII, Madrid Spain.

Abstract:

Despite being a relatively new field, nanoscience is in the forefront of many scientific areas. The nanometer scale change the materials properties, hence slight changes in their size or coating can dramatically modify their physical, chemical, and biological properties. Subsequently, nanomaterials (NM) show two sides, the first one offer attractive properties for industry, medical and electronics applications, but the another one poses several questions marks about their biological effects that recall the evaluation of their potential harmful effects for protecting both humans and environment. One effective model to be used for this aim is *Drosophila melanogaster* (Ong et al., 2015) as an *in vivo* model. The usage of *Drosophila* in the study of the biological interactions of NM has been recently increasing (Alaraby et al., 2015). Notably, *Drosophila* shows a high sensitivity in front of changes in the NM properties, not only to change in the chemical composition of NM as different nanoparticle elements and different coating or to the physically variations in size, shape and surface area, but also to exposure conditions and concentration range. Moreover, *Drosophila* can be used as effective sensitive bio-monitor to determine the shedding ions from NM and their physical interactions. In addition, *Drosophila* offer a perfect model to measure the NM effects in all life stages from embryo, up to adult stage passing with transitional stages, in a relative short time. Furthermore it can be used to determine the role of intestine as a barrier to protect against NM. Importantly, the use of *D. melanogaster* is ethically less controversial than using other higher in vivo model organisms (Alaraby et al., 2015).

Keywords: *Drosophila*, in vivo model, nanomaterial.

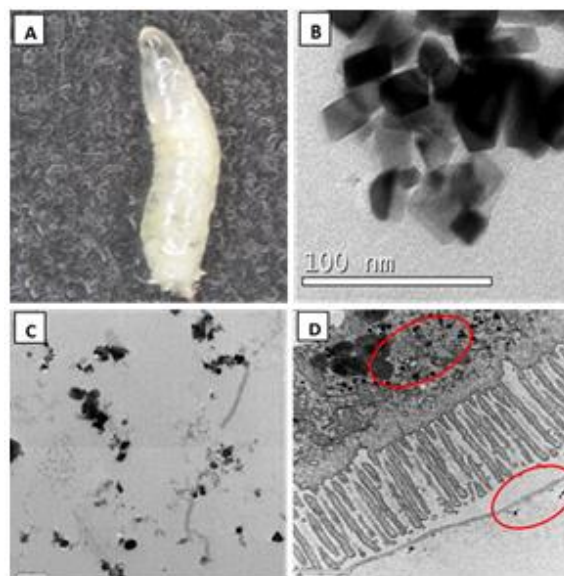


Figure 1: Show *Drosophila* larva (A) and cerium nanoparticles; in suspension (B), distributed inside midgut lumen (C) or attached to peritrophic membrane and inside larval cellular cytoplasm (D).

References

1. Alaraby, M., Hernández, A., Annangi, B., Demir, E., Bach, J., Rubio, L., Creus, A., and Marcos, R. (2015) Antioxidant and antigenotoxic properties of CeO₂ NPs and cerium sulphate: Studies with *Drosophila melanogaster* as a promising in vivo model, *Nanotoxicology*, 9, 749-59.
2. Ong, C., Yung, L. Y. L., Cai, Y., Bay, B. H., and Baeg, G. H. (2015) *Drosophila melanogaster* as a model organism to study nanotoxicity, *Nanotoxicology*, 9, 396-403.

Determination for Stability Constant of Silver-DMSA Nanoparticles

S. Srisung^{1,*}, N. Wasukan,^{1,2} K. Kulthong², R. Maniratanachote²

¹Srinakharinwirot University, Department of Chemistry, Bangkok, Thailand

²National Nanotechnology Center, National Science and Technology Development Agency, Pathumthani, Thailand

Abstract:

Silver, both in the nano- as well as in other forms, is used in many applications which the risks associated with human or environmental exposure to an engineered nanomaterial are chiefly determined in part by the release and transformation. Silver nanoparticles (AgNPs) are increasing utilization in commercial products due to its antibacterial effect causing the industrial concern has raised to environment. For these problem solutions, a wide range of scientific approach in physics, chemistry are related sciences is involved. Dimercaptosuccinic acid (DMSA) is known to be one of the effective chelating reagents for heavy metal ions. This ligand is a very important in used as a treatment and removal for metals toxicity. Assessment of binding strengths in a AgNPs-DMSA complex is necessary for useful comparisons of binding ligand. The proton dissociation constants of the ligands and the stability constant of their complexes with Ag⁺ and AgNPs have been determined spectrophotometrically. The selectivity towards silver compared with the other heavy metal ions (M²⁺) were investigated and the data reveal that the stoichiometric for all complexes were prepared in different molar ratio. Moreover, the characterization of AgNPs-DMSA complexes was supported by scanning electron microscopy (SEM) and transmission electron microscopy (TEM). Therefore, this method can be useful to qualify the behavior of silver in both form.

Keywords: silver nanoparticles, dimercaptosuccinic acid, stability constant, spectrophotometrically, scanning electron microscopy

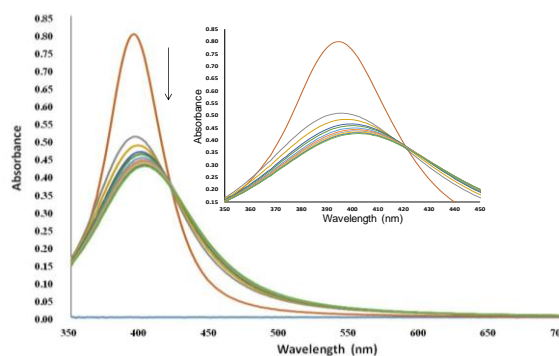


Figure 1: Changes in the UV-Vis absorption spectrum of DMSA upon addition of AgNPs.

References:

1. Jahromi, E.Z., Gailer J., Pickering I.J., George, G.N. (2014), Structural characterization of Cd²⁺ complexes in solution with DMSA and DMPS, *J. Inorg. Biochem.*, 136, 99-106.
2. Zaluzhna, O., Brightful, L., Allison, T.C., Tong, Y.J. (2011), Spectroscopic evidence of a bidentate-binding of meso-2,3-dimercaptosuccinic acid on silver nanoclusters, *Chem. Phys. Lett.*, 509, 148-151.

Legal Metrology Framework for Nanotechnology in Australia

Sheila Devasahayam

Federation University Australia, Victoria 3350 Australia
Email:sdevasahayam@federation.edu.au

Abstract:

This work explores the feasibility of legal metrology (LM) as a platform to address the impact of nanotechnology (NT) on legal and social-economic aspects. It considers whether a LM framework needs to be developed for NT and the associated benefits and risks.

NT applies scientific knowledge to control and utilize matter at the nano-scale, where size-related properties and phenomena can emerge. It is a convergent platform of many disciplines with a value to the global economy predicted at US \$1 trillion by 2015. It has now come under strong scrutiny due to the potential risks posed to Health Safety and Environment (HSE). It is anticipated that nanometrology as a tool must enable industry to meet regulations and demonstrate that nanotechnologies are safe with regard to HSE.

NT's interdisciplinary nature requires many measurement systems involving physical, biological and chemical measurements. Nanometrology develops measurement infrastructure and standards for NT to assist the industries to capitalise on commercialisation opportunities, and contribute to effective HSE regulatory frameworks for nanotechnologies. Australia coordinates the physico-chemical safety testing programme for selected manufactured nano-materials (MNs), run by the Working Party on Manufactured Nano-materials of the Organisation for Economic Co-operation and Development.

Current fragmented regulatory regimes across the world, whilst considered adequate, have been identified to have potential gaps which would prevent comprehensive regulation of NT. There is now a general consensus for an internationally integrated NT governance approach to address the ethical, legal and social aspects.

LM's objectives relate to harmonised regulation and measurements, and not exclusive to meas-

urement range or technology, such as macro, micro, meso, nano, or space and biotechnologies. Legal metrology's scope concerning the HSE measurements as well as the trade measurements seems to be the ideal platform to address the impact of NT.

Effects of Different Printing Ink Binders on Printability and Biodegradability of Polylactic Acid Film

S. Netpradit,^{1*} S. Binraman,¹ and C. Ladmai,²

¹ Department of Printing and Packaging Technology, King Mongkut's University of Technology Thonburi, Thailand

² Printing Engineering Institute, Siam University, Thailand

Abstract: Polylactic acid (PLA) film is a biodegradable aliphatic polyester derived from renewable resources and becomes famous for application as flexible packaging to counteract problem in landfill waste management. Although printing on packaging is important for sale promotion, the printing ink should be non-impact to the biodegradability of packaging waste which can be composted into CO₂, water and biomass in soil after disposal by landfill. The objectives of this research were to compare the printability and biodegradability trend of PLA film printed with different ink binders which were nitrocellulose, Para rubber latex and acrylic resin. After the water-based ink samples were applied on the non-surface treated PLA film by the bar coater, the printability and ink film properties were determined. The results showed that the ink of nitrocellulose resin was the best transferred on the PLA film with the highest optical density and gloss. The adhesion and rub resistance of nitrocellulose ink film were as good as acrylic ink film while the Para rubber film was poor in abrasion resistant. For biodegradability analysis after composting simulation in soil for 93 days, the PLA samples with natural resin of nitrocellulose ink and para rubber ink had more accumulated CO₂ emission than did the samples with acrylic ink. The SEM micrographs were also taken and showed that surface of PLA film seem to be decomposed and the trend was more pronounced on the printed PLA film with Para rubber latex and nitrocellulose than acrylic resin, respectively. The mechanical properties and molecular weight of the PLA film were also decreased after biodegradability testing and these results were significantly shown by printing with nitrocellulose ink, indicating that the natural-based resins were better applied for printing on the biodegradable film than did the petroleum-based resin.

Keywords: printing ink binder, printability, biodegradability, polylactic acid film, nitrocellulose, Para rubber latex, acrylic resin

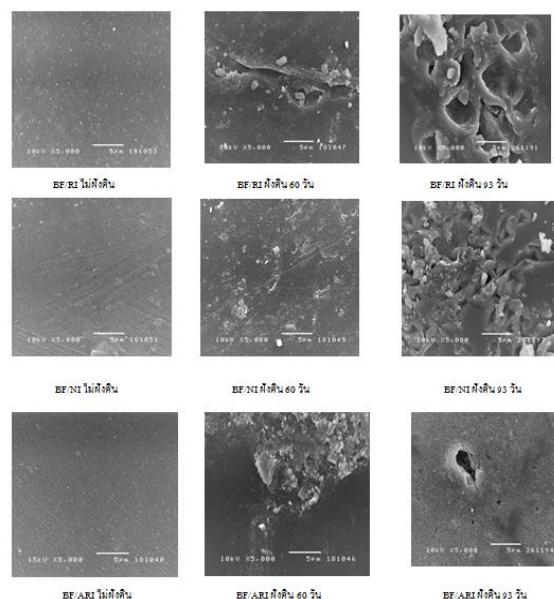


Figure 1: Figure illustrating the SEM micrographs of PLA film printed with Para rubber ink (top), nitrocellulose ink (middle) and acrylic resin ink (bottom) which were initial printed and decomposed in soil for 60 days and 93 days, respectively.

References:

1. Rudeekit, Y., Leejakpai, T., Euaphantasate, N. and Kongsuwan, K. (2006) Comparative Degradable of Biodegradable Plastic by Aerobic Microorganism Using ASTM D5338-98(03) and ASTM D5338-98(03) as Standard Methods, *The 4th Thailand Materials Science and Technology Conference*, 31 March - 1 April, Thailand Science Park Convention Center.
2. A. Ashwin Kumar, Karthick, K. and K.P. Arumugam (2011) Biodegradable Polymers and Its Applications, *Int. J. Bioscience, Biochemistry and Bioinformatics*, 1 (3), September, 2011, 173-176

Effect of the supply air supporting the shaping of the exhaust air flow during the processing of nanomaterials

T. Jankowski,^{1*}

¹Central Institute for Labour Protection – National Research Institute, Department of Chemical and Aerosol Hazards, Warsaw, Poland

Abstract: Important aspect of safe operation during the processing of engineered nanomaterials is to prevent risks in indoor dust contamination.

Elimination or reduction exposure to harmful dust generated in the production process it should be implemented through the use of effective devices for capture dust directly from the emission sources and air distribution to prevent the spread of pollutants in the workspace.

Changing the approach to the protection against the risk to nanoparticles should be related to the modeling of air distribution through local exhaust ventilation used directly at the source of emission of nano-objects supported by supply air ventilation in the room.

The article presents the results of studies which aim was to demonstrate the effect of the application of the supply air supporting the shaping of the exhaust air flow during the cutting of nanomaterials. A study was performed in three variants of supporting of exhaust ventilation.

In the study, commercially available stainless steel covered with a layer of silver nanoparticles subjected to machining by cutting. Silver nanoparticles were bound chemically to the surface of the stainless steel and heat-set. The results were compared with the results of velocity and turbulence intensity of the air surrounding the emission source using only a local exhaust ventilation.

On the basis of the results showed a significant effect of changes in the variant ventilation parameters associated with the distribution of ventilation air in the workspace source of air pollutant emissions (Fig. 1). The air velocity of the ambient of emission sources and intensity of flow turbulence discharged from the workspace emissions have an impact on the emission intensity of nanoparticles and effectiveness of ventilation systems (Fig. 2).

Keywords: nanomaterials, pollutants, nanosilver, air velocity, air flow, ventilation.

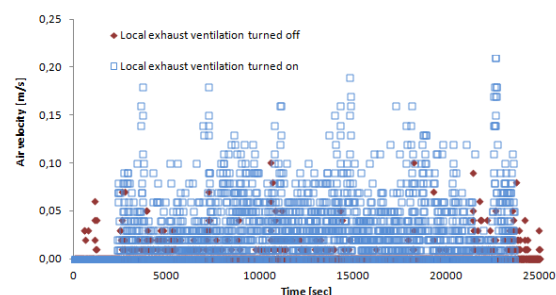


Figure 1: Figure presents air velocity distribution in the emission source of nanoparticles.

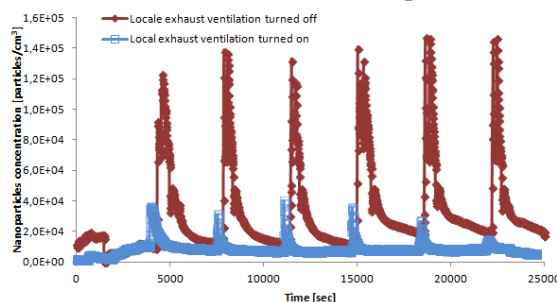


Figure 2: Figure illustrating the changes in efficiency of ventilation and number pollutant concentration from tests carried out in nanomaterials machining.

References:

- Lee, M., McClellan, W. (2007) Reduction of nanoparticle exposure to welding aerosols by modification of the ventilation system in a workplace. *J. Nanopart. Res.*, 9, 127–136.
- ISO/TS 12901-2:2014 Nanotechnologies — Occupational risk management applied to engineered nanomaterials. Part 2.

Acknowledgments

This paper has been prepared on the basis of the results of research task II.P.03 carried out within the National Programme “Improvement of safety and working conditions” partly supported in 2014-2016 within the scope of research and development by the Ministry of Science and Higher Education. Central Institute for Labour Protection - National Research Institute has been the Programme main coordinator.

High stability metal nanoparticles for healthcare applications

Emad El-Meliigy

National Research Centre, Ceramics Dept., 12622 El-Tahrir Str., Dokki, Cairo, Egypt,
Email:emadmeliigy@hotmail.com

Abstract:

Nanomedicine is a challenging science employing nanoscale devices in monitoring, and controlling the cell functions in the biological systems. It has the ability to operate on the same small scale as the intimate biochemical functions inside the living cells. The materials currently used in medical treatment are limited by their effectiveness in the treatment and diagnosis of diseases such as infections, diabetes, and cancer and offers potential solutions to improving the medical diagnosis and therapy. For example: utilizing nanomedicine, it could be possible to get rid of bacterial infection in minutes, rather than weeks by direct delivery of antibiotics directly to cells.[1]

The current work aims at targeting the synthesis of metal nanoparticles and nanocomposite, with excellent tissue compatibility and safety profiles essential for their successful utilization in the human body.

This work involved the synthesis of metal nanoparticles by chemical synthesis and freeze drying. The nanoparticles were characterized by XRD and DTA, and TEM. The prepared nanoparticles; including silver, selenium, copper and iron nanoparticles, were prepared using different synthesis techniques and different conditions of preparation.

The results showed that the particle size of metal nanoparticles is found to be <50nms. The results show crystalline metal nanoparticles with high stability and narrow particle size distribution, with size less than 50nms prepared on the commercial scale. For example: copper nanoparticles with high crystallinity are shown in Fig.1.

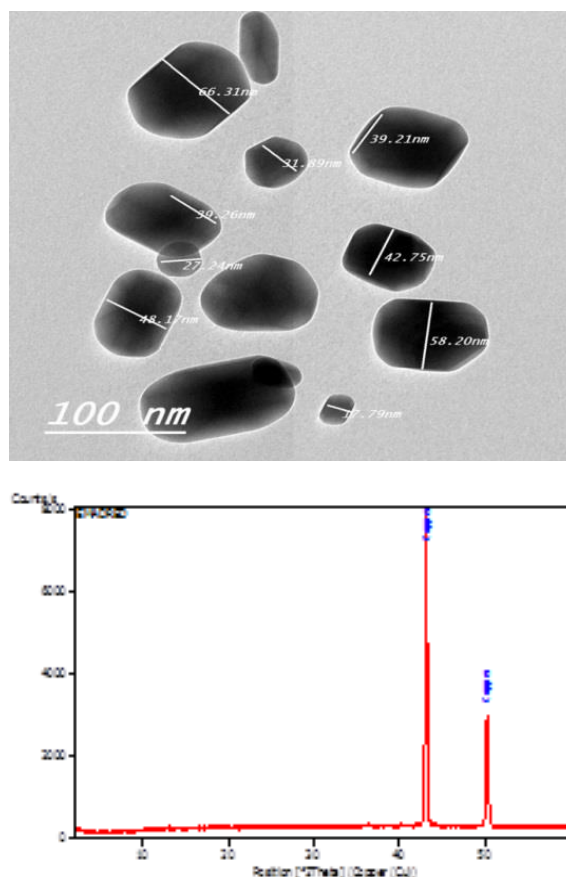


Figure 1: TEM and XRD of copper nanoparticles less than 50nm

References:

B. K. Park, S. Jeong, D. Kim, J. Moon, S. Lim and J. Kim, Synthesis and size control of monodisperse copper nanoparticles by polyol method, *Journal of Colloid and Interface Science* 311 (2007) 417–424

Acknowledgments

This project is supported financially by the Science and Technology Development Fund (STDF), Egypt, Grant No: 5150.

Overview of available data of occupational exposure to manufactured nanomaterials, approaches and needs

S. Bau^{1*}, O. Witschger¹

¹ Institut National de Recherche et de Sécurité, Department of Pollutant Metrology, Laboratory of Aerosol Metrology, Vandoeuvre lès Nancy, France

Abstract:

Manufactured nanomaterials present new challenges to understanding, predicting, and managing potential risks to workers, consumers and the environment (Houdy *et al.*, 2011). In the recent years, concerns about the risks associated with nanomaterials have led to a significant increase in toxicology studies (Stebounova *et al.*, 2012), whose results have raised issues of concern. In that context, the prospective widespread usage of nanomaterials calls for an assessment of the possible release and exposure to workers in industrial and academic workplaces.

The aims of this lecture are (i) to provide an overview of the occupational inhalation exposure in the workplaces where nanomaterials are manufactured and used, and (ii) to identify, to our point of view, the still existing shortcomings and to propose strategies to overcome them.

The up-to-date overview mainly relies on the analysis of 50 peer-reviewed publications that have been identified over the period 2004 – 2013, among which more than half published in the last 4 years. The choice is deliberately focused on publications that describe studies based on real workplaces with potential exposure data on nanomaterials, not publications with potential exposure to incidental nanoparticles. As an illustration, Figure 1 gives an overview of the distribution of the selected publications according to the main activity of the workplaces visited.

Many of the earlier studies have an explorative character, whether in terms of instruments used or approaches to measurement or analysis of the data, while the most recent studies provide more relevant information for the interpretation of the exposure.

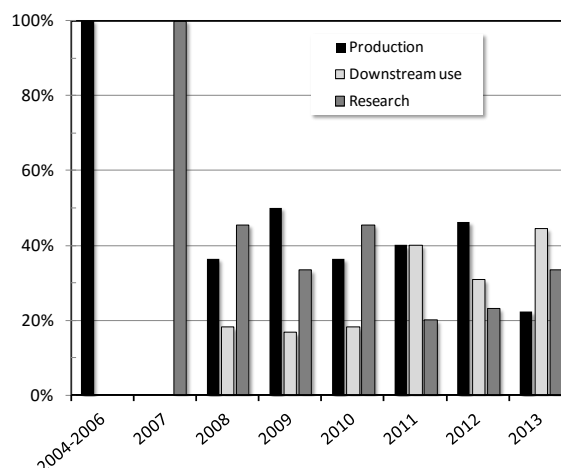


Figure 1: Overview of the distribution of publications according to the main activity of the visited workplaces for the period 2004 – 2013.

Examples of occupational exposure assessment will be provided. Situations such as big bag discharging, filling and closing, as well as dry sandpapering of pieces exposed to nanomaterials will be discussed in the presentation.

Keywords: occupational exposure, measurement strategy, manufactured nanomaterial.

References:

1. Houdy P, Lahmani M, Marano F (eds) (2011). *Nanoethics and Nanotoxicology*, Springer-Verlag Berlin Heidelberg, 620p.
2. Stebounova LV, Morgan H, Grassian VH, Brenner S (2012) *Wiley Interdisciplinary Reviews: Nanomedicine and Nanobiotechnology*, 4, 310-321.

Nanotech France 2016 Session IV

Nano Electronics / Nano Photonics

NANOSCALE MAGNETIC SKYRMIONS – A NEW TWIST FOR SPINTRONICS

ROLAND WIESENDANGER

Interdisciplinary Nanoscience Center Hamburg, University of Hamburg, D-20355 Hamburg

Abstract:

Nanoscale magnetic knots, called skyrmions, are novel types of localized non-collinear spin textures which offer great potential for future magnetic memory and logic devices [1]. The twisting in the skyrmions' magnetization profile leads to a gain in energy with respect to a homogeneously magnetized, ferromagnetic state. As a result of this magnetization twisting, skyrmions have non-trivial topological properties, described by a topological charge, and are topologically protected against a transition into topologically trivial states. The energetics of skyrmionic states is explained by the Dzyaloshinskii-Moriya interaction [2] being relevant in material systems exhibiting large spin-orbit coupling and a lack of inversion symmetry, in contrast to magnetic bubble domains which are stabilized by dipolar magnetic interactions.

Skyrmion lattices were initially observed in bulk non-centrosymmetric materials based on neutron diffraction experiments and Lorentz microscopy observations. However, recent experimental and theoretical work has focused on atomic- and nanolayers of magnetic materials with intrinsic or interface-induced chiral interactions, thereby achieving full compatibility with state-of-the-art technology which has been developed over the past decades in the field of GMR- and TMR-based devices. It has been shown both experimentally and theoretically that magnetic skyrmions in ultrathin film systems can be as small as one nanometer in diameter [3] and that their properties can largely be tuned by the choice of the substrate and overlayer materials [4].

Atomic-resolution spin-polarized scanning tunneling microscopy (SP-STM) and spectroscopy [5] has proven to be an invaluable tool for revealing the atomic-scale properties of ultimately small skyrmions [6-9]. By locally injecting spin-polarized electrons from an atomically sharp SP-STM tip, we are able to write and delete individual skyrmions one-by-one, making use of spin-transfer torque exerted by the injected high-energy spin-polarized electrons [4]. Switching

rate and direction can be controlled by the parameters used for current injection. Alternatively, individual skyrmions can be created and deleted by local electric fields [10], which can be of great advantage in view of energy-saving skyrmionic device concepts. The subsequent detection of the written skyrmions can also be achieved by electrical means rather than by using a magnetic sensing element [11]. The demonstration of various methods for the creation and annihilation as well as the detection of individual nanoscale skyrmions highlight their great potential for future spintronic devices making use of individual topological charges as information carriers.

Keywords:

Spintronics, skyrmionics, magnetic memory and logic devices, atomic-resolution magnetic microscopy and spectroscopy, spin-polarized STM

References

1. A. Fert et al., *Nature Nanotechnology* 8, 152 (2013).
2. A. A. Khajetoorians et al., *Nature Commun.* 7, 10620 (2016).
3. S. Heinze et al., *Nature Physics* 7, 713 (2011).
4. N. Romming et al., *Science* 341, 6146 (2013).
5. R. Wiesendanger, *Rev. Mod. Phys.* 81, 1495 (2009).
6. N. Romming et al., *Phys. Rev. Lett.* 114, 177203 (2015).
7. K. von Bergmann et al., *Nano Lett.* 15, 3280 (2015).
8. A. Sonntag et al., *Phys. Rev. Lett.* 113, 077202 (2014).
9. J. Brede et al., *Nature Nanotechnology* 9, 1018 (2014).
10. P.-J. Hsu et al., <http://arxiv.org/abs/1601.02935>.
11. C. Hanneken et al., *Nature Nanotechnology* 10, 1039 (2015).

Density of states and electrical properties of nanocrystalline Co^{2+} and Ta^{5+} substituted barium bismuth niobate

Prasanta Dhak¹, Atreyee Kundu², Mrinal Kanti Adak,³ Debasis Dhak,³ and Anja O. Sjøstad¹

¹Centre for Materials Science and Nanotechnology, Department of Chemistry, University of Oslo, Blindern, N-0315 Oslo, Norway

²Department of Biological Sciences, Presidency University, Kolkata 700073, India

³Department of Chemistry, Sidho-Kanho-Birsha University, Purulia 723101, India

Abstract: Bi-based layered perovskite ferroelectric (BLSF) materials are widely investigated because of its high Curie temperature (T_c), fatigue free, low sintering temperature, and environmentally suitability. The investigation of electrical conductivity is very significant for the ferroelectric compounds as many physical properties like dielectric, ferroelectric, and piezoelectric are dependent on the nature and extent of conductivity of the materials. Complex impedance spectroscopy is considered to be a great experimental technique to interface between the electrical and structural properties like dielectric behavior of crystalline as well as amorphous materials. For dielectric materials, most of the electrical properties are greatly influenced by doping of metal ions or chemical compositions and powder characteristics such as particle size, morphology, purity etc, become critical to control. There are many reports aiming to improve the dielectric and ferroelectric properties of $\text{BaBi}_2\text{Nb}_2\text{O}_9$ by doping different metal ions in suitable sites. To the best of our knowledge, till date, no studies are available on impedance spectroscopy of Co^{2+} and Ta^{5+} substituted $\text{BaBi}_2\text{Nb}_2\text{O}_9$ respectively at A and B site ions.

In this present work, nanocrystalline Co^{2+} and Ta^{5+} substituted barium bismuth niobate $\text{Ba}_{0.5}\text{Co}_{0.5}\text{Bi}_2\text{NbTaO}_9$ (BCBNT) was synthesized by a chemically based route. Powder X-ray diffraction (XRD) confirmed the samples to be phase pure with tetragonal crystal structure. Average crystallite and particle sizes were found to be 33 nm and 40 nm, as analyzed through XRD and transmission electron microscopy (TEM) respectively. Field emission scanning electron microscopy (FESEM) was used for microstructural investigation of samples sintered at 950°C for 4h. The investigation revealed that the material was exhibiting high dielectric constant value of 1017 at Curie temperature (T_c), 500°C when measured at 10 kHz. Impedance spectroscopy analysis showed that above 425°C, the ma-

terial exhibited both bulk and grain boundary conductivities which were evidenced from FESEM studies. Density of states, minimum hopping distance, binding energy etc. were studied along with other electrical properties from impedance analysis. Hysteresis behavior was also investigated using polarization study.

Keywords: Nanomaterials; Chemical Route; Dielectrics; Ferroelectrics; Impedance; Density of States|

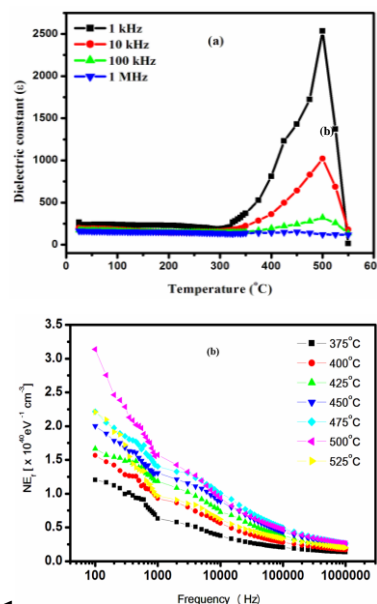


Figure.1. variation of (a) dielectric constant with temperature at different frequency and (b) dependence of density of states, $N(E_F)$ at Fermi level on frequency at various temperatures for BCBNT measured at different frequency

References:

1. Park, B. H.; Kang, B. S.; Bu, S. D.; Noh, T. W.; Lee, J.; Jo, W, (1999) Lanthanum-substituted bismuth titanate for use in non-volatile memories *Nature* 401, 682.
2. Dhak, P., Dhak, D.; Das, M.; Pramanik, K.; Pramanik, P, Impedance spectroscopy study of LaMnO_3 modified BaTiO_3 ceramics (2009) *Mat. Sci. Eng. B.* 164, 165.

Self-powered high photoresponse ultraviolet photodetector based on dual ion beam sputtered Ga doped ZnO

Pankaj Sharma, Rohit Singh, Ritesh Bhardwaj, and Shaibal Mukherjee*

Hybrid Nanodevice Research Group (HNRG), Electrical Engineering, Indian Institute of Technology, Indore 452020, India

[*shaibal@iiti.ac.in](mailto:shaibal@iiti.ac.in)

Abstract: In recent times, the research on ZnO based ultraviolet (UV) photodetectors (PDs) have gained interest due to its unique properties such as direct wide band gap of 3.37 eV, large exciton binding energy of 60 meV, high radiation hardness and hence they find place in civil and defence applications such as air quality monitoring, flame detection, UV communications and missile warning systems.¹ ZnO films for UV PDs have been deposited by various techniques such as magnetron sputtering, molecular beam epitaxy, and pulse laser deposition etc.² Since almost all kind of photodetectors requires external supply for their operation, it is highly desired to have PDs based on self-powered mechanism. In this work, we present the feasibility of realizing a highly sensitive and self powered UV photodetector by exploring the photoconducting properties of Ga doped ZnO (GZO) thin films.

GZO based ultraviolet photodetectors were fabricated by dual ion beam sputtering (DIBS) in metal-semiconductor-metal structure. The room-temperature operable PD demonstrated responsivity of 58 mAW⁻¹ at zero bias, which is 15 times larger than that reported on similar material grown by other physical vapour deposition process^{3, 4}, with the external (EQE) and internal (IQE) quantum efficiency values of ~22.5% and 37.4% respectively. The unbiased photodetection is attributed to the tunnelling of electrons due to heavy doping of GZO and built-in electric field due to different barriers at two metal semiconductor contacts. The asymmetry in electrodes was investigated by temperature-dependent current-voltage measurements. These PDs are critical in terms of energy saving point of view and are preferred for long-term monitoring of air-pollution and wastewater. Fig 1 shows the photoresponse of fabricated GZO photodetector at room temperature.

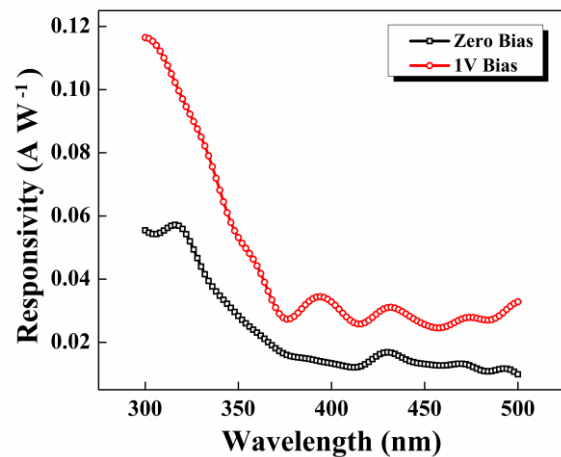


Fig 1. Photoresponse of GZO photodetector

Keywords: GZO, Dual Ion Beam Sputtering, Photoresponse, EQE, IQE, Tunnelling.

References:

1. Yang, C.-C.; Su, Y.-K.; Hsiao, C.-H.; Young, S.-J.; Kao, T.-H.; Chuang, M.-Y.; Huang, Y.-C.; Wang, B.-C.; Wu, S.-L. *IEEE PHOTONICS TECHNOLOGY LETTERS* **2014**, 26, (13).
2. Çalışkan, D.; Bütün, B.; Çakır, M. C.; Özcan, Ş.; Özbay, E. *Applied Physics Letters* **2014**, 105, (16), 161108.
3. Jiang, D. L.; Li, L.; Chen, H. Y.; Gao, H.; Qiao, Q.; Xu, Z. K.; Jiao, S. J. *Applied Physics Letters* **2015**, 106, (17), 171103.
4. Chen, H.-Y.; Liu, K.-W.; Chen, X.; Zhang, Z.-Z.; Fan, M.-M.; Jiang, M.-M.; Xie, X.-H.; Zhao, H.-F.; Shen, D.-Z. *J. Mater. Chem. C* **2014**, 2, (45), 9689-9694.

Acknowledgment:

This work is partially supported CSIR. We are thankful to Sophisticated Instrument Centre (SIC) at IIT Indore. Dr. Shaibal Mukherjee is thankful to Deity YFRF award.

Perovskite Oxide Spin Filters

Bhagwati Prasad,^{a,b,*} and Mark G. Blamire^a

^aDepartment of Materials Science and Metallurgy, University of Cambridge, 27 Charles Babbage Road, Cambridge, CB3 0FS, UK

^bMax Planck Institute for Solid State Research, Heisenbergstr. 1, D-70569 Stuttgart, Germany
Email: b.prasad@fkf.mpg.de

Abstract:

The simple growth process and better stability of the perovskite oxide heterostructures make them a promising candidate for the realization of many novel spintronic effects and devices. Integration of ferromagnetic insulating (FMI) manganite thin films as spin filter into these heterostructure systems has emerged a novel way to generate a highly spin-polarised current [1,2]. In this work, the spin-filtering effect through an ultrathin $\text{Sm}_{0.75}\text{Sr}_{0.25}\text{MnO}_3$ (SSMO) FMI barrier in epitaxial oxide nanopillar tunnel junctions fabricated by the Focused Ion Beam (FIB) nano-machining technique has been demonstrated. The fabricated spin filter tunnel junctions exhibited a spin-polarization of up to 75% at 5K, which is nearly double to that reported in oxide based junctions. The spin filter effect was also verified by measuring the tunnel magnetoresistance (TMR) response of the SSMO-based quasimagnetic tunnel junctions [3]. A highly unconventional bias-dependent TMR response was observed in these devices with two different behaviours in two different thickness regimes of the barrier layer for the first time. These results demonstrate the role of many novel phenomena, including electric-field-dependent spin polarization, Coulomb blockade and spin accumulation. Nearly 100% spin-polarised current has been generated from the fully magnetic manganite tunnel junctions. Introducing the FMI manganite barrier in magnetic tunnel junctions allows the device to operate in three-resistance states. These wide varieties of novel findings observed in this work open the way for the discovery of new spintronic devices by exploiting the many degree of freedom of perovskite manganite heterostructure systems.

Keywords Perovskite oxides; Spintronics; Manganites; Spin-filters; Magnetic tunnel junctions.

References:

- [1] T. Harada, I. Ohkubo, M. Lippmaa, Y. Sakurai, Y. Matsumoto, S. Muto, H. Koinuma, M. Oshima, *Phys. Rev. Lett.* **2012**, 109, 076602.
- [2] B. Prasad, M. Egilmez, F. Schoofs, T. Fix, M. E. Vickers, W. Zhang, J. Jian, H. Wang, M. G. Blamire, *Nano Lett.* **2014**, 14, 2789.
- [3] B. Prasad, W. Zhang, J. Jian, H. Wang, M. G. Blamire, *Adv. Mater.* **2015**, 27, 3079.

New fundamental effects in single molecular circuitry

Albert C. Aragonès,^{1,*} N. Darwish,² F. Sanz,¹ Elsieo Ruiz³ and I. Díez-Pérez¹

¹ Departament de Química Física, Universitat de Barcelona, Diagonal 645 and Institut de Bioenginyeria de Catalunya (IBEC), Baldori Reixac 15-21, 08028 Barcelona, Catalonia, Spain.

² Nanochemistry Research Institute Department of Chemistry, Faculty of Science & Engineering, Curtin University, Perth, Australia.

³ Departament de Química Inorgànica and Institut de Química Teòrica i Computacional, Universitat de Barcelona, Diagonal 645, 08028 Barcelona, Catalonia, Spain.

Abstract: Inspired by the proposal that single molecules will be functional elements of future nanoelectronic and photovoltaic devices, there exists considerable interest in understanding charge transport in individual molecular backbones.¹ To investigate charge transport in single-molecule devices, we exploit scanning tunneling microscopy-based approaches in the *break-junction* mode (STM-BJ).

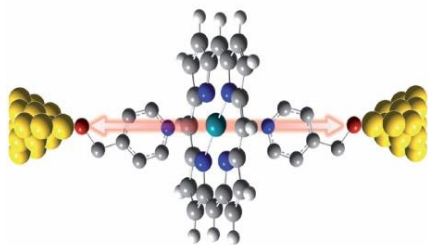


Figure 1: Molecular wire through the metal.

The first block of this seminar will present a novel way to form highly conductive and tunable molecular wires exploiting supramolecular chemistry schemes. Single metalloporphyrin rings are wired from its metallic center by using strong Lewis bases, resulting in an increase of the conductivity of three orders of magnitude versus previous single-porphyrin wires. This novel platform of wiring individual porphyrins mimics the way nature exploits these systems by orienting the perpendicular porphyrin axis as the easy axis for electron/energy transfer (*Fig. 1*).²

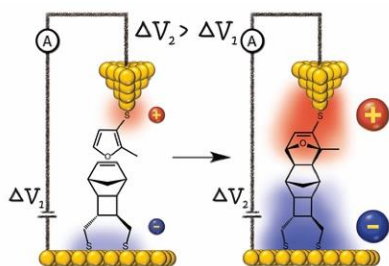


Figure 2: Single-molecular reactor

In the second block, we will demonstrate the use of such approaches to study basic mechanisms in chemical catalysis at the nanoscale. We have designed a surface model system to probe electric

field catalysis of a Diels-Alder reaction by delivering an oriented electrical field-stimulus across two reactants (*Fig. 2*). This method enable studying chemical reactions at the single-molecule level.³

For the last block, we will focus on spin-dependent transport in such single-molecule devices. We will show that the interfacial magnetism or *spininterface*, resulting from the interaction between a magnetic molecule and a metal surface, becomes the key pillar to engineering nanoscale molecular devices with novel functionalities, such as a *spinfilter*-based switch (*Fig. 3*).⁴

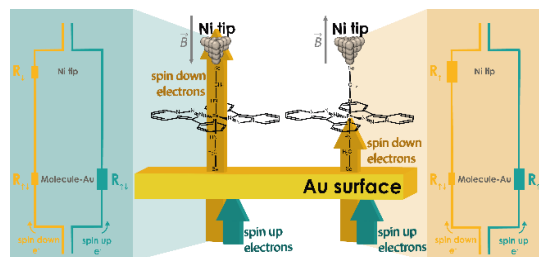


Figure 3: Fe-complex as a spintronic-switch

Keywords: single-molecule junctions, STM break-junction, metalloporphyrins, electrocatalysis, spin-crossover complexes, magnetoresistance, spininterface, spin orbit coupling.

References:

1. Tao, N. J. (2006) Electron Transport in Molecular Junctions *Nat. Nanotechnol.*, 1 (3), 173–181.
2. Aragonès, A. C. et al. (2014) Orientation by Coordination of Metalloporphyrins. *Nano Lett.*, 14 (8), 4751–4756.
3. Aragonès, A. C. et al. (2016) Electrostatic Catalysis of a Diels–Alder Reaction. *Nature*, 531 (7592), 88–91.
4. Aragonès, A. C. et al. (2016) Large Conductance Switching in a Single-Molecule Device through Room Temperature Spin-Dependent Transport. *Nano Lett.*, 16 (1), 218–226.

Synaptic Weight Modulation and Logic Function Learning with Electro-grafted Nano Organic Memristors

Y-P. Lin,¹ C.H. Bennett,² D. Chabi,² D. Vodenicarevic,² D. Querlioz,² T. Cabaret,¹ A. Balan,¹ B. Jous-
selme¹, C. Gamrat,³ J-O. Klein,² V. Derycke¹

¹ LICSEN, NIMBE, CEA, CNRS, Université Paris-Saclay, CEA Saclay 91191 Gif-sur-Yvette Cedex, France

² Université Paris-Sud, IEF (UMR CNRS 8622), F-91405 Orsay, France

³ Laboratoire d'intégration de systèmes et de technologies, CEA Saclay, Gif-sur-Yvette F-91191, France, Contact: yu-pu.lin@cea.fr

Abstract: Neuromorphic computing has gained important attention since it is an efficient way to handle advanced cognitive tasks such as image recognition and classification. Hardware implementation of an artificial neural network (ANN) requires arrays of scalable memory elements to act as artificial synapses. Memristors, which are two-terminal analog memory devices, are excellent candidates for this application as their tunable resistance could be used to code and store synaptic weights with, in principle, low power consumption. In this work, we studied metal-organic-metal memristors in which the organic layer is a dense and robust electro-grafted thin film of redox complexes. The process allows fabricating planar and vertical junctions, as well as small crossbar arrays. The unipolar devices display non-volatile multi-level conductivity states with high R_{MAX}/R_{MIN} ratio and two distinct thresholds. The characteristics of individual memristors were characterized in depth with respect to the targeted synaptic function. We notably showed that they possess the Spike Timing-Dependent Plasticity (STDP) property (their conductivity evolves as a function of the time-delay between incoming pulses at both terminals), which is critical for future applications in neuromorphic circuits based on unsupervised learning. In parallel, we implemented a series of memristors as synapses in a simple prototype: a mixed circuit with the neuron implemented with conventional electronics. This ANN is able to learn linearly separable 3-input logic functions through an iterative supervised learning algorithm inspired by the Widrow-Hoff rule.

Keywords: spike timing-dependent plasticity, electro-grafting, organic memristors, supervised learning, neuromorphic circuit.

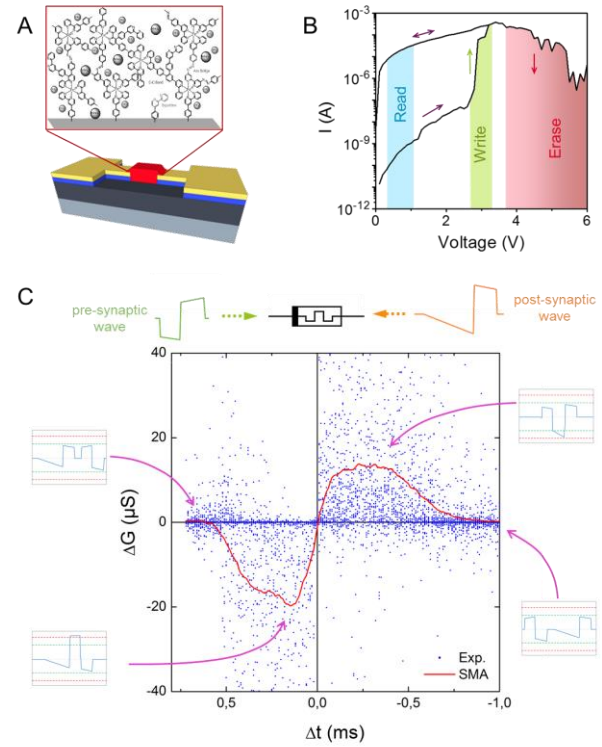


Figure 1: A) Planar structure of the organic memristor and schematic of the electro-grafted thin film of redox complexes. B) Unipolar switching behavior of single memristor. C) Cumulative STDP property of single organic memristor during ~4300 sequentially-applied voltage pulses with random time-delay of pre/post-synaptic input.

References:

1. Bennett C.H., Chabi D., Cabaret T., Jous-
selme B., Derycke V., Querlioz D., Klein J.-O., (2015) Supervised Learning with Organic Memristor Devices and Prospects for Neural Crossbar Arrays, *Nano-Arch 2015 IEEE/ACM International Symposium*, 181.
2. Cabaret T., (2014) Etude, réalisation et caractérisation de memristors organiques électro-graftés en tant que nanosynapses de circuits neuro-inspirés, *Thesis*.

Quantum Interference Effect In Anthraquinone Solid State Junctions

M. L. Della Rocca,¹ C. Bessis,¹ C. Barraud,¹ P. Martin,² J.-C. Lacroix,² T. Markussen,³ P. Lafarge¹

¹Université Paris Diderot, Sorbonne Paris Cité, MPQ, UMR 7162 CNRS, 75205 Paris Cedex 13, France

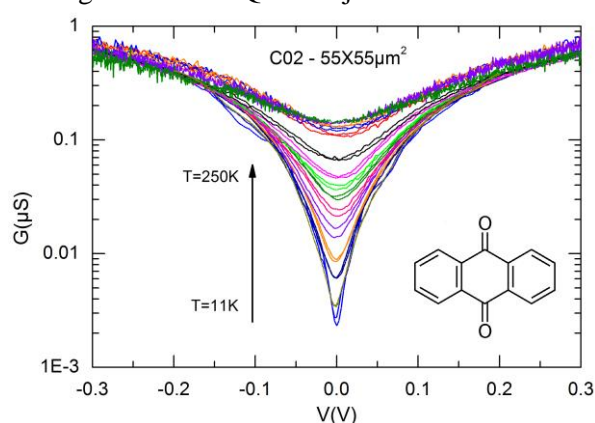
²Université Paris Diderot, Sorbonne Paris Cité, ITODYS, UMR 7086 CNRS, 75205 Paris Cedex 13, France

³QuantumWise A/S, Fruebjergvej 3, Box 4, DK-2100 Copenhagen, Denmark

Abstract: Quantum interference results from the wave properties of electrons and is a well-known quantum effect in mesoscopic physics.¹ The ability to control quantum interference at the molecular level could improve knowledge of electron transport through molecular systems and provide novel electronic behavior of molecular junctions. This subject has recently attracted great interest, both theoretically² and experimentally³. Such effect is predicted to occur with cross-conjugated molecules, systems composed of three unsaturated groups, two of which are conjugated to the third but not conjugated to each other. The anthraquinone (AQ) molecule (inset of Figure 1) is intrinsically cross-conjugated as long as contact between the bottom and top electrodes involves the two peripheral aromatic rings. The expected signature of quantum interference in transport through a molecule is a reduction of the transmission resulting from destructive interference, with a clear antiresonance at the energy where interference occurs.

I will present our investigation of quantum interference on AQ molecular layers embedded in large-area solid-state devices⁴. We have found direct experimental evidence of a large quantum interference effect through measurement of the differential conductance. We have demonstrated that quantum interferences are present at room temperature and are enhanced as temperature is lowered for molecular layers thicker than a monolayer (Figure1). Furthermore, the experimental signature of the electron-phonon coupling appears at low temperature as the major source of decoherence, extinguishing interference effects⁵. The visibility and robustness of this quantum effect on large area junction confirms the dominant intramolecular charge transport mechanism occurring in the molecular layer, and it paves the way for the development of practical devices based on the control of the coherent electron transport through conjugated systems.

Figure 1: Measured conductance G as function of voltage V for an AQ-based junction with an area



of $30 \times 30 \mu\text{m}^2$ for different temperatures ranging from 11K to 250K. A pronounced antiresonance is present at low voltage. Inset: Structure of an AQ molecule.

Keywords: molecular electronics, quantum interference, electron-phonon interaction, electronic transport.

References:

- ¹Nazarov, Y.V., Blanter, Y. (2009), Quantum Transport: Introduction to Nanoscience, Cambridge University Press.
- ²Solomon, G.C., Andrews, D.Q., Ratner, M.A. (2011), Charge and Exciton Transport through Molecular Wires, Eds L.D.A. Siebbeles, F.C. Grozema, Wiley-VCH: Weinheim.
- ³Guedon, C.M., Valkenier, H., Markussen, T., Thygesen, K.S., Hummelen, J.C., van der Molen, S.J., (2012), *Nat. Nanotechnol.*, 7, 305.
- ⁴Rabache, V., Chaste, J., Petit, P., Della Rocca, M.L., Martin, P., Lacroix, J.C., McCreery, R.L., Lafarge, P., (2013) *J. Am. Chem. Soc.* 135, 10218.
- ⁵Bessis, C., Della Rocca, M.L., Barraud, C., Martin, P., Lacroix, J.C., Markussen, T., Lafarge, P., (2016), *Sci. Rep.* 6, 20899.

Impact of Surface Modification of ITO Bottom Electrode on Switching Characteristics of ZnO-based Transparent Resistive Memory Devices Fabricated on Polymer Substrate

F. M. Simanjuntak,^{1*} T. Y. Tseng²

¹Department of Materials Science & Engineering Department, National Chiao Tung University, Taiwan

²Department of Electronics Engineering and Institute of Electronics, National Chiao Tung University, Taiwan

Abstract:

The influence of ultraviolet/ozone (UVO) surface modified bottom electrode on resistive switching characteristics Al-doped ZnO/ZnO/Indium Tin Oxide (ITO) transparent resistive memory devices fabricated on flexible substrate was investigated. The importance of surface treated bottom electrode is simply overlooked in RRAM fabrication process, whereas, the surface condition of bottom electrode (BE)/below layer will highly affect the property/quality of the grown films above it. Thus, may alter the electrical properties and device reliability. Based on our results, RF sputtered ZnO crystallinity is degraded when it is deposited on long exposure surface treated amorphous ITO, as shown in Fig. 1 (a) and (b). However, the preferred (002) orientation is still observed in all samples, which is an advantage for ion diffusion across the resistive layer (Simanjuntak *et al.*, 2015). The (002) orientation will limit the occurrence of branches conducting filaments which leads to uniform/stable switching. In order to fabricate sandwich structure device, 150 μm in diameter of AZO top electrode is deposited on the films. Consequently, highly transparent devices (transparency of approximately 85% at visible wavelength) has been successfully fabricated as depicted in Fig. 1 (c). Both non- and treated UVO BE devices show clockwise bipolar switching mode as shown in Fig (a) and (b), respectively. Obvious enhancement of memory properties of treated devices is exhibited. In this study, we first propose a simple surface treatment method to improve device performance. Further materials analysis have been conducted to explain this phenomena.

Keywords: resistive memory, RRAM, surface treatment, ultraviolet/ozone, transparent electronic devices.

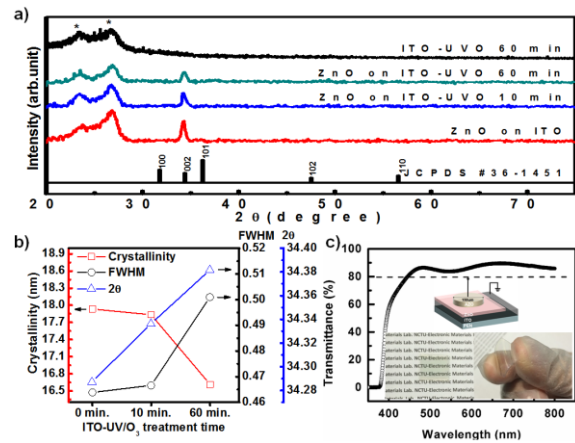


Figure 1: X-Ray diffraction analysis of the deposited films grown on various condition of surface treated ITO/substrate (a) and ZnO crystallinity changes due to the surface treated ITO/substrate (b). (c) Highly transparent devices (transmittance of more than 80% at visible wavelength of 550 nm). Insets show the schematic of single device structure and photograph of the fabricated devices.

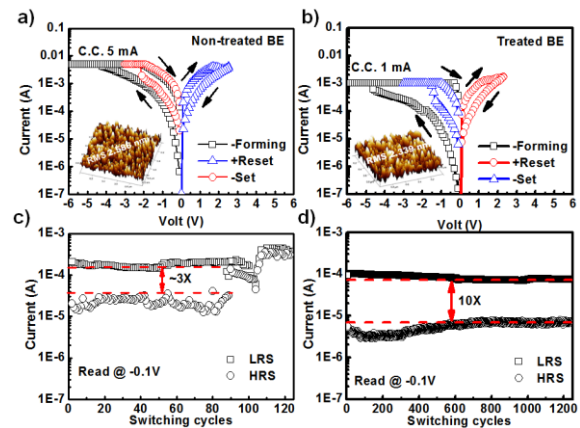


Figure 2: I-V curve of non-treated BE device (a) and treated BE device (b). (c) and (d) endurance performance of device (a) and (b), respectively.

References:

Simanjuntak, F. M., Panda, D., Tsai, T.L., Lin, C. A., Wei, K. H., Tseng Y. T. (2015) Enhanced switching uniformity in AZO/ZnO_{1-x}/ITO transparent resistive memory devices by bipolar double forming, *Applied Physics Letter*.

Synthesis of ZrO₂ films by spray pyrolysis ultrasonic presenting the up conversion phenomenon

P. E. Ortiz-Ortega,^{1*} M García-Hipólito.¹

¹Instituto de Investigaciones en Material, UNAM., Department of Electronics, Mexico City, MEXICO.

Abstract:

Up conversion is an optical process that involves the conversion of lower-energy photons into higher-energy photons. Remarkable properties of the phenomenon in rare earth as a narrow bandwidth, a long-time emission, anti-Stokes emission. This characteristics had been applied to design lasers, solar cells, and analytic sensors and so on (Alves, Bergmann, & Berutti, 2013; Chen & Zhao, 2012; Zhou, Liu, Feng, Sun, & Li, 2015). The main purpose was synthesize films by spray pyrolysis method presenting the up conversion phenomenon in particular for Er³⁺ and Yb³⁺. Films was synthesized by a solution of 0.05 M of ZrO₂ in deionized water and the variation of deposition temperature was from 450°C to 600°C. X ray diffraction found that films crystallized at 500°C and 550°C. The photoluminescence found two emission bands by up conversion at 544 nm and 654 nm for doped films by Er³⁺ at 1% (De la Rosa-Cruz et al., 2003). Percent concentration of co-doped Yb³⁺ was changed at 0.5%, 1%, 3% and 5%. The films with the best intensity was synthesized by ZrO₂:Er³⁺(1%) with Yb³⁺ at 3% and 5% whom presenting two bands at 550 nm and 656 nm. The band at 550 nm decreased in comparison with the band at 656 nm with a percentage rise of Yb³⁺ concentration. This results are partial and the main implication is the synthesis of films doped with Er³⁺ and co-doped with Yb³⁺ whom presented up-conversion as the works in dust with the same materials (De la Rosa-Cruz et al., 2003; Sun, Gao, & Huang, 2014).

Keywords: thin, Erbium, Yterbium, Zirconia, spray pyrolysis ultrasonic, x ray diffraction, photoluminescence, dopants, narrow bandwidth.

References:

- Alves, A., Bergmann, C. P., & Berutti, F. A. (2013). Novel Synthesis and Characterization of Nanostructured Materials. Springer. http://doi.org/10.1007/978-3-642-41275-2_2
- Chen, J., & Zhao, J. X. (2012). Upconversion Nanomaterials: Synthesis, Mechanism, and Applications in Sensing. *Sensors*, 12(12), 2414–2435. <http://doi.org/10.3390/s120302414>
- De la Rosa-Cruz, E., Díaz-Torres, L. a., Rodríguez-Rojas, R. a., Meneses-Nava, M. a., Barbosa-García, O., & Salas, P. (2003). Luminescence and visible upconversion in nanocrystalline ZrO₂:Er³⁺. *Applied Physics Letters*, 83(24), 4903. <http://doi.org/10.1063/1.1632020>
- Sun, L., Gao, F., & Huang, Q. (2014). White upconversion photoluminescence for Er³⁺–Tm³⁺–Yb³⁺ tri-codoped bismuth titanate ferroelectric thin films. *Journal of Alloys and Compounds*, 588, 158–162. <http://doi.org/10.1016/j.jallcom.2013.11.009>
- Zhou, J., Liu, Q., Feng, W., Sun, Y., & Li, F. (2015). Upconversion luminescent materials: Advances and applications. *Chemical Reviews*, 115(1), 395–465. <http://doi.org/10.1021/cr400478f>

Use of Nanobiomechanics robots to tackle HIV virus

AMIT VOHRA

Deputy Engineer, Bharat Electronics Limited, Ghaziabad

amitvohra@bel.co.in, Birbal.vohra@gmail.com

Abstract:

AIDS – Acquired Immune Deficiency Disease is a disease related to human immune system and is caused by HIV virus -Human Immune Deficiency Virus. Till the date a number of researches has undergone to cure AIDS and still under execution. Some even proposed some drugs to cure it, but their side effects are uncountable. In this paper described a proposed research which can be used to tackle with this incurable disease.

AIDS by itself is not a killer disease. The cause of AIDS is the HIV virus that is capable of destroying the immune system. Thereby the host system is vulnerable to small diseases which will turn into a fatal one but actually it is not a fatal disease. The HIV virus attack the WBC's by converting them into the HIV. Thereby all the WBC's are converted into HIV, so the immune system will fail. This is the reason for the death of the patient.

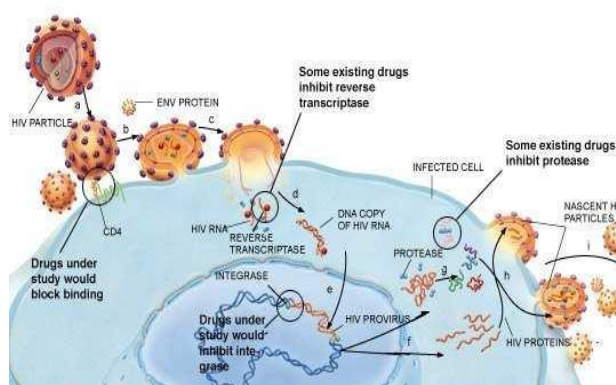


Figure1: Figure illustrating the reaction between end proteins on membranes of HIV and T-CELLS which causes the rest of the DNA segment of HIV to enter into T – CELL to enter WBC and destroys it. The interaction with CD4 is just an initiation of path for reacting with CCR5 which then leads to complete reaction.

The idea proposed here is to design a NANOBIOMECHANIC robot which will prevent the HIV to interact with immune system.

By observing that how the virus affects and interacts with the membrane proteins to enter in WBC the paper describes the ways to rig the HIV virus.

The nanobiomechanic robot comprises the methods of treatment of virus.

The nanobiomechanic robot is comprised of biotic sensors, converters, magnetic particle which will work as a whole for the treatment.

Keywords: Nanobiomechanics, cytotoxins, CD4 cells, biosensors, biological converters, magnetic particles.

References:

- Adachi, A., Gendelman, H. E., Koenig, S., Folks, T., Willey, R., Rabson, A. & Martin, M. A. (1986). J. Virol. 59, 284±291.
Brooks, I., Watts, D. G., Sonesson, K. K. & Hensley, P. (1994). Methods Enzymol. 240, 459±478. BruÈnger, A. T. (1992a). Nature (London), 355, 472±475.
Cell functioning : LAGREINGE

Conjugated Polyrotaxanes: A Critical Assessment of Photo-physical Properties in Correlation with the Effect of the Nature of Host Molecules Encapsulation

A. Farcas,¹ A.-M. Resmerita,¹ P.-H. Aubert²

¹ Petru Poni Institute of Macromolecular Chemistry, 700487 Iasi, Romania

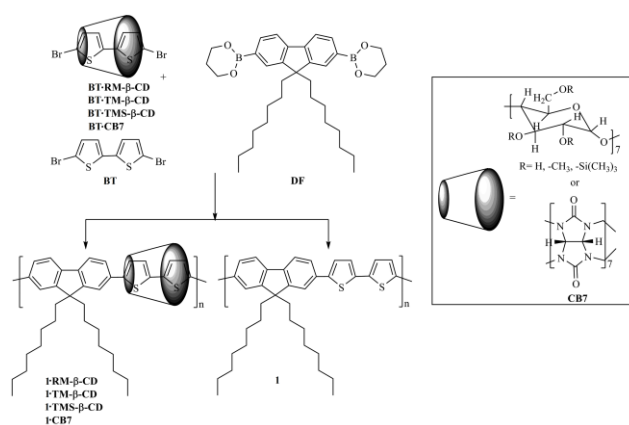
² Laboratoire de Physicochimie des Polymères et des Interfaces (EA 2528), Institut des Matériaux, Université de Cergy-Pontoise, F-95031 Cergy-Pontoise Cedex, France

Abstract:

In the past decade, the field of polymer science has witnessed remarkable innovations and progress, alongside major advances in the complementary field of supramolecular science, which offer great opportunity for new concepts, new materials with unique properties and novel practical applications. Among the wide range of possibilities, the construction of mechanically interlocked assemblies such as conjugated polyrotaxanes (CPr) provides an alternative to the modification of the polymer backbone with substituents, which not only leads to soluble CPs, but allows the “insulation” of individual molecular wires (IMWs). Rotaxane formation provides an efficient strategy to reduce CP's intermolecular interactions by threading a individual π -conjugate backbone through macrocycle rings. Previous studies have shown that the aggregation tendency of CP and quenched luminescence in the solid films can be inhibited by encapsulation of polymer chains. In addition, this strategy has been shown to increase both optical and electronic properties of CPr's compared with films of the non-rotaxinated polymers.^[1,2]

In this presentation, the influence of the nature of the host molecules on the optical and electrochemical behavior, surface topography, as well as transport properties of poly(9,9-dioctylfluorene-*alt*-bithiophene) main-chain polyrotaxanes (Scheme 1) will be reported. Also, a comparison between these properties and those of the corresponding non-rotaxane counterparts will be provided.

Keywords: host-guest system, conjugated polyrotaxanes, macrocycles, fluorescence, fibers, surfaces, optoelectronic applications.



Scheme 1. Synthesis of main-chain polyrotaxanes and their non-rotaxane counterparts

References:

1. Farcas, A., Aubert, P.-H., Mohanty, J., Lazar, A. I., Cantin, S., Nau, W. M. (2014), Effect of permethylated β -cyclodextrin on the photophysical properties of poly[2,7-(9,9-dioctylfluorene)-*alt*-(5,5'-bithiophene)] main-chain Polyrotaxanes, *J. Polym. Sci. Part A: Polym. Chem.*, 52, 460-471.
2. Farcas, A., Aubert, P.-H., Mohanty, J., Lazar, A. I., Cantin, S., and Nau, W. M. (2015), Molecular wire formation from poly[2,7-(9,9-dioctylfluorene)-*alt*-(5,5'-bithiophene)/cucurbit[7]uril] polyrotaxane copolymer, *Eur. Polym. J.*, 62, 124-129.

Acknowledgements: This research was supported by a grant of the Romanian National Authority for Scientific Research, CNCS – UEFISCDI, project number PN-II-ID-PCE-2011-3-0035. A. F. acknowledges financial support from Institute d'Etude Avancées (IEA), University of Cergy-Pontoise, France.

Designing High Performance Digital Logic NOT Gate Using Single Electron Box (SEB) Nano-Devices

Davoud Bahrepour

Mashhad Branch, Islamic Azad University, Mashhad, Iran

Abstract:

The continuing scaling down of CMOS circuits has led researchers to build new devices with nano dimensions, whose behavior will be interpreted based on quantum mechanics [1]. Single-electron devices (SEDs) are promising candidates for future VLSI applications, due to their ultra small dimensions and lower power consumption. In most SED based digital logic designs, a single gate is introduced and its performance discussed. While in the SET based circuits the fan out of a designed gate circuit should be measured and discussed. In the other words, cascaded SET based designs must work properly and the next stage(s) should be driven by previous stage. In this paper, a digital logic NOT gate based on single electron box (Figure 1) which is introduced in [2] reviewed. This gate utilizes in series and by connecting two of this NOT gate a buffer circuit is achieved (Figure 2). In order to achieve better performance the designed NOT gate circuit is improved by the use of scaling process [3]. The scaling factors are:

$$CSF \triangleq \frac{C_{T,new}}{C_{T,old}} \quad (1)$$

$$RSF \triangleq \frac{R_{T,new}}{R_{T,old}} \quad (2)$$

where CSF is the capacitance scaling factor, $C_{T,new}$ is the total capacitor in the new technology, $C_{T,old}$ is the total capacitor in the old technology, RSF is the tunneling resistance factor, $R_{T,new}$ is the tunneling resistance in the new technology, and $R_{T,old}$ is the tunneling resistance in the old technology. Scaling process changes the voltage, resistance and capacitance values and lead to better switching speed and better bit error rate (BER), however, it does not change the logic function. By the use of SIMON simulator [4] the correct operation of the new design is illustrated.

Keywords: digital logic NOT gate, single-electron devices, fan out, switching speed, bit error rate.

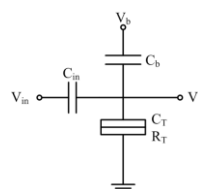


Figure 1: A simple NOT gate circuit based on a SEB.

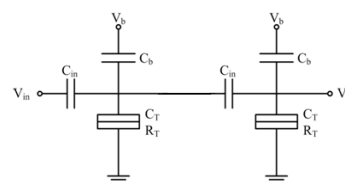


Figure 2: Cascading two NOT gate circuits based on a SEB (buffer gate). By changing the voltage, resistance and capacitance values better performance will achieve.

References:

1. Likharev K. K. (1999), Single-Electron Devices and Their Applications, *Proceeding of the IEEE*, vol. 87, No. 4, 606–632.
2. Rehan S. E. (2011), The design of logic gates using Single Electron Box (SEB) Nano-Devices, *Design & Technology of Integrated Systems in Nanoscale Era (DTIS), 2011 6th International Conference on*, 1-6.
3. Sharifi M. J. , Bahrepour D. (2011), Introducing a technology index concept and optimum performance design procedure for single-electron-device based circuits, *Microelectronics Journal*, Volume 42, Issue 7, July 2011, 942-949.
4. Wasshuber C., Kosina H., Selberherr S., (1997), SIMON - A Simulator for Single-Electron Tunnel Devices and Circuits, *IEEE Transactions on Computer-Aided Design*, Vol. 16, 937–944.

InnovNano France 2016: Industrial Session

Graphene based supercapacitors: results and perspectives

P. Bondavalli,¹ G. Pognon,¹

¹Thales Research and Technology, Palaiseau, France

Abstract:

Supercapacitors are electrochemical energy storage devices that combine the high energy-storage-capability of conventional batteries with the high power-delivery-capability of conventional capacitors. In this contribution we will show the results of our group recently obtained on supercapacitors with electrodes obtained using mixtures of carbonaceous nanomaterials (carbon nanotubes (CNTs), graphite, graphene, oxidised graphene). The electrode fabrication has been performed using a new dynamic spray-gun based deposition process set-up at Thales Research and Technology (patented). First, we systematically studied the effect of the relative concentrations of Multi-Walled Carbon Nanotubes (MWCNTs) and graphite on the energy and power density. We obtained a power increase of a factor 2.5 compared to barely MWCNTs based electrodes for a mixture composed by 75% of graphite [1]. This effect is related with the improvement of the mesoporous distribution of the composites and to the increase of the conductance as pointed out by Coleman et al. [2]. After these results, we decided to test water as a solvent in order to reduce the heating temperature and to obtain a green type process without toxic solvents. To achieve stable suspensions we oxidised the graphene and the CNTs before putting them in water. We observed that changing the Graphene Oxide concentrations we obtained different value of capacitance and energy. The best results were obtained with 90% of GO and 10% of CNTs [3]. We obtained 120F/g and a power of 30kW/Kg. The importance of these results is that it is the first time that these performances have been obtained for graphene related materials using an industrial fabrication suitable technique that can be implemented in roll-to-roll production. In this way we were able to fabricate stable suspensions in less than one hour compared to three days using NMP. All these results demonstrate the strong potential to obtaining high performance devices using an industrially suitable fabrication technique. Finally, new results using mixtures of Carbon nanofibers and graphene will be shown. These new composite

allow to use ionic liquid as electrolytes and so to increase dramatically the energy stored in the device without reducing the power.

Keywords: Graphene, Carbon Nanotubes, Energy, supercapacitors, Deposition method, Carbon Nanofibers.

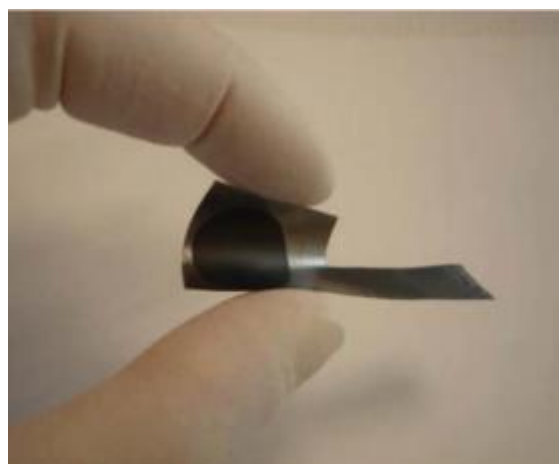


Figure 1: Figure illustrating a flexible supercapacitors obtained using spray-gun deposition method.

References:

1. Supercapacitor electrode based on mixtures of graphite and carbon nanotubes deposited using a new dynamic air-brush deposition technique, P Bondavalli, C.Delfaure, P.Legagneux, D.Pribat JECS 160 (4) A1-A6, **2013**
2. Non-faradic carbon nanotubes based supercapacitors : state of the art, P.Bondavalli, D.Pribat, C.Delfaure, P.Legagneux, L.Baron, L.Gorintin, J-P. Schnell, Eur. Phys. J. Appl. Phys. 60,10401, **2012**
3. Graphene-based technologies for energy applications, challenges and perspectives, Etienne Quesnel, Frédéric Roux, Paolo Bondavalli et al., *2D Materials* 08/2015; 2(3):030204.

Graphenea Roadmap: Wafer Scale Integration

Iñigo Charola

Business Development Director, Graphenea

i.charola@graphenea.com

Abstract

Graphenea aims to develop the potential of graphene for electronic systems by means of combining large scale graphene synthesis and conventional CMOS technology into an industrial compatible process. If wafer scale integration is available, many applications will be realized on commercial scale (logic, HF, optoelectronics, telecommunications, sensors and flexible electronics). Graphenea objective is to meet industry demand of a demonstrator made with actually compatible CMOS processes, then spill-over to other applications will be possible and broad adoption will begin

Speaker Biography (Inigo Charola) Iñigo Charola is Business Development Director at Graphenea. He has an extensive experience in industrial related products at marketing and sales positions. He started his career at ASSA ABLOY, a global leader in security products, then as Sales and Marketing Director at an industrial processes private company. Before joining Graphenea he is been working in the Electronic Manufacturing Services industry as a Sales Director. He holds a Bachelor's Degree in Business Administration from University of Wales, a Master in Marketing and Sales Management from ESIC and an Executive MBA from Deusto Business School.

Company Profile (Graphenea) Graphenea is the leading graphene producer. Graphenea supplies CVD graphene wafers and Graphene Oxide materials for industrial applications. Graphenea develops custom materials in joint development for specific applications.

Static Multiple Light Scattering to monitor protein aggregation and pigments dispersibility

C. Tisserand,^{1,*} G. Brambilla¹, P. Bru¹, G. Meunier¹

¹Formulacion, 10 Impasse Borde Basse, 31240 L'Union, France

Abstract:

A technique of Static Multiple Light Scattering (SMLS) is proposed to measure mean particles size in a large range of concentration between 0.0001 and 95%, for sizes between 10 nm and 100 μm by Turbiscan LAB technology. Turbiscan consists in sending a light source (880nm) and acquiring backscattered and transmitted signal. The signal intensity enables to measure directly the mean spherical equivalent diameter (d), knowing refractive index of continuous (n_c) and dispersed phase (n_p) and the particles concentration (φ) according to the Mie theory:

$$d = f(BS \text{ (or } T), \varphi, n_p, n_c)$$

with BS for Backscattering Intensity and T for Transmission Intensity.

This technique has the advantage to measure in one click, without sample preparation or dilution, the mean particles size and so the dispersibility efficiency particularly for concentrated suspensions. Other optical techniques such as DLS or PTA can perform this measurement but only at a very high dilution which denatures the agglomerates and give an erroneous size of the native particles.

In this paper, we present different complete studies:

- mean size measurement of various products, comparison of SMLS with SEM/TEM microscopy,
- dispersibility characterization of pigments,
- protein aggregation monitoring versus histidine concentration

Keywords: protein, pigments, coating, static multiple light scattering, aggregation, dispersibility, mean size

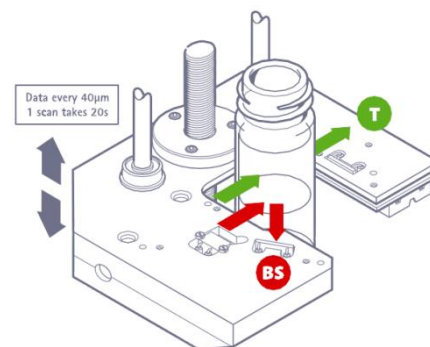


Figure 1: Principle of measurement of Turbiscan®

References:

- M. Wulff-Pérez, J. de Vicente, A. Martín-Rodríguez, M. J. Gálvez-Ruiz, *Int. J. Pharm.*, 2012, 423, 161-166
- A. Pizzino, M. Catté, E. Van Heckea, J.-L. Salager, J.-M. Aubry, *Coll. Surf.*, 2009, 338, 148-154
- D. Seo, W. Yoon, S. Park, J. Kim, J. Kim, *Coll. Surf. A*, 2008, 313-314

Bulk graphene production and application in composites, energy and coatings

J. Gomez,^{1*} J. Perez,¹ E. Villaro,^{2,3}

¹ Avanzare Innovacion Tecnologica S.L., Navarrete, Spain ² Instituto de Tecnologías Químicas Emergentes de La Rioja; San Francisco, 11 Navarrete, Spain. ³ Departamento de Química Inorgánica y Técnica, UNED. Senda del Rey, 9, Madrid, Spain.
julio@avanzare.es

Abstract:

The bulk graphene market will exponentially grow in the next few years. Its applications in composites will be the largest segment, followed by energy storage applications.[1]

Different synthetic methods can be used for the production of graphene and graphene related materials.

Several reviews analyzed the applications of the different graphene and related products in energy [4, 1b] and in composites applications.[5, 1b]

In this presentation, 3 different methods for the production of bulk graphene or reduce graphene oxide: liquid exfoliation, reduced graphene oxides and high expansion were compared with other production methods and products in the market.

The complete characterization of graphene and highly reduce graphene oxide using TEM, SEM, AFM, XPS, DRX, Laser diffraction, surface area and pore size analysis (Figure 1), etc will be presented.

Different types of graphene materials with variation in lateral size, defects and defects concentration, thickness, etc, have been used to obtain graphene-thermoplastic and thermoset composites. The different effects of the incorporation of liquid exfoliated graphene, highly reduced graphene oxide and graphene nanoplatelets on electrical, thermal conductivity and fire retardant properties of epoxy were investigated.

Related to electrical properties, some of these composites show lower percolation threshold limits than the previously reported values, also obtaining ultralow percolation limits (Figure 2), opening a new range of applications and markets.

Other factors as processing technique, the compatibility between graphene and matrix and dispersion have an extremely high importance in the results. Vertical and horizontal casting experiment (Figure 3) has been performed to observe

the segregation of the graphene in the polymer matrix.

The use of different graphene materials and decorated graphene materials in energy applications, from anodes and cathodes of batteries to supercapacitors with ultrahigh energy density, will be also presented. .

Keywords: graphene production, graphene oxide, composite, coatings, energy applications.

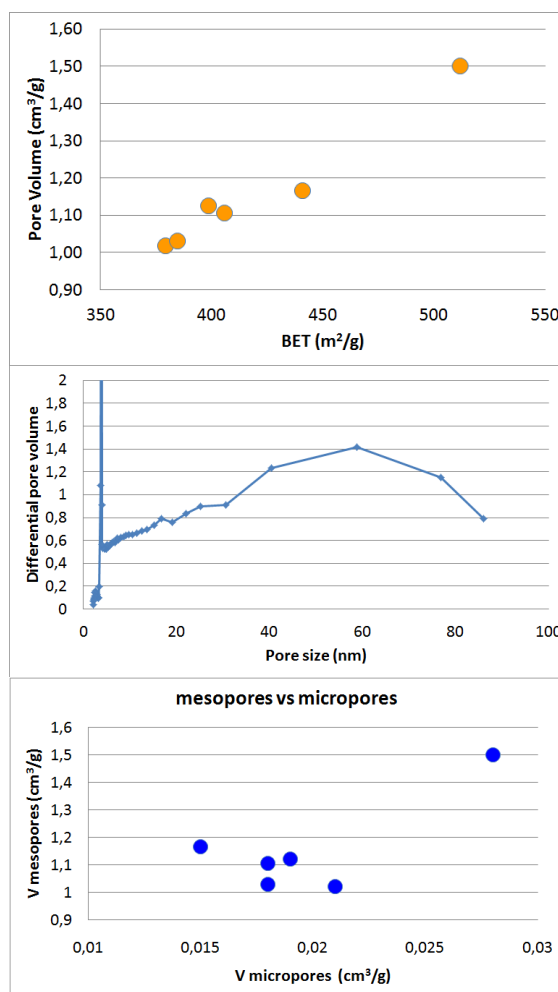


Figure 1: Pore size analysis, distribution and micro/mesoporous distribution for different HRGO prepared by thermochemical methods.

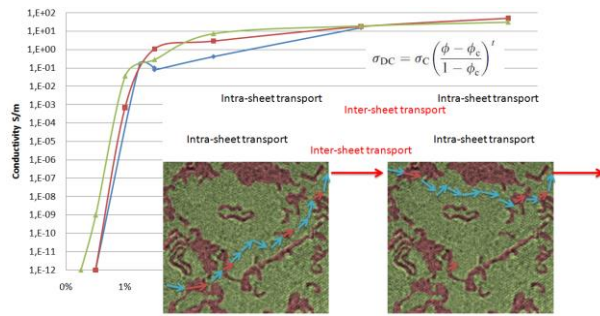


Figure 2: Electric percolation and Scheme of the transport in a composite.

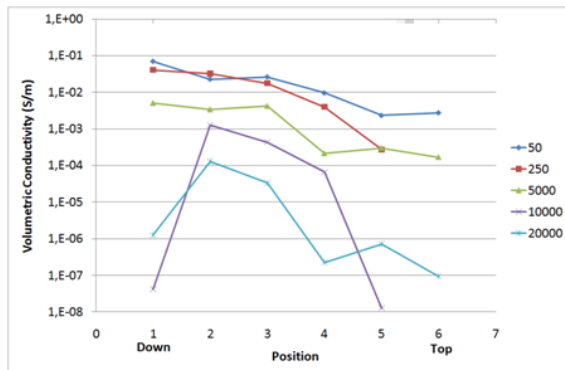


Figure 3: Influence of processing on the electrical conductivity of epoxy-HRGO composites.

References:

1. a) Zh Ma, R. Kozarsky, M. Holman., GRAPHENE MARKET UPDATE. LUX RESEARCH (2014). b) Ferrari A Cet al Nanoscale 7 (2015) 4598–810, c) M. Peplow, Nature 522, (2015), 268
2. W. Ren, H.-M. Cheng, Nature Nanotechnology 9, (2014) 726–730
3. P. Wick et all, Angew. Chem. Int. Ed. 53 (2014)7714–7718. b) R. Hurt et all, Carbon, 65 (2013) 1-6
4. The role of graphene for electrochemical energy storage. Nature Materials 14 (2015) 271–279.
5. a) P Samorì, I A Kinloch, X Feng and V Palermo, 2D Mater. 2 (2015) 030205 b) R. J. Young, I. A. Kinloch, L. G., Kosty. S. Novoselov, Composites Science and Technology, 72 (2012) 1459–1476

Graphene: the early commercialisation prospects

Ray Gibbs
CEO Hatydale Graphene Industries Plc

Abstract:

Graphene has been hailed as the new wonder material, yet commercial progress remains slow to the industrial observer. Ray Gibbs CEO of Haydale will take you through what they are doing to rapidly grow the Graphene space and why the near term wins are really not that far away and bigger than some researchers and commentators think.

The key to commercialisation is to

- fully understand the base materials and their price/performance criteria;
- focus on key market drivers in markets renowned for early adoption of new technology- most likely unregulated;
- to establish a robust supply chain; and
- gain independent credibility for the technical claims.

Keywords: Graphene commercialisation

3D Printing Sets New Standards in Microfabrication

A. Legant¹

¹Nanoscribe GmbH, Eggenstein-Leopoldshafen, Germany

Abstract:

The technique of two-photon polymerization (TPP) allows for additive manufacturing based on 3D digital models with sub-micrometer feature sizes and resolution. In addition, 2D and 2.5D topologies can be fabricated with ultra-high aspect ratios and outstanding design freedom with a resolution between electron beam and UV lithography. This enables additive as well as subtractive maskless lithography beyond the limits of grayscale lithography or the limitations of diamond milling. This talk gives an overview on the technology, its performance and highlights both scientific disruptive breakthroughs as well as enabled applications in industry.

A simple workflow including the use of STL data as standard secures a rapid transformation of virtual models into physical objects. This closes the gap to conventional stereolithography formerly considered as highest resolution 3D printing technique.

The range of applications is wide spread: In optics and photonics, TPP is - among others - used for the fabrication of photonic crystals materials [1] and optical cloaks [2], photonic colors or high-precision micro-optics. As one industrial application example, wafer-level micro-optics and photonic multi-chip integration [3] will be discussed.

Mechanical engineers are enabled to design unique mechanical characteristics previously unachievable by shaping complex microtrusses. Ultra-light, yet strong [4] or auxetic materials as well as unfeelability cloaks [5] have been published.

Unique designs and precision open new applications in microfluidics: Filters, mixers, complex nozzles, micro-robots [6] or micro-needles for painless drug delivery exemplify the challenges that can be overcome by 3D printing on the micro- to mesoscale.

Keywords: 3D microprinting, Two-photon polymerization, highest precision additive manufacturing, microscale fabrication, 3D laser lithography



Figure 1: The Figure illustrates meso-scale printing with sub-micrometer feature sizes.

References:

- [1] N. Muller et al., “Silicon Hyperuniform Disordered Photonic Materials with a Pronounced Gap in the Shortwave Infrared”, *Advanced Optical Materials* 2, 115–119 (2014).
- [2] T. Ergin et al., “Three-dimensional invisibility cloak at optical wavelengths”, *Science* 328, 337–339 (2010)
- [3] N. Lindenmann et al., “Photonic wire bonding: a novel concept for chip-scale interconnects”, *Optics Expr.* 20, 17667 (2012).
- [4] D. Jang et al. “Fabrication and Deformation of Three-Dimensional Hollow Ceramic Nanostructures”, *Nature Materials* 12, 893 (2013).
- [5] T. Bückmann et al. “An elasto-mechanical unfeelability cloak made of pentamode metamaterials”, *Nature Communications* 5, 4130 (2014).
- [6] Cellular Cargo Delivery: Toward Assisted Fertilization by Sperm-Carrying Micromotors, M. Medina-Sánchez et al., *Nano Letters*, 2016, 16 (1)

Graphene grown on SiC substrates for applications in electronics

L. Serrano^{1,2}, A. García-García^{1,3}, A. Ballestar^{1,2}, J. M. de Teresa^{2,4,5}, M. R. Ibarra^{2,5}, P. Godignon³

¹ Graphene Nanotech, S.L., Miguel Villanueva 3, 26001 Logroño, Spain

² INA, LMA, Universidad de Zaragoza, Mariano Esquillor, 50018 Zaragoza, Spain

³ CNM-IMB-CSIC, Campus UAB, Bellaterra, 08193 Barcelona, Spain

⁴ ICMA, Universidad de Zaragoza, 50009 Zaragoza, Spain

⁵ Departamento Física de la Materia Condensada, Universidad de Zaragoza, 50009 Zaragoza, Spain

Abstract:

Since the isolation of graphene became accessible and the investigation of its properties revealed outstanding features [1], a large number of companies aiming the production of graphene-based materials and devices appeared in order to develop a new and powerful technology. However, the fabrication process of high quality graphene in an industrial scale remains as an open issue. The growth of graphene on Silicon Carbide (SiC) wafers is one of the most promising routes for both production and integration into planar technology electronic applications [2-3].

In the present work we study the epitaxial graphene growth on top of different types of SiC substrates. Of particular interest for electronic applications are those in which a bottom gate is ready to be used and prepared prior to graphene growth. Processes of implantation of nitrogen atoms at a controlled depth have been used in order to fabricate such substrate. We investigated the properties of the graphene grown on top of them by means of non-invasive techniques, e.g. Raman spectroscopy and optical and atomic force microscopy (AFM), and completed the characterization with High Resolution Transmission Electron Microscopy (HRTEM) and transport measurements. As a result, we found that high quality single layer graphene is covering ~85% of the substrate and it appears to be a good candidate for the development of bottom gated devices based on graphene in an industrial scale.

Keywords: graphene, Silicon Carbide, SiC, field effect gate transistors, FET, bottom gate, optics, electronics, high frequency, biosensors.

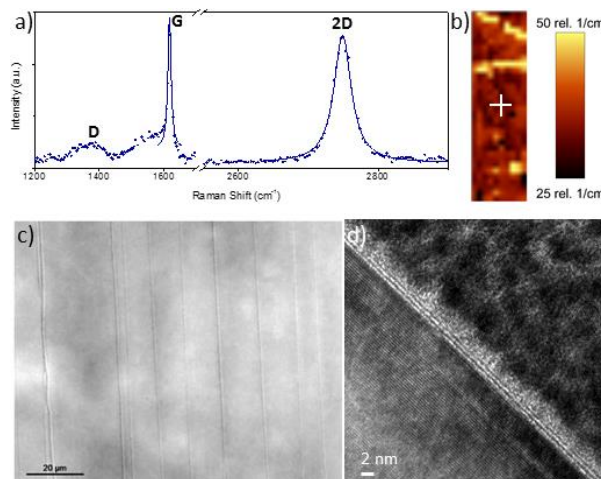


Figure 1: a-b) Raman results obtained on graphene grown on an implanted SiC substrate. a) Raman spectra measured at the position indicated by the white cross in b). b) Mapping of the FWHM of the 2D peak, in which only the yellow dots indicate positions where graphene is not found, as it can be inferred from the color scale to the right. c) Optical Image of a sample surface. Note the large width of the observed terraces. d) HRTEM image of a sample, in which the presence of one graphene layer and the buffer layer are clearly seen (dark lines on the center of the image).

References:

- [1] Novoselov, K. S., Fal'ko V. I. Colombo L., Gellert P. R., Schwab M. G. and Kim K. (2012). "A roadmap for graphene." *Nature* 490(7419): 192-200.
- [2] First, P. N., de Heer, W. A., Seyller, T., Berger C., Strosio, J. A., Moon, J-S. (2011). "Epitaxial Graphenes on Silicon Carbide." *MRS Bulletin* 35(04): 296-305.
- [3] Waldmann, D., Jobst, J., Speck, F., Seyller, T., Krieger, M. and Weber, H. B. (2011). "Bottom-gated epitaxial graphene." *Nat Mater* 10(5): 357-360.

NanoMetrology France 2016 Session I
Methodologies for NanoMaterials
Characterization

Exact solutions for the axial pressure profiles in channels with Maxwell slip flow

A. C. Hoffmann,^{1*} S. Karakitsiou,¹ B. Holst¹

¹University of Bergen, Dept. of Physics and Technology, Bergen, Norway

Abstract:

An upsurge in the development of micro- and nanoelectromechanical devices [1] has kindled renewed interest in the flow of fluids at moderately high Knudsen numbers through channels and crevices. Another reason for this renewed interest is the flow in shale reservoirs, where the pore size is extremely small, and the prediction of flow and permeability depends on accurate models. In many modern applications, such as MEMS and NEMS, namely micro- and nanoelectromechanical devices, it is important to know the pressure profile in channel flow at Knudsen numbers in the Maxwell slip regime.

An explicit expression for the axial pressure profile in a cylindrical channel with Maxwell slip flow of a gas is derived in a direct and transparent way from first principles. The resulting expressions, which only involve the inlet and outlet pressures and the channel dimensions, are given for use in modelling or simulations of channel flows at Knudsen numbers in the range 10^{-3} –0.1. The expression is shown to be correct by deriving from it an expression for the mass flow through the channel, which is shown to be identical to the known expression for the mass flow through cylindrical channels with Maxwell slip flow. The developed expression makes it possible to assess the effects of the involved physical parameters directly (see e.g. Figure 1). The same method may be used for deriving pressure profiles for Maxwell slip flow in other types of nano-sized channels, e.g. flat rectangular channels with large aspect ratio.

Keywords: nanochannels, pressure profile, Maxwell slip flow, MEMS, NEMS

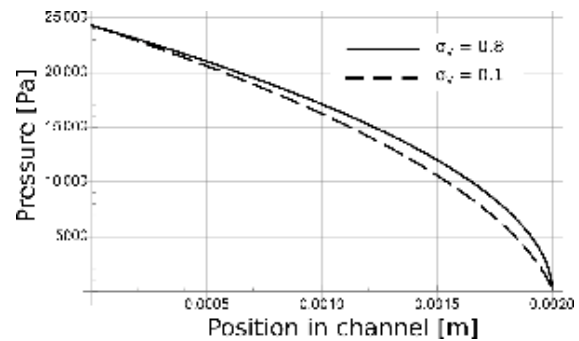


Figure 1: Figure showing the effect of the accommodation coefficient (the fraction of molecules undergoing diffuse rather than specular reflection at the tube wall), σ_v , on the pressure profile in a cylindrical channel with Maxwell slip flow. The mass flow through the channel increases by 23% when changing the accommodation coefficient from the standard value of 0.8 to 0.1.

References:

Nishanth Dongari, Ashutosh Sharma, and Franz Durst. (2009) Pressure-driven diffusive gas flows in micro-channels: from the knudsen to the continuum regimes. *Microfluidics and Nanofluidics*, **6**:679–692.

Dynamic identification of perforated MEMS devices by the continuous wavelet transform

J. Lardiès¹, T.P. Le²

¹Institut FEMTO-ST, DMA, Université de Bourgogne Franche-Comté, 2500 Besançon, France

²Laboratoire Navier, Université Paris Est, 77455 Marne-la-Vallée, France

Abstract: Micro electro mechanical systems (MEMS) are built using integrated circuits and include movable parts such as membranes, plates, beams and other mechanical components. The structural parts differ between applications and perforated microplates are often used in micromechanical squeeze film dampers to reduce the damping and spring forces due to the fluid flow inside and around the microstructure. Identification of the damping caused by surrounding fluid and by the dissipations in the material is very important to predict the dynamic response of the microsystem and to estimate some important parameters such as the quality factor, the switching time and the release time. Many methods have been proposed to calculate the squeeze-film damping in perforated micro systems. In particular G. De Pasquale and T. Veijola (2008) used numerical strategies and the software ANSYS to estimate the gas damping in perforated MEMS. It was shown that ANSYS results contained a systematic error at small perforations and were not usable for large perforations. A method was proposed by J. Lardiès (2015) to estimate the modal parameters of a micro structure using the subspace approach and the damping coefficient was obtained by eigendecomposition of the transition matrix. In this communication we propose a time-frequency method (Le *et al.*, 2015) based in the use of the wavelet transform (WT) to identify the dynamic parameters (in particular the modal parameters) of a perforated microplate (Figure 1). The perforated microplate area is $A = 3.127 \times 10^{-8} \text{ m}^2$ and its mass is $m = 3.814 \times 10^{-9} \text{ kg}$. The dynamic measurements are conducted in time domain by means of a laser vibrometer (details are given in the communication). We obtain then the displacement of the center of the MEMS (Figure 2). The WT of this response is used for dynamic parameters identification. A procedure to obtain the skeleton of the WT is presented in the communication and it is shown that from the skeleton we can identify the dynamic parameters of the perforated microplate. With our approach it is not necessary to use the excitation force, only output measurements in the time domain are used. Numerical examples and an experimental example of a perforated microplate are presented. Figure 3 shows the amplitude (in logarithm form) and the phase of the skeleton of the W.T. used to identify the dynamic parameters.

Values of these parameters will be presented in the communication.



Figure 1. Experimental test on the perforated microplate with a laser vibrometer

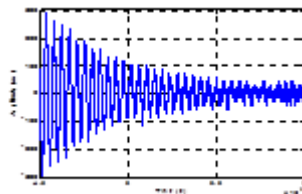


Figure 2. Displacement response of the perforated microplate

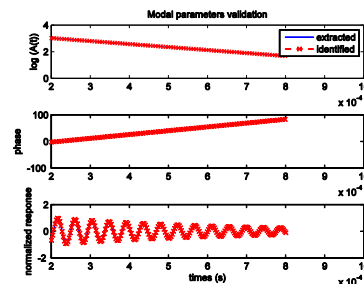


Figure 3. Amplitude and phase of the wavelet transform. Normalized reconstituted displacement of the perforated microplate

Keywords: MEMS, microplate, oscillating system, dynamic response, wavelet transform, modal parameters, experimental identification.

References:

1. De Pasquale, G. and Veijola, T. (2008) Comparative numerical study of FEM methods solving gas damping in perforated MEMS devices, *Microfluid Nanofluid* 5, 517-528.
2. Lardiès, J (2015) Modal parameter identification of perforated microplates from output data only, *Nanotech France 2015*.
3. Le T.P. and Argoul P. (2015) Distinction between harmonic and structural components in ambient tests using the time-frequency domain decomposition technique, *Mechanical Systems and Signal Processing* 52, 29-45.

General atomistic approach for modeling metal-semiconductor interfaces using density functional theory and non-equilibrium Green's function

Daniele Stradi,^{1,2} Umberto Martinez,² Anders Blom,² Mads Brandbyge,¹ and Kurt Stokbro²

¹Center for Nanostructured Graphene (CNG), Department of Micro- and Nanotechnology (DTU Nanotech), Ørstedes Plads, Building 345B, DK-2800 Kongens Lyngby, Denmark

²Quantumwise A/S, Fruebjergvej 3, Postbox 4, DK-2100 Copenhagen, Denmark

Abstract:

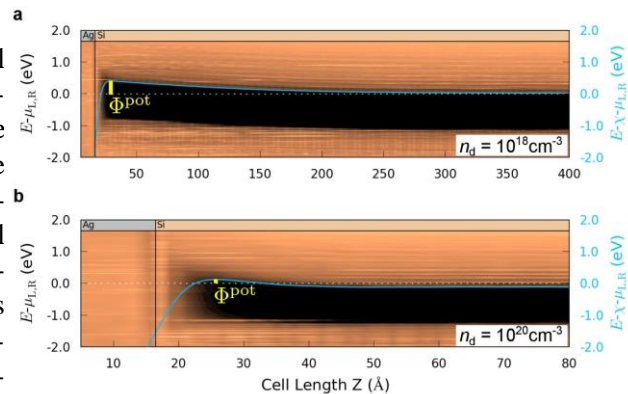
Metal-semiconductor (M-SC) contacts play a pivotal role in a broad range of technologically relevant devices. Still, their characterization at the atomic-scale remains a delicate issue. One of the reasons is that the present understanding relies either on simplified analytical models often parametrized using experimental data [1], or on electronic structure simulations describing the interface using simple slab calculations [2]. Here we propose a general strategy to model realistic M-SC interfaces by using density functional theory (DFT) in combination with the non-equilibrium Green's function (NEGF) method as implemented in the Atomistix ToolKit (ATK) simulation software [3]. An accurate description of both sides of the interface is achieved by using a meta-GGA functional [4] optimally tuned to reproduce the SC measured band-gap, and a spatially dependent effective scheme to account for the presence of doping in the SC side. Compared to previous computational methods [2], the present approach has the important advantages of (i) treating the system using the appropriate boundary conditions and (ii) allowing for a direct comparison between theory and experiments by simulating the I-V characteristics of the interface. We apply this methodology to an Ag/Si interface relevant for solar cell applications, and test the reliability of traditional strategies [1,2] to describe its properties [5].

Keywords: device simulations, density functional theory, metal-semiconductor interfaces, Schottky barrier.

Figure 1: Local density of states for a Ag(100)/Si(100) device along the direction normal to the Ag/Si interface plane, for two different doping densities of the Si side of the interface, $n_d=10^{18} \text{ cm}^{-3}$ and $n_d=10^{20} \text{ cm}^{-3}$. The light-blue lines show the electrostatic potential relative to the metal fermi energy and the chemical potential of bulk silicon. The yellow vertical lines indicate the Schottky barrier at the interface.

References:

- [1] S. M. Sze and K. N. Kwok, *Physics of Semiconductor Devices: 3rd edition* (Wiley, 2006)
- [2] C. G. van de Walle and R. M. Martin, *Phys. Rev. B* **35**, 8154 (1987)
- [3] “Atomistix ToolKit version 2015.0”, QuantumWise A/S (www.quantumwise.com)
- [4] F. Tran and P. Blaha, *Phys. Rev. Lett.* **102**, 226401 (2009)
- [5] D. Stradi et al. <http://arxiv.org/abs/1601.04651>



Sidewall Roughness of Nanoelectronic and Nanophotonic Structures: Metrological Challenges and their Critical Role in Applications

V. Constantoudis,^{1,2,*} G. Patsis^{2,3}, and E. Gogolides^{1,2}

¹Institute of Nanoscience and Nanotechnology., NCSR Demokritos, Aghia Paraskevi, Greece

²Nanometrisis P.C., Aghia Paraskevi, Greece

³Department of Electronic Engineering, Technological Educational Institution, Athens, Greece

Abstract:

The reliable performance of several nanoelectronic and nanophotonic devices depends critically on the dimensions of the nanostructures they contain. Deviations from the designed size and shape cause degradation effects and reduce dramatically their yield. This is the reason why the measurement and characterization of these dimensional deviations have been a great challenge of nanometrology. In this work, we present a concise review of the recent advances and open issues on one of the most common type of size and shape deviation: the sidewall roughness of linear and cylindrical nanostructures, which in the jargon of semiconductor manufacturing is usually called Line or Contact Edge Roughness (LER/CER) (see Fig.1). The presentation is separated in three parts. In the first, we focus on the measurement techniques used for the measurement of sidewall roughness (SEM, AFM and scatterometry) and discuss their comparative pros and cons with respect to the accuracy of the measurement. In the second part, we describe the mathematical methods and parameters (pdf moments, Fourier spectrum, correlation and fractal analysis) proposed for the characterization of the acquired roughness measurements in view of their relevance to the fabrication conditions and device operation. Finally, we elaborate the challenges and issues raised by the recent advances in nanolithography (Multiple patterning techniques, Directed Self Assembly Lithography) to produce features with widths <10nm and present the recent results of the relevant work of our group to address these and explore their solutions.

Keywords: sidewall roughness, Line Edge Roughness, Contact Edge Roughness, nanolithography, nanoelectronics, nanophotonics.

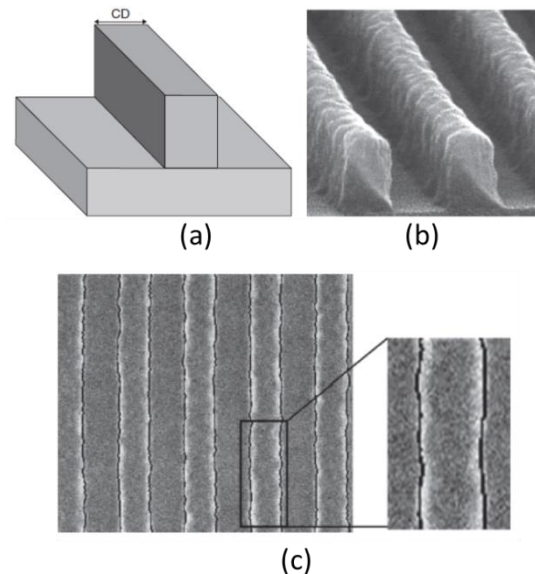


Figure 1: a) Ideal Shape of a line nanostructure on a substrate with totally smooth sidewalls, b) an SEM image of real line structure where the roughness of sidewalls is evident and c) the extraction of line edge roughness from a top-down SEM image.

References:

Constantoudis, V., Gogolides, E., Patsis, G.P. (2013), Sidewall roughness in nanolithography: Origins, metrology and device effects *Nanolithography: The Art of Fabricating Nanoelectronic and Nanophotonic Devices and Systems*, pp. 503-537

Constantoudis, V., Kuppaswamy, V.-K.M., Gogolides, E. (2013), Effects of image noise on contact edge roughness and critical dimension uniformity measurement in synthesized scanning electron microscope images *Journal of Micro/Nanolithography, MEMS, and MOEMS*, 12 (1), art. no. 13005

Implementation of Process Analytical Technology for the multi-sectoral manufacturing of nanoparticles by wet milling

C. Vairon,¹ D. Bordeaux,¹ A. Blasco,²

¹SDTech, Alès, France, ²Malvern Instruments, Malvern, United-Kingdom

Abstract:

The demand for nanoparticles has been rapidly increasing with the widening of nanomaterials applications from construction and coatings to energy, food, cosmetic and pharmaceutical industries. After an intensive innovation phase the transfer to industrial production brings new challenges. The online characterization of manufactured nanoparticles brings major advantages in a context where material's costs and quality are preponderant. This study will focus on the top-down manufacturing of nanoparticles and nanosuspensions by wet milling process. The objectives of the process analytical technology (PAT) in this case are numerous: reduction of the analytical time and costs, pollution and risk reduction by avoiding nanoparticles samples transport, fast interaction with the process to avoid nonconformity and downtime, optimisation of the required process energy, better knowledge of the process by real-time information without sampling bias, automated processes. The key-information required during the nano-milling process were identified. The particle-size distribution (PSD) and its evolution during the milling process is the most critical information (end-user specification, milling efficiency, possible agglomeration phenomenon between nanoparticles). On the other hand, the rheology and the turbidity of the suspensions are linked to the PSD changes. The sensitivity range and the measuring limits such as the nanoparticle concentration in liquid were studied. The integrated measurement through Dynamic Light Scattering (DLS) and Static Light Scattering (SLS) addresses the challenges of the PAT in universal nano-milling processes: very short measuring time, non-destructive testing or reduced sampled quantities, wide measuring range and reproducibility. The data acquisition enables the interconnection between the process and the analyser. The installation will provide useful information for the industrial scale-up of the process and its application to a wide variety of materials at nanoscale.

Keywords: PAT, online measurement, nanosuspensions, particle size distribution, rheology, SLS, DLS, nano-milling, automated process

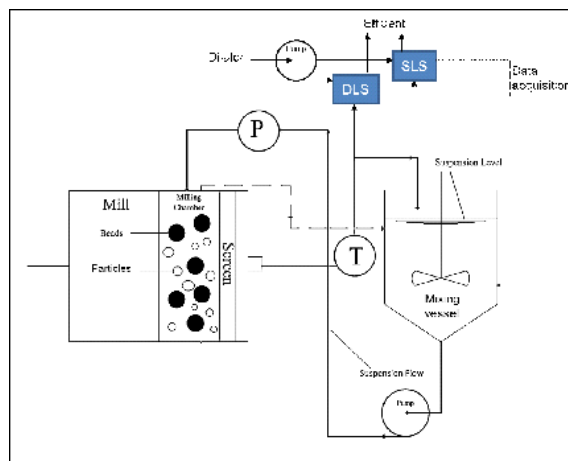


Figure 1: Figure illustrating the PAT system with the wet-milling equipment, the mixing vessel and the DLS, SLS and rheology measurement equipment.

References:

1. Roberts, I. (2001) In-line and on-line rheology measurement, *Instrumentation and Sensors for the Food Industry*, In Press.
2. Wang, X. Z., Liu, L., Li, R. F., Tweedie, R. J., Primrose, K., Corbett, J., McNeil-Watson, F. K. (2009), Online characterization of nanoparticle suspensions using dynamic light scattering, ultrasound spectroscopy and process tomography, *Chemical Engineering Research and Design*, 87, 874-884.

A SAXS/WAXS LABORATORY INSTRUMENT FOR NANOMATERIALS CHARACTERIZATION

Olivier Taché, Antoine Thill, David Carrière, Fabienne Testard, Olivier Spalla
LIONS, NIMBE, CEA, Université Paris Saclay, CEA Saclay, 91191
Gif-sur-Yvette, France.

Abstract:

Small Angle X-ray Scattering (SAXS) allows traceable measurements of size, size distribution, surface area, concentration and shape of nanomaterials in solutions, powders and in bulk materials.

We present here a custom-made state-of-the-art SAXS laboratory instrument (see Figure 1) based on Mo X-ray generator. Its design has been thought and optimized for the wide angles (WAXS) for investigate nanostructured material in particular in the size range from below 1 nm to above 20 nm.

The X-ray generator is a molybdenum (17 keV) rotating anode. A combination of a multilayer collimating mirror and a patented hybrid slits gives us a very sharp and high purity beam for a laboratory setup, with a size of 1x1 mm² and a flux of 10⁸ photons/s.

The motorized sample holder can load 20 capillaries, a temperature controlled system or a circulation environment system for kinetic studies.

A vacuum chamber is placed behind whose output window diameter is designed for the 2D image plate Mar345 detector. The accessible q-range is $q_{min} = 0.03 \text{ \AA}^{-1}$ to $q_{max} = 3 \text{ \AA}^{-1}$.

A special attention was given to the complete data treatment processing (absolute intensities, uncertainties, reference samples, calibration,...), enable us to make traceable measurements.

Combining molybdenum energy and the state-of-art experimental setup provide us with a very powerful tool for nanomaterial studies [2][3].

We present here some results obtained with this experiment for inter-laboratories characterization studies in particular of silver nanoparticles, and Si nanoparticles.

Keywords: nanomaterials, nanoparticles, characterization, size and size distribution, nanoparticles concentration, inter-laboratories studies

Figure 1: photographic view of the SAXS-WAXS setup.

Figure 2 : SAXS datagram of silver nanoparticle (blue) and the fit model (red)

References:

Taché O. and al.

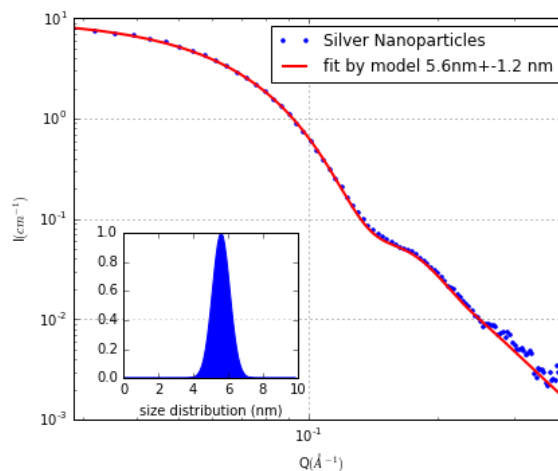
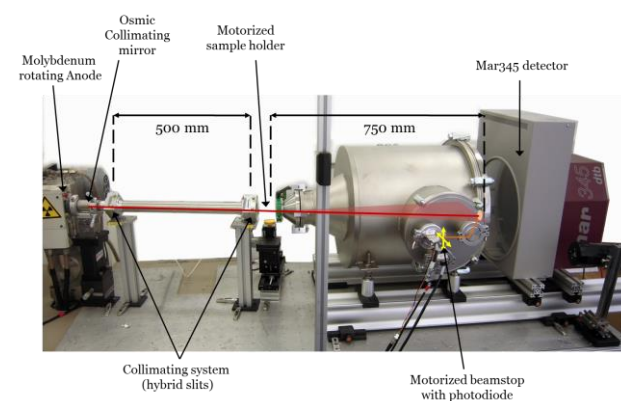
MOMAC: A SAXS/WAXS laboratory instrument dedicated to nanomaterials

Reviw Sci. Instr., In Press.

Fleury B. and al.

Gold Nanoparticle Internal Structure and Symmetry Probed by Unified Small-Angle X-ray Scattering and X-ray Diffraction Coupled with Molecular Dynamics Analysis

Nanoletter 2015



MEMS for in-situ TEM nanoscience on dry and wet samples

L. Jalabert,^{1,2,*} T. Ishida,³ T. Sato,³ M. Egawa,³ G. Valet,³ S. Volz,⁴ H. Fujita³

¹LIMMS-CNRS/IIS-University of Tokyo, Tokyo, Japan

²LAAS-CNRS, Toulouse, France

³IIS-University of Tokyo, Japan

⁴Ecole Centrale Paris and CNRS, UPR 288 (EM2C), Chatenay-Malabry, France

Abstract:

The combinaison of MEMS and in-situ Transmission Electron Microscopy offers unprecedented insights on atomic or nanoscale phenomena occurring in dry and more recently in wet environments. MEMS overcomes technical challenges in integrating mechanical elements into the tiny space of TEM holder, adding versatility, high integration level, and low cost. Several examples of MEMS in TEM studies are presented. Using a pair of electrostatic actuators, silicon opposing tips within a nanogap can be actuated until the contact, and we observed in real-time the elongation of nanojunction for different materials including Si, Au, Pt, Ag. Additional integration of double actuators allows sliding capabilities for studying nanoscale friction in single Ag nanojunction. Nanoscale heat transfer through a few silicon atoms was also achieved by integrating micro-resistances on the generic MEMS device. A prototype of cryogenic TEM holder was developed with Hitachi and Gatan to operate MEMS from 90K to 360K, and tested to evaluate heat transfer through a diamond-like carbon nanowire made by FIB-CVD method. The field of MEMS in TEM expanded a lot with the capability to encapsulate liquids between electron transparent windows, also called TEM liquid-cell. We present real-time video of nanoscale Au electroplating, as well as a new liquid-cell concept for merging droplets for applications in chemistry, catalysis, and bio-chemistry.

Keywords: MEMS, in-situ TEM, nanojunction, elongation, friction, heat transfer, DLC-nanowire, cryogenic TEM holder, liquid-cell TEM.

Characterization of nanomaterials by A4F-UV-MALLS-ICPMS, Sp-ICPMS and DLS: Application to foodstuff, consumer products, environmental and medicinal samples

M.Menta^{1*} I. de La Calle,^{1,2} M.Klein¹

¹Ultra-Traces Analyses Aquitaine, Pau, France

²Universidad de Vigo, Departamento de Química Analytica y Alimentaria, Vigo, Spain

Abstract:

Nanomaterials (NM) open huge prospects for innovation in different fields such as medicine, electronics, cosmetics and materials. However, their uses raise questions about possible risks to the environment and humans. The development of suitable protocols for the physicochemical characterization (size distribution, shape and chemical composition) of such materials is a fundamental issue for coming years. To meet the needs of various industrial producing or using NM, UT2A has developed new analytical approaches. The first one is focused on the determination of the size distribution of nano-scale particles using Dynamic Light Scattering detector (DLS) and a splitting system (by size and weight) such as Asymmetrical Flow Field Flow Fractionation hyphenated with a Multi Angle Laser Light Scattering detector (A4F-MALLS). The second approach is based on a comprehensive physicochemical characterization made by the combination of A4F-MALLS with an Inductively Coupled Plasma Mass Spectrometer (ICP-MS). The Single Particle-ICPMS has also been used to characterize NM. This study is first focused on the characterization of NM in consumer products such as sunscreens, candies or juices. The results obtained by the different analytical approaches are also discussed. Then the same techniques were used for environmental (colloids), industrial (aeronautical surface treatment and effluent process) and pharmaceutical applications. This work has enabled to develop and validate an approach to global physicochemical characterization of nanomaterials in complex matrices.

Keywords: nanomaterials, physicochemical characterization, analytical development, industrial and environmental applications

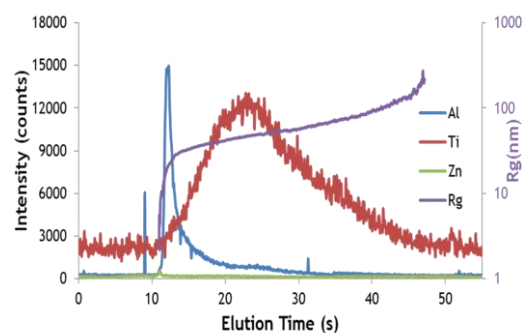


Figure 1: Physicochemical characterization (size, size distribution, composition and quantification) of metallic nanoparticles in sunscreens by A4F-MALLS-ICPMS.

Mixture of Au NPs of 30, 50 and 100 nm

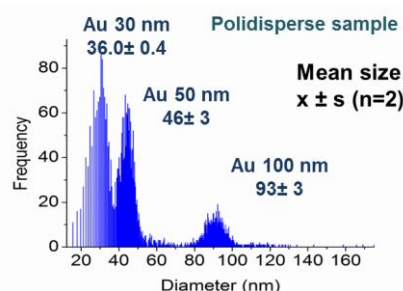


Figure 2: Characterization of gold nanoparticles by Sp-ICPMS.

References:

- Da Silva, B.F., Pérez, S., Gardinalli, P., Singhal, R.K., Modesto, A.A., Barceló, D. (2011) Analytical chemistry of metallic nanoparticles in natural environments, *Trends Anal. Chem.*, 30(8), 1327-1336.
- Weinberg, H., Galyean, A., Leopold, M. (2011), Evaluating engineered nanoparticles in natural waters, *Trends Anal. Chem.*, 30(1); 72-83.

Design of experiment for uncertainty evaluation of nanoparticle diameter measurements with AFM

B. De Boeck¹, J. Pétry¹, N. Sebaihi¹, M. Dobre¹

¹SMD, FPS Economy, Koning Albert II-laan 16, 1000 Brussels, Belgium

Abstract: Dimensional characterization of nanoparticles is getting increasingly important in nanotechnology research for regulation, legislation and many applications arising in industry and health. In practice, dimensional measurements are often not comparable because they lack traceability and a reliable uncertainty evaluation. Traceability can be reached by calibration of measurements through certified reference grids or materials. Nevertheless, a reliable measurement uncertainty evaluation is indispensable to make any statement about the measurand. In this paper, we describe a methodology to calibrate Atomic Force Microscopy (AFM) diameter measurements and to evaluate the corresponding uncertainty by performing a series of experiments.

The measurand we want to quantify in a traceable way is defined as the height (in meter) of a set of nanoparticles, deposited on a flat mica surface. The AFM output parameter which is a natural measurement for this measurand is the maximal measured z-value of a particle in the coordinate system of the AFM. Since the commercial AFM we use is not directly traceable to the meter, we need to use reference grids of step heights to perform measurement calibrations. The ISO norm 11952:2014 describes the standardized approach to perform calibrations of scanning-probe microscopes. Generally, 3 groups of influencing factors have to be investigated in detail to take into account (by controlling or correcting for them and by adding them in the uncertainty evaluation): intrinsic influences (determined by the instrument characteristics), extrinsic influences (caused by the ambient conditions) and the effects of operation and image analysis. We have minimized the effect of these influencing factors by following well-defined procedures under intermediate precision conditions. The remaining variation of all kinds of influencing effects under these conditions is assessed by performing a series of measurements and analyzing the resulting data. This remaining variation corresponds to intra-laboratory precision uncertainty. The series of measurements is intelligently chosen by using a Design of Experiment (DOE) approach. This approach is a practical alternative to traditional measurement uncertainty evaluation through a measurement equation since the underlying physics are too complex to derive such model. Our

approach is nevertheless fully compliant with the GUM.

The measurement calibration is performed on short-term and with multiple calibration points to avoid stability and linearity problems. The calibration correction on the maximal z-values we obtain from the microscope yields traceable particle heights. It is important to use reference grids with step heights that cover the desired application range. Hence, if the height range of the concerning nanoparticles is expected to be between 20nm and 80nm, relevant reference grids are those with step heights in this range. The measurement model for this multiple point calibration is a piecewise linear function. For every two reference grids R1 and R2, we have the line segment (1)

$$h_a = \frac{h_{R1;a} - h_{R2;a}}{h_{R1;m} - h_{R2;m}} \left(h_m - \frac{h_{R1;m} + h_{R2;m}}{2} \right) + (h_{R1;a} + h_{R2;a})/2$$

to model the relationship between actual (traceable) height h_a and measured maximal z-value h_m of a nanoparticle for measured maximal z-values between $h_{R1;m}$ and $h_{R2;m}$. We denote $h_{R1;a}$ for the certified and $h_{R1;m}$ for the measured step height of reference grid R1. Similar notation is used for R2. To obtain a complete uncertainty evaluation for h_a , the individual uncertainty contributions of the individual quantities have to be evaluated. For h_m , $h_{R1;m}$ and $h_{R2;m}$, we use the DOE methodology. To assess the intra-laboratory precision under intermediate precision conditions, we vary all parameters that may influence our measurements (and fall under the imposed conditions) through an extensive series of measurements. To appropriately capture all variation present, we fit the experimental data to a random effects model. The solution of such mixed model can be obtained using frequentist or Bayesian methodology. By all means, an intra-laboratory precision uncertainty is obtained for the measured reference grids and nanoparticle height which together with the uncertainties on the certified step heights of the reference grids leads to a complete measurement uncertainty evaluation through measurement model (1).

Keywords: AFM, measurement uncertainty, GUM, nanoparticles, mixed effects model.

Local resistance imaging on soft materials by conducting probe atomic force microscopy in intermittent contact mode

Aymeric Vecchiola^{1,2}, Pascal Chrétien¹, Karim Bouzehouane², Olivier Schneegans¹, Pierre Seneor², Sergio Tatay³, and Frédéric Houzé¹

¹ Lab. Génie électrique et électronique de Paris (GeePs), UMR 8507 CNRS-CentraleSupélec, Paris-Sud and UPMC Universities, 11 rue Joliot-Curie, Plateau de Moulon, 91192 Gif-sur-Yvette Cedex, France.

² Unité Mixte de Physique CNRS-Thales UMR 137, 1 avenue Augustin Fresnel, 91767 Palaiseau, France.

³ Molecular Science Institute, University of Valencia, 46980 Paterna, Spain.

Abstract:

Local electrical measurements by atomic force microscopy (AFM) have become an essential tool, both for the characterization of materials, structures and devices at smaller and smaller scale, than for more fundamental studies of nanostructures and nano-objects properties. Those measurements are generally done in contact mode, that can alter soft samples (molecular electronics, organic solar cells...) or weakly anchored nano-objects (nanotubes, nanoparticles...). In order to overcome these difficulties, we recently developed an imaging technique allowing local electrical resistance measurements in a low-frequency intermittent contact mode with a wide range, home-made sensing device based on the Resiscope module¹. After a brief description of the operating principle, we will present some significant results and compare them with existing solutions. First, we will focus on academic samples consisting of self-assembled monolayers of alkanethiol with different chain lengths deposited on gold substrates, that are ideal model systems to demonstrate the capabilities of our instrument. Then, we will present results obtained on various molecular spintronics research samples as well as some carbon-based materials.

Keywords: Atomic Force Microscopy, intermittent contact mode, local electrical measurements, soft materials, Resiscope.

Figure 1: Schematic view of an x 1-Resiscope implementation for local resistance measurements in intermittent contact mode (example of a sinusoidal actuation). The small graph on left side shows the successive phases of a deflection versus time curve: tip approach without interaction ①, jump-to-contact ②, maximum of repulsive force ③, adhesion peak at withdrawal ④, jump-off and free cantilever oscillation ⑤.

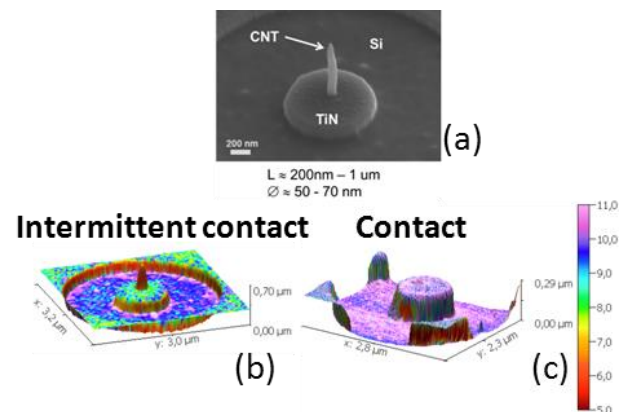
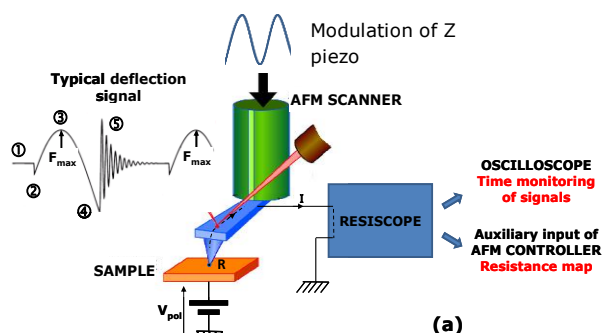


Figure 2: (a) SEM image of vertical carbon nanotube. (b) 3D image of topography with electrical representation in colour in intermittent contact mode (10 nN). The NTC stay bond after even after several scans. (c) Same representation on another NTC, in contact mode (5 nN). The NTC was snatch by the tip at the first scan.

References:

¹ O. Schneegans, P. Chrétien, F. Houzé, *Patents* WO-2011138738A1 (2011) ; EP-2567245A1 (2013).



Continuous monitoring of tip radius during atomic force microscopy imaging using higher harmonics

E. Rull Trinidad,¹ F. Gramazio², M. Lorenzoni³, F. Pérez-Murano³, U. Staufer,¹ J. Fraxedas²

¹ Group of Micro and Nano Engineering, Department of Precision and Microsystems Engineering, Technical University of Delft, Mekelweg 2, 2628CD Delft, The Netherlands

² Catalan Institute of Nanoscience and Nanotechnology (ICN2), CSIC and The Barcelona Institute of Science and Technology, Campus UAB, Bellaterra, 08193 Barcelona, Spain

³ Instituto de Microelectrónica de Barcelona (IMB-CNM, CSIC), Campus UAB, 08193 Barcelona, Spain

Abstract:

The accurate determination of nanomechanical properties of surfaces by Atomic Force Microscopy (AFM) depends to a large extent both on the shape and radius of the used cantilever tips. Even in the gentle amplitude modulation (AM) dynamic mode both parameters become irreversibly modified due to the mechanical contact with the surface in the MHz frequency range. Thus, the possibility to monitor in-situ and in-operando the tip state would represent a major advantage when interpreting the experimental results. Here, we present a continuous tip monitoring method based on the simultaneous acquisition of several higher harmonics, which are generated in the repulsive regime as a result of the nonlinear interactions between the tip and the studied surface. We have used a multi-frequency analysis technique using advanced lock-in instrumentation which permits recording extremely small signals (well below 1 nm amplitudes) above the first flexural eigenmode of the cantilever. Figure 1 shows the evolution of the mean value of the amplitude of the 6th (top) and 7th (bottom) harmonics, respectively, during the acquisition of 150 amplitude images. We ascribe the observed increase of both amplitudes to the increase of the tip radius based on numerical simulations using the Virtual Environment for Dynamic AFM (VEDA) open code (Kirakofe *et al.*, 2012). Note that the increase is more accused in the first images, where the tip is sharper (below 10 nm). Thus, the simultaneous acquisition of higher harmonic images allows the continuously control of the state of the tip.

Keywords: atomic force microscopy, amplitude modulation, tip monitoring, higher harmonics, computer simulations, nanometrology.

This work has been performed within the aim4np project (Automated in-line Metrology for Nanoscale Production), which is supported by the EC through a grant (contract Nr. 309558) within the 7th Framework Program NMP Call 2012.1.4-3 on Nanoscale mechanical metrology for industrial processes and products (Patent pending). ICN2 acknowledges support of the

Spanish MINECO through the Severo Ochoa Centers of Excellence Program under Grant SEV-2013-0295. IMB-CNM, CSIC acknowledges the grant CSD2010-00024.

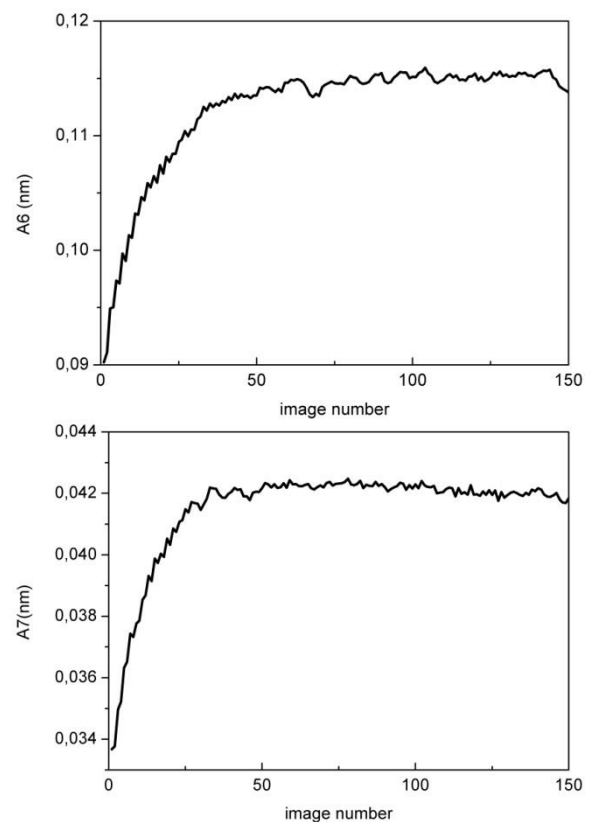


Figure 1: Evolution of the mean value of the amplitude of the 6th (top) and 7th (bottom) harmonics over 150 amplitude images. The estimated cantilever parameters are $k=26.12$ N/m, $f=166.92$ kHz and $Q=517.56$ with $A_0=32.5$ nm and $A_{sp}=0.45 \times A_0$, where A_0 and A_{sp} represent the free oscillation amplitude and amplitude setpoint, respectively. The sample was a TiN film with an estimated Young's modulus of $E_{TiN}=600$ GPa.

References:

Kirakofe, D., Melcher, J. Rahman, A., (2012), Gaining insight into the physics of dynamic atomic force microscopy in complex environments using the VEDA simulator, *Rev. Sci. Instrum.* 83, 013702.

Measurement uncertainty evaluation of a metrological AFM by modeling its position measurement system

P. Ceria, S. Ducourtieux, Y. Boukellal, A. Allard
LNE – Laboratoire National de métrologie et d'Essais – France

Abstract:

At present where nanotechnology is growing worldwide, measurement accuracy at the nanometer scale becomes an essential challenge to improve the performance and the quality of nanoproducts. To meet the specific needs in the field of dimensional nanometrology, LNE (French national metrology institute) integrally designed a metrological Atomic Force Microscope (mAFM) as shown on the figure 1.

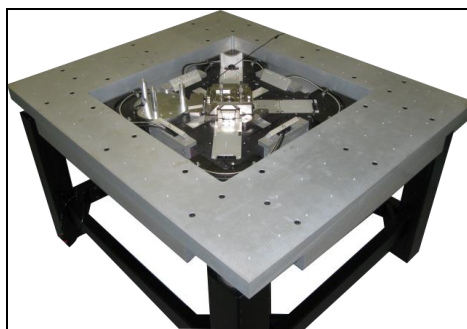


Figure 1: Photo of the LNE's mAFM.

The main objective of this future French reference instrument is to ensure the traceability to the meter as defined by the International System of Units (SI). It will be devoted to the calibration of scanning probe microscopes (SPM) and scanning electron microscopes (SEM). To measure the tip to sample relative position, this instrument uses an original configuration with four double path differential interferometers whose He-Ne laser sources are frequency-calibrated.

During the calibration process of transfer standards, the mAFM issues a calibration certificate with a measurement uncertainty. This uncertainty is determined by propagating the uncertainty associated with each input quantity which perturbs the measurement result, as for example the beam misalignment, the metrology frame dilatation, the instrument drift, etc. The measurement uncertainty is important because it gives an indication on the dispersion of the mAFM measurements. For the LNE's mAFM, the evaluation of the uncertainty budget is complex and unfortunately

some components can't be experimentally determined. To overcome this difficulty, a numerical model of the geometry position measurement system (Virtual AFM) has been developed under Matlab.

This model takes into account the position drift of the reference prism, the parasitic rotation of the mobile prism, the positioning error and dilatation of the prisms, the shape and orthogonality of all the mirrors (eight in total), the sample thickness, the structural frame dilatation and its bending deformation, the Abbe offset and cosine error of each interferometer (sixteen beams). This model enables the use of components evaluated experimentally. A sensitivity analysis is performed to identify which of these considered input quantities are important regarding the variance of mAFM measurements, including potential interactions that could arise. A Morris' design is used to this extent and will lead to consider non influential quantities as fixed parameters. The next step consists in calculating Sobol's indices in order to quantify their contributions to the variance of the XYZ positions and provide the overall uncertainty budget.

Finally, the measurement uncertainty is evaluated using Monte Carlo methods, according to the principles of the Supplement 1 of the GUM. The algorithm is executed virtually on a parallel computer with 32 cores of the LNE cluster to reduce calculation time.

The given presentation will introduce the different modeling steps, some typical examples of contributions evaluated by the model and the results obtained for the LNE's mAFM in terms of measurement uncertainty.

Acknowledgements: This research has been performed within the EMRP project, "Metrology for movement and positioning in six degrees of freedom (6DoF)." The EMRP is jointly funded by the EMRP participating countries within EURAMET and the European Union.

Quantitative X-ray Resolution of the Atomic Structure of Metal Oxide Nanotubes: the Imogolite Case

M.-S. Amara¹, S. Rouzière¹, E. Paineau¹, E. Poli², J. D. Elliott², G. Teobaldi² and P. Launois¹

¹Laboratoire de Physique des Solides, CNRS, Univ. Paris Sud, Univ. Paris Saclay, France

²Stephenson Institute for Renewable Energy, Department of Chemistry, University of Liverpool, UK

Abstract:

Accurate determination of the atomic structure of a nanoobject is essential for understanding and eventual optimization of properties and functions. Imogolites, the only metal oxide tubular clays with a diameter of the order of the nanometer, are considered as promising candidates for molecular recognition applications. However, more than forty years after the seminal article of Cradwick and coworkers which gave clues on their structure, it has not been precisely determined.

Here we show that it is possible to resolve quantitatively the atomic structure of metal oxide imogolite nanotubes (figure 1(a)) via the combination of small and wide angle X-ray scattering. We will present the specific strategy developed to minimize interatomic distortions and to account for both small and wide angle X-ray scattering data (figure 1(b)). Fitting of the experimental data reveals the circumference of aluminosilicate, $(\text{Al}_2\text{SiO}_7\text{H}_4)_N$, and aluminogermanate, $(\text{Al}_2\text{GeO}_7\text{H}_4)_M$, imogolite nanotubes to be composed by $N=13$ and $M=22$ units, in flagrant disagreement with previous computational suggestions. We developed a phenomenological model to understand and conciliate this apparent contradiction. Moreover, we performed linear-scaling density functional theory simulations which confirm the fitted structures to be mechanically stable.

The transferability of the introduced methodology anticipates straightforward application towards quantitative structural resolution for newly-discovered imogolite-type nanotubes (double-walled nanotubes or functionalized nanotubes), as well as for other inorganic nanotubes and bio-compatible tubular clays such as halloysites.

Keywords: inorganic nanotubes, imogolite, metal-oxide structure, small-angle X-ray scattering, wide-angle X-ray scattering, linear-scaling density functional theory

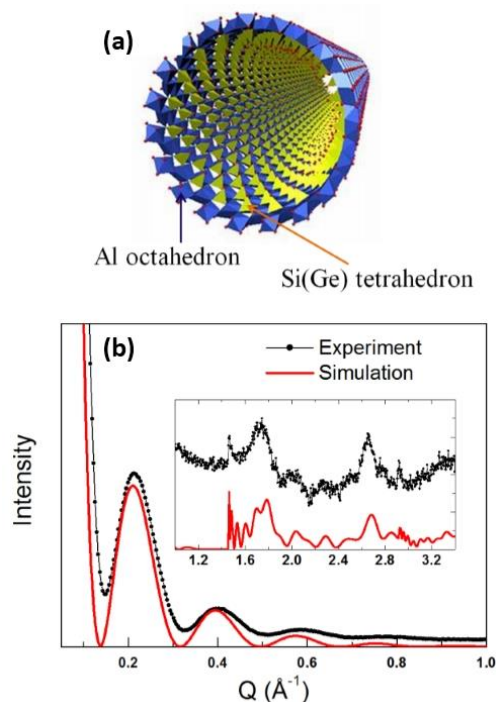


Figure 1: (a) An imogolite nanotube $\text{Al}_2\text{Si}(\text{Ge})\text{O}_7\text{H}_4$, with AlO_6 octahedra and $\text{Si}(\text{Ge})\text{O}_4$ tetrahedra; (b) X-ray scattering pattern of $\text{Al}_2\text{GeO}_7\text{H}_4$ nanotubes, together with its simulation for the refined structure.

References:

- Cradwick, P. et al (1972), Imogolite, a hydrated aluminosilicate of tubular structure, *Nature* 240, 187-189
- Duarte, H. A. et al (2012), Clay Mineral Nanotubes: Stability, Structure and Properties, *Rijeka : INTECH Open Access Publisher*
- Kang, D.Y. et al (2014), Direct Synthesis of single-walled aluminosilicate nanotubes with enhanced molecular absorption selectivity, *Nat. Comm.* 5:3342
- Amara, M. S. et al (2015), Hybrid, Tunable-Diameter, Metal Oxide Nanotubes for Trapping of Organic Molecules, *Chem. Mater.* 27, 1488-1494

Water in Single-Walled Carbon Nanotubes: structural and dynamical analyses

E. Paineau¹, S. Dalla-Bernardina², J.B. Brubach², S. Rouzière¹, P. Judeinstein³, S. Rols⁴, P. Roy² and P. Launois¹

¹Laboratoire de Physique des Solides, CNRS, Univ. Paris Sud, Univ. Paris Saclay, France

²Synchrotron SOLEIL, Saint-Aubin, France

³Laboratoire Léon Brillouin, CNRS-CEA, Gif-sur-Yvette, France

⁴Institut Laue-Langevin, Grenoble, France

Abstract:

Fast water transport inside carbon nanotubes (CNT) is a highly topical issue in fundamental research, while related applications are already under consideration in environmental and energy fields. A substantial set of simulation and theoretical works have pointed out two important parameters for filling hydrophobic nanochannels, namely curvature effects or the strong modification of the hydrogen-bond (HB) network. In contrast, experimental publications are rather scarce.

Here, we report the first experimental analysis of water structure and H-bond network during CNT filling. Experiments were performed on single-walled carbon nanotubes (SWCNT) with diameters between 1 and 2 nm, as they are ultimate one-dimensional carbon nanochannels. We present in-situ monitoring of water filling of SWCNT at room temperature, using X-ray scattering (XRS) and infra-red (IR) spectroscopy. A systematic method is developed to determine the water radial density profile from XRS measurements, which reveals a progressive structuration with increasing the filling rate. Furthermore, IR spectroscopy gives evidence for a large proportion of loosely bonded water molecules inside SWCNTs, even for fully hydrated nanotubes (figure 1). These results are discussed with respect to theoretical and simulation studies in the literature. The present experimental data provide a solid reference for the elaboration of an energetic model accounting for the properties of water in hydrophobic nanoconfinement. They could also be relevant with respect to the unimpeded permeation of water through graphene-based membranes, or in other fields such a biology, where the extreme permeability to water of aquaporins, those membrane proteins that form nanopores, is crucial for many physiological processes.

Keywords: nanofluidics, carbon nanotubes, water, X-ray scattering, infra-red spectroscopy

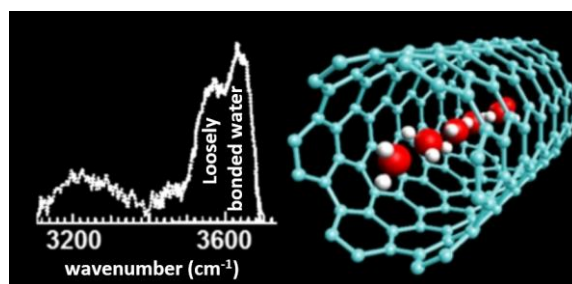


Figure 1: Left: the O-H stretching band of nanoconfined water; right: single-file water inside narrow carbon nanotubes.

References:

- Lee, B. et al (2015), A carbon nanotube wall membrane for water treatment, *Nature Comm.*, 6: 7109
- Park, H. G., Jung, Y. (2014), Carbon Nanofluidics of Rapid Water Transport for Energy Applications, *Chem. Soc. Rev.* 43, 565-576
- Falk, K. et al (2010), Molecular Origin of Fast Water Transport in Carbon Nanotube Membranes: Superlubricity versus Curvature Dependent Friction, *Nano Lett.* 10, 4067-4073
- Joseph, S., Aluru, N. R. (2008), Why Are Carbon Nanotubes Fast Transporters of Water? *Nano Lett.* 8, 452-458
- Paineau, E. et al. (2013), X-ray Scattering Determination of the Structure of Water during Carbon Nanotube Filling *Nano Lett.* 4, 1751-1756

An Accurate Reconvergent Fanout Aware Algorithm for nano-Circuits Reliability Ranking

W. Ibrahim,* H. Amer,^{1,2}

UAE University, College of Information Technology, Al Ain, UAE

Abstract:

CMOS devices have always been subject to a steady reduction in feature size. However, as the feature size is approaching the deca-nanometer mark, the industry is currently facing several fundamental limitations. One of the major limitations is the severe static and dynamic parameter fluctuations [1]. These fluctuations will inevitably reduce reliability at device, gate, and system levels [2], [3]. Hence, having manufacturing processes that achieve 100% correctness with future nano-devices will not be only extremely costly, but might be also plainly impossible. Consequently, future circuits will have to rely on less than perfect devices and compensate for the anticipated transient and permanent failures by incorporating redundancy at the architectural level [4], [5].

The well-known approach for developing fault-tolerant architectures is to incorporate space, time, or information redundancy. Unfortunately, incorporating any of the above redundancy schemes to enhance reliability, will inevitably affect the design area, power, and delay figures. Therefore, accurate reliability estimation is becoming essential for future nano-circuits [6]. New accurate and efficient simulation algorithms are needed for estimating the overall reliability of different architectures, and selecting the one that best optimizes the trades-off between reliability and the classical delay, power, and area design parameters.

Several tools have been proposed in the literature to calculate the circuit probability of failure (PF_{CIR}) [7]–[12]. However, these tools are usually used to estimate the average PF_{CIR} or the PF_{CIR} associated with a specific input vector. None of these tools, to the best knowledge of the authors, has tried to identify the worst reliability vector (WRV), i.e., the input vector associated with the maximum PF_{CIR} (PF_{MAX}). This aspect cannot be ignored, as PF_{MAX} could be orders of magnitude higher than the average PF_{CIR} (PF_{AVG}) [13]. Fig. 1 shows a histogram for the difference between PF_{MAX} and PF_{AVG} for 298 different output signals selected from ISCAS’85 benchmark. It shows that PF_{MAX} could be 150 times higher

than PF_{AVG} . Therefore, identifying the WRV is essential or future circuit design. Circuit designers should ensure that the circuit is still operating within the allowable reliability margin even when the WRV is applied to the primary inputs.

However, identifying the WRV could be complicated. The massive size of today’s digital circuits, and the complexity of interconnects make the accurate calculation of the PF_{CIR} associated with the individual input vectors a challenging and time-consuming task. In a similar problem, Bobba et al. proved that identifying the worst leakage power input vector is an NP-hard problem [14]. Moreover, for digital circuits with few input signals, WRV can be identified by using brute-force search to check the PF_{CIR} associated with each input vector. However, as the number of primary inputs increases, the number of possible input vectors (search space) increases exponentially. Consequently, simple brute-force search is impossible to implement even for relatively small circuit with 32 primary inputs (i.e. 2^{32} input vectors).

It is important to mention that circuit designer are usually not interested in the PF_{CIR} associated with individual input vectors. However, they are highly interested in the PF_{CIR} associated with the WRV to ensure that the circuit operates within the predefined reliability margin during the worst case condition. Therefore, instead of calculating the complicated and time consuming PF_{CIR} for each input vector, reliability enabled EDA tool

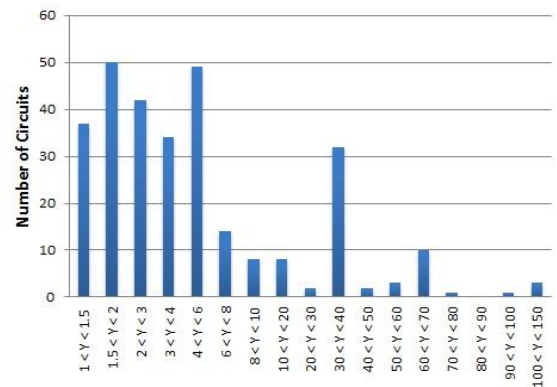


Fig. 1. Distribution of the ratio between the worst and the average PF_{OUT} ($Y = PF_{MAX} / PF_{AVG}$) for 298 ISCAS’85 output signals

could rely on a more efficient metric to rank the individual input vectors with respect to their reliabilities. The new reliability metric should be more efficient than PF_{CIR} , and should be able to rank the input vectors similar to their ranking with respect to PF_{CIR} . Using this metric, the EDA tool will be able to efficiently and accurately identify the WRV , while exact PF_{CIR} is only calculated for the identified WRV .

In this paper a highly accurate, reconvergent fanout aware algorithm is proposed for input vectors reliability ranking. Simulation results show that the input vector ranking using the new metric is identical and much more efficient than PF_{CIR} , and more accurate and efficient than other ranking algorithms currently proposed in the literature.

Keywords: nano-circuits, reliability, input vectors ranking, heuristic algorithms

References:

1. A. Asenov, Statistical device variability and its impact on design," *Proc. IEEE Int. Symp. Asynch. Circ. & Sys.*, Newcastle, UK, Apr. 2008, pp. xv–xvi.
2. S. Borkar, "Designing reliable systems from unreliable components: The challenges of transistor variability and degradation," *IEEE Micro*, vol. 25, Nov.-Dec. 2005, pp. 10–16.
3. J.W. McPherson, "Scaling-Induced Reductions in CMOS Reliability Margins and the Escalating Need for Increased Design-In Reliability Efforts," *Intl. Symp. Quality Elect. Design*, San Jose, CA, USA, Mar. 2001, pp. 123–30.
4. M. Hamamatsu, T. Tsuchiya, and T. Kikuno, "On the reliability of cascaded TMR systems," *Proc. Pacific Rim Intl. Symp. Dependable Comput.*, Tokyo, Japan, Dec. 2010, pp. 184–190.
5. T. Li, M. Shafique, J. A. Ambrose, S. Rehman, J. Henkel, and S. Parameswaran, "RASTER: runtime adaptive spatial/temporal error resiliency for embedded processors," *Proc. Design Automation Conf.*, Austin, Texas, USA, Jun. 2013, Article 62.
6. V. Beiu, and W. Ibrahim, "On computing nano-architectures using unreliable nano-devices," Chp. 12 in S. E. Lyshevski (Ed.): *Handbook of Nano and Molecular Electronics*, London, UK: Taylor & Francis, May 2007.
7. K. N. Patel, I. L. Markov, and J. P. Hayes, "Evaluating circuit reliability under probabilistic gate-level fault models," *Proc. Intl. Workshop Logic Synthesis*, Laguna Beach, CA, USA, May 2003, pp. 59–64.
8. J. Han, H. Chen, J. Liang, P. Zhu, Z. Yang, and F. Lombardi, "A Stochastic Computational Approach for Accurate and Efficient Reliability Evaluation," *IEEE Trans. Comp.*, vol. 99, 2012; pp. 1–14.
9. T. Rejimon, and S. Bhanja, "An accurate probabilistic model for error detection," *Proc. Intl. Conf. VLSI Design*, Kolkata, India, Jan. 2005, pp. 717–722.
10. N. Mohyuddin, E. Pakbaznia, M. Pedram, "Probabilistic error propagation in logic circuits using the Boolean difference calculus," *Proc. IEEE Intl. Conf. Comp. Design*, Lake Tahoe, CA, USA, Oct. 2008, pp. 7–13.
11. M. R. Choudhury, and K. Mohanram, "Accurate and scalable reliability analysis of logic circuits," *Proc. Design Autom. & Test Europe*, Nice, France, Apr., 2007, pp. 1454–1459.
12. H. Chen and J. Han, "Stochastic computational models for accurate reliability evaluation of logic circuits," *Proc. IEEE/ACM Great Lakes Symp. on VLSI*, Providence, RI, USA, May 2010, pp. 61–66.
13. W. Ibrahim, V. Beiu, and H. Amer, "How much input vectors affect nano-circuit reliability estimates," *Proc. IEEE Conf. Nanotech.*, Genoa, Italy, Jun. 2009, pp. 699–702.
14. S. Bobba, i.N. Hajj, "Maximum Leakage Power Estimation for CMOS Circuits", *IEEE Int. Workshop on Low Power Design*, Como, Italy, Mar. 1999, pp. 116–124.

Modeling and Analysis of scatterometry with high-harmonic-generation EUV source

Yi-sha Ku,* Yi-Chang Chen, Chia-Liang Yeh, Yi-Chen Hsieh, Chia-Hung Cho, Chun-Wei Lo
Center for Measurement Standards, Industrial Technology Research Institute, Bldg. 12, 321 Kuang Fu Rd 2., Hsinchu, Taiwan

Abstract:

For advanced semiconductor production the features sizes is smaller than tens of nanometer, the capability of scatterometry to extract detailed critical dimension (CD) geometric information will require a move to shorter measurement wavelengths [1]. The short wavelength of Extreme UltraViolet (EUV) radiation is advantages since it give rise to a number of diffraction orders scattered from the features of tens nanometers and increases the sensitivity to accurately extract topographic profile information from nano-scale periodic structures. In this paper, we discuss the particular attention to use polychromatic High Harmonic Generation (HHG) in EUV range for the novel applications of modeled based EUV scatterometer. Compared to synchrotrons and x-ray free electron lasers that also provide light source with short wavelength range, high harmonic beam provide an output that exhibits a high degree of spatial coherence, but they are small scale, and their unique characteristic of multiple-order output can be tailored to single or multiple orders for the experimental requirements [2].

We extend the previous scatterometry work by employing harmonic emission consisting of a few harmonic orders, namely 15-35 nm in EUV to illuminate periodic structures for diffractive imaging. In contrast to two major types of existing scatterometry tools are variable-angle scatterometers and the specular spectroscopic scatterometers, the EUV scatterometer we propose is designed to measure intensity of the multi-order diffraction at a fixed incident angle and multiple laser-like wavelengths. The sample with periodic structures itself serves as an optical grating to disperse the HHG onto a CCD camera, and the well separated higher order diffraction are more informative than the zero order diffraction which just along the single specular direction as the measurement wavelength range is held fixed in visible or UV. This type of non-zero order diffraction information, coupled with a very efficient Rigorous Coupled Wave Analysis (RCWA) implementation, seems

to be adequate for detailed reconstruction of the profiles of nano-scale periodic gratings. The extraction of a CD profile can be viewed as an optimization problem. A novel approach is to find a profile whose simulated higher order diffraction responses match the measured responses to enable 3D structure profile reconstruction.

Keywords: Extreme UltraViolet, scatterometry, High Harmonic Generation, Rigorous Coupled Wave Analysis.

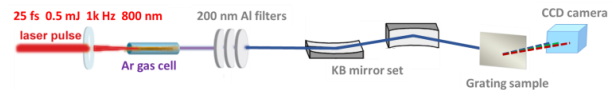


Figure 1: Schematic diagram of EUV scatterometer geometry.

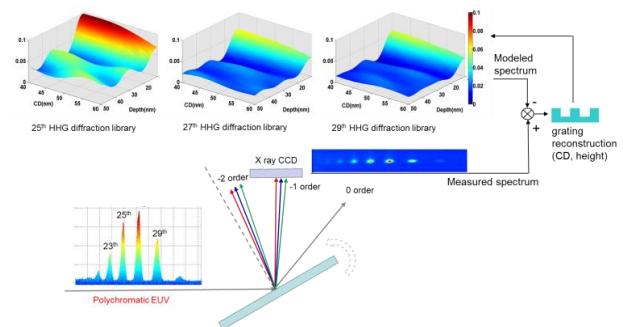


Figure 2: Schematic diagram of EUV scatterometry measurement algorithm and library match process.

References:

1. F. L. Terry, Jr., "Accuracy Limitations in Specular-Mode Optical Topography Extraction," *Proc. SPIE 5038*, 557 (2003).
2. C. Bressler and M. Cherguiet., "Ultrafast X-ray Absorption Spectroscopy," *Chem. Rev.* 104, 1781 (2004).

Influence of the probe-surface contact area on AFM tribological investigation of nanopatterned Si surfaces

A. Rota¹, E. Serpini^{1,2}, G. C. Gazzadi¹, S. Valeri^{1,2,3}

¹ CNR Istituto di Nanoscienze, Centro S3, Via Campi 213/A – 41125 Modena, Italy

² Dipartimento di Scienze Fisiche, Informatiche e Matematiche - Università di Modena e Reggio Emilia, Via Campi 213/A – 41125 Modena, Italy

³ Centro Interdipartimentale per la Ricerca Applicata e i Servizi nel settore della Meccanica Avanzata e della Motoristica - Università di Modena e Reggio Emilia, Via Vignolese, 905/b - 41125 Modena (Italy).

Abstract:

One of the most promising methods to control friction, wear and adhesion concern the modification of surface morphology by means of patterning techniques. Depending on the size of the surface texture and on the applied load, different tribological properties arise. At the microscale the effects of patterning on tribological parameters were extensively studied [1-5], showing that the contact area plays the dominant role in friction, adhesion and wettability. In particular, many studies report on the effect of micro-patterning in increasing/decreasing the wettability in already hydrophilic/hydrophobic surfaces. At the nano-scale the tribological behaviour of patterned surfaces has not been completely understood [6]. The difficulty in studying the tribological behaviour of nano-patterns can be related to the instability of the contact area between the probe and the surface, which becomes very critical in case of very short and small nano-structures.

In this study we show how the variation of the local radius of curvature can be very frequent, leading to different tribological outputs in the case of very small nano-structures. The adhesion and the coefficient of friction of ordered arrays of 1D linear protrusions of Si were studied by means of AFM, using a home-made Si rounded tip. The nano-patterns were fabricated by Focused Ion Beam working in very low-ion dose mode, taking advantage of the amorphization-related swelling effect. To limit the experimental errors, an ad-hoc measurement procedure and data analysis have been adopted. After the estimation of the local radius of curvature, we are able to show that adhesion and friction are influenced by the contact area and by a hydrophobic effect induced by the nano-structures. Depending on the shape of the nano-features, one contribution dominates on the other: the contact area in

the case 1D protrusions, the hydrophobic effect in the case of 1D grooves [7].

This research has been supported by Fondazione Cassa di Risparmio di Modena.

Keywords: nano-patterning, AFM, coefficient of friction, adhesion, contact area, hydrophobicity.

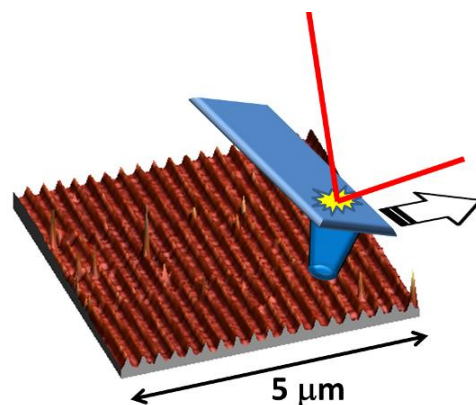


Figure 1: sketch representing the AFM tribological characterization procedure of the nanopatterned Si surface.

References:

- [1] Burton B. *et al*, Nano Lett. 2005, 5, 8, 1607-1613.
- [2] Hu Y.-Z. *et al*, Comprehensive Nanoscience and Technology, ISBN: 978-0-12-374396-1, Vol. 3: Nanostructured Surfaces, (2010) 383.
- [3] Wang, Y. *et al.*, Colloids and Surfaces A: Physicochem. Eng. Aspects 2010, 372, 139-145.
- [4] Pham D. *et al*, Surf. Eng. 2011, 27, 4, 286-293..
- [5] Zhao W. *et al*, Q., Colloids and Surfaces A: Physicochem. Eng. Aspects 428 (2013) 70– 78.
- [6] Marchetto D. *et al*, Wear 268 (2010) 488.
- [7] Rota A. *et al*, Langmuir 2013, 29, 5286.

Simultaneous Topographical, Spectroscopic and Electrical Mapping at the Nanoscale

Alina Zoladek-Lemanczyk¹, Naresh Kumar¹, Anne A. Y. Guilbert², Sachetan M. Tuladhar², Thomas Kirchartz^{2,3,4}, Bob C. Schroeder⁵, Iain McCulloch^{5,6}, Jenny Nelson², Debdulal Roy¹ and Fernando A. Castro¹

¹National Physical Laboratory, Teddington, Middlesex, U.K. TW11 0LW,

²Department of Physics, Imperial College London, London, U.K. SW7 2AZ,

³IEK-5 Photovoltaik, Forschungszentrum Juelich 52425, Germany,

⁴Faculty of Engineering and CENIDE, University of Duisburg-Essen, 9 Carl-Benz-Strasse 199, 47057 Duisburg, Germany,

⁵Department of Chemistry, Imperial College London, London, U.K. SW7 2AZ,

⁶SPERC, King Abdullah University of Science and Technology (KAUST), Thuwal, 23955-6900, Saudi Arabia.

Abstract:

The simultaneous non-destructive chemical and physical characterisation of materials at the nanoscale is an essential and highly sought after capability. For optoelectronic devices, the key functions of interest are optical and electrical. Although significant progress in instrumentation has been made recently, most existing analytical methods can measure only either spectroscopic or electrical information but not both simultaneously. Furthermore, high resolution is rarely achieved in all three dimensions at the same time. Here we demonstrate a new method that allows simultaneous non-destructive measurement of topographical, chemical, optical and electrical properties with nanoscale resolution by combining nano-optical spectroscopy (plasmonic signal enhancement) with atomic-force microscopy electrical modes in a single experiment.

As a proof of concept we apply this new method to the organic solar cell blend C8SiIDT-BT:ICMA. We are able to identify a hierarchical 3D nanostructure and directly correlate local composition to photocurrent generation and collection, including the direct identification of impurities within nanoscopic domains of operating solar cells. Such ability to directly measure the impact of nanostructure on optoelectronic function at the same time is unique and solves the critical issue of trying to find the same location when using a sequence of experiments to obtain the different properties. Not only is this task extremely difficult (sometimes impossible) but it can also lead to contamination and/or degradation when samples are moved from one instru-

ment to another, leading to false results and conclusions.

This is the first demonstration of the powerful combination of tip-enhanced optical spectroscopy (TEOS) and photoconductive atomic force microscopy in a single experiment. We believe the approach shown here will pave the way to the development of new methods for investigation of a range of scientific problems where different electrical properties can be measured simultaneously with the identification of the chemical sub-surface components or impurities affecting them.

Keywords: Solar cell, polymer blend, photocurrent, Tip-enhanced optical spectroscopy, TEOS, TERS, PC-AFM.

Interaction between Hybrid Inclusions mediated by surfactant membranes

E. Azar¹ and D. Constantin¹

¹ Laboratoire de Physique des solides, CNRS, UMR 8502, 91405 Orsay, France

Abstract:

We perform a systematic investigation of the interaction between hydrophobic inorganic particles (butyl-functionalized tin oxide clusters) inserted in highly aligned lamellar phases of a zwitterionic surfactant as a function of particle concentration and temperature.

The SAXS measurements (with the beam incident along the layer normal) give access to the in-plane signal $I(q_r)$ (at $q_z=0$) of the two-dimensional fluid formed by the inclusions within the bilayer. The background-subtracted intensity divided by the form factor of the particles yields the structure factor $S(q)$, shown in Figure 1 for 30 °C, 70 °C and 100 °C (the highest temperature reached) at various surface fraction of inclusions η .

The differences are visible: at high temperature, the flattening of the primary peak and a small-angle upturn indicate a more attractive interaction. By numerically solving the Ornstein-Zernicke equation [1]–[3], we extract from the structure factor the membrane-mediated interaction potential $V(r)$, determined by the elastic properties of the membrane.

We will fit the experimental data using analytical and numerical models for the membrane-mediated interaction between inclusions, developed in collaboration with a theory team of the MSC laboratory in Paris (J.-B. Fournier and P. Galatola.) [4]. The comparison should yield a detailed image of the elastic properties of the membranes, as well as of their temperature dependence.

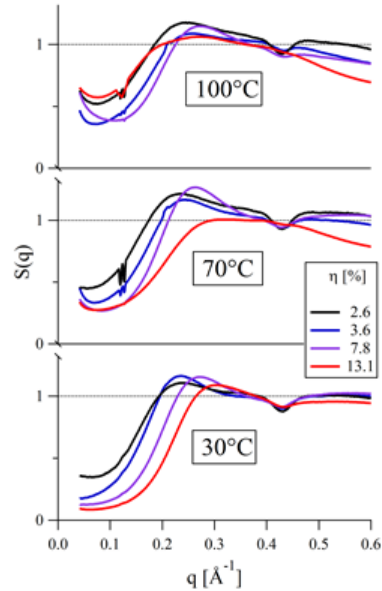


Figure 1: Two-dimensional structure factor of the particle fluid within the membrane, for selected concentrations and at different temperatures. The small dip around 0.4 Å⁻¹ is due to imperfect subtraction of the peak from a kapton window.

References:

1. D. Constantin, “The interaction of hybrid nanoparticles inserted within surfactant bilayers.,” *J. Chem. Phys.*, vol. 133(14), 144901, 2010.
2. D. Constantin, “Membrane-mediated repulsion between gramicidin pores.,” *Biochim. Biophys. Acta*, vol. 1788(9), pp. 1782–9, 2009.
3. D. Constantin, B. Pansu, M. Impérator, and P. Davidson, “Repulsion Between Inorganic Particles Inserted Within Surfactant Bilayers,” *Phys. Rev. Lett.* vol. 101(9), 098101, 2008.
4. A.-F. Bitbol, D. Constantin, and J.-B. Fournier, “Bilayer elasticity at the nanoscale: the need for new terms.,” *PLoS One*, vol. 7(11), e48306, 2012.

Micro to Atomic Scale Observations on Nano-sized Y-TZP Powder Produced by One-Step Hydrothermal Route

A. Yurdakul¹ H. Gocmez¹ H. Yurdakul^{1*}

¹Dumlupinar University, Department of Material Science and Engineering, Kutahya, TURKEY

Abstract:

Hydrothermal is one of the appropriate and practical methods to obtain narrow particle size distribution with weak agglomeration as well as high purity and homogenous nano-sized zirconia powder within a short time. Tetragonal zirconia powders were synthesized from zirconium acetate in dilute acetic acid as a precursor under hydrothermal conditions. 3 mol % yttrium chloride hexahydrate ($Y_2Cl_3 \cdot 6H_2O$) as a stabilizer and urea $CO(NH_2)_2$ were added as a mineralizer into the solution at convenient pH values. The precursor was heat treated in a reactor at 180 °C for 12-48 h to obtain pure t- ZrO_2 nanocrystals. To prevent agglomeration anionic dispersant was used and examined the zeta potential parameter. Zirconia pellet was prepared with cold isostatic pressing using polyvinyl butyral as a binder, polyethylene glycol (PEG) and stearic acid as a plasticizer and lubricant, respectively. Heat treatment was applied 1500 °C for 2 h. Dense zirconia ceramics are characterized in detail by Scanning Electron Microscopy, X-Ray diffraction and Transmission Electron Microscopy at atomic scale.

Keywords: hydrothermal, nano particle, Y-TZP, characterization.

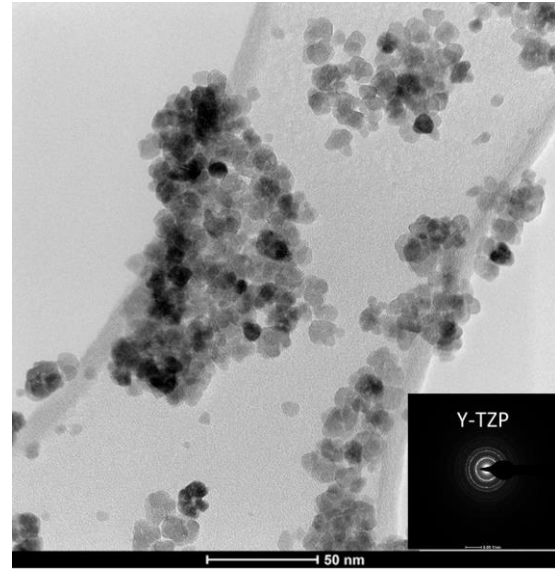


Figure 1: TEM observation of Y-TZP powder synthesized by the hydrothermal method.

References:

1. Somiya, S. ve Akiba, T., (1999), A bibliography , Journal of the European Ceramic Society, 19, 81-87.
2. Suchanek, W.L. ve Riman, R.E., (2006), Hydrothermal Synthesis of Advanced Ceramic Powders, Advances in Science and Technology, cilt.45, 184-193.

First steps towards instantaneous positioning of Nanorobots equipped with graphene antenna in large scaled nano-systems

Dermas Moffo¹, Philippe Canalda,¹

¹Femto-st Institute (UMR CNRS 6174). Department of Complex Systems, University of Bourgogne-Franche-Comté, Monbéliard, FRANCE – {Surname.Name}@femto-st.fr

Abstract: The development of new materials such as graphene, a sheet of the thickness of one atom, consisting of carbon atoms arranged in a hexagonal pattern, enables the fabrication of new nano-devices. The expected frequency of nano-transmitters and nano-graphen-based antennas is of the order of terahertz, resulting in nano-wireless communications between nanorobots [1]. Nano- robots with these means are used in different applications to carry out actions or for the construction of 2D and 3D smart-forms (programmable matter – Claytronics[2]).

These applications often require (to be completed), a precise knowledge of the position of the nanorobot. In many cases, it is more useful to have a local information on the relative position of nanorobots and their orientation, than a global position (or absolute position) of each robot. Previous work on nanorobots micropositioning are either stochastic [3] and based on probabilistic approaches, which give better results on a small sample, but produce a larger error due to accumulation with a large scale; either deterministic and are based on geometrical considerations to calculate accurately the position of each item. In this work, we propose a model of a smartgrid (orthogonal and hexagonal lattice) of nanorobots regular geometry, and their connectors (actuators and sensors for displacement and other actions) communicating by contact. Based on this model, we propose a mixed positioning algorithm (absolute and relative) in 2D and 3D without mobility of nodes in a group ranging in size from thousands to millions of items, based on neighborly relations and on geometrical considerations to calculate accurately the position of each item, and then distribute it to all the elements of a large grid. Then by simulation we perform a functional validation of our algorithm, and a validation of the scalability of our algorithm on an orthogonal grids of one million nodes.

Keywords: 2D and 3D Nano-localization, relative and global positioning, Nano-systems, localization algorithm, simulation.

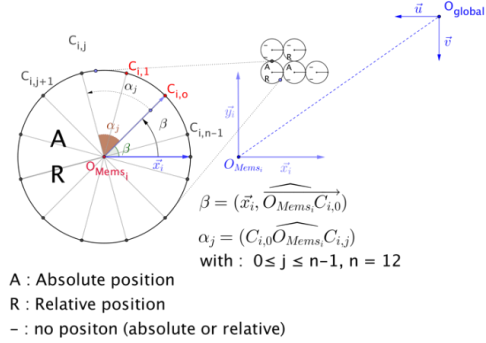


Figure 1: Mems regular geometry (nanorobot) + connectors form, within an orthogonal grid, in an absolute reference frame environment.

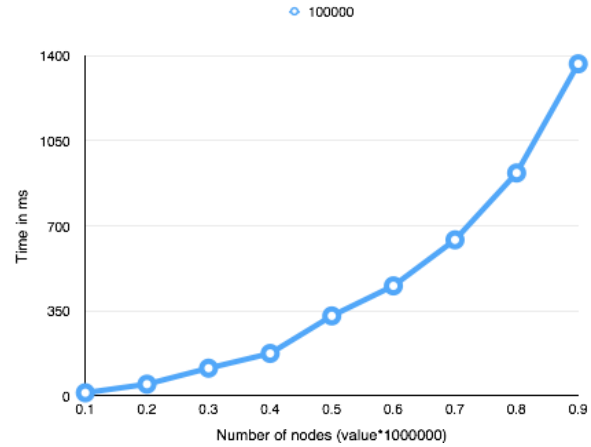


Figure 2: Average simulation time for positioning a set of nanorobots whose size ranges from 100000 to 900000.

References:

1. Jornet, J. M., Akyildiz, I. F. "The internet of multimedia nano-things". Nano Communication Networks, 3(4), 242-251, 2012.
2. Goldstein, S. C., Mowry, T. C." Claytronics: A scalable basis for future robots". Published in the proceedings of RoboSphere 2004, <http://repository.cmu.edu/compsci>, 6pages.
3. Funiak, S., Pillai, P., Campbell, J., & Goldstein, S. C. (2007). Internal Localization of Modular Robot Ensembles. Published In the public access proceeding of Workshop on Self-Reconfiguring Modular Robotics at the IEEE International Conference on Intelligent Robots and Systems (IROS) '07, <http://repository.cmu.edu/compsci>, 6 pages.

Nanometrology France 2016
Symposium on Nanospectroscopy

Nanospectroscopy of optical antennas and coupled hybrid antenna-nanoemitter-structures

M. Fleischer

Eberhard Karls University Tübingen, Institute for Applied Physics, Tübingen, Germany

Abstract:

Plasmonic nanostructures that act as optical nanoantennas for visible light offer interesting opportunities for locally concentrating and enhancing the electric near-field of an incident light wave, or of spectrally tuning the antenna characteristics via their size, shape and material.

These properties are increasingly employed for the development of high-resolution optical microscopy and nanospectroscopy. Using various nanofabrication techniques, suitable antenna structures can be prepared for surface-enhanced Raman spectroscopy (SERS), optical near-field scanning probes, or nano-optical (bio-)sensors. By combining the antenna structures with a second component in hybrid configurations, such as quantum dots, fluorescent molecules, or organic thin-films, the antennas can be employed to modify the absorption and emission characteristics of these objects in the coupled system. Key challenges in this context are the optimization of the antenna properties in view of the envisaged application, as well as achieving selective coupling of the nano-emitters to the high near-field regions of individual antennas.

In this presentation the top-down nanofabrication of different optical antennas by various nanolithographic techniques, combined with etch-mask transfer, will be demonstrated. Conical nanoantennas offer narrow, high near-field intensity hotspots near their tip apexes. Different procedures for selectively coupling few or single nano-emitters to these tips will be shown. Applications of different hybrid antenna configurations for absorption enhancement in organic thin films, emission enhancement and lifetime reduction of single quantum dots coupled to nanocones, and biosensing through plasmon resonance shifts after integration in a microfluidic environment will be illustrated.

Keywords: plasmonic nanostructures, optical antennas, nanofabrication, nanospectroscopy, surface enhanced Raman spectroscopy, hybrid nanostructures, nano-emitters, quantum dots.

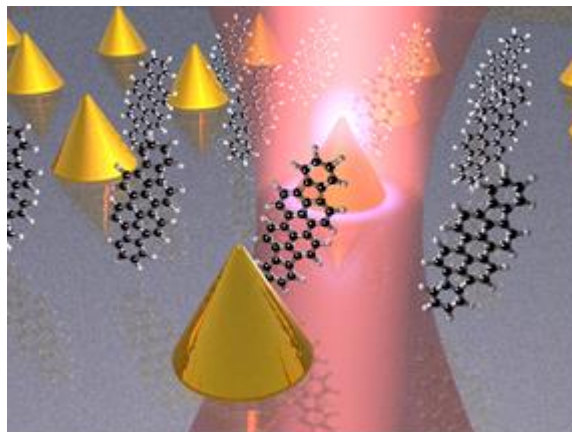


Figure 1: Schematic illustration of spectroscopic investigation of optical antennas and organic molecules (not to scale), courtesy of D.A. Gollmer.

References:

1. Schäfer, C., Gollmer, D.A., Horrer, A., Fulmes, J., Weber-Bargioni, A., Cabrini, S., Schuck, P.J., Kern, D.P., Fleischer, M. (2013), Single particle plasmon resonance study of 3D conical nanoantennas, *Nanoscale* 5, 7861-7866.
2. Schäfer, C., Kern, D.P., Fleischer, M. (2015), Capturing molecules with plasmonic nanotips in microfluidic channels by dielectrophoresis, *Lab Chip* 15, 1066-1071.
3. Fulmes, J., Jäger, R., Bräuer, A., Schäfer, C., Jäger, S., Gollmer, D.A., Horrer, A., Nadler, E., Chassé, T., Zhang, D., Meixner, A.J., Kern, D.P., Fleischer, M. (2015), Self-aligned placement and detection of quantum dots on the tips of individual conical plasmonic nanostructures, *Nanoscale* 7, 14691-14696.
4. Horrer, A., Krieg, K., Freudenberger, K., Rau, S., Leidner, L., Gauglitz, G., Kern, D.P., Fleischer, M. (2015), Plasmonic vertical dimer arrays as elements for biosensing, *Anal. Bioanal. Chem.* 407(27), 8225-8231.

This work was performed in the context of the COST Action MP1302 Nanospectroscopy.

Nanospectroscopy with Silver Nanowires

S. Mackowski^{1,2,*}

¹Nicolaus Copernicus University, Institute of Physics, Torun, Poland

²Baltic Institute of Technology, Gdynia, Poland

Abstract:

Silver nanowires are among the most interesting plasmonic nanostructures. They not only induce metal - enhanced fluorescence of located nearby emitters, but can also be used as nanoscale conductors or energy waveguides. In the presentation I will describe several recent results obtained for hybrid nanostructures composed of silver nanowires. Among the most important is strong, wavelength dependent, fluorescence enhancement observed for natural photosynthetic complexes coupled to silver nanowires. Particularly interesting are results obtained for photosynthetic complexes bioconjugated with the nanowires, as in this way we achieve the ultimate control of the morphology of the structure. For such systems we were able to use wide-field fluorescence imaging to monitor the conjugation process in the real time. Another aspect of using silver nanowires in hybrid nanostructures concerns coupling polymers considered building blocks of organic solar cells. In such a system, we obtained two-fold increase of the P3HT absorption. Finally, I will describe observations obtained for rare earth-doped nanocrystals coupled to the silver nanowires. As these systems feature reasonably efficient up-conversion upon infrared excitation, we demonstrate that this process can also be enhanced by the presence of the nanowires. The experimental results obtained for nanostructures composed of silver nanowires, demonstrate excellent optical properties of these plasmonic structures, as well as unique versatility of possible applications.

Keywords: silver nanowires, fluorescence imaging, real-time conjugation, energy propagation, plasmonic networks.

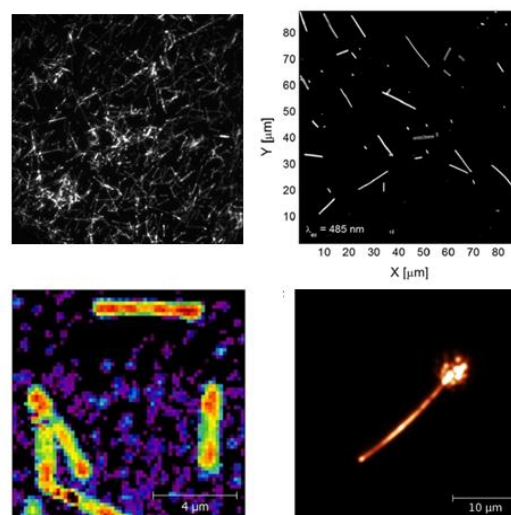


Figure 1: Examples of photosynthetic complexes, P3HT polymer and up-converting nanoparticles coupled with silver nanowires. The last panel shows propagation of energy in a silver nanowire-nanocrystal hybrid.

References:

1. S. Mackowski, "Metallic nanoparticles coupled to photosynthetic complexes", Smart Nanoparticles Technology ,InTech Publishing (2012) 3-28
2. D. Piatkowski, N. Hartmann, T. Macabelli, M. Nyk, S. Mackowski, A. Hartschuh, Nanoscale **7**, 1479–1484 (2015)
3. K. Smolarek, B. Ebenhoch, N. Czechowski, A. Prymaczek, M. Twardowska, I.D.W. Samuel, S. Mackowski, Applied Physics Letters **103**, 203302/1-4 (2013)
4. N. Hartmann, D. Piatkowski, R. Ciesielski, S. Mackowski, A. Hartschuh, ASC Nano **7**, 10257-10262 (2013)
5. M. Olejnik, B. Krajnik, D. Kowalska, M. Twardowska, N. Czechowski, E. Hofmann, S. Mackowski, Applied Physics Letters **102**, 083703/1-5 (2013)
6. S. Mackowski, S. Wörmke, A.J. Maier, T.H.P. Brotsudarmo, H. Harutyunyan, A. Hartschuh, A.O. Govorov, H. Scheer, C. Bräuchle, Nano Letters **8**, 558-564 (2008)

Addressing Challenges in Fabrication of Nanoscale Interstices at Molecular resolutions for Nanospectroscopies

S. Krishnamoorthy

Materials Research and Technology (MRT), Luxembourg Institute of Science and Technology, 41, Rue du Brill, L-4422, Belvaux, Luxembourg; sivashankar.krishnamoorthy@list.lu

Abstract:

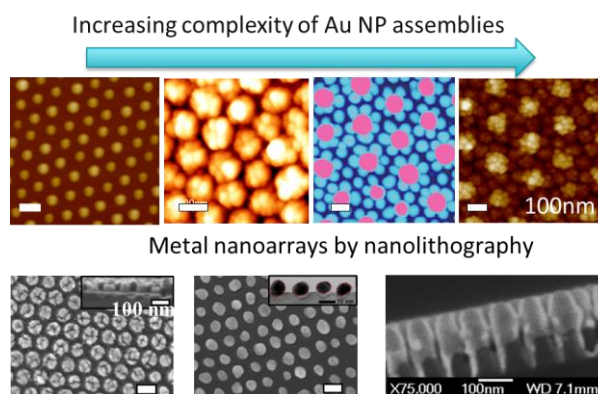
Noble metal nanostructures have been long sought as means to concentrate, direct, and transform electromagnetic fields at nanoscale volumes to advantage in light based devices including photovoltaics, optoelectronics, sub-wavelength optical communications and biomedicine. The geometric impact on the EM field profile can be shaped to advantage by precise control over repeating patterns of nanoscale gaps and curvatures at the metal-dielectric interface. The talk would present issues and challenges in attaining this goal, and present self-assembly approaches as a means to attain metal nanoarrays at ultra-high resolutions. Besides shaping EM field profiles, a systematic control at molecular resolutions is a pre-requisite for applications like bio sensing, due to the simultaneous influence of the geometry on optical/spectroscopic properties as well as biomolecular adsorption characteristics. The talk would focus on the use of colloids and copolymers, to achieve such systematic control within nanoarrays taking advantage of electrostatic attraction, replication and/or selective deposition.

Keywords: plasmonics, nanolithography, self-assembly, nanoarray, nanoparticle arrays, nanogaps, design rules, surface-enhanced Raman spectroscopy

Figure 1: Figure illustrating the metal nanoarrays fabricated using a combination of approaches involving self-assembly of copolymers and colloidal structures, and pattern-transfer approaches.

References:

1. V. Suresh, M. P. Srinivasan and S. Krishnamoorthy* (2013), Hierarchically built Hetero Superstructure Arrays with Structurally Controlled Material Compositions, *ACS Nano*, 7(9), 7513.
2. S. Dinda, F.L. Yap, V. Suresh, R. K. Gupta, D. Das, S. Krishnamoorthy* (2013), Quantitative detection with Surface Enhanced Raman Scattering (SERS) using self-assembled gold nanoparticle cluster arrays, *Aust. J. Chem.* 66(9), 1034
3. F. L. Yap, P. Thoniyot*, S. Krishnan and S. Krishnamoorthy* (2012), Nanoparticle Cluster Arrays for High-Performance SERS Through Directed Self-Assembly on Flat Substrates and on Optical Fibers, *ACS Nano*, 6 (3), 2056-2070.



Real-time sensing of chemical and biological species into individual cells with single-molecule resolution

P. Actis

University of Leeds, School of Electronic and Electrical Engineering, Leeds, UK

Abstract:

It is increasingly appreciated that physiological and pathological processes within the human body are controlled by complex cell-cell interactions within the context of a dynamic micro-environment. Current methods are inadequate to monitor the multiple interactions and dissect the contributions of single cells to disease processes. Furthermore these methods either study cells post-mortem, which prevents analysis of dynamic changes in the cell's 'omics over time, or they do not maintain the natural environment of a cell in heterogeneous tissues.

Scanning Ion Conductance Microscopy (SICM) is a scanning probe technique ideally suited for topographical imaging of living cells in culture. The operation of SICM relies on an ion current that flows between an electrode inside a nanopipette and another electrode in an external bath solution. The magnitude of this ion current depends on the nanopipette-sample separation, and it is utilised as a feedback signal to maintain a constant nanopipette-sample separation and to generate topographic information. I will discuss the application of SICM as an interventional tool to allow nondestructive manipulation of living cells, including real-time sensing of chemical and biological species into individual cells with single-molecule resolution.

I will then discuss the development of multifunctional nanoprobe based on nanopipettes and their application as intracellular nanosensors. I will conclude by highlighting the potential application of such nanoprobe to the field of nanospectroscopy.

Keywords: single-cell analysis, nanopore, nanopipette, electrochemistry

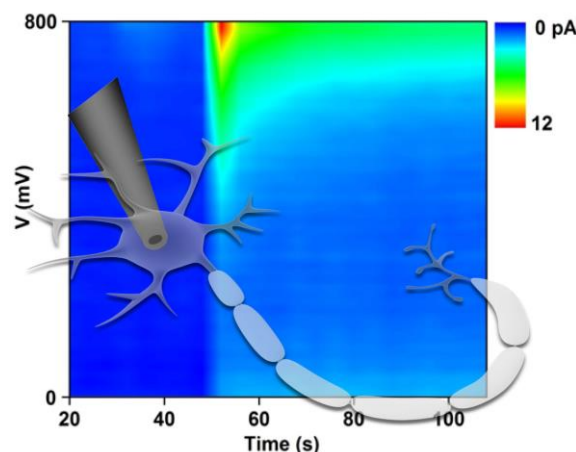


Figure 1: Electrochemical analysis of a living cell with a nanoelectrode

References:

- P. Actis et al (2013), Compartmental genomics in living cells revealed by single-cell nanobiopsy, *ACS Nano*, 8 (1), 546-553
- P. Actis et al (2014), Electrochemical nanoprobe for single-cell analysis, *ACS Nano*, 8 (1), 875-884
- A. Ivanov et al (2015), On-Demand Delivery of Single DNA Molecules Using Nanopipets, *ACS Nano*, 9 (4), 3587-3595

Resonant Surface-enhanced Raman Scattering by Optical Phonons in CdSe Nanocrystals on Metal Nanocluster Arrays

Alexander G. Milekhin^{1,2}, Volodymyr M. Dzhagan³, Dietrich R.T. Zahn³

¹A.V. Rzhanov Institute of Semiconductor Physics, pr. Lavrentjeva, 13, 630090 Novosibirsk, Russia

²Novosibirsk State University, Pirogov str. 2, 630090 Novosibirsk, Russia

³Semiconductor Physics, Technische Universität Chemnitz, D-09107 Chemnitz, Germany

Abstract:

Here we present the results on an investigation of resonant Stokes and anti-Stokes surface-enhanced Raman scattering (SERS) by optical phonons in colloidal CdSe nanocrystals (NCs) homogeneously deposited on arrays of Au nanoclusters using the Langmuir–Blodgett technology. The thickness of deposited NCs, determined by transmission and scanning electron microscopy, amounts to approximately 1 monolayer. Special attention is paid to the determination of the localized surface plasmon resonance (LSPR) energy in the arrays of Au nanoclusters as a function of the nanocluster size by means of micro-ellipsometry. SERS by optical phonons in CdSe NCs shows a significant enhancement factor with a maximal value of 2×10^3 which depends resonantly on the Au nanocluster size and thus on the LSPR energy. The deposition of CdSe NCs on the arrays of Au nanocluster dimers enabled us to study the polarization dependence of SERS. It was found that a maximal SERS signal is observed for the light polarization along the dimer axis. Finally, SERS by optical phonons was observed for CdSe NCs deposited on structures with a single Au dimer. A difference of the LO phonon energy is observed for CdSe NCs on different single dimers. This effect is explained as the confinement-induced shift which depends on the CdSe nanocrystal size and indicates quasi-single NC Raman spectra being obtained.

Keywords: resonant surface-enhanced Raman scattering, metal nanocluster arrays, colloidal CdSe nanocrystals, localized surface plasmon resonance, micro-ellipsometry, quasi-single nanocrystal Raman spectra

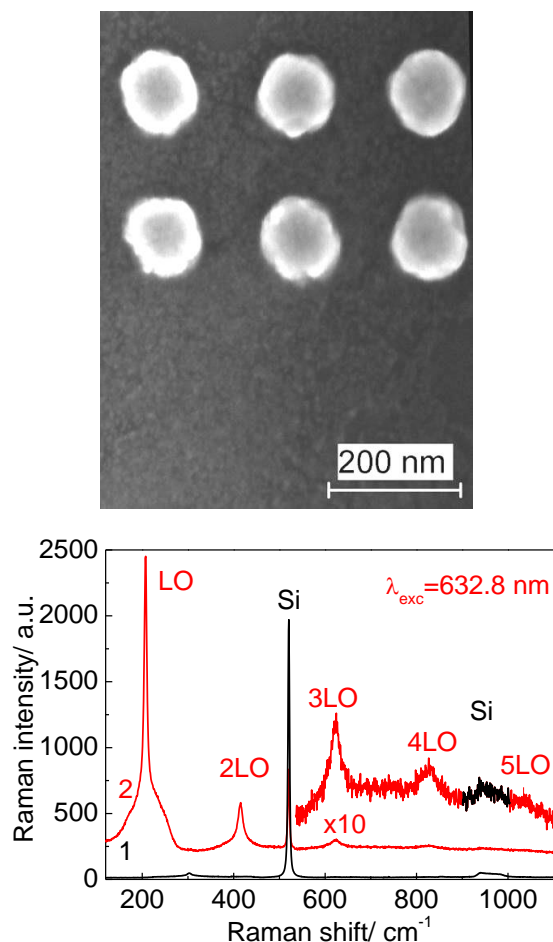


Figure 1: top: Typical SEM image of 1 monolayer of CdSe NCs deposited on a Au nanocluster array. White circular areas with a diameter of about 100 nm refer to Au nanoclusters. bottom: Raman spectra of CdSe NCs on bare Si (curve 1) and SERS spectra on arrays of Au nanoclusters with diameters of 76 nm (curve 2), measured with $\lambda_{exc} = 632.8 \text{ nm}$.

Approaching single molecule detection using plasmonic nanogaps

Addison R. L. Marshall¹, Jamie Stokes¹, Jean-Sebastien Bouillard^{1,2} and Ali M. Adawi¹

¹Department of Physics and Mathematics, University of Hull, Cottingham Road, Hull HU6 7RX, United Kingdom

²Department of Physics, King's College London, Strand, London WC2R 2LS, United Kingdom

Abstract:

Plasmonic technology, referring to the study of specific surface electromagnetic waves resulting from the coupling of photons and collective electron oscillations in metals, has seen a rapidly increasing interest over the past two decades. Combining key advantages directly linked to their nature, such as high field confinement, strong field enhancement, with polarisation and spectral selectivity, plasmonic systems promise many applications encompassing bio- and chemical sensing, signal guiding and manipulation on subwavelength scales, and extend to include photonic devices with enhanced performances, such as photodetectors, solar cells and light emitting diodes.

Plasmonic nano-gaps, arising from the strong coupling of a metal nanoparticle and metal film, offer a surprisingly powerful way to control and enhance light-matter interactions at the nanoscale despite their simple fabrication. Here we explore in details the plasmonic nano-gaps and gauge more specifically their Surface Enhanced Raman Spectroscopy (SERS) potential. SERS offers non-invasive label free detection characteristics from these structures and provides a molecular fingerprint from the analyte under investigation therefore allowing for highly specific sensing. The very large field enhancements obtainable in the plasmonic nano-gaps make them ideally suited for SERS which relies on strong field enhancements to counterbalance the relatively small cross-sections involved in Raman scattering.

We present an in-depth study of the plasmonic nano-gap optical properties as a function of various parameters, including the gap thickness. We determine different enhancement regimes corresponding to different mode hybridisations within the plasmonic cavity and successfully measure the SERS signal from single molecule in a polymer host matrix.

In parallel, FDTD calculations were used to corroborate the experimental results and to determine the nano-gap optical properties, including the spa-

tial extension of the hot spot and the corresponding local field enhancement within the nanocavity. Using the knowledge developed by this study, we propose a figure of merit for the application of plasmonic nano-gaps to SERS based devices.

This paper demonstrates the huge SERS potential plasmonic nanogaps and proves their single molecules capability using relatively minimalist structures.

Colloidal Gold Nanostructures for Plasmonics

M. Y. Khaywah,^{1*} S. Marguet,¹

¹NIMBE, CEA, CNRS, Université Paris-Saclay, CEA Saclay 91191 Gif-sur-Yvette, France

Abstract:

Gold at the nanoscale is a **plasmonic material** that has been proven effective in the development of new tools and improved-devices for Energy, Health and Information-Technology in the visible and near-IR ranges. Gold nanoparticles (AuNPs) can now be readily synthesized in large quantities and high quality thanks to significant advances in colloidal chemistry over the past decade. **Assembly of AuNPs leads to the appearance of new or enhanced plasmonic properties, still relatively poorly explored**, and is therefore particularly promising for industrial-scale production of cost-effective devices.

The **uniformity of size and morphology** of the nanoparticles **as building blocks is essential for the achievement of large-area assemblies**. Our group has been developed an expertise in the synthesis of monodispersed size- and shape-controlled gold NPs (see poster). Among the anisotropic shapes, triangles and plates are of particular interest. Indeed, the hot spot induced by six tips of self-assembly triangles exhibits an unprecedented enhanced electromagnetic field. Triangles can assemble in the edge-to-edge fashion or through face to face interactions (fig.1) and plates can form ordered columnar aggregates.

In this study, we report the spontaneous self-assembly of gold NPs of various shapes (rod, sphere, decahedron, triangle, cube, plate) by simply evaporating concentrated NPs dispersions on non-patterned substrates. This straightforward drop-casting method leads to the formation of an organized-ring at the periphery of the deposit (see fig.1). Key parameters related to a controlled-deposition are discussed i.e. the orientation of the particles with respect to the substrate, the procurement of large organized-areas, the removal of the surfactant and the degree of reproducibility.

In the literature, the applications of such 2D and 3D-arrays of gold NPs are currently related to **SERS studies** (for a very sensitive detection

of organic molecules and for anti-counterfeiting devices), 3D-metamaterials and ultra-thin metasurfaces, involving either spherical or rod-shaped NPs. Studies with non-commercial shapes such as “nanocubes”, “nanotriangles”, and “platelets” are still very scarce. Our next purpose is to study **the influence of the morphology and the effects of the substrate** (metallic or dielectric) upon the properties of these assemblies in collaboration with physicists.

Keywords: gold-nanoparticles, gold-nanoplates, spontaneous self-assembly, plasmonics

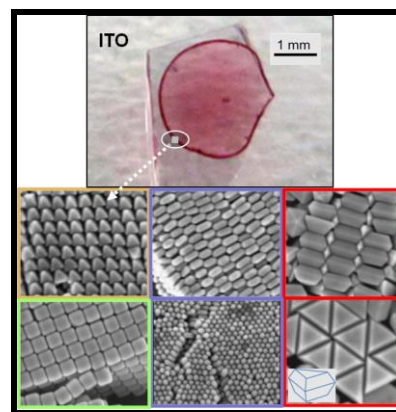


Figure 1: top to bottom: - formation of a ring of Au@CTAB NPs during the slow evaporation of the droplet; - SEM images of 3D-assemblies of gold NPs of various shapes obtained with this method.

References:

- E. Le Moal et al. (2013) “An electrically excited nanoscale light source with active angular control of the emitted light,” *Nano Lett.* 13, 4198-4205
- M. Haggui et al. (2012) “Spatial Confinement of Electromagnetic Hot and Cold Spots in Gold Nanocubes”, *ACS Nano.* 6(2) , 1299-1307

Intermixing length measurement with up to sub-nm accuracy by XEDS spectrum imaging

E Carbo-Argibay¹, C. Afonso², M. S. Claro³, D. G. Stroppa^{1,*}

¹International Iberian Nanotechnology Laboratory, 4715-330 Braga, Portugal.

²Department of Informatics, University of Minho, 4715-057 Braga, Portugal.

³Institute of Physics, University of São Paulo, 05508-090 São Paulo, Brasil.

Abstract:

Outstanding properties emerge at the interfaces of heterogeneous materials, so that their engineering offers promising prospects for achieving novel functional structures. The design and realization of highly-controlled interfaces requires reliable characterization techniques with high spatial and resolution chemical sensitivity, and X-rays Energy Dispersive Spectroscopy Spectrum Imaging (XEDS-SI) has been used qualitatively for this purpose with ample success. This work presents the data processing and signal quantitative analysis from XEDS-SI datasets obtained by aberration-corrected Scanning Transmission Electron Microscopy (STEM). A strategy consisting of successive XEDS-SI dataset breakdown with decreasing binning sizes was explored to improve the chemical mapping spatial resolution up to the XEDS signal to noise significance limit. The use of anisotropic binning maximized the chemical analysis spatial resolution across the interfaces, allowing for an accurate measurement of the intermixing layer and projected roughness at the interface of heterogeneous nanostructured materials.

Keywords: Interfaces, interdiffusion, chemical analysis, TEM.

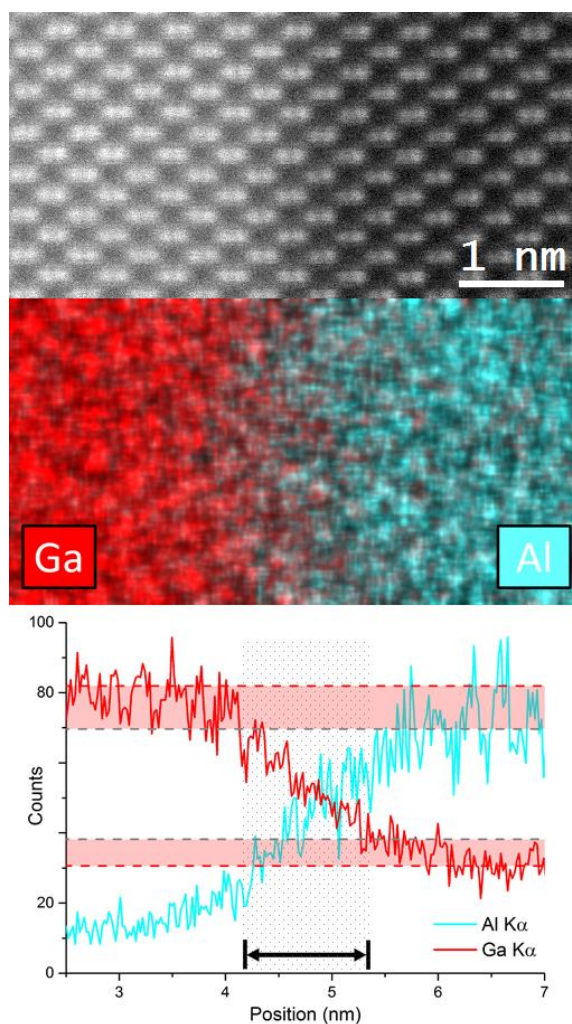


Figure 1: (top) Atomic resolution High Angle Annular Dark Field (HAADF) from a GaAs-AlGaAs heterostructure interface. (mid) Qualitative color map indicating the Ga-K α and Al-K α signal distribution from a XEDS-SI experiment. (bottom) Ga-K α and Al-K α profiles accross the interface and assessment of the intermixing layer dimension – 1.2 ± 0.1 nm (2σ).

High resolution solid state NMR spectroscopy in surface organometallic chemistry: access to molecular understanding of active sites of well-defined heterogeneous catalysts.

Edy Abou-Hamad¹ and Jean-Marie Basset¹

¹ KAUST Catalysis Center (KCC) King Abdullah University of Science and Technology, Thuwal, Saudi Arabia

Abstract:

Among various measurements techniques, Nuclear Magnetic Resonance (NMR) is an extremely powerful tool for the identification of chemical composition and the determination of molecular structure. Because of its versatility it is widely applied in chemistry, materials science, and biomedical research. At KAUST, we boast an NMR lab housing 5 Solid State NMR spectrometers from Bruker include one of the world's first Bruker 900MHz Wide-Bore magnets, coupled with a huge range of accessories that would allow break-through research. High resolutions NMR provide a range of exquisitely precise tools to characterize well-defined active sites in heterogeneous catalysis. Implementation of high resolution and 2D solid state NMR techniques helped to identify surface structures at a molecular level, which is a key to implementing structure–reactivity relationships and rational developments in heterogeneous catalysis. It is clear that these methods also have the potential for extensive further developments and applications, for example towards understanding more complex systems (complex oxide materials, active sites with paramagnetic or quadrupolar centres), probing the dynamics of surface species (access to mobility of active sites), and to monitor the active sites as a function of time. 2D high resolution and 2D spectra shows the power of this technique to characterize the well-defined heterogeneous catalysts prepared by surface organometallic chemistry.

Keywords: heterogeneous catalysis, surface organometallic chemistry, solid-state NMR,

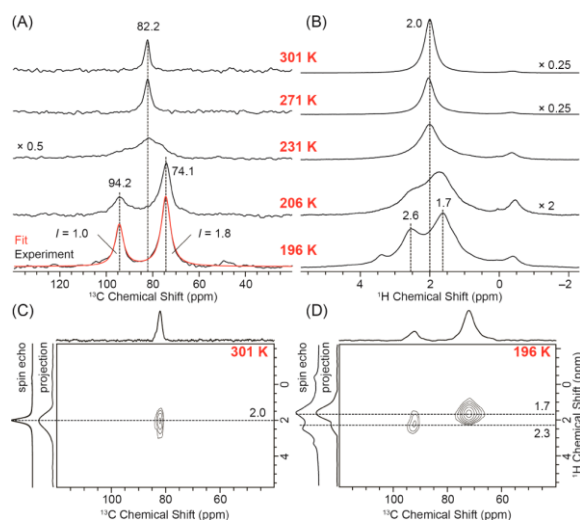


Figure 1: Variable-temperature ^{13}C CP/MAS, ^1H spin-echo, two-dimensional ^1H – ^{13}C dipolar HETCOR NMR spectra MAS solid-state NMR spectra of $\equiv\text{Si-O-W}(\text{Me})_5$

References:

- Chen, Y., Abou-hamad, E., Hamieh, A., Hamzaoui B., Emsley, L., Basset, J.M. (2015) Alkane Metathesis with $[(\equiv\text{SiO})\text{Ta}(\text{=CH}_2)\text{Me}_2]/[(\equiv\text{SiO})_2\text{Ta}(\text{=CH}_2)\text{Me}]$ Generated from Well-Defined Surface Organometallic Complex $[(\equiv\text{SiO})\text{Ta}^V\text{Me}_4]$ *J.Am.Chem.Soc.*, 137, 588–591
- Samantaray, K. M., Callens, E., Abou-Hamad, E., Rossini, J. A., Widdifield, C. M., Dey, R., Emsley, L., Jean-Marie Basset, J. M., (2014) WMe6 Tamed by Silica: Si–O–WMe5 as an efficient, Well-Defined Species for Alkane Metathesis, Leading to the Observation of a Supported W–Methyl/Methyldiyne Species *J.Am.Chem.Soc.*, 136, 1054–106

Aluminum plasmonics for UV nanooptics

J. Martin,¹ D. Khlopin,¹ F. F. Zhang,¹ Silvère Schuermans,¹ D. Gérard,¹ J. Proust¹ and J. Plain¹

¹Institut Charles Delaunay - Laboratoire de nanotechnologies et d'instrumentation optique, UMR CNRS 6281, Université de Technologie de Troyes, France

Abstract: An electromagnetic field is able to produce a collective oscillation of free electrons at a metal surface. This allows light to be concentrated in volumes smaller than its wavelength. The resulting waves, called surface plasmons¹ can be applied in various technological applications such as ultra-sensitive sensing², Surface Enhanced Raman Spectroscopy (SERS)³, or metal-enhanced fluorescence⁴, to only name a few. For several decades plasmonics has been almost exclusively studied in the visible region by using nanoparticles made of gold or silver as these noble metals support LSPR only in the visible and near-IR range. Nevertheless, emerging applications will require the extension of nanoplasmonics toward higher energies, in the UV-range. Aluminum is one of the most appealing metal for pushing plasmonics up to ultraviolet energies. The subsequent applications in the field of nanooptics are various. This metal is therefore a highly promising material for commercial applications in the field of nanooptics from the infrared to ultraviolet. As a consequence, aluminum (or UV) plasmonics has emerged quite recently. Aluminium plasmonics has been demonstrated efficient for numerous potential applications including non-linear optics⁵, enhanced fluorescence⁶, UV-SERS⁷, optoelectronics^{8,9} (plasmonic assisted lasing, by coupling Al with wide bandgap semiconductors such as GaN), photocatalysis¹⁰, structural colors¹¹ and data storage¹². In this talk, we will discuss about the recent advances in aluminum plasmonics. Different preparation methods developed in the laboratory to obtain aluminum nanostructures will be presented with their optical and morphological characterizations. Both advantages and issue of aluminum as a plasmonic material will be part of the presentation.

Keywords: ultraviolet, plasmonics, aluminum, localized surface plasmon resonance

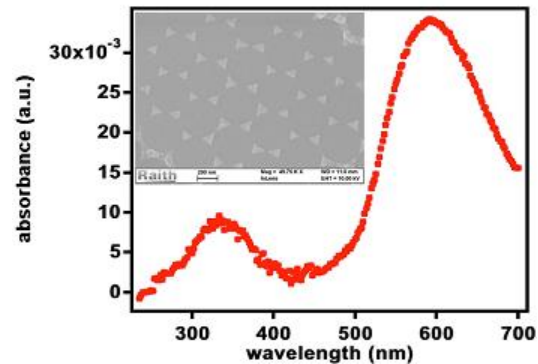


Figure 1: Aluminum nanotriangles made by nanosphere lithography (SEM image in the inset, scalebar 200 nm) and their corresponding extinction spectra unveiling their UV and visible optical properties.

References:

1. A. V. Zayats, I. I. Smolyaninov, and A. A. Maradudin 2005 Phys. Rep. **408**, 131–314
2. A. V. Kabashin, P. Evans, S. Pastkovsky, W. Hendren, G. A. Wurtz, R. Atkinson, R. J. Pollard, V. A. Podolskiy, and A. V. Zayats 2009 Nat. Mater. **8**, 867–871
3. F. De Angelis, F. Gentile, F. Mecarini, G. Das, M. Moretti, P. Candeloro, M. L. Coluccio, G. Cojoc, A. Accardo, C. Liberale, R. P. Zaccaria, G. Perozziello, L. Tirinato, A. Toma, G. Cuda, R. Cingolani, and E. Di Fabrizio 2001 Nat. Photonics **5**, 682–687
4. D. Gerard, J. Wenger, N. Bonod, E. Popov, H. Rigneault, F. Mahdavi, S. Blair, J. Dintinger, and T. W. Ebbesen 2008 Phys. Rev. B **77**, 045413
5. Krause D, Teplin C W and Rogers C T 2004 J. Appl. Phys. **96** 3626
6. Forestiere C, Handin A and Dal Negro L 2014 Plasmonics **9** 715–25
7. Jha S K, Ahmed Z, Agio M, Ekinici Y and Löffler J F 2012 J. Am. Chem. Soc. **134** 1966–9
8. Zhang Q, Li G, Liu X, Qian F, Li Y, Sum T C, Lieber C M and Xiong Q 2014 Nat. Commun. **5** 5953
9. Lawrie B, Kim K W, Norton D and Haglund R 2012 Nano Lett. **12** 6152–7
10. Honda M, Kumamoto Y, Taguchi A, Saito Y and Kawata S 2014 Appl. Phys. Lett. **104** 061108
11. Tan S J, Zhang L, Zhu D, Goh X M, Wang Y M, Kumar K, Qiu C W and Yang J K W 2014 Nano Lett. **14** 4023–9

12.Miao L, Stoddart P R and Hsiang T Y 2014
Nanotechnology **25** 295202

Scanning Tunneling Spectroscopy approaches for Nano-structures characterization

Borislav Naydenov, Jing Li, P. Barimar, and John J. Boland

Centre for Research on Adaptive Nanostructures and Nanodevices (CRANN) & School of Chemistry, Trinity College Dublin, Dublin 2, Ireland

Abstract:

Silicon-On-Insulator (SOI) layers and patterned structures are investigated using low-temperature scanning tunneling spectroscopy (STS). Different STS methods like field emission [1] (see Fig.1) and variable-height [2] spectroscopy were applied to study SOI layer with various thicknesses. Significant shifts of the density of states (DOS) with the thickness were detected for annealed samples. These shifts in the LDOS are attributed to an increase of the band gap of the thin layer. Similar changes in the electronic structure of SOI nanowires (see Fig.2) were observed by combined study using Scanning Tunneling and Atomic Force Microscopies (STM/AFM).

Keyword: Scanning tunneling spectroscopy (STS), Silicon-On-Insulator (SOI), Si band gap.

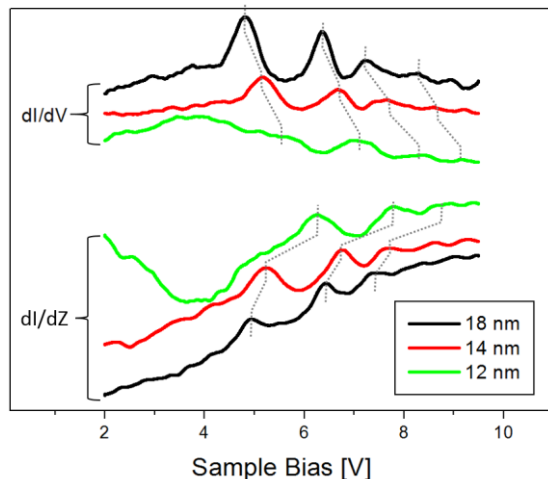


Fig.1 Field emission spectra taken on annealed SOI-layer with varying thicknesses.



Fig.2 STM and STS images of annealed SOI-wire.

References:

- [1] R.S. Becker, J.A. Golovchenko, and B.S. Swartzentruber, Electronic Interferometry at Crystal Surfaces, *Phys. Rev. Lett.* **55**, 09987 (1985); G. Binnig, K.H. Frank, H. Fuchs, N. Garcia, B. Reihl, H. Rohrer, F. Salvan, and A.R. Williams, Tunneling Spectroscopy and inverse photoemission: Image and field states, *Phys. Rev. Lett.* **55**, 09991 (1985)
- [2] B. Naydenov and John J. Boland, Variable-height scanning tunneling spectroscopy for local density of states recovery based on the one-dimensional WKB approximation, *Phys. Rev. B* **82**, 245411 (2010).
- [3] B. Naydenov, Jing Li, P. Barimar, and John J. Boland, *in preparation*.

Material optical properties by spectroscopic ellipsometry of thin particulate films

O. Zhuromskyy,^{1,*} S. Golkar,² I. Spies,² R. Klupp-Taylor,² U. Peschel,³

¹Institute of Optics, Information and Photonics, University of Erlangen-Nürnberg, Germany

²Institute of Particle Technology, University of Erlangen-Nürnberg, Germany

³Institute of Solid State Theory and Optics, University of Jena, Germany

Abstract:

Optical properties of materials are crucial for building predictive models for light-matter interaction. For many important optical materials the book by Palik is a reliable source of wavelength dependent complex refractive indexes. The majority of the data sets reported there were measured on macroscopic samples and represent pure, bulk material properties. However, in certain cases, especially when dealing with nano sized objects, the Palik data might deviate from those of the synthesized materials. And, the question “What are the optical properties of the material constituting our nano structures?” sometimes is not that easy to answer. We apply spectroscopic ellipsometry to study optical properties of goethite nano particles. Goethite is a material that is not found as bulk crystals, and thus, its optical properties can only be determined from particulate systems, as reported by Maedas. Particles coming out of our synthesis are of spherical shape, making the handling easier if compared to the rod shaped particles typical for goethite. It is quite a difficult task to form particulate films with subwavelength accuracy using dip coating or droplet drying technique. The non uniformity of the film thickness is immediately translated into inaccuracy of the extracted optical parameters. The particulate films used in our measurements were manufactured by the Langmuir-Blodgett technique, and as it can be seen in Figure 1, are basically dense monolayers of particles. In addition to the excellent uniformity across the entire substrate, which was verified by SEM screening, the material density in the film can be computed from purely geometric considerations, whereas for thicker films obtaining the material density is a challenge. The mean particle diameter of about 70nm ensures that there is no diffraction on the particles and the films are seen by the light as effective media. Thus, the optical properties of goethite can be obtained from the effective refractive indexes of the films with the help of Maxwell-Garnett equation. Due to the small size of the structure, the accuracy of the

obtained material parameters can be verified by directly simulating light reflection from the particulate film using the superposition T-matrix method. We believe that our approach can be easily extended to other material systems and in combination with T-matrix method to particle diameters of up to micrometer.

Keywords: refractive index, material parameters, spectroscopic ellipsometry, effective medium theory, langmuir-blodgett films, light scattering, T-matrix.

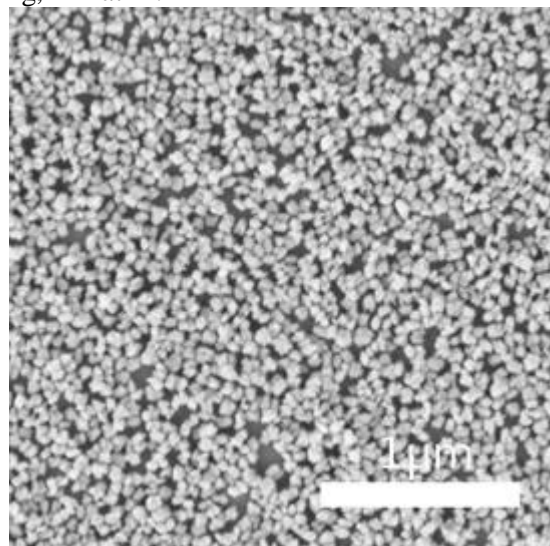


Figure 1: SEM image of the Langmuir-Blodgett monolayer of goethite particles.

References:

1. Palik, E.D. (1997) Handbook of Optical Constants of Solids, Academic Press Inc.
2. Maeda, H., Maeda, Y. (2011) Spectroscopic Ellipsometry Study on Refractive Index Spectra of Colloidal β -FeOOH Nanorods with Their Self-Assembled Thin Films, *Langmuir* 27 (6), 2895-2903.
3. Mishchenko, M.I., L.D. Travis, and D.W. Mackowski, T-matrix computations of light scattering by nonspherical particles: A review, *J. Quant. Spectrosc. Radiat. Transfer* 55, 535-575..

Investigation of Diamond-Like Carbon Films Physical Properties Using Multifractal Analysis

N. Margaryan, Zh. Panosyan, A. Mailyan, S. Voskanyan

National Polytechnic University of Armenia, Halotechnics basic laboratory, Yerevan, Armenia

Abstract:

The process of forming the semiconductor layers for modern electronic devices is accompanied by a process of self-organization at the nano and micro levels. A promising approach to describe such self-similar state to the surface is the multifractal analysis. The methodology of multifractal parameterization of structures of materials is based on the fundamental principles of self-similarity, stochastic and fractal broken symmetry structures of natural materials. It uses a set of self-similar measures in Euclidean space, so can more accurately describe the characteristics of the material. The property of self-similarity quantitatively expressed using the concept of fractal dimension. To determine the fractal dimension of the fractal and other parameters, we used obtained atomic force microscopy images for chemical vapor deposited diamond-like carbon nanofilms (Figure 1). One of the important physical parameters of the nanofilms is surface energy, which we can calculate using the results obtained by multifractal analysis. These results allow us to propose a mathematical expression that gives an opportunity to evaluate the surface energy of the film, due to the presence of fractal structure on its surface. Surface energy we calculated by the experiment and results were compared with the results of multifractal method. The dependence of multifractal parameters on the deposition duration and other technological parameters was revealed.

Keywords: AFM, multifractal analysis, diamond-like carbon, CVD technology, surface potential.

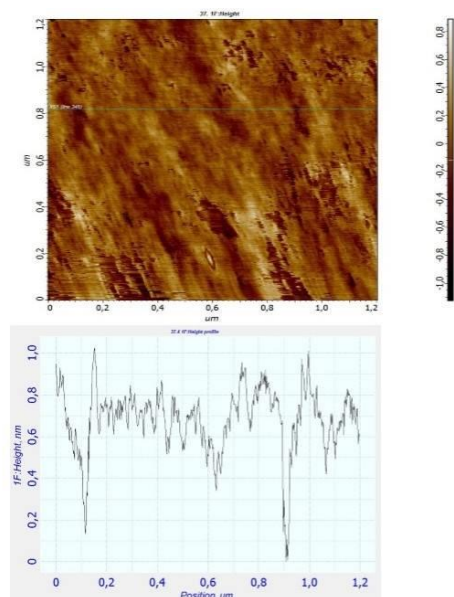


Figure 1: AFM image of a sample of DLC grown on Ge substrate (upper panel) and cross sectional profile of thickness across the green line on the image (lower panel).

References:

1. Panosyan Zh. R., Darbasyan A.T., Voskanyan S.S., Yengibaryan Y. V. (2014), Method for preparation of transparent conductive diamond-like carbon films and mechanisms of conductivity formation. *Journal of Contemporary Physics*, Vol. 49, No. 6, 286-292.
2. Moskvina P., Krizhanivskiy V., Rashkovetskiy L., (2014), Multifractal analysis of areas of spatial forms on surface of $Zn_x Cd_{1-x}$ Te-Si (111) heterocompositions, *Journal of Crystal Growth*, 404, 204-209.
3. Yadav R.P., Singh U. B., Mittal A.K. & Swivedi S. (2014) Investigating the nanostructured gold thin films using the multifractal analysis, *Applied Physics A*, 117, 2159-2166

**Nanometrology France 2016
Symposium on Detection, location &
quantification of nanomaterials and by-
product released from nano-enable
products**

Towards a Better Understanding of Interaction Mechanisms and Thermodynamic Properties of Nanomaterials Interacting with BioMacromolecules.

S. Stoll,^{1*} F. Loosli,¹ O. Oriekhova,¹ F. Carnal,¹ A. Clavier,¹

¹University of Geneva, Environmental Physical Chemistry, Geneva, Switzerland

Abstract:

Interactions between isolated or aggregated nanoparticles with, in particular, natural organic matter such as biopolymers (polysaccharides, proteins) and humic substances in aquatic systems, are often resulting in surface coating, that will strongly alter their dynamic properties and bioavailability. The extend to which manufactured nanoparticles form such complexes or agglomerates will depend on the balance between the attractive and repulsive forces among the nanoparticles as well as between them and the environmental matrix.

Novel and original approaches are presented to investigate and quantify the interaction mechanisms between nanoparticles and biopolymers. The first one is Isothermal Titration Calorimetry allowing the measurements of the exchanged heat during binding processes. Such quantitative and thermodynamic information is often missing to get an insight into the thermodynamic association properties and mechanisms of adsorption and agglomeration. Changes of enthalpy, entropy and total free energy, as well as reaction stoichiometry and affinity binding constant can be calculated indicating the importance and balance of enthalpic and entropic effects. The second approach is related to computer modelling. In particular Monte Carlo simulations constitute a powerful approach to get an insight into the interaction processes between nanoparticles and aquagenic compounds since the effect of many parameters can be investigated in a systematic way (nanoparticle size, nanoparticle surface charge density, nanoparticle surface hydrophobicity, dispersion medium properties, biomacromolecule chemistry, etc). The formation of a complex between a protein and a charged nanoparticle in presence of explicit counterions will be presented. In all cases, we will show that the presence of one nanoparticle is found to deeply change the bi

omacromolecule structure and electrostatic properties.

Keywords: Interaction mechanisms, surface coating, Isothermal titration, Monte Carlo Simulations.

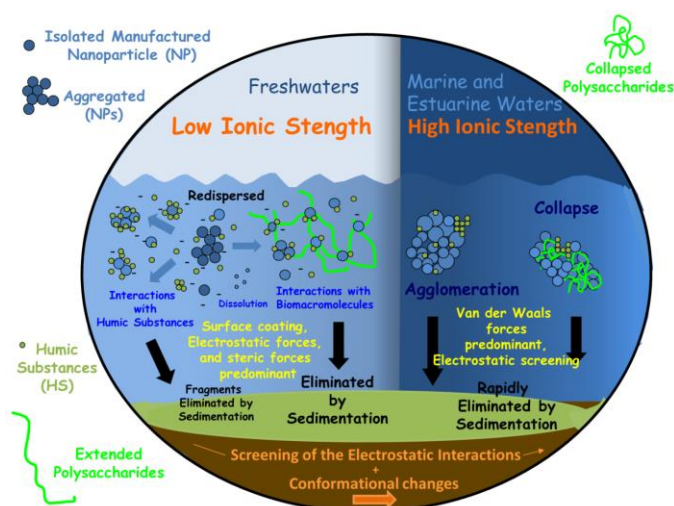


Figure 1: Possible transformation processes of nanoparticles in aquatic systems.

References:

1. Loosli, F., Vitorazi, L., Berret, J.-F., Stoll, S. (2015) Towards a better understanding on agglomeration mechanisms and thermodynamic properties of TiO₂ nanoparticles interacting with natural organic Matter, *Water Res.*, 80, 139–148.
2. Carnal, F., Clavier, A., Stoll, S., (2015) Modelling the interaction processes between nanoparticles and biomacromolecules of variable hydrophobicity: Monte Carlo simulations, *Env. Sci. : Nano*, 327-339

Silver Nanoparticles in managed waste facilities: From metallic to sulfidic and back again.

R. Kaegi,^{1*} C. Meier,² A. Voegelin,¹ A. Pradas del Real,³ G. Sarret, and C.R. Mueller,⁴

¹Eawag, Swiss Federal Institute of Aquatic Science and Technology, Duebendorf, Switzerland

²Zhaw, Zurich University of Applied Sciences, Winterthur, Switzerland

³ISTerre (Institut des Sciences de la Terre), Université Grenoble Alpes and CNRS, France

⁴ETH Zurich, Laboratory of Energy Science and Engineering, Zurich, Switzerland

Abstract:

Transformations of metallic silver nanoparticles (AgNP) critically affect their antimicrobial efficacy. Although particle specific effects have been postulated, the toxicity of AgNP has been largely attributed to the release of ionic silver. Due to the limited solubility of silver sulfide (Ag₂S) under relevant environmental conditions, the sulfidation of AgNP has been identified as a key transformation, strongly mitigating the effects of AgNP after their release.

The beginning of the sulfidation of AgNP in sewer systems has been reported from lab- and full-scale experiments. The ongoing sulfidation and the efficient removal of AgNP from the wastewater results in the accumulation of almost completely sulfidized AgNP in the sewage sludge. After anaerobic sludge treatment, no metallic Ag is detected anymore and Ag is mainly present as Ag₂S, but a minor fraction of Ag bound to thiol groups and/or present as an amorphous Ag₂S-species is consistently observed.

In France, UK, and the USA, sewage sludge is used as fertilizer in agriculture. In Switzerland and in Germany, sewage sludge is incinerated preferably in fluidized bed reactors. To investigate the behavior of AgNP during the mono-incineration, we incinerated digested sludge containing sulfidized AgNP in a lab-scale fluidized bed reactor. The reactor was operated at 800 °C in an atmosphere of 4 % O₂, 12 % CO₂, 84% N₂ with 300 ppm SO₂ and humidified to 30% H₂O and thus closely mimicked the condition is a full-scale fluidized bed reactor. Ash particles collected after only 1 minute of reaction time revealed that Ag was dominantly present as metallic, spherical particles < 50 nm (Figure 1). Thus, the incineration very efficiently transforms sulfidized AgNP back into metallic AgNP. This raises a number of questions: Do these incidentally formed AgNP have different properties than the engineered AgNP that were used in consumer products and how can these incidentally formed

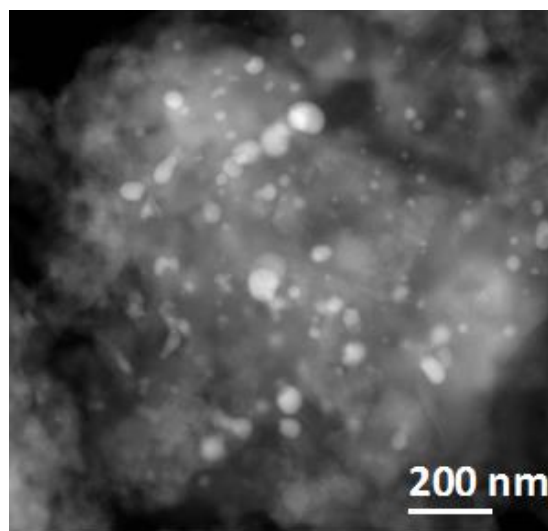


Figure 1: TEM image of a sewage sludge ash sample collected after 1 minute at 800°C. The white dots represent AgNP.

AgNP be distinguished analytically from engineered AgNP? How should these incidentally formed AgNP, which went through a sulfidation in the WWTP but originated from engineered AgNP, be treated in a fate model? Are these incidentally formed AgNP firmly incorporated into the ash matrix or may they be mobilized upon contact with water, for example during storage in a landfill?

Keywords: Sulfidation, silver nanoparticles, wastewater treatment, incineration

References:

Meier, C., Voegelin, A., et al., (2016) Transformation of Silver Nanoparticles in Sewage Sludge during Incineration, *ES&T*, In Press.

Rules and rates of release from nano-enabled products

N. Neubauer

BASF SE, Material Physics, GMC/R, Carl-Bosch-Strasse 38, 67056 Ludwigshafen, Germany

Abstract:

Release assessment regards the detachment of fragments from a larger whole, such as consumer products, and additionally considers release mechanism, form of the released entity, release scenario, probability of release, and lifecycle simulation, if relevant. Key parameters which mainly influence release are chemical aging intensity (photolysis, hydrolysis, leaching), processing (sanding, drilling), matrix properties (soft or brittle) and nanomaterial properties (particulate or fibrous). Systematic series of release studies allow a ranking (and possibly even a grouping) of the probability and characteristics of release from nano-enabled products.

Based on protocol optimization and inter-laboratory validation by MARINA (FP7), nanoGEM (BMBF), and the NanoRelease (US, CAN, EU) initiative, we report on quantitative release rates from real-world value-chains: automotive parts, consumer appliances, wood coatings. Original data from BASF and the *SUN* (FP7) project shows that release rates are hierarchically determined by decreasing importance of aging > process > matrix > nanomaterial. Many release phenomena are matrix-dominated with released fragments which resemble primarily those of the matrix, modulated by properties of the nanomaterial. Accordingly, also the physical-chemical and toxicological properties of fragments are dominated by the matrix. Specifically for weathering, the matrix (various polymers, epoxies, cement) determines releases across 5 orders of magnitude from 100 mg release per MJ of UV energy (cements) down to 0.002 mg/MJ (polyethylenes), with less than a factor of 10 up- or down-modulation by the embedded metal-oxide, carbonaceous, or organic nanomaterials (Wohleben and Neubauer, 2016).

Keywords: release, nano-enabled products, aging, processing, matrix, nanomaterial,

References:

Wohleben, W., Neubauer, N. (2016) Quantitative rates of release from weathered nanocomposites are determined across 5 orders of magnitude by the matrix, modulated by the embedded nanomaterial. *NanoImpact* 1, 39–45

Response of microbial communities and plant to metal oxide- and carbon-based nanomaterials in a plant-soil-based system

C. Santaella^{1,2,*}, B. Collin^{1,2}, M. Hamidat, M. Barakat^{1,2}, P. Ortet^{1,2}, W. Achouak^{1,2}

¹ Aix-Marseille Université, CEA, CNRS, Biosciences and biotechnology Institute of Aix-Marseille BIAM, DRF, UMR 7265, LEMIRE, CEA Cadarache, St-Paul-lez-Durance, France

² GDRI iCEINT, international Consortium for the Environmental Implication of Nanotechnology, CNRS-Duke University, F-13545 Aix-en-Provence, France

Abstract:

Several classes of nanomaterials (NMs) are globally manufactured in hundred to thousands of metric tons per year. NMs are considered to be emergent contaminants, with specific endpoints in soils and sediments. Current knowledge on NMs on soil-based ecosystem comes from exposure to concentrations that are far from those predicted in soil or even in biosolids.

We have examined the impact of different NMs based on metal oxide, CeO₂ and TiO₂, and carbon based NMs (carbon nanotubes, CNTs), on a simple-track terrestrial ecosystem based on a microbe-soil-plant network.

Our issues were twofold: i) Can we modulate the impact of NMs by designing their properties through their physicochemical properties (particle size, shape, crystalline phase, coating...)? ii) Do NMs with very different chemistry and properties trigger common responses on a plant-soil-microbe system?

The NMs were added to a soil at a concentration of 1 mg.kg⁻¹, a concentration approaching the current maximal estimations of NMs concentration in soils through modeling. The plant selected was Canola (*Brassica napus*), an oil-producing plant. We examined the response of three different compartments that form the system, *i.e.* the unplanted soil, the rhizosphere and the plant roots. We analyzed microbial enzymatic activities for carbon, nitrogen, phosphorus recycling and the microbial community structure by pyrosequencing of 16S rRNA gene.

The presentation will focus on how NMs differentially alter microbial activities and/or microbial communities structure depending on the chemistry and physico-chemistry of the NMs, and the compartment (unplanted, rhizosphere or root) considered. We will provide some tracks to evaluate to what extent the design of the NMs can modulate the impact and some trends shared by NMs with different reactivity.

Keywords: nanomaterials, design, soil, rhizosphere, microbiota, plant response, biotransformation, soil ecosystem.



Figure 1: Localization of CeO₂ NMs on a plant root. The pixels in red denote the presence of NMs. Root hairs were targets in the interaction between the plant and NMs. Root hairs are important because they increase the surface for nutrients and water absorption. Root cap and root hairs are also preferred localizations for bacteria on plant roots, which suggests likely plant-bacteria-NMs interactions. We are tempting to address these interactions and their impacts on a plant-soil-bacteria based system.

References:

1. Nowack, B., Ranville, J. F., Diamond, S., Gallego-Urrea, J. A., Metcalfe, C., Rose, J., ... & Klaine, S. J. (2012). Potential scenarios for nanomaterial release and subsequent alteration in the environment. *Environmental Toxicology and Chemistry*, 31, 50-59.
2. Gottschalk, F., Lassen, C., Kjoelholt, J., Christensen, F., & Nowack, B. (2015). Modeling flows and concentrations of nine engineered nanomaterials in the Danish environment. *International journal of environmental research and public health*, 12, 5581-5602.

Effect of chemical transformations of silver in nanoAg-enabled textiles on their antimicrobial efficacy and release

G. Lowry,^{1,2,*} T. Dankovich,^{1,2}

¹ Carnegie Mellon University, Department of Civil & Env. Eng., Pittsburgh, USA

² Center for Environmental Implications of Nanotechnology (CEINT), Pittsburgh, USA

Abstract:

This research project seeks to understand the effect of aging under different use and end of life scenarios on the chemical transformation of silver nanoparticles in consumer textile products, and the subsequent effect on functional performance of such products. This is accomplished through various stress tests including exposures to artificial sweat and end-of-life chemical exposures. These exposure scenarios represent realistic, but ‘worst-case’ scenarios to better understand if commonly used life-cycle assumptions, such as an immediate release of total Ag-content and duration of antimicrobial efficacy, are valid in certain circumstances. Several fabrics were chosen to be models for various attachment methods for silver nanoparticles, silver metals, and silver chlorides. Silver loading ranged from low ppm levels to as high as 0.4 wt%. The silver containing fabrics were exposed to extreme environmental chemical scenarios, including chloride, sulfide, and acetic acid, and were subsequently analyzed with extended x-ray absorption fine structure spectroscopy (EXAFS) for nano-material transformations, and silver release was quantified with ICP-MS. The functional performance of such textiles post worse-case exposure was assessed to determine what, if any chemical exposure has a detrimental effect on efficacy of antibacterial performance. The potential for determination of the most robust method to incorporate silver into textiles, and the appropriate loadings, for sustained long-term performance under the most strident conditions is discussed.

Keywords: environmental nanotechnology, safe by design, nano-enabled products.

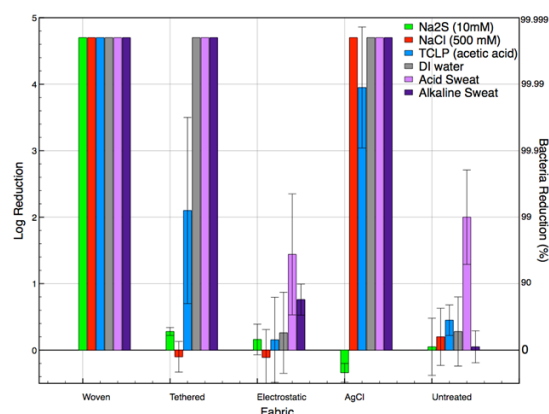


Figure 1: E. coli antibacterial efficacy of silver embedded textiles post-corrosive treatments. A) Comparison of log and percent reduction of E. coli bacteria after 24 hours of incubation on various textile surfaces. B) Efficacy of silver embedded textiles with respect to remaining silver content on the textile surfaces.

Multi-scale X-ray computed-tomography for the 3D detection and location of nanomaterials in manufactured materials and complex media

P. Chaurand,^{1,2} D. Borschneck,^{1,2} V. Vidal^{1,2}, C. Levard^{1,2}, L. Scifo^{1,2}, J. Perrin³ and J. Rose^{1,2}

¹CEREGE, UM 34, Aix-Marseille Univ., CNRS, IRD, Aix en Provence, FRANCE

²Labex SERENADE, Aix en Provence, FRANCE

³IMBE, UMR 7263 Aix-Marseille Univ., CNRS, IRD, Univ. d'Avignon, Marseille, FRANCE

Abstract:

X-ray computed tomography (CT) is a powerful 3D imaging technique for the in-situ and non-destructive investigation of the inner structure of an object. This relatively recent technique has tremendously evolved over the past decade with much more sensitive detection systems and increased spatial resolution. Indeed it is now possible to reach spatial resolution of tens of nanometers with synchrotron X-ray source but also with lab-based systems (nano-CT). Reaching such high spatial resolution made CT a valuable technique for the 3D detection and location of nanomaterials, their aggregates and agglomerates (NOAA) in manufactured materials (wood coating, polymers ..) and in complex and/or natural media (plants, organisms, organs ...).

The Nano-ID¹ platform, installed at CEREGE (Aix en Provence, France), is equipped with two CT systems and offers the opportunity to perform multi-scale analysis on a same sample, i.e. 3D imaging with a spatial resolution from 50 μm to 50 nm.

For example, in a study focusing on the aging of wood-coating containing CeO_2 nanomaterials and associated NOAA released, multi-scale micro and nano-CT gave the keys to identify NOAA distribution in non-aged materials and their behavior during aging. In the field of “safer-by-design” production or eco-conception, the accurate distribution of NOAA and their residues in complex matrixes is of particular interest to understand the transfer mechanisms between the different environmental compartments;

We also demonstrated the relevance of multi-scale micro-CT (down to submicron-scale) to detect and locate CeO_2 -based NOAA within soft tissues (e.g. mouse lung tissues) after in vivo exposure and artefact-reduced sample preparation procedure. This capability is gaining interest especially since the scientific community

cautiously address the potential risk of NOAA for humans and living organisms.

Keywords: micro and nano-CT, multi-scale 3D imaging, in-situ and non destructive technique, nanomaterials, their aggregates and agglomerates (NOAA), wood coating aging, release mechanisms, biodistribution, soft tissue, lung architecture.

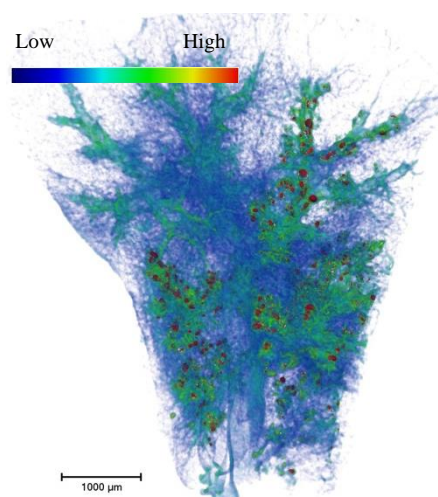


Figure 1: 3D image of a lung lobe of mouse exposed to CeO_2 nanomaterials obtained by micro-CT (voxel size of 14,32 μm). Dense nanonanomaterials are false-colored in red.

References:

1. Nano-ID platform was funded by the « Investissements d'Avenir » French Government program of the French National Research Agency (ANR) through the EQUIPEX project ANR-10-EQPX-39-01.

Indoor mesocosms: an integrated approach to assess the environmental risks of nanomaterials

Mélanie Auffan^{1,2*}, Marie Tella^{1,2}, Lenka Brousset^{2,3}, Catherine Santaella^{2,4}, Jerome Rose^{1,2},
Alain Thiéry^{2,4,5}, Jean-Yves Bottero^{1,2}

¹ CNRS, Aix-Marseille Université, CEREGE UM34, UMR 7330, Aix en Provence, France. ² GDRi iCEINT, Aix en Provence, France.

³ CNRS, Aix-Marseille Université, CNRS, IMBE, UMR 7263, Marseille, France.

⁴ CNRS, Aix-Marseille Université, CEA Cadarache DSV / IBEB / SBVME, LEMiRE, UMR 7265, Saint Paul lez Durance, France.

Abstract:

Headway has been made in exploring the potential impacts of engineered nanomaterials (ENMs) on human health. However, investigation of the roles of nano-scale objects towards evolutionary change, environmental disturbance, ecosystem structure and function have lagged behind the advances in fabricating, measuring and manipulating materials at the nano-scale. Moreover, current approaches to assess the ENMs environmental safety are based on classical ecotoxicology approaches, which are not always adequate for ENMs. For instance, most of the research only concerns the hazard but rarely the exposure to ENMs that plays a pivotal role to understand their environmental risks. The exposure depends on various properties; some of them are those of colloids (*e.g.* hetero-, homo-aggregation, adsorption of organic matter), while others are characteristic of nano-size (*e.g.* redox transformation, dissolution and ubiquist mineralogy).

We will present an innovative design offering physico-chemists, (micro)biologists, and ecologists the possibility of conceiving robust experiments to study the exposure and impacts of engineered nanomaterials as well as mechanistic concepts at various time and spatial scales. This system is based on modular, intermediate size (60 L), indoor aquatic mesocosms (Auffan et al. 2014). It is adjustable to several ecosystems as lotic, lentic, estuarine, or lagoon environments (Tella et al. 2014, Tella et al. 2015).

Keywords: Mesocosms, realistic exposure condition, ecotoxicology, nanomaterials, ecosystems.

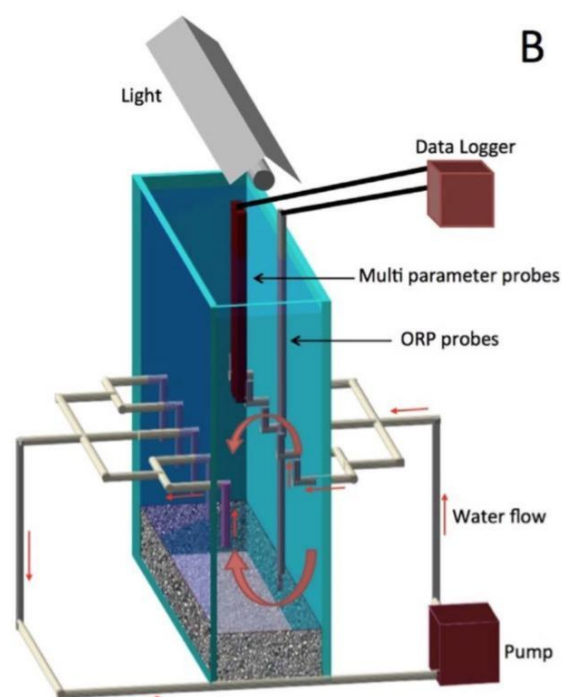


Figure 1: Schematics of the indoor aquatic mesocosms. Tank of 750 3 200 3 600 mm.

References:

1. Auffan M et al. (2014) An Adaptable Mesocosm Platform for Performing Integrated Assessments of Nanomaterial Risk in Complex Environmental Systems. *Scientific reports* 4: 5608.
2. Tella M et al. (2014) Transfer, Transformation and Impacts of Ceria Nanomaterials in Aquatic Mesocosms Simulating a Pond Ecosystem. *Environmental Science & Technology* 48: 9004–9013.
3. Tella M et al. (2015) Chronic Dosing of a Simulated Pond Ecosystem in Indoor Aquatic Mesocosms: Fate and Transport of CeO₂ Nanoparticles. *Environmental Science: Nano* 2: 653–663.

Effect of nanoceria biotransformation in activated sludge on the microbiota associated to canola roots

B. Collin^{1,2*}, E. Doelsch³, M. Auffan^{2,4}, N. Roche⁵, M. Barakat^{1,2}, P. Ortet^{1,2}, W. Achouak^{1,2}, C. Santaella^{1,2}

¹ Aix-Marseille Université, CEA, CNRS, Biosciences and biotechnology Institute of Aix-Marseille BIAM, DRF, UMR 7265, LEMIRE, CEA Cadarache, St-Paul-lez-Durance, France

² GDRi iCEINT, international Consortium for the Environmental Implication of Nanotechnology, CNRS-Duke University, F-13545 Aix-en-Provence, France

³ CIRAD, UPR Recyclage et risque, F-34398 Montpellier, France

⁴ Aix-Marseille Université, CNRS, IRD, CEREGE UM34, 13545 Aix en Provence, France

⁵ Aix-Marseille Université, CNRS, M2P2, Traitement des Eaux et des Déchets, UMR 7340, 13545 Aix-en-Provence, France

Abstract:

Recent interest in the environmental fate and effects of manufactured CeO₂ nanomaterials (NMs) has stemmed from its expanded use for a variety of applications. The majority of these NMs will end up in wastewater treatment plants (WWTP) where they will partition to sewage sludge during wastewater treatment, and ultimately re-enter the environment through the application of biosolids to agricultural soils.¹ Thus, soil may serve as a primary sink for NMs accumulation in the environment, in which NMs may enter food webs or cause direct toxicity to plants, microbial communities, or other soil organisms.

This project aims to study (i) the impact of CeO₂ NMs biotransformation on a soil-plant-microbe system using realistic exposure modes and (ii) the interaction between NMs and trace elements such as Cd, Pb, Zn, Ni, which are present both in the biosolid and in the soil.

Pristine CeO₂ NMs were first aged in a laboratory-scale activated sludge reactor during 5 weeks. The biosolid enriched NMs was then amended to a sandy loam soil at environmentally relevant concentration: 1 mg.kg⁻¹ CeO₂. Four treatments were performed: control soil, soil amended with 1 mg.kg⁻¹ pristine CeO₂ NMs, control biosolid without NMs, biosolid enriched NMs. The plant selected was Canola (*Brassica napus*), an oil-producing plant.

Bulk Ce L3-edge X-ray absorption spectroscopy (XAS) was performed in the biosolid before culture in order to evaluate the NMs transformation in the reactor (Figure 1). After the culture, elemental concentrations were measured in the plant parts by ICP-AES, and their distribution in roots by laser ablation ICP-MS. Root bacterial community structure was characterized by sequenc-

ing of 16S rRNA gene (Illumina MiSeq) in order to understand the impact of the biotransformation of CeO₂ NMs on the microbiota. Our presentation will focus on how CeO₂ NMs biotransformation modulates the interactions in the plant-soil-microbes system.

Keywords: biotransformation, heavy metal, nanomaterials, soil, rhizosphere, microbiota, plant response, soil ecosystem.

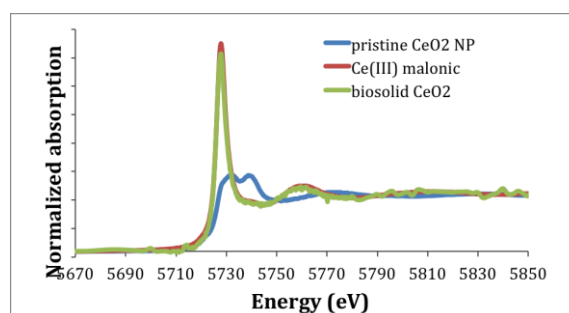


Figure 1:

Experimental XANES spectra at the Ce L3-edge of the Ce present in the biosolid after 5 weeks in the bioreactor contaminated with pristine CeO₂ NMs (green spectra). XANES spectra of the initial pristine CeO₂ NPs and the Ce(III) malonic are provided for reference. This figure shows that Ce, initially present as Ce(IV) in the nanoparticles, were reduced in the bioreactor, and formed Ce(III) complexes in the biosolid.

References:

1. Gottschalk, F., Lassen, C., Kjoelholm, J., Christensen, F., & Nowack, B. (2015). Modeling flows and concentrations of nine engineered nanomaterials in the Danish environment. *International journal of environmental research and public health*, 12, 5581-5602.

Some challenges and solutions for detecting engineered nanoparticles in environmental samples

M. Hadioui,¹ K. Proulx¹, L. Frechette-Viens¹, T. Theoret¹, K.J. Wilkinson^{1,*}

¹ Biophysical Environmental Chemistry Group, Dept. of Chemistry, University of Montreal, Montreal, QC, Canada

Abstract:

The main problems associated with the detection and characterization of engineered nanoparticles (ENP) in the environment are that the concentrations are low and it is often very difficult to distinguish ENP from the environmental matrices in which they are found. In this work, we have focused our efforts on optimizing and developing rigorous techniques to determine ENP sizes and distinguish the ENP from their aggregates and dissolution products. Single particle inductively coupled plasma mass spectrometry (SP-ICPMS) has been our method of choice in aqueous matrices while hyperspectral analysis of darkfield images has generally been employed for solid phase samples. Lower particle size detection limits have been attained by the on-line coupling of an ion exchange column (IEC) with SP-ICPMS (IEC-SP-ICPMS). The IEC effectively removes the continuous signal of dissolved metal, allowing for both lower detection limits and an improved resolution of solutions containing multiple particles. This technique was shown to be particularly useful for metal based nanoparticles with high solubilities. Hydrodynamic chromatography (HDC) has also been coupled to SP-ICPMS in order to detect ENP in environmental samples, including river waters and wastewater effluents. The role of adsorption has been specifically examined. Finally, some work on the detection of ENP in solid samples such as biosolids and sediments will be presented in order to help better understand the fate of the ENP in complex samples.

Keywords: nanomaterials, single particle inductively coupled plasma spectrometry, hydrodynamic chromatography, silver, rare earth metals, zinc oxide

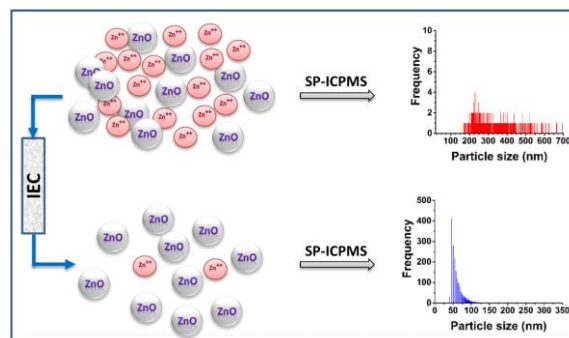


Figure 1: Figure illustrating the influence of an ion exchange resin on the particle size determinations for a ZnO nanoparticle

References:

1. Proulx, K., M. Hadioui and K.J. Wilkinson. 2016. The use of hydrodynamic chromatography and single particle ICPMS to detect nanosilver in municipal wastewaters. In press: *Analytical and Bioanalytical Chemistry*.
2. Hadioui, M., V. Merdzan and K.J. Wilkinson. 2015. Detection and characterization of ZnO nanoparticles in surface and waste waters using single particle ICPMS. *Environ. Sci. Technol.* 49: 6141–6148.
3. Hadioui, M., C. Peyrot and K.J. Wilkinson. 2014. Improvements to Single Particle ICPMS by the on-line coupling of ion exchange resins. *Anal. Chem.* 86(10):4668–4674.

Behavior of Engineered CeO₂ Nanoparticles Released in Aquatic Systems

O. Oriekhova,* S. Stoll,

Institute F.-A. Forel, University of Geneva, Faculty of Science,
Uni Carl Vogt, Group of Environmental Physical Chemistry, Geneva, Switzerland

Abstract:

Cerium dioxide nanoparticles (CeO₂ NPs) are widely used in many consumer products due to their catalytic and oxidative properties. The growing consumption of such products is constantly increasing the presence of CeO₂ NPs in the environment including natural water sources such as rivers or lakes. The NPs behavior in aquatic system is influenced by many factors including water chemistry, presence of natural colloids and biota (Loosli et al., 2015). Despite the number of researches which have been conducted in this area, the fate of CeO₂ NPs in aquatic systems is not clearly understood. In our work we investigated the behavior of CeO₂ NPs in various environmental conditions. Different physicochemical methods and techniques, such as dynamic light scattering (DLS), nanoparticle tracking analysis (NTA), scanning electron microscopy (SEM), acid-base titration (Oriekhova et al., 2014), were used to characterize CeO₂ NPs. Then the influence of the physicochemical properties of aqueous medium such as variable ionic strengths, pH, and presence of natural polyelectrolytes, on CeO₂ NPs hetero-aggregation was investigated (Figure 1). In particular, the influence of natural organic matter on the NPs stability was assessed (Oriekhova et al., 2016). Then the behavior of NPs in artificial medium that mimic the composition of natural waters was studied and comparison was made by considering Lake Geneva water. We found that natural organic matter and ionic composition of water are strongly modifying the surface of CeO₂ NPs. Such a coating influences their hetero-aggregation behavior and stability in environmentally changing conditions. Our study covers the interdisciplinary domains between colloidal, physical and environmental chemistry and the results are important not only for a better understanding of NPs fate and transport but also for their elimination from aquatic systems (water treatment processes) and evaluation of their ecotoxicity.

Keywords: CeO₂ nanoparticle, fulvic acids, hetero-aggregation, ionic strength effect,

stability of nanoparticles, dynamic light scattering, nanoparticle tracking analysis, scanning electron microscopy.

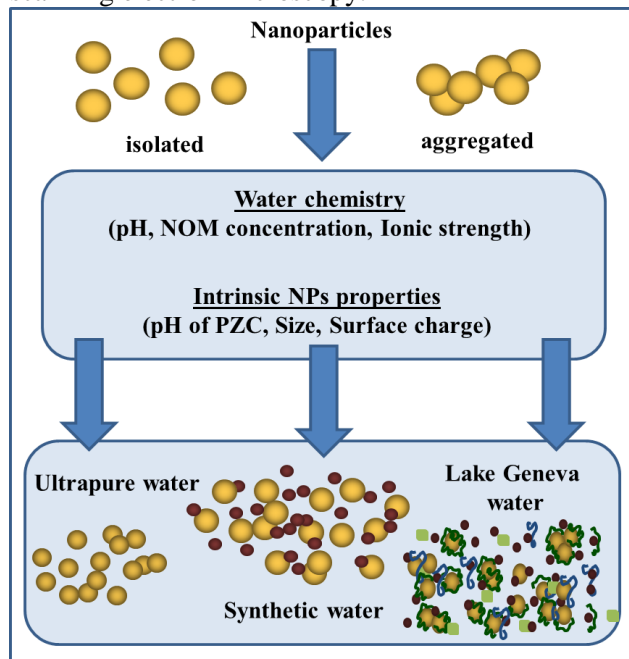


Figure 1: Schematic illustration of the behavior of engineered nanoparticles, isolated or aggregated, released in aquatic system. This figure is demonstrating the possible scenarios of NPs behavior in ultrapure, synthetic and natural water, taking into account various parameters (such as water chemistry and intrinsic NPs properties).

References:

1. Loosli, F., Le Coustumer, P., Stoll, S. (2015), Effect of electrolyte valency, alginate concentration and pH on engineered TiO₂ nanoparticle stability in aqueous solution, *Sci. Total Environ.*, 535, 28-34.
2. Oriekhova, O., Stoll, S. (2014). Investigation of FeCl₃ induced coagulation processes using electrophoretic measurement, nanoparticle tracking analysis and dynamic light scattering: Importance of pH and colloid surface charge, *Colloids Surf. Physicochem. Eng. Asp.*, 461, 212–219.
3. Oriekhova, O., Stoll, S. (2016), Effects of pH and fulvic acids concentration on the stability of fulvic acids – cerium (IV) oxide nanoparticle complexes, *Chemosphere*, 144, 131–137.

Elucidation of standard specimen preparation techniques of nano-enabled products for characterization using field-emission scanning electron microscope

A. Sohrabi,^{1,2,*}

¹Sharif University of Technology. Institute for Nanoscience and Nanotechnology, Tehran, IRAN

²Iranian Nanotechnology Initiative Council (INIC), Tehran, IRAN

Abstract:

Nano-enabled products are the products which includes nano-objects. Our research focuses on a science-based understanding of nanomaterial properties and effects, alongside development of improved measurement and testing methods.

Taking into consideration our activity on surface analysis of nanomaterials using FEG-SEM and more specifically, our research on sample preparation methods to obtain effective micrographs, which is becoming increasingly important since nanomaterials are comprised into a large degree of surfaces which have a significant impact on the overall properties and behaviours of these materials. The need and importance of adequate characterization of the surfaces of nanomaterials has been highlighted by many organisations. In this paper in order to better expalining of sample preparation techniques, nanomaterials are categorized due to the nature of them:

- 1) Polymeric, biological and carbomous
- 2) Metallic
- 3) Ceramic and semiconductor

In each section it is divided into five physical states:

- a) Emulsion or colloids
- b) Powders
- c) Thin film coatings
- d) Bulky paper or ultrathin films
- e) Bulk nanomaterials

In determining the appropriate sampling strategy, the following interlinking factors should be considered together: stability of the complex matrix, stability of the nano-object, stability of the nano-object in the complex matrix. It should be mentioned that the more accurate sample preparation techniques is applied, the more effective imaging is obtained using field emission gun scanning electron microscope.

Keywords: Field emission gun scanning electron microscope, sample preparation, nano-objects, nanomaterials, emulsion, colloid, powders, thin films, bulky paper, ultrathin films, bulk materials

References:

Yong Yang, Jie Lan, Xiaochun Li, Study on bulk aluminum matrix nano-composite fabricated by ultrasonic dispersion of nano-sized SiC particles in molten aluminum alloy, Materials Science and Engineering: A, Volume 380, Issues 1–2, 25 August 2004, Pages 378-383

A. Bogner, G. Thollet, D. Basset, P.-H. Jouneau, C. Gauthier, Wet STEM: A new development in environmental SEM for imaging nano-objects included in a liquid phase, Ultramicroscopy, Volume 104, Issues 3–4, October 2005, Pages 290-301

Influence of nano-TiO₂ with Different Crystalline Phases on Bioaccumulation of Perfluorooctanesulfonate by Fishes Living in Different Water Layers

L.Y. Zhu*, L.W. Qiang

College of Environmental Science and Engineering, Nankai University, Tianjin 300071, People's Republic of China

Abstract:

Nano-titanium dioxide (nano-TiO₂) has been widely used in commercial products and found in aquatic environment. It is expected to affect the environmental fate and bioavailability of organic pollutants dynamically in the environment. Perfluorooctanesulfonate (PFOS) is a typical new emerging environmental pollutant. A novel semi-static multilayer microcosm was set up to investigate the impacts of nano-TiO₂ on PFOS bioaccumulation in fish species [*Danio rerio* (*D. rerio*), *Ctenopharyngodon idella* (*C. idella*), *Hypostomus plecostomus* (*H. plecostomus*)] living in different vertical layers. As a result of aggregation and deposition, the concentration of TiO₂ increased from upper to bottom layers in the water column. Concomitantly, due to adsorption of PFOS on the nano-TiO₂ particles, PFOS also displayed an increasing trend from upper to bottom layer. Owing to ingestion of the TiO₂-PFOS complexes, more PFOS was taken-up by fish. With the aid of intestinal fluid, PFOS was readily released from TiO₂ particles and absorbed by fish. As a result, accumulation of PFOS in whole fish was facilitated and the bioaccumulation factors of PFOS in *D. rerio*, *C. idella* and *H. plecostomus* were 3.01, 2.42 and 1.11 times of that in the groups without TiO₂. However, TiO₂ aggregates were too large to penetrate biological membranes to participate body circulation, and no significant accumulation of TiO₂ was observed in fish muscle. The bioaccumulation of PFOS was much more promoted by anatase than rutile, which was mainly accounted by the greater adsorption capacity of anatase to PFOS and slower elimination rate of anatase from fish. The whole-body PFOS concentration in zebrafish was enhanced by 59.0% for anatase and 25.4% for rutile after equilibrium. The results suggested that the ecological risk of PFOS could be enhanced due to the presence of nano-TiO₂ in wa-

ter.

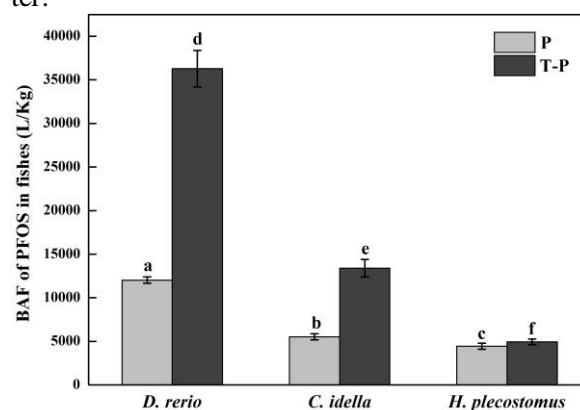


Figure 1: The BAFs of PFOS in the three fish species in the PFOS and TiO₂-PFOS groups. Bars with different letters above them are significantly different ($p < 0.05$).

Keywords: anatase nano-TiO₂, rutile nano-TiO₂, PFOS, aggregation, bioaccumulation, zebrafish.

References:

- Boyle D, Al-Bairuty GA, Henry TB, Handy RD. (2013), Critical comparison of intravenous injection of TiO₂ nanoparticles with waterborne and dietary exposures concludes minimal environmentally-relevant toxicity in juvenile rainbow trout *oncorhynchus mykiss*. *Environ. Pollut.*, 182, 70-79.
- Chen GX, Liu XY, Su CM. (2012), Distinct effects of humic acid on transport and retention of TiO₂ rutile nanoparticles in saturated sand columns. *Environ. Sci. Technol.*, 46, 7142-7150.

Assessing the heteroaggregation of manufactured nanoparticles with naturally occurring colloids in a typical surface water

D. Slomberg¹, J. Labille^{1,*}, A. Praetorius², C. Harns³, J.-Y. Bottero¹, P. Ollivier⁴, M. Scheringer², N. Sani-Kast², S. Ilina⁴, J. Brant³

¹Labex Serenade, CEREGE, Aix-Marseille Université, BP80, 13545 Aix en Provence cedex 4, France

²Institute for Chemical and Bioengineering, ETH Zurich, 8093 Zurich, Switzerland

³University of Wyoming, Department of Civil and Architectural Engineering, Laramie, WY 82071

⁴BRGM, UMR 7327, BP 36009, 45060 Orléans, France

Abstract:

To assess the risk posed by nanotechnology-enabled products, the likelihood of engineered nanoparticle (NP) exposure through aqueous media must be considered, as it is a receptacle of these materials throughout their lifecycle. The predicted concentrations of engineered NPs in surface water systems are expected in the $\mu\text{g/L}$ level and consequently, the probability that NPs interact with each other may be lower relative to their collision frequency with naturally occurring colloids present at substantially higher concentrations. Colloids may strongly affect the fate and transport of NPs via heteroaggregation processes. Thus, fate models aimed at predicting NP behaviour and concentration profiles must account for this heteroaggregation (1). A NP-colloid sticking efficiency, α_{hetero} , is well suited as an input for such fate models, but remains a challenge to determine experimentally. Here, we present a novel method for determining α_{hetero} at environmentally relevant NP concentrations by using a combination of laser diffraction measurements and aggregation modeling based on the Smoluchowski equation (2,3). Interactions between TiO_2 NPs (15 nm) and different types of larger mineral colloids (i.e., silica microspheres, smectite clay, and natural riverine suspended particulate matter) were used to demonstrate this new approach (4). Studies were conducted at low NP concentrations (0.1 to 4 mg/L) with regard to the colloid occurrence (100 mg/L) to develop realistic fate scenarios for surface water systems. The NP/colloid number ratio was found to be a critical component in the heteroaggregation mechanism and the effects of ionic strength, pH, and natural organic matter on NP heteroaggregation were also explored. Our data show that at relevant concentrations, NP behaviour is mainly driven by heteroaggregation with colloids, while homoaggregation remains negligible. The dimensionless α_{hetero} value is a key parameter needed to

feed environmental fate models that are of high importance in the field of risk assessment of engineered NPs. Work funded by the French ANR and Swiss FOPH as NANOHETER in the frame of ERA-NET SIINN.

Keywords: nanoparticle fate, natural colloids

References:

1. Sani-Kast N. Scheringer M., et al. (2015) Addressing the Complexity of Water Chemistry in Environmental Fate Modeling for Engineered Nanoparticles, *Science of the Total Environment*, 535 (SI) 150-159
2. Praetorius A., Labille J., et al. (2014), Heteroaggregation of titanium dioxide nanoparticles with model natural colloids under environmentally relevant conditions, *Environ. Sci. Technol.* 48, 10690-10698
3. Labille J., Harns C., et al. (2015) Heteroaggregation of titanium dioxide nanoparticles with natural clay colloids. *Environ. Sci. Technol.* 49 (11) 6608-6616
4. Slomberg D, Ollivier P., et al. (2016) Characterization of suspended particulate matter in the Rhône River: Insights into analogue selection. *Environmental Chemistry*, in press

Behavior of engineered nanomaterials from marketed tiles under standardized abrasion conditions.

C. Bressot¹, O. Aguerre-Chariol¹, C., Pagnoux², M., Morgeneyer³

¹Institut National de l'Environnement Industriel et des Risques (INERIS) Verneuil en Halatte, France,

²ENSCI – SPCTS – Limoges, France

³Sorbonne Universités, Université de Technologie de Compiègne (UTC)Compiègne, France

Abstract:

The study presented here focuses on marketed anti-bacterial tiles whose emissivity of (nano) particles due to abrasion has yet barely been investigated [1,2]. The tiles have been characterized regarding their surface properties and composition throughout their life cycle, *i.e.* from their use until the end-of-life. In contrast to conventional tiles, their surfaces happen to be uneven. Titanium dioxide is found in the depressions these being protected from abrasion. at the surface, thus protected by the hilly areas against abrasion on the surface of tile. Furthermore, a deposition technique has been put in place by producers allowing coating of the aforementioned marketed tiles with titanium, thus rendering them similar to those available on the market. It consists of depositing titanium dioxide on the surface to be fixed later on the ceramic surface using thermal treatments. Besides the intermittent deposition of nano-TiO₂, the major modification on the state of surface can lead to a greater emissivity during its use.

The tests reveal the aerosolization of inhalable micronic and submicronic particles that can subjected to be released in the environment from antibacterial tiles.

The generated aerosol is mainly dominated by so called nanoobjects, agglomerates and aggregates (NOAAs) where titanium is widely detected but at low concentrations, which is in accordance with the relatively low nano-titanium dioxide presence on the tile surface. No free and isolated nano-TiO₂ particles have been released.

This emission of NOAAs can be attributed to (i) the intermittent deposition on the tile surface which may be less resistant to abrasion as compared to the uncoated tile surface, (ii) the specific mechanical resistance of the nanocoating and (iii) the change in the surface morphology where the irregular surface facilitates not only deposition of nano-TiO₂ suspension but also the wrench of tile pieces during the abrasion. Long term duration weathering under standardized and documented conditions [3] lead to the formation of submicronic and compact NOAAs. No growth in emission due to weather stress has been detected.

Keywords: Tiles, aerosol emission, abrasion, anti-bacterial, weather, nanomaterial, TiO₂.

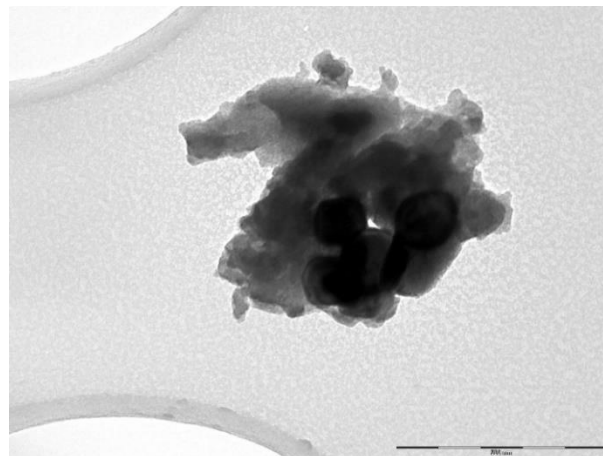


Figure 1: Example of a nanoparticle observed after abrading a weathered tile containing nano-TiO₂.

Acknowledgments

The authors would like to thank the French Ministry of Environment, and ANSES (Nano-data Project, APR ANSES 2012).

References:

1. Froggett, S.J.; Clancy, S.F.; Boverhof, D.R.; Canady, R.A. A review and perspective of existing research on the release of nanomaterials from solid nanocomposites. *Particle & Fibre Toxicology* **2014**, *11*, 1-28.
2. Sánchez, E.; García-Ten, J.; Sanz, V.; Moreno, A. Review: Porcelain tile: Almost 30 years of steady scientific-technological evolution. *Ceramics International* **2010**, *36*, 831-845.
3. Shandilya, N.; Le Bihan, O.; Bressot, C.; Morgeneyer, M. Emission of titanium dioxide nanoparticles from building materials to the environment by wear and weather. *Environ Sci Technol* **2015**, *49*, 2163-2170.

Marine plastic litters: the unanalyzed nano-fraction

Julien Gigault¹, Boris Pedrono², Benoît Maxit², and Alexandra Ter Halle³

¹ Environnements et Paléo-Environnements Océaniques et Continentaux, French National Center of Scientific Research (CNRS, UMR 5805), 351 Cours de la Libération, 33405 Talence Cedex, France
E-mail: julien.gigault@u-bordeaux.fr

² Cordouan Technologies, Cité de la Photonique, 11 Avenue de Canteranne, 33600 Pessac, France

³ Laboratoire des Interactions Moléculaires et réactivité Chimique et Photochimique (IMRCP), UMR CNRS 5623, Université Paul Sabatier-UPS, Bâtiment 2R1, 3ème étage, 118, route de Narbonne, 31062 Toulouse Cedex 09, France
E-mail: ter-halle@chimie.ups-tlse.fr

Abstract:

In this work, we present for the first time undeniable evidence of nano-plastic occurrence due to solar light degradation of marine micro-plastics under controlled and environmentally representative conditions. As observed during our recent expedition (Expedition 7th Continent), plastic pollution will be one of the most challenging ecological threats for the next generation.

Up to now, all studies have focused on the environmental and the economic impact of millimeter scale plastics. These plastics can be visualized, collected and studied. We are not aware of any studies reporting the possibilities of nano-plastics in marine water.

Here, we developed for the first time a new solar reactor equipped with an *in situ* DLS device to investigate the possibility of the formation of nano-plastics from millimeter scale plastics. With this system, correlated with electronic microscopy observations, we identified for the first time the presence of plastics at the nano-scale in water due to UV degradation. Based on our observations large fractal nano-plastic particles (i.e., >100 nm) are produced by UV light after the initial formation of the smallest nano-plastic particles (i.e., <100 nm).

These results show the new potential hazards of plastic waste at the nanoscale, which had not been taken into account previously.

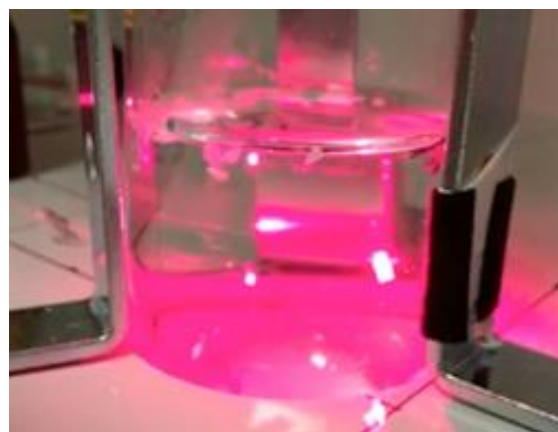


Figure 1: DLS monitoring of micro-plastics degradation under UV solar light

References:

1. S. Morét-Ferguson, K. L. Law, G. Proskurowski, E. K. Murphy, E. E. Peacock and C. M. Reddy, Mar. Pollut. Bull., 2010, 60, 1873–1878.
2. V. Hidalgo-Ruz, L. Gutow, R. C. Thompson and M. Thiel, Environ. Sci. Technol., 2012, 46, 3060–3075.

Challenges on fate, behavior and effects of nanomaterials in the marine environment

C. Mouneyrac,^{1,2}

¹LUNAM Université, Université Catholique de l'Ouest, Laboratoire Mer, Molécules et Santé (MMS), Angers, France

²International Consortium for the Environmental Implications of Nanotechnology (iCEINT), Aix en Provence, France

Abstract:

The fast growth of nanotechnologies has brought new industrial and business opportunities and leads inevitably to the appearance of nanomaterials (NMs) in the aquatic environment which represents the major sink of anthropogenic contaminants. The assessment of risks related to NMs in the estuarine/marine environment represents a real challenge for ecotoxicologists. The complexity of physico-chemical properties of NMs may result in different and unpredictable interactions with biological systems as compared with their bulk counterparts. The first studies were mainly conducted with freshwater species using standard ecotoxicity tests with less than 20% of published papers on marine species (Cattaneo et al., 2009). During the last decade, publications on ecotoxicity of NMs in marine species such as bivalves, polychaetes has risen considerably (up to 38% of the total published papers) focusing on NMs accumulation, sub-lethal effects and mechanisms of action. However, still major scientific gaps need to be filled. A multidisciplinary approach combining physico-chemical, biological and nanoparticle-analysis expertise is necessary to understand: i) how does the marine environment into which engineered metal nanoparticles are released affect their physicochemical properties and their (bio)reactivity? ii) how does this interaction nanoparticle/medium modify their ability to penetrate organisms (speciation, bioavailability) and exert toxicity? Multiple case studies will be presented on the fate and behaviour of NMs in coastal-estuarine environments and their toxicity effects using different experimental approach (microcosms vs mesocosms, short-term vs long term studies) on species which have a key role in the structure and functioning of estuarine ecosystems.

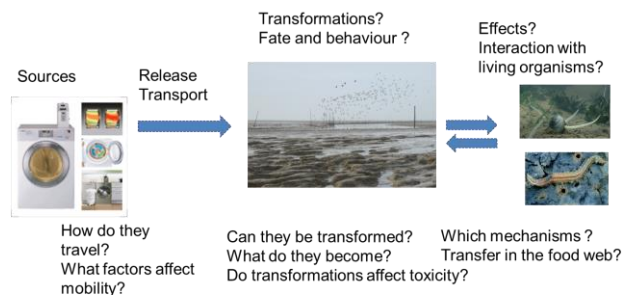


Figure 1: Figure illustrating the main questions on the environmental impacts of nanomaterials in marine ecosystems.

Keywords: nanomaterials, marine environment, behavior in seawater, uptake and accumulation, trophic transfer, biomarkers, bivalves, polychaetes, sediment, mesocosms.

References:

Cattaneo, A.G., Gornati, R., Chiriva-Internati, M., Bernardini, G. (2009). Ecotoxicology of nanomaterials: the role of invertebrate testing. *Invertebr. Surviv.* J. 6, 78–97.

Sulfidation pathways of Silver Nanoparticles in the presence of Humic Acid

Basilius Thalmann¹, Andreas Voegelin¹, Eberhard Morgenroth^{1,2} and Ralf Kaegi¹

¹Eawag, Swiss Federal Institute of Aquatic Science and Technology, CH-8600 Dübendorf

²ETH Zürich, Institute of Environmental Engineering, CH-8093 Zürich, Switzerland

Abstract:

Silver nanoparticles (Ag-NP) are applied to a wide range of consumer products due to the well-known antimicrobial activity of Ag⁺. During the use these particles are likely to be released to the urban wastewater system. Due to their toxicity toward higher organism, they are of environmental concern.¹ However, recent studies in wastewater systems have shown that the Ag-NP undergo transformations, most importantly sulfidation to nanoscale silver sulfide (Ag₂S-NP).² Ag₂S is several orders of magnitude less toxic than metallic Ag-NP.³

However, the reaction rates are currently unknown and the pathways of the Ag-NP sulfidation are only poorly understood. Furthermore, the influence of humic acid (HA) on the transformation has not been studied to date. We, therefore, investigated the sulfidation of Ag-NP reacted with bisulfide (HS⁻) in the absence and presence of HA and evaluated different kinetic models to describe the observed reaction kinetics.

Citrate-stabilized Ag-NP of different sizes (20 – 200 nm) buffered to pH 7.5 were reacted with an excess of HS⁻ in the absence of HA as well as at HA concentrations ranging from 50 to 1000 mg L⁻¹. The metallic and sulfidic fraction of Ag-NP after selected reaction times was determined by X-ray absorption spectroscopy (XAS). The metallic fraction decreased faster with decreasing Ag-NP size and increasing HA concentration. To elaborate possible reaction pathways four kinetic models were evaluated. Results revealed that the experimental data were best described with a diffusion-limited solid-state reaction model (parabolic rate law). The calculated half-life times of the Ag-NP ranged from minutes to hours.

Increasing sulfidation rates observed with increasing HA concentrations may be explained by the adsorption of HA onto the Ag-NP surface facilitating the access of HS⁻ to the particle surface.

To reveal the reaction pathways partially sulfidized Ag-NP were investigated by analytical

transmission electron microscopy (TEM). In the presence of HA, initially formed concentric core-shell Ag⁰-Ag₂S structures developed into hollow Ag₂S nanoparticles with increasing reaction time, possibly via the Kirkendall effect. In the absence of HA, the Ag-NP sulfidation resulted in asymmetric Ag₂S-Ag⁰ structures.

Our results indicate that the sulfidation rate of Ag-NP is limited by the available Ag-NP surface and the diffusion of Ag through an Ag₂S layer formed at the surface of the Ag-NP.

Keywords: Silver Nanoparticles, Sulfidation, Kinetics, XAS

References:

1. F. Gottschalk, T. Sonderer, R. W. Scholz and B. Nowack, *Environmental science & technology*, 2009, **43**, 9216-9222.
2. R. Kaegi, A. Voegelin, C. Ort, B. Sinnet, B. Thalmann, J. Krismer, H. Hagendorfer, M. Elumelu and E. Mueller, *Water Res.*, 2013, **47**, 3866-3877.
3. B. C. Reinsch, C. Levard, Z. Li, R. Ma, A. Wise, K. B. Gregory, G. E. Brown, Jr. and G. V. Lowry, *Environmental science & technology*, 2012, **46**, 6992-7000.

Mechanism of CuO/ZnO nanoparticle sulfidation: Insights from electron microscopy

A. Gogos,^{1*} B. Thalmann¹ and
R. Kaegi,¹

¹Eawag, Swiss Federal Institute of Aquatic Science and Technology, 8600 Duebendorf, Switzerland

Abstract:

Besides their manifold use in the fields of catalysis, electronics and energy, copper oxide nanoparticles (CuO NPs) are increasingly used in a variety of biocide applications, such as wood preservation, anti-fouling coatings and agricultural pesticides [1]. CuO NPs from specific applications will be directly released to the wastewater stream and reach a wastewater treatment plant (WWTP). Also, zinc oxide nanoparticles (ZnO NPs), which enter the water stream mainly from personal care products, will end up in WWTPs. The sulfidation of chalcophile elements, such as Cu and Zn, favored by the elevated concentration of bisulfide (HS^-) in wastewater systems [2], will strongly influence the speciation and the bioavailability of these elements in (treated) wastewater.

In this paper, we, therefore, investigate the sulfidation of CuO and ZnO-NP, in the presence of HS^- under oxic conditions buffered to pH 8. Reacted ZnO- and CuO-NP were collected at selected time points and characterized using scanning transmission electron microscopy in combination with energy dispersive X-ray (EDX) analysis.

After a reaction time of only 15 min, CuO NPs already show distinct core-shell structures indicating a rather rapid sulfidation (Figure 1). More detailed investigations of the reacted particles revealed a CuO-core encapsulated in a void which was surrounded by a CuS shell. These complex 3-layer structures were not observed in comparable experiments conducted with Ag-NP, where mostly central voids were observed [3]. In experiments conducted with ZnO NP, only a thin layer of ZnS formed at the surface of the ZnO-NP after 15 min (Figure 1). The results from this study suggest widely different sulfidation pathways and probably different reaction rates for different metal(oxides), which have to be taken into consideration when assessing the fate of the respective NP.

Keywords: nanomaterials, transformation, wastewater, environment, energy dispersive X-ray spectroscopy

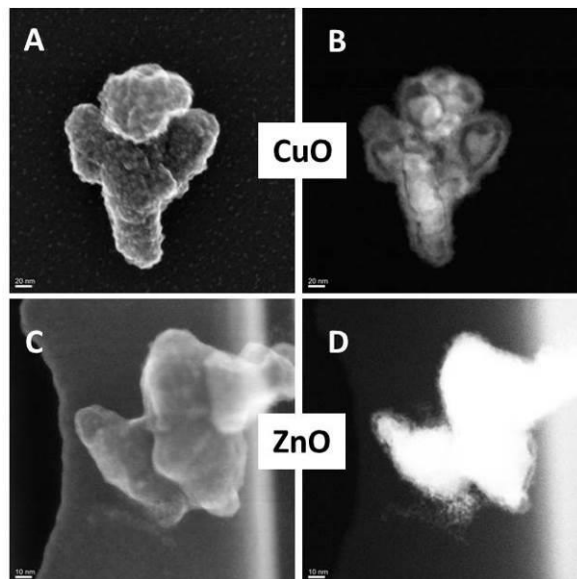


Figure 1: STEM micrographs (left panel secondary electron image, right panel high angle annular dark field image) of CuO (A, B) and ZnO (C, D) NPs after 15 min of reaction time with HS^- .

References:

1. Kiaune, L. and N. Singhasemanon, *Pesticidal copper (I) oxide: environmental fate and aquatic toxicity*, in *Reviews of Environmental Contamination and Toxicology Volume 213*. 2011, Springer. p. 1-26.
2. Kaegi, R., et al., *Behavior of Metallic Silver Nanoparticles in a Pilot Wastewater Treatment Plant*. *Environmental Science & Technology*, 2011. **45**(9): p. 3902-3908.
3. Thalmann, B., et al., *Effect of humic acid on the kinetics of silver nanoparticle sulfidation*. *Environmental Science: Nano*, 2016. **3**(1): p. 203-212.

Development of the first generation of hybrid metrology algorithms dedicated to nanoparticles measurement with AFM and SEM techniques

A.Dervillé^{1,2}, A.Delvallée³, S.Martinez¹, D.Pauwels¹, A.Labrosse¹, S.Ducourtieux³, N.Feltin³, L.Devoille³, Y.Zimmermann¹, J.Foucher¹, G.Favre³

¹ POLLEN Metrology, France, ²Université Grenoble Alpes, Laboratoire Jean Kuntzmann (LJK), France

³Laboratoire National de Métrologie et d'Essais (LNE), France

Abstract: For years, semiconductor industries have been using nanomaterials in a daily basis. Nowadays « nanos » are starting to be integrated in fundamental research, R&D, pilot lines and even in production in many other industries. Nanomaterials are even more present in products of daily provided by pharmaceutical, cosmetic, aeronautic, chemical, textile and food industries, among others. The nanoparticles are the primary structures of nanomaterials. The main challenges in their implementation are related to the rigorous quality control of processes which require specific metrology techniques. These techniques leads to R&D cost management and high yield production security. Thus, we focus this work on improving the analysis of nanoparticles.

Two standard techniques are commonly used by many laboratories and industries for dimensional characterization of nanoparticles: Atomic Force Microscopy (AFM) and Scanning Electron Microscopy (SEM). The main advantage from AFM is the topological information whereas the SEM provides a lateral information. These techniques are complementary and the fusion of both measurements is an active area of research because of 1- the artifacts on raw data induced from each approach, 2 - the mismatch between the AFM and SEM images on the same location and 3- the difficulty of estimating the measurement uncertainties due to their acquisition at different axes. These characteristics lead to a limited accuracy on the detection, location and quantification of nanoparticles. In this paper we propose a novel approach of AFM and SEM data fusion for the analysis of nanoparticles. Our proposed approach is divided in three steps. The first one concerns the preprocessing of the AFM images which show some tilt and bow introduced by the microscope. The main challenge is to level the AFM data without affecting nanoparticles as illustrated in figure 1. In this purpose, we developed a new algorithm and we also propose a new criterion to assess the quality of the leveling step.

The second one is a new algorithm to measure the diameter of nanoparticles separately with AFM and SEM, including accurate uncertainties assessment. The third part is the fusion of both techniques to minimize the uncertainties. In this sense, we consider two approaches according to their applications. One approach is the combination of two different sets of measurements from AFM and SEM collected at different locations from the same sample. The other one is the fusion of the AFM and SEM sets acquired at the same location. Up to now, the registration between the two acquisition techniques is not an evident task but this approach allows a 3D reconstruction of the nanoparticle in a traceable way. The results in our image data sets validate the combination of AFM and SEM with defined uncertainties for the analysis of nanoparticles. We conclude that the proposed approach based on the fusion of AFM and SEM could increase the accuracy of nanomaterials analysis.

Keywords: nanometrology, AFM, SEM, data fusion, hybrid metrology, accuracy, uncertainties, nanoparticles

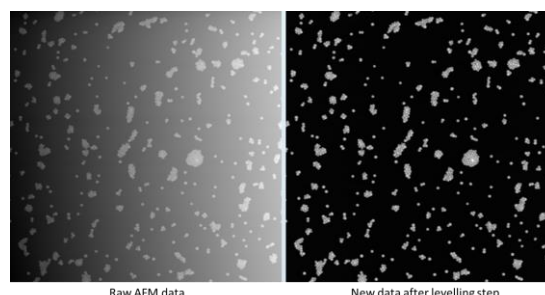


Figure 1: Figure illustrating raw AFM image of nanoparticles and the same image after an automated levelling step.

References:

1. M. Raposo, Q. Ferreira, P.A. Ribeiro (2007) A Guide for Atomic Force Microscopy Analysis of SoftCondensed Matter, *Microscopy Book Series*,

Toward the direct quantification of dissolution and aggregation of AgNPs using AF4-UVD-MALLS-ICP-MS and Cryo-TEM analysis

I.A.M Worms^{1,2*}, A. Arnould², R. Soulas², J-F. Damlencourt², S. Motellier,² E. Mintz¹,
I. Michaud-Soret¹, D. Truffier-Boutry²

¹CEA-Grenoble, UMR5249 CEA/CNRS/Univ. Grenoble Alpes, DRF/BIG/LCBM/ BioMet

²CEA-Grenoble, DRT/ LITEN / DTNM / SEN / LR2N

Abstract:

Physicochemical factors (e.g. pH, I, chelators) are known to affect silver nanoparticles (AgNPs) stability in aqueous solution. In particular, organothiols¹ have been shown to induced either their surface dissolution and/or their aggregation. However, a simultaneous quantification of both processes for polydisperse suspensions can be limited by artefacts arising from the use of simple techniques and methods. Those include (i) Changes in surface plasmon resonance (SPR) signal operating during surface adsorption of chelators and aggregation of AgNPs² for the quantification of dissolution the process (ii) Overestimation of hydrodynamic *radii* using light scattering techniques^{2,3} (iii) Difficulty in the separation of the dissolved, nanoparticulate and aggregate silver forms by classical fractionation techniques. The use of hyphenated techniques able to do so such as asymmetrical flow field-flow fractionation (AF4), in combination to on-line detectors whom give the size (Multi Angle Laser Light Scattering (MALLS) and the quantity of associated metals (ICP-MS), is thus very promising. In this study, the effect of glutathione (GSH), D-penicillamine (D-Pen) and L-cysteine (Cys) on AgNPs stability was quantified by the use of AF4-UVD-MALLS-ICP-MS. Some analytical details regarding the limitation of the technique are given (e.g. membrane interaction, ICP-MS detection; influence of intrinsic SPR signal on gyration *radii* determination by MALLS). The results are compared to micrographs of suspensions obtained by cryo-TEM (Figure 1) and the complementarity of both techniques to assess the fate of AgNPs is further discussed.

Keywords: AgNPs dissolution, AgNPs aggregation, AF4-ICP-MS, Cryo-TEM.

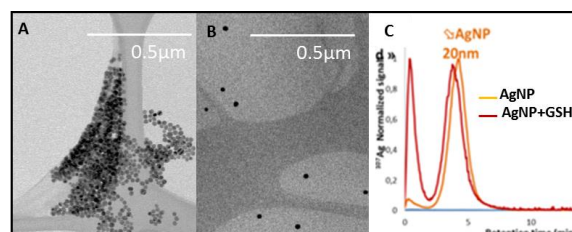


Figure 1: Examples of AgNPs suspension micrographs recorded on TEM Osiris FEI after (A) dry deposition or (B) cryo-fixation; and (C) AF4 fractograms of disperse AgNPs samples recorded by ICP-MS for ¹⁰⁷Ag silver isotope .

References:

1. Siriwardana, K., Wang, A., Gadogbe, M., Collier, W. E., Fitzkee, N. C., & Zhang, D. (2015), Studying the effects of cysteine residues on protein interactions with silver nanoparticles. *J. Phys. Chem. C*, 119(5), 2910–2916.
2. Baalousha, M., Nur Y., Römer, I., Tejamaya, M., Lead, J.R., (2013), Effect of monovalent and divalent cations, anions and fulvic acid on aggregation of citrate-coated silver nanoparticles, *Sci. Total. Environ.*, 454-455, 119-131.
3. Tomaszewska E., Soliwoda K., Kadziola, K., Tkacz-Szczesna B., Celichowski, G., Cichomski, M., Szmaja, W., Grobelny, J. (2013), Detection limits of DLS and UV-Vis spectroscopy in characterization of polydisperse nanoparticles, *J. Nanomater.*

Particle Size Distribution Analysis of Complex Fe₂O₃ Nanoparticle Aggregates Embedded in High Density Polyethylene Matrix

T. Uusimäki¹, T. Wagner², E. Verleysen³, P. Müller⁴ and R. Kägi¹

¹ETH, Eawag, Dübendorf, Switzerland

²University of Applied Science and Arts Dortmund, Dortmund, Germany

³CODA-SERVA, Brussel, Belgium

⁴BASF SE, Ludwigshafen, Germany

Abstract:

The European Commission's recommendation for a definition of a nanomaterial requires the determination of primary particles sizes of the materials under investigation. Electron microscopy is commonly referred to as the confirmatory method for particle size distribution determination. However on complex nanoparticle agglomerates and aggregates it is difficult to identify the primary particles. In this study, an automatic determination of particle sizes with complex aggregated samples is proposed to derive a reliable number based particle size distribution. As a proof of principle, a sample of Fe₂O₃ nanoparticle aggregates embedded in high density polyethylene matrix was used. Different sample preparation methods, such as cryo-microtomy and focused ion beam milling, were applied. Electron tomography was performed to compare the segmentation of the 2D micrographs to the reconstructed 3D structure. A custom made particle analysis software was used to identify primary particles.

The comparison of the segmented 2D images with the reconstructed 3D particles revealed substantial limitations of the segmentation algorithms. Most reliable results were obtained, when using the so-called 'single particle mode', in which only non-agglomerated (primary) particles are considered.

Keywords: nanoparticles, iron oxide, particle size distribution, electron tomography, agglomerates, aggregates, TEM

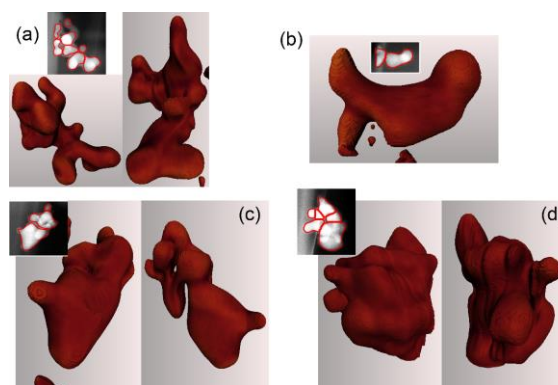


Figure 1: 2D segmentation results as compared to the 3D Fe₂O₃ aggregates visualized as triangulated surfaces. The left images are positioned approximately on the same projection direction as the original 2D images. The right-hand images are vertically rotated anti-clockwise 150° degrees

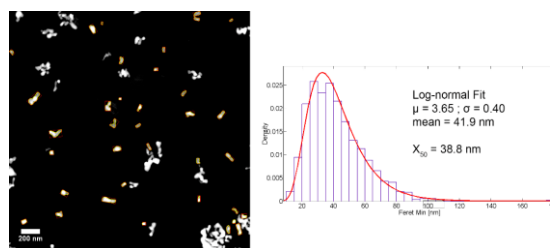


Figure 2: STEM dark field image of the Fe₂O₃ nanoparticles with segmentation results using the single particle mode and the particle size distribution with mean and median feret min values.

Combination of micro- and nano- computed X-ray tomography for the characterization of nanomaterial-plant interactions

C. Levard,^{1*} A.E. Pradas del Real,^{2,3} A. Avellan,¹ F. Schwab,¹ P. Chaurand,¹ D. Borschneck,¹ V. Vidal,¹ M. Auffan,¹ G. Sarret² and J. Rose¹

¹ Aix-Marseille Université, CNRS, IRD, CEREGE UM34, 13545, Aix en Provence, France

² ISTerre (Institut des Sciences de la Terre), Université Grenoble Alpes, CNRS, Grenoble, France

³ ID21, ESRF-The European Synchrotron, CS40220, 38043 Grenoble Cedex 9, France

Abstract:

Plants are directly exposed to natural and engineered nanomaterials (ENMs) in the atmospheric, terrestrial and aquatic compartments, which potentially leads to phytotoxicity, accumulation and transfer in the food chain [1, 2]. As an example, the application of sewage sludge on agricultural soils that contain manufactured Ag NPs [3] exposes plants to these ENMs. Although plants are essential components of eco- and agro-systems, knowledge about Ag-ENM-plant interactions is scarce.

One major reason for this lack of knowledge is the difficulty of characterizing ENM in plant tissues without disturbing the sample. Most of available techniques are highly invasive and need extensive sample preparation which can lead to measurement artifacts. As an example, transmission electron microscopy requires fixation, staining, drying, resin embedding, and microtoming before visualization. Here, we present how X-ray computed tomography (CT) can provide 3-dimensional information to better understand ENM uptake, translocation in plants, and phytotoxicity with minimal sample preparation. The combination of both micro- and nano- resolved X-ray CT has allowed to semi-quantitatively analyze the nanoparticle accumulation and distribution in plants as well as anatomical responses when plants are exposed to ENMs at subacute exposure concentrations. Three studies will be presented including *M. sativa*, *A. thaliana* and *T. aestivum* exposed to Au, Ag, and Ag₂S ENMs.

Keywords: Nanomaterial-plant interactions, bioaccumulation, bioavailability, internalization, micro- and nano- X-ray computed tomography. Ag, Au and Ag₂S nanoparticles.

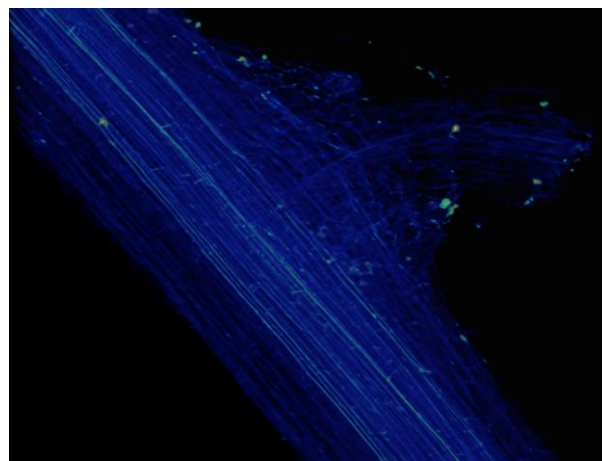


Figure 1: 3D image of the root of a wheat plant exposed to Ag₂S-ENMs. Bright dots correspond to the denser material identified as Ag using other complementary techniques. Root diameter is 300 μm .

References:

- [1] Gardea-Torresdey, J. L.; Rico, C. M.; White, J. C., Trophic transfer, transformation, and impact of engineered nanomaterials in terrestrial environments. *Environmental Science & Technology* **2014**, 48, (5), 2526-2540.
- [2] Ma, C.; White, J. C.; Dhankher, O. P.; Xing, B., Metal-based Nanotoxicity and Detoxification Pathways in Higher Plants. *Environmental Science & Technology* **2015**.
- [3] Meier, C.; Voegelin, A.; Pradas del Real, A. E.; Sarret, G.; Mueller, C. R.; Kaegi, R., Transformation of Silver Nanoparticles in Sewage Sludge during Incineration. *Environmental Science & Technology* **2016**.

Piezo-Resistive Sensing Active (PRSA) Probes integrated into a Nanomeasuring Machine (NMM-1)

A. El Melegy,^{1,3,*} T. Hausotte,¹ M. A. Younes², M. Amer³

¹Friedrich Alexander University Erlangen-Nürnberg (FAU), Institute of Manufacturing Metrology (FMT), Erlangen, Germany

²Alexandria University, Faculty of Engineering, Alexandria, Egypt.

³National Institute for Standard (NIS), Engineering and Surface Metrology Laboratory (ESML), El Giza, Egypt.

Abstract: Atomic force microscopes (AFM) are instruments for the measurement of topographic surface features in the nanoscale. Nanoscale surface features are reconstructed through scanning the surface by silicon cantilevers. The main drawbacks of conventional AFMs are mainly design constraints due to the size of the optical deflection measurement system, the difficulty of alignment of the laser spot focused on the cantilever backside and the limited scanning range. The recent use of self-sensing piezo-resistive cantilevers has led to the development of self-sensing and self-actuating cantilevers and eliminated the need for the optical deflection measurement [3]. To overcome the limitation on the measurement range, a new measuring system has been developed where a piezo-resistive sensing active (PRSA) cantilever is integrated into a nanomeasuring machine (NMM-1) which extends the lateral scanning area up to 25 mm by 25 mm (Figure 1). Factors affecting performance and accuracy of the developed AFM-system have been investigated and compared to other long-range AFM-systems [4,2,5,1]. The integrated system was successfully used for measuring a glass scale with a spacing of 8 μm and 100 nm feature height and a standard step height of 119 nm height and 5 μm step width. The system resolution and measurement repeatability have been investigated.

Keywords: Nanometrology – Atomic Force Microscopy (AFM) – Self-Sensing Cantilever - Nanomeasuring Machine (NMM)

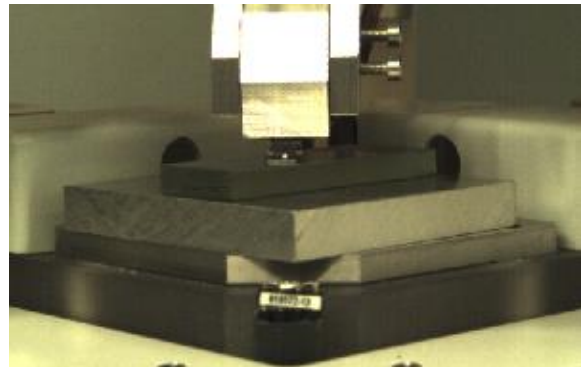


Figure 1: The new AFM system is illustrated. A self-sensing piezo resistive cantilever using the Electro-mechanical setup is integrated into the Nano-Measuring Machine (NMM-1).

References:

1. Gaoliang Dai, Wolfgang Häbeler-Grohne, Dorothee Hüser, Helmut Wolff, Hans-Ulrich Danzebrink, Ludger Koenders, and Harald Bosse, (2011) Development of a 3d-afm for true 3d measurements of nanostructures. *Measurement science and technology*, 22:094009(10pp).
2. Gaoliang Dai, Frank Pohlenz, Hans-Ulrich Danzebrink, Min Xu, Klaus Hasche, and Günter Wilkening, (2004) Metrological large range scanning probe microscope. *Review of scientific instruments*, 75(4).
3. Michael Leitner, Georg E. Fantner, Ernest J. Fantner, Katerina Ivanova, Tzvetan Ivanov, Ivo Rangelow, Andreas Ebner, Martina Rangl, Jilin Tang, and Peter Hinterdorfer, (2012) Increased imaging speed and force sensitivity for bio-applications with small cantilevers using a conventional afm setup. *Micron*, 43(12):1399–1407.
4. Nataliya Vorbringer-Dorozhovets, Tino Hausotte, Eberhard Manske, Jing-Chung Shen, and Gerd Jäger, (2011) Novel control scheme for a high-speed metrological scanning probe microscope. *Meas. Sci. Technol.*, 22:094012 (7pp).
5. Jian Zhao, Tong Guo, Long Ma, Xing Fu, and Xiaotang Hu, (June 2011) Metrological atomic force microscope with self-sensing measuring head. *Sensors and Actuators A: Physical*, 167(2):267–272.

Green way of Synthesizing fluorescent zinc oxide nanoparticles and its biomedical studies - A step towards green nanoscience.

Puja Kumari¹, Manjusha Kushwaha¹, Anwar mallick^{1*}, Suresh kr. Verma^{2*}

¹ P.G Department of Biotechnology, Vinoba Bhave University, Hazaribag, Jharkhand, India

² School of Biotechnology, KIIT University, Bhubaneswar, India

Abstract:

Zinc oxide nanoparticles are one of the most eye catching among the recent nanotechnological research(1). Fluorescent metal nanoparticles (ZnO) have been proved to be a key tool for different biotechnological research because of its vast application like drug targeting and cellular trafficking. Zinc oxide nanoparticles are generally synthesized by different methods and used by tagging with fluorescent dye or antibody. Moreover these nanoparticles are less stable and have short life span. In current work, we have synthesized novel fluorescent zinc oxide nanoparticles using green synthesis method where the plant extract has been used as a reducing as well as stabilizing agent in the synthesis(2). These fluorescent zinc oxide nanoparticles bear fluorescent property permanently and have capacity to be used for many biotechnological applications. Moreover, green synthesis method have advantage over conventional method involving chemical reducing agent often associated with environmental toxicity. The synthesized nanoparticles were characterized by UV-Visible Spectrophotometry(UV-VIS), Dynamic Light Scattering (DLS) ,Fluorescent microscopy and Scanning Electron Microscope(SEM). Further, we have investigated the antibacterial and cytotoxic effect of these nanoparticles against bacterial cell (*E.coli*) and mammalian cell line (HCT116) respectively. The results were satisfactory and found to be open new dimension in synthesis and application of fluorescent nanoparticle.

Keywords: Fluorescent ZnO nanoparticles; antibacterial effect; Cytotoxicity ,biomedical applications, Antibacterial effects.

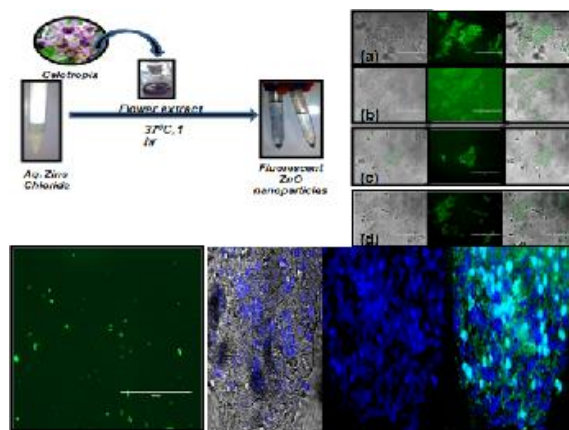


Figure 1: Figure illustrating a novel and green way of preparing fluorescent Zinc oxide nanoparticles with help of natural flora . A illustrative way is presented presenting the characterization of nanoparticles and their probable use in particle trafficking as a biological application.

References

1. Douglas M. Smith, Jakub K. Simon & James R. Baker Jr (2013), Applications of nanotechnology for immunology *Nature Reviews Immunology* 13,592–605.
2. Kaushik N. Thakkar, Snehit S. Mhatre, Rasesh Y. Parikh(2010), Biological synthesis of metallic nanoparticles, *Nanomedicine: Nanotechnology, Biology and Medicine*,6, 2, 257–262.
3. Raman Preet Singh, Poduri Ramarao,(2012) Cellular uptake, intracellular trafficking and cytotoxicity of silver nanoparticles *Toxicology Letters* 213, 2, Pages 249–259.

Adsorption properties of DOX antibiotic from aqueous solutions onto pristine and magnetized carbon nanotubes.

A. Terechshenko^{1,2}, K.Korzhybayeva^{1,2}, M.R.Babaa^{1,2}, Jorge O. Oña-Ruales³ and Z. Bakenov^{1,2}

¹Institute of Batteries LLC, 53 Kabanbay Batyr Ave, Astana, 010000, Kazakhstan

²Nazarbayev University, 53 Kabanbay Batyr Ave, Astana, 010000, Kazakhstan

³National Institute of Standards and Technology (NIST), Gaithersburg, MD 20899, United States

Abstract:

The presence of antibiotics in aquatic environments has been recognized as an issue warranting consideration. Increasing concerns have been raised regarding the potential risks of antibiotics to human and ecological health due to their extensive use. More efficient and cost-effective adsorbents are urgently needed and are the focus of intense research effort. Previous studies have demonstrated that carbon nanotubes can be used as effective adsorbent materials to remove organic contaminants [2].

In this study, magnetic multi-walled carbon nanotubes (MMWNTs) were synthesized from iron salt solution [3]. Pristine, oxidized and magnetized MWNTs were characterized by scanning electron microscopy (SEM), Fourier transform infrared spectroscopy (FT-IR), and X-ray diffraction (XRD). The three solid samples were then investigated for the adsorption of doxycycline antibiotic (DOX) from aqueous solutions. The influence of adsorbent mass, contact time, the temperature and the pH on the adsorption of DOX on the three types of solids was investigated by conducting a series of batch adsorption experiments. The equilibrium data at different temperatures were fitted with the Langmuir, Freundlich, Tempkin, Redlich-Peterson models. Adsorption results showed that the maximum percentage removal of DOX from aqueous solution by pristine, oxidized and magnetized MWCNT's were 99.39%, 78.79% and 94.68% respectively.

Our results indicate that surface properties and aqueous solution chemistry play important roles in DOX adsorption on MWCNTs.

Keywords: adsorption, pristine MWCNT, oxidized MWCNT, magnetized MWCNT, water treatment, antibiotics, doxycycline, multi-walled carbon nanotubes, nanotechnology

References:

1. Mauter, M.S.; Elimelech, M. Environmental applications of carbon-based nanomaterials. *Environ. Sci. Technol.* 2008, 42, 5843–5859.
2. Liangliang Ji et al., Adsorption of tetracycline on single-walled and multi-walled carbon nanotubes as affected by aqueous solution chemistry. *Environmental Toxicology and Chemistry*. 2010, 19 : 2713-2719
3. Fazelirad H, Ranjbar M, Taher M, Sargazi Gh Preparation of magnetic multi-walled carbon nanotubes for an efficient adsorption and spectrophotometric determination of amoxicillin. *Journal of Industrial and Engineering Chemistry*. 2015, 21: 889–892.

Acknowledgements:

This work was supported by the Research Grant of Nazarbayev University.

NanoMatEn 2016 Session I

NanoEnergy

Multi-functional Thin Films for Solar Energy Utilization

Junhui He

Functional Nanomaterials Laboratory, Center for Micro/Nanomaterials and Technology, Technical Institute of Physics and Chemistry, Chinese Academy of Sciences, Zhongguancundonglu 29, Haidianqu, Beijing 100190, China.

Abstract:

Multi-functional thin films are attracting much attention because of their wide potential applications in energy and environmental applications. In this talk, we will present our recent efforts towards self-cleaning antireflective thin films for solar energy utilization, including superhydrophilic, superhydrophobic and superamphiphobic antireflective thin films. The multifunctional thin films not only show high transmittance and self-cleaning function, but good mechanical strength as well. These unique characteristics endow the multifunctional thin films with great potential for solar energy utilization, such as varied solar cells.

Acknowledgements:

This work was supported by the National High Technology Research and Development Program (“863” Program) of China (Grant no. 2011AA050525), the Knowledge Innovation Program of the Chinese Academy of Sciences (CAS) (Grant nos KGCX2-YW-370, KGCX2-EW-304-2), the National Natural Science Foundation of China (Grant no. 21271177), and Key Laboratory of Space Energy Conversion Technology, TIPC, CAS

References:

1. L. Yao, J. He, Prog. Mater. Sci. 61, 94-143 (2014).
2. Z. Geng, J. He, Adv. Mater. Interfaces, 1500196 (2015).
3. L. Yao, J. He, Z. Geng, T. Ren, Nanoscale 7, 13125-13134 (2015).
4. Z. Geng, J. He, L. Xu, L. Yao, J. Mater. Chem. A 1, 8721-8724 (2013).
5. Z. Geng, J. He, J. Mater. Chem. A 2, 16601-16607 (2014).

Comparative study of PN, PIN and new Schottky based InGaN thin films solar cells

A. Adaine ^{1,2}, S. Ould Saad Hamady ^{1,2,*}, N. Fressengeas ^{1,2}

¹ Université de Lorraine, Laboratoire Matériaux Optiques, Photonique et Systèmes, Metz, F-57070, France

² Laboratoire Matériaux Optiques, Photonique et Systèmes, CentraleSupélec, Université Paris-Saclay, Metz, F-57070, France

* sidi.hamady@univ-lorraine.fr

Abstract:

The Indium Gallium Nitride III-N alloy has the required potentialities to be a material of choice used in the next generation high efficiency solar cells. Indeed, the mere change in its Indium composition allows its absorption to cover the whole solar spectrum. One of InGaN main challenges remains today its p-doping. We therefore propose a comparative study between PN and PIN thin films structures, alongside new Schottky based designs which allow the removal of the difficult p-layer.

A mathematically rigorous multi-criteria structure optimization associated to a 2D simulation based on actually measured physical parameters and precise models lead to theoretical efficiencies of 17.8%, 19.0%, 18.2% and 19.8% respectively for the PN, PIN, Schottky and a new proposed Metal-IN (MIN) Schottky based structure. Figure 1 shows the current-voltage characteristics of the optimal MIN solar cell, the Schottky one being shown for comparison purposes. The tolerance that is allowed on each parameter for each of the proposed cells has been thoroughly studied. These studies have shown that the new MIN structure exhibits high fabrication tolerances. This is particularly true for the n-doping of its n-layer, which can be raised enough, without loss of efficiency, to realize good low resistance ohmic contacts.

Therefore, these new InGaN Schottky Based Solar Cells (SBSC) are shown to be efficient and tolerant alternatives to the conventional structures, allowing the removal of the p-type doping of InGaN while giving photovoltaic (PV) performances comparable to the highest reported thin films Solar Cell efficiencies.

Keywords: Solar Cell, Photovoltaics, Thin Films, InGaN, Schottky, Simulation.

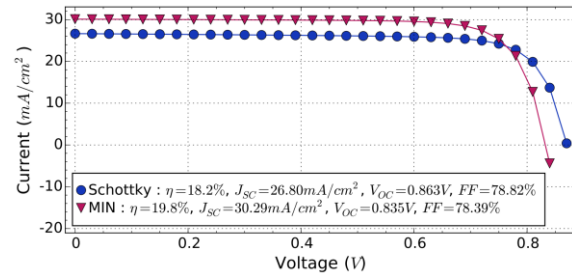


Figure 1: Current-voltage characteristic for the InGaN MIN solar cell compared to the Schottky one.

References:

Green, M. A., Emery, K., Hishikawa, Y., Warta, W., Dunlop, E. D. (2015), Solar cell efficiency tables (Version 45), *Progress in Photovoltaics: Research and Applications*, 23 (1), 1–9.

Ould Saad Hamady, S., Adaine, A., Fressengeas N. (2016), Numerical Simulation of InGaN Schottky Solar Cell, *Materials Science in Semiconductor Processing*, 41, 219-225.

Hybrid Heterojunction PEDOT:PSS/GaAs Thin Film Solar Cells Via Wafer-Bonding Technique

K.W. Sun,^{1,2,*}

¹Department of Applied Chemistry, National Chiao Tung University, Hsinchu, Taiwan

²Department of Electronics Engineering, National Chiao Tung University, Hsinchu, Taiwan

Abstract:

The expensive fabrication processes and materials for crystalline Si solar cells limit the wide application of photovoltaics. The fabrication of p-n junctions for Si involves furnace diffusion, which is expensive and requires very high temperatures ($\sim 1000^\circ\text{C}$). Therefore, hybrid solar cells that combine semiconductor and conjugated polymers at low temperatures provide an alternative to simplify the fabrication processes and reduce costs (Chen *et al.*, 2013, Lin *et al.*, 2015). The conjugated polymer called PEDOT:PSS is the most widely used organic material for hybrid solar cell devices. PEDOT:PSS is transparent, conductive (1000 S/cm), and can produce a heterojunction with semiconductors. Thus, the efficiency of the hybrid PEDOT:PSS/semiconductor solar cell is comparable with a conventional semiconductor p-n junction solar cell in principle. With a recent record of GaAs p-n junction solar cell achieving 28.8%, PEDOT:PSS/GaAs hybrid heterojunction solar cell can offer an alternative route to provide more affordable solar power than current semiconductor technology. Herein we demonstrate the fabrication of a wafer-scale solution-processed PEDOT:PSS/GaAs thin film solar cell by using wafer bonding and chemical wet etching techniques. Figure 1 shows the schematic of the wafer-bonded GaAs thin film on a conducting Si substrate. An Al back contact was deposited on the substrate. A thin layer of PEDOT:PSS was spin-coated on the sample to form a p⁺-n heterojunction. Finally 100 nm-thick Al front electrodes are thermally evaporated through a patterned shadow mask which contains one bus bar connecting several finger electrodes. The best thin film hybrid solar cells reached an excellent power conversion efficiency of 8.93% when an additional p⁺ Al_{0.3}Ga_{0.7}As epi-layer is deposited on the surface of the solar cells to provide a front-surface field (Figure 2). However, we uncovered that the bonding materials was able to diffuse into the GaAs thin film during the wafer-bonding stage, which led to the decrease in efficiency. Dependence of the cell efficiency on GaAs thin film thickness was also investigated. GaAs-based hybrid solar cells are promising for thinning process due to the combined advantages of high absorption in inorganic semiconductors and large-area solution process in organic materials.

Keywords: hybrid, heterojunction, solar cell, wafer bonding, thin film, front-surface field, back-surface field.

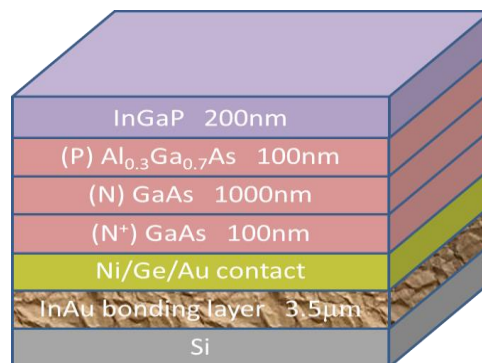


Figure 1: Illustration of the wafer-bonded GaAs thin film on Si.

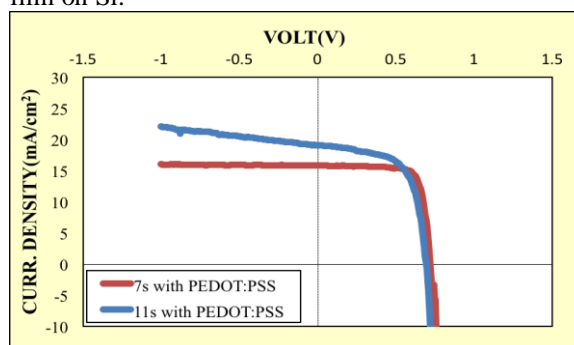


Figure 2 J-V characteristics of the PEDOT:PSS/GaAs thin film solar cells. Our best device shows a V_{oc} , J_{sc} , FF, and conversion efficiency of 0.722 V, 15.83 mA, 0.781, and 8.93, respectively.

References:

- Chen, J.Y., Yu, M.-H., Chang, S.-F., Sun, K.W. (2013) Highly efficient poly(3,4-ethylenedioxythiophene):poly(styrenesulfonate)/Si hybrid solar cells with imprinted nanopyramid structures, *Appl. Phys. Lett.*, 103, 133901.
- Chen, J.Y., Con, C., Yu, M.-H., Cui, B., Sun, K.W. (2013) Efficient enhancement of PEDOT:PSS/Si hybrid solar cells by using nanostructured radial junction and antireflection surface, *ACS Appl. Mater. Interfaces*, 5, 7552-7558.
- Lin, C.H., Sun, K.W., Liu, Q.M., Shirai, H., Lee, C.P. (2015), Poly(3,4-ethylenedioxythiophene):poly(styrenesulfonate)/GaAs hybrid solar cells with 13% power conversion efficiency using front- and back-surface field, *Opt. Express*, 32, 20-31.

Role of methylammonium molecules on the electronic transport properties of organometallic perovskite $\text{CH}_3\text{NH}_3\text{PbI}_3$

G. R. Berdiyorov, F. El-Mellouhi, M. E. Madjet, F. H. Alharbi, and S. N. Rashkeev
Qatar Environment and Energy Research Institute, Hamad Bin Khalifa University, Qatar Foundation,
Doha, Qatar

Abstract:

Organometallic lead-halide perovskites, such as methylammonium (MA) lead iodide (MAPbI_3), have attracted new interest in the past few years as promising light harvesting materials with the solar conversion efficiency already exceeding 20% [1]. The organic cations play an important role in determining the structural, electronic and optical properties of organometallic perovskites. For example, orientational rotation of the cations results in dynamic direct-to-indirect transition in the band gap, which suppresses considerably the charge carrier recombination [2]. In addition, ferroelectric domain walls can be formed due to the permanent dipole moment of the MA molecules, which can assist separation of electrons and holes and reduce their recombination due to charge segregation [3, 4]. Despite recent extensive research, the role of organic cations in defining the excellent photovoltaic performance of these materials is not, however, fully understood. In this work we used first-principles density-functional theory in combination with the nonequilibrium Green's function formalism to study the electronic transport properties of MAPbI_3 in different ferroelectric states. We consider the cubic crystalline phase of MAPbI_3 in order to reduce the structural changes induced by the organic base. Electronic transport in homogeneous ferroelectric or antiferroelectric phases both of which do not contain any charged domain walls is quite similar (Fig. 1). However, the electronic transport in the system can be increased by an order of magnitude along the charged domain walls. Such an enhancement of electronic transport originates from smaller variations of the electrostatic potential profile along the domain walls, whereas the effect of internal octahedral reorganization is negligibly small in this crystal phase of the material. This fact may provide a tool for tuning transport properties of such hybrid materials by manipulating molecular cations having dipole moment.

We also present results on the electronic transport and optical properties of all-inorganic perovskite material CsPbI_3 . Effect of bulk water on the charge carrier dynamics in organometallic halide perovskites will also be discussed.

Keywords: Lead-halide perovskites, organic cations, solar cells, density-functional theory, electronic transport, domain walls.

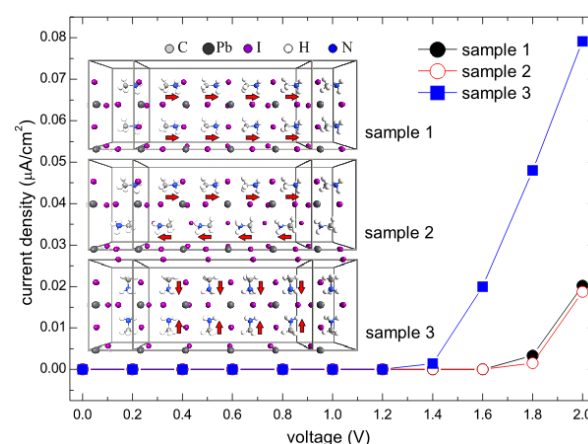


Figure 1: Current-voltage characteristics of MAPbI_3 for different orientations of the MA molecules. Insets: device geometries: cubic lattice structure of organometallic perovskite MAPbI_3 for different orientations of the organic molecules. Periodic boundary conditions are applied along the x - and y -directions and electronic transport occurs along the z -direction through the metallic electrodes. Arrows indicate the direction of the dipole moment of the organic cations.

References:

1. M. A. Green, K. Emery, Y. Hishikawa, W. Warta, E. D. Dunlop, *Prog. Photovoltaics Res. Appl.* **23**, 1 (2015).
2. C. Motta, F. El-Mellouhi, S. Kais, N. Tabet, F. Alharbi, and S. Sanvito, *Nat. Commun.* **6**, 7026 (2015).
3. S. Liu, F. Zheng, N. Z. Koocher, H. Takenaka, F. Wang, and A. M. Rappe, *J. Phys. Chem. Lett.* **6**, 693 (2015).
4. A. Walsh, *J. Phys. Chem. C* **119**, 5755 (2015).
5. G. R. Berdiyorov, F. El-Mellouhi, M. E. Madjet, F. H. Alharbi, and S. N. Rashkeev, *Applied Physics Letters* **108**, 053901 (2016).

Surface Modification for Enhancing Perovskite Solar Cell Performance

Weili Yu,¹ Tom Wu,² Aram Amassian^{1,*}

¹Solar and Photovoltaic Engineering Research Center (SPERC), King Abdullah University of Science and Technology (KAUST), 4700 KAUST, Thuwal 23955-6900, Saudi Arabia.

²Material Science and Engineering, King Abdullah University of Science and Technology (KAUST), 4700 Thuwal, 23955-6900, Saudi Arabia.

Abstract:

Organic–inorganic hybrid perovskites (in particular $\text{CH}_3\text{NH}_3\text{PbX}_3$, where $\text{X} = \text{I}, \text{Br}, \text{Cl}$) solar cells are attracting more interest due to their increasing power conversion efficiency (PCE) as results of the broad absorption, large carrier diffusion length, suitable for large scale processing, etc[1]. Now the certified PCE of perovskite solar cells has increased by several folds in a few years to above 20% [2]. In both planar and meso-porous structured perovskite solar cells, charge transporting materials play critical roles in the extraction and collection of photo-excited carriers. Specifically, it is still challenging to develop low cost and environmental friendly hole transporting materials (HTMs), which are key for effectively extracting holes from the perovskite layer while preventing electrons from recombination. Recently, we have demonstrated that Cu_2O thin films could serve as an efficient HTM for efficient perovskite solar cells[3]. Here, we further declare that the PCE can be improved by modifying the surface of Cu_2O with a small molecule with bifunctional groups, Glycine.

Cu_2O is a typical p-type semiconductor, and has merits such as low cost, chemical and thermal stability, as well as high work function. As a result, Cu_2O has potential applications in photo-electrochemistry, magnetoelectrics and superconductor, etc. In this research, we confirmed that Glycine modified Cu_2O thin films can improve the power conversion efficiency (PCE), which might due to the optimized surface morphology (see **Figure 1**. AFM images), interfacial energy level bending, strengthened electronic coupling. Our results showed that surface modification of HTM layer is an effective process for making efficient perovskite solar cells. This method is simple, suitable for large scale processing and easy to control thickness. The optical and electrical properties of Cu_2O films (before and after modification) were systematically characterized. Our findings strongly support that transition metal oxide, in case of Cu_2O here, are promising inorganic HTMs for industrial-scale solar cell applications, and surface

modification will be necessary for achieving higher performance.

Keywords: perovskite, solar cell, hole transporting materials, copper oxide, surface modification, photovoltaics.

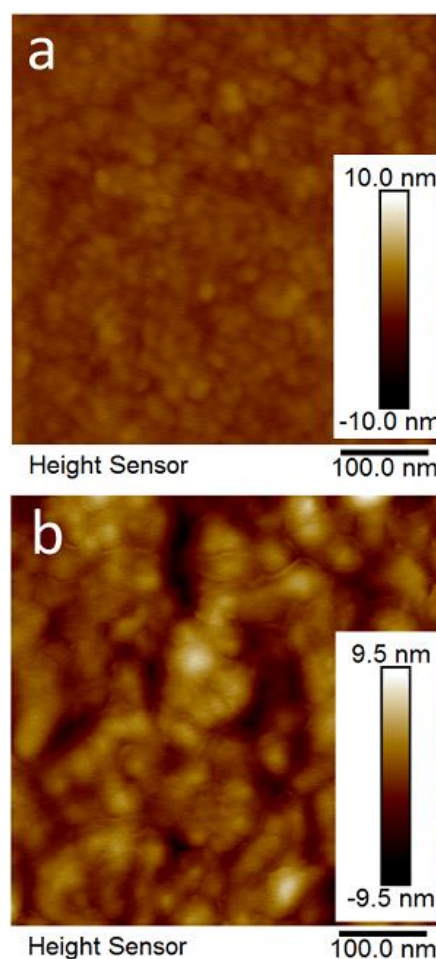


Figure 1. a) The AFM image of Cu_2O layer; b) The AFM image of Cu_2O layer after modifying with Glycine.

References:

- [1] M. Antonietta Loi and J. C. Hummelen, *Nature Materials* 2013, 12, 1087-1089.
- [2] W. S. Yang, J. H. Noh, N. J. Jeon, Y. C. Kim, S. Ryu, J. Seo and S. Seok, *Science* 2015, 348, 1234-1237
- [3] W. Yu, F. Li, H. Wang, E. Alarousu, Y. Chen, B. Lin, L. Wang, M. N. Hedhili, Y. Li, K. Wu, X. Wang, O. F. Mohammed, and Tom Wu, *Nanoscale* 2016

The TiO₂-dye interface in DSSCs: comparing single crystals and thin films and deposition methods, sensitized in UHV and liquid solution

Z. Besharat,^{1,2,*} R. Alvarez Asencio¹, M. Götelid², M. Johnson¹, M. W. Rutland¹

¹ KTH Royal Institute of Technology, Department of Chemistry, Division of Surface and Corrosion Science, Stockholm SE-100 44, Sweden

² KTH Royal Institute of Technology, Department of Material Physics, MNF, ICT, Stockholm SE-164 40, Sweden

Abstract:

The urgent needs of world to replace fossil fuels with renewable energy sources in order to reduce the amount of greenhouse gases strongly motivates research in the field. Photovoltaic solar cells is one potential solution. In the dye sensitized solar cells (DSSCs), photo absorption induces charge excitation in the dye, which later is transferred to the TiO₂ substrate. The TiO₂ is nano structured in order to adsorb maximal amount of dye and maximize the photo absorption. Also, aggregation of dye into large clusters or multilayer films leads to reduced efficiency. Simply, adsorption, bonding and (mono) layer formation of the photo sensitive dye is crucial and much work has been put into detailed understanding of these interfaces [1]. However, one essential issue is how to relate work done under realistic conditions with work done under ultra high vacuum (UHV). In this work we compare thin layers of dye deposited from a dilute liquid solution with deposition through sublimation in UHV. We use synchrotron based x-ray photoelectron spectroscopy (XPS) to evaluate the sublimated thin films and to compare with samples prepared in solution. Further, the amount of adsorbed dye in solution was monitored by quartz crystal microbalance (QCM) in-situ liquid until reaching the monolayer. The structure and mechanical properties of the dye film was investigated by atomic force microscopy (AFM) in the peakforce quantitative nanoscale mechanical (QNM) mode. Results from QCM shows a nice Langmuir adsorption in solution. The XPS comparison shows that the sublimated films and the solution made ones are very similar. Thus, UHV studies can be relevant for understanding realistically prepared samples.

Keywords: QNM AFM, XPS, QCM, DSSCs and UHV

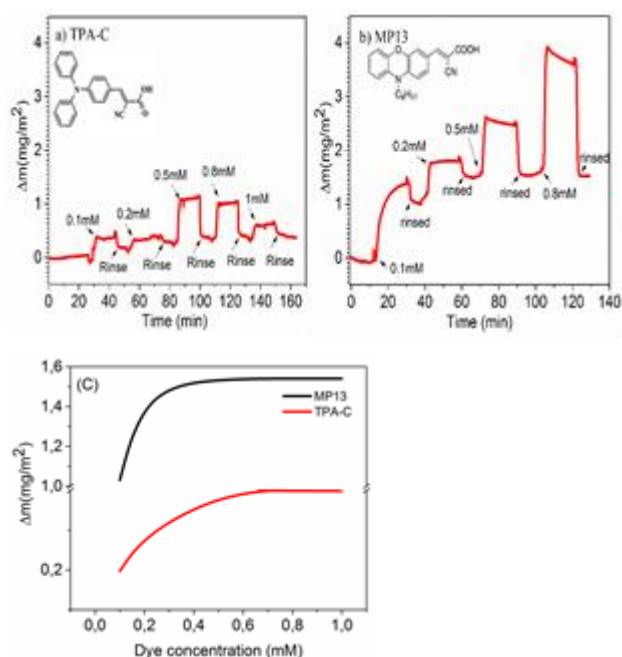


Figure 1: a, b) shows the mass changes due to adsorption of a) TPA-C ,b) MP13 on TiO₂ QCM-D sensor and c) shows the mass changes of both dye vs the concentration of dye in the solution.

References:

1. H.A. Harms, et al, Phys. Chem. Chem. Phys. 14 (2012) 9037
2. S. Yu, et al, J Chem. Phys. 133 (2010) 224704

Photoelectric and Photothermoelectric Material of SBA-15/K-OMS-2 on Photoelectrochemical Solar Cell Application

Chiu-Hsuan Lee,¹ Je-Lueng Shie,^{2,*} Yen Li,² Ching-Yuan Chang,¹

¹National Taiwan University, Graduate Institute of Environmental Engineering, Taipei, Taiwan

²National I-Lan University, Department of Environmental Engineering, Yi-Lan, Taiwan

Abstract:

The purpose of this study is to investigate the feasibility of the applications of the thermos-material (TM), and photo-thermoelectric material (PTEM), thereof, to be the thermal photovoltaic material (TPM) or photoelectric material (PEM) for photoelectrochemical solar cell (PECSC). In this study, the macro molecular zeolite (Santa Barbara Amorphous 15 (SBA-15) and Nanorod molecular sieve (Octahedral manganese potassium cryptomelane, K-OMS-2) (Figure 1) were fabricated and the simulated thermos-reactor can be offered as the light heat source with feasible temperature for target conversion as well as evaluation of thermos-current parameter of thermoelectric figure of merit (TFOM). Furthermore, PTEM process was also used to test the photo-current production curve (I-V curve) from PECSC. At the same time, SBA-15 and SBA-15/K-OMS-2 as the electrode of PECSC, named as SPECSC and SKOPECSC, were also set to test the open-circuited output voltage (V_{oc}), short-circuited output current (I_{sc}), fill factor (FF) and maximum output power (P_{max}) as well as evaluated and discussed. The operation parameters and influential factors, for example, the temperature of PTEM, type and intensity of indoor light radiation (BLED, WLED and UVLED), fabrication method of PECSC, coating type etc. were carried out, meanwhile, the characteristic analyses (EA, TEM-EDS, XRD, FEG-TEM, XPS, FTIR, NMR, etc.) of SBA-15 and K-OMS-2 were also examined in order to find the optimum conditions for the most effective material and treatment method in the indoor light recovery utilization.

Keywords: Photoelectric and Photothermoelectric material, photoelectrochemical solar cell, SBA-15, K-OMS-2, UVLED.

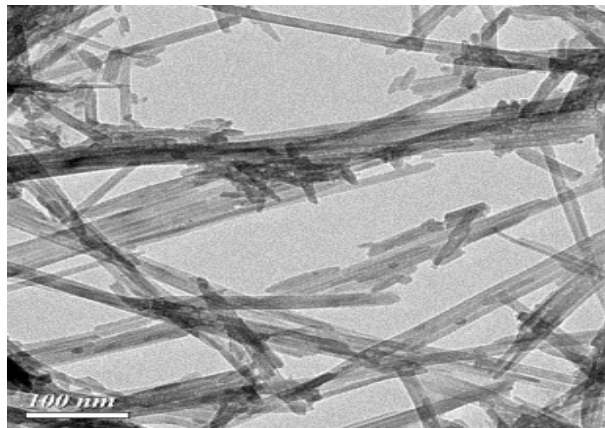


Figure 1: Figure illustrating the TEM images of K-OMS-2 : 38,000x.

References:

- Li, Y., Hou, J., Liu, L., Lv, H., Zhao, X. (2013) Tuning the K^+ Concentration in the Tunnel of OMS-2 Nanorods Leads to a Significant Enhancement of the Catalytic Activity for Benzene Oxidation, *Environ. Sci. Technol.*, 47 (23), 13730–13736.
- Shie, J.L., Lee, C.H., Chiou, C.S., Chang, C.T., Chang, C.C., Chang, C.Y. (2008) Photodegradation Kinetics of Formaldehyde Using Light Sources of UVA, UVC and UVLED in the Presence of Composed Silver Titanium Oxide Photocatalyst, *J. Hazard. Mater.*, 155(1-2), 164-172.

Aluminum-Carbon Nanotube Nanocomposite for Silicon Solar Cell Back Metallization

K. El-Rafei,¹ A. Esawi,¹ O. Tobail,² A. Klingner³

¹The American University in Cairo, Department of Mechanical Engineering, Cairo, Egypt

²Cairo University, Egypt Nanotechnology Center (EGNC), Cairo, Egypt

³German University in Cairo, Department of Physics, Cairo, Egypt

Abstract:

There is a global trend towards reducing the thickness of the silicon wafers used in the manufacturing of solar cell panels. This will result in the improvement of the electrical efficiency of the panel on one hand, and on the other there is the reduction in cost as it was found that nearly half of the manufacturing cost of the panel could be attributed to the silicon wafer (Soon-gil et al., 2010). A silicon panel has the silicon wafer in the middle along with a silver paste screen printed on the front side and similarly an aluminium one on the back side of the wafer. The co-firing of both pastes at high temperature up to 900°C for a short time is done in order to fix both metals to the wafer at both sides so that after co-firing both metals constitute the cell positive and negative electrodes. A problem arises because of this high temperature process, which together with the later soldering of the cells to assemble a module, causes the bowing of the solar cell. This bow is mainly due to the difference of the coefficient of thermal expansion (CTE) of the back side Al paste and the Si wafer. Silicon has $CTE = 2.6 \times 10^{-6} \text{ }^{\circ}\text{C}^{-1}$, while Al has $CTE = 22.2 \times 10^{-6} \text{ }^{\circ}\text{C}^{-1}$, meaning that for a given increase of 1 °C in temperature, Aluminum will expand around 8.5 times more than the Silicon wafer to which it is attached, thus bowing will result as one side tries to stretch more than the other constraining it.

The aim of this research is to replace the aluminium paste with another material with a lower CTE thus minimizing the bowing problem.

Keywords: Carbon nanotubes, Coefficient of Thermal Expansion, Solar Panel, Bowing problem, Aluminium Paste

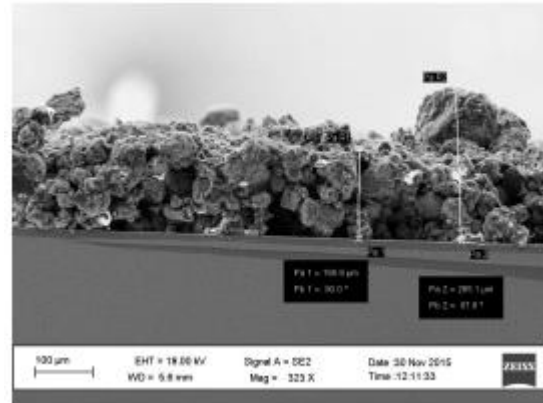


Figure 1: SEM cross sectional image of a silicon wafer coated with Al-10wt% CNT paste.

The proposed replacement is a nanocomposite, using Aluminum as the matrix and multi-walled carbon nano-tubes (CNT) as the filler. Several samples were prepared with different proportions of CNT, 2% CNT-Al, 5% CNT-Al and 10% CNT-Al. The CTE of these samples were measured using a dilatometer, the results contrasted against 2 control samples: Milled and Unmilled Aluminum. It was shown that adding CNTs to Aluminium resulted in a reduction of the CTE by 2.7%, 12.7% and 18.6% for the 2%, 5% and 10% CNT-Al composites respectively. CNT-Al composite pastes were printed on the wafers using a spin coater, and then were fired at 160°C. The bow and warp were measured using a Wafer Geometry Gauge device. It was found that the CNT-Al pastes led to a reduction in the warp developed.

References:

Soon-gil Kim, In-jae Lee, Kim, S., Jun-phill Eom, Jin-gyeong Park, Sun-mi Lee, . . . Joo-won Lee. (2010). Enhancing the solar cell efficiency with optimized metal paste, IEEE-NANO, 2010, 1151-1155.

Co-based mesoporous spinels for oxygen evolution reaction in alkaline medium

A. Habrioux,^{1,*} I. Abidat,¹ C. Canaff,¹ D. Dambournet,² J. Rousseau,¹ O. Borkiewicz,³ C. Morais,¹ C. Comminges,¹ T. Napporn,¹ K.B. Kokoh¹

¹ University of Poitiers, IC2MP UMR-CNRS 7285, 4 rue Michel Brunet, B27, TSA 51106, 86073 Poitiers Cedex 9, France

² CNRS, UMR 8234, PHENIX, F-75005, Paris, France

³ X-ray Science Division, Advanced Photon Source, Argonne National Laboratory, Argonne, Illinois 60439, USA

Abstract:

Stabilization of atmospheric CO₂ amount in the upcoming years requires a transition towards a new energetic grid involving the large scale use of renewable resources. As these energies are intermittent, it is required to implement costly effective and efficient electricity storage systems. These latter systems will allow converting intermittent renewable energies into sustainable energetic vectors (hydrogen, electron). For this purpose, the oxygen evolution reaction (OER) plays an important role. OER possesses a sluggish kinetics that can be enhanced by using a catalyst exhibiting reliable surface composition and morphostructural properties. Additionally, in order to limit the use of scarce noble metals, the synthesis of efficient 3d transition metal oxide-based catalysts is of interest. These materials are indeed known to be capable of improving the OER kinetics in alkaline medium. The activity and stability of such materials are intimately related to their morphostructural properties. In this way, the synthesis of well-defined catalysts is of utmost importance and can be performed using nanocasting approach. In this presentation, oxygen deficient M_xCo_{3-x}O_{4-δ} (where M = Ni, Mn) materials have been synthesized by replicating ordered mesoporous silica templates (KIT-6, SBA-15). The activity of these materials towards OER (Figure 1) has been correlated with their chemical composition and morphostructural properties. A particular attention has been carried out to restructuring phenomena occurring upon potential cycling. For particular chemical compositions, it was shown that the formation of a very active surface layer was responsible for improving the catalytic activity of the catalysts towards the OER.¹

Keywords: mesoporous silica, oxygen evolution reaction, nanocasting, surface restructuring

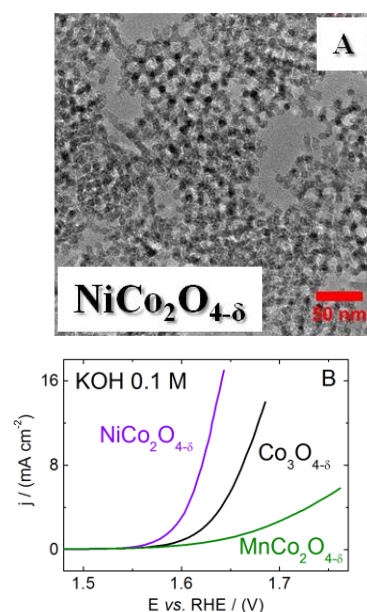


Figure 1: A) Low-magnification transmission electron microscopy image of NiCo₂O_{4-δ} catalyst obtained by replicating a KIT-6 mesoporous silica template. B) Polarization curves obtained with mesoporous Co₃O_{4-δ}, NiCo₂O_{4-δ} and MnCo₂O_{4-δ} oxides synthesized using nanocasting technique (KOH 0.1 mol L⁻¹, 20 °C). Scan rate = 5 mV s⁻¹

References:

1. Abidat, I., Bouchenafa-Saib, N., Habrioux, A., Comminges, C., Canaff, C., Rousseau, J., Napporn, T.W., Dambournet, D., Borkiewicz, O., Kokoh, K.B., (2015), Electrochemically induced surface modifications of mesoporous spinels (Co₃O_{4-δ}, MnCo₂O_{4-δ}, NiCo₂O_{4-δ}) as the origin of the OER activity and stability in alkaline medium, *J. Mater. Chem. A*, 3, 17433-17444.

Coupled surface-plasmon/thermoelectric power generators based on TCO nanowires

A. Catellani,¹ A. Ruini,^{1,2} M. Buongiorno Nardelli,³ and A. Calzolari,^{1,3}

¹Istituto Nanoscienze CNR-NANO-S3, I-41125 Modena, IT

²Dip. Fisica, informatica e Matematica, Univ. Modena e Reggio Emilia, I-41125, Modena IT

³Department of Physics, University of North Texas, Denton, TX 76203, USA

Abstract:

Sunlight energy conversion throughout exciton dissociation in nanoscale systems (e.g. nanoparticles, nanowires, tetrapods, hierarchical structures, etc.) is a valuable alternative to carbon-based sources for green and low cost power generators. Yet, the shrinking of the solar cell dimensions causes relevant problems, especially for the local thermal dissipation that limits the efficiency of photovoltaic systems. On the contrary, thermophotovoltaic converters, which directly convert the energy of photons emitted by a thermal source into electrical energy, are limited to photons with energy above the bandgap, thus reducing the range of solar spectrum available for photoconversion. The design of mixed architectures that could positively exploit both light and heat conversion would represent an important step forward in the realization of more efficient devices. Particularly promising are recent prototypical systems that couple a plasmonic heater to a thermoelectric device [1] for the realization of power generators (Fig. 1). Here, using calculations from first principles, we demonstrate that In-doped ZnO nanowires [2] exhibit the unique property of being simultaneously thermoelectric transparent conducting oxides (TCOs) [3] and low-loss plasmonic materials in the near-IR and visible range [5]. The analysis of their geometrical and optoelectronic properties shows that In doping does not perturb significantly the structure of the nanowire, while gives rise to a good electrical conductivity. The calculated charge density injected into the conduction band of the host ($> 10^{19} \text{ cm}^{-3}$) is sufficient to sustain a surface-plasmon excitation, whose energy decay could generate a temperature gradient in the wire. This effect, coupled with the quenching of the thermal conductivity due to surface scattering and the enhanced thermoelectric figure of merit with respect to the bulk material, establishes the potential of In-doped ZnO nanowires as novel nanostructured energy converters in the form plasmon-heater/thermoelectric generators [2].

Keywords: transparent conducting oxide, thermoelectric materials, plasmonics, power generators, nanowires, In-doped ZnO, first principles simulations.

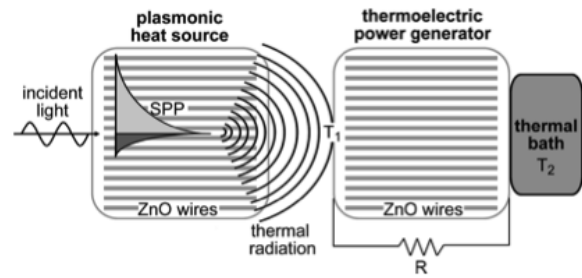


Figure 1: Schematic model of a coupled surface-plasmon/thermoelectric power generator based on ZnO nanowires..

References:

1. Y. Xiong, R. Long, D. Liu, X. Zhong, C. Wang, Z.-Y. Li and Y. Xie, (2012), Solar energy conversion with tunable plasmonic nanostructures for thermoelectric devices, *Nanoscale*, 4, 4416–4420.
2. A. Catellani, A. Ruini, M. B. Nardelli and A. Calzolari, (2015), Unconventional co-existence of plasmon and thermoelectric activity in In:ZnO nanowires, *RSC Advances*, 5, 44865-44872.
3. M. Bazzani, A. Neroni, A. Calzolari, A. Catellani, (2011), Optoelectronic properties of Al:ZnO: Critical dosage for an optimal transparent conductive oxide, *Appl. Phys. Lett.*, 98, 121907.
4. A. Calzolari, A. Ruini, and A. Catellani, (2014), Transparent conductive oxides as near-IR plasmonic materials: the case of Al-doped ZnO derivatives, *ACS Photonics*, 1, 703-709.

Core-shell Ni-NiF₂ as cathode materials for secondary lithium batteries

L. DOUBTSOF, L. JOUFFRET, P. BONNET, K. GUERIN
Clermont Université. Institut de Chimie de Clermont-Ferrand.
UMR CNRS 6296 Aubière Cedex. France

Abstract:

Choosing the best cathode material used in a Li-ion battery is one of the most crucial issues in achieving higher energy densities, since the energy density is directly correlated to the specific capacity associated with that cathode material [1]. Conversion based cathode materials tend to exhibit substantially high capacities, due to the fact that essentially all the possible oxidation states of the compound during the redox reaction can be used. Transition metal fluorides have recently been investigated as potential cathode materials because of their high electronegativity. [2] However there are very few studies on NiF₂ based conversion cathode materials in terms of the conversion mechanism and electrochemical properties, due to its poor electrochemical properties compared to other metal fluorides [3, 4]. It has been recently demonstrated that NiO doped NiF₂ exhibited slightly higher conversion potential and better reversibility due to the doping of NiO phase, presumably due to the relatively high electronic conductivity. The nucleation sites of Ni were reduced by the presence of the NiO phase in NiF₂ and the kinetics of conversion reaction involving the nucleation and growth of Ni particles was enhanced in NiO-doped NiF₂ [4]. In this study, NiF₂ metal fluorides have been prepared by an original route where nickel nanoparticles are fluorinated under pure molecular fluorine gas. Managing the fluorination conditions allows to control the amount of fluorinated nickel and to get partial conversion of nanoparticles of nickel into NiF₂. For such purpose, Ni nanoparticles of median diameter of 50 nm were purchased and fluorinated at temperatures ranged in between room temperature and 450°C. It was then possible to get different proportions of NiF₂ shell onto Ni core. The structure of Ni-doped NiF₂ was investigated by X-ray diffraction (XRD) and the texture by transmission electron microscopy (MET) (Figure 1).

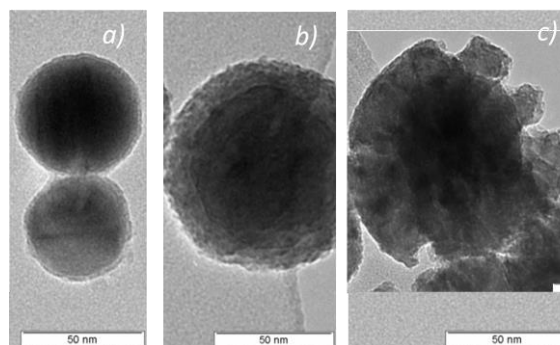


Figure 1: TEM images of pristine Ni nanoparticles a), fluorinated at 200°C b) and fluorinated at 300°C c)

Structural data obtained by XRD combined with the weight uptake evolution got at the end of the fluorination show first the progressive formation of a NiF₂ shell which appears as amorphous until 250°C i.e. a weight percentage of NiF₂ lower than 24%. Then, the proportion of NiF₂ and Ni phases becomes only the same by XRD and weight uptake as soon as the NiF₂ phase is perfectly crystallized i.e. for fluorination temperature higher than 400°C. The coherence lengths of each phase evolve with the fluorination temperature.

Finally, performances got by galvanostatic measurements on those materials used as electrode in secondary lithium battery are different owing to the nanostructure and very promising.

Keywords: nanomaterial, core-shell particle, fluorination, nickel fluoride, secondary lithium battery.

References:

1. J.M. Tarascon, M. Armand, *Nature* 414 (2001) 359.
2. P. Poizot, S. Laruelle, S. Grugeon, L. Dupont, J.M. Tarascon, *Nature* 407 (2000) 496.
3. H. Zhang, Y.N. Zhou, Q. Sun, Z.W. Fu, *Solid State Sci.* 10 (2008) 1166.
4. D. H. Lee, K. J. Carroll, S. Calvin, S. Jin, Y. S. Meng, *Electrochimica Acta* 59 (2012) 213

Ultra-Thin copper oxide nanowires grown by atmospheric pressure afterglow for water splitting application

A. Imam^{1*}, T. Gries¹, K. Hussein², T. Belmonte¹

¹ Lorraine University, Jean Lamour institute, CP2S, UMR CNRS 7198, Nancy, France.

² Lebanese University, Faculty of sciences (section III), Department of applied physics, Tripoli, Lebanon.

Abstract:

To produce hydrogen by water splitting, a photocatalyst must be used to dissociate water into hydrogen and oxygen under solar irradiation. As photocatalyst, iron oxide and copper oxide were chosen because they have relatively narrow band gaps (2.2 eV), which gives them the advantage of harvesting a larger part of the visible spectrum compared with other oxides like TiO₂. But on the other hand, the positions of their band gaps are not suitable to produce hydrogen and oxygen simultaneously, because these two semiconductors (p-type for CuO and n-type for Fe₂O₃) have band gaps with one positive edge below 1.23 eV. The solution proposed here is to use quantum size effects to extend the band gap so as to get it spanned over the reduction and oxidation water potentials and thus, to produce hydrogen and oxygen simultaneously. Quantum size effects occur only in very small nanowires, with diameters smaller than ~3 nm. To elaborate these nanostructures, we used a micro-afterglow produced downstream an argon-oxygen microwave plasma at atmospheric pressure. The micro-afterglow is a very oxidizing medium for it contains concentrations of oxygen atoms of a few 10¹⁴ cm⁻³ and a high concentration of excited oxygen molecules like O₂(a¹Δ_g). The presence of these species at moderate temperature can discriminate the growth rates of iron oxide along different directions, which promotes the emergence of nanostructures. The elaborated nanostructures, grown on pure iron and pure copper samples, were too large to exhibit quantum size effects but the differences in their morphologies guided us to mix them. Modifications in the growth mechanism of nanostructures were thus expected, making us capable of modifying the nanostructures sizes by tuning alloy compositions. Mixtures of copper and iron either as alloys or as stacks of layers

gave outstanding results after oxidation, making it possible to control the morphologies of thus-grown nanowires and to decrease their diameter down to 5 nm.

Keywords: Nanowires, water splitting, photocatalyst, plasma, afterglow, quantum confinement.

References:

1. Liao, C.H., Huang, C.W., Wu, J.C.S. (2012) Hydrogen production from semiconductor-based photocatalysis via water splitting, *Catalysts* **2**.
2. Yu, J., Hai, Y., Jaroniec, M. (2011) Photocatalytic hydrogen production over CuO-modified titania, *J. Colloid. Interf. Sci.* **357**
3. Altaaweel, A., Filipič, G., Gries, T., Belmonte, T. (2014) Controlled growth of copper oxide nanostructures by atmospheric pressure micro-afterglow, *Journal of Crystal Growth* **407**.

Energy transfer between up-converting nanocrystals and organic polymer

Justyna Grzelak,^{1*} Kamil Ciszak,¹ Marcin Nyk,² Dawid Piatkowski,¹ Sebastian Mackowski,¹

¹Institute of Physics, Faculty of Physics, Astronomy and Informatics, Nicolaus Copernicus University, Grudziadzka 5/7, 87-100 Torun, Poland

²Institute of Physical and Theoretical Chemistry, Wrocław University of Technology, Wybrzeże Wyspińskiego 27, 50-370 Wrocław, Poland

Abstract:

We study interactions between up-converting nanocrystals and Poly(9,9-dioctylfluorene-alt-benzothiadiazole) (F8BT) polymer, which is one of the most commonly used building block in bulk heterojunction solar cell [1]. The promising candidates for sensitizing organic solar cells to infrared radiation are up-converting materials [2,3], however this requires developing conditions for energy transfer to occur between these nanostructures. We report on single fluorescence microscopy of colloidal up-converting NaYF₄ nanocrystals (20-nm-large) doped with rare-earth ions (Er³⁺ and Yb³⁺) [4] mixed with the F8BT polymer. We also prepared a sample containing only the NaYF₄:Er³⁺/Yb³⁺ nanocrystals with identical concentration as a reference sample. To enable energy transfer between nanostructured one of the emission bands of the nanocrystals (centered at 550 nm) overlaps with the absorption of the F8BT polymer. For excitation we used solid-state near infrared laser (980 nm). The nanostructure containing nanocrystals mixed directly into the F8BT layer, was studied by means of high-resolution luminescence microscopy, both in continuous-wave and time-resolved modes. We demonstrate that energy transfer is efficiently transferred from the nanocrystals to polymer by probing luminescence properties of individual nanocrystals. The life-time of nanocrystal emission decreases for nanocrystals embedded in F8BT polymer as compared to a reference sample, what proves efficient non-radiative energy transfer from the nanocrystals to the polymer layer. The intensity of polymer emission, like F8BT or P3HT, can be further enhanced by an order of magnitude using metallic nanoparticles with plasmon resonance matching the absorption of nanocrystals [5]. These results are important for improving the spectral response of organic bulk

heterojunction solar cells, in particular in the infrared region.

This work was supported by project DEC-2013/09/D/ST3/03746 from the National Science Center and by the National Research and Development Center (NCBiR) under Grant ORGANOMET No: PBS2/A5/40/2014.

Keywords: up-conversion, nanocrystals, rare earth ions, solar cells, polymers, fluorescence microscopy

References:

- [1] John Chappel, *Nature Materials* **2**, 616 – 621 (2003)
- [2] D. Piatkowski, *ACS Nano*, **7(11)**, pp 10257-10262 (2013)
- [3] D. Piatkowski, *Nanoscale*, **7**, 1479-1484 (2015)
- [4] J. Grzelak, *Appl. Phys. Lett.*, **105**, 163114 (2014)
- [5] K. Smolarek, *Appl. Phys. Lett.*, **103**, 203302 (2013)

Energy Harvesting with Decorative Colour Specific Windows

B. Fisher,^{1,*} E. New,¹ D. Kutsarov¹, V. Stolojan¹, S. R. P. Silva¹

¹Advanced Technology Institute, Department of Electrical and Electronic Engineering, University of Surrey, GU2 7HX.

Abstract:

Organic solar cells (OSCs) can be light-weight, flexible, and semi-transparent (Jayawardena, 2013; He, 2012); they can also be integrated into architectural elements, such as windows (He, 2012; Schmidt, 2009), where reducing glare, providing decorative ambiance and harvesting energy in office buildings can be achieved simultaneously. Energy harvesting from coloured windows with power conversion efficiencies of around 0.5-2.8% (Schmidt, 2009) has been reported. Using a one-dimensional simulation (the transfer matrix method) (He, 2012; Pettersson, 1999; Jung, 2011), we show that we can tune the thicknesses of the components of the OSC to create bespoke devices that transmit a given quantity of light, having a specific colour and to have optimum energy harvesting capabilities. In Figure 1, we demonstrate this by designing a Red, Green and a Blue solar cell, each with 50% transmissivity and around 2% power conversion efficiency, increasing to more than 4% with 30% transmissivity. This shows that OSCs can be integrated into architectural designs, leading to a new generation of energy efficient with ambient control buildings.

Keywords: transfer matrix method, semi-transparent solar cells, organic solar cells, organic photovoltaics, energy harvesting, power conversion efficiency.



Figure 1: Illustrates different coloured semi-transparent OSCs (red, green and blue), all having an average transmissivity of 50%. The RGB values that have been used are Red (213, 148, 147), Green (200, 210, 172), and Blue (173, 182, 199). Each of the images shows the approximated power conversion efficiency for the materials used.

References:

1. He, Z. et al., 2012. Enhanced power-conversion efficiency in polymer solar cells using an inverted device structure. *Nature Photonics*, 6(9), pp.591–595.
2. Jayawardena, K.D.G.I. et al. 2013 ‘Inorganics - in - Organics’: Recent Developments and Outlook for 4G Polymer Solar Cells. *Nanoscale*, 5(18), pp.8411.
3. Jung, S. et al., 2011. Optical modeling and analysis of organic solar cells with coherent multilayers and Incoherent glass substrate using generalized transfer matrix method. *Jpn.J.Appl.Phys*, 50(12), pp. 122301.
4. Pettersson, L.A.A., Roman, L.S. & Inganas, O., 1999. Modeling photocurrent action spectra of photovoltaic devices based on organic thin films. *Journal of Applied Physics*, 86(1), pp.487–496.
5. Schmidt, H. et al., 2009. Efficient semitransparent inverted organic solar cells with indium tin oxide top electrode. *Applied Physics Letters*, 94(24), pp.21–24.

Enhanced Thermal Conductivity of Nanofluids Containing Two-Dimensional Materials

Dongju Lee¹, Gyoungja Lee¹, Jin-Ju Park¹, and Minku Lee^{1,*}

¹Nuclear Materials Development Division, Korea Atomic Energy Research Institute, Daejeon, Republic of Korea

Abstract:

Heat transfer fluids plays an important role in diverse fields in transport, electronic, solar cells, and nuclear cooling systems, etc. The increasing thermal loads in applications require advanced operational fluids. In recent years, two-dimensional (2D) materials such as graphene and hexagonal boron nitride (h-BN) with high mechanical strength and thermal conductivity have been tried in fluids for heat transfer improvement. However, 2D materials with high specific surface area are prone to form irreversible aggregation due to van der Waals interactions. Thus, stable dispersion of the 2D materials in the fluids are essential problems to be solved for the effective utilization. We report the synthesis and characterization of stable high thermal conductivity nanofluids using exfoliated h-BN and graphene oxide (GO) in ethylene glycol (EG) without surfactants. Exfoliated h-BN and graphene oxide effectively be used to achieve remarkable thermal conductivity improvement of the nanofluids. The thermal conductivity enhancement depends strongly on the volume fraction of exfoliated h-BN and GO and increases with the increasing loading. With exfoliated h-BN as fillers, thermal conductivity of the nanofluids can be effectively improved with maintaining its electrical insulation. (Figure 1) Moreover, the thermal conductivity of the BN-EG nanofluids remains almost constant for five days, indicating their high stability. In addition, we will introduce the viscosity the nanofluids with concentration and temperature. This study will enable us to discuss advanced nanofluids containing 2D materials that can be applied in various thermal management applications.

Keywords: nanofluid, boron nitride, graphene oxide, thermal conductivity, viscosity.

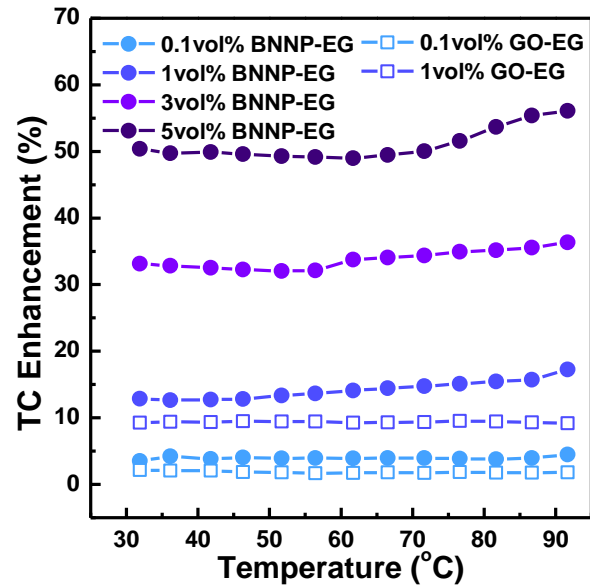


Figure 1: Thermal conductivity enhancement of BNNP-EG and GO-EG nanofluids with concentration and temperature.

Nanofluids with enhanced thermal properties: an experimental and theoretical analysis

Javier Navas,¹ Antonio Sánchez-Coronilla,² Elisa I. Martín,³ Roberto Gómez-Villarejo,¹ Miriam Te-
ruel,¹ Juan Jesús Gallardo,¹ Teresa Aguilar,¹ Rodrigo Alcántara,¹ Concha Fernández-Lorenzo,¹ Joaquín
Martín-Calleja¹

¹Cádiz University, Department of Physical Chemistry, Cádiz, Spain

²Seville University, Department of Physical Chemistry, Seville, Spain.

³Seville University, Department of Chemical Engineering, Seville, Spain.

Abstract:

Concentrating Solar Power (CSP) is one of the most interesting option as renewable energy today. One option in order to improve the efficiency of these plants is to enhance the properties of the heat thermal fluid (HTF) used. Thus, one of the research lines of greater interest is the use of nanofluids to enhance the thermal properties of HTFs, because of the incorporation of solids into these fluids improves several thermal properties such as thermal conductivity or the heat transfer coefficient. In this work, we report nanofluids based on metallic nanoparticles, and we analysed the effect of the presence of the nanoparticles in different properties such as density, viscosity, and thermal properties, that is isobaric specific heat, thermal conductivity, and thermal diffusivity. So, in function of the nanoparticle nature, the enhancement of the HTF properties were different. Also, in order to understand the behaviour of the nanofluidic systems, dynamic molecular analysis were performed. The structural and dynamic properties of the nanofluids were analysed. From, radial distribution function and the spatial distribution function analysis, the structural properties of the systems were studied. In turn, the thermal properties were estimated from theoretical calculations, and the same trend obtained from the experimental results were observed, which validates the methodology proposed. Thus, this study provides us with a better understanding of how the HTF molecules are rearranged around the metal, leading to an enhancement of the thermal properties.

Keywords: nanofluids, Concentrating Solar Power, Dynamic Molecular, heat transfer fluid, specific heat, thermal conductivity, nanoparticles.

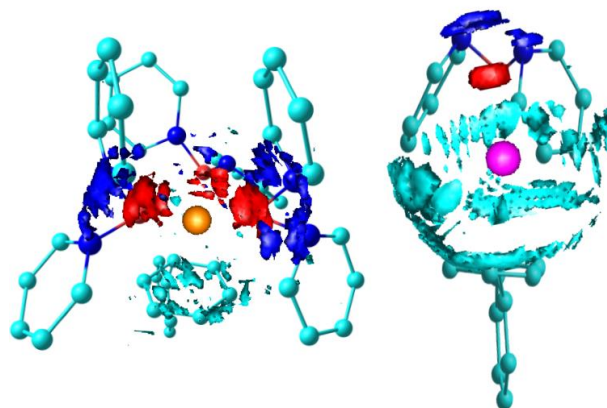


Figure 1: The metal-fluid interactions lead to a different behaviour of the thermal properties of nanofluids based on metallic nanoparticles and the eutectic mixture of diphenyl oxide and biphenyl as base fluid.

References:

- Yoo, D. H., Hong, K. S., Yang, H. S. (2007) Study of thermal conductivity of nanofluids for the application of heat transfer fluids, *Thermochim. Acta*, 455, 66-69.
- Singh, D., Timofeeva, E. V., Moravek, M. Cingarapu, S. R., Yu, W. H., Fischer, T., Mathur, S. (2014) Use of the metallic nanoparticles to improve the thermophysical properties of the organic heat transfer fluids used in concentrated solar power, *Sol. Energy*, 105, 468-478.

New Composites “LiCl/vermiculite” for Sorptive Heat Storage

A.D. Grekova,^{1,2,*} L.G. Gordeeva,^{1,2} Y.I. Aristov^{1,2}

¹Boreskov Institute of Catalysis, Novosibirsk, Russia

²Novosibirsk State University, Novosibirsk, Russia

Abstract:

The renewable energy sources are inexhaustible, but the main barrier to their successful implementation is a mismatch between the production of and demand for the energy they generate [1]. Sorption heat storage (SHS) is a promising way towards efficient use of the renewable energy sources. SHS process consists of two main stages, namely, charging (heat accumulation) during endothermic desorption process, and discharging (heat release) during exothermic sorption. Among adsorbents suggested for SHS, the composites “salt in porous matrix” (CSPM) are considered promising due to their high Heat Storage Capacity (HSC) and tunable sorption behavior [2]. This paper addresses the intent synthesis of novel CSPMs, adapted for two SHS cycles: long-term (LT), or seasonal, and short-term (ST), or daily, heat storage. Expanded vermiculite was used as a host matrix with large pore volume ($V_p = 2.7 \text{ cm}^3/\text{g}$), and LiCl as an active salt. Firstly, the analysis of operating conditions of two selected SHS cycles was performed. Then, the LiCl/vermiculite composites were synthesised for these cycles by dry impregnation method; water and methanol sorption on these materials was studied. Finally, the HSC of the new sorbents was evaluated. The XRD pattern of LiCl/vermiculite shows that LiCl forms well-crystallized phase (cubic lattice Fm-3m) in the vermiculite pores with the coherently scattering domains of 100 nm size. Isobars of water and methanol sorption on these composites are S-shaped curves. At high temperature, the sorption is minor; at decreasing temperature the sorption steeply rises indicating the formation of $\text{LiCl} \cdot n\text{H}_2\text{O}$ ($n = 1, 2$) and $\text{LiCl} \cdot 3\text{CH}_3\text{OH}$ complexes. The new composites exchange 0.75 and 0.65 g/g of water under conditions of ST and LT cycles, respectively. The appropriate values for methanol equal 1.08 and 0.88 g/g. The isosteric heat of water ($57 \pm 3 \text{ kJ/mol}$) and methanol ($41 \pm 3 \text{ kJ/mol}$) sorption are calculated. For LiCl(35 wt.)/vermiculite – methanol no sorption-desorption hysteresis, typical of the bulky salt, is observed. For LiCl(35 wt.)/vermiculite

– water the hysteresis does not exceed 5°C , that is acceptable for SHS.

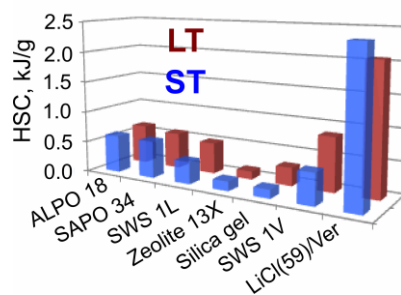


Figure 1: The HSC for different sorbents under ST and LT cycles conditions (working fluid - water).

The working pair LiCl(59 wt.)/vermiculite possesses higher HSC equal to 2.1 and 2.4 kJ/g under conditions of LT and ST cycles, respectively. These values are superior to appropriate HSCs (0.13 – 0.87 kJ/g) reported for the common and innovative adsorbents proposed for SHS [1]. This demonstrates that the new composites hold much promise for SHS and their utilization can promote a broader implementation of this emerging technology.

Acknowledgment: The study was partially supported by the RFBR (project 15-53-53096). Grekova A.D. thanks the Ministry of Education and Science of the Russian Federation (the Russian President's Scholarship SP-3769.2016.1)

Keywords: sorption heat storage, LiCl, vermiculite, methanol, water.

References:

1. Yu, N., Wang, R. Z., Wang, L.W. (2013) Sorption thermal storage for solar energy. *Prog. Energy Comb. Sci.*, 39, 489-514.
2. Gordeeva, L.G., Aristov, Yu.I. (2012) Composites “salt inside porous matrix” for adsorption heat transformation: a current state of the art and new trends. *Int. J. Low Carbon Technol.*, 7, 288-302.

Pseudocapacitive Study of Nickel Oxide Nanomaterials for Electrochemical Energy storage

L. Meda*, J. Adkins, C. Arnold

Xavier Univresity of Louisiana, Department of Chemistry, New Orleans, LA USA

Abstract:

Supercapacitors deliver a higher power density than batteries, but the latter stores more capacity.¹ Combining the attributes of supercapacitors and batteries are needed for future electronics. One approach is to synthesize pseudocapacitive storage materials with both characteristics. Pseudocapacitive or hybrid materials offer opportunities to tackle much needed improvements in the performance of energy storage devices. Using a low-pressure chemical vapor deposition (CVD) process, nanostructured Ni-based electrodes pure NiO and NiO/Ni(OH)₂ mixture were directly deposited on stainless steel current collectors. Powder X-ray diffraction revealed the deposited materials have (111) preferred growth for NiO and (102) preferred growth for NiO/Ni(OH)₂ samples. FESEM revealed differences in morphology for the materials, but all deposited materials were nanosized in scale. The relationships of the electrochemical properties and morphology were also investigated in order to design Ni-based oxide electrodes that exhibit overall superior electrochemical properties including pseudocapacitor. Galvanostatic charge-discharge and cyclic voltammetry experiments were performed in these two materials in the range of 0.1 – 4.0 V versus Li/Li⁺ in 1:1:1 molar ratio of EC/PC/DMC. The electrochemical performance of the NiO and NiO/Ni(OH)₂, which behave as a pseudocapacitor, will be discussed.

Keywords: Pseudocapacitor, NiO, lithium ion battery, CVD

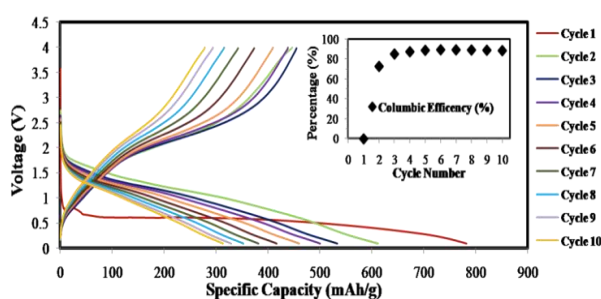
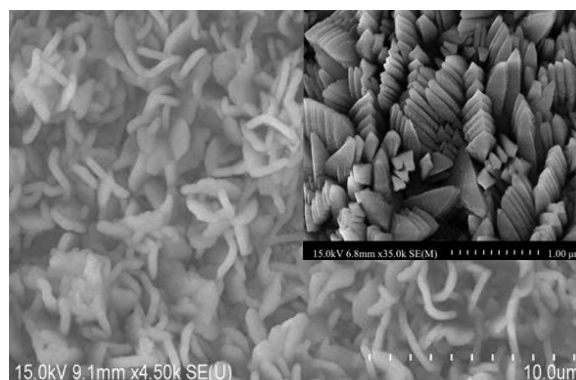


Figure 1. FESEM image of NiO after galvanostatic charge/discharge curves for the first 10 cycles of annealed NiO. The as-deposited NiO is shown on the inset . The charge/discharge curves are shown as well as the Coulombic Efficiency.

References

1. Augustyn, V., Simon, P., & Dunn, B. 2014. Pseudocapacitive oxide materials for high-rate electrochemical energy storage. *Energy & Environmental Science*, 7, 1597-1614.

NanoMatEn 2016 Session II
Nanotechnology for Environmental
applications

Effect of Sb segregation on conductance and catalytic activity at Pt/Sb-doped SnO₂ interface: a synergetic computational and experimental study

Qiang Fu¹, Luis César Colmenares Rausseo², Umberto Martinez³, Paul Inge Dahl², Juan Maria García Lastra¹, Per Erik Vullum², Ingeborg-Helene Svenum², and Tejs Vegge^{*1}

¹Department of Energy Conversion and Storage, Technical University of Denmark, Fysikvej, 2800 Kongens Lyngby, Denmark

²SINTEF Materials and Chemistry, NO0-7465 Trondheim, Norway

³QuantumWise A/S, Fruebjergvej 3, Postbox 4, 2100 Copenhagen, Denmark

Abstract:

In this work, the effect of Sb segregation on the conductance and catalytic activity at Pt/Antimony doped tin dioxide (ATO) interface was investigated through a combined computational and experimental study. It was found that Sb-dopant atoms prefer to segregate toward the ATO/Pt interface. The deposited Pt catalysts, interestingly, not only promote Sb segregation, but also suppress the occurrence of Sb³⁺ species, a charge carrier neutralizer at the interface. The conductivity of ATO was found to increase, to a magnitude close to that of activated carbon, with an increment of Sb concentration before reaching a saturation point around 10%, and then decrease, indicating that Sb enrichment at the ATO surface may not always favor an increment of the electric current.

Keywords: atomistic simulations, density functional theory, electronic transport properties, NEGF, fuel cells, energy storage

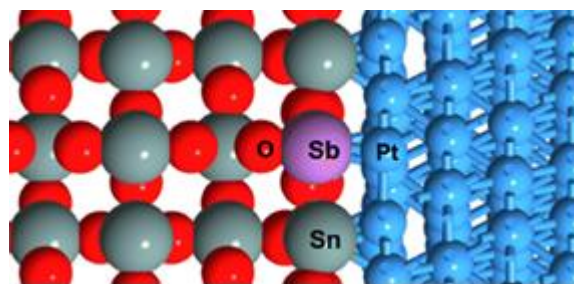


Figure 1: Antimony-doped tin dioxide (ATO) interface as modeled in ATK.

References:

1. ACS Appl. Mater. Interfaces, 2015, 7, 27782
2. Atomistic Toolkit 2015, QuantumWise A/S (www.quantumwise.com).

Au@Pt Core-shell Mesoporous Nanoballs and Nanoparticles as Efficient Electrocatalysts for formic acid and glucose oxidation

T.W. Napporn^{1*}, Y. Holade¹, A. Lehoux², H. Remita², K. B. Kokoh¹ and

¹IC2MP, UMR CNRS 7285 Université de Poitiers, 4, rue Michel Brunet, B27, TSA 51106, 86073 Poitiers Cedex 09, France

²Laboratoire de Chimie Physique, UMR 8000-CNRS Université Paris-Sud, Université Paris-Saclay, 91405 Orsay Cedex, France

Abstract:

Platinum (Pt) electrocatalyst exhibits sluggish kinetics toward organics electrooxidation and oxygen reduction reaction. This represents a major obstacle to a more widespread use of the polymer electrolyte membrane (PEM) fuel cells. Currently, Pt nanoparticles (NPs) dispersed on carbon supports (Pt/C) are used as electrode materials. The carbon support corrosion process, the aggregation of Pt NPs, and their dissolution lead to significant loss of the electrochemical surface area (ECSA). For improving the performance of such Pt/C catalysts, unsupported Pt nanoscale materials were found to exhibit interesting properties like their high active surface area. Therefore novel synthesis routes are proposed to elaborate more active and cleaner materials for energy conversion and storage systems. Compared to chemical reducing processes that follow a diffusion front, radiolysis presents the advantage of inducing homogeneous nucleation and growth in the whole volume of the irradiated sample. Metal nanoparticles including 1D, 2D and 3D nanostructures can be directly synthesized in surfactant mesophases. In the present work, supportless Pt, Au@Pt 3D-porous nanostructures (PtNBs and Au@PtNBs), and Au-core-Pt-shell nanoparticles (Au₅₀Pt₅₀NPs) were synthesized. The radiolytic synthesis provides a high control on the size, morphology, and composition of the nanoparticles. Nanoballs, 85 ± 5 nm for PtNBs and 75 ± 5 nm for Au@PtNBs, are formed by 3D-interconnected nanowires leading to a giant mesoporous structure. The high catalytic activity of these nanostructures toward organic electrooxidation was highlighted in aqueous media and attributed to their particular core-shell structure. The Au@PtNBs mesoporous materials exhibit improved kinetics toward glucose and formic acid electrooxidation compared to their counterpart PtNBs and Au₅₀Pt₅₀NPs respectively.

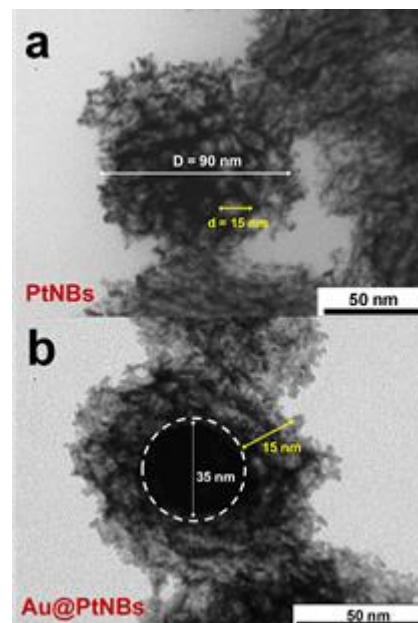


Figure 1: Figure 1 illustrating (a) single PtNB of about $D = 90$ nm, highlighting pore construction, $d = 15$ nm. (b) HRTEM image of Au@PtNBs formed by a large core made of gold and a porous Pt shell.

Keywords: Electrocatalysts, Radiolysis, core-shell, Nanoparticles, Gold, Platinum, oxidation of Glucose and formic Acid, Fuel cells..

References:

Holade Y., Lehoux A., Remita H., Kokoh KB., W. Napporn TW. (2015) Au@Pt Core-Shell Mesoporous Nanoballs and Nanoparticles as Efficient Electrocatalysts toward Formic Acid and Glucose Oxidation, *J. Phys. Chem. C*, 119 (49) 27529–27539

First insight into fluorinated Pt/carbon aerogels as more corrosion-resistant electrocatalysts for Proton Exchange Membrane Fuel Cells Cathodes

Y. Ahmad¹, S. Berthon-Fabry^{*2}, L. Dubau^{3,4}, K. Guerin¹, M. Chatenet^{3,4}

¹ Institut de Chimie de Clermont-Ferrand, Clermont Université, Université Blaise Pascal, BP 10448, 63000 Clermont-Ferrand, France

² MINES ParisTech, PSL Research University PERSEE-Centre procédés, énergies renouvelables et systèmes énergétiques, CS 10207 rue Claude Daunesse, 06904 Sophia Antipolis Cedex, France

³ LEPMI, University of Grenoble Alpes, 38000 Grenoble, France

⁴ CNRS, LEPMI, 38000 Grenoble, France

Abstract:

Proton exchange membrane fuel cells (PEMFC) are devices that convert chemical energy into electricity in a clean and efficient manner. They can be used in automotive, nomad, or stationary applications without emission of pollutants (neither gas nor particles). After several decades of scientific and technological improvements, the PEMFC technology is now mature and starts to be deployed on the field, but some drawbacks must be overcome; in particular, their durability in operation must be increased. The durability strongly depends on the technical choice of the PEMFC manufacturer (bipolar plates, membrane, and quality of the hydrogen) but also especially the resistance to degradation of the carbon support and the catalyst and the water management. This study evaluates the fluorination of a carbon aerogel and gives first insights into its durability when used as platinum electrocatalyst substrate for proton exchange membrane fuel cell (PEMFC) cathodes. Fluorine has been introduced before or after platinum deposition (Figure 1). The different electrocatalysts are physico-chemically and electrochemically characterized, and the results discussed by comparison with commercial Pt/XC72 from E-Tek. The results demonstrate that the level of fluorination of the carbon aerogel can be controlled. The fluorination modifies the texture of the carbons by increasing the pore size and decreasing the specific surface area, but the textures remain appropriate for PEMFC applications. Two fluorination sites are observed, leading to both high covalent C-F bonds and weakened ones, the quantity of which depends on whether the

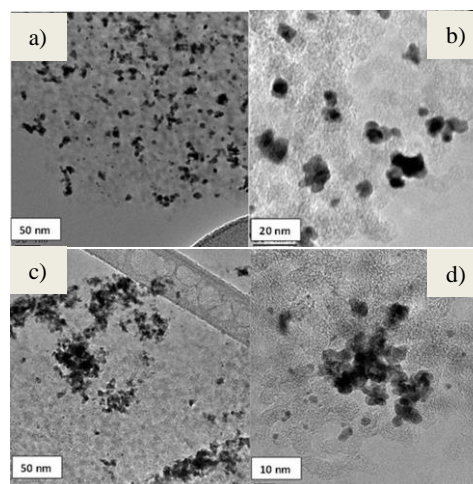


Figure 1. TEM pictures of the Pt-CA (a,b) and Pt/F-CA (c,d) electrocatalysts

treatment is done before or after platinum deposition. The order of the different treatments is very important. Indeed, the presence of platinum contributes to the fluorination mechanism, but leads to amorphous platinum, which is demonstrated rather inactive towards the oxygen reduction reaction. On the contrary, a better durability was demonstrated for the fluorinated and then platinized catalyst compared both to the same but not fluorinated catalyst and to the reference commercial material (based on the loss of the electrochemical real surface area after accelerated stress tests).

Keywords: Carbon aerogel, Fluorination, Electrocatalysts, Durability, PEMFC

Label-Free Surface Plasmon Resonance Biosensing with Titanium Nitride Thinfilm

S.P. Ng, G. Qiu, Z. Deng, C.M.L. Wu*

City University of Hong Kong, Department of Physics and Materials Science, Hong Kong SAR, China

Abstract:

State-of-the-art label-free biosensors employing surface plasmon resonance (SPR) technology are governed by two critical components, namely, 1) the plasmonic material responding to refractive index alteration on the sensing surface, and 2) surface functionalization by specific antibody so that the corresponding antigen can be captured and detected accordingly. While gold is the dominating plasmonic material, it is also expensive, fragile and incompatible with existing complementary metal-oxide-semiconductor (CMOS) fabrication technology. Thus, the scope to miniaturize chip-scale gold-based SPR devices is rather limited. Recently, we observed the renaissance of novel titanium nitride (TiN) plasmonic material, which is durable and CMOS compatible. It is thought that TiN may address some of the above-mentioned limitations. In this presentation, we fabricated TiN thinfilm of various thicknesses on glass (TiNG) by magnetron sputtering. It was found that with nominal TiN thickness of 30 nm, the refractive index resolution attains approximately 1.9×10^{-7} RIU, which is comparable to the performance of gold film. We have also attempted direct detection of biotin with the TiNG biosensor and monitored the subsequent biotin-streptavidin conjugation. As it was found that the biotin-TiN affinity is one order of magnitude better than that of biotin-gold, we were able to detect biotin directly to $1.2 \mu\text{g}\cdot\text{mL}^{-1}$ ($4.9 \mu\text{M}$) at flow rate of $5 \mu\text{L}\cdot\text{min}^{-1}$ in label-free manner. Thus, the detection limit of biotin is two orders of magnitude better than existing SPR devices. We have also explored the biotin-TiN interaction with periodic density functional theory via computational simulation and found that the exceptional biotin-TiN affinity may be due to the formation of both S-Ti and O-Ti bonds, whereas only S-Au bonds were formed on gold. In conclusion, we have proved that TiNG is a convincing alternative to existing gold-based SPR biosensors by both experimental and theoretical investigations.

Keywords: Immunosensors, surface plasmon resonance biosensing, label-free, titanium nitride thinfilm, biotin-streptavidin conjugation, direct detection.

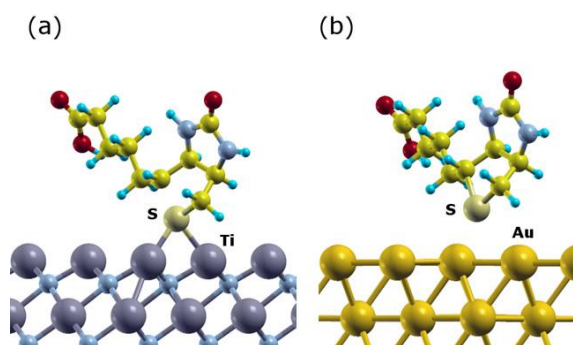


Figure 1: a) Absorption of biotin to the TiN (200) surface with formation of two S-Ti bonds and the adsorption energy is estimated to be -3.2 eV using DFT geometrical optimization, b) the absorption of biotin to the Au (111) surface is also calculated and it is found to be -0.8 eV which is much weaker and no S-Au chemical bond is formed.

References:

1. Naik, G.V., Shalae, V.M., Boltasseva, A., Alternative Plasmonic Materials: Beyond Gold and Silver, *Adv. Mater.* 25, 3264-3294.
2. Kabashin, A.V., Evans, P., Pastkovsky, S., Hendren, W., Wurtz, G.A., Atkinson, R., Pollard, R., Podolskiy, V.A., and Zayats, A.V., Plasmonic nanorod metamaterials for biosensing, *Nat. Mater.* 8, 867-871.

Effect of calcination temperature on photocatalytic activity of $\text{TiO}_2/\text{Bi}_x\text{O}_y$ Nanofibers in the photodegradation of Acid Orange 7 (AO7) under visible light irradiation

Juay Jermyn,¹ Siew Siang Lee,¹ Benny Yong Liang Tan,¹ Hongwei Bai,¹ Darren Delai Sun,¹
¹Nanyang Technological University

Abstract:

Currently, it is still a challenge to utilise Titanium Dioxide (TiO_2) to photocatalytically degrade dye wastewater under solar irradiation. This is due to the wide band gap of TiO_2 material (3.2 eV) which can only be activated by UV light irradiation. Bismuth (Bi) is one of the candidate that aids in the extension of TiO_2 nanomaterials photoactivity into visible light region but little has been studied on how the visible light photoactivity of these composite changes with its calcination temperature. In this study, 3 mol% Bismuth (Xu et al., 2011) was used to synthesis $\text{TiO}_2/\text{Bi}_x\text{O}_y$ nanofibers via a facile electrospinning (Bai et al., 2012). The composite nanofibers were calcined at 550°C, 650°C, 750°C, 850°C respectively and were characterised using XRD, FESEM and TEM. Subsequently, the photocatalytic activity of the composite nanofibers were studied with respect to its calcination temperature. The results illustrated in Figure 1b substantiates that Bi was successfully incorporated into TiO_2 which facilitates the extension of its activity into the visible light region (Wu, Lu, & Li, 2009). Moreover, from the photodegradation experiment, it revealed that the composite nanofibers exhibited higher activity than pure TiO_2 nanofibers in the degradation of Acid Orange 7 (AO7) under visible light irradiation. The analytical outcomes indicate that the $\text{TiO}_2/\text{Bi}_x\text{O}_y$ nanofibers calcined at 850°C exhibited highest photoactivity. This suggests that the phase transformation of TiO_2 between its anatase and rutile phase plays a significant part in enhancing the photoactivity of the $\text{TiO}_2/\text{Bi}_x\text{O}_y$ nanofibers.

Keywords: $\text{TiO}_2/\text{Bi}_x\text{O}_y$, Nanofibers, Electrospinning, Visible Light, photocatalytic oxidation, Dye wastewater, Acid Orange 7, Temperature,

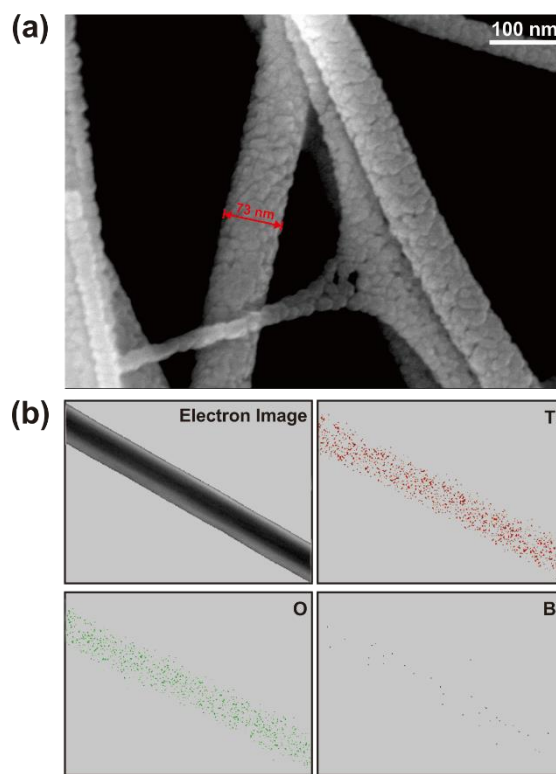


Figure 1: (a) FESEM image of $\text{TiO}_2/\text{Bi}_x\text{O}_y$ nanofibers (b) EDX dispersion pattern of the $\text{TiO}_2/\text{Bi}_x\text{O}_y$ nanofibers indicating the successful incorporation of Bismuth into the TiO_2 nanofibers.

References:

1. Bai, H., Juay, J., Liu, Z., Song, X., Lee, S. S., & Sun, D. D. (2012). Hierarchical $\text{SrTiO}_3/\text{TiO}_2$ nanofibers heterostructures with high efficiency in photocatalytic H_2 generation. *Applied Catalysis B: Environmental*, 125, 367-374.
2. Wu, Y., Lu, G., & Li, S. (2009). The Doping Effect of Bi on TiO_2 for Photocatalytic Hydrogen Generation and Photodecolorization of Rhodamine B. *The Journal of Physical Chemistry C*, 113(22), 9950-9955.
3. Xu, J., Wang, W., Shang, M., Gao, E., Zhang, Z., & Ren, J. (2011). Electrospun nanofibers of Bi-doped TiO_2 with high photocatalytic activity under visible light irradiation. *Journal of hazardous materials*, 196, 426-430.

Facile Synthesis of Highly Efficient One-Dimensional Plasmonic Photocatalysts

Jinyan Xiong¹, Zhen Li^{*,1,2}

¹ Institute for Superconducting & Electronic Materials, The University of Wollongong, NSW 2500, Australia.

² School of Radiation Medicine and Radiation Protection, Collaborative Innovation Center of Radiation Medicine of Jiangsu Higher Education Institutions, Soochow University, 199 Ren Ai Road, Suzhou Industrial Park, Suzhou 215123, China.

Abstract: Semiconductor photocatalysis have attracted considerable attention in recent years due to their great potential indevelopment of renewable and clean energy, as well as in environmental protection and remediation. The limited visible-light absorption and high recombination rate of electron-hole pairs of the commonly used semiconductor photocatalysts such as TiO₂, ZnO, Cu₂O, CdS, however, hinder their practical applications. Modification of photocatalysts with novel plasmonic metals to form metal/semiconductor heterostructures has been considered as a promising strategy to enhance their photocatalytic performance. Compared with other noble metals, one-dimensional (1D) Ag nanowires are more attractive because of their high electrical and thermal conductivity, antibacterial characteristics, low cost, nontoxicity, and a wealth of optical and photoelectrochemical properties directly related to their geometry-dependent surface plasmon resonances, which makes them very popular for fabrication of advanced semiconductor/noble metal nanophotocatalysts. Herein, we chose semiconductor oxides such as ZnO and Cu₂O as an example of photocatalysts, and investigated the optimum ratio of ZnO/Cu₂O to Ag nanostructures (Xiong *et al.*; 2014) and their performance. The resultant 1D Ag@ZnO/Cu₂O core-shell nanowires prepared by a facile and general ambient strategy exhibited much higher photocatalytic activity and stability towards degradation of organic contaminants than Ag@ZnO/Cu₂O core-shell nanoparticles and pure ZnO/Cu₂O nanocrystals under solar light irradiation. The core-shell 1D Ag@CdS nanowires also exhibit better photocatalytic performance than pure CdS. In addition, the 1D Ag-Ag₂S hybrid nanowires showed excellent dye adsorption performance, although the catalytic activity was not significantly enhanced.

Furthermore, they also exhibited potential applications in other areas such as lithium ion batteries and SESR detection of pollutants (Xiong *et al.*; 2015). It is expected this work not only provide a simple and general strategy to synthe-

size 1D Ag-oxides/sulfides heteronanostructured photocatalysts but also explore the potential applications of such 1D heterostructures in the field of energy.

Keywords: Ag@Cu₂O, Ag@ZnO, Ag@CdS, Ag-Ag₂S, one-dimensional structure, core-shell nanowires, plasmonic photocatalysts.

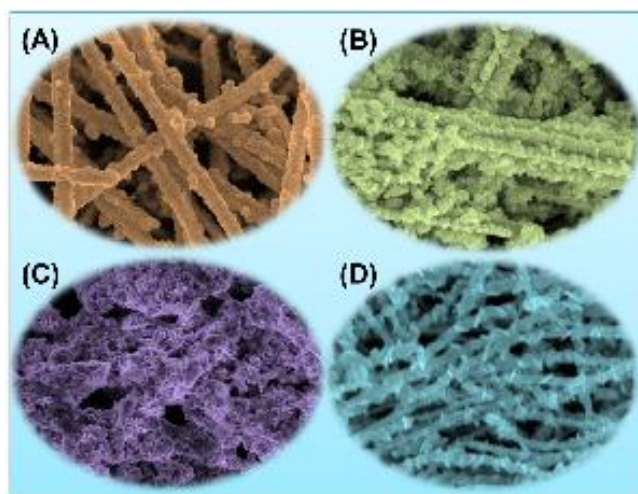


Figure 1: SEM images of 1D Ag@Cu₂O nanowires (A), Ag@ZnO nanowires (B), Ag@CdS nanowires (C), Ag-Ag₂S nanowires (D).

Acknowledgement

The authors gratefully acknowledge financial support from the Australian Research Council (ARC) through the Discovery Projects DP 130102274 and DP130102699, and from ISEM at UOW. The authors also acknowledge the use of the facilities in the UOW Electron Microscopy Centre.

References:

1. Xiong, J., Li, Z., Chen, J., Zhang, S., Wang, L., Dou, S. (2014), Facile Synthesis of Highly Efficient One-Dimensional Plasmonic Photocatalysts through Ag@Cu₂O Core-Shell Heteronanowires, *ACS Appl. Mater. Interfaces*, 6, 15716-15725.
2. Xiong, J., Han, C., Li, W., Sun, Q., Chen, J., Chou, S., Li, Z., Dou, S. (2016), Ambient Synthesis of a Multifunctional 1D/2D Hierarchical Ag-Ag₂S Nanowire/Nanosheet Heterostructure with Diverse Applications, *CrystEngComm*, 18, 930-937.

Analytical TEM study on the behavior of CeO₂ nanoparticles in Sb-V-CeO₂/TiO₂ catalysts for NH₃-SCR

Young Eun Jeong,^{1,2} Pullur Anil Kumar,² Kwan-young Lee,¹ Heon Phil Ha,^{2,*}

¹ Korea university, Department of Chemical and Biological Engineering, Seoul, Republic of Korea

² Korea Institute of Science and Technology, Materials Architecturing Research Center, Seoul, Republic of Korea

Abstract:

Selective catalytic reduction (SCR) with NH₃ is well known for the abatement of NO_x from the stationary power sources, ships and automobiles [1]. Commercially, WO₃ (or MoO₃)-V₂O₅-TiO₂ based catalysts are well established at narrow operating temperatures (300-400°C) [2].

Recently, *Ha et al.* promoted Sb added V₂O₅/TiO₂ catalysts that showed remarkably efficient sulfur resistance at low temperature (<250°C) compared to the WO₃-V₂O₅/TiO₂ commercial catalyst [3]. Furthermore, added Sb-V₂O₅-10% CeO₂/TiO₂ (SbVCT) catalyst showed almost 90% of NO_x conversion in the 800ppm SO₂ and 6% H₂O at 220°C [4]. Additionally, the SbVCT catalyst after sulfation pretreatment indicated higher both catalytic activity and physico-chemical properties than non-sulfated catalyst [5]. At 500°C sulfation, the catalytic activity was improved by surface acidity and sulfur toluene in relation with the Ce³⁺/Ce⁴⁺ ratio and formation of strong bulk-like sulfate species on the surface, which are mainly due to CeO₂ added. [6]. Therefore, from now on, the study of SbVCT catalyst is focused on only the performance through the various Ce ionic states. In this study, we will mainly discuss about the CeO₂ nanoparticle behavior on SbVCT catalyst and sulfated catalyst by TEM analysis. **Figure 1** shows the STEM images of the SbVCT catalyst. **Figure 1(a)** displays the fresh SbVCT catalyst with 2-4nm size of CeO₂ clusters formed on the anatase TiO₂ particles while the CeO₂ nanoparticles were dispersed well after sulfation at 500°C for 1hr in **Figure 1(b)**. The dispersion of CeO₂ on SbVCT sulfated catalyst revealed higher the NO_x conversion in low temperature range between 180 and 250°C than fresh catalyst (**Figure 2**). **Figure 3** exhibits SO₂-DRIFTS analysis carried out on the surface sulfate species formed on the 10% CeO₂/TiO₂ (CT) Sb-10% CeO₂/TiO₂ (SbCT), V-10% CeO₂/TiO₂ (VCT) and SbVCT catalysts. The SbVCT catalyst shows the highest spectra intensity of the band at 1267cm⁻¹, which indicates strong bulk-like sulfate species compare with others [7]. From the supported results, the CeO₂ nanoparticles behavior on the SbVCT catalyst has relationship with catalytic activity

after sulfation due to the following reasons : (i) highly dispersive CeO₂ nanoparticles on surface, (ii) synergetic effects of metal oxide compound owing to increasing total acidity and redox properties. The CeO₂ behavior and catalytic properties on SbVCT catalyst were thoroughly characterized by TEM with EDS mapping analysis, BET surface area, in situ DRIFT spectrometer, H₂-temperature programmed reduction, thermogravimetric analysis, and X-ray photoelectron spectroscopy.

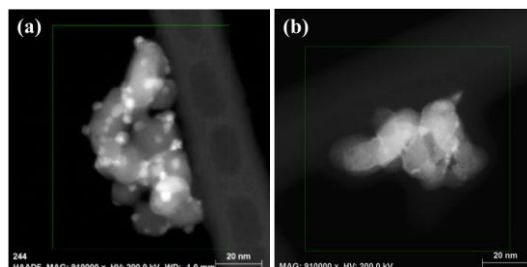


Figure 1: STEM image of the (a) fresh, (b) sulfated SbVCT catalyst.

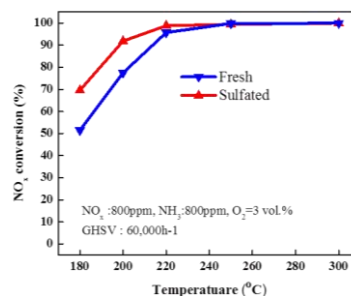


Figure 2: NO_x conversion of SbVCT catalysts

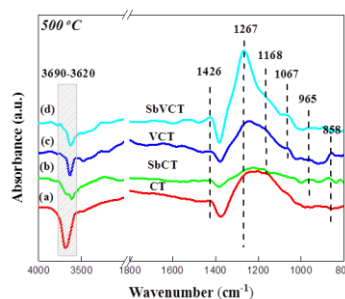


Figure 3: DRIFT spectra of catalysts exposed to 1000ppm SO₂+ 3vol. O₂ for 30min at 500°C.

Keywords: CeO₂ nanoparticles, TEM, EDS mapping, NH₃-SCR.

Photodegradation of Ofloxacin with nano-go/m Composite and it's reuse

P. Alicanoğlu,^{1*} D. T. Sponza,²

¹Pamukkale University, Department of Environmental Engineering, Denizli, Turkey

²Dokuz Eylul University, Department of Environmental Engineering, Izmir, Turkey

Abstract: Pharmaceuticals, newly recognized classes of environmental pollutants, are becoming increasingly problematic contaminants of either surface water or ground water around industrial and residential communities (Kyzas et al., 2015). Among widespread used antibiotics, fluoroquinolone antibiotics (FQ) are an important type with undetectable biodegradability (Kagle et al., 2009). Within the large class of FQs, ofloxacin (OFL) is used to treat urinary and respiratory tract infections in humans and animals (Goyne et al., 2005). Chemically, OFL, a fluorinated carboxyquinolone, is the racemate, (\pm)-9-fluoro-2,3-dihydro-3-methyl-10-(4-methyl-1-piperazinyl)-7-oxo-7H-pyrido[1,2,3-de]-1,4-benzoxazine-6-carboxylic acid (Min et al., 2011). In receiving environments, low concentrations of antibiotic traces can cause resistance to microorganisms (Bhandari et al., 2008). Concentrations OFL in wastewaters have been obtained to range from ng to mg L⁻¹ (Larsson et al., 2007), thus OFL removal from wastewater has become important. Graphene oxide (GO) with large quantities of oxygen atoms on the surface are present in the forms of epoxy, hydroxyl, and carboxyl groups. These functional groups make GO hydrophilic and suitable to be an adsorbent (Gao et al., 2012). Especially, some iron oxide nanomaterials composited with GO as magnetic adsorbents were a better solution (Mostofizadeh et al., 2011). Thus, the combination of GO with magnetic nanoparticles (Nano-GO/M) to produce a magnetic graphene-based composite and it will be separated from the matrix rapidly and easily by an external magnetic field. This study aims to investigate the removal of OFL at increasing concentrations (1, 3, 5, 25, 100, 500 and 1000 mg/L), at increasing irradiation times and at acidic (pH=4), neutral and alkaline (pH=10) conditions via photodegradation process by using UV light and sunlight. Also photodegradation products of OFL (POF (9-piperazino ofloxacin) and MOF (des-methyl ofloxacin) were investigated during the UV light process. The Nano-GO/M was prepared under laboratory conditions. The surface properties of the Nano-GO/M composite was investigated by a scanning electron microscope (SEM), fourier transform infra-

red spectroscopy (FTIR) and x-ray diffraction (XRD). For maximum OFL removal (93%) the optimum Nano-GO/M concentration was found to be 0.5 g/L at 1 mg/L OFL concentration, at pH of 6.5, at a UV power of 300 W and at a temperature of 21°C after 60 min retention time by UV light. For maximum OFL removal (82%) the optimum Nano-GO/M concentration was found to be 2 g/L at 1 mg/L OFL concentration, at pH of 6.5, after 350 min irradiation time, at 35°C \pm 5°C and with a power of 80 W sunlight. In this study, six sequential treatment steps were investigated for determination of reusability of Nano-GO/M composite. 0.5 g/L Nano-GO/M composite were used for six times under specified operational conditions (60 min, 300 W UV, 100 mg/L OFL, pH 6.5 and room temperature).

Keywords: Fluoroquinolone, Ofloxacin, Graphene, Magnetite, Nano composite, Photodegradation, UV irradiation, Sunlight

References:

1. Bhandari, A., Close, L. I., Kim, W., Hunter, R. P., Koch, D. E., Surampalli, R. Y. (2008) Occurrence of ciprofloxacin, sulfamethoxazole, and azithromycin in municipal wastewater treatment plants. *Practice Periodical of Hazardous, Toxic, and Radioactive Waste Management*, 12(4), 275–281.
2. Gao, Y., Zhang, L., Huang, H., Hu, J., Shah, S., Su, X. (2012). Adsorption and removal of tetracycline antibiotics from aqueous solution by graphene oxide. *J. Colloid Interface Sci.*, 1, 540–546.
3. Goyne, K. W., Chorover, J., Kubicki, J. D., Zimmerman, A. R., Brantley S. (2005) Sorption of the antibiotic ofloxacin to mesoporous and nonporous alumina and silica. *Journal of Colloid and Interface Science*, 283, 160–170.
4. Kagle, J., Porter, A.W., Murdoch, R.W., Rivera-Cancel, G., Hay, A.G. (2009) Biodegradation of pharmaceutical and personal care products. *Adv. Appl. Microbiol.*, 67, 65–108.
5. Kyzas, G., Fu, J., Lazaridis, N., Bikiaris, D., Matis, K. (2015) New approaches on the removal of pharmaceuticals from wastewaters with adsorbent materials. *Journal of Molecular Liquids*, 209, 87–93.
6. Larsson, D.G., Pedro, C., Paxeus, N. (2007). Effluent from drug manufactures contains extremely high levels of pharmaceuticals. *J. Hazard. Mater.*, 148, 751–755.
7. Min, X., Zhao-Rong, M., Liang, H., Feng-Juan, C., Zheng-zhi, Z. (2011) Spectroscopic studies on the interaction between Pr(III) complex of an ofloxacin derivative and bovine serum albumin or DNA- *Spectrochimica Acta Part A: Molecular and Biomolecular Spectroscopy*, 78, 503–511.
8. Mostofizadeh, A., Li, Y., Song, B., Huang, Y. (2011). Synthesis, properties, and applications of low dimensional carbon-related nanomaterials. *J. Nanomater.*, 68, 50-81.

Nanostructures as Catalysts for H₂O₂ Electrogeneration and Degradation of Organic Pollutants

M. C. Santos¹

¹ LEMN – CCNH - Universidade Federal do ABC, UFABC, Santo André, SP, Brazil.

Abstract: Electrogeneration of H₂O₂ is one of the most important processes today for production of this molecule with low cost and without storage and transport. H₂O₂ is recognized as both a good and an environmental friendly in Electrochemical Advanced Oxidative Processes (EAOPs). The use of nanostructures and modification of carbonaceous materials for H₂O₂ electrogeneration and degradation of organic pollutants using Advanced Oxidative Processes has been extensively studied by our group [1 - 5]. The main materials are related to: 1) carbon materials modified with functional groups by acidic and alkaline treatment and 2) nanomaterials modifying carbon support. The effects of increasing H₂O₂ electrogeneration are associated to the surface properties of the two materials above which are completely different from those ones of pure carbon for the activity toward H₂O₂. For this reason, we have been developing changes of the carbon materials with acidic and alkaline treatment [1], using nanostructures of different oxides and metals with very small amounts on carbon and base materials for H₂O₂ electrogeneration and electrochemical degradation of Dipirone, Phenol, Evans Blue and Ciprofloxacin [2 - 6]. The main goal of this work is to discuss the modification of the carbon properties such as hydrophilicity, conductivity, structure and composition of the surface species when we prepare both different carbon treatments and different proportions of nanostructures with several oxides and metals on carbon. With rotating ring-disk experiments is clearly indicated that ring currents (due to peroxide electrogeneration) are the highest using carbon modified materials with acidic treatment and nanostructures such as: CeO₂/C (4%), WO₃/C (1%), W@Au/C (1%) and nanospheres of TiO₂ covered with gold nanoparticles on carbon). For dipirone one can observe using different EAOPs very good results as CeO₂/C 4% gas diffusion electrode GDE which produced 331 mg L⁻¹ of H₂O₂ while Vulcan carbon produced 108 mg L⁻¹, more than three times higher, since Ce(III) and Ce(IV) species on carbon in similar concentration facilitated the formation of H₂O₂. Electro-Fenton process mineralized 57 % of the dipirone in 5 min at -1.1 V. Regarding

phenol 1% WO₃/C produced 585 mg L⁻¹ of H₂O₂ while Vulcan carbon produced 100 mg L⁻¹. Lower quantities of metal on carbon supports are more efficient for H₂O₂ formation. WO₃/C material exhibits surface acidity by the presence of W⁶⁺ and oxygenated species. Acid surface provides hydrophilicity and higher activity in ORR for H₂O₂ production. Photo-electro-Fenton allowed 75 % phenol mineralization following 12 h of electrolysis.

Keywords: Hydrogen peroxide electrogeneration, Oxygen reduction reaction, Nanostructures, Degradation of organic pollutants.

References:

1. Moraes, A., Assumpção M. H. M. T.; Simões F. C., Hammer, P., Lanza, M. R. V., Santos, M.C. (2016) Surface and Catalytic effects on Treated Carbon Materials for Hydrogen Peroxide Electrogeneration. *Electrocatalysis*, 7, 60-69.
2. Assumpção, M.H.M.T., Moraes, A., De Souza, R.F.B., REIS, R.M., Rocha, R.S., Gaubeur, I., Calegari, M.L., Hammer, P., Lanza, M.R.V., Santos, M.C. (2013) Degradation of Dipyrone via Advanced Oxidation Processes using a Cerium Nanostructured Electrocatalyst Material. *Applied Catalysis. A, General*, 462, 256-261.
3. Assumpção, M. H. M. T., De Souza, R. F. B., Reis, R. M., Rocha, R. S., Steter, J. R., Hammer, P., Gaubeur, I., Calegari, M. L., Lanza, M. R. V., Santos, M.C. (2013). Low Tungsten Content of Nanostructured Material supported on Carbon for the Degradation of Phenol. *Applied Catalysis. B, Environmental*, 142-143, 479-486.
4. Antonin, V. S., Garcia-Segura, S., Santos, M.C., Brillas, E. (2015). Degradation of Evans Blue diazo dye by electrochemical processes based on Fenton's reaction chemistry. *Journal of Electroanalytical Chemistry*, 747, 1-11.
5. Antonin, V. S., Santos, M. C., Garcia-Segura, S., E Brillas (2015). Electrochemical incineration of the antibiotic ciprofloxacin in sulfate medium and synthetic urine matrix. *Water Research*, 83, 31-41.

Designing efficient bimetallic photocatalysts for hydrogen production

Eran Aronovitch^{1*}, Philip Kalisman², Lothar Houben³, Lilac Amirav², Maya Bar-Sadan^{1*}

¹ Department of Chemistry, Ben-Gurion University of the Negev, Beer-Sheva, Israel

² Schulich Faculty of Chemistry, The Russell Berrie Nanotechnology Institute, and The Nancy and Stephen Grand Technion Energy Program; Technion – Israel Institute of Technology, Haifa 32000, Israel

³ Peter Grünberg Institut 5 and Ernst Ruska-Centre for Microscopy and Spectroscopy with Electrons, Forschungszentrum Jülich GmbH, 52425 Jülich, Germany.

Abstract:

The search for alternative clean and renewable energy source is a major pressing issue. One promising direction is the use of semiconductor nanoparticles as photocatalysts which absorb the solar radiation and produce hydrogen from water. Upon radiation, excited electrons and holes are created. They then migrate to the surface and react with the aqueous solution. Efficient photocatalysts should maintain charge separation of the holes and electrons and contain different sites for oxidation and reduction. Usually a small metallic particle is deposited on the semiconductor which acts as an electron sink and a reduction site for protons. Hybrid core-shell structures such as CdS@CdSe increase the charge separation and reduce the particle dissolution by confining the holes to the core and leaving the electrons delocalized over the entire structure. A bimetallic co-catalyst composed of metals such as gold and palladium should improve the photocatalytic activity of the system. Such bimetallic particles possess the ability to attract electrons from the semiconductor and discharge them into the aqueous solution more efficiently than each of the metals on their own. Here we use the CdSe@CdS-Au/Pd system as a case study to explore the effect of the inner structure of the bimetallic tip on the photocatalytic performance. In addition we study the dynamic processes which occur during photocatalysis. For this aim we used high resolution energy dispersive spectroscopy (EDS) for the system characterization and an online GC equipped setup for the long duration photocatalytic hydrogen evolution measurements.

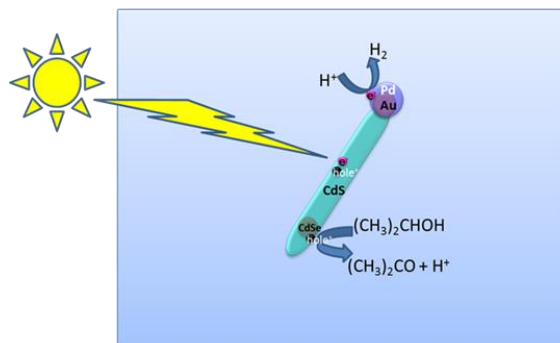


Figure 1: Figure illustrating the hydrogen evolution process and the roles of the photocatalysts' different components; light harvesting CdS rod, charge carriers attractors: CdSe core and bimetallic tip, and reduction site for protons - the bimetallic tip.

Keywords: HR-STEM, photocatalysis, water splitting, nano-hetero structures, hydrogen evolution catalyst.

Reference:

1. Aronovitch, E.; Kalisman, P.; Mangel, S.; Houben, L.; Amirav, L.; Bar-Sadan*, M.; Designing Bimetallic Co-catalysts: A Party of Two. *J. Phys. Chem. Lett.* 6, 3760 (2015).
2. Kalisman, P.; Houben, L.; Aronovitch, E.; Kauffmann, Y.; Bar Sadan, M.; Amirav, L.; The Golden Gate to Photocatalytic Hydrogen Production. *J. Mater. Chem. A*, 3, 19679-19682 (2015).

Enhancing Cuprous Oxide Stability for Hydrogen Evolution

J. Azevedo^{1*}, S.D. Tilley², M. Schreier³, M. Stefik⁴, L. Steier³, P. Dias¹, C.T. Sousa⁵, J.P. Araújo⁵,
M.T. Mayer³, M. Graetzel³, A. Mendes^{1**}
¹LEPABE, Porto, 4200-465, Portugal
²UZH, Zurich, 8092, Switzerland
³EPFL, LPI, Lausanne, 1015, Switzerland
⁴University of South Carolina, 29208, USA
⁵IFIMUP, Porto, 4169-007, Portugal

Abstract: The possibility of producing chemical fuels from solar energy has become increasingly attractive as sustainable, clean and efficient solution to our ever-growing energy demands. Photo-electrochemical (PEC) water splitting has been much improved since the first reports in the 70s¹ and nowadays researchers aim to find inexpensive, efficient and stable materials to perform PEC water splitting. Cuprous oxide, Cu₂O, is very interesting since it has a 2 eV bandgap with favorable energy band positions, good conductivity and it can be processed with low-cost methods such as electrodeposition. Cu₂O has been proven an efficient material with current densities up to 7.5 mA cm⁻² under AM 1.5 illumination and biased at 0 V_{RHE}² nevertheless it is not stable in contact with the electrolyte, decomposing completely after few minutes. For real applications, much more is required and new strategies are needed to overcome this limitation. In this work, we focus on improving the Cu₂O stability up to ~60 h with only 10 % loss. Electrodeposition and atomic layer deposition (ALD) were used to synthesize the Cu₂O and for over-layer deposition, respectively, and are here described.³ A simple low-cost solution was developed to greatly enhance the Cu₂O photocathode stability. Steam treatments employed on Cu₂O/AZO/TiO₂ photocathodes allow for stability improvement using both RuO₂ and Pt catalysts.⁴ Not only did we obtain enhanced stabilities in both cases, we also uncovered the critical importance of morphological changes of the surface in generating these high-stability photocathodes. The most used protection layer for Cu₂O is still TiO₂.^{2,3,4} In this study it was discovered that ALD deposited SnO₂ is a promising candidate overlayer for stabilizing photocathodes for hydrogen evolution.

Keywords: water splitting; cuprous oxide; steam treatment; stability; protective layer.

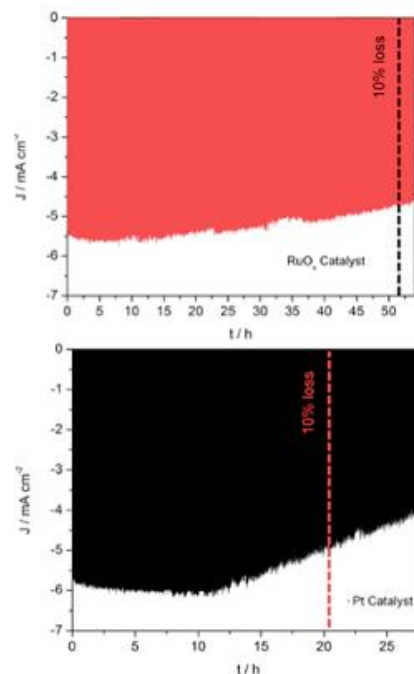


Figure 1: Performance of a composite Cu₂O photocathode after steam treatment: chronoamperometric stability measurement biased at 0 V_{RHE} in pH 5.0 phosphate-sulfate electrolyte under light chopping with (b) RuO_x and (c) Pt as catalyst.

The performance and stability were influenced by the film thickness, post-deposition steam treatment, and the nature of the heterojunction interface. The optimized device exhibited great stability, maintaining 90 % of its initial photocurrent after 57 h of sustained photoelectrochemical water reduction. These new results open a much-needed window to make this semiconductor a strong competitor for solar water splitting applications.

References:

1. A.Fujishima, K. Honda, *Nature*, 238(3), 37-38, 1972.
2. A. Paracchino, V. Laporte, K. Sivula, M. Graetzel, E. Thimsen, *Nature Materials*, 10(6), 456-461, 2011.
3. S.D. Tilley, M. Schreier, J. Azevedo, M. Stefik, M. Graetzel, *Advanced Functional Materials*, 24(3), 303-311, 2014.
4. J.Azevedo, L. Steier, P. Dias, M. Stefik, C.T. Sousa, J.P. Araujo, A. Mendes, M. Graetzel, S.D. Tilley, *Energy & Environmental Science*, 7, 4044-4052, 2014.

Preparation of Basic Type of Activated Alumina Supports for Using in Production and Separation of Hydrogen

M. Duran, F.N. Tüzün

Hitit University, Department of Chemical Engineering, 19100, Çorum, Turkey

Abstract:

Hydrogen permeable membranes are highly attractive in the membrane gas separation field due to the importance of hydrogen (Lee et al., 2004). However, there has been great interest for catalytic membranes providing the production and separation of hydrogen at the same time (Kurungot et al., 2003 and Lee, D., Hacırlıoğlu, P., Oyama, S.T., 2004). This study contains the development of basic activated alumina supports employed in the preparation of membrane reactors for hydrogen production and separation. For this reason, three different basic types of activated alumina supports were developed by using three different Si/Al molar ratio at two different calcination temperatures. Supports developed are in disc shape having the diameter of 21 mm with the thickness of 1 mm (Figure 1). Then, effect of different Si/Al molar ratio and annealing temperature variations on supports was explored with the usage of BET instrument. Surface area and pore diameter of supports changed around 1.99-2.17 m²/g and 2.13-2.39 nm respectively as a consequence of calcination temperature of 1200°C. Surface area and pore diameter of supports also increased around 54.08-67.66 m²/g and 6.41-6.52 nm by reducing the calcination temperature to 600°C.

Keywords: basic type activated alumina, porous alumina support, hydrogen production and separation, binder



Figure 1: Figure indicates the support sample manufactured with having the disc shape in terms of diameter of 21 mm and thickness of 1 mm

References:

1. Lee, D. et al. (2004) Synthesis, characterization and gas permeation properties of a hydrogen permeable silica membrane supported on porous alumina, *Journal of Membrane Science*, 231, 117-126 .
2. Kurungot, S. , Yamaguchi, T. , Nakao, S.(2003) Rh / γ -Al₂O₃ catalytic layer integrated with sol-gel synthesized microporous silica membrane for compact membrane reactor applications, *Catalysis Letters*, 86(4), 273-278 .
3. Lee, D., Hacırlıoğlu, P., Oyama, S.T.(2004) The effect of pressure in membrane reactors: trade-off in permeability and equilibrium conversion in the catalytic reforming of CH₄ with CO₂ at high pressure, *Topics in Catalysis*, 29(1-2), 45-57.

On the applicability of Johnson-Mehl-Avrami-Kolmogorov (JMAK) approach in explaining the hydrogen sorption kinetics in nanocrystalline magnesium hydride

S. Shriniwasan^{1*}, A. Gangrade¹, N.K. Gor¹, H.-Y. Tien², M. Tanniru², F. Ebrahimi² and S.S.V. Tatiparti^{1,2}

¹ Indian Institute of Technology Bombay, Department of Energy Science and Engineering, Mumbai-400076, India.

² University of Florida, Materials Science and Engineering Department, Gainesville, FL 32611, USA.

Abstract:

Magnesium hydride (MgH_2) can be a promising material for on-board hydrogen storage due to its high gravimetric capacity (7.6 wt. %). However, its applicability is hindered by the slow kinetics of hydrogen absorption and desorption ('sorption'). During sorption the nucleation of the growing phase is followed by its interfacial and diffusional growth. One or more of these phenomena can be rate limiting, thus deciding the overall kinetics. To enhance the kinetics it is necessary to understand the sorption mechanisms. Hydrogen sorption mechanism in $\text{Mg}(\text{H}_2)$ is studied using Johnson-Mehl-Avrami-Kolmogorov (JMAK) equation represented as $\alpha = 1 - \exp(-kt^n)$, where α is the converted fraction of the growing phase, k is the kinetic factor which gives information about the nucleation density (N_o), interface velocity (U) and growth dimensionality of the growing phase (n). Interestingly, the very detailed analysis presented here shows that n , k change with time which in turn affect N_o and U . Investigations on hydrogen sorption mechanism in nanocrystalline MgH_2 (~80 nm) were carried out through absorption/desorption experiments at several temperatures (150 – 400 °C). It was observed that n decreases with time. A transition from interfacial to diffusional growth during sorption was observed as suggested by a change in the interface velocity by ~2 orders; decrease in the estimated diffusion coefficients (Fick's 2nd law) by ~2-5 orders. The changes in these kinetic parameters are supported by microscopic analysis (HRTEM, SEM). Microscopic analysis reveals that the change in morphology of the growing phase (formation of core-shell structure) results in the decrease of growth dimensionality (n). The changing n was further used in explaining the trends in the nucleation density (N_o) and the kinetic factor (k). These trends were explained by developing several mathematical functions for interfacial and diffusional regime. The present analysis shows that the applicability of the JMAK approach and its related equations

change with the changing kinetic mechanisms of sorption in nanocrystalline MgH_2 .

Keywords: MgH_2 , hydrogen sorption, JMAK, interfacial growth, diffusional growth.

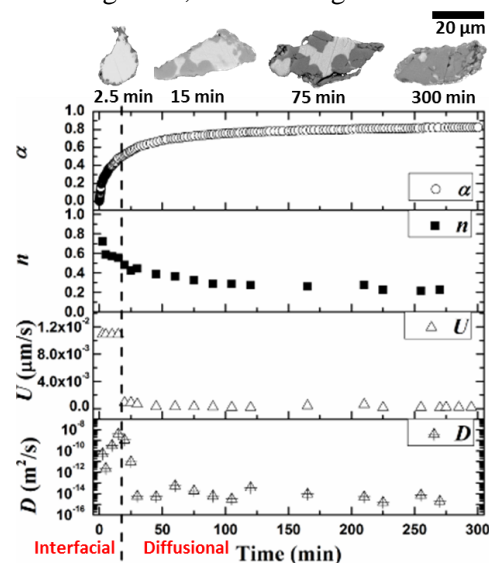


Figure 1: Transition from interfacial to diffusional growth represented in terms of the n , U and D and microscopic images for hydrogen absorption in Mg at 210 °C and $P_{\text{H}_2}=1$ MPa.

References:

1. S. Shriniwasan, H.-Y. Tien, M. Tanniru, F. Ebrahimi, S.S.V. Tatiparti, *Mater. Lett.*, **161** (2015), 271-274.
2. S. Shriniwasan, H. Goswami, H.-Y. Tien, M. Tanniru, F. Ebrahimi, S.S.V. Tatiparti, *Int. J. Hydrogen Energy*, **40** (2015), 13518-13529.

Improving the Adhesion Capacity of Foliar Nitrogen Fertilizer through Nano networks

D. Cai^{1,2,*}, N. Zhong³, P. Zhao³, Z. Wu^{1,2,*}

¹ Key Laboratory of Ion Beam Bioengineering, Hefei Institutes of Physical Science, Chinese Academy of Sciences, Hefei, Anhui 230031, Rep. of China

² Bioenergy Forest Research Centre of State Forestry Administration, Hefei 230031, Rep. of China

³ Institute of Microbiology, Chinese Academy of Sciences, Beijing 100101, Rep. of China

*Corresponding authors. Tel.: +86-551-65595143; Fax: +86-551-65591413. E-mail addresses: dqcai@ipp.ac.cn (D. Cai), zywu@ipp.ac.cn (Z. Wu)

Abstract:

Traditional foliar nitrogen fertilizer (TFNF) on crop leaves tends to discharge into environment through rainwater washing, leaching, and volatilization, resulting in severe pollution. Hence, it is important to improve the adhesion capacity of FNF. This work describes a loss-control foliar nitrogen fertilizer (LCFNF) by adding attapulgite (ATP) irradiated by high-energy electron beam (HEEB), as a loss control agent (LCA), to TFNF. LCA possesses a micro/nano networks structure and thus could bind a large amount of nitrogen to form fertilizer-ATP complex which could be then retained by the rough surface of crop leaves to increase the adhesion ability of TFNF. Therefore, LCFNF displayed lower loss amount and higher utilization efficiency compared with TFNF. This work provides a facile method to decrease the loss of TFNF and thus lower the environment pollution risk.

Keywords: foliar nitrogen fertilizer, attapulgite, biochar and biosilica, adhesion, loss control.

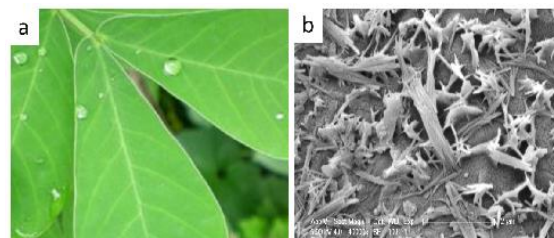


Figure 1: (a) Digital photo of peanut leaf; (b) SEM image of LCFNF. LCA possesses a micro/nano networks structure and thus could bind a large amount of nitrogen to form fertilizer-ATP complex which could be then retained by the rough surface of crop leaves to increase the adhesion ability of TFNF.

References:

1. Cai, D., Wu, Z., Jiang, J., Wu, Y., Feng, H., Brown, I., Chu, P., Yu, Z. (2014), Controlling nitrogen migration through micro-nano networks, *Sci. Rep.*, 4, 3665-3672.
2. Finney, K., Meyer, J., Smith, F., Fryer, H. (1957), Effect of foliar spraying of pawnee wheat with urea solutions on yield, protein content, and protein quality, *Agron. J.*, 49, 341-347.
3. Fernandez, V., Ebert, G. (2005), Foliar iron fertilization: a critical review, *J. Plant Nutr.*, 28, 2113-2124.
4. Matocha, M., Krutz, L., Reddy, K., Senseman, S., Locke, M., Steinriede, R., Palmer, E. (2006), Foliar washoff potential and surface runoff losses of trifloxysulfuron in cotton, *J. Agric. Food Chem.*, 54, 5498-5502.

Development of an “anti-bug” Bicomponent Fibre

M. Bischoff¹, G. Seide¹, T. Gries¹

¹Institut für Textiltechnik, RWTH Aachen University, Aachen, Germany

Abstract:

Nowadays crop spraying is mostly done with pesticides, which harm crop enemies, but can also interfere with the human body. Silica particles (SiO_2) in the nanometer and micrometer scale offer a physical way to combat insects without harming humans and other mammals. Thereby, they allow to forego pesticides, which can harm the environment. As silica particles are supplied as a powder or in a suspension to farmers, the silica use in large scale agriculture is not sufficient due to erosion through wind and rain.

When silica is implemented in a textile's surface (uncovered by polymer), particles are locally bound and do resist erosion, but can function against bugs. By choosing polypropylene as a matrix polymer, the production of an inexpensive agritextile with an “anti-bug” effect is made possible. In the Symposium the results of

1) preliminary experiments from lab scale extruded filaments (Figure 1 and 2) and of

2) compound development and investigation as well as selection and furthermore

3) the fibre manufacturing on a pilot scale melt spinning line and fibre investigation will be shown. For the compound manufacture, a selected number of investigated silica particles are shown (3 out of 8, different sizes in the nano and micron range: small, medium and large) and results of filler content and filter testing are portrayed and explained. In the following, one particle type is selected for the fibre manufacture in a semi-industrial scale. In a melt-spinning process, bicomponent fibres are manufactured. These fibres consist of a virgin polypropylene core and a functionalized silica sheath as shown in graph 1. In the Symposium both the manufacturing characteristics and varied parameter will be shown as well as their influence on the fibre characteristics are investigated.

Keywords: agriculture, environment, textile, silica, insects, protection

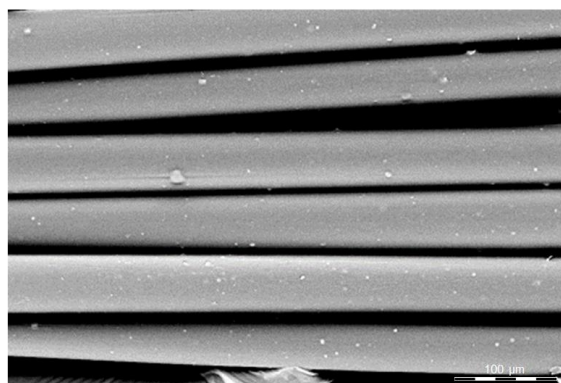


Figure 1: PP fibre with 5,2 wt.% Aerosil R812

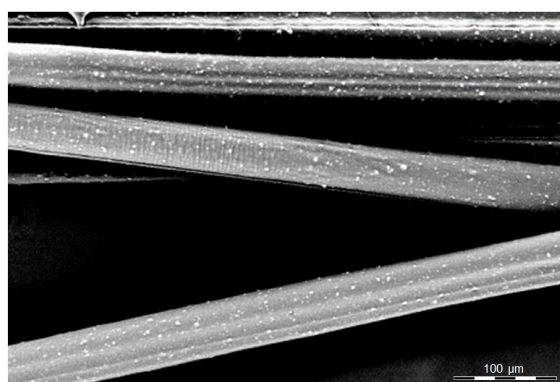
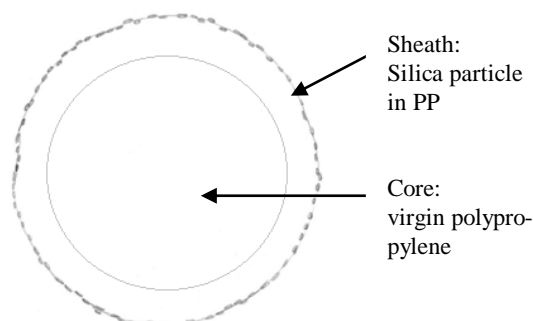


Figure 2: PP fibre with 4,5 wt% Syloid 244



Graph 1: Bicomponent fibre with virgin polypropylene core and functionalized sheath

References:

John, H. (2011) Untersuchungen zur Wirksamkeit synthetisch-amorpher Kieselsäure gegen den Glänzendschwarzen Getreideschimmelkäfer Dissertation, Leipzig

Molecularly Imprinted Polymer Nano layers for the electrochemical detection of pesticides

S. Bouden,¹ V. Bertagna,¹ B. Cagnon,¹ C. Vautrin-UI¹

¹ ICMN, Laboratoire Interfaces, Confinement, Matériaux et Nanostructure UMR 73 74 Université d'Orléans – CNRS 1B rue de la Férolierie, 45071 Orléans Cedex 2, France

Abstract:

The use of many pesticides in agriculture is responsible for their release into the environment and these substances have a negative impact on the ecosystem. In fact, their degradation products and their metabolites are toxic toward living organisms. Furthermore, the monitoring of the quality of groundwater and surface water showed many aquifers contamination by these pollutants. It is therefore crucial to develop rapid, sensitive and selective technical analysis for the *in-situ* monitoring of these pollutants in real-time. Modified surfaces by Molecular Imprinted Polymers (MIPs) are a cross-linked polymers which contain specific cavities corresponding to a template molecule imprint. MIPs based nano layers have become an important tool for sensing applications (Figure 1). In fact, MIPs have high selectivity, and are very stable, robust, easy to obtain and low cost, which make them interesting especially for *in-situ* sensing devices. Furthermore, the combination of the large selectivity of MIPs nano layers with the high sensitivity of the electrochemical methods enables to reach high analytical performances. In this context, our aim is to develop modified carbon electrodes by thin films of molecularly imprinted polypyrrole (PPy) for electrochemical detection of selected pesticides such as Isoproturon. The pesticide molecule-imprinted PPy is electrochemically prepared on glassy carbon and on screen printed electrodes in aqueous solutions of pyrrole and template molecule. Cyclic voltammetry and chronoamperometry are compared as electropolymerization methods and electrochemical parameters such as electrodeposition time, electrodeposition potential, scan number and scan rate are studied. The specific and selective recognition of the targeted molecule by the imprinted PPy is showed by comparison with results obtained on non-imprinted PPy. The modified electrodes are characterized by IRTF and microscopy (AFM, SEM).

Finally, electrochemical detection of pesticides is achieved by square wave voltammetry after a preconcentration first step.

Keywords: MIPs nanolayers, pesticides pollutants, electropolymerization, electrochemical sensor, MIPs/ Carbon sensor, electrochemical layer characterization, molecular recognition.

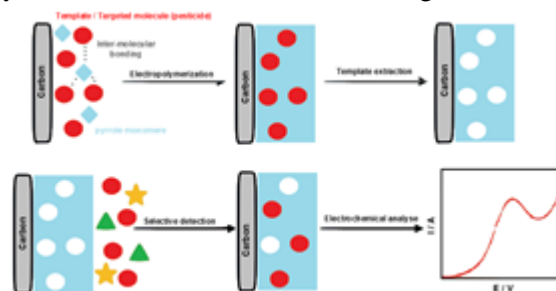


Figure 1: Figure illustrating the development of a MIPs/ Carbon sensor.

References:

1. Sharma, P. S., Dabrowski, M., Souza, F. D., Kutner, W. (2013) Surface development of molecularly imprinted polymer films to enhance sensing signals, *TrAC.*, 51, 146-157.
2. Suryanarayanan, V., Wu, C. T., Ho, K. C. (2010) Molecularly imprinted electrochemical sensors, *Electroanalysis*, 22, 1795-1811.
3. da Silva, H., Pacheco, J. G., MCS Magalhães, J. (2014) MIP-graphene-modified glassy carbon electrode for the determination of trimethoprim, *Biosens. Bioelectron.*, 52, 56-61.

Carbon Nanofibers–Ionic Liquid Composite Sensors For Detection of Trace Heavy Metals

Larbi. OULARBI,^{1,2} Mamia. EL RHAZI,¹ Mireille. TURMINE,²

¹University Hassan II Casablanca, Faculty of Science and Technology, Laboratory of Physical Chemistry & Bioorganic Chemistry, Mohammedia Morocco

²Sorbonne University, UPMC Univ Paris 06, CNRS, Laboratoire Interfaces et Systèmes Electrochimiques, 4 place Jussieu, F-75005, Paris, France

Abstract

Heavy metal contaminations is one of the major problems for environment and human health due to high toxicity, are also a major environmental contaminants found in air, soil and drinking water. Among of them, lead ion Pb^{2+} is one of the most toxic environmental pollutants even at very low concentrations [1]. Considering the severe toxicity of lead ion, developing sensitive and selective strategies for Pb^{2+} detection has been of great concern in the past decades as well as recent years. The electroanalytical techniques are one of the most techniques used for detection and analysis of trace heavy metals ions, because of their attractive features, including easiness, robustness and their low cost. During the last decades, different approaches have been used to develop high-performance electrochemical sensors based on modified electrodes by carbon nanomaterials (CNMs). Carbon nanofibers (CNFs) are one of them and have recently attracted much attention in diverse application areas especially in electroanalysis and biosensing owing to their unique characteristics such as excellent electrical and thermal conductivities, high chemical and mechanical stability, and large specific area [2]. Room Temperature Ionic Liquids (RTILs) are a new class of purely ionic, salt-like materials that are liquid at unusual low temperatures. Because of their high stability, fair electrical conductivity, and very low vapor pressure, ILs hold a great promise for green chemistry applications in general and for electrochemical applications in particular [3]. In the present work a new composite electrode has been fabricated by using CNFs and an ionic liquid, 1-ethyl-3-methylimidazolium bis(tri-fluoro-methylsulfonyl)imide, [EMIM][NTf2]. This electrode shows very attractive electrochemical performances compared to other conventional electrodes using graphite and mineral oil, notably improved sensitivity and stability. The interface properties of obtained composite were characterized by cyclic voltammetry (CV), electrochemical impedance spectroscopy (EIS), and the morphology was examined by scanning electron mi-

croscopy (SEM-FEG). This new composite demonstrated interesting performances for lead detection, and also a better sensibility, and stability.

Keywords: Carbon nanofibers, Room Temperature Ionic Liquids, Electrochemical sensors, Lead detection.

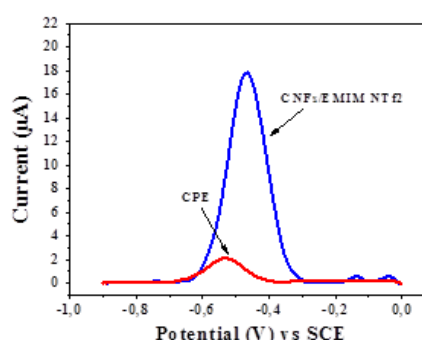


Figure1: Anodic Stripping Square Wave Voltammetry (ASSWV) for 50 ppb Pb^{2+} in 0.1 M acetate buffer at the CPE and CNFs/EMIM NTf2 electrode. Deposition potential: -1.1 V, deposition time: 2 min.

References

- [1] A. C. Todd, J.G. Wetmur, J.M. Moline, J.H. Godbold, S.M. Levin, and P.J. Landrigan. (1996) "Unraveling the Chronic Toxicity of Lead: An Essential Priority for Environmental Health," *Environ. Health Perspect.*, vol. 104, pp. 141–146.
- [2] D. Zhao, T. Wang, D. Han, C. Rusinek, A.J. Steckl, and W. R. Heineman. (2015) "Electrospun Carbon Nanofiber Modified Electrodes for Stripping Voltammetry," *Anal. Chem.*, vol. 87, no. 18, pp. 9315–9321.
- [3] J. G. Huddleston, A. E. Visser, W. M. Reichert, H. D. Willauer, G. A. Broker, R. D. Rogers. (2001), "Characterization and comparison of hydrophilic and hydrophobic room temperature ionic liquids incorporating the imidazolium cation," *Green Chem.*, vol. 3, no. 4, pp. 156–164.

Zero valent iron nanoparticles for remediation of soils contaminated with heavy metals

Olga Cortes¹, Susana Machado², Nádia Vital¹, Helena Gouveia¹, Vítor Correia³, Tomás Albergaria², Cristina Delerue Matos²

¹ISQ, Taguspark – Oeiras, Portugal;

²REQUIMTE/LAQV, Instituto Superior de Engenharia do Porto, Instituto Politécnico do Porto, Porto, Portugal

³Geoplano Consultores, SA, Lisboa, Portugal

Abstract:

Zero-valent iron nanoparticles (nZVIs) have become extremely popular, in the last decade, for environmental remediation. Their size and high surface area makes them a highly reactive agent for degrading a wide range of pollutants in contaminated soils (Machado et al, 2015).

There are two distinct approaches for synthesizing nZVIs: the top-down and the bottom-up. The former transforms micro and macro materials in nanosized materials using mechanical and/or chemical processes while the latter promotes the growth of the particles through chemical reactions (Hoag et al. 2009). In the bottom-up approach the innovative green method, that uses natural extract as reducing agent to produce nZVI, can be highlighted due to its advantages. Among them it can be stressed the fact that the natural extract can act as a capping agent that protects the iron nanoparticles from premature oxidation and agglomeration. In addition, it can be used as a source of nutrients and microorganisms for a possible bioremediation. The increasing interest in these green based-methods requires in-depth studies that would allow to evaluate their efficiencies when compared to already commercially available nZVI products. Following this, the main objective of this work was to simulate, at a laboratory scale, the remediation of soils contaminated with Zinc and Chromium (VI), comparing the efficiencies of two distinct types of nZVIs: the green and the commercial ones (Nanofer 25s). Different sets of column tests were performed in heavy metal contaminated soils collected at Parque Empresarial do Barreiro, Lisbon, Portugal. In each set of tests a distinct parameter was studied: nZVI dosage, reaction time and sequence of injection. Preliminary results allowed concluding that both nZVIs (commercial and green) are efficient to remediate the soils contaminated with Zinc and Chromium, validating the green nZVI as an alternative method. Further full-scale ecosystem studies addressing integrative risk assessment and life cycle assessment approaches are needed to guarantee a

responsible and sustainable use of the green-based method.

Keywords: zero-valent iron, nanoparticles, soil, chromium, zinc, green.

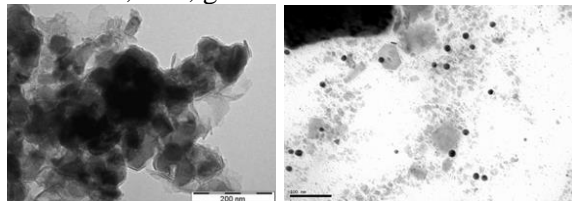


Figure 1: Transmission electron microscopy (TEM) analysis of the Nanofer 25s (left) and green nZVI (right).

Acknowledgements:

This work received financial support from the European Union (FEDER funds through COMPETE) and National Funds (FCT, Fundação para a Ciência e a Tecnologia) through projects UID/QUI/50006/2013.

References:

1. Machado, S., Pacheco, J.G., Nouws, H.P.A., Albergaria J.T., C. Delerue-Matos C. (2015) Characterization of green zero-valent iron nanoparticles produced with tree leaf extracts, *Sci. Total. Environ.*, 533, 76–81.
2. Hoag, G.E., Collins, J.B., Holcomb, J.L. et al (2009) Degradation of bromothymol blue by ‘greener’ nano-scale zero-valent iron synthesized using tea polyphenols, *J Mater Chem*, 19, 8671–8677.

Development of nano-porous geopolymer for passive cooling systems

M. Alshaaer^{1,*}, J. Alkafawein², Y. Al-Fayez², T. Fahmy¹, M. Zamorano Toro³, M. Martín Morales⁴

¹ Department of Physics, Prince Sattam Bin Abdul Aziz University, 11942 Alkharj, Saudi Arabia

² Department of Chemistry, King Faisal University, Al-Ahsa, Saudi Arabia

³ Department of Civil Engineering, University of Granada, 18071 Granada, Spain

⁴ Department of Building Construction, University of Granada, 18071 Granada, Spain

Abstract:

This work aims to investigate the use of alkali activated metakaolinite from natural kaolinitic soil as precursors for the production of Nano-porous geopolymer cement for passive cooling systems. Nano – porous geopolymer cement was synthesized using metakaolinite, and alkaline activators, namely sodium silicate (Na_2SiO_3) and sodium hydroxide. For metakaolinite preparation, Kaolinitic soil sample was collected from kaolin deposit (Saudi Arabia), which is located in Riyadh region. XRD analysis showed that kaolinite phase, was diminished due calcination and geopolymerization. The produced geopolymer cement exhibited a flexural strength of 12.3MPa, and compressive strength of 32MPa and 44.2MPa under immersed and dry conditions. The microstructure of the produced geopolymer was characterized by formation of Nano-porous network as shown by the SEM images. The general evaluation of the produced geopolymer cement from kaolinitic soil indicates its potential for a number of applications including green construction materials, and passive cooling .

Keywords: Nano-porous, Geopolymers, Kaolinite, SEM, Construction, Minerals, Water absorption, Strength.

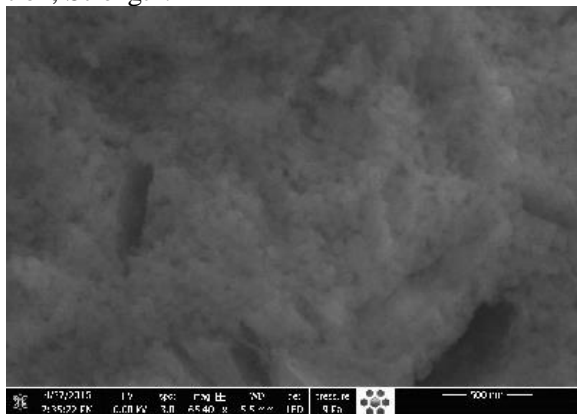


Figure 1: Figure illustrating the SEM image of Nano-porous network of the geopolymer.

Acknowledgments:

The financial support of the project “Development of functional geopolymer – based construction materials for passive cooling of buildings” funded under the contract number (AT-34- 211) by the King Abdulaziz City for Science and Technology KACST within the Research Grants Program is gratefully acknowledged.

References:

1. Davidovits, J., Geopolymer chemistry and sustainable development. The Poly(sialate) terminology: a very useful and simple model for the promotion and understanding of green-chemistry. In: Davidovits J., ed. Proc. of the World Congress Geopolymer, Saint Quentin, France, 28 June – 1 July 2005: p. 9-15.
2. Alshaaer, M., Two-phase geopolymerization of kaolinite-based geopolymers, Applied Clay Science, 86, 2013, 162–168
3. Khale, D., Chaudhary, R., Mechanism of geopolymerization and factors influencing its development: a review, J. Mater. Sci. 42, 2007, 729–746.
4. Alshaaer, M., El-Eswed, B., Yousef, R.I., Khalili, F., Rahier, H., Development of functional geopolymers for water purification, and construction purposes. Journal of Saudi Chemical Society, DOI:10.1016/j.jscs.2012.09.012, 2012.
5. Yousef, R., El-Eswed, B., Alshaaer, M., Khalili, F., Rahier, H., Degree of reactivity of two kaolinitic minerals in alkali solution using zeolitic tuff or silica sand filler, Ceram. Int., 36 (6), 2012, 5061–5067.

Novel Zeolite-Polyurethane Membrane for Environmental Applications

H. Shehu,^{1,2} E. Gobina,^{1,2}

¹Robert Gordon University., School of Engineering, Aberdeen, UK

²Center for Process Intergration and Membrane Technology, RGU, Aberdeen, UK

Abstract:

There has been great concern in the emissions of Volatile Organic Compounds (VOCs) from oil and process industries in the recent years. Different countries in the world have regulations in place that tightly control these emissions. In many countries emissions of VOCs and Non-Methane Volatile Organic Compounds (NMVOCs) are not subject to control. The separation of hydrocarbons from gas mixtures is one of the major objectives of chemical and petrochemical industries. There are various methods that these industries employ to achieve good separation. These include adsorption, rectification, membrane technology and use of cryogenics. Modern membrane technology can also be used in implementing Process intensification (PI) which is an innovative design method that is aimed at decreasing production cost, waste generated and size of equipment used as well as energy utilization. This research has reviewed the current technology that is being used for the control of VOC emissions from shuttle tankers and also investigated the feasibility of the use of membrane technology to separate and recover the hydrocarbon gases under various experimental conditions.

The aim of this research is to identify and modify separation membranes for optimum selectivity for lighter hydrocarbons recovery from crude oil shuttle tanker transportation and the feasibility of using the modified membrane for natural gas processing. This research work looks at the effect of polyurethane polymer on the separations of CO₂, CH₄ and C₃H₈ through a zeolite/polyurethane mixed matrix membrane was evaluated. The dip-coating method was used for the preparation of Y-type zeolite. A methodology based on the modification of ceramic inorganic membranes using different types of support with the aim to achieving high selectivity for the hydrocarbons has been developed. Polyurethane-zeolite nanoparticles were prepared by solution blending and casting method. Physical properties of the polyurethane and the zeolite/polyurethane mixed matrix membrane were investigated by Scanning Electron Microscope (SEM), Fourier Transfer Infra-Red (FTIR) and

Nitrogen physisorption analyses. This confirmed the homogenous and nanoscale distribution of zeolite particles in the polyurethane-zeolite nanocomposite membrane. The Nitrogen physisorption measurements showed the hysteresis isotherm of the membrane corresponding to type IV and V that is indicative of a mesoporous membrane. The surface area and the pore size was determined using the Barrett, Joyner, Halenda (BJH) desorption method which showed a pore diameter of 3.320 nm, pore volume of 0.31 ccg⁻¹ and surface area of 43.583m²g⁻¹. Single gas permeation tests were carried out at a pressure range of 0.01 to 0.1 MPa. The membrane showed a permeance of CH₄ to be in the range of 5.189 x 10⁻⁷ to 1.78 x 10⁻⁵ mols⁻¹m⁻²Pa⁻¹ and a CH₄/C₃H₈ selectivity of 3.5 at 293 K with the molar flux of the gases having an average linear regression coefficient value of R² = 0.9892. On the basis of the results obtained it can be concluded that for the recovery of volatile organic compounds the use of the zeolite/polyurethane membrane can be competitive.

References:

Burggraaf A. Single gas permeation of thin zeolite (MFI) membranes: theory and analysis of experimental observations. *Journal of Membrane Science*. 1999; 155(1):45-65.

Flue Gases Capturing Capacity of Nano-porous organic Materials

Ruh Ullah¹, Mert Atılhan^{1*} and Cafer T. Yavuz^{2*}

¹Department of Chemical Engineering, Qatar University, Doha, Qatar

²EEWS Graduate School, Korean Advanced Institute of Science and Technology (KAIST), Daejeon, Republic of Korea

Abstract:

Pre-combustion flue gas capture has been emerged as an efficient alternative to circumvent the costly procedures of materials regeneration utilized by the energy industry for CO₂ capture and separation. Stability of the porous structure and repeated use at high pressure and high temperature are among the essential requirements for the efficient materials to be used for industrial level CO₂ separation. Herein we report the CO₂ adsorption-desorption performance of nanoporous covalent organic polymers (COPs), which can operate efficiently and repeatedly at elevated pressure of 200 bars and above. Since, pre-combustion capture also requires removal of hydrogen along with CO₂; therefore, nanoporous COP was also tested for hydrogen removal at high pressure. COP material prepared with simple technique from building block monomers of cyanuric chloride and linked with 1,3-bis(4-piperidinyl)propane has enough surface area and pore volume which makes the material capable to store large quantity of syngas at high temperature and pressure. Results indicated that the newly synthesized COP material can adsorb exceptionally large quantity of CO₂ and very little hydrogen at 200 bars and 35 °C. Additionally, the adsorption isotherm was exactly matching with the desorption isotherm, suggesting that material has excellent adsorption-desorption characteristics. Similarly, the material has shown very stable performance when used repeatedly and alternatively for CO₂ and hydrogen after regeneration at 50 °C. The capturing performance of material was also investigated for other gases like methane and nitrogen at various pressures and temperatures. Experimental results revealed that COP material has exceptional CO₂ adsorption efficiency, very good selectivity, and strong stability and can be manufacture with simple techniques. Upon comparing with the very recently investigated materials such as amine modified SBA-15 and poly-benzimidazole materials, it was concluded that covalent organic polymers prepared from cyanuric chloride possess extremely high CO₂ capturing capacity at elevated pressure. Based on their very high stability and

excellent capturing capacity the materials can be tested for large scale applications in IGCC. Lastly, material is economically attractive when it is compared with the commercially available materials and has exceptional performance contrary to activated carbon, metal organic frame work and monoethanol amine

Keywords: High pressure, CO₂ Capture. Materials for Pre-combustion gases separation

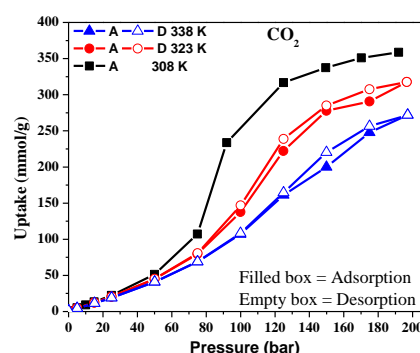


Figure 1: CO₂ adsorption-desorption isotherms at three different temperatures obtained with magnetic suspension balance.

References:

- Del Regno, A., et al., Polymers of Intrinsic Microporosity Containing Tröger Base for CO₂ Capture. *Industrial & Engineering Chemistry Research*, 2013. 52(47): p. 16939-16950.
- Ullah, R., et al., Insights of CO₂ adsorption performance of amine impregnated mesoporous silica (SBA-15) at wide range pressure and temperature conditions. *International Journal of Greenhouse Gas Control*, 2015. 43: p. 22-32.
- Ullah, R., et al., Synthesis, characterization and evaluation of porous polybenzimidazole materials for CO₂ adsorption at high pressures. *Adsorption*, 2016: p. 1-14.

Acknowledgements.

This paper was made possible by the support of Qatar National Research Fund, National Priorities Research Program grant (NPRP 6 - 330 - 2 - 140).

NanoMatEn 2016 Symposium on Nanotechnology for Photovoltaics

High efficiency thin film photovoltaic cells in novel light confinement architectures

Jordi Martorell^{1,2}

¹ ICFO-Institut de Ciències Fotoniques, The Barcelona Institute of Science and Technology, 08860 Castelldefels (Barcelona), Spain

² Departament de Física, Universitat Politècnica de Catalunya, Terrassa, Spain

Abstract:

An optimal light absorption in the active layer of thin film light harvesting devices has for many years challenged scientists in the area of solar cell research. The approaches followed may be grouped into two categories that consider: Anti-reflection configurations to reduce the amount of light that is reflected by the device top layers; Light trapping to limit the amount of light ejected by the structure. The former has been applied to several types of devices with considerable success, but the latter one has not been shown to be critical in any record performing thin film cell architecture yet.

Here, we will present a new optical cavity configuration that can confine light effectively in a large wavelength range close to 400 nm. The new elements we incorporate to a standard 1-D optical cavity lead to a smeared resonance behavior which is no longer limited to the fundamental and harmonics of such cavity. We consider a PTB7-Th: PC₇₁BM organic solar cell integrated within this new cavity and demonstrate that PECs higher than 11% can be reached. We demonstrate that the cavity concept we propose is quite universal in terms of the materials needed for its fabrication as well as the type of cells where it is applicable. In addition, we will also discuss a new fiber plate configuration for thin film cells where confining the light that is incident at an orthogonal direction is achieved effectively.^{1,2}

Keywords: Light harvesting, light trapping, thin film photovoltaics, optical cavity enhanced absorption, photonic fiber plate, whispering gallery, organic, polymer, perovskite, hybrid cells.

References:

1. Marina Mariano, Francisco J. Rodríguez, Pablo Romero-Gomez, Gregory Kozyreff and Jordi Martorell, Light coupling into the Whispering Gallery Modes of a fiber array thin film solar cell for fixed partial Sun tracking, *Scientific Reports* 4, Art. No.: 4959, May 2014.
2. Marina Mariano, Gregory Kozyreff, Luis G. Gerling, Pablo Romero-Gomez, Joaquim Puigdollers, Jorge Bravo-Abad, and Jordi Martorell, Intermittent Chaos for an Ergodic Light trapping in a Photonic Fiber Plate, submitted.

Nano-architectures and organic-inorganic hybrid material combinations for novel photovoltaic device concepts

S. Christiansen^{1,2}, S. Schmitt^{1,2}, S. Jäckle^{1,2}, G. Sarau^{1,2}, M. Göbelt², R. Keding², M. Mattiza¹, B. Hoffmann², M. Latzel²

¹ Helmholtz-Zentrum Berlin für Materialien, Institut Nanoarchitekturen für die Energieumwandlung, und Energie GmbH, Berlin, Germany

² Max-Planck-Institute for the Science of Light, Christiansen Research Group, Erlangen, Germany

Abstract: The implementation of tailored nano-architectures into conventional as well as novel material combinations for photovoltaic devices can improve photovoltaic (PV) cells by optimizing charge generation, separation and extraction. The charge generation in solar cells can be tuned by using lowly reflective materials such as nano-patterned layers which can contribute to an enhanced absorption through enhanced scattering and if geometries of nano-structures permit even through photonic coupling. While already large arrays of homogenous silicon nanowires (SiNWs) or – inverted cones (SiNCs), produced by reactive ion etching combined with nano-sphere-lithography, can substantially increase the absorption of thin film silicon on glass [1], vertical light-funnel arrays composed of SiNCs show even superior absorption properties [2]. These nanostructures optimized with respect to their optical behavior show large surfaces which require proper passivation and more importantly, good charge extraction concepts. Tunnel-oxides deposited by atomic layer deposition (ALD) show proven passivation capacities. The highly p-conducting polymer PEDOT:PSS forms a nearly perfect hybrid hole selective contact to silicon leading to power conversion efficiencies of 14% on planar n-type silicon [3]. Of course, these hybrid contacts can also be combined with nanostructured material. Last but not least, the charge extraction concepts seek for novel cheap, transparent and highly conductive materials replacing conventional metal grid-electrodes. Alternatives can be solution-processed Ag-nanowire networks, stabilized and protected by e.g. ALD deposited aluminum doped ZnO, showing solar cells with high short circuit currents, low resistivity and small amounts of metal [4]. The present paper will present the optical behavior of individual and arrays of SiNWs and SiNCs using finite difference time domain (FDTD) simulations and will derive design rules

for PV optimized ensembles of Si nanostructures. Moreover, experimental confirmation of simulation results will be presented. Here, nano-probing of individual nano-structures and ensembles will be presented based on a powerful electron-microscopy platform to carry out correlative microscopy and spectroscopies.

Keywords: Advanced Nanomaterials, Nanomaterials Fabrication, Characterization and Tools, Nanoscale Electronics, Nanotech for Energy and Environment, Nano Applications

References:

1. Schmitt, S.; Schechtel, F.; Amkreutz, D.; Bashouti, M.; Srivastava, S.K.; Hoffmann, B.; Diecker, C.; Spiecker, E.; Rech, B.; Christiansen, S.H.; Nano Letters 12, 2012, 4050
2. Shalev, G.; Schmitt, S.; Embrechts, H.; Brönstrup, G.; Christiansen, S.; Scientific Reports 5, 2015, 8570

Metal Oxide Nanorod Arrays Fabricated by Solution Processes for Applications in Hybrid Photovoltaic Cells

Surawut Chuangchote^{1,2,*}, Witchaya Arpavate³, Navadol Laosiripojana^{1,2}, Takashi Sagawa⁴

¹The Joint Graduate School of Energy and Environment, King Mongkut's University of Technology Thonburi, 126 Prachauthit Rd., Bangmod, Tungkru, Bangkok 10140, Thailand.

²Centre of Excellence on Energy Technology and Environment, Science and Technology Postgraduate Education and Research Development Office, Bangkok Thailand.

³Faculty of Engineering, Rajamangala University of Technology Phra Nakhon, 1381 Pracharat1 Rd., Bangsue, Bangkok 10800, Thailand

⁴Graduate School of Energy Science, Kyoto University, Yoshida-honmachi, Sakyo-ku, Kyoto 606-8501, Japan

Abstract:

Organic photovoltaic cells (OPVs) have recently become a great attention due to the simple process and the cheaper production cost compared with silicon solar cells. However, photoconversion efficiencies of OPVs are still low compared with inorganic photovoltaic cells because of low mobility to transfer excited electrons or holes in OPVs. In order to overcome the low mobility of carriers and improve the cell efficiencies, hybrid solar cells combined organic material as an electron donor and inorganic material as an electron acceptor have been studied. Recently, metal oxide nanorod arrays, e.g. ZnO arrays, are normally used as inorganic semiconductor acceptor in hybrid solar cells due to their several favorable properties, such as high electron mobility and wide bandgap. Among the various techniques to fabricate one-dimensional ZnO nanostructure, hydrothermal method gets a lot of attention and extensive uses, because it is a simple technique that can operate at low temperature and ambient pressure. Moreover, there is no requirement of special equipment and substrate in hydrothermal method. In this work, ZnO nanorod arrays have been synthesized on seed-coated transparent conducting oxide (TCO) substrates by hydrothermal method from different thickness of seed layers. The obtained ZnO nanorods were investigated by Scanning electron microscope (SEM) and X-ray diffractometer (XRD) to study the influence of different seed layer thicknesses on the orientation of nanorods. The experimental results demonstrate that the thickness of seed layers has roles on the density, diameter, and vertical alignment of ZnO nanorods. SEM images show that the morphologies of ZnO nanorods are hexagonal wurtzite structures and ZnO nanorods are denser with increasing seed layer thickness. XRD pattern shows that ZnO nanorods are grown along the vertical direction at suitable seed layer thick-

ness. The well-aligned ZnO nanorods from the suitable seed layer thickness were applied as an electron transporting layer in hybrid photovoltaic cells. Various surface modifications were carried out on ZnO nanorods, i.e. TiO₂ nanotube arrays using ZnO nanorods as templates by liquid phase deposition methods, addition of a layer of TiO₂ nanofilm, and addition of nanoparticles (TiCl₄ treatment). Photovoltaic properties and power conversion efficiency of devices made of typical and modified metal oxide nanorod arrays were investigated.

Keywords: metal oxide nanorod, solution process, hydrothermal method, seed layer, hybrid photovoltaic cell

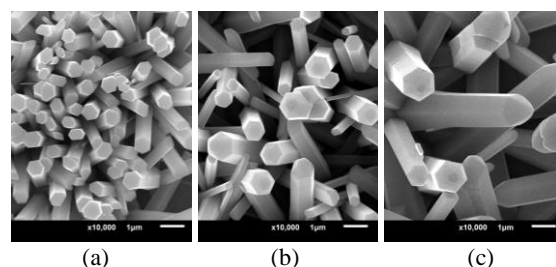


Figure 1: SEM images of ZnO nanorod arrays grown on various seed layer thicknesses: (a) 1, (b) 2, and (c) 3 seed layer(s).

Boosting impact of nanometric Ge layers on the synthesis and performance in $\text{Cu}_2\text{ZnSnSe}_4$ solar cells

Paul Pistor^{1,*}, Sergio Giraldo,¹ Markus Neuschitzer,¹ M. PlacidiAlejandro Pérez-Rodríguez,^{1,2} Edgardo Saucedo¹

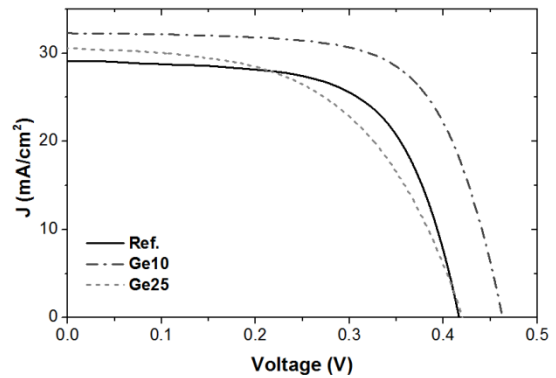
¹ IREC – Catalonia Institute for Energy Research, 08930 Sant Adrià de Besòs, Barcelona, Spain

² IN²UB, Universitat de Barcelona, C. Martí Franquès 1, 08028 Barcelona, Spain

Abstract:

Recently, we reported the beneficial effects of the incorporation of small amounts of Ge into $\text{Cu}_2\text{ZnSnSe}_4$ (CZTSe) based solar cell absorbers synthesized in a sequential process (sputtering of metallic precursors and selenization in a selenium atmosphere). We have proven the impact of the nanometric Ge layers on crystal growth, doping density and alkali metal diffusion dynamics. These findings have ultimately led to a boost in power conversion efficiencies enabling us to surpass 10 %. The nanometric Ge layers are applied during the metallic Cu, Zn,Sn precursor deposition prior to the selenization of the absorbers. While the addition of the nanometric Ge layer (10-20nm) improves all solar cell parameters, we find the highest impact on the open circuit voltage. Thanks to the nano-engineering with Ge, we were able to drastically reduce the voltage losses in our devices and achieve open circuit voltages of nearly 500 mV. In this presentation, we summarize our recent results and our current understanding and the origins of this surprisingly efficient nanometric surface modification. We focus on the optimum preparation condition and the main impact the Ge incorporation has on the opto-electronic behaviour of the device. We will then shed light on the interaction between germanium and sodium. As it is widely known, Na is a very important dopant in kesterite which plays an essential role in the doping level control. We demonstrate that during the annealing process, a Ge-Se liquid phase is formed which dissolves preferably Na-related phases modifying the content of this last element in the CZTSe absorber, and impacting notably on the electrical properties of the layers and concomitantly on the devices performance. We support our Ge-Na interaction model with experiments using Na-free substrates, showing the importance of accurately control the Na content when Ge is used to increase the efficiency of CZTSe based solar cells.

Keywords: Thin Film Photovoltaics, Sustainable Next Generation PV, Earth Abundant, Kesterite Solar Cells, Voltage Loss Minimization, Ge Nanolayer, Surface Modification.



Sample	Eff. (%)	V _{oc} (mV)	J _{sc} (mA.cm ⁻²)	FF (%)	R _s (Ω.cm ²)	R _{sh} (Ω.cm ²)	N _{cv} (cm ⁻³)	SCR (μm)
Ref	7.7	417	29.1	63.8	0.7	333	2x10 ¹⁶	0.15
Ge10	10.0	463	32.3	66.9	0.9	734	3x10 ¹⁶	0.10
Ge25	6.9	420	30.5	53.6	1.3	252	4x10 ¹⁵	0.32

Figure 1: IV characteristics and solar cell parameters obtained for solar cells with different amounts of Ge (Ref: no Ge, Ge10: 10 nm Ge, Ge25: 25 nm Ge) applied on top of the metallic precursor step prior to selenization.

References:

1. S. Giraldo, M. Neuschitzer, T. Thersleff, S. López-Marino, Y. Sanchez, H. Xie, M. Colina, M. Placidi, P. Pistor, P., V. Izquierdo-Roca et al. "Large Efficiency Improvement in $\text{Cu}_2\text{ZnSnSe}_4$ Solar Cells by Introducing a Superficial Ge Nanolayer" *Adv. Energy Mater.*, Wiley-Blackwell, 2015.
2. S. Giraldo, M. Placidi, M. Neuschitzer, P. Pistor, A. Pérez-Rodríguez, E. Saucedo. " $\text{Cu}_2\text{ZnSnSe}_4$ -Based Solar Cells With Efficiency Exceeding 10% by Adding a Superficial Ge Nanolayer: The Interaction Between Ge and Na", *IEEE J. Photov.*, 2016.

Thin Epitaxial Silicon Foils Using Porous-Silicon-Based Lift-Off for Photovoltaic Application

I. Gordon

IMEC, Photovoltaics Department, Leuven, Belgium

Abstract:

In order to reduce the material cost for silicon solar cells, several research groups are investigating the feasibility of making cells on very thin monocrystalline silicon foils. Imec proposed in the past the so-called i^2 -module approach, which allows for the module-level processing (many cells in parallel) of solar cells on thin silicon foils that are bonded to a glass superstrate. The silicon substrates used for this concept are high-quality epitaxial foils lifted off from a parent silicon substrate using porous silicon made by electrochemical etching (see Figure 1). The porous-silicon lift-off approach is one of the promising “direct wafering” routes that could potentially replace traditional wafers, made by ingot casting and wire sawing, to create substrates with a thickness well below 100 μm and without kerf losses. This contribution first of all deals with the latest optimization of the foil fabrication in order to create foils that combine high material quality with a high detachment yield. The quality of the resulting epitaxial foil strongly depends on the smoothness of the seed. Therefore, adapted reorganization processes for the porous silicon seed and detachment layers are proposed. In this way, we have managed to obtain 100 μm thick silicon foils with effective lifetimes up to 1.3ms, and 40 μm thick foils with effective lifetimes up to 700 μs . We will also review the current status of the process development for solar cells made from these thin foils. Two approaches are presented. In the first approach, heterojunction solar cells are fabricated on freestanding epitaxial wafers of 40 μm thickness. In the second approach, heterojunction back-contacted cells are fabricated on thin foils that are bonded to a glass superstrate. Challenges for device processing and limitations in cell performance will be discussed.

Finally, we will show how nanophotonics can be used to improve the solar cells made from these thin silicon foils by nanotexturing the front surface of the foils which leads to increased current densities in the devices.

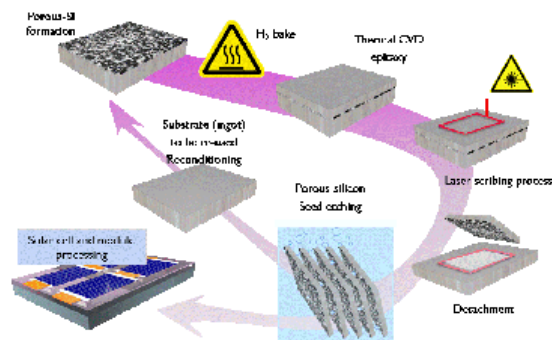


Figure 1: Figure illustrating the envisaged process flow, starting with a silicon substrate on which an epitaxial layer is grown, which is lifted off from the substrate and then processed into a working solar device while the starting substrate is re-used again.

Keywords: Silicon solar cells, epitaxy, porous-silicon, lift-off, kerfless wafering, heterojunctions, nanophotonics.

Electric and Photovoltaic Behavior of Novel Few Layer α -MoTe₂ / MoS₂ Dichalcogenide Heterojunction

Atiye Pezeshki,^{1,*} Prof. Seongil Im¹

¹ Yonsei university institute of physics and applied physics, Seoul, Korea

Abstract:

Transition-metal dichalcogenides (TMDs) are two dimensional (2D) nanomaterial with the common formula MX₂. In general, M atoms are sandwiched between X atoms to form a single layer, and each layer can be stacked together via van der Waals forces, which make 2D TMDs easily cleaved by scotch tape or other similar techniques. Among TMD families with ultra-thin layers, molybdenum disulfide (MoS₂) is a well-known semiconductors with their bandgaps of more than 1.2 eV; their band gap increases to 1.8 eV for monolayer and band properties changes from indirect to direct type. As one of quite recent 2D materials, molybdenum ditelluride (α -MoTe₂) has also been attracting attention due to its optical and electrical properties. Monolayer α -MoTe₂ exhibits a direct optical bandgap of 1.10 eV, while its bulk form becomes an indirect semiconductor with the band gap of 0.88~1.0 eV. MoTe₂-based homo- or hetero-junction p-n diode has not been reported yet although p-n diode is one of the basic building blocks for electronics and optoelectronics. In fact, forming two different types of conduction in the same nanoflake might not be easy. So, heterojunction p-n diode studies have always been preferred but limited to n-MoS₂/p-Si bulk, n-MoS₂/p- WSe₂ and n-MoS₂/p-BP (black phosphorous) systems, to the best of our knowledge.

In the present study, we attempted van der Waals heterojunction p-n diode fabrication by direct imprinting technique transferring p-type α -MoTe₂ onto n-type MoS₂ nanoflake, since in this way we would achieve Mo-based dichalcogene 2D p-n diode which appears novel in view of using the same transition metal for both p- and n-type. Pt electrode appeared very good for ohmic contact with p-type α -MoTe₂ even without thermal annealing. Our few-layered α -MoTe₂/MoS₂ p-n diode demonstrates low voltage opera-

tion at 5 V and high reasonable ON/OFF current ratio of $10^3 \sim 4 \times 10^3$ ($\sim 4 \times 10^3$ on SiO₂/Si and $\sim 10^3$ on glass substrate) along with good ideality factors of 1.06~1.34. Kilohertz fast dynamic rectification was achieved in the dark while dynamic photovoltaic switching was also exhibited under red, green, blue LEDs, and 800 nm infrared laser. We regard that our new 2D p-n diode is quite promising in the prospects of nano-electronics and optoelectronics.

Keywords: MoS₂, MoTe₂, Photovoltaic effect, P-n Diode, Van der Waals heterojunction

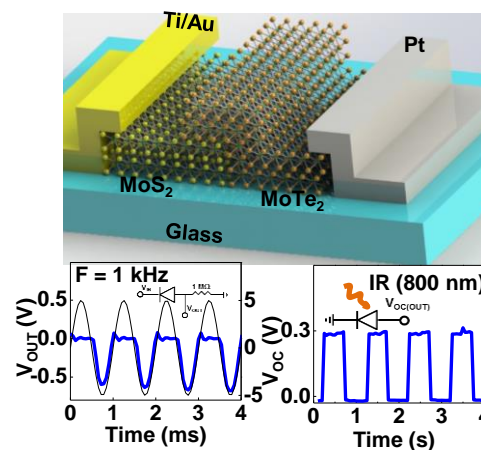


Figure 1: This figure shows the 3D schematic of our van der Waals 2D p-n diode on glass substrate.

Zinc selenide as a potential Cd-free buffer nanolayer for CZTSe solar cells

M. Placidi¹, M. Espindola-Rodriguez¹, H. Xie¹, F. Oliva¹, Y. Sanchez¹, M. Neuschitzer¹, S. Giraldo¹, I. Becerril-Romero¹, P. Pistor¹, V. Izquierdo-Roca¹, E. Saucedo¹, A. Pérez-Rodríguez^{1,2}

¹Catalonia Institute for Energy Research (IREC), Sant Adrià del Besòs (Barcelona), Spain

²IN²UB, Departament d'Electrònica, Universitat de Barcelona, Barcelona, Spain

Abstract:

A way of achieving via a dual step method the formation of Cd free chalcogenide buffer nanolayers for chalcogenide thin film solar cells is proposed in this work. More particularly the case of ZnSe buffer for CZTSe absorber was investigated through the deposition of a very thin zinc oxide layer onto CZTSe and subsequent selenization at low temperatures to form ZnSe without deterioration of the absorber. The preliminary characterizations of ZnSe/CZTSe solar cells with different ZnSe thicknesses show promising results achieving 3.8% efficiency on a first set of experiments.

High efficiency chalcogenide solar cells are based in the formation of a pn heterojunction between the p-type chalcogenide absorber and an n-type nanometric buffer layer. Cadmium sulfide (CdS) is the most common used buffer layer for thin film photovoltaics, mainly for historical reasons, since it was the first working buffer layer with CdTe solar cells. However, the toxicity of Cd stimulated the research of alternative Cd-free buffer layers, the most commonly reported being sulfide ones such as ZnS, In₂S₃, Zn(O,S) and Zn(O,OH)S. Similarly to CdS, chemical bath deposition (CBD) was used to prepare them, which can complicate the deposition of equivalent selenide buffers, for which hazardous selenide chemical precursors (such as selenourea) are required. One way of avoiding the use of dangerous chemical precursors relies on other safer methods to prepare selenide buffers. In this work a process for preparing cadmium-free ZnSe buffer onto the absorber is presented, based on a dual step consisting on the sputtering deposition of zinc oxide followed by a rapid selenization. Cu₂ZnSnSe₄ (CZTSe) kesterite absorbers were prepared following the same process than described in [1]. Several thicknesses of zinc oxide (around 5, 10, 25 and 50 nm) were deposited onto the surface of the CZTSe layers which was etched using KMnO₄ and (NH₄)₂S [2,3]. The samples were labeled ZnSe-0 (no ZnSe layer), ZnSe-1, ZnSe-2, ZnSe-5 and ZnSe-10 respectively, the numbers corresponding to the deposition time (in minutes) of

the ZnO (i.e. ZnSe-1 means 1 min of ZnO deposition, giving around 5 nm). Just after the ZnO deposition, the samples were selenized at 400°C at atmospheric pressure during 15 min. The solar cells were then completed by depositing on top an i-ZnO layer followed by an ITO layer.

No efficiency in CZTSe solar cells was obtained without ZnSe buffer layer. However, for very thin layers of ZnSe (the initial ZnO thickness was between 5 and 10 nm) the devices exhibited a clear solar cell behaviour, despite a low fill factor (around 40%). An efficiency of 3.8% was obtained for a ZnSe thickness around 10 nm, with an open circuit voltage (V_{oc}) and short circuit current density (J_{sc}) values of 357 mV and 26 mA/cm² respectively. When the ZnSe thickness increased, the efficiency considerably reduced, probably due to elevated recombinations in the thick ZnSe layer (as confirmed in the quantum efficiency behaviour, not shown here). Further characterizations are currently being performed to optimize the process synthesis of the buffer and improve the devices efficiency.

Keywords: free-cadmium buffers, zinc selenide, thin film solar cells, kesterite solar cells.

References:

- 1.- S. Giraldo et al., Adv. Energy Materials (2015) doi: 10.1002/aenm.201501070.
- 2.- S. López-Marino et al., Chemistry – A European Journal 19, 14814 (2013).
- 3.- H. Xie et al., ACS Appl. Mater. Interfaces 6, 12744 (2014).

SURMOFs and CNCs as novel tuneable Materials for Optical, Photonic as well as for Solar Energy Materials

E. Redel^{1*}

¹ Institut für Funktionelle Grenzflächen (IFG), Karlsruhe Institute of Technology (KIT),
Hermann-v.-Helmholtz-Platz-1, D-76344 Eggenstein-Leopoldshafen

Abstract:

Here I will present a particularly interesting class of surface-anchored (metal-organic frameworks and coordination network compounds) materials SURMOFs and CNCs for the fabrication e.g. of 1D (Photonic Band Gap) PBG materials [1] as optical sensors, low-*k* dielectric thin films [2], optoelectronic/ electrochromic switchable coatings/devices [3] PV devices [4] or as future artificial Light-Harnessing (LH) antenna array assemblies as well as monolithic up- and down conversion architectures. Since these materials are highly porous and the size of their pores are highly adjustable, they can be further functionalized (e.g. with different metal/oxo connectors or clusters linked with various organic linkers) e.g. in order to specifically bind target analytes (optical sensing), to electrically load and unload small ions (optoelectronic applications) as well as to act as photon traps, which are able to efficiently absorb, transport and harness light energy over an artificial LH antenna array. In addition, the RI (Refractive Index) as well as the optical properties of SURMOF and CNC materials can be tailored – a fact which makes these materials ideally suited for photonic, optical, optoelectronic, light-harnessing as well as for future solar energy systems like photocatalytic and PV applications.

Keywords: SURMOFs, porous thin films, artificial light harnessing, optics and photonics, PV applications, photocatalysis.

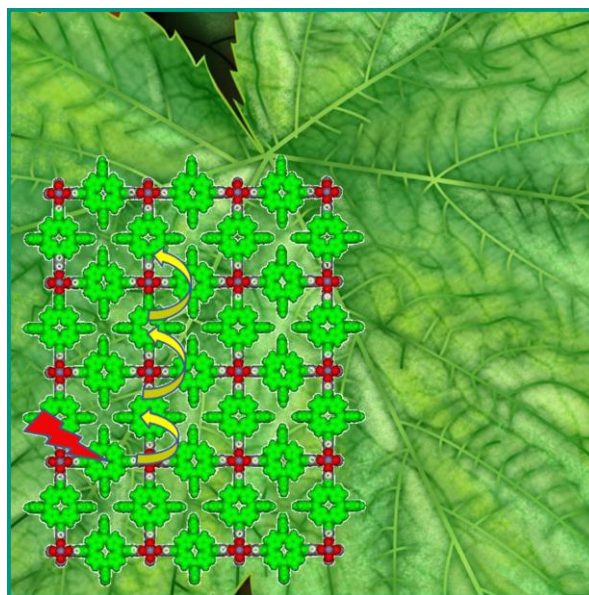


Figure 1. Schematic Drawing of an artificial supramolecular LH array for photocatalytic and/or PV applications.

References:

- [1] J. Liu, E. Redel, S. Walheim, Z. Wang, V. Oberst, J. Liu, S. Heissler, A. Welle, M. Moosmann, T.Scherer, M. Bruns, H. Gliemann, Ch. Wöll *Chemistry of Materials (ACS)* **2015**, *27*, **1991-1996**.
- [2] E. Redel, Z. Wang, S. Walheim, J. Liu, H. Gliemann, Ch. Wöll, *App. Physics Lett.* **2013**, *103*, 091903 [3] J. Liu, W. Zhou, S. Walheim, Z. Wang, P. Lindemann, S. Heissler, J. Liu, P. G. Weidler, T. Schimmel, Ch. Wöll, E. Redel *Optics Express (OSA)* **2015**, *23*, 13725-13733.
- [4] J. Liu, W. Zhou, J. Liu, I. Howard, G. Kilibarda, S. Schlabach, D. Couprey, M. Addicoat, S. Yoneda, Y. Tsutsui, T. Sakurai, S. Seki, Z. Wang, P. Lindemann, E. Redel, T. Heine, C. Wöll

VIP* \equiv *Very Important Paper* (Angewandte Front Cover Issue 2015-54/25**)

Angewandte Chemie International Edition (Wiley-VCH) **2015**, *54*, 7441.

NanoMatEn 2016 Session III

Nanotechnology for water treatment

Nanotechnology for cleaning water: redox reactions the way out?

J. Dutta

Functional Materials Division Materials- and Nano Physics Department, KTH Royal Institute of Technology-Sweden

Abstract:

Due to continuous population growth in the world, water scarcity is an important area to find an immediate answer. Environmental pollution and industrialization in global scale have led to pollution of available water and thus hygienically friendly purification technologies are the need of the hour. Cost-effective treatment of pollutants requires the transformation of hazardous substances into benign forms. Nanotechnology based filters utilizing photocatalytic processes that activate the antimicrobial properties under sunlight and Capacitive Deionization techniques promise as an interesting alternative for effective degradation of organics and removal of dissolved ions from water.

Development of these techniques would make it possible to install delocalized systems with very little capital investment and operation and maintenance costs.

Functional nanostructured materials for water treatment and desalination

Mirko Faccini¹, Diego Morillo Martín¹, Marcel Boerrigter¹

¹LEITAT Technological Center, C/ de la Innovació, 2 · 08225 Terrassa (Barcelona)

Abstract: Nanotechnology has the potential to contribute to long-term water quality, availability, and viability of water resources, such as through the use of advanced filtration materials that enable greater water reuse, recycling, and desalinization. In this talk, we will give an overview of the latest advances made at LEITAT in the development of nanostructured materials and membranes for water treatment. We will provide examples of the innovations in fundamental science, engineering and technology with the highest potential to foster a breakthrough in sustainable water technologies, including:

- i. Photocatalytic hollow-fiber membranes to prevent fouling in water desalination reverse osmosis systems.
- ii. High surface area nanofibers for the decontamination of water polluted with toxic and heavy metals and the recovery of valuable metals.
- iii. Nanostructured materials for oil spill remediation.
- iv. Microbial electrochemical cells as emerging technology for low-energy desalination and simultaneous wastewater treatment.

Keywords: Nanotechnology, Nanomaterials, Water Treatment, Desalination, Nanofibers, Membranes, Drinking water.

Acknowledgements:

The research leading to these results has received funding from the European Union's Seventh Framework Programme (FP7/2007-2013) under grant agreement N°308439.

References:



<http://www.nawades.eu/>

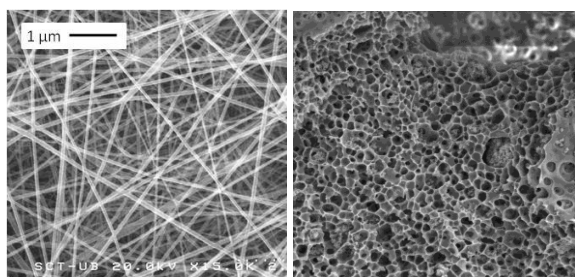


Figure 1: Representative SEM image of nanostructured membranes.

Decontamination of wastewater using nanocarbon compounds insert in diatomite mesoporous structure

E. Flores,¹ O. Enriquez,¹ J. De la Cruz¹, A. López¹, G.Poma^{1,2}, M.Quintana^{1,2}

¹ Engineering and Technological University, Department of Chemical Industrial Engineering, Lima, Peru

²National University of Engineering, School of Physical Engineering, Faculty of Science, Lima, Peru

Abstract:

There is a wide variety of techniques for the removal of heavy metals from wastewater. These techniques are useful but some of them are not economically available. Herein, we have synthesized a diatomite earth and graphene compound material. This material was obtained by continuous stirring of diatomite earth in a suspended graphene solution. Diatomite earth was taken from Piura locality (Peru) and graphene was synthesized in a lab from Merck graphite. In this research, we carried out a comparative study about the relationship of the diatomite distribution size used, stirring time required to produce the material and graphene concentration of the solution. Finally we study the behavior of this compound material to decontamination of heavy metals in wastewater.

Keywords: diatomite, graphene, heavy metals, water decontamination.

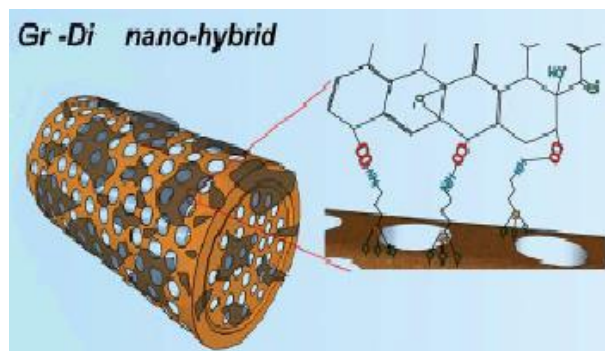


Figure 1: Figure illustrating the possible bending between diatomites and graphene. The synthesized graphene covers the diatomites surface. (Gr=graphene, Di=diatomites)

References:

1. Kumeria, T., Bariana, M., Altalhi, T., Kurkuri, M., Gibson, C., Yang, W. & d. Losic (2013) Graphene oxide decorated diatom silica particles as new nano-hibryds: towards smart natural drug microcarriers. *J. Mater. Chem. B*, 6302- 6311
2. Khraisheh, M., Al-degs, Y., Mcminn, W., (2004) Remediation of wastewater containing heavy metals using raw and modified diatomite. *Chem. Eng.J.*, 89, 177-184.

Functionalization of glassy carbon electrode by amines electro-chemical oxidation for micro-pollutants detection in water

David Pally¹, Moslem Alaaeddine¹, Benoît Cagnon¹, Valérie Bertagna^{1*}, Roland Benoit¹, Fetah Podvorica¹, Christine Vautrin-UI¹

¹ Univesity of Orleans-CNRS,ICMN - Interfaces, Confinement, Matériaux et Nanostructures Orléans, France

Abstract:

Good chemical status of European water is defined in terms of compliance with all the quality standards established for chemical substances at European level in the European Water Framework Directives (WFD) ¹. Implementation of the WFD needs the monitoring of 45 micro-pollutants belonging to several chemical groups such as metal, HAP, pesticide, hormone...For now, all the controls need on site sampling then analysis in laboratory that require costly apparatus. Consequently, the spatial and temporal cover of the monitoring plan remains inadequate. The improvement of water quality involves the implementation of self-powered on-site devices of analysis with remote data collection. Electrochemical sensors are good candidate to meet these specifications. However the improvement of the sensibility, the robustness and the selectivity of the electrode is essential to allow the development and the validation of the electrochemical sensors as standard tools for water monitoring. Within this context, our works deal with the development of functionalized carbon electrodes for micro-pollutants detection in aqueous media. Especially we have shown that electro-grafted carboxy-carbon electrode via reduction of diazonium are able to detect metallic micro-pollutants such as Cu(II), Pb(II), U(VI) or Cd(II) at ppb levels². In this presentation, the electro-oxidation of several amines is explored as functionalization way to improved selectivity and sensibility of glassy carbon electrode used for lead detection. Since 1990, electro-oxidation of primary and aromatic amines is known to be able to grafted organic layer on carbon, noble metal and semi-conductor. Less used as surface modification method than the electro-reduction of diazonium salt, this way allows grafting of covalent layer and is an powerful alternative to functionalize carbon surface by aliphatic or aromatic groups. In the present work, we functionalized glassy carbon electrode by carboxyl groups via oxidation of the corresponding amines and we will show their potential application to trace lead detection. Evidence of the grafted layer at the

electrode surface was investigated via electro-chemical signal study of the ferri cyanide probe. XPS and FTIR characterization are used to show the presence of the carboxyl function on the glassy carbon grafted surface. The rough-ness and the homogeneity of the grafted layer are explored by AFM. Analytical performances of the carboxy grafted glassy carbon electrode will be established for the analysis of lead aqueous solution. Finally a comparison will be proposed between the performances of the grafted electrode obtained via electro-oxidation of amines and electro-reduction of the corresponding diazonium salts.

Keywords: amine electrooxidation, lead detection, micropollutant, diazonium electroreduction

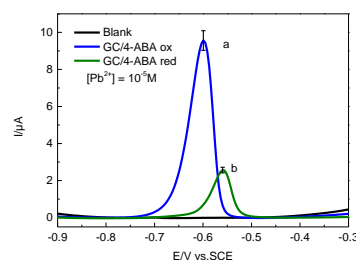


Figure 1: Square wave Adsorptive stripping voltammetry in Pb(II) trace solution glassy carbon electrode functionalized a) via **4-aminobenzoic acid** electro-oxidation b) **4-aminobenzoic acid diazonium** electro-reduction

References:

1. Directive 2000/60/CE, Official Journal of the European Union.
2. Bouden, S., Chaussé, A., Dorbes, S., El Tall, O., Bellakhal, N., Dachraoui, M., Vautrin-UI, C., (2013) Trace lead analysis based on carbon-screen-printed-electrodesmodified via 4-carboxy-phenyl diazonium salt electro-reduction Talanta , 106, 414-421.

PVDF UF hollow-fiber membrane production as pre-treatment system in Water Desalination Reverse Osmosis Unit

Alberto Figoli¹, Omar Saoncella¹, Song Xue², Silvia Simone¹, Francesco Galiano¹, Marcel Boerrigter³, Christiane Chaumette², Mirko Faccini³, Enrico Drioli¹

¹Institute on Membrane Technology, ITM-CNR, Via P. Bucci Cubo 17/C, 87036 Rende (CS) Italy

²Fraunhofer IGB, Nobelstrasse 12, 70569 Stuttgart, Germany

³LEITAT, C/ de la Innovació, 2 · 08225 Terrassa (Barcelona)

Abstract:

Membrane processes are widely accepted as more economic, environmental-friendly and sustainable alternatives to several industrial processes. Although these technologies offer several advantages, both in terms of costs and of reduced environmental impact, and are in perfect agreement with the philosophy of process intensification [1], fouling and, above all, biofouling, still represents one of the main drawback in water membrane applications. Fouling negatively affects the plant productivity and offering additional resistance to transport. Consequently, operational costs increase; while, membrane life-time reduces. Moreover, fouling makes necessary the use of chemical agents for cleaning; hence, one of the main advantages of any membrane process, i.e. the un-necessity of additional chemicals, is lost. Therefore, different strategies have been developed for overcoming this problem, such as physical and chemical cleaning (i.e. back flushing, or treatment with sodium hypochlorite, enzymes etc.), improvement of the system fluid-dynamic conditions and/or membrane modification. In particular, the membrane modification is part of the present work, polyvinylidene fluoride (PVDF) hollow-fiber membranes loaded with TiO₂ have been produced and tested for water treatment. As already largely discussed in literature, the immobilization of TiO₂ photocatalyst in a polymeric membrane represents an interesting and viable approach for reducing fouling in membranes. In this work, different TiO₂ concentrations were homogeneously dispersed into the polymeric matrix to evaluate the influence of the amount of TiO₂ on the membrane characteristics. Different PVDF concentrations and pore forming additives have been added to modulate the membrane morphology and properties. The produced

membranes have been, then, characterised and fouling tests by using UV light have been also performed. The results demonstrated the stability of the membrane produced and potentiality of this approach as antifouling approach.

Keywords: Membrane preparation, hollow-fiber, TiO₂ nanoparticles, fouling, desalination

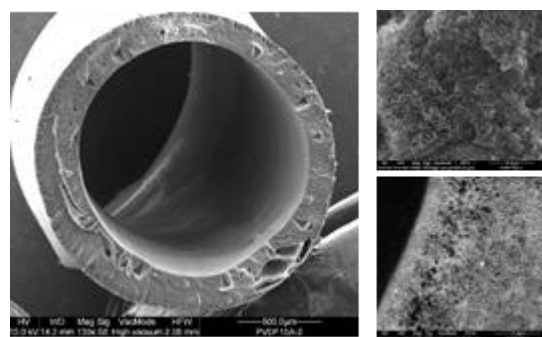


Figure 1: Figure illustrating the PVDF hollow-fiber membranes loaded TiO₂.

Acknowledgements:

The research leading to these results has received funding from the European Union's Seventh Framework Programme (FP7/2007-2013) under grant agreement N°308439.

References:

1. <http://www.nawades.eu/>

Development of Alumina-Carbon Nanotubes Porous Membranes Using Spark Plasma Sintering Process for Water Purification

T. Laoui,^{1,*} H. K. Shahzad,¹ M. A. Hussein,¹ F. Patel,¹ N. Al Aqeeli,¹ M. A. Atieh,²

¹ King Fahd University of Petroleum and Minerals, Mechanical Engineering Dept., Dhahran, Saudi Arabia

² Qatar Environment and Energy Research Institute, HBKU, Qatar Foundation, Doha, Qatar

Abstract:

Owing to their superior characteristics, porous ceramic membranes have been used for water filtration for decades. The objective of this research is to develop porous alumina-carbon nanotubes composite membranes for sustainable water purification, via the removal of heavy metal ions from polluted water through adsorption. In the present study, porous alumina-carbon nanotubes composite membranes, containing different amount of carbon nanotubes (CNTs), are synthesized by spark plasma sintering (SPS) technique through controlled process parameters including compaction pressure, sintering temperature and time. Because of CNTs inertness and relatively high specific surface area for physical adsorption, they are selected as adsorbent material, in addition to alumina, for heavy metal ions. For membrane preparation, CNTs are first dispersed in a mixture of Arabic gum and sodium dodecyl sulfate (SDS) dissolved in water followed by sonication. Then, alumina powder is added to this solution to obtain a homogeneous physical mixture of alumina and CNTs powders, which is then dried and sintered using SPS. For comparison, alumina is also sintered without the addition of CNTs. The effects of SPS parameters, including sintering temperature; holding time and pressure, on the developed microstructure of the composite membranes and porosity are studied. The porous membranes are characterized using x-ray diffraction, scanning electron microscopy, contact angle and porosity measurement.

The dispersion of CNTs in alumina matrix, and the membrane pore size are evaluated. The prepared membranes are tested for pure water flux transport as well as for their capacity to adsorb heavy metal ions. The membrane characteristics are also correlated with the SPS parameters and amount of CNTs. The results of this study indicate that these membranes offer excellent potential for the removal of heavy metals from water.

Keywords: carbon nanotubes, alumina, porous membranes, composite membranes, spark plasma sintering, heavy metal removal, water purification applications.

The efficient separation of oil-water emulsions with a flexible, superhydrophilic and self-cleaning TiO₂/Fe₂O₃ membrane

Benny Yong Liang Tan^a, Jermyn Juay^a, Jeremy Koon Keong Ang^a, Zhaoyang Liu^b, Darren Sun^{a*}

^a School of Civil and Environmental Engineering, Nanyang Technological University

^b Qatar Environmental and Energy Research Institute

Abstract:

The discovery of efficient self-cleaning oil-water separation membrane has been in urge demand due to the daily production of oily wastewater[1]. Currently, the available options for oil-water separation are not sustainable and are prone to fouling. TiO₂ material has been realised for its intrinsic superhydrophilic and underwater superoleophobic properties. However, its self-cleaning property and efficiency in separating oil from water have been restricted by its large band gap and the nanostructures formation respectively. Thus, this study introduces a hierarchical TiO₂/Fe₂O₃ nano-fabric constructed membrane, which possess with a high oil-water separation ability coupled with self-cleaning phenomenon. The analytical results showed that the TiO₂/Fe₂O₃ membrane portrayed excellent oil-water separation capability owing to its interconnected delicate network[2]. Furthermore, its enlarged specific surface area promotes the formation of more-water layers represented by its high water capture percentage (WCP), which improve the underwater superoleophobic interface. As compared to the primary TiO₂ nanowire membrane, this novel membrane illustrated a better self-cleaning ability, in which it is able to remove the oleic acid accumulated on its surface, and concurrently regaining its superhydrophilic property in a shorter period of time under UV light irradiation. This superior photodegradation property can be attributed to two main characteristics possessed by the TiO₂/Fe₂O₃ membrane: 1) the high light harvesting capability contributed by the multiple reflections of incident light; and 2) superior photo-generated electron collection feature resulted from the hierarchical formation of TiO₂/Fe₂O₃ nano-fabric structure[3]. Moreover, the mechanical flexible characteristic of this novel membrane endows its opportunity to be employed in wider industrial employments.

Keywords: TiO₂/Fe₂O₃ nano-fabric; flexible oil-water separation membrane; self-cleaning properties; superhydrophilic and underwater superoleophobic interface; photodegradation

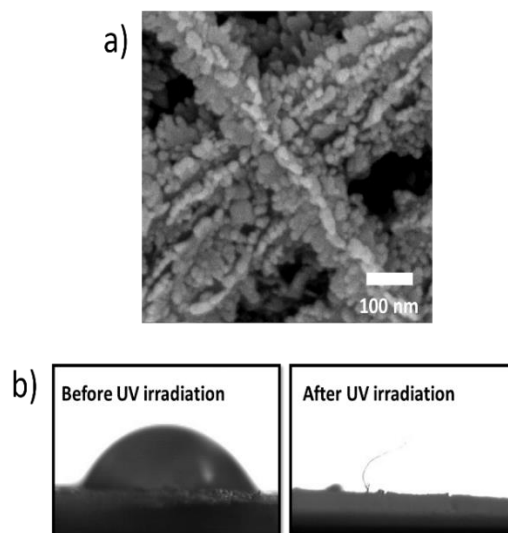


Figure 1: (a) FESEM image of TiO₂/Fe₂O₃ nano-fabric (b) Video snapshots of the water contact measurement (right) before UV irradiation and (left) after UV irradiation indicating recovery cycle of the contaminated TiO₂/Fe₂O₃ membrane

References

1. Asatekin, A.M. Mayes, Oil Industry Wastewater Treatment with Fouling Resistant Membranes Containing Amphiphilic Comb Copolymers, *Environmental Science & Technology*, 43 (2009) 4487-4492.
2. [2] B.Y.L. Tan, M.H. Tai, J. Juay, Z. Liu, D. Sun, A study on the performance of self-cleaning oil-water separation membrane formed by various TiO₂ nanostructures, *Separation and Purification Technology*, 156, Part 3 (2015) 942-951.
3. P. Gao, A. Li, D.D. Sun, W.J. Ng, Effects of various TiO₂ nanostructures and graphene oxide on photocatalytic activity of TiO₂, *Journal of Hazardous Materials*, 279 (2014) 96-104

Nanostructure formation, characterization and application of banana peels nanosorbent in mine water treatment

¹Opeyemi Atiba-Oyewo*, ¹Maurice S. Onyango, ^{2,3}Christian Wolkersdorfer

¹Department of Chemical, Metallurgical and Materials Engineering, Tshwane University of Technology, Pretoria 0001, South Africa

²SARChI Chair for Mine Water Management, Department of Environmental, Water, and Earth Sciences, Tshwane University of Technology, Pretoria 0001, South Africa

³Finnish Professor, Lappeenranta University of Technology, Laboratory of Green Chemistry, Sammonkatu 12, 50130 Mikkeli, Finland

Abstract:

This paper describes the preparation and performance of banana peels nanosorbent for the removal of actinides from mine water. The sorbent before and after adsorption samples were characterised by X-ray diffraction (XRD), Fourier transform infra-red (FTIR), Scanning electron microscopy (SEM) while the amount of actinides adsorbed was determined by inductively coupled plasma optical emission spectroscopy. Results revealed the appearance of fibres in before and after adsorption sorbent samples. The functional groups responsible for the banana peels capability to coordinate and remove metal ions, such as the carboxylic and amine groups, were identified at absorption bands of 1730 and 889 cm^{-1} , respectively, via FTIR analysis. Adsorption isotherm results demonstrated that the adsorption process was endothermic in both uranium and thorium. The Langmuir maximum adsorption capacity was 30.8 mg g^{-1} for uranium and 45.6 mg g^{-1} for thorium. The results obtained indicate that nanostructured banana peel is a potential adsorbent for radioactive removal from mine water. However, the choice of this sorbent material for any application will depend on the water matrix to be treated and therefore more research must be done.

Keywords banana peels, mechanical milling, nanostructure, adsorption, actinides



Figure 1: Figure illustrating the base material we are tempting to create novel media from to solve problem involving waste water problem: A certain functional group was targetted from this agricultural waste which responsible for its ability to coordinate metal ions

References:

1. Bakiya, L. K. & Sudha, P. N. 2012. Adsorption of Copper (II) ion onto chitosan/sisal/banana fiber hybrid composite. *J. Environ. Sci*, 3, 453.
2. Castro, R. S. D., caetano, L., Ferreira, G., Padilha, P. M., saeki, M. J., Zara, L. F., Martines, M. A. U. & Castro, G. R. 2011. Banana Peel Applied to the Solid Phase Extraction of Copper and Lead from River Water: Preconcentration of Metal Ions with a Fruit Waste. *Ind. Eng. Chem. Res.*, 50, 3446-3451.
3. Arup, R. & Jayanta, B. 2015. *Nanotechnology in industrial wastewater treatment*, 12 Caxton street, London, IWA Publishing.

Fabrication of hematite photoanode for solar water splitting by using pulsed laser deposition

Chih-Ping Yen,^{1,2} Yan-Jin Li,³ Shr-Jie Luo,³ Jyhpyng Wang,^{1,2,4} Chung-Jen Tseng,³ Szu-yuan Chen^{1,4}

¹Institute of Atomic and Molecular Sciences, Academia Sinica, Taipei, Taiwan

²Department of Physics, National Taiwan University, Taipei, Taiwan

³Department of Mechanical Engineering, National Central University, Jhongli, Taiwan

⁴Department of Physics, National Central University, Jhongli, Taiwan

Abstract:

Solar hydrogen production is promising as a clean and sustainable energy source. An ideal material for solar water splitting should have the properties such as proper band edge positions, small band gap for good light harvesting, good electron and hole transport characteristics, high electrochemical charge-transfer rate, and high chemical stability. For hematite, however, the low electron mobility, short hole diffusion length, and the sluggish oxygen evolution reaction pose severe limitation on its application, although it possesses a suitable band gap and good chemical stability. These shortcomings could be overcome by (1) employing of n-type doping to increase electron conductivity and to create a depletion region for effective separation of electrons and holes (Cao *et al.*, 2010 and Lee *et al.*, 2014) and (2) fabrication of a nano-porous structure in the hematite film to increase its electrochemically active surface area. (Lee *et al.*, 2014)

In this work, we used pulsed laser deposition in an atmosphere consisting of nitrogen and oxygen gases to prepare Ti-doped α -Fe₂O₃ (hematite) thin films composed of an array of nanorods formed by stacking of nanoparticles on FTO substrates. The films were annealed *in situ* during and after deposition at 500 °C for 4 hours in total. The target-to-substrate distance, nitrogen gas pressure, and oxygen gas pressure were optimized to maximize simultaneously the specific surface area and electron-doping concentration of the hematite film, leading to a high photocurrent density. The dependences of the film characteristics on these control parameters could be explained by cooperative control over nanoparticle formation and oxygen dissipation in the ablation plume to attain the desired mesoscopic morphology and defect identity.

Key words: solar water splitting, hematite photoanode, pulsed laser deposition, defect chemistry

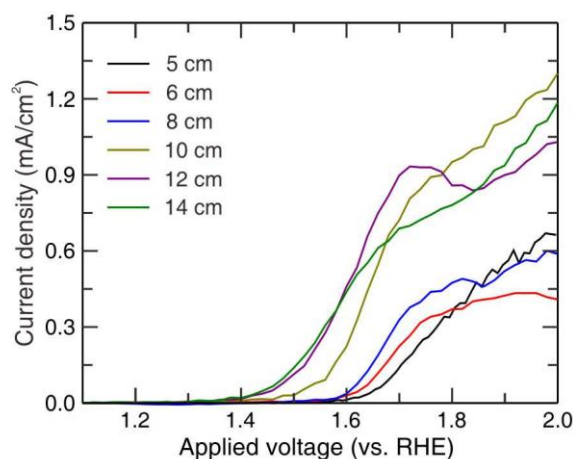


Figure 1: J-V curves of the hematite photoanodes deposited in an atmosphere of 30 mtorr oxygen at various target-to-substrate distances. The photoanode deposited at a target-to-substrate distance of 14 cm exhibits the lowest onset potential and highest photocurrent.

References:

1. Lee, M.H., Park, J.H., Han, H.S., Song, H.J., Cho, I.S., Noh, J.H., Hong, K.S. (2014), Nanostructured Ti-doped hematite (α -Fe₂O₃) photoanodes for efficient photoelectrochemical water oxidation, *Int. J. Hydrogen Energy*, 39, 17501-17507.
2. Cao, J., Kako, T., Kikugawa, N., Ye, J. (2010), Photoanodic properties of pulsed-laser-deposited α -Fe₂O₃ electrode, *J. Phys. D: Appl. Phys.*, 43, 325101-325107.

Molecular Dynamics-Continuum Hybrid Simulation of Water Transport through Carbon Nanotube Membranes

A. Kudaikulov,¹ A. Kaltayev,¹ C. Josserand,²

¹Al-Farabi Kazakh National University, Department of Mechanics, Almaty, Kazakhstan

²Sorbonne Universités, Institut D'Alembert, CNRS and UPMC UMR 7190, 4 place Jussieu, 75005 Paris, France

Abstract:

Nanotechnology holds great potential in advancing water and wastewater treatment to improve treatment efficiency as well as to augment water supply through safe use of unconventional water sources. Various types of nanomaterials, such as nanoadsorbents, nanometals, nanomembranes, and photocatalysts, have been utilized in water treatment applications. However, the prediction of the fluid mass flow rate and heat transfer in nanoscale systems presents a major barrier to their design. The existence of non-continuum effects, such as molecular layering and velocity slip near to liquid–solid interfaces, seemingly precludes efficient continuum computational fluid dynamics (CFD). On the other hand, more accurate molecular dynamics (MD) simulations can be extremely costly in terms of the computational resources they require. In this paper we used the molecular dynamics-continuum hybrid simulation to investigate the water transport through carbon nanotube (CNT) membranes (Figure 1). We present a procedure for using molecular dynamics (MD) simulations to provide essential fluid and interface properties for subsequent use in computational fluid dynamics (CFD) calculations of nanoscale fluid flows. Comparison with full-scale MD simulations demonstrate that these enhanced CFD simulations providing good flow field results in a range of complex geometries at the nanoscale.

Keywords: computational fluid dynamics, molecular dynamics, hybrid methods, carbon nanotube membranes, non-continuum effects, molecular layer, slip flow.

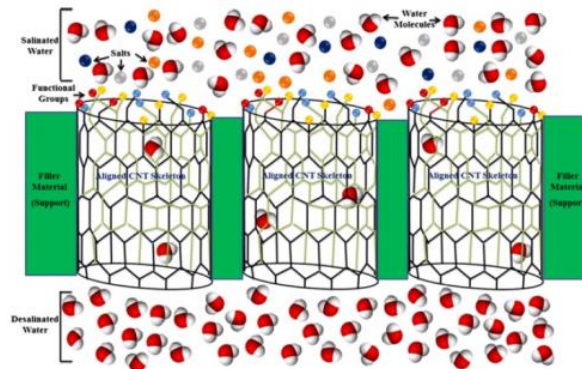


Figure 1: Carbon nanotube membranes (CNT).

References:

David, M., Duncan, A., Matthew, K., William, D., Jason, M. (2015) Molecular dynamics pre-simulations for nanoscale computational fluid dynamics, *Microfluidics and Nanofluidics*, Volume 18, Issue 3, 461-474.

Xiaolei, Q., Pedro, J., Qilin, L. (2013), Applications of nanotechnology in water and wastewater treatment, *Water Research*, Volume 47, Issue 12, 3931-3946.

Titanium Dioxide-Based Nanocatalysts Constructed from Natural Sources for Photocatalytic Wastewater Treatment

Patiya Kemacheevakul^{1*}, Surawut Chuangchote^{2,3,*}

¹Department of Environmental Engineering, Faculty of Engineering, King Mongkut's University of Technology Thonburi, 126 Pracha-uthit Road, Bangmod, Tungkru, Bangkok 10140, Thailand.

²The Joint Graduate School of Energy and Environment, King Mongkut's University of Technology Thonburi, 126 Prachauthit Rd., Bangmod, Tungkru, Bangkok 10140, Thailand.

³Centre of Excellence on Energy Technology and Environment, Science and Technology Postgraduate Education and Research Development Office, Bangkok Thailand.

Abstract:

Sustainable pollutant destruction and energy production are two of the areas in which intense research is being carried out. Photocatalysis can be defined as a catalytic reaction involving the production of a catalyst by absorption of light. Semiconductor-mediated photocatalysis is a well-established technique for pollutant degradation and hydrogen production by water splitting. Nano-structured titanium dioxide (TiO₂) is a multifunctional semiconductor photocatalyst that can be an energy catalyst (in water splitting to produce hydrogen fuel), an environmental catalyst (in water and air purification), or an electron transport medium in dye-sensitized solar cells. Photocatalytic water and air purification using nano-structured TiO₂ is a predominant advanced oxidation process because of its efficiency and eco-friendliness. Recently, dyes and poisonous metals are extremely used in the textiles industries. Unfortunately, they are stable to light and are non-biodegradable. In order to reduce the risk of environmental pollution from such waste, it is necessary to treat them before discharging to the environment. Today, more than 10,000 dyes have been incorporated in the color index. The removal of hazardous materials, e.g. dyes, poisonous metals, and toxic organic and inorganic substances from wastewater is very difficult. There are various methods for removal of organic and inorganic compounds from the wastewater, such as filtration, electrolysis, precipitation, ion exchange, and adsorption process. Among the above-mentioned methods, photocatalysis is highly effective and cheap process than the other methods. In this work, TiO₂-based nanocatalysts were synthesized from Thai natural sources, i.e. TiO₂ nanostructures from natural minerals and hydroxyapatite-supported TiO₂ catalysts from chicken bones. For TiO₂ nanostructures from natural minerals, the minerals were washed by 10 M NaOH aqueous solution (5 times) before synthesis. For hydroxyapatite-supported TiO₂ catalysts, chicken bones were

boiled at 100 °C, dried, and grinded prior to mixing with TiO₂ precursors. The prepared samples were characterized by X-ray fluorescence (XRF), X-ray diffraction, scanning electron microscopy (SEM), transmission electron microscopy (TEM), and nitrogen adsorption (for Brunauer-Emmett-Teller (BET) specific surface area). Photocatalytic degradation of a model dye, i.e. methylene blue, in water by synthesized TiO₂-based catalysts was studied. It was found that nanofibers fabricated from leucoxene minerals showed the highest photocatalytic activity, indicating the high surface area and good crystallinity of the fibers, while the synthesized hydroxyapatite-supported TiO₂ catalysts showed comparable photocatalytic activity with commercial hydroxyapatite-supported ones.

Keywords: dye wastewater, wastewater treatment, photocatalysis, titanium dioxide, natural mineral, hydroxyapatite

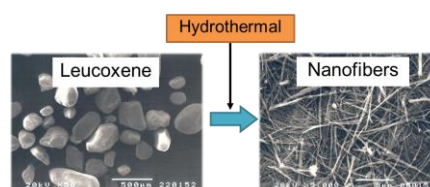


Figure 1: SEM images of natural mineral (leucoxene, left) and nanofibers fabricated from leucoxene (right).

Magnetic Nanoparticles Stabilized by Lignocellulosic Waste as Green Adsorbent For Cr(VI) Removal from Waste Water

I.L.A. Ouma,* A.E. Ofomaja, E.B. Naidoo,

Vaal University of Technology, Biosorption and Wastewater Treatment Research Laboratory,
Vanderbijlpark, South Africa

Abstract:

The application of nanotechnology in water and wastewater treatment has been a topic of interest the past few years. Nanoparticles especially iron oxide magnetic nanoparticles have certain advantages over conventional adsorbents which include large surface area to volume ratio, high reactivity, ability to be functionalized, low diffusion resistance when applied in a packed column and the ability to be separated from treated water by applying a magnetic field (Peng *et al.*, 2014). Nanoparticles have sizes in the nanometer scale and are highly charged leading to agglomeration (size increase) and ultimately loss of desired surface properties. Therefore, to keep them as stable dispersions, avoid agglomeration and loss of surface properties, capping agents need to be added to nanoparticle surfaces (Cheraghipour *et al.*, 2013). Various capping agents have been applied to stabilize nanoparticles in aqueous solution and these includes silica, ligands of nitrogen containing organic chemicals, and polyfunctional organic acids. In this work, pine cone powder obtained from biocompatible agricultural waste materials was used to stabilize iron oxide magnetic nanoparticles to form a nanocomposite which was used for adsorption of Cr(IV) from water. The powder was pre-treated with Fenton's reagent to oxidise some of the surface groups and provide more binding sites for iron oxide while also eliminating soluble organic components which may lead to contamination of the treated water (Argun *et al.*, 2008). Iron oxide magnetic nanoparticles were prepared via the co-precipitation method and the nanocomposite was prepared by precipitation of iron oxide in the presence of pine cone powder. The prepared nanoparticles and nanocomposite were characterized using FTIR, XRD, SEM, TEM and TGA. The amount of Cr(IV) in solution was determined using UV-Vis spectroscopy. It was observed that stabilizing the nanoparticles with pine cone powder improved the chromium uptake by up to 32% and allowed them to be more stable and minimize agglomeration.

Keywords: adsorption, nanoparticles, nanocomposite, co-precipitation.

References:

1. Argun, M.E., Dursun, S., Karatas, M., Gürü, M. (2008), Activation of pine cone using Fenton oxidation for Cd(II) and Pb(II) removal. *Bioresour. Technol.*, 99, 8691–8.
2. Cheraghipour, E., Tamaddon, a. M., Javadpour, S., Bruce, I.J. (2013), PEG conjugated citrate-capped magnetite nanoparticles for biomedical applications. *J. Magn. Magn. Mater.*, 328, 91–95.
3. Peng, X., Xu, F., Zhang, W., Wang, J., Zeng, C., Niu, M., Chmielewska, E. (2014), Magnetic Fe₃O₄ @ silica-xanthan gum composites for aqueous removal and recovery of Pb²⁺. *Colloids Surfaces A Physicochem. Eng. Asp.*, 443, 27–36.

EGF 2016: Plenary session I

Supramolecular approaches to 2-D materials: from complex structures to sophisticated functions

Paolo Samorì

ISIS, Université de Strasbourg & CNRS, 8 allée Gaspard Monge, 67000 Strasbourg, France.

Abstract:

Supramolecularly engineered hybrid materials containing graphene are key multifunctional systems for applications in (opto)electronics and energy. The tuning of their dynamic physical and chemical properties can be achieved via tailored covalent or non-covalent interactions with ad-hoc macromolecules.[1] My lecture will review our recent findings on:

(i) The harnessing of the yield of exfoliation of graphene in liquid media by mastering the supramolecular approach via the combination with suitably designed functional molecules possessing high affinity for the graphene surface, leading ultimately to the bottom-up formation of optically responsive graphene based nanocomposites for electronics.[2]

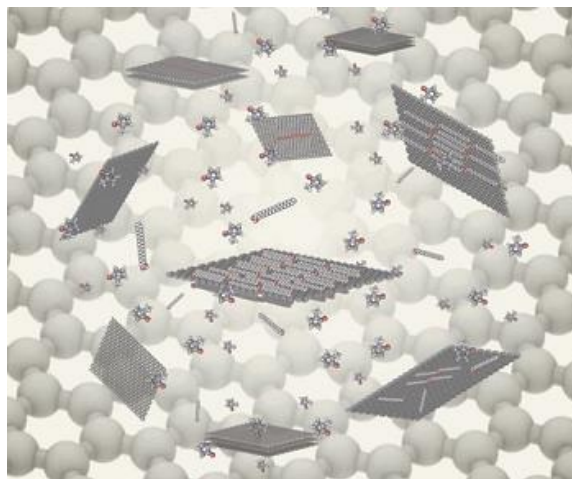
(ii) The tuning of the graphene properties by combining them with organic semiconductors as a strategy both to promote hole mobility in an otherwise electron transporting material and to exploit the tunable ionization energy of thermally annealed liquid phase exfoliated graphene to modulate the transport regime as well as to fabricate new memory devices.[3]

(iii) The bottom-up formation of graphene based 3D covalent frameworks with tunable intersheet distance, exhibiting large specific surface areas which determine extremely high performance in supercapacitors.[4]

(iv) The local thermal reduction of graphene oxide using a laser writer in order to develop very smooth, ultra thin, highly transparent and extremely conducting reduced graphene oxide patterns that can operate as highly sensitive ozone sensor.

Our approaches provide a glimpse on the chemist's toolbox to generate multifunctional graphene based nanocomposites with ad-hoc properties to address societal needs in electronics and energy applications.

Keywords: graphene, supramolecular chemistry, switches, memories, multifunctional devices.



References:

1. A. Ciesielski, P. Samorì, *Chem. Soc. Rev.* **2014**, 43, 381–398. (b) A. Ciesielski, P. Samorì, *Adv. Mater.* **2016** in press (DOI: 10.1002/adma.201505371).
2. (a) A. Ciesielski, S. Haar, M. El Gemayel, H. Yang, J. Clough, G. Melinte, M. Gobbi, E. Orgiu, M.V. Nardi, G. Ligorio, V. Palermo, N. Koch, O. Ersen, C. Casiraghi, P. Samorì, *Angew. Chem. Int. Ed.* **2014**, 53, 10355–10361. (b) S. Haar, A. Ciesielski, J. Clough, H. Yang, R. Mazzaro, F. Richard, S. Conti, N. Merstorf, M. Cecchini, V. Morandi, C. Casiraghi, P. Samorì, *Small* **2015**, 11, 1691–1702. (c) M. Döbbelin, S. Haar, M. Bruna, S. Osella, F. Richard, A. Minoia, R. Mazzaro, E. Adi Prasetyanto, L. De Cola, V. Morandi, R. Lazzaroni, A.C. Ferrari, D. Beljonne, A. Ciesielski, P. Samorì, *Nat. Commun.* **2016**, 7, 11090. (d) X. Zhang, L. Hou, P. Samorì, *Nat. Commun.* **2016**, 7, 11118.
3. (a) M. El Gemayel, S. Haar, F. Liscio, A. Schlierf, G. Melinte, S. Milita, O. Ersen, A. Ciesielski, V. Palermo, P. Samorì, *Adv. Mater.* **2014**, 26, 4814–4819. (b) T. Mosciatti, S. Haar, F. Liscio, A. Ciesielski, E. Orgiu, P. Samorì, *ACS Nano*, **2015**, 9, 2357–2367.
4. X. Zhang, A. Ciesielski, F. Richard, P. Chen, E. Adi Prasetyanto, L. De Cola, P. Samorì, *Small* **2016**, 12, 1044–1052.

Water-based 2D-crystal Inks: from Production to Devices

Cinzia Casiraghi

School of Chemistry, University of Manchester, UK

Abstract:

The isolation of various two-dimensional (2D) materials allows for the possibility to combine them into heterostructures. Such a concept can be used to study particular phenomena such as the metal-insulator transition [1], Coulomb drag [2], Hofstadter's butterfly [3], or to make functional devices such as tunnel diodes [4], tunneling transistors [5,6], photodetectors [7] and light emitters [8].

The range of functionalities and performance are likely to be further improved by increasing the number of components in the heterostructure and by improving their electronic quality. Such complex heterostructures are currently fabricated by using mechanically exfoliated 2D crystals. Therefore, alternative low cost and mass-scalable methods should be utilized to bring the attractive qualities of 2D crystal based heterostructures into real-life applications.

I will show that the ink-based technology is suitable for fabrication of low cost and flexible devices based on heterostructures of arbitrary complexity [9]. The success of this technology does not only depend on the performance of the devices, but also on the nature of the ink. Currently, 2D crystal inks are mostly based on organic solvents [10], which are toxic, expensive and have high boiling point, which affects post-processing. Water is very attractive as solvent, but it is not able to exfoliate graphite and it is also not suitable for inkjet printing, which is a very attractive technique for flexible electronics.

We recently developed a method to produce highly concentrated and oxygen-free graphene dispersions in water [11]. Furthermore, by modifying the exfoliation process, we have been able to produce water-based inks compatible with ink-jet printing technology. The method can be extended to make 2D crystal inks of any layered material (hBN, MoS₂, WS₂, etc [12]), making possible to build a whole heterostructure by inkjet printing different water-based 2D crystal inks [13].

Keywords: graphene, 2D materials, inks, ink-jet printing, heterostructures, photodetectors, flexible electronics.

References:

1. L. A. Ponomarenko et al, Nature Physics 7, 958 (2011)
2. R. V. Gorbachev et al, Nature Physics 8, 896 (2012)
3. L. A. Ponomarenko et al, Nature 497, 594 (2013)
4. L. Britnell et al, Nano Lett., 12, 1707 (2012)
5. L. Britnell et al, Science, 335, 947 (2012)
6. T. Georgiou et al, Nature Nanotech., 8, 100 (2013)
7. L. Britnell et al, Science, 340, 1311 (2013)
8. F. Withers et al, Nature Materials, 14, 301 (2015)
9. F. Withers et al, Nano Letters, 14, 3987 (2014)
10. J. N. Coleman et al., Science 331, 568 (2011)
11. H. Yang et al, Carbon, DOI: 10.1016/j.carbon.2012.11.022
12. H. Yang et al, 2D materials, 1 (1), 011012 (2014)
13. Filed patents; Mc Manus et al, Nature Nanotechnology, *Submitted*

PN Junction Based Devices in Ultra-Clean Graphene

P. Rickhaus¹, Ming-Hao Liu², P. Makk¹, M. Jung¹, C. Handschin¹, S. Zihlmann¹, E. Tovari³, R. Maurand¹, M. Weiss¹, K. Richter² and C. Schönenberger¹

¹ Dept. of Physics, University of Basel, Klingelbergstr. 81, Basel, CH-4056 Switzerland

² Institute of Physics, University of Regensburg, Germany

³ Dept of Physics, Budapest University of Technology and Economics, Hungary

Abstract:

Encapsulated or suspended graphene offers a promising platform for **electron optical devices** due the ballistic nature of electron transport. In graphene gapless **pn interfaces** can be formed by electrostatic gating, showing intriguing effects like a negative index of refraction and tunneling with perfect transmission (Klein tunneling). We have developed a versatile technology that allows to suspend graphene and complement it with arbitrary bottom and top-gate structures. Using current annealing we demonstrate **exceptional high mobilities** in monolayer graphene approaching 10^2 m²/Vs. These suspended devices are **ballistic over micrometer length scales** and display intriguing interference patterns in the electrical conductance when different gate potentials and magnetic fields are applied. Specifically, ballistic electric graphene pn-devices, both suspended and encapsulated, will be discussed, in which one can study **electric analogs** of a **mirror**, a **guiding fiber**, and **Fabry-Perot resonators**, well known in optics. There are great similarities between the propagation of light in a dielectric and electrons in graphene, but also differences. In particular, a negative refractive index is straightforward to realize in graphene, but hard in optics. If time permits, we will discuss recent results on microwave absorption in suspended bilayer graphene shedding light on thermoelectrics, as well as GHz mechanical resonances in suspended pn devices.

Keywords: graphene, ballistic transport, electronic properties, flexible electronics and mechanics, electron optics, nanoelectronics, quantum electronics, spintronics

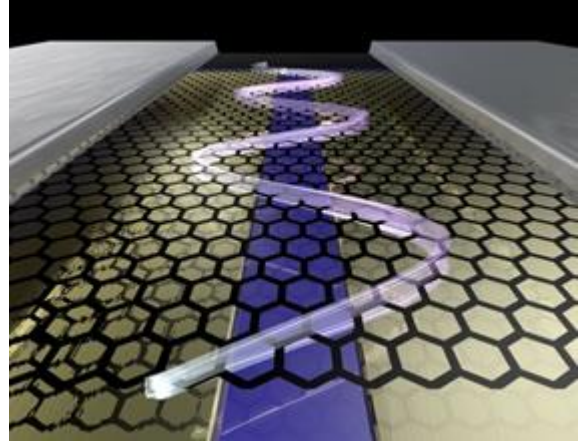


Figure 1: Illustration of electron guiding along a pn junction in graphene in a small magnetic field.

References:

1. P. Rickhaus et al. *Ballistic interferences in suspended graphene*, Nature Comm. 4, 2342 (2013).
2. R. Maurand et al. *Fabrication of ballistic suspended graphene with local-gating*, Carbon 79:486–492 (2014).
3. P. Rickhaus, Ming-Hao Liu, P. Makk, R. Maurand, S. Hess, S. Zihlmann, M. Weiss, K. Richter, and C. Schönenberger, *Guiding of Electrons in a Few-Mode Ballistic Graphene Channel*, Nano Lett. 15, 5819 (2015).
4. Min-Hao Liu et al. *Scalable tight-binding model for graphene*, Phys. Rev. Lett. 114:036601 (2015)
5. P. Rickhaus et al. *Snake trajectories in ultra-clean graphene p–n junctions*, Nature Comm. 6, 6470 (2015).
6. P. Rickhaus et al., Appl. Phys. Lett. 107, 251901 (2015).

2-D Nanocarbons: Attraction, Reality and Future

Zhongfan Liu

Center for Nanochemistry, Beijing Science and Engineering Center for Nanocarbons, College of Chemistry and Molecular Engineering, Peking University, Beijing 100871, China; zfliu@pku.edu.cn

Abstract:

Carbon element has a great number of allotropes, covering the traditional three dimensional (3-D) diamond and graphite, 2-D graphene, 1-D carbon nanotubes and 0-D fullerenes. Recently, graphyne, a new 2-D carbon allotrope family formed by sp and sp^2 hybridization carbon atoms also comes into the stage. Theoretical calculations further indicate that there may exist a *penta*-graphene, formed by a huge number of carbon pentagons in a 2-D fashion instead of the hexagon structure of graphene. Therefore, 2-D nanocarbons including graphene, graphyne, etc have created a new category of carbon allotropes which attract increasing attentions. We have been working on the controlled synthesis of 2-D nanocarbons for many years. Systematic studies have been done on the chemical vapor deposition (CVD) of high quality graphene on various solid substrates ranging from metals (Cu, Ni, Cu-Ni alloy, Pt, Ru, Rh, Ir, Pd), groups IV-VI early transition metal carbides, to dielectric substrates (*h*-BN, STO, glass, NaCl).

We also made a great effort for the controlled synthesis of graphdiyne, a representative member of the graphyne family. A brief overview will be made in the talk following a general concept of CVD process engineering by highlighting the catalyst design, super graphene glass and scalable production techniques of graphene and various applications as well as the Glaser-Hay coupling synthesis of graphdiyne nanowalls on Cu foils and foams.

Keywords: graphene, graphyne, chemical vapor deposition (CVD), super graphene glass, scalable production techniques

Effects of morphology and surface chemistry of graphite nanoplates on dispersion and network formation in polypropylene melts

R. M. Santos¹ and J. A. Covas^{1*}

¹Institute for Polymers and Composites/I3N, University of Minho,
Campus de Azurém, 4800-058 Guimarães, Portugal
jcovas@dep.uminho.pt

Abstract:

Currently, the improvement of the thermal and electrical conductivity of polymers for advanced engineering applications involves the incorporation of particles based on carbon allotropes, including carbon nanotubes, graphite, graphene and its derivatives¹. Graphite nanoplates (GnP), a 2-dimensional hexagonal structure of sp^2 hybridized carbon atoms with open edges, obtained by intercalation and exfoliation of natural flake graphite, is a promising low cost alternative to carbon-based reinforcements. In practice, the dispersion of GnP in polymer media has proven to be difficult, due to their strong π - π interactions and/or lack of functionalities at the surface². When nanocomposites are prepared by melt mixing - a technique that is readily scalable to industrial production, a number of process and material (polymer and filler) parameters influence the outcome. In the case of GnP, surface modification, aspect ratio (L/D), agglomerate density and strength, are particularly important³. Moreover, the stability of the dispersion level depends on the prevailing thermomechanical stresses².

Therefore, the present work investigates the effects of morphology and surface chemistry of graphite nanoplates on their dispersion behavior and network in PP melts. For this purpose, three commercial GnP grades were chemically modified *via* 1,3 dipolar cycloaddition of azomethine ylides and further covalent bonded to polypropylene-*graft*-maleic anhydride (PP-*g*-MA), in order to enhance interfacial bonding with the matrix. Nanocomposites were prepared in a prototype small-scale extensional mixer, under pre-defined temperature and flow rate. The mixer consists of a first sequence of convergent/divergent flow sections inducing a strong extensional component, followed by a chamber with constant cross-section (where relaxation can develop) and a second series of convergent/divergent channels. Samples can be collected along the axis for subsequent characterization (optical microscopy and dielectric spectroscopy). Figure 1 shows the typical evolution of dispersion (in terms of the area Ratio) along the axis of the mixer for the three GnP tested. Dispersion, re-

agglomeration and dispersion (with a distinct rate) are clearly visible.

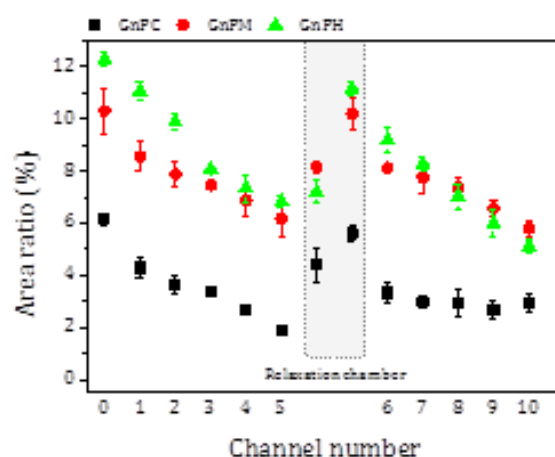


Figure 1: Evolution of dispersion (area ratio) along the axis of the mixer of PP nanocomposites with 2 wt. % of as-received GnP.

Keywords: nanocomposites, melt mixing, dispersion, electrical conductivity.

References:

1. Kuilla, T. *et al* (2010) Recent advances in graphene based polymer composites, *Prog. Polym. Sci.* 35, 1350–1375.
2. Santos, R. M., Vilaverde, C., Cunha, E., Paiva, M. C. & Covas, J. A. (2015) Probing dispersion and re-agglomeration phenomena upon melt-mixing of polymer-functionalized graphite nanoplates, *Soft Matter* 12, 77–86.
3. Beate Krause, G. P. (2009) Correlation of carbon nanotube dispersability in aqueous surfactant solutions and polymers, *Carbon* 47, 602–612.

Exploring Graphene Plasmonics for Novel Applications: From Tunable Absorption Enhancement to Strong Optical Forces

Jianfa Zhang, Wenbin Liu, Zhihong Zhu, Chucai Guo, Ken Liu, Xiaodong Yuan, Shiqiao Qin
National University of Defense Technology, Changsha, China

Abstract:

Graphene shows promising potential in optics and optoelectronics. Among the many novel properties, its plasmonic characteristics are particularly attractive. The low-loss intrinsic plasmons in graphene exhibit strong spatial confinement and remarkable enhancement of local electromagnetic fields. Moreover, the Fermi energy and optical conductivity of graphene can be tuned via chemical or electrostatic doping and this type of tunability can be rarely achieved in traditional plasmonic materials such as gold and silver. Thus graphene plasmons may be explored for a variety of tunable and compact infrared and THz optical devices. Here two potential applications are introduced.

Figure 1(a) shows the simulated optical spectra of an array of doped graphene nanodisks. In the spectral range, a plasmonic dipole resonance is excited and a large proportion of incident light is trapped in the vicinity of the graphene nanodisks which leads to strong field enhancements. Figure 1 (b) is the schematic of a proposed photodetector using graphene plasmonics for light trapping, where tunable absorption enhancement up to tens of times can be realized in the surrounding absorptive layer of graphene nanostructures at the plasmonic resonances. Polarization control and related functionalities will also be studied. This may lead to a new generation of photodetectors with high efficiency and tunable spectral selectivity in the mid-infrared and THz ranges. Fig. 1(c) shows the schematic of optical trapping of nanoparticles with graphene plasmonics. Due to the large field gradients of graphene plasmons, giant optical forces will be exerted on nanoparticles in the near proximity of graphene nanostructures under the illumination of infrared light. The advantages and challenges of using graphene plasmonics for optical nanotweezers will be discussed.

Keywords: graphene plasmonics, light trapping, absorption enhancement, optical forces.

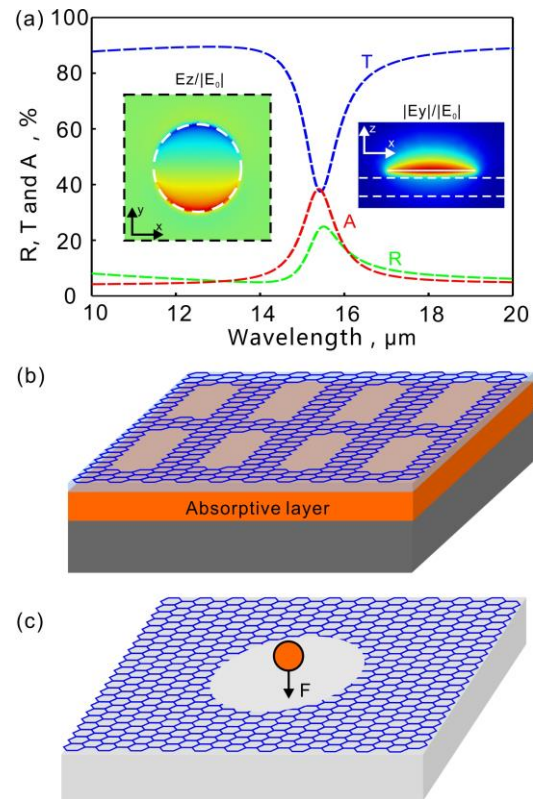


Figure 1: Strong light-matter interactions with graphene plasmonics and the applications. (a) Optical spectra of graphene nanodisks and field distributions at the plasmonic resonance; (b) Tunable absorption enhancement; (c) Giant optical forces exerted on a nanoparticle;

References:

1. Zhang, J. , MacDonald, K. F., Zheludev, N. I. (2012) Optical gecko toe: Optically controlled attractive near-field forces between plasmonic metamaterials and dielectric or metal surfaces, *Phys. Rev. B* 85, 205123.
2. Zhang, J., Guo, C., Liu, K., Zhu, Z., Ye, W., Yuan, X., Qin, S. (2014) Coherent perfect absorption and transparency in a nanostructured graphene film, *Opt. Express* 22, 12,524–12,532.
3. Zhang, J., Zhu, Z., Liu, W., Yuan, X., Qin, S. (2015) Towards photodetection with high efficiency and tunable spectral selectivity: graphene plasmonics for light trapping and absorption engineering, *Nanoscale* 7, 13530–13536.

Scalable Few Layer Graphene Production by Graphite Exfoliation in Liquids

C. Damm,^{1*} T. J. Nacken,¹ H. Xing,¹ Y. Hambal,¹ W. Peukert¹

¹Institute of Particle Technology, Friedrich-Alexander-University Erlangen-Nürnberg, Erlangen, Germany

Abstract:

Industrial application of Graphene and Few Layer Graphene (FLG) requires inexpensive, green and scalable production methods. Stirred media Graphite delamination is a simple and well-scalable liquid-phase exfoliation method and does not require expensive or dangerous feed materials (Nacken *et al.*; 2015; Damm *et al.*; 2015). The Graphite exfoliation is achieved by interaction of the Graphite particles with ZrO₂ beads acting as delamination media (Figure 1). We report the influence of different process parameters (size of ZrO₂ beads, stirrer rotation speed, feed Graphite concentration) on the yield, degree of delamination and quality of the formed product based on the statistical Raman-spectroscopic characterization of the processed materials. The size of the ZrO₂ beads and therefore the kinetic energy transferred to the Graphite particles during collision as well as the solvent viscosity have major impact on defect generation. For bead sizes < 50 µm and/or increased solvent viscosity exfoliation dominates over lateral particle fracture (Figure 1) and therefore FLG (of typically 2-4 layers) with low defect concentration is obtained. A FLG production rate up to ~ 0.3 g/h was achieved for a 200 mL batch. The scalability of stirred media delamination is demonstrated by increasing the batch size by the factor of 10. Moreover, we show that shear-induced Graphite exfoliation as demonstrated for low-viscous Graphite suspensions by Paton *et al.*; 2014 and Liu *et al.*; 2014, is also useful for highly viscous Graphite master batches. We will show how to achieve highly efficient Graphite exfoliation without any product contamination. Product suspensions with FLG concentrations up to 5 g/L were obtained from the processed master batches corresponding to a production rate up to 1.2 g/h for a 500 mL batch.

Keywords: Liquid-phase Graphite exfoliation, Few Layer Graphene, Stirred media mill, Statistical Raman-spectroscopy.

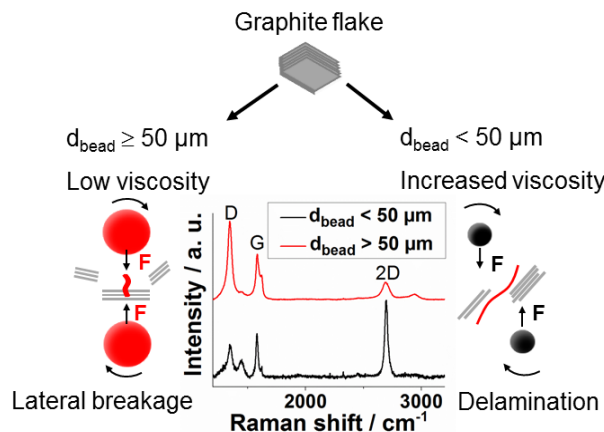


Figure 1: General scheme of stirred media Graphite delamination due to collision with ZrO₂ beads (Nacken *et al.*; 2015). Large beads (50 µm or larger) transfer a too high amount of kinetic energy to the Graphite particles leading to lateral fracture and defect formation (left side). For bead sizes < 50 µm and/or increased solvent viscosity the kinetic energy is below the critical value for defect generation. In this case exfoliation dominates over lateral fracture and FLG of high quality is obtained (right side).

References:

1. Damm, C., Nacken, T. J., Peukert, W. (2015) Quantitative evaluation of delamination of graphite by wet media milling, *Carbon*, 81, 284-294.
2. Liu, L., Shen, Z., Yi, M., Zhang, X., Ma S. (2014) A green, rapid and size-controlled production of high-quality graphene sheets by hydrodynamic forces, *RSC Adv.*, 69, 36464–36470.
3. Nacken, T. J., Damm, C., Xing, H., Rüger, A., Peukert, W. (2015) Determination of quantitative structure-property and structure-process relationships for graphene production in water, *Nano Res.*, 8, 1865-1881.
4. Paton, K.R., Varrla, E., Backes, C., Smith, R.J., Khan, U., O'Neill, A. et al. (2014) Scalable production of large quantities of defect-free few-layer graphene by shear exfoliation in liquids, *Nat. Mater.*, 6, 624–630.

**EGF 2016 Session I:
Graphene and 2D Materials
Synthesis, characterization and
properties**

CVD-grown large-area monolayer MoS₂ using H₂S

D. Dumcenco^{1,*}, D. Ovchinnikov¹, O. Lopez-Sanchez¹, P. Gillet², D. T. L. Alexander³, S. Lazar⁴, A. Radenovic⁵, A. Kis¹

¹Electrical Engineering Institute, EPFL, Lausanne, Switzerland

²Institute of Condensed Matter Physics, EPFL, Lausanne, Switzerland

³Interdisciplinary Center for Electron Microscopy, EPFL, Lausanne, Switzerland

⁴FEI Electron Optics, Eindhoven, Netherlands

⁵Institute of Bioengineering, EPFL, Lausanne, Switzerland

Abstract:

Because of the unique two-dimensional (2D) nature, molybdenum disulfide (MoS₂) has attracted extensive attention for a variety of next generation electrical and optoelectronic device applications. This material has a crystalline structure consisting of covalently bonded layers weakly coupled to each other by weak van der Waals forces in the bulk form. By scotch tape or liquid-phase exfoliation monolayer MoS₂ can be easily obtained. Using mechanical exfoliation from bulk samples, versatile devices were demonstrated on 2D MoS₂ crystals. However, exfoliation is not scalable for large-scale device fabrication resulting from the absence of controllable thickness, size and uniformity of the 2D film. Up to date, chemical vapor deposition (CVD) is the most promising method to synthesize monolayer MoS₂ from triangular islands up to hundreds of micrometers in size to a large film scale. We report on the growth of MoS₂ using H₂S as a gas-phase sulfur precursor. Depending on the H₂S:H₂ ratio in the reaction gas mixture and temperature at which they are introduced during growth, it allows controlling the domain growth direction of domains in both vertical (perpendicular to the substrate plane) and horizontal (within the substrate plane). Different characterization techniques such as optical and atomic force microscopy, scanning transmission electron microscopy, Raman and photoluminescence spectroscopy demonstrate the formation of monolayer triangular-shape domains with a regular atomic structure of a hexagonal symmetry. Field-effect transistors fabricated on MoS₂ domains show mobility similar to previously reported exfoliated and CVD-grown materials.

Keywords: MoS₂, monolayer, CVD.

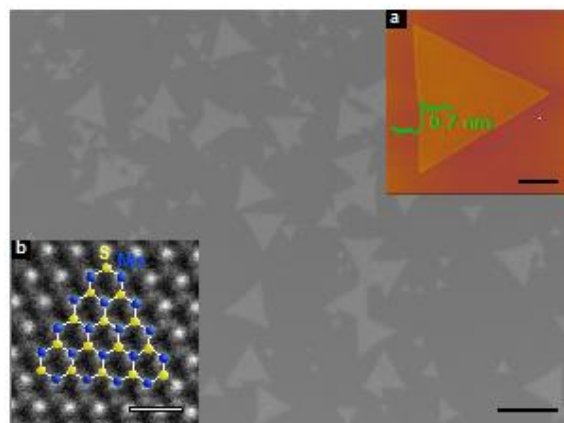


Figure 1: Optical microscopy image of the sample showing incomplete coverage area with isolated MoS₂ islands. Scale bar length is 10 μm. Original optical images were converted to greyscale. Inset (a): Atomic force microscope image showing a monolayer MoS₂ island. Scale bar length is 2 μm. Inset (b): Scanning transmission electron microscopy image of monolayer MoS₂ lattice with structural model overlaid. Scale bar length is 500 pm.

References:

- Dumcenco, D., Ovchinnikov, D., Marinov, K., Lazić, P., Gibertini, M., Marzari, N., Lopez-Sanchez, O., Kung, Y.-C., Krasnozhan, D., Chen, M.-W., Bertolazzi, S., Gillet, P., Fontcuberta i Morral, A., Radenovic, A., Kis, A. (2015) Large-Area Epitaxial Monolayer MoS₂, *ACS Nano*, 9, 4611-4620.
- Dumcenco, D., Ovchinnikov, D., Lopez-Sanchez, O., Gillet, P., Alexander, D., Lazar, S., Radenovic, A., Kis, A. (2015) Large-area MoS₂ grown using H₂S as the sulphur source, *2D Materials*, 2, 044005.

Centimeter-scale synthesis of ultrathin layered MoO₃ by van der Waals epitaxy

Aday J. Molina-Mendoza^{1*}, José L. Lado², Joshua Island³, Miguel Angel Niño⁴, Lucía Aballe⁵, Michael Foerster⁵, Flavio Y. Bruno⁶, Herre S. J. van der Zant³, Gabino Rubio-Bollinger^{1,7}, Nicolás Agrait^{1,4,7}, Emilio M. Perez⁴, Joaquín Fernández-Rossier², and Andres Castellanos-Gomez⁴

¹Departamento de Física de la Materia Condensada, Universidad Autónoma de Madrid, Campus de Cantoblanco, E-28049, Madrid, Spain.

²International Iberian Nanotechnology Laboratory (INL), Av. Mestre Jose Veiga, 4715-330, Braga, Portugal

³Kavli Institute of Nanoscience, Delft University of Technology, Lorentzweg 1, 2628 CJ Delft, The Netherlands

⁴Instituto Madrileño de Estudios Avanzados en Nanociencia (IMDEA-nanociencia), Campus de Cantoblanco, E-28049 Madrid, Spain

⁵ALBA Synchrotron Light Facility, Carretera BP 1413, Km. 3.3, Cerdanyola del Vallés, Barcelona 08290, Spain

⁶Department of Quantum Matter Physics, University of Geneva, 24 Quai Ernest-Ansermet, 1211 Genève 4, Switzerland

⁷Condensed Matter Physics Center (IFIMAC), Universidad Autónoma de Madrid, E-28049 Madrid, Spain

Abstract: Molybdenum trioxide nanosheets (MoO₃), recently isolated by mechanical exfoliation of bulk α -MoO₃ layered crystals, is a relatively low-bandgap oxide (>2.7 eV) making it very attractive for applications requiring a transparent material in the visible part of the spectrum (Kalantar-zadeh et al., 2010), and for devices such as field effect transistors and photodetectors (Balendhran et al., 2013). However, a method for the large scale synthesis of this novel 2D material is still not well established. We report on the large-scale synthesis of highly oriented ultrathin MoO₃ layers using an atmospheric pressure, van der Waals epitaxy growth on muscovite mica substrates (Wang et al., 2014), with thicknesses ranging from 1.4 nm (two layers) up to a few nanometers. The crystals can be easily transferred to an arbitrary substrate (such as SiO₂) by a deterministic transfer method and extensively characterized to demonstrate the high quality of the resulting crystal. We also study the electronic band structure of the material by density functional theory calculations demonstrating that bulk MoO₃ has a rather weak electronic inter-layer interaction and thus it presents a monolayer-like band structure. Finally, we fabricate large-area field-effect devices (10 μ m by 110 μ m in lateral dimensions), finding responsivities of 30 mA \cdot W⁻¹ for a laser power density of 13 mW \cdot cm⁻² in the UV region of the spectrum

Keywords: two-dimensional materials · molybdenum oxide · van der Waals epitaxy · UV photodetector

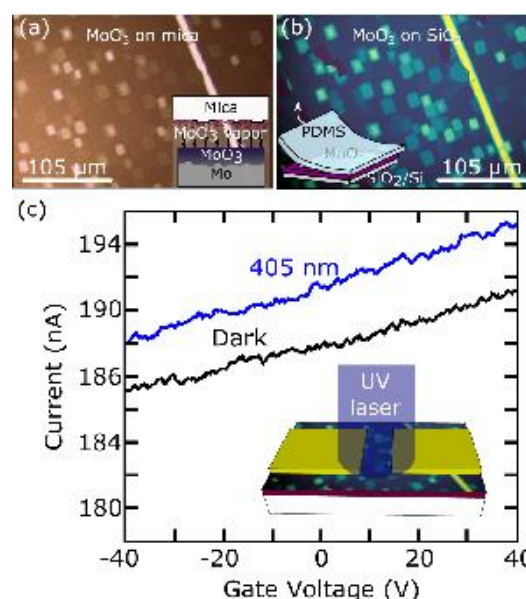


Figure 1: MoO₃ extended layer (a) as-grown on mica (inset: drawing of the growth process) and (b) transferred to a SiO₂ (inset: drawing of the transfer method). (c) Source-drain current for a fixed V_b as a function of the back-gate voltage (inset: drawing of a MoO₃ UV-photodetector)

References:

1. Kalantar-zadeh, K.; Tang, J.; Wang, M.; Wang, K. L.; Shailos, A.; Galatsis, K.; Kojima, R.; Strong, V.; Lech, A.; Wlodarski, W.; Kaner, R. B. (2010) Synthesis of nanometre-thick MoO₃ sheets. *Nanoscale*, 2, 429-433.
2. Balendhran, S.; Deng, J.; Ou, J. Z.; Walia, S.; Scott, J.; Tang, J.; Wang, K. L.; Field, M. R.; Russo, S.; Zhuiykov, S.; Strano, M. S.; Medhekar, N.; Sriram, S.; Bhaskaran, M.; Kalantar-zadeh, K. (2013) Enhanced Charge Carrier Mobility in Two-Dimensional High Dielectric Molybdenum Oxide. *Advanced Materials*, 25, 109-114
3. Wang, Q.; Safdar, M.; Xu, K.; Mirza, M.; Wang, Z.; He, J. (2014) Van der Waals Epitaxy and Photoreponse of Hexagonal Tellurium Nanoplates on Flexible Mica Sheets. *ACS Nano*, 8, 7497-7505.

Plasma-assisted CVD graphene synthesis and characterization on nickel substrates

P. Pop-Ghe,^{1*} L. Krückemeier,¹ N. Wöhrl,¹ V. Buck¹

¹University of Duisburg-Essen, Faculty of Physics and CENIDE, Duisburg, Germany

Abstract:

This work presents the synthesis of graphene by plasma-assisted chemical vapour deposition on polycrystalline nickel foils. It is initiated by the comparison of the mechanisms in CVD and plasma-assisted CVD on a nickel substrate and focusses on the development of a growth model for both sides of the substrate within the experimental results. In detail, the differences in graphene growth at the front and at the back side of the substrate are investigated and correlated to specific influence factors. It is shown that growth mode as well as expansion and quality of graphene sheets can be adjusted by process temperature and time respectively since carbon solubility and diffusion in nickel both hold strong temperature and time dependencies. The strong time dependence of graphene growth is further indicative of a reconstructional nature of graphene formation, which is further discussed in the developed growth model. In addition the influence of the substrate is investigated by comparing results from graphene growth on polycrystalline nickel foils and nickel single crystal(111) substrates, as well as graphene on nickel (synthesized graphene) and silicon dioxide substrates (transferred graphene). Raman mappings are demonstrated to confirm the quality of the synthesized graphene.

Keywords: graphene growth, PECVD, growth mechanisms, carbon diffusion and solubility in nickel, graphene growth model, temperature dependence, Raman mapping, surface plasma, nickel substrates

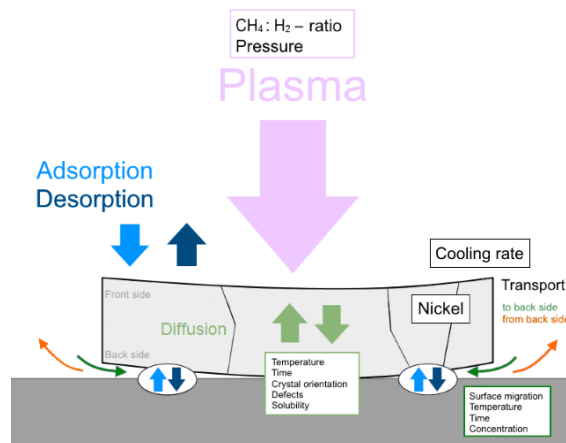


Figure 1: Schematic summary of the most important mechanisms and influence factors in PACVD growth of graphene concerning the front and the back side of the substrate respectively. All of the depicted direction arrows refer to the movement of carbon species.

References:

- M. Losurdo, M. M. Giangregorio, P. Capezzuto and G. Bruno (2011), Graphene CVD growth on copper and nickel: role of hydrogen in kinetics and structure, *Physical Chemistry Chemical Physics*, 13, 20836.
- G. Kalita, K. Wakita and M. Umeno (2012), Low temperature growth of graphene film by microwave assisted surface wave plasma CVD for transparent electrode application, *RSC Advances*, 2, 2815.

A Record-Breaking Mobility For CVD Graphene By Suppressing The Effect Of Charged Impurities

R. Nashed,^{1,*} K. Brenner,² A. Naeemi¹

¹ Georgia Institute of Technology, School of Electrical and Computer Engineering, Atlanta, USA

² Harper Labs LLC., Atlanta, USA

Abstract:

We have developed a simple, two-step lithography process to fabricate CVD graphene devices in a manner that is compatible with wafer-scale CMOS. Record-breaking electron and hole mobilities of 25,600 and 23,700 cm²/Vs, respectively, are achieved with high symmetry and low intrinsic doping. To the best of our knowledge, the highest reported mobility for CVD-grown graphene has been 11,000 cm²/V.s [1]. Figure 1a summarizes the fabrication process of the CVD graphene devices. The first step is patterning the graphene sheet into 30 μm × 10 μm rectangles using electron beam lithography with 2% HSQ as an etch mask. The channel length was intentionally made much larger than the typical mean free path of graphene to account for scattering and demonstrate the high quality of the fabricated devices. Next, the metal contacts are patterned using the positive-tone resist ZEP520. Prior to deposition of the metal, a BOE etch is used to clear the HSQ and allow contact with the graphene. Finally, Ti/Au with a 20/80 nm thickness is deposited by e-beam evaporation and a standard liftoff. We believe that the improvement in the charge carrier mobility is largely due to using HSQ as a top dielectric layer for several reasons. Firstly, using a high-k medium was shown to fix the Dirac point at zero V_g, where V_g is the back gate voltage, and lead to a sharp R-V_g curve; hence improving mobility[2]. This is due to the dielectric screening of charged impurities by the high-k material. The Fourier transform of the potential of a charged impurity is given by [3]:

$$V_i^0(q) = \frac{2pe^2}{kq} \quad (1)$$

where k is proportional to the screening (dielectric) constant, which is the average dielectric constant of the material below and above the graphene sheet. In the absence of HSQ, the average dielectric constant is given by averaging the dielectric constant of SiO₂ ($k_{SiO_2}=3.9$) and that of air ($k_{air}=1$); that is $k_{avg}=(3.9+1)/2 \approx 2.5$.

Adding HSQ ($k_{HSQ}=4$) increases the average dielectric constant to ~ 4 . From equation (1), the potential created by the charged impurities is reduced and hence the force felt by an electron moving from the source to the drain of the graphene transistor is reduced, which in turn minimizes scattering. Furthermore, we believe that HSQ helps pin down the graphene to SiO₂ and hence minimizes the charged impurities (mainly O₂ and H₂O) trapped between graphene and SiO₂; thus reduces scattering and improves mobility. Figure 1b shows the transfer characteristics of a typical device measured at room temperature.

Keywords: CVD Graphene, Interconnects, Dielectric Screening, Electron mobility

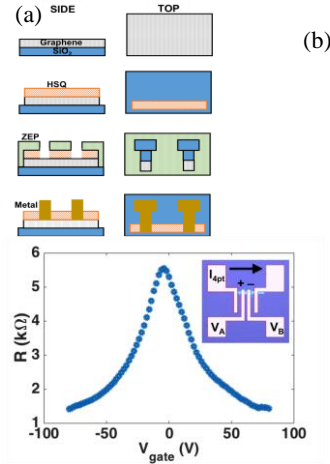


Figure 1: (a) The general process flow for a dielectrically pinned CVD graphene. First, the starting material is CVD graphene on SiO₂. Next, EBL is used to pattern the graphene with HSQ. Next, the HSQ pattern is transferred into the graphene via a plasma etch. Next, a second EBL layer with ZEP is used to pattern via and contact pads. Next, the vias are opened by clearing the HSQ using a wet etch. Next, contact metal is deposited using E-Beam. Finally, the excess metal is removed using a standard liftoff procedure, (b) Transfer characteristics from four-point measurements on a typical pinned CVD graphene device. An optical image of the device is shown in the inset. Four-point testing is performed by passing an excitation current around the outer pads and measuring the voltage drop across the inner pads.

Chemical Kinetics during CVD Growth of Graphene

S. Farhat¹, I. Hinkov², H-A. Mehedi¹ and A. Gicquel¹

¹ Laboratoire des Sciences des Procédés et des Matériaux, CNRS, LSPM – UPR 3407, Université Paris 13, PRES Sorbonne-Paris-Cité, Villetaneuse, 93430, France

² Département de Génie Chimique, Université de Technologie Chimique et de Métallurgie, Sofia 1756, Bulgaria

Abstract:

Efforts to obtain high-quality graphene film over a large area have been hampered by the lack of quantitative understanding of the gas phase chemistry as well as the nucleation and growth mechanisms at the scale and quality required for applications. To date, among graphene synthesis methods, only chemical vapor deposition (CVD) method has shown the capability for growing high-quality graphene film [1]. The quality and continuity of the graphene being affected by numerous process parameters such as growth temperature, hydrocarbon concentration, pressure and cooling rate. Also, the graphene growth mechanism is significantly affected by catalyst type, structure, quality, and carbon solubility. However, synthesizing a single-layer graphene and controlling the quality of the graphene film are very challenging due to the multiplicity of the growth conditions. Complementary in-situ metrology approach including XPS, XRD, Raman and ESEM have been proposed to study Graphene-catalyst interactions during the synthesis [1]. Computer modeling could be supportive in understanding CVD graphene growth mechanism. In this article, we report on some of the fundamental chemical and physical processes responsible for the deposition of graphene by plasma enhanced chemical vapor deposition (PECVD). In order to investigate the effect of the process parameters on the graphene growth, graphene were grown by plasma decomposition of a mixture of methane and hydrogen over different catalysts (Co, Ni and Cu). During cooling from high temperature, carbon atoms segregate to the catalyst surface, causing graphene islands to nucleate. Using a thermochemical mathematical model, we calculate the local concentration of carbon precursors on the surface resulting from the reactions taking place inside the plasma. The model includes species and energy equations for analyzing specific conditions for graphene growth in a microwave plasma reactor by extending classical chemistry formulation to non-equilibrium plasma reactors that include (H_2 / CH_4) gas-phase reactions, surface-recombination and detailed power deposition with inelastic and elastic collision losses [2]. To understand the effect of the macroscopic process parameters on graphene growth, a two dimension (2D) model with reduced kinetics has been also developed and implemented in the commercial computational fluid dynamics (CFD) software ANSYS Fluent [3]. Simulations were performed to determine the gas phase fields for temperature and species concentration (Figure 1-a) as well as the surface-species coverage. Hydrocarbon species such as C_2H_2 , CH_3 are likely to be key deposition species influencing graphene growth on the substrate. If the amount of bulk carbon is sufficiently high, a single layer of graphene can nucleate and grow from carbon segregating on metals during cooling. At higher bulk concentrations, multilayers of graphene can precipitate.

A model representing CVD graphene growth on cobalt thin films by dissolution-precipitation mechanism will be presented. Our results indicates that substrate temperature as well as hydrocarbon injection time affects spatially and time resolved diffusion of carbon in bulk cobalt thereby controlling graphene nucleation and growth (Figure 1-b).

Keywords: Graphene - PECVD - Modeling - Plasma - Kinetics -

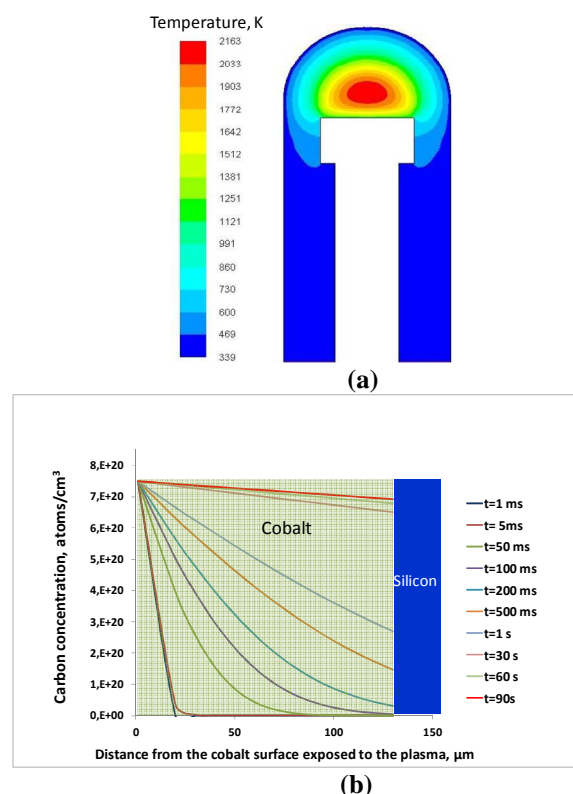


Figure 1: (a) Calculated contours of temperature during PECVD graphene deposition. (b) Spatially and time resolved diffusion of carbon in Cobalt.

References:

- [1] Hofmann S., Braeuninger-Weimer P., Weatherup R.S., CVD-Enabled Graphene Manufacture and Technology, *J. Phys. Chem. Lett.* 6, 2714 (2015).
- [2] Scott, C. D., S. Farhat, A. Gicquel, K. Hassouni, M. Lefebvre, "Finding Electron Temperature in a Hydrogen Microwave Discharge Plasma", *Journal of Thermophysics and Heat Transfer*, vol. 10, No. 3, 426-435, 10 pages, (1996).
- [3] ANSYS, Inc. (2010, November). ANSYS Workbench User's Guide. Canonsburg, Pennsylvania, United States of America.

Optimized Synthesis of Graphene by Cobalt-Catalyzed Decomposition of Methane with Plasma-Enhanced CVD

H.-A. Mehedi¹, B. Baudrillart¹, D. Alloyeau², C. Ricolleau², J. Lagoutte², A. Gicquel¹, S. Farhat¹

¹Laboratoire des Sciences des Procédés et des Matériaux, CNRS, LSPM – UPR 3407, Université Paris 13, PRES Sorbonne-Paris-Cité, Villetaneuse, 93430, France

²Laboratoire Matériaux et Phénomènes Quantiques, CNRS, UMR 7162, Université Paris Diderot, Bâtiment Condorcet, Paris, 75205, France

Abstract:

The reduced thermal load and the possibility to industrially scale-up the plasma-enhanced CVD (PECVD) process makes it a very attractive alternative to the thermal CVD process with respect to future's graphene production. However, PECVD graphene, in general, displays significant D-band, thus with quality still not equivalent to exfoliated or thermal CVD graphene. In addition, the process space for graphene-PECVD growth is usually complex, very wide and depends on many factors, from substrate choice, to specific growth conditions, as well as variables not under direct control. Many experiments need to be performed for reaching at the optimum conditions. Here, we report the optimization of PECVD process for the synthesis of graphene films by cobalt-catalyzed decomposition of methane. In order to find the most appropriate experimental conditions for the realization of thin, high-grade films, eight experiments suitably designed and performed using Taguchi experimental design technique. The influence of temperature (700–890 °C), synthesis duration (30–90 sec), methane flow (1–10 sccm) and microwave power (300–400 watt) on the number of graphene layers and defect density in the graphitic lattice was ranked by monitoring the intensity of the 2D and D-bands relative to the G-band in the Raman spectra. After critical examination and adjusting of the conditions predicted to give optimal results, a continuous film of monolayer graphene was obtained, as characterized by Raman spectroscopy (Figure 1a). The optimal setting allows us to realize graphene deposition up to 2 inch surface coverage. Graphene samples were further characterized with STM and HRTEM (Figure 1b and c) after their transfer on the TEM grid and gold/mica substrates respectively, using bubbling transfer approach. Analysis of PECVD process optimization with Taguchi software 'Qualitek-4' coupled to theoretical modeling of plasma chemistry will also be discussed.

Keywords: Plasma-enhanced-CVD, Taguchi experimental design, Qualitek-4 software, Bubbling transfer of graphene, Raman spectroscopy, Transport properties of graphene, Theoretical modeling.

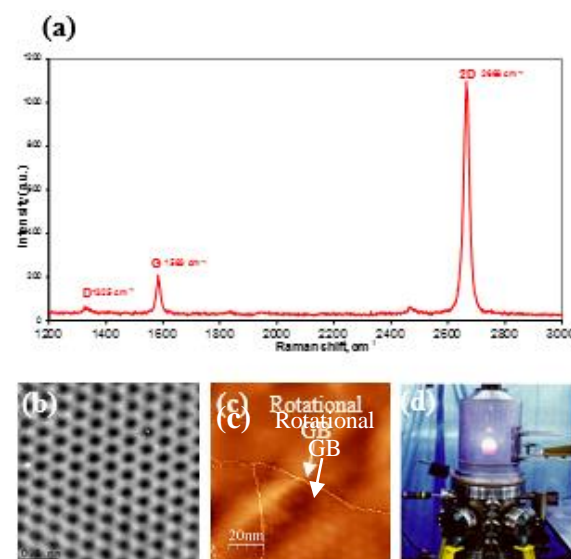


Figure 1: (a) Raman spectrum of the films deposited with optimal PECVD process conditions displaying characteristic Raman of SLG with the $I_{2D}/I_G \sim 5$; (b) HRTEM image confirming deposition of SLG; (c) STM image at 4K displaying well-defined rotational grain boundaries and (d) photograph of the Bell Jar type PECVD reactor used in this study.

References:

- Bonaccorso, F., Lombardo, A., Hasan, T., Sun, Z., Colombo, L., Ferrari, A. C. (2012), Production and processing of graphene and 2d crystals, *Materials Today*, 15, 564–589.
- Singh, H. (2012), Taguchi optimization of process parameters: a review and case, *Int. J. Adv. Eng. Res. Stud.*, I, 39–41.

Tuning the nature of nitrogen atoms in N-containing RGO: Enhanced thermal oxidation stability by nitrogen doping.

Stefania Sandoval,^{a*} Nitesh Kumar,^b A. Sundaresan,^b C. N. R. Rao,^b Amparo Fuertes^a and Gerard Tobias^a

^aInstitut de Ciència de Materials de Barcelona (ICMAB-CSIC), Campus de la UAB, 08193 Bellaterra (Barcelona), Spain

^bJNCASR, Jakkur P.O., Bangalore- 560064

Abstract:

N-containing reduced graphene oxide (RGO) samples have been prepared by ammonolysis of GO.¹ The nitrogen content (up to 14.7 wt. %), as well as the level of reduction have been tailored by tuning the annealing conditions of the reaction. The employed methodology allows expanding the capabilities of the synthetic approach to afford not only N-doping (at high temperature) but also to introduce amine and amide moieties at 100 °C (Figure 1). The presence of N within the structure of RGO confers the material interesting properties including a much greater thermal stability against oxidation by air² and a higher dispersability in aqueous media than GO.³ The observed thermal stability is closely related to the temperature of synthesis and the nitrogen content. The combustion reaction of N-doped RGO with nitrogen atoms occupying different coordination environments (pyridinic, pyrrolic, and graphitic) is analyzed against a graphene fragment (undoped) from a thermodynamic point of view. In agreement with the experimental observations, the combustion of undoped graphene turns out to be more spontaneous than when nitrogen atoms are present. Employing several complementary techniques it is possible to properly assess the nature of the nitrogen atoms present in the sample. The presented characterization protocol benefits from the physical and chemical properties of the nitrogen bearing RGO to unambiguously discern between N-bearing aliphatic functionalities and N-doping.[3]

This work opens up new possibilities for tailoring the properties of graphene and related systems, further expanding their range of application.

Keywords: Graphene oxide, functionalization, nitrogen doping, ammonolysis, reduction, thermal stability, dispersability.

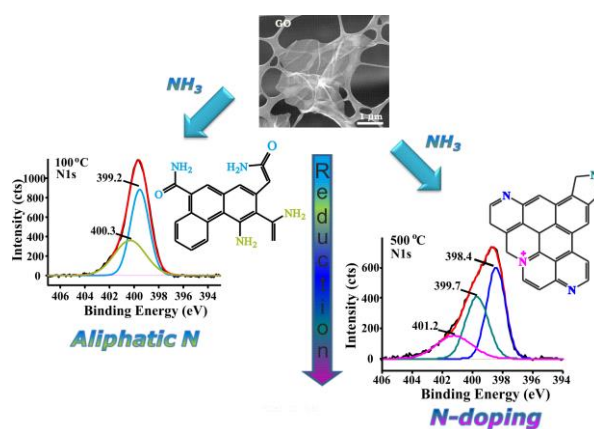


Figure 1: The nature of the N atoms within the RGO structure as well as the level of reduction is tailored by ammonolysis of GO at different temperatures.

References:

1. Marcano DC, Kosynkin DV, Berlin JM, Sinitskii A, Sun Z, Slesarev A, et al. Improved Synthesis of Graphene Oxide. *ACS Nano*. **2010**;4(8):4806-14.
2. Sandoval, S.; Kumar, N.; Sundaresan, A.; Rao, C. N. R.; Fuertes, A.; Tobias, G. Tuning the nature of nitrogen atoms in N-containing reduced graphene oxide. *Carbon*, **2016**, 96, 594.
3. Sandoval, S.; Kumar, N.; Sundaresan, A.; Rao, C. N. R.; Fuertes, A.; Tobias, G. Enhanced thermal oxidation stability of reduced graphene oxide by nitrogen doping. *Chemistry – A European Journal*, **2014**, 20, 11999.

Towards High Quality Graphene Flakes by Electrochemical Exfoliation of Graphite With Multifunctional Electrolytes

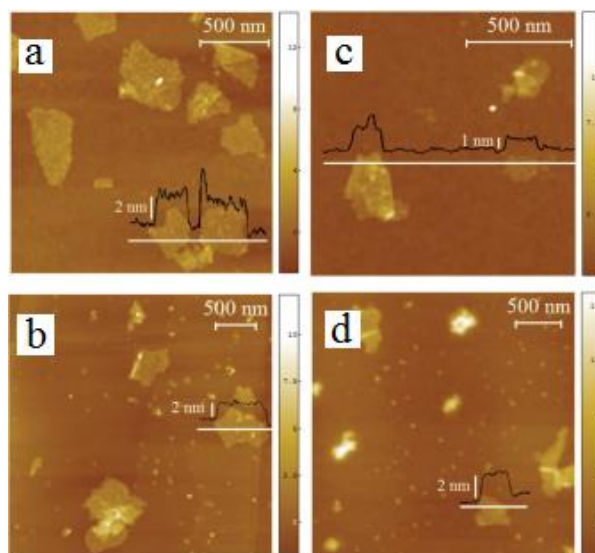
J.M. Munuera, J.I. Paredes, S. Villar-Rodil, M. Ayán-Varela, A. Martínez-Alonso, J.M.D. Tascón

Instituto Nacional del Carbón, INCAR-CSIC, Apartado 73, 33080 Oviedo, Spain

Abstract:

Anodic exfoliation of graphite in water under anodic potential is an attractive and cost-effective method for the mass production of. However, it also suffers from several drawbacks, including the oxidation and structural degradation of the graphene flakes that is usually associated to this electrochemical approach. To overcome these limitations, especially selected multifunctional electrolytes are used here for the anodic preparation of graphene flakes. Such electrolytes are anions with an amphiphilic character (mostly aromatic hydrocarbons functionalized with sulfonate groups) and are shown to play various relevant roles. Thus, in addition to acting as intercalating electrolyte that triggers the exfoliation of graphite into graphene flakes, they are simultaneously used as a surfactant to colloidal stabilize the exfoliated flakes in aqueous and as a sacrificial agent that is able to prevent to a large extent the oxidation of the graphene flakes during exfoliation and. Importantly, this strategy even affords anodically exfoliated graphenes of a quality comparable to that of flakes produced by direct, ultrasound- or shear-induced exfoliation of graphite in the liquid phase (i.e., flakes that are almost oxide- and defect-free). Furthermore, these multifunctional electrolytes are employed as linkers to favour the anchoring of platinum nanoparticles on the flakes, yielding functional hybrids with good catalytic activity towards the reduction of nitroarenes. A rationale that accounts for the multifunctional nature of these electrolytes (i.e., their ability as intercalating species, colloidal dispersant and sacrificial agent) is provided as well. Taken together, the present results open the prospect of anodic exfoliation as a competitive method for the production of very high quality graphene flakes.

Keywords: graphene, graphene production, Pt nanoparticles, catalysis, aromatic sulfonate.



graphene flakes prepared with 0.1 M sodium sulfate (a), 0.01 M sodium pyrene tetrasulfonate (b), 0.05 M sodium benzene disulfonate (c) and 0.2 M sodium naphthalene disulfonate (d). A typical line profile taken along the marked white line is shown superimposed on each image.

References:

- (1) J. M. Munuera, J. I. Paredes, S. Villar-Rodil, M. Ayán-Varela, A. Martínez-Alonso and J. M. D. Tascón (2016) Electrolytic exfoliation of graphite in water with multifunctional electrolytes: en route towards high quality, oxide-free graphene flakes Nanoscale, (2016), DOI: 10.1039/c5nr06882g

Acknowledgements

Financial support from the Spanish Ministerio de Economía y Competitividad (MINECO) and the European Regional Development Fund (ERDF) through project MAT2011-26399 is gratefully acknowledged. Partial funding by Plan de Ciencia, Tecnología e Innovación (PCTI) 2013–2017 del Principado de Asturias and the ERDF (project GRUPIN14-056) is also acknowledged. J. M. M. and M. A.-V. are grateful to the Spanish Ministerio de Educación, Cultura y Deporte (MECD) and MINECO, respectively, for their pre-doctoral contracts.

Figure 1: Representative AFM images of

Deoxygenation of Graphene Oxide by Metalorganic Compounds

N. Jalagonia,¹ T. Kuchukhidze,¹ N. Jalabadze,³ V. Tsitsishvili,² R. Chedia,^{1,2}

¹Ilia Vekua Sukhumi Institute of Physics and Technology, Tbilisi, Georgia

²Iv. Javakhishvili Tbilisi State University, P. Melikishvili Institute of Physical and Organic Chemistry, Tbilisi, Georgia

³Georgian Technical University, Tbilisi, Georgia

Abstract:

Graphene oxide, obtained by oxidation of graphite contains oxygen functional groups (-COOH, -OH, -O-O-, -CHO), after reduction of which reduced graphene oxide (rGO) is received, in which C:O ratio increases due to partial removal of oxygen atoms (deoxygenation). Many organic and inorganic compounds are used as reducers. As a result of reduction oxygen-containing graphene functional groups OH groups are formed. Thus structure of rGO is defective due to existence of sp^3 carbon atoms. Transition of sp^3 state in sp^2 might conduct in a result of treatment of rGO by metal amides, hydride and metal-organic compounds. Using of soluble metalorganic compounds ($RMgCl$, AlR_3 , $ClAlR_2$ etc.) in aprotic solvents is more perspective. In a result of treatment (2–24 hrs, 50–90°C, Ar) of graphene oxide suspension in aprotic solvents by metal-organic compounds, hydrocarbonyls RH is excreted and graphene oxide, functionalized by alumoorganic compounds have been received, which contains -Al-O-C (sp^3) bonds. Such kinds of compounds after heating (>500°C) in inert environment or in vacuum are decomposed, this means that oxygen atoms existed in graphene transform in Al_2O_3 phase, thus deoxygenation of graphene oxide takes place. Similarly interact calcium organic compounds. By variation of metal-organic compounds it is possible to include any metal-oxide or metalorganic fragments in structure of graphene oxide (functionalization). Purposed method is a possibility of increasing C:O ratio in graphene oxide. It is possible to obtain multi-functional graphene structure containing powdary composites by the developed method.

By using this method, we have obtained graphene structure containing pressing powdary composites [graphene]-O-AlR-O- $[Al_2O_3]$, where graphene oxide and alumina were connected by alumoorganic compounds. Powder composites

consolidation has been conducted by SPS method (at 1450–1700°C) for 5–10 minutes.

During the work the following devices have been used: SPS synthesis device, Glow box, Electronic scanning microscopes Nikon ECLIPSE LV 150, Analysette 12 Dyna sizer, planetary mill Pulverisette 7 premium line, SHIMADZU Dynamic Ultra Micro Hardness Tester DUH-211S.

Keywords: graphene oxide, deoxygenation, functionalization, alumoorganic compounds.

References:

1. Craciun M. F., Khrapach I., Barnes M. D., Russo S. (2013), Properties and applications of chemically functionalized graphene. *J. Phys.: Condens. Matter*, 25, 423201, doi:10.1088/0953-8984/25/42/423201
3. Yuhai Hu, Xueliang Sun. (2013), Chemically functionalized graphene and their applications in Electrochemical energy conversion and storage. *Nanotechnology and Nanomaterials*. Book edited by Mahmood Aliofkhazraei.
2. Gutierrez-Gonzalez C.F., Smirnov A., Centeno A., Fernandez A., Alonso B., Rocha V.G., (2015), Torrecillas R., Zurutuza A., Bartolome J.F.. Wear behavior of graphene/alumina composite. *J. Ceramics International*, 41(6), 7434–7438.

Functionalization of Graphene by [2+1] Cycloaddition Reaction at Ambient Conditions

Abbas Faghani¹, Rainer Haag, Mohsen Adeli*^{1,2}

¹*Institut für Chemie und Biochemie Organische Chemie, Freie Universität Berlin, Takustr. 3, 14195 Berlin, Germany.*

²*Department of Chemistry, Faculty of Science, Lotestan University, Khorram Abad, Iran.*

Abstract:

Functionalization of TRGO is a well-known strategy to increase its processability and to construct 2D surfaces with novel properties [1-3]. Among various methods for covalent functionalization of TRGO, nitrene [2+1] cycloaddition reaction is one of the most useful approaches to conjugate a variety of functional groups onto its surface [4-7]. However, this approach required temperatures as high as 160 °C, due to the low chemical reactivity of TRGO, and control over the functionality and surface structure of the obtained 2D nanomaterials is challenging [4, 8]. In this work, we report for the first time on a gram-scale, controlled, and reproducible method for asymmetric functionalization of graphene by one-pot nitrene [2+1] cycloaddition reaction at ambient conditions. Taking advantages of this methods, construction of graphene based 2D surfaces with preserved physicochemical properties and well-defined structure for advanced applications is possible (Figure 1).

Keywords: Graphene, Functionalization, controlled post-functionalization.

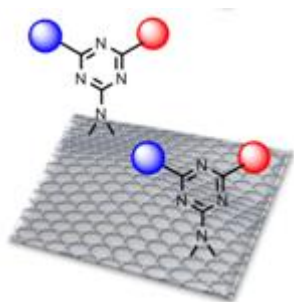


Figure 1. Controlled post-functionalization of graphene to obtain well-defined 2D nanomaterials.

References:

1. Georgakilas, V., et al., *Functionalization of Graphene: Covalent and Non-Covalent Approaches, Derivatives and Applications*. Chemical Reviews, 2012. **112**(11): p. 6156-6214.
2. Maleki, M., et al., *Enzymatic functionalization of nanomaterials: A strategy for engineering their surfaces*. Polymer, 2013. **54**(18): p. 4802-4806.
3. Movahedi, S., et al., *Edge-functionalization of graphene by polyglycerol; A way to change its flat topology*. Polymer, 2013. **54**(12): p. 2917-2925.
4. Strom, T.A., et al., *Nitrene addition to exfoliated graphene: a one-step route to highly functionalized graphene*. Chemical Communications, 2010. **46**(23): p. 4097-4099.
5. Vadukumpully, S., et al., *Functionalization of surfactant wrapped graphene nanosheets with alkylazides for enhanced dispersibility*. Nanoscale, 2011. **3**(1): p. 303-308.
6. Holzinger, M., et al., *[2+1] cycloaddition for cross-linking SWCNTs*. Carbon, 2004. **42**(5-6): p. 941-947.
7. Choi, J., et al., *Covalent Functionalization of Epitaxial Graphene by Azidotrimethylsilane*. The Journal of Physical Chemistry C, 2009. **113**(22): p. 9433-9435.
8. Han, J. and C. Gao, *Functionalization of carbon nanotubes and other nanocarbons by azide chemistry*. Nano-Micro Letters, 2010. **2**(3): p. 213-226.

A facile and scalable way to produce reduced graphene oxide/epoxy nanocomposites

Ganiu B. Olowojoba¹, Sotirios Kopsidas¹, Salvador Eslava^{2,3}, Eduardo S. Gutierrez², Anthony J. Kinloch¹, Cecilia Mattevi², Victoria G. Rocha² and Ambrose C. Taylor¹

¹Mechanics of Materials Division, Department of Mechanical Engineering, Imperial College London, London, UK

²Centre for Advanced Structural Ceramics, Department of Materials, Imperial College London, London, UK

³Department of Chemical Engineering, University of Bath, Bath, UK

Abstract:

Graphene has become a prime target for use as a filler material in the development of multifunctional composites due to its excellent mechanical, thermal, electrical and optical properties. However, challenges still remain in obtaining a good dispersion of the filler material and good interfacial properties between graphene and the matrix polymer. These problems arise from the inert nature of graphene. Previous research has focused on using graphene oxide (GO) reduced externally, either by using hazardous chemical reagents such as hydrazine or via thermal or electrochemical reduction strategies, for synthesizing graphene/epoxy nanocomposites. In the present work, use is made of (a) the increased interplanar spacing between the sheets which make up a GO nanoplatelet (i.e. 0.6 – 1.1 nm, compared to the spacing in graphite nanoplatelets (GNPs) of 0.34 nm), and (b) the enhanced compatibility between the oxygen-containing functional groups (OCFGs) present on the GO surface and the matrix epoxy, to achieve a good dispersion of reduced graphene oxide (rGO) in the composite via in-situ processing. In-situ processing, followed by in-situ thermal reduction of the GO to rGO while the epoxy is simultaneously cured, can indeed remove most of the OCFGs (although some such groups, which are attached to the edges of the GO require higher temperatures to thermally dissociate). An examination of the morphology of such rGO/epoxy nanocomposites via electron microscopy reveals a good dispersion of rGO may be achieved throughout the epoxy polymer matrix.

Although reductions in the glass transition temperature were recorded, good improvements in the storage moduli of the composites were observed. Good improvements in the tensile

moduli were also observed, even though this was accompanied by a decrease in the tensile

fracture strength of the epoxy nanocomposites. The observed decrease in the glass transition temperature and the tensile strength were attributed to the decrease in crosslink density and defects present in the polymer nanocomposites. The thermal instability of the composites was also found to increase with increasing rGO content, owing to the undissociated OCFGs present in the partially-reduced graphene oxide. A marked increase in the thermal conductivity was however observed in the nanocomposites due to the excellent thermal conductivity and dispersion of the rGO in the epoxy matrix. The results obtained show that it is possible to tune the properties of an epoxy polymer with a simple and viable method of GO addition.

Benzoxazine-functionalized graphene oxide for synthesis of new nanocomposites

I. Biru,¹ C. Damian¹, S. A. Garea¹, H. Iovu,^{1,*}

¹ Advanced Polymer Materials Group, University Politehnica of Bucharest, Romania

Abstract:

In this paper was proposed an original route to synthesize new benzoxazine – functionalized graphene oxide monomers (GO-BZ). The new method consists in the growth of the benzoxazine rings directly on the graphene oxide (GO) surface. In order to obtain the GO-BZ monomers the chlorination method using SOCl_2 was employed. Firstly, the carboxylic groups from graphene oxide surface are acylated and then treated with a hydroxyamine (TYR) in order to synthesize the hydroxilic groups on graphene oxide (Figure 1). These groups react further on with amine and formaldehyde to give the benzoxazine rings (Figure 2) which are polymerized in order to produce the polybenzoxazine matrix which will include the graphene oxide's exfoliated layers within the polymer. Finally a nano structure with strong bonds between the graphene sheets and the polybenzoxazine chains is achieved. The formation of multi-benzoxazine functionalized graphene oxide was checked by FT-IR, ^1H -NMR, TGA, Raman spectrometry, XRD, HR-TEM and XPS analysis.

Keywords: graphene oxide, benzoxazine, covalent functionalization, ring opening polymerization, graphene sheets exfoliation.

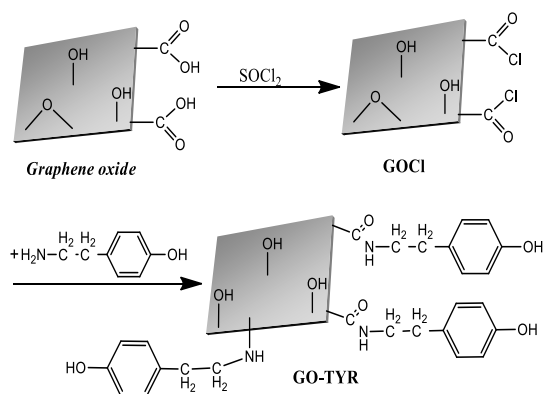


Figure 1: Figure illustrating the synthesis route of OH-functionalized graphene oxide

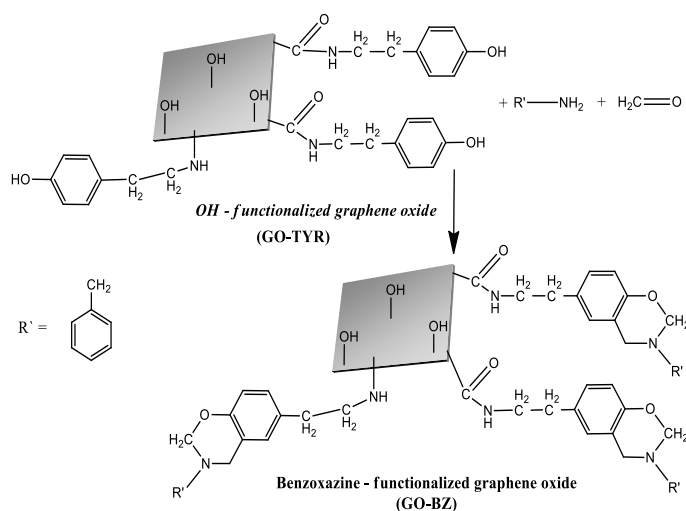


Figure 2: Figure illustrating the synthesis of multi-benzoxazine functionalized graphene oxide proper chemically modified. The benzoxazine rings previously obtained will be subsequently polymerized to produce the polybenzoxazine structure including the graphene oxide sheets exfoliated within the polymer mass. The benzoxazine polymerization may take place either between the rings of the same GO layer (“in-graphene” polymerization) or between the rings of two neighbors of GO layers (“out-graphene” polymerization), in the end obtaining a nanostructure with strong bonds between the graphene sheets and the polybenzoxazine chains.

References:

- Zu, Y., Murali, S., Cai, W., Ruoff, R. S. *et al.* (2010), Graphene and Graphene Oxide: Synthesis, Properties and Applications: Advanced Materials, Vol. 22, pp. 3906-3924 (1-19).
- Arza, C. R., Ishida, H., Maurer, F. H. (2014), Quantifying Dispersion in Graphene Oxide/Reactive Benzoxazine Monomer Nanocomposites: Macromolecules, Vol. 47, pp. 3685-3692.

Electrodeposition process of graphene nano-plates on open-cells aluminum foams – a critical review

A. Simoncini^{1,*}, V. Tagliaferri¹, N. Ucciardello¹

¹ University of Rome “Tor Vergata”, Dipartimento di Ingegneria dell’Impresa “Mario Lucertini”, Via del Politecnico 1, Rome 00133, Italy

Abstract:

Thanks to its particular planar structure, graphene is characterized by unique properties, such as excellent chemical inactivity, high electrical and thermal conductivity, high optical transparency, extraordinary flexibility and high mechanical resistance, which make it suitable in a very wide range of applications. This review details the state of the art in graphene coating and surface modification technologies, applied to aluminum open-cells foams for the improvement of their thermal, mechanical and chemical behavior (Figure 1). Metallic foams are highly porous materials, which present complex structure of three-dimensional open cells. The experimental findings revealed that the metal foams, electroplated with graphene, were characterized by a higher mechanical resistance and thermal conductivity and low process costs, making these materials very promising in many technological fields (A. Antenucci et al.; 2013, 2015). The topics covered include surface modification, electrochemical plating, galvanic measures, thermo-graphic and mechanical analysis

Keywords: Graphene electro-deposition; Open-cells aluminum foams; Thermal and mechanical characterization; Galvanic measures

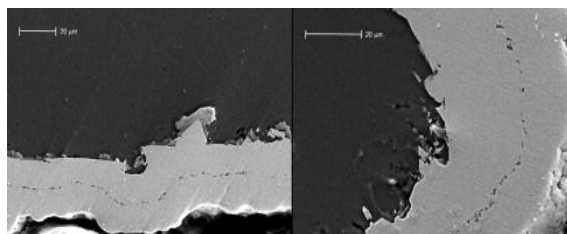


Figure 1: SEM image of the combined electrodeposition process of copper and graphene nano-plates on aluminum foam substrate.

References:

1. Antenucci, A., Guarino, S., Tagliaferri, V., Ucciardello N. (2013) Improvement of the mechanical and thermal characteristics of open cell aluminum foams by the electrodeposition of Cu, *Mater. Des.*, 59, 124-129.
2. Antenucci, A., Guarino, S., Tagliaferri, V., Ucciardello N. (2015) Electro-deposition of graphene on aluminium open cell metal foams, *Mater. Des.*, 71, 78-84.

Optimization of In-Situ Polymerization Process of Graphene Nano-Platelet Composites

B. Yang, J. Doucette and P. Mertiny*

University of Alberta, Mechanical Engineering, Edmonton, Alberta, Canada

Abstract: Multifunctional nano-composites (NCs) are ad-vanced polymers that, by addition of fillers, gain specific property enhancements. Unique properties, such as electrical conductance or swelling reduction, that do not exist in the base polymers can be introduced (Oskouyi & Mertiny 2011; Kraus 1964). Hence, the range of usage can be expanded for the already much diversified application of polymers. The fabrication process of NCs is generally not a trivial “mix-and-stir” approach; additional processes must be implemented to aid the dispersion and distribution of agglomerated particles in a viscous environment. In-situ polymerization is an effective method where the polymer resin and nano-filler are dispersed in a solvent, mixed, and then re-solidified, while concurrently removing the solvent (Ishida et al., 2000). Two critical parameter to this process are solution viscosity (Ahmed et al., 2015) and nano-filler dispersion (Hernandez et al., 2008). In addition, mechanical properties, such as the NC modulus of elasticity, are also of significance to the final material functionality (Van et al., 2001). Therefore, the creation of a NC will need to consider three major aspects: the specific property enhancement of the NC, the parameters of in-situ polymerization, and the mechanical properties toward functionality. An initial optimization framework is proposed herein to advance and guide the creation process of multifunctional NCs via in-situ polymerization. This study aims to determine the optimal filler fraction of graphene-nano-platelet in a NC that satisfies all the mechanical and manufacturing constraints while maximizing or minimizing an objective function representing a specific enhanced property. Solution viscosity, the nano-filler dispersion and the material elastic modulus will constitute the set of constraints that will be assessed using analytical descriptions. The optimization objectives will be on maximizing both electrical conductivity (Oskouyi & Mertiny 2011) and swelling reduction (Kraus 1964). In addition, the shadow price per constraint – the amount by which the objective function will vary per unit change in the parameter’s upper or lower limit – will be studied. More specifically, the range of constraint restrictions that will promote the largest change for the ob-

jective function per unit change in constraint will be determined. The optimization framework will initially be completed by a linear programming, shown in Figure 1, followed by a comparison towards non-linear optimization for accuracy and ease of use.

Keywords: Optimization, shadow price, nano-composite, graphene nano-platelets, in-situ polymerization, swelling reduction, electric conductivity.

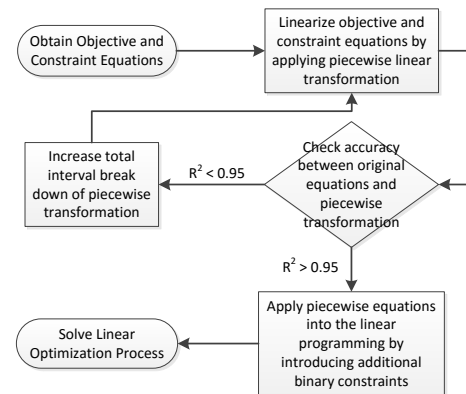


Figure 1: Process diagram for initial linear optimization framework for in-situ polymerization.

References:

1. Oskouyi, A. B., & Mertiny, P. (2011). Monte Carlo model for the study of percolation thresholds in composites filled with circular conductive nano-disks. *Procedia Engineering*, 10, 403-408.
2. Kraus, G. (1963). Swelling of filler-reinforced vulcanizates. *Journal of Applied Polymer Science*, 7(3), 861-871.
3. Ishida, H., Campbell, S., & Blackwell, J. (2000). General approach to nanocomposite preparation. *Chemistry of Materials*, 12(5), 1260-1267.
4. Ahmed, N., Asirvatham, L. G., & Wongwises, S. Effect of volume concentration and temperature on viscosity and surface tension of graphene–water nanofluid for heat transfer applications. *Journal of Thermal Analysis and Calorimetry*, 1-11.
5. Hernandez, Y., Nicolosi, V., Lotya, M., Blighe, F. M., Sun, Z., De, S., ... & Boland, J. J. (2008). High-yield production of graphene by liquid-phase exfoliation of graphite. *Nature nanotechnology*, 3(9), 563-568.
6. Van Es, M., Xiqiao, F., Van Turnhout, J., & Van der Giessen, E. (2001). Comparing polymer-clay nanocomposites with conventional composites using composite modeling. *Speciality Polymer Additives: Principles and Applications*, 484.

Multilayered Membranes based on Graphene and Natural Polymers for Biomedical Applications

M. C. Paiva,^{1*} E. Cunha,¹ D. Moura,^{1,2,3} C. Silva,^{1,2,3} M. F. Proença,⁴ N. Alves^{2,3}

¹ IPC/i3N-Institute for Polymers and Composites, University of Minho, Campus of Azurém, 4800-058 Guimarães, Portugal

² 3B's Research Group – Biomaterials, Biodegradables and Biomimetics, University of Minho, Headquarters of the European Institute of Excellence on Tissue Engineering and Regenerative Medicine. AvePark, 4806-909, Caldas das Taipas, Guimarães, Portugal.

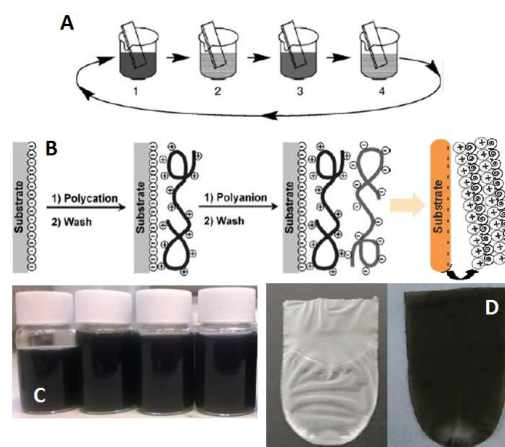
³ ICVS/3B's PT Government Associate Laboratory, Braga/Guimarães, Portugal

⁴ Departamento de Química, Universidade do Minho, Campus de Gualtar, 4710-057 Braga, Portugal

Abstract:

Natural polymers are adequate for biomedical applications due to their optimal biocompatibility and biodegradability. The applications are often limited by their low mechanical performance, and solutions to this problem include the production of composites with a reinforcing phase. Recently, the incorporation of graphene-based materials is showing high potential due to the outstanding mechanical and electrical properties of these materials. Typical graphene-based materials used are obtained by exfoliation of graphite using covalent or a non-covalent methods. The covalent approach is based on the extensive oxidation of graphite followed by exfoliation of the graphene oxide (GO) formed. GO has lower mechanical performance than graphene, and is not electrically conductive, but these properties may be partially recovered by reduction of GO (rGO). The non-covalent approach is based on stabilizer-assisted liquid phase exfoliation, by physical adsorption of suitable molecules on the graphene surface, such as surfactants or biomolecules, through van der Waals forces, electrostatic interactions or π - π stacking. This approach may lead to the formation of few-layer (FLG) or multi-layer graphene (MLG), leaving intact the electrical and mechanical properties of the material. The work presented here reports the production of GO, FLG and MLG in aqueous suspension, and their characterization by STEM, Raman and UV-visible spectroscopies, and zeta potential measurement. GO was produced using the modified Hummers method, while FLG and MLG were produced by liquid-phase exfoliation with an aqueous solution of chemically modified pyrene. Pyrene was functionalized in our lab to introduce a moiety containing carboxylic acid, making it water-soluble and stabilizing the aqueous suspension of FLG and MLG. A strategy was established to produce layer-by-layer (LbL) membranes based on the graphene derivative

suspensions produced and polyanion or polycation forms of water soluble natural polymers, namely alginate (ALG) and chitosan (CHI) (Figure 1). The mechanical and electrical properties of the free-standing membranes produced by LbL were characterized. The graphene distribution across the membrane area was mapped by Raman microscopy. The biocompatibility and biodegradability of the developed membranes were tested. The results obtained show great promise for biomedical applications, including wound healing, cardiac and bone tissue engineering.



Keywords: graphene oxide, few-layer graphene, layer-by-layer film forming, Raman spectroscopy, biomedical applications.

Figure 1: Figure illustrating the layer-by-layer technique (A and B), the stable suspensions of GO (C) and the free-standing membranes obtained (D).

References:

Hummers, W.S., Offeman, R.E. (1958) Preparation of graphitic oxide. *Journal of the American Chemical Society*, 80, 1339.

Antimicrobial properties of RGO modified with Polysulfone Brushes and their nanocomposites

Peña-Bahamonde, J.², Nguyen, H.¹, San Miguel, V.², Cabanelas, J.C.², Rodrigues, D.¹

¹. Department of Civil and Environmental Engineering, University of Houston, Houston, TX (USA)

². Department of Science and Engineering of materials, Universidad Carlos III de Madrid. Leganes. Madrid (Spain)

Abstract:

There is a widespread interest in incorporating nanomaterials in polymer matrices to produce biocompatible polymers with antimicrobial properties for applications in water treatment, food packaging, and biomedical devices.^{1,2} The incorporation of nanomaterials into polymer matrices has been shown to generate novel properties to the individual polymer components. Therein lies the special interest to study the biocompatibility of reduced graphene oxide (RGO) in polysulfones (PSUs).

PSUs are high-temperature thermoplastic polymers that exhibit great chemical inertness, enhanced oxidative resistance, thermal and hydrolytic stability, as well as high mechanical strength. Additionally, PSUs might be easily processed as a film and thus, they are good candidates for different applications, such as gas separation, hemodialysis, nano/ultra-filtration, adhesives for metal to metal bonds, membranes for fuel cells, drug delivery, or matrices for fiber reinforced composites.^{3,4}

Recently, different studies have confirmed that reduced graphene oxide (RGO) and its nanocomposites are good candidates for biomedical and environmental applications,^{5,6} even so they need to present both low cytotoxicity to human cells and suitable antimicrobial properties. To the best of our knowledge, biocompatibility studies with RGO modified with polymer brushes have not been reported so far.

In this work, we describe the preparation and characterization of nanocomposites made of modified RGO with polysulfone brushes⁷ of two different sizes of the polymer chain dispersed in a polysulfone matrix. Cytotoxicity and antimicrobial properties of the nanocomposites were investigated in order to determine its suitability as an antimicrobial agent in biomedical and industrial settings (Figure 1). Furthermore, degradability assays of the samples in wastewater were carried out.

Nanocomposites with different concentrations of RGO modified with polysulfone brushes of different sizes were tested to determine the most toxic concentrations to both, Gram-positive and Gram-negative microorganisms. The preliminary results with *B. subtilis* show microbial inactivation of nearly 90% after exposure to the polymer modified nanosheets for three hours (Figure 2). Nanocomposites (RGO/PSU) with 3 wt% RGO also showed a de-

crease in bacterial growth and in the biofilm formation.

Nanocomposites immersed and exposed to raw wastewater did not degrade after 1 month, which suggests that this material is resistant to biodeterioration and can be useful for applications in food packaging.

Keywords: nanocomposites, graphene oxide, polysulfones, antimicrobial properties.

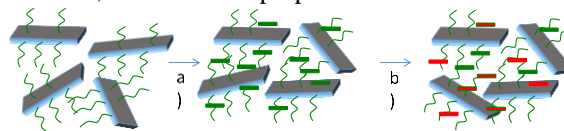


Figure 1: a) schematic representation of the RGO modified with polysulfone brushes in contact with microorganisms, b) representation of dead bacteria (red color) after three hours of exposure to the nanocomposite.

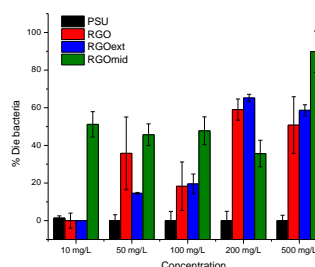


Figure 2: Percentage inactivation of *B. subtilis* after 3 h of exposure to nanomaterials with different concentrations.

References:

1. I. E. Mejias Carpio, C. M. Santos, X. Wei and D. F. Rodrigues (2012) *Nanoscale*, **4**, 4746-4756.
2. S. Liu, T. H. Zeng, M. Hofmann, E. Burcombe, J. Wei, R. Jiang, J. Kong and Y. Chen (2011) *ACS Nano*, **5**, 6971-6980.
3. P.T. McGrail (1996) *Polym. Int.*, **41**, 103-121.
4. D. Cemil, A.T. Mehmet and Y. Yusuf (2013) *Polym. Int.*, **62**, 991-1007.
5. O. Akhavan and E. Ghaderi. (2010) *ACS Nano*, **4**, 5731-5736.
6. C.S. Sean, D. Rodrigues (2015) *Carbon*, **91**, 122-143.
7. H. He and C. Gao (2010) *Chem. Mater.*, **22**, 5054-5064.

Room-temperature positive magnetoresistance in functionalized graphene grown by CVD

O.V. Kononenko,^{1,2,*} V. N. Matveev,¹ V.I. Levashov,¹ V.T. Volkov¹

¹ Institute of Microelectronics Technology and High Purity Materials, Russian Academy of Sciences, Chernogolovka, Moscow District 142432, Russia

² National University of Science and Technology "MISiS", 4, Leninsky pr., Moscow, 119049, Russia

Abstract:

Recently magnetoresistance (MR), the change in electrical resistance upon application of magnetic fields, in graphene has attracted a lot of attention both theoretically and experimentally [1, 2]. A large value of MR at room temperature is necessary for practical applications. A positive MR up to 120% is observed in multilayer epitaxial graphene [3], and a MR up to 100% is obtained from sandwiched chemical vapor deposition graphene samples [4]. A linear and quadratic MR of 60%, at 300 K and a magnetic field of 14 T, are reported in chemical vapour deposition grown few-layer graphene with the current perpendicular to the film plane [5].

In this work graphene was grown by the CVD method with a short-time acetylene inflow [6] on Fe films deposited by laser ablation. Two-terminal structures with Pt electrodes were fabricated from the graphene. Two types of structures were used for MR measurements. First is a quasi suspended graphene fabricated by etching of Fe film and second is graphene transferred on an oxidized silicon substrate. After fabrication graphene structures were exposed in $\text{Fe}(\text{NO}_3)_3 \times 9 \text{H}_2\text{O}$ aqueous solution up to 6 days.

MR in graphene was experimentally investigated by varying magnetic-field strength from 0 to 0.45 T.

MR was defined as $([R(B)-R(0)]/R(0)) \times 100\%$. A maximum value of observed magnetoresistance was about 70% in a normal magnetic field of 0.45 T. Measured magnetoresistance was positive with a quadratic magnetic-field (B) dependence in fields up to 0.08 T and about linear dependence in fields up to 0.45 T.

Keywords: graphene, chemical vapor deposition, magnetoresistance.

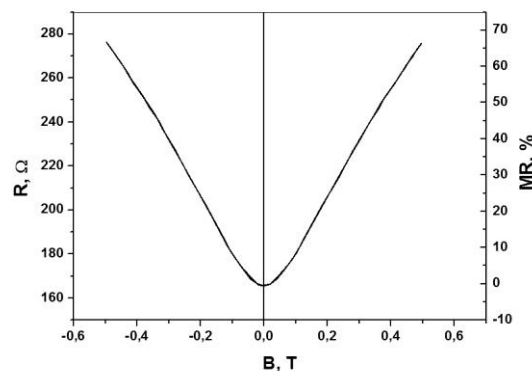


Figure 1: MR of the graphene structure measured at room temperature with perpendicular magnetic field.

O.V.K. gratefully acknowledge the financial support of the Ministry of Education and Science of the Russian Federation in the framework of Increase Competitiveness Program of NUST «MISiS» (№ K1-2015-046)

References:

1. G. Yu. Vasil'eva, P. S. Alekseev, Yu. L. Ivanov, Yu. B. Vasil'ev, D. Smirnov, H. Schmidt, R. J. Haug, F. Gouider, G. Nachtwei, *JETP Letters* (2012) **96**, 471.
2. Z.-M. Liao, Y.-B. Zhou, H.-C. Wu, B.-H. Han, D.-P. Yu, *EPL* (2011) **94**, 57004.
3. A. L. Friedman *et al.*, *Nano. Lett.* **10**, 3962 (2010).
4. Z.-M. Liao, H.-C. Wu, S. Kumar, G. S. Duesberg, Y.-B. Zhou, G. L. W. Cross, I. V. Shvets, and D.-P. Yu, *Adv. Mater.* **24**, 1862 (2012).
5. Liao, Z.-M. *et al.* Large magnetoresistance in few layer graphene stacks with current perpendicular to plane geometry. *Adv. Mater.* **24**, 1862–1866 (2012).
6. O.V. Kononenko, V.N. Matveev, D.P. Field, D.V. Matveev, S.I. Bozhko, D.V. Roshchupkin, E.E. Vdovin, A.N. Baranov, *Nanosystems: Physics, Chemistry, Mathematics* (2014) **5**, 117.

Defects in irradiated graphene on metallic substrates

I. Shchedrina¹, C. Corbel¹, N. Ollier¹, O. Cavani¹, T. Wade¹, M. Konczykowski¹, Jean-Philippe Renault², Jalal Ghilan³, Hyacinthe Randriamahazaka³, C.S. Cojocaru⁴, I. Florea⁴, B. Geffroy^{4,5}

¹ LSI, Ecole Polytechnique, CEA, CNRS, Université Paris-Saclay, 91128, Palaiseau, France

² NIMBE, CEA Saclay, IRAMIS, 91191 Gif sur Yvette, France

³ Université Paris Diderot, Sorbonne Paris Cité, ITODYS, UMR 7086 CNRS, 75202 Paris, France

⁴ LPICM, CNRS, Ecole Polytechnique, Université Paris Saclay, 91128, Palaiseau, France

⁵ LICSEN, NIMBE, CEA, CNRS, Université Paris-Saclay, CEA Saclay 91191 Gif-sur-Yvette Cedex, France

Abstract:

The reactivity of graphene surface and its homogeneity are expected to be strongly dependent on the chemical and structural defects that, as reported in literature, can be induced by various treatments, including irradiation [Teweldebrhan2009, Kotakoski2011, Giannazzo2011].

The nature and thermal stability of chemical and structural changes induced by light and electron irradiation are investigated in single layers of graphene deposited on metallic substrates. The present work is focused on surface changes and heterogeneity appearance induced by irradiation and revealed in Raman and photoluminescence spectra at the micro-scale. The aim is to investigate more specifically the evolution of the Raman and Photoluminescence spectra before, during and after the different types of irradiation and their correlation. Irradiation tests are performed both in dry and wet conditions.

As illustrated in Fig.1 for UV irradiation, the evolution of the Raman spectra reveals a strong dependency on the irradiation conditions (light wavelength, electron energy, flux, irradiation dose). Similar behavior was found by other authors [Pimenta2007, Teweldebrhan2009] using different irradiation conditions. Moreover, as illustrated in Fig.2, the Raman and the photoluminescence spectra vary independently. The effect of graphene substrates evolution is also discussed in comparison with HOPG behavior.

Keywords: graphene, irradiation, UV, Raman spectroscopy, photoluminescence

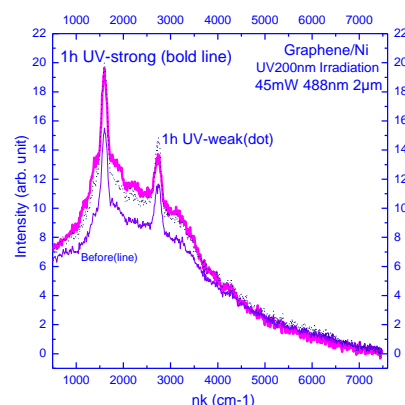


Figure 1: Raman and Photoluminescence spectra (spot 2 μm , laser wavelength 488nm, intensity 45mW) in single layer Graphene/Ni before and after 1 hour of ultra-violet (200nm) irradiation at low and high flux

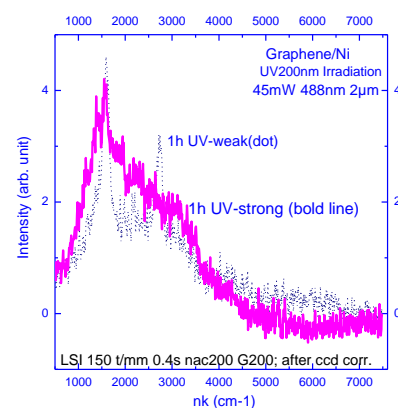


Figure 2: Raman and PL spectra (spot 2 μm , laser wavelength 488nm, intensity 45mW) after normalization to reference spectra in single layer Graphene/Ni: effect of the flux of ultra-violet (200nm) irradiation

References:

1. Teweldebrhan D. et al. Appl. Phys. Lett., 94,013101–013103, (2009)
2. Kotakoski J. et al. PRL 106, 105505 (2011)
3. Giannazzo F. et al. Nanoscale Research Letters (2011)
4. Pimenta M ;A. et al. Phys. Chem. Chem. Phys., 9, 1276-1290 (2007)

High porosity Graphene/Fe₃O₄ scaffolds for Electromagnetic Interference Shielding

M. González,¹ J. Pozuelo¹, J. Baselga¹

¹ Materials Science and Engineering and Chemical Engineering Department, University Carlos III of Madrid (IAAB), Spain

Abstract:

The interest on microwave absorbing and shielding materials is ever-increasing because of the growing environmental pollution from electromagnetic radiation due to the rapid development of communication technology.

Graphene sheets are reported as high-performance absorbing materials because of their much better intrinsic properties compared with traditional materials [1]. Graphene is an ideal substrate for dispersing nanoparticles due to its large surface-area ratio per unit mass and its high temperature stability [2]. The functionalization of graphene with Fe₃O₄ nanoparticles can improve the electromagnetic wave absorption property increasing the complex permeability values due to the large saturation magnetization of Fe₃O₄ [3].

In this work, we have prepared and characterized reduced Graphene oxide (rGO) and rGO/Fe₃O₄ porous scaffolds. A simple modified hydrothermal treatment has been used for the preparation of the macroporous scaffolds. This method involves preparing a stable aqueous emulsion of graphene oxide (GO) containing hexane droplets. This is possible due to GO amphiphilicity, which can act as emulsion stabilizer. For this reason, during hydrothermal process, GO sheets are reduced and assembled around hexane droplets to form a 3D network. The surface of graphene sheets has been decorated with magnetite nanoparticles using a microwave based method

An exhaustive structural characterization (Figure 1) of rGO and rGO/Fe₃O₄ scaffolds was carried out. SEM images show that the macroporous ($\geq 200 \mu\text{m}$) morphology remains unaltered after modification with Fe₃O₄. TEM images show an homogeneous growth of the nanoparticles over the graphene sheet with an average diameter of $4.68 \pm 1.07 \text{ nm}$. DC conductivity measurements show that magnetite increases the conductivity of the scaffolds. These results agree with the electromagnetic characterization: rGO scaffold shows a higher absorption power than rGO/Fe₃O₄ scaffold. However, the shielding efficiency due to absorption is better for rGO/Fe₃O₄ scaffold.

Keywords: Graphene, Magnetite, Macroporosity, Dielectric Properties, Electromagnetic Characterization, Shielding effectiveness, Epoxy Resin, Nanocomposites.

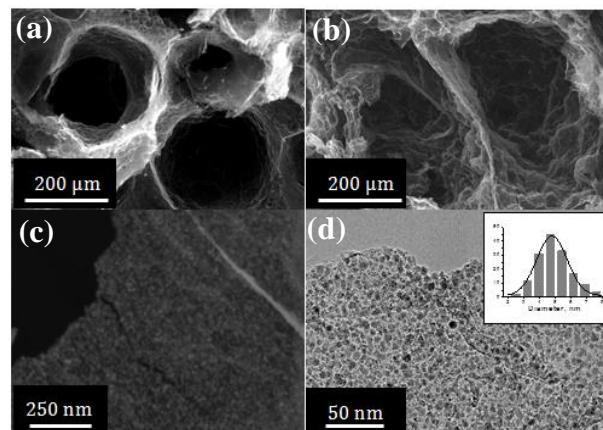


Figure 1: SEM images of: (a) rGO scaffold and (b) rGO/Fe₃O₄ scaffold. (c) FE-SEM image of a decorated Graphene sheet (c). (d) TEM image of a decorated graphene sheet with magnetite nanoparticles; insert: particle size distribution.

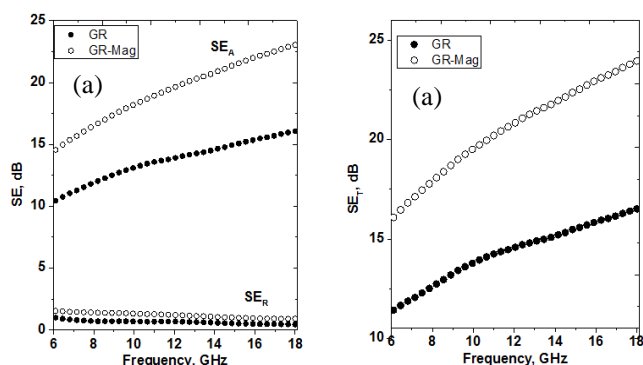


Figure 2: (a) Absorption, SE_A and reflection, SE_R coefficients for both scaffolds. (b) Total electromagnetic shielding efficiency, SE_T for composites.

References:

- [1] Lee, S. H., Lee, D. H., Lee, W. J., Kim, S.O. (2011) Tailored Assembly of Carbon Nanotubes and Graphene, *Adv. Funct. Mater.*, 21, 1338.
- [2] Saha, S. K., Chandrakanth R. C., Krishnamurthy H. R., Waghmare U. V. (2009) Mechanisms of molecular doping of graphene: A first-principles study. *Phys. Rev. B Condens. Matter.*, 80, 6, 155414-155419.
- [3] Sun, G., Dong, B., Cao, M., Wei, B., Hu, C. (2011) . Hierarchical Dendrite-Like Magnetic Materials of Fe₃O₄, γ-Fe₂O₃, and Fe with High Performance of Microwave Absorption. *Chem. Mater.* 23, 1587–1593.

Effect of Post-Exfoliation Annealing and Ultrasonic Treatments on Mechanically Exfoliated MoS₂

P. Budania,^{1,*} N. Mitchell,¹ D. McNeill¹

¹School of Electronics, Electrical Engineering and Computer Science, Queen's University, Belfast, UK

Abstract:

A study is presented on post-exfoliation thermal annealing in air and ultrasonic treatments performed on mechanically exfoliated MoS₂ flakes on oxidised silicon substrates. Post-exfoliation treatments on mechanically exfoliated graphene have been previously reported to enable formation of large area single-layer nanosheets of graphene (Pang *et al.*, 2010).

Ultra-sonication of MoS₂ flakes on SiO₂ without prior annealing resulted in almost complete removal of flakes, indicating weak bonding at the MoS₂/SiO₂ interface Figure 1(a). Thermal annealing at 270 °C prior to ultrasonic treatment was found to significantly increase the interface adhesion and prevent removal of MoS₂ flakes. We consider that the improved adhesion is due to effusion of water vapour and other impurities from the interface resulting in greater contact area. Samples were also annealed in the range of 75 °C to 175 °C followed by ultrasonic treatment. This resulted in small residual MoS₂ fragments due to breakage and/or partial removal of overlying MoS₂ flakes. Increase in annealing temperature to 460 °C, resulted in decomposition of MoS₂ (Lu *et al.*, 2013).

Contrary to post-exfoliation experiments on graphene, we observed that whilst the adhesion of MoS₂ is considerably enhanced upon annealing, no single-layer MoS₂ flakes resulted. Although the two materials have very similar interlayer van der Waals interaction, the corrugation upon annealing on oxide substrates is not identical. We believe that the dissimilarity in corrugation due to structural difference in the materials. Interplanar interaction between out of plane Mo and S atoms gives MoS₂ a higher bending rigidity (Jiang *et al.*, 2013) in comparison to graphene which is a single layer of carbon atoms. The adhesion of a thick MoS₂ flake to the oxide substrate is illustrated in Figure 1(b). Adhesion is reduced due to low contact area. Therefore, ultrasonic treatment without prior annealing of the sample results in removal of all top layers of the flake but sometimes a few bottom layers remain adhered to the substrate only at places where it was in contact prior to sonication. This results in

non-uniform and discontinuous fragments on the substrate.

Keywords: mechanical exfoliation, MoS₂, post-exfoliation, thermal annealing, ultrasonic cleaning, interface adhesion.

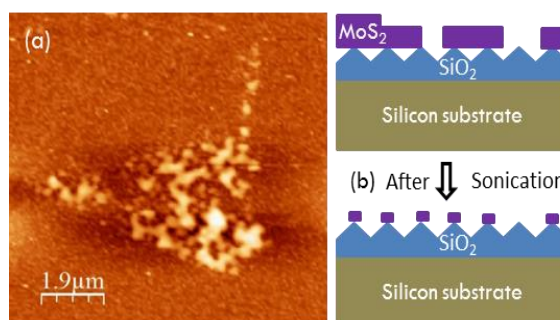


Figure 1: (a) AFM image of region where a MoS₂ flake has come off the substrate leaving non-continuous fragments of MoS₂. (b) representation of a thick MoS₂ flake on oxide substrate.

References:

- Pang, S., Englert, J. M., Tsao, H. N., Hernandez, Y., Hirsch, A., Feng, X., Müllen, K. (2010), Extrinsic Corrugation-Assisted Mechanical Exfoliation of Monolayer Graphene, *Adv. Mater.*, 10, 5374-5377.
- Lu, X., Utama, M. I. B., Zhang, J., Zhao, Y., Xiong, Q. (2013), Layer-by-layer thinning of MoS₂ by thermal annealing, *Nanoscale*, 5, 8904.
- Jiang, J.-W., Qi, Z., Park, H. S., Rabczuk, T. (2013), Elastic bending modulus of single-layer molybdenum disulfide (MoS₂): finite thickness effect, *Nanotechnology*, 24, 435705.

EGF 2016: Plenary session II

2D Materials: technology, standards and science

Antonio H. Castro Neto

Director, Centre for Advanced 2D Materials and Graphene Research Centre
National University of Singapore, Singapore

Abstract:

Over the last five years the physics of two-dimensional (2D) materials and heterostructures based on such crystals has been developing extremely fast. From one hand, with new 2D materials, more and more truly 2D physics started to appear (Kosterlitz-Thouless (KT) behaviour, 2D excitons, commensurate-incommensurate transition, etc). From another - we see the appearance of novel heterostructure devices - tunnelling transistors, resonant tunnelling diodes, light emitting diodes, etc.

Composed from individual 2D crystals, such devices utilise the unique properties of those crystals to create functionalities which were not accessible to us in other heterostructures. In this talk I will review the properties of novel 2D crystals and how those properties are used in new heterostructure devices

Graphene-based Platforms for Biosensing Applications

Arben Merkoçi

Catalan Institute of Nanoscience and Nanotechnology (ICN2), CSIC and The Barcelona Institute of Science and Technology, Campus UAB, Bellaterra, 08193 Barcelona, Spain

E-mail: arben.merkoci@icn.cat
www.nanobiosensors.org www.icn.cat

Abstract:

There is an increasing demand for biosensing systems based on simple electrical/optical transducing schemes able to achieve cost efficient detection. Among the various biosensing system performance requirements the high sensitivity and selectivity of the response are crucial for applications in diagnostics. Due to the fact that the analytes to be detected in clinical, environmental or food sample are present in very low concentrations the need for biosensing systems that can detect with high sensitivity and selectivity that include very low detection limits along with high reproducibility is an important challenge. To overcome the difficulties in accomplishing all these requirements the main efforts are driven toward signal amplification and noise reduction of biosensing systems by the incorporation of nanomaterials. Since graphene exhibits innovative mechanical, electrical, thermal and optical properties this two-dimensional material is increasingly attracting attention and it is under active research. Graphene-based materials (GBMs) display advantageous characteristics to be used in biosensing platforms due to their interesting properties such as excellent capabilities for direct wiring with biomolecules, heterogeneous chemical and electronic structure, the possibility to be processed in solution and the availability to be tuned as insulator, semiconductor or semi-metal. Moreover, GBMs such as graphene oxide (GO) bears the photoluminescence property with energy transfer donor/acceptor molecules exposed in a planar surface and even can be proposed as a universal highly efficient long-range quencher, which is opening the way to several unprecedented biosensing strategies. The rationale behind the use of GO and GBMs in optical and electrochemical biosensing is being studied and explored. We are developing simple, sensitive, selective and rapid biosensing platforms based on the advantageous properties of GBMs while used as electrochemical transducers or revealing agents in a variety of biosensing systems. Examples related to diagnostics applications including bacteria and other analytes (ex. contaminants) detection

will be shown. The developed devices and strategies are intended to be of low cost while offering high analytical performance in screening scenarios beside other applications. Special emphasis will be given to (nano)paper/plastic-based platforms that operate in microarray or lateral flow formats with interest for various detections.

Keywords: graphene, graphene oxide, biosensors, diagnostics

References:

1. Morales-Narváez, E., Merkoçi, A. (2012), Graphene oxide as an optical biosensing platform, *Adv. Mater.*, 24, 3298–3308.
2. Morales-Narvez, E., Hassan, A-R., Merkoçi, A. (2013), Graphene Oxide as a Pathogen-Revealing Agent: Sensing with a Digital-Like Response, *Ang. Chem.* 52, 13779–13783.
3. Morales-Narváez, E., Golmohammadi, H., Naghdi, T., Yousefi, H., Kostiv, U., Horak, D., Pourreza, N., Merkoçi, A. (2015), Nanopaper as an Optical Sensing Platform, *ACS Nano*, 9, 7296–7305
4. Morales-Narváez, E., Naghdi, T., Zor, E., Merkoçi, A. (2015), Photoluminescent Lateral-Flow Immunoassay Revealed by Graphene Oxide: Highly Sensitive Paper-Based Pathogen Detection, *Anal. Chem.*, 87, 8573–8577
5. Gravagnuolo, A. M., Morales-Narváez, E., Matos, C. R. S., Longobardi, S., Giardina, P., Merkoçi, A. (2015), On-the-Spot Immobilization of Quantum Dots, Graphene Oxide, and Proteins via Hydrophobins, *Adv. Funct. Mat.* 25, 6084–6092
6. Baptista-Pires, L., Mayorga-Martínez, M.M., Medina-Sanchez, M., Monton, H., Merkoçi, A. (2016) Water Activated Graphene Oxide Transfer Using Wax Printed Membranes for Fast Patterning of a Touch Sensitive Device”, *ACS Nano*, 10, 853–860

Carbon Based Nano-Materials/Devices

Kwang S. Kim¹

¹ Department of Chemistry, Ulsan National Institute of Science and Technology, Ulsan 44919, Rep. of Korea

Abstract: To design novel molecules and materials, it is of importance to understand inherent molecular properties, intermolecular interactions, and dynamic/transport properties of molecular systems [1,2]. Here, I describe how we have designed functional nanomaterials and nanodevices using graphene and organic molecules. These include intriguing receptors/sensors [3], selective fluorescence sensing for RNA over DNA [4], gate-controlled gas storage [5], large-scale graphene [6], and graphene functionalization towards energy storage, water remediation [7], and fuel cell catalysts [8]. I discuss novel assembling phenomena of diverse nanostructures of conjugated organic molecules and the utilization of the resulting unusual functional characteristics as devices. Novel nano-optics phenomena are presented based on self-assembled nano-scale lenses which show near-field focusing and magnification beyond the diffraction limit [9]. Some ballistic electron/spin transport phenomena in molecular electronic/spintronic devices and graphene nanoribbon spin valves are discussed based on non-equilibrium Green function theory [10]. By utilizing Fano-resonance driven 2D molecular electronics spectroscopy using graphene nanoribbon, the quantum conductance spectra of a graphene nanoribbon placed across a fluidic nanochannel can lead to fast DNA sequencing including cancerous methylated nucleobases detection [11,12].

Keywords: molecular interactions, sensing, nanolens, graphene, supermagnetoresistance, gas storage, fuel cell, DNA sequencing, spintronics, 2D molecular electronics spectroscopy.

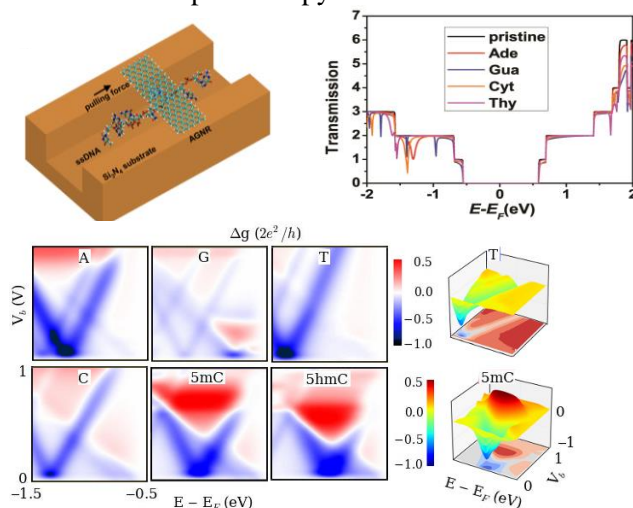


Figure 1: DNA sequencing and cancerous DNA recognition with a graphene-based nanochannel device based on Fano resonance driven Two Dimensional Molecular Electronics Spectroscopy (2D MES) for molecular fingerprinting.

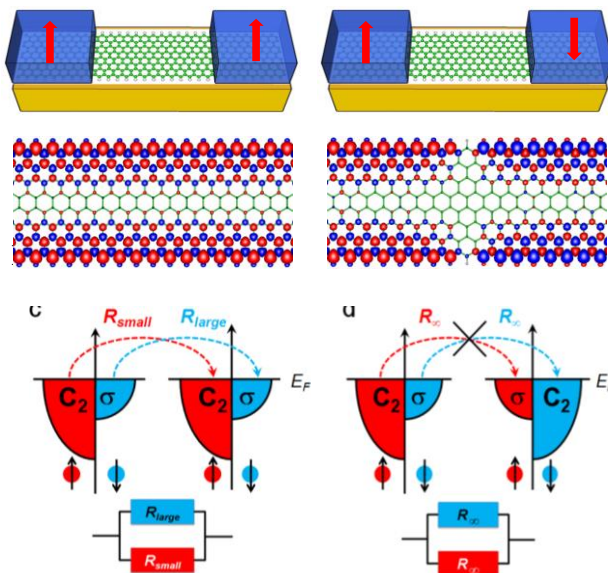


Figure 2: Supermagneto-resistance of spin-valve device using graphene nanoribbon.

References:

- Georgakilas, V. et al. *Chem. Rev.* **2012**, *112*, 6156.
- Cho, Y. et al. *Acc. Chem. Res.* **2014**, *47*, 3321..
- Y Chun et al. *Nature Commun.* **2013**, *4*, 1797.
- Shirinfar, B. et al. *J. Am. Chem. Soc.* **2013**, *135*, 90.
- Baeck S. B. et al. *Proc Natl Acad Sci.* **2015**, *112*, 14156.
- Kim, K. S. et al. *Nature* **2009**, *457*, 706.
- Chandra, V. et al. *ACS Nano* **2010**, *4*, 3979.
- Tiwari, J. N. et al. *Nature Commun.* **2013**, *4*, 2221.
- Lee, J. Y. et al. *Nature* **2009**, *460*, 498.
- Kim, W. Y. et al. *Nature Nanotechnol.* **2008**, *3*, 408.
- Min, S. K. et al. *Nature Nanotechnol.* **2011**, *6*, 162.
- Rajan, A. C. et al. *ACS Nano* **2014**, *8*, 1827.

Reaction kinetics of Stone - Wales rotation in graphene

A. Chuvilin^{1,2}, S. T. Skowron³, V. O. Koroteev^{4,5}, M. Baldoni³, S. Lopatin⁶, A. Zurutuza⁷, E. Bichoutskaia³

¹ CIC nanoGUNE Consolider, Donostia-San Sebastian, Spain

² IKERBASQUE Basque Foundation for Science, Bilbao, Spain

³ School of Chemistry, University of Nottingham, Nottingham, UK

⁴ Nikolaev Institute of Inorganic Chemistry, SB RAS, Novosibirsk, Russia

⁵ Novosibirsk State University, Novosibirsk, Russia

⁶ King Abdullah University of Science & Technology, Thuwal, Saudi Arabia

⁷ Graphenea S.A., Donostia-San Sebastian, Spain

Abstract:

The raise of nanoscience and nanotechnology and necessity to characterize the structure of individual objects consisting of a countable number of atoms determined the shift of structure characterization paradigm from bulk methods like X-ray diffractometry to local high resolution methods like electron microscopy. The similar shift in paradigm is urging now in chemistry – chemical processes defining structure and properties of nanoscale and low dimensional objects often constitute a negligible part of the total volume of the material, and thus their assessment by experimental bulk chemical methods is often impossible. The new concept is provided by the time resolved electron microscopy allowing for direct observation of atomic rearrangements.

We are developing the methodology [1] to apply the formalism and approaches of the classical chemical kinetics for the quantitative description of atomistic processes observable in the microscope. We show that a proper statistical treatment of the data obtained in a range of experimental conditions allows determining the threshold energies for radiation induced reactions. But not only that: we show that true activation energies for thermally activated reaction pathways for individual defects can be estimated as well.

We apply this methodology for reactions of point defects in graphene. The cross-sections and threshold energies of irreversible (atom emission) and reversible (bond rotation, see Figure 1) processes are measured. Observation of statistically significant number of events at variable experimental conditions allows decoupling of radiation induced and thermal reaction pathways and obtaining independent estimations of cross-sections and activation energies for direct and backwards rotations. The cross-sections of direct rotation were found to be in a decent agreement with theoretical estimations. Interestingly the backwards

rotation is characterized by very high cross-section exceeding theoretical values by 3-4 orders of magnitude. The values obtained rule out electron-nucleus collision as the main mechanism of energy transfer from electron beam to the sample. We speculate that the energy is transferred through electron-electron interactions via strong coupling of excited electron states with the phonon modes localized around the defect.

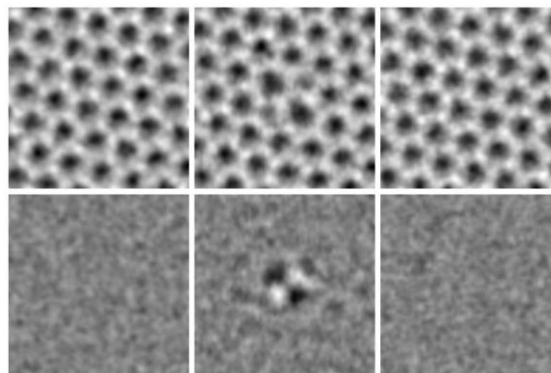


Figure 1: Sequence of electron microscopy images showing the bond rotation reaction in graphene. The upper row – unprocessed images of the graphene lattice separated by time slices of 1s. The lower row – the same images filtered in order to remove the pattern of the lattice.

Keywords: graphene, Stone-Wales transformation, reaction kinetics, electron microscopy, atomistic chemistry.

References:

1. S.T. Skowron, V.O. Koroteev, M. Baldoni, S. Lopatin, A. Zurutuza, A. Chuvilin, E. Besley (2016) Reaction Kinetics of Bond Rotations in Graphene, *Carbon*, Accepted.

Ultrafast Generation of Plasmon Polaritons in High Mobility Graphene

D.N. Basov,^{1,2}

¹ Department of Physics, University of California San Diego, USA

² Department of Physics, Columbia University, New York, NY, USA

Abstract:

The stunning success of metal-based plasmonics for manipulating light at the nanoscale has been empowered by imaginative designs and advanced nano-fabrication. However, the fundamental optical and electronic properties of elemental metals, the prevailing plasmonic media, are difficult to alter using external stimuli. This limitation is particularly restrictive in applications that require ultrafast modification of the plasmonic response at sub-picosecond time scales. This handicap has prompted the search for alternative plasmonic media, with graphene emerging as one of the most capable candidates. We resolved, visualized and elucidated the properties of non-equilibrium photo-induced plasmons in a high mobility graphene monolayer. We succeeded in switching on plasmons on demand with femtosecond optical pulses in a specimen of graphene that does not show plasmonic response at equilibrium.

We examined the real space aspects of plasmon polariton generation and propagation under femtosecond photo-excitation using a novel ultrafast nano-infrared technique that fuses direct plasmon imaging with spectroscopy. Pump-probe nano-spectroscopy data in infrared frequencies, in combination with static nano-imaging results on plasmon propagation, reveal novel aspects of carrier relaxation in heterostructures based on high purity graphene.

Keywords: graphene, nano-optics, plasmonics, pump-probe, nano-imaging.

References:

1. G. X. Ni, L. Wang, M. D. Goldflam, M. Wagner, Z. Fei, A. S. McLeod, M. K. Liu, F. Keilmann, B. Özyilmaz, A. H. Castro Neto, J. Hone, M. M. Fogler and D. N. Basov “*Ultrafast optical switching of infrared plasmon polaritons in high-mobility graphene*” *Nature Photonics* 10, 244 (2016)

Design and fabrication of Graphene based platforms for Raman sensing

Leo Álvarez-Fraga¹, Félix Jimenez-Villacorta¹, Esteban Climent-Pascual¹

Rafael Ramírez-Jiménez^{2,1}, Carlos Prieto¹ and Alicia de Andrés¹,

¹ Instituto de Ciencia de Materiales de Madrid, Consejo Superior de Investigaciones Científicas. Cantoblanco 28049 Madrid, Spain

² Departamento de Física, Escuela Politécnica Superior, Universidad Carlos III de Madrid, Avenida Universidad 30, Leganés, 28911 Madrid, Spain

Abstract:

The detection of protein biomarkers secreted by tumors at early stages for preventive cancer medicine is of vital relevance but their extremely low concentration in blood and the presence of mixtures of proteins makes difficult their detection. Raman spectroscopy meets the required specificity criterion since the vibrational spectrum of every component of a biological specimen is a specific signature that can be used for its identification. Moreover, compared to magnetic resonance imaging, Raman micro-spectroscopy has the ability of visualizing morphological details in cells and tissues on a much higher spatial resolution. Also, no external markers are required, it has a sub-micron resolution and quite good penetration depth. Nevertheless, Raman spectroscopy is strongly limited by its sensitivity. For the last years, a great effort is underway to increase Raman intensity mainly by enhancing the Raman signal by localized surface plasmon resonances from metal nanoparticles (NPs), but these SERS platforms deal with problems such as the NPs stability, their interaction with the analyte and the adsorption, distribution and arrangement of the probed molecules on the substrate. Another enhancement process is the use of excitation wavelengths in resonant conditions for the sensed molecule, in general using ultra-violet lasers. Recently, the Raman signal of graphene has been shown to increase significantly due to the constructive interference processes in graphene/SiO₂/Si. Graphene has several roles to play in optical sensing since it provides a bio-compatible surface adequate for many organic and bio materials and also a protection of the metal NPs increasing the stability of the system.

Our aim is the fabrication of different architectures of SERS substrates that combine different enhancement processes of Raman signal in one

multilayered hybrid system based on graphene. We will present our approaches to the different Raman enhancement processes. In particular we will show the formation of graphene protected ruthenium ultrathin films with controlled size and shape of the particles with different characteristics of the Ru plasmon resonance adequate for UV-SERS. The structure, determined by synchrotron radiation diffraction, and the preferential orientation of Ru nanostructured films depend on the substrate, thermal history as well as on the synthesis of the graphene toplayer.

We have explored the limit of ultrasmall Ag nanoparticles (4 nm) to study their interaction with graphene and the SERS amplification capabilities. The Ag nanoparticles are very efficiently doping graphene with electrons and inducing strain in the graphene lattice.

We will also demonstrate that long term oxidation of the copper foil used as catalyst for graphene synthesis by chemical vapor deposition leads to the formation of Cu/air/graphene bubbles. The bubbles produce an enhancement of the graphene Raman signal up to 70. Moreover, the transfer matrix method used to simulate the multi-reflection processes predicts amplification factors up to 11000 for graphene/air/aluminum systems. The results of these approaches pave the way to the design and fabrication of extremely sensitive graphene based bio-compatible platforms by combining the different Raman enhancement processes.

Keywords: Raman spectroscopy, graphene, plasmons, interference processes, SERS, optical sensing, metallic nanoparticles, AFM

Imaging and spectroscopy on the 10-nm length scale

M. Eisele
neaspec GmbH, Martinsried, Germany

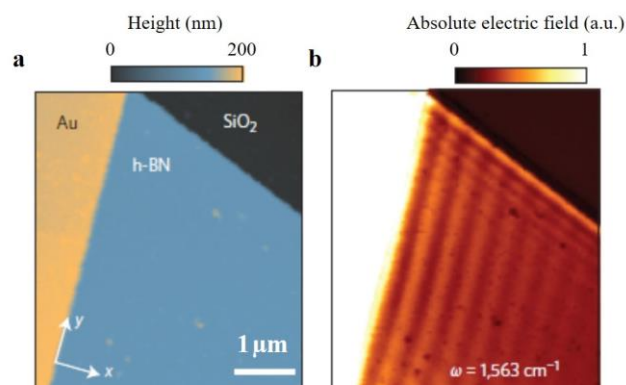
Abstract:

Single-layer materials like graphene, boron-nitride or transition-metal dichalcogenides are of rising interest for novel plasmonic and optoelectronic applications due to their unique characteristics and their broad application range. Being highly sensitive to the local environment, their properties can, however, strongly vary on the nanometer length scale, severely limiting the macroscopic performance of such novel devices. The desire to understand and resolve existing limitations calls for analysis tools, which are capable of measuring the optical and electronic properties on the 10-nanometer length scale.

This talk introduces the latest achievements of our neaSNOM microscope, combining the spatial resolution of scattering-type scanning near-field optical microscopy (s-SNOM) with the analytical power of infrared spectroscopy. This technique has already proven itself vital for modern nanoscopy and has been used in applications such as chemical identification [1], free-carrier profiling [2], or the direct mapping of propagating graphene plasmons [3,4] and phonon polaritons in boron nitride [5-8]. The neaSNOM microscope has been used to directly trace the optical properties of e.g. single layer materials within the entire mid-infrared spectral range with unprecedented spatial resolution. Key information like the local conductivity, intrinsic electron-doping, absorption or the complex-valued refractive index can now routinely be extracted using this technology.

Additionally, the highly flexible design of the neaSNOM microscope enables a complete new level of correlation microscopy: near-field microscopy in combination with time-resolved measurements [9,10] or photocurrent nanoscopy [11] are just two prime examples.

Keywords: Graphene, near-field microscope, s-SNOM, nanoscale, time-resolved photocurrent nanoscopy, spectroscopy, nano-FTIR.



Application: **a**, Topography of a 55-nm-thick gold film on a 135-nm-thick hexagonal boron-nitride slab on a SiO₂ substrate. **b**, Infrared near-field image of the electric field at a frequency of 1563 cm⁻¹, revealing hyperbolic phonon polaritons launched at the gold edge, as well as hyperbolic phonon polaritons launched by the tip of the near-field microscope and reflected by the hexagonal boron-nitride edge. Figures taken from [5].

References:

- [1] F. Huth *et al.*, Nano Lett. **12**, 3973 (2012)
- [2] J. M. Stiegler *et al.*, Nano Lett. **10**, 1387 (2010)
- [3] J. Chen *et al.*, Nature **487**, 77 (2012)
- [4] Z. Fei *et al.*, Nature **487**, 82 (2012)
- [5] S. Dai *et al.*, Science **343**, 1125 (2014)
- [6] S. Dai *et al.*, Nature Comm. **6**, 6963 (2015)
- [7] P. Li *et al.*, Nature Comm. **6**, 7507 (2015)
- [8] E. Yoxall *et al.*, Nature Photon. **9**, 674 (2015)
- [9] M. Eisele *et al.*, Nature Photon. **8**, 841 (2014)
- [10] M. Wagner *et al.*, Nano Lett. **14**, 894 (2014)
- [11] A. Woessner *et al.*, arXiv:1508.07864v1

EGF 2016- Session II
Graphene and 2D Materials
characterization and properties

Graphene nanoplatelets for thermally conductive polymer nanocomposites via melt reactive extrusion

A. Fina¹, S. Colonna¹, O. Monticelli², M. Tortello³, R.S. Gonnelli³, J. Gomez⁴, M. Pavese³, F. Giorgis³, G. Saracco³

1- Dipartimento di Scienza Applicata e Tecnologia, Politecnico di Torino, 15121 Alessandria, Italy

2- Dipartimento di Chimica e Chimica Industriale, Università di Genova, 16146 Genova, Italy

3- Dipartimento di Scienza Applicata e Tecnologia, Politecnico di Torino, 10129 Torino, Italy

4- AVANZARE Innovacion Tecnologica S.L., 26370 Navarrete (La Rioja), Spain

Abstract:

As the exploitation of graphene in materials for large scale application is still very much limited by the amount and quality of graphenes available, for large scale bulk applications in polymer nanocomposites, multilayer graphenes or graphene nanoplatelets (GNP) are currently the most interesting graphene-based materials. Thermal conductivities for graphenes were reported in the wide range of about 1500 to 6000 W/mK; however, thermal properties of graphene-based materials may decrease dramatically as a function of the number of layers, the density of topological defects, re-hybridization defects as well as on the presence of impurities.

In this paper, different types of GNPs were thoroughly characterized both in terms of chemical/physical properties and in terms of thermal properties of individual flakes. Two selected GNPs were annealed at 1700°C in vacuum for 1 h to reduce defectivity of the graphenic structure, evidencing that thermal annealing can considerably reduce the amount of defects, as consistently proven by Raman measurements, X-ray photoelectron spectroscopy, X-ray diffraction and thermogravimetry. Thermal conductivity improvement of individual GNP upon annealing was confirmed by scanning thermal microscopy, a scanning probe technique which allows to measure thermal properties at the nanoscale and at the same time achieving information on the morphology, with a spatial resolution of a few tens of nanometers, simultaneously with the topography and lateral force maps, thus combining in a single measurement, properties that cannot be observed at the same time with other techniques.

Both pristine and annealed GNPs were used to prepare polymer nanocomposites, via a melt reactive extrusion process. In particular, GNPs were pre-dispersed in cyclic oligomers of polybutylene terephthalate (CBT) followed by catalyzed ring-opening polymerization of CBT in extrusion. This technique allowed to obtain significantly improved dispersion of GNP compared

to conventional melt processing methods, thanks to facile distribution of GNP in CBT and further dispersion as a result of high shear applied once viscosity increase during polymerization. Thermal conductivity results showed significant variability as a function of GNP properties, particularly in terms of defectivity, surface area and lateral dimensions (Figure 1). Furthermore, a dramatic two- to three-fold increase in the thermal conductivity of the nanocomposite was observed in the presence of annealed GNP compared to pristine ones (Figure 1), evidencing the importance of using low defectivity nanoflakes. Thermal conductivity of about 1.7 W/mK, i.e. one order of magnitude higher than for pristine polymer, was obtained with 10%wt of annealed GNPs, which is in line with state of the art nanocomposites prepared by more complex and less upscalable in situ polymerization processes.

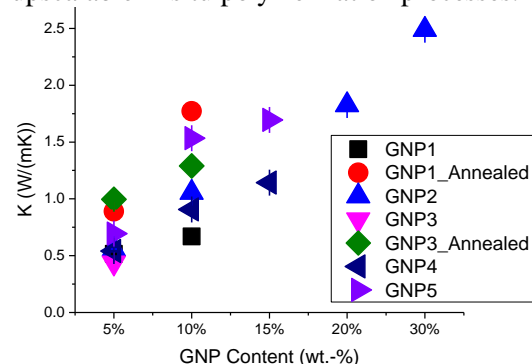


Figure 1: Thermal conductivity values for polymer nanocomposites embedding different types of GNPs or high temperature-annealed GNPs, as a function of % loadings

Keywords: thermally conductive polymer nanocomposites, graphene nanoplates, scanning thermal microscopy

Reduced Graphene Oxide Enhances Horseradish Peroxidase Stability by Serving as Radical Scavenger and Redox Mediator

Chengdong Zhang^{1*}, Silong Chen¹, Pedro J. J. Alvarez² and Wei Chen¹

¹College of Environmental Science and Engineering, Nankai University, China

²Dept. of Civil and Environmental Engineering, Rice University, USA

Abstract:

Graphene-based nanomaterials have been widely studied as high-performance matrices for enzyme immobilization and in the development of biosensors. Surface O-functionalities of graphene induce changes in chemical reactivity and electronic conductivity of nanomaterials and may interfere with enzymatic processes; however, the mechanisms are not fully understood. Here, we compare the effects of three commercially available graphene-based nanomaterials, namely a graphene, a graphene oxide, and a reduced graphene oxide, on the activity/stability of horseradish peroxidase. Both graphene and graphene oxide significantly reduced enzyme stability by altering enzyme conformation, which was evidence by circular dichroism spectroscopy. However, reduced graphene oxide improved stability up to 7-fold. This increased stability was attributed to the capability of reduced graphene oxide to quench superoxide anion radical, which was primarily responsible for the enzyme deactivation. The basal plane of reduced graphene oxide, mainly through the quinone moieties, may act as a redox mediator to facilitate enzymatic turnover. These results indicate that graphene-based nanomaterials, when appropriately functionalized, have great potential to enhance enzyme engineering and enzyme-based biosensing.

Keywords: Reduced graphene oxide, horseradish peroxidase, radical scavenger, redox mediator.

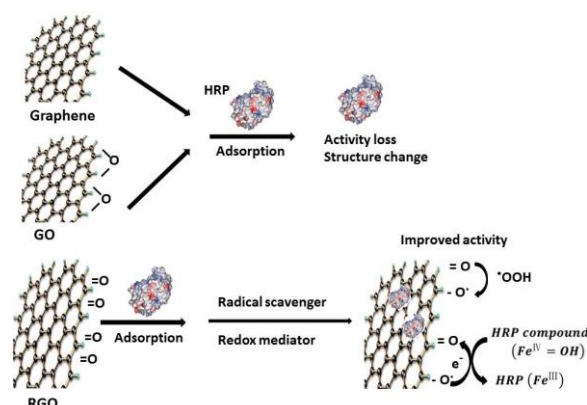


Figure 1 Effects of graphene-based nanomaterials on HRP activity and related mechanisms.

References:

Zhang, C., Chen, S., Alvarez, P., Chen, W. (2015) Reduced Graphene Oxide Enhances Horseradish Peroxidase Stability by Serving as Radical Scavenger and Redox Mediator, *Carbon*, 94,531-538.

Ab-initio calculations and simple models of electronic excitations in 2D materials and heterostructures

Kristian Sommer Thygesen

Center for Nanostructured Graphene (CNG), Department of Physics, Technical University of Denmark, Fysikvej 1, Kgs. Lyngby, Denmark

Abstract:

Many-body calculations based on the GW approximation to the electron self-energy and the Bethe-Salpeter equation (BSE) for the density response function are powerful methods for predicting band structures and optical excitations in real materials from first principles. We illustrate the high accuracy obtained by these methods through examples from our computational 2D materials database [1]. In 2D materials electron-electron interaction effects are particularly important because of the weak dielectric screening resulting in large self-energy corrections to band energies and strong excitonic effects. We show that the exciton binding energy can be approximated by a simple 2D Hydrogenic model taking an effective 2D dielectric constant and the exciton mass as input. Remarkably, the exciton binding energy depends only weakly on the exciton mass, and consequently the binding energy is found to scale directly with the size of the band gap – an effect unique to 2D excitons [2]. The simple Hydrogenic model also allows us to obtain the field-induced dissociation rates of 2D excitons by the technique of complex scaling to compute resonance life times. We show that the dissociation rates can be tuned significantly by embedding the active 2D material in a van der Waals heterostructures [3]. In general, periodic ab-initio calculations for van der Waals heterostructures are complicated by the incommensurable nature of the interfaces.

We show that by neglecting the effect of hybridization and thus assuming a purely electrostatic coupling between the layers, it is possible to compute the dielectric properties of large incommensurable van der Waals heterostructures from the dielectric function of the individual layers [4]. The latter can be calculated once and for all and stored in a database. We illustrate how the Quantum Electrostatic Heterostructure (QEH) model can be used as a tool for modeling excitons, plasmons, and optical properties of van der Waals heterostructures [5].

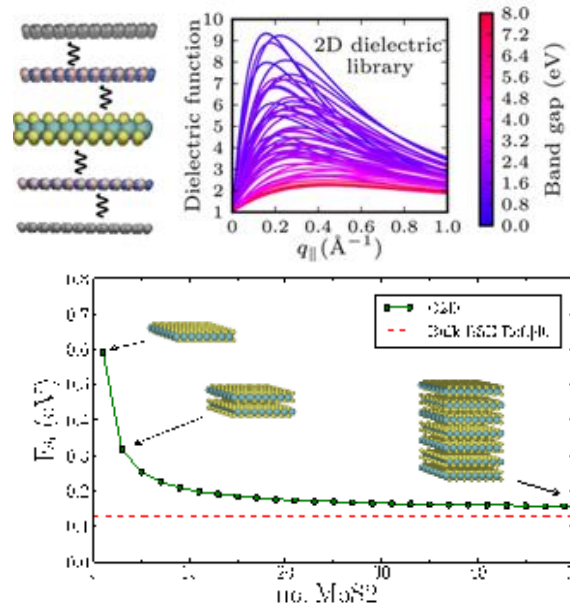


Figure: Top: The QEH model calculates the dielectric function of a vdWH from the dielectric functions of the individual 2D crystals assuming a pure Coulombic interaction between the layers. Middle: Static dielectric function of 50 semiconducting TMDs. bottom: Exciton binding energy in MoS₂ slabs of varying thickness. The exciton is calculated using a (quasi-)2D Hydrogen model with screened electron-hole interaction obtained from the QEH model. The results are seen to converge towards the bulk result showing the importance of dielectric screening relative to quantum confinement (not taken into account).

References:

1. F. A. Rasmussen and K. S. Thygesen, "Computational 2D Materials Database: Electronic Structure of Transition-Metal Dichalcogenides and Oxides", *J. Phys. Chem. C* 119, 13169 (2015)
2. Thomas Olsen, Simone Latini, Filip Rasmussen, and Kristian S. Thygesen, "Simple screened hydrogen model of excitons in two-dimensional materials", *Phys. Rev. Lett.* 116, 056401 (2016)
3. Sten Haastrup, Simone Latini, and K. S. Thygesen, "Field-induced dissociation of excitons in MoS₂/hBN heterostructures", *arXiv*
4. K. Andersen, S. Latini, and K. S. Thygesen, "Dielectric Genome of van der Waals Heterostructures", *Nano Letters* 15, 4616 (2015)
5. S. Latini, T. Olsen, and K. S. Thygesen, "Excitons in van der Waals heterostructures: The important role of dielectric screening", *Phys. Rev. B* 92, 245123 (2015)

Mechanical Property Enhancement of In-Situ Synthesized Three-Dimensional Network Graphene Reinforced Copper Nanocomposites

X. Zhang,¹ C.N.He,^{1,*} N.Q. Zhao,^{1,*}

¹Tianjin University, School of Materials Science and Engineering and Tianjin Key Laboratory of Composites and Functional Materials, Tianjin, P.R. China

Abstract:

Graphene has been emerging as an attractive reinforcement for composites due to its unique mechanical and electrical properties as well as its two-dimensional structure. It is a great challenge to efficiently combine the graphene with metal matrix for achieving excellent mechanical and physical performance of the metal matrix composite. In this work, we propose an easy and scalable strategy to *in situ* synthesizing the high-quality and well dispersed three-dimensional network graphene (3DNG) in copper matrix by chemical vapour deposition (CVD) method. The typical process involves using a water-soluble NaCl as the template, $\text{Cu}(\text{NO}_3)_2 \cdot 3\text{H}_2\text{O}$ as metal source and glucose ($\text{C}_6\text{H}_{12}\text{O}_6$) as solid carbon source, and the procedure of freeze drying was employed to get the homogeneous distributed mixtures of $\text{Cu}(\text{NO}_3)_2$ and $\text{C}_6\text{H}_{12}\text{O}_6$ on the flat surface of the intervals inside NaCl self-assembly. During the CVD process, the 3DNG with ultrathin thickness was *in situ* grown on the surface of NaCl self-assembly, followed by water washing for NaCl removal. The adjustable and dramatically enhanced mechanical properties of 3DNG/Cu composites have been obtained by varying the volume fraction of the reinforcement through an impregnation-annealing-hot pressing strategy. The *in-situ* CVD method for producing 3DNG/Cu composites exhibits a promising strategy for developing its structural and functional applications.

Keywords: three-dimensional network graphene, copper, metal matrix composites, toughness, chemical vapour deposition

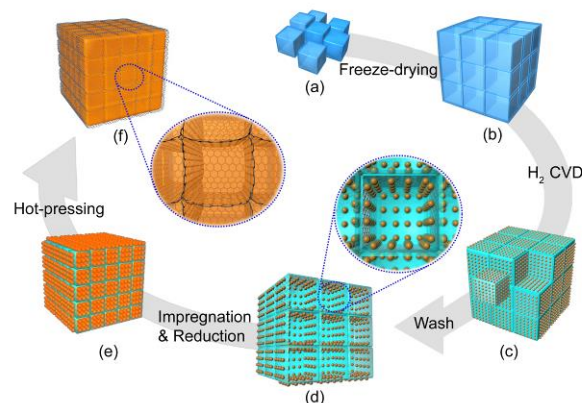


Figure 1: Schematic illustration of the synthesizing process for 3DNG/Cu bulk composites. (a) $\text{Cu}(\text{NO}_3)_2$ - $\text{C}_6\text{H}_{12}\text{O}_6$ -coated NaCl particles. (b) $\text{Cu}(\text{NO}_3)_2$ - $\text{C}_6\text{H}_{12}\text{O}_6$ -coated NaCl self-assembly. (c) Cu NPs-3DNG coated NaCl self-assembly. (d) 3DNG decorated with Cu NPs. (e) Cu particles wrapped 3DNG powders. (f) 3DNG/Cu bulk composites.

References:

1. Stankovich, S., Dikin, D.A., Dommett, G.H.B., et al(2006), Graphene-based composite materials, *Nature*, 442, 282.
2. Hwang, J., Yoon, T., Jin, S.H., Lee, J., et al(2013), Enhanced mechanical properties of graphene/copper nanocomposites using a molecular-level mixing process, *Adv. Mater.*, 25:6724-6729.

Next-Generation of Graphene Composites: Surface-Modified GO with Tunable Flake Orientation

M. Wåhlander,^{1*} F. Nilsson¹, A. Carlmark¹, S. Edmondson², E. Malmström¹

¹KTH Royal Institute of Technology, Department of Fibre and Polymer Technology, Stockholm, Sweden

²University of Manchester, School of Materials, Oxford Road, Manchester, UK

Abstract:

The extraordinary properties of graphene have made graphene-based fillers extremely popular for inclusion in composite materials.¹ In this work we have demonstrated a novel and efficient route to synthesize “next-generation graphene composite” materials without the need of polymeric matrices. Robust and hydrophobic matrix-free composites of grafted graphene oxide (GO), with well-dispersed flakes in isotropic and nematic states, are hereby characterized. The matrix-free GO-composites demonstrated superior thermal properties and new optical and barrier effects. This is the first instance a cationic macroinitiator (MI) has been immobilized on anionic GO and subsequently grafted with hydrophobic polymer grafts. Densely grafted brushes of PBA, PBMA and PMMA with a wide range of average graft molar masses (M_n : 1 – 440 kDa) were polymerized by a surface-initiated controlled radical precipitation polymerization technique from the statistically composed MI.

Transparent and translucent matrix-free GO-composites were melt processed directly from polymer-grafted GO. After processing, birefringence was observed, attributed to the nematic alignment of grafted GO. Permeability models for composites were developed which predicted the isotropic or nematic states of GO from the experimental oxygen permeability data. The storage modulus of the matrix-free GO-composites increased with GO-content, while the significant increases in the thermal stability and the glass transition temperature were dependent on graft length.

These robust and tunable matrix-free GO-composites are promising candidates for a range of applications, such as selective membranes and sensors.^{2, 3}

Keywords: Matrix-free graphene oxide composites; surface-initiated controlled radical polymerization; isotropic and nematic state; giant Maltese cross; oxygen permeability model; tunable thermomechanical properties.

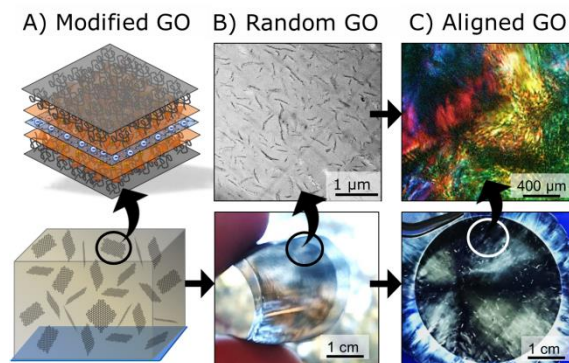


Figure 1: A) Illustrations of the surface-modified GOs which isotropically assemble in organic solvents, and B) form solid matrix-free GO-composites, with random orientation of flakes, when dried. The densely grafted polymer brushes provide low-friction flow during melt-processing while preventing the GOs to aggregate. In C), the majority of modified GOs have aligned in the direction of the flow after processing of flexible or stiff films. The alignment could be observed between crossed polarizers as a single giant Maltese cross covering the entire film (3.4 cm in diameter).

References:

1. A. C. Ferrari, F. Bonaccorso, V. Fal'ko, K. S. Novoselov, S. Roche, P. Boggild, S. Borini, F. H. L. Koppens, V. Palermo, N. Pugno and etal, (2015) *Nanoscale*, **7**, 4598-4810.
2. J. Yang, C. Liu, L. Gao, J. Wang, Y. Xu and R. He, (2015) *RSC Adv.*, **5**, 101049-101054.
3. M. Zhang, Y. Li, Z. Su and G. Wei, (2015) *Polym. Chem.*, **6**, 6107-6124.

Tunable Magnetism of Adatoms adsorbed on Bilayer Graphene

D. Nafday^{1,2}, M. Kabir^{3*} and T. Saha Dasgupta¹

¹S.N. Bose National Center for Basic Sciences, Kolkata

²Indian Institute of Science Education and Research, Kolkata

³Indian Institute of Science Education and Research, Pune

Abstract:

The controlled opening of band gaps in bilayer graphene through application of external electric field has brought into focus this material for its possible application to spintronics.[1]. Atoms adsorbed on bilayer graphene have garnered interest as the influence of an electric field modifies the electronic states of the bilayer graphene as well as shifts the adatom energy states relative to that of the graphene energy states. Employing first principle calculations, we study the effect of external electric field on three different adatoms Na, Cu and Fe. For the case of Na and Cu adatoms it was observed that application of electric field, lead to formation of local magnetic moment in the latter case (Cu) and destruction of magnetic moment in the former case (Na). This indicates to the possibility of switching on or off of local magnetic moments of single adatoms placed on bilayer graphene via an external electric field applied perpendicular graphene[2]. A similar calculation was done for Fe adatom and Fe dimer on bilayer graphene. We show that application of external electric field is able to modulate the charge and spin states of the adatom. States ranging from $3d$, $S=2$ to $3d$, $S=0$ have been observed for Fe adatom as shown in figure, which are inaccessible under normal condition. In the case of Fe dimer, the ground state was found to be ferromagnetically coupled. However, a ferrimagnetically coupled state driven by structural changes was found to stabilize ~ 0.25 eV higher than the ferromagnetic ground state. We show that by applying a small external electric field it was possible to switch the magnetic coupling from ferromagnetic to ferrimagnetic.[3]

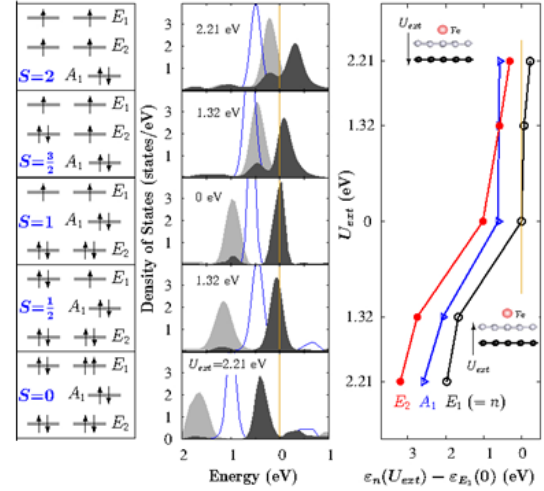


Figure: Left panel: The non spin polarized LDA density of states for single Fe adatom onBLG/SiO2 projected onto Fe-E2 (light shaded), Fe-E1 (dark shaded) and Fe-A1(unshaded) states, corresponding to different applied electric field. The zero of the energy is set at Fermi energy in each panel. The corresponding nominal occupancies of Fe d states are shown by side which determine the charge and spin state of Fe. Right panel: The energy positions of E2, E1 and A1 states measured with respect to the position of E1 at zero electric field.

References:

1. E. V. Castro, K. S. Novoselov et al , PRL 99, 216802 (2007)
2. Dhani Nafday and T. Saha-Dasgupta, Physical Review B 88, 205422 (2013)
3. Dhani Nafday and T. Saha-Dasgupta, Physical Review B 93, 045433 (2016)

Ultrafast optics in graphene

K. Liu^{1*}, J.F. Zhang¹, Z.H. Zhu¹, C.C. Guo¹, X.D. Yuan¹, W.M. Ye and S.Q. Qin¹

¹ College of Optoelectronic Science and Engineering, National University of Defense Technology, Changsha, Hunan 410073, China

*E-mail: liukener@163.com.

Abstract:

Graphene is a monolayer material without bandgap and with linear symmetrical energy-momentum dispersion relationship. The absorbance of light by graphene related with the unique electrical properties has been well studied and graphene shows a broadband linear absorbance of 2.3%, which is related to the fine structure constant. Here we show the reverse process, broadband photon emission from graphene, which has been seldom studied. The ultrafast hot carrier relaxation and lack of bandgap lead to a very low emission efficiency of graphene. But we achieve bright multicolored frequency-upconverted photoluminescence (Figure. 1) and THz emission from graphene by femtosecond laser injection. The results can be explained by linear carrier collision mechanism in graphene and reveals strong hot carrier multiplication and hot carrier scattering in graphene, and could also help to study the population inversion of graphene so that graphene can be used as a on-chip broadband lasing material.

Graphene has an ultra-large Kerr coefficient which is 6 orders larger than that of silicon and 8 orders larger than that of silica. We report the ultrafast pulse propagation in a hybrid graphene/silicon ridge waveguide. With only one layer of graphene transferred on the silicon ridge waveguide, the effective Kerr coefficient of the hybrid waveguide could be enhanced several times. After propagation in the hybrid waveguide, great spectral broadening was observed due to self-phase modulation (Figure. 2). The results demonstrate the ultra-large Kerr coefficient of graphene, and provide a new method to enhance the nonlinear coefficient to design CMOS-compatible nonlinear devices.

Keywords: graphene, photoluminescence, THz emission, linear carrier collision, carrier multiplication, ultra-large Kerr coefficient, ultrafast pulse propagation, hybrid graphene/silicon ridge waveguide.

Figure 1: SEM image of the graphene/silicon hybrid waveguide (left) and the photoluminescence image captured by CCD (right). The figure shows broadband photon emission from graphene.

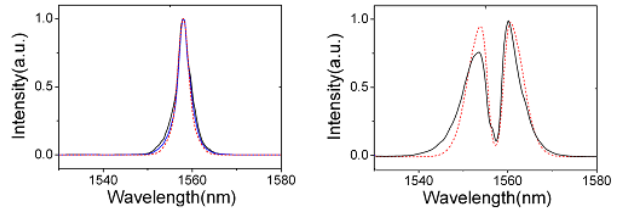
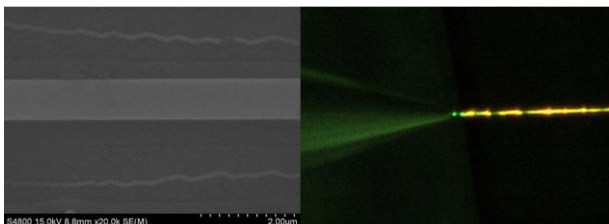


Figure 2: Experimentally measured and numerically calculated spectra of ultrafast pulses propagation along silicon ridge waveguide (left) and graphene/silicon hybrid waveguide (right). The figure shows the hybrid structure has an enhanced Kerr coefficient.

References:

1. Liu, K., Zhu, Z. H., Li, X. J., Zhang, J. F., Yuan, X. D., Guo, C. C. & Qin, S. Q. (2015). Bright Multicolored photoluminescence of hybrid graphene/silicon optoelectronics. *ACS Photonics*, 2(7), 797-804.
2. Liu, K., Zhang, J. F., Xu, W., Zhu, Z. H., Guo, C. C., Li, X. J. & Qin, S. Q. (2015). Ultra-fast pulse propagation in nonlinear graphene/silicon ridge waveguide. *Scientific reports*, 5, 16734.



Graphynes: from Competitors to Graphene to Atomic Sieves and Scatters

Francesc Viñes,¹ Montserrat Manadé,¹ Sunkung Kim,² Pablo Gamallo,¹ Jin Yong Lee,² Francesc Illas¹
N. Surname,^{1,2,*} B. Someone,^{1,2}

¹ Departament de Química Física & Institut de Química Teòrica i Computacional (IQTCUB), Universitat de Barcelona, c/Martí i Franquès 1, 08028 Barcelona, Spain

² Department of Chemistry, Sungkyunkwan University, Suwon, 440-746, Korea

Abstract:

Graphynes, 2D carbon allotropes containing sp^2 and sp bonds, have lately driven much attention because of the versatility in manipulating their physicochemical properties according to the sp^2/sp ratio and the particular periodic arrangement, and also because they display anisotropic Dirac cones (Figure), charge carrier mobility in principle better than graphene, and, depending on the graphyne, even self-doping [1].

Graphene and graphyne are considered as a supports for transition metals, for instance, in catalysis. Here we present a systematic Density Functional Theory (DFT) study, including dispersive forces, on the interaction of *all* Transition Metals (TMs) on graphene and graphyne, with the accent put on the trends of interaction, structural aspects, as well as electronic properties [2]. TMs are found to strongly attach on graphene, except d^5 and d^{10} ones (Figure). Diffusion is found to be easy on graphene, despite some exceptions. TMs magnetic moment is decimated, yet still prevails in many TMs. On graphene TMs aggregation is possible, yet hindered since adsorbed TM are normally charged, and so coulombic repulsion prevents so.

On γ -graphyne TMs attach with a much more stronger strength compared to graphene. Moreover, the interaction with d^5 metals is not negligible, and only d^{10} TMs can be considered physisorbed. Apart from that, TMs prefer to reside over or inside the larger cavities. Indeed, in some cases the metal atom prefers to be inserted in the cavity becoming a part of the 2D structure. Aside from that, and similarly to graphene, TMs n-dope γ -graphyne, and the magnetic moment is reduced but kept in many cases. Note that diffusion does not seem to be prevented in these cases, and, especially on small TMs, the γ -graphyne can allow its trespassing, while this step is prohibited for larger metal atoms, thus, acting as an atomic sieve.

For some metals (Sc, Y, La, Co, Ni, Cu), the adsorption energy of their isolated atoms on γ -graphyne is larger than on the corresponding bulk, at low coverage (medium in some metals).

This points for γ -graphyne to be a metal adatom scatter, allowing to have isolated metal atom, in particular position, with a peculiar electronic state (in the case of Co even having a given magnetic moment). These systems are of high interest for spintronics, having a particular pattern of magnets, or even as an excellent support for the so-called single-atom catalysts [4].

Keywords: Graphene · Graphyne · Dirac Cones · Transition Metal Atoms · Electronic Structure.

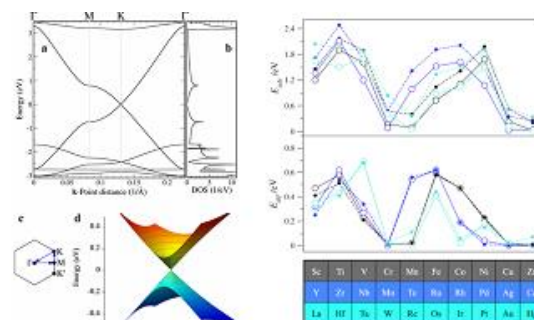


Figure: Graphyne bandstructure showing the Dirac cones at K (left), and d series trends of adsorption and diffusion energies of transition metal atoms on graphene (right)

References:

- [1] Daniel Malko, Christian Neiss, Francesc Viñes, Andreas Görling, Phys. Rev. Lett., **108** (2012) 086804.
- [2] Montserrat Manadé, Francesc Viñes, Francesc Illas, Carbon, **95** (2015) 525.
- [3] Sunkung Kim, Francesc Viñes, Antonio Ruíz, Pablo Gamallo, Jin Yong Lee, Francesc Illas, Carbon, *submitted*.
- [4] Sunkung Kim, Francesc Viñes, Pablo Gamallo, Jin Yong Lee, Francesc Illas, Nanoletters, *submitted*.

Combination of the PDCs Route with the SPS Process to Easily Obtain Large and Pure h-BN Nanosheets

Y. Li^{1,2}, S. Yuan^{1,2}, P. Steyer^{1*}, B. Toury², V. Garnier¹, A. Brioude², C. Journet²

¹Laboratoire Matériaux Ingénierie et Science, UMR CNRS 5510, INSA de Lyon, Université de Lyon, F-69621, Villeurbanne, France.

²Laboratoire des Multimatériaux et Interfaces, CNRS, UMR 5615, Université Lyon 1, Université de Lyon, F-69622, Villeurbanne, France.

Abstract:

With the continuous development of the electronic devices field, research on 2D nanomaterials has developed remarkably in the past few years. Especially, widespread interest in graphene has been driven by its excellent capacity for charge transport within the atomic plane.¹ However, the promising future development of practical graphene devices seems therefore strongly linked to the nature of the substrate. One of the most suitable substrates appears to be the hexagonal variety of boron nitride (*h*-BN, also called “white graphite”), which is isostructural and isoelectronic of graphene, with a lattice matching that of graphene.

As a consequence, the development of a novel source for highly crystallized *h*-BN crystals, suitable for a further exfoliation, is a prime scientific issue. This presentation proposes a promising approach to synthesize pure and well-crystallized *h*-BN flakes, which can be easily exfoliated into BN nanosheets. This new accessible production process represents a relevant alternative source of supply in response to the increasing need of high quality BNNSs. The synthesis strategy to prepare pure *h*-BN is based on a unique combination of the Polymer Derived Ceramics² (PDCs) route from the polyborazylène precursor, with the Spark Plasma Sintering (SPS) process³. Through a multi-scale chemical and structural investigation (XRD, SEM, TEM, EELS, Raman), it is clearly shown that obtained flakes are large (fig. 1), defect-free and well-crystallized, which are key-characteristics for a subsequent exfoliation into relevant BNNSs.

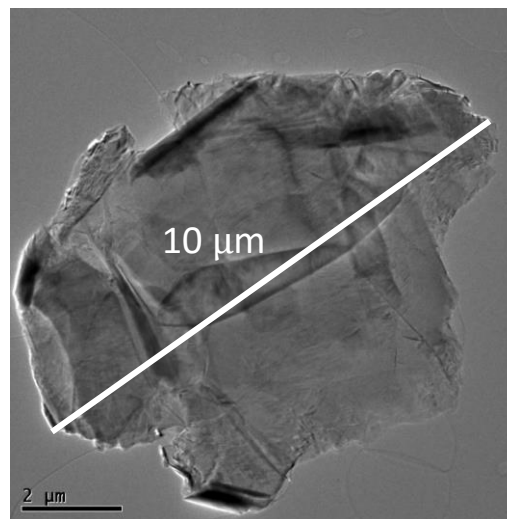


Figure 1: TEM bright field micrograph attesting the large dimension of *h*-BN flake resulting from the PDCs/SPS dual process

Keywords:

hexagonal boron nitride, graphene-like material, 2D material, PDCs, SPS, Raman, TEM

References:

1. K. S. Novoselov, A. K. Geim, S. V. Morozov, S. V. Dubonos, Y. Zhang, D. Jiang, “Two-dimensional gas of massless Dirac fermions in graphene”, *Nature* **2005**, 438, 197.
2. S. Yuan, B. Toury, C. Journet, A. Brioude, “Synthesis of hexagonal boron nitride graphene-like few layers”, *Nanoscale*, **2014**, 6, 7838.
3. S. Yuan, S. Linas, C. Journet, P. Steyer, V. Garnier, G. Bonnefont, A. Brioude, B. Toury, “Pure and crystallised 2D Boron Nitride sheets synthesized via a novel process coupling both PDCs and SPS methods”, *Scientific Reports*, **2016**, In press.

Graphene based Electrically Tunable Hybrid Plasmonic-photonic Waveguide with Low-loss and Nano-scale Optical Confinement

Lalit Singh, Sulabh and Mukesh Kumar

Integrated Photonics Laboratory, Department of Electrical Engineering, Indian Institute of Technology Indore, India

Abstract: Graphene has emerged as a potential material for various applications including integrated electronics and photonics [1]. Plasmonics response of graphene can be promising in realizing nano photonic devices [2]. Hybrid Plasmonic (HP) waveguide is advantageous in optical confinement beyond diffraction limit with larger propagation length [3]. The propagation loss of Plasmonics waveguide can be reduced by introducing a high index layer below the confinement layer [4]. Unique properties of graphene can be utilized to further improve the performance of HP waveguide for large scale photonic integration [5]. In this paper, a novel design of Graphene based on Electrically Tunable HP waveguide for low-loss and nano-scale optical confinement is proposed. On the application of electric field on graphene, contribution of metallic loss in HP waveguide decreases because of the coupling of SPP and optical mode through graphene. The effective refractive index of hybrid mode is tuned electrically. The proposed design is shown in Fig.1 which consists of Graphene layer between gold and dielectric layer followed by high index layer of silicon. Few layers of Graphene are taken with thickness of 1-nm [5]. Thickness of silicon layer, SiO₂ and gold layer is 100-nm, 10-nm and 200-nm respectively. Width of silicon and dielectric layer is 200-nm. Fig.2 (a) shows the effect of change in applied field on propagation length. SPP and optical modes get decoupled when applied voltage is below 1.5 volt. On application of electric field Fermi-level of graphene shifts which causes a change in dielectric constant of graphene leading to a change in effective index of the guided HP mode [5]. In conclusion the presence of graphene provides a way to tune the effective refractive index of proposed waveguide device. The presence of graphene also reduces metallic losses and hence a large propagation length of 11-mm and low loss of 0.36 dB/mm is reported. The proposed design can be potential candidate in realizing nanophotonic devices for applications in optical communication and cell-level sensing.

Keywords: hybrid plasmonic waveguide, Graphene, nano-scale optical confinement.

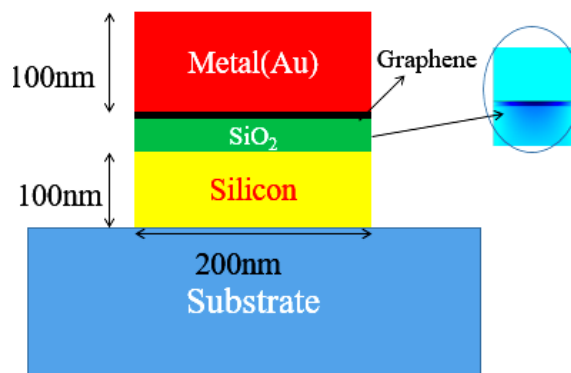


Fig.1 Schematic of the proposed design. Inset shows confinement of light through the graphene in dielectric.

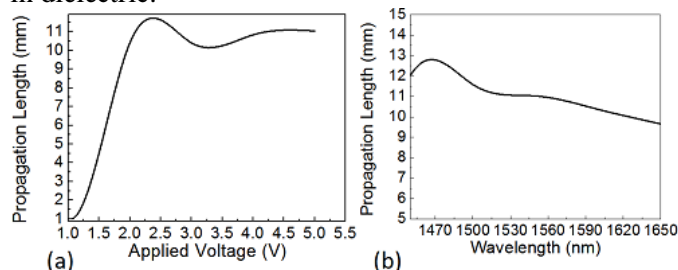


Fig.2 (a) Effect of change in applied voltage on propagation length when voltage is applied to graphene. **(b)** Effect of change in wavelength on propagation length when 5 volts is applied to graphene.

Fig.2 (b) shows wavelength dependence of propagation length when electric field is applied on the graphene. Wideband property of graphene is observed. Acceptable propagation length is seen between wavelength range from 1450-nm to 1650-nm. The propagation-loss at 1450-nm is reported to be 0.36 dB/mm when 5 volts is applied.

Acknowledgement- The work is supported by the grant (#22/680/14/EMRII) of Council of Scientific and Industrial Research (CSIR), Government of India.

References :

1. K. S. Novoselov, , Nature 490, 192–200 (2012)
2. Ming Liu et. al.64-67 Nature, Vol 474, 2 June (2011)
3. R. F. Oulton, V. J. Sorger, D. A. Genov, D. F. P. Pile, and X. Zhang, Nat. Photonics 2, 496–500 (2008).
4. T. Sharma and M. Kumar, Appl.Opt.53(9) (2014)1954.
5. J. K. Thind, M. Kumar and B. K. Kaushik; IEEE Journal of Quantum Electronics Volume 51 issue 10 Oct. (2015).

Electrochemically exfoliated graphite for solution-processed transparent conductive electrodes.

A.Ly^{*1,2}, P. Viville², and R. Lazzaroni^{1,2}

¹University of Mons – UMONS- CMN (Laboratory for Chemistry of Novel Materials), 20, Place du Parc, 7000, Mons, Belgium

² Materia Nova, 1 Avenue Nicolas Copernic, 7000, Mons, Belgium

Abstract:

One of the main issues that currently slows down the commercialization of Organic Photovoltaics and Organic Light Emitting diodes is the high cost-efficiency ratio, related to the product and the fabrication processes. In particular, the costs associated with the fabrication conditions of Indium Tin Oxide (ITO) electrodes, the scarcity of indium and the lack of flexibility of ITO has stimulated intensive research in recent years to replace ITO by cost-effective solution-processed transparent conductive electrodes (TCE).

Graphene represents, in that framework, a valuable alternative to ITO due to its excellent intrinsic electrical conductivity, optical transparency, thermal and mechanical stability and flexibility.

Its production by intercalation/exfoliation methods is therefore extensively studied. In this work, we present an efficient method based on electrochemical exfoliation of Highly Oriented Pyrolytic Graphite (HOPG) to produce stable dispersions of few layers graphene.

In our setup, HOPG is used as the anode and platinum as the cathode and the electrochemical reactions take place in concentrated or diluted acid electrolytes. Depending on the used electrolytes, the chemical reactions allow to end in various levels of intercalation. In certain conditions, water oxidation allows to separate the graphene layers. The graphite is first intercalated and is finally exfoliated.

In this work, we study the morphology and the chemical composition of thin films produced from dispersions of electrochemically produced few layers graphene. We show that the method can produce until ~1nm-thick graphene layers with micrometric lateral dimensions with high yields.

For a better understanding of the sp^3 defects arising from this electrochemical method, we also study the intercalation and the exfoliation processes by in situ Raman spectroscopy in order to discriminate between the two processes and to allow, at the end, a better control of the exfoliation process.

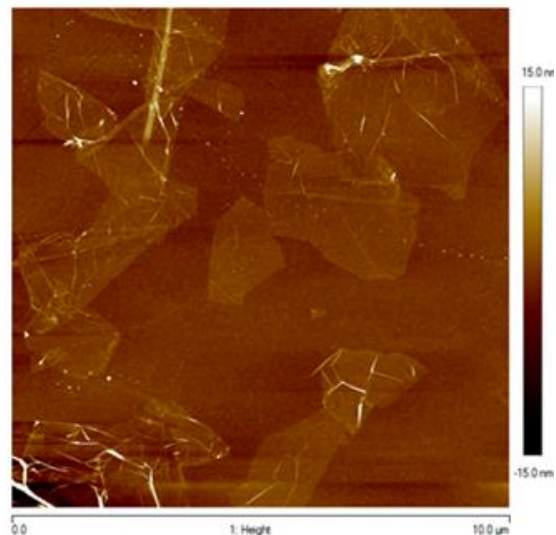


Figure 1: 10x10 μm^2 Tapping mode AFM (TMAFM) imaging of a spray coated film obtained from a graphene dispersion in DMF after electrochemical intercalation/exfoliation. The images highlight micrometer-sized sheets with a 1 nm average thickness.

From a statistical analysis of the Raman spectroscopy results on exfoliated sheets we demonstrate exfoliation conditions that significantly lowers the sp^3 defects on the exfoliated sheets.

Keywords: Graphene, graphite exfoliation, Raman spectroscopy, graphene functionalization, transparent conductive coating.

Discontinuous bilayer graphene chemiresistors

P. Krauß,¹ J. J. Schneider^{1,*}

¹Technische Universität Darmstadt, Eduard-Zintl-Institut für Anorganische und Physikalische Chemie, Darmstadt, Germany

Abstract:

The application of graphene in sensors for the detection of toxic gases has been widely explored due to its unique structure and electronic properties. To improve the gas sensing characteristics of pristine graphene, e.g. sensitivity and selectivity, latest research focuses on defective and functionalized graphene materials for sensor devices (Randeniya *et al.*, 2013). We introduce a modified transfer technique of graphene grown by chemical vapor deposition (CVD), which allows tearing of a single, continuous graphene layer into discontinuous but closely spaced graphene flakes. Applying the modified etching process, discontinuous bilayer graphene chemiresistors are fabricated by selective deposition of two graphene layers, which is the minimum number required to span the sensor's electrodes (Figure 1). The gas sensing characteristics of the as-fabricated chemiresistors towards nitrogen dioxide, ammonia and sulfur dioxide were analyzed in the temperature range of 30 to 200 °C. An increased sensitivity compared to pristine graphene and defective graphene confirms their high level of structural defects without additional post-processing (Paul *et al.*, 2012). As the number of interacting layers can be controlled precisely by the modified transfer process, the sensor's response is highly reproducible for different devices. Additionally, we analyzed the effects of further functionalization on the gas sensing characteristics of the discontinuous bilayer graphene chemiresistors by carbon dioxide plasma and the deposition of iron oxide nanoparticles (Babu *et al.*, 2014).

Keywords: modified transfer technique, discontinuous bilayer graphene, chemiresistors, toxic gases, carbon dioxide plasma, iron oxide nanoparticles.

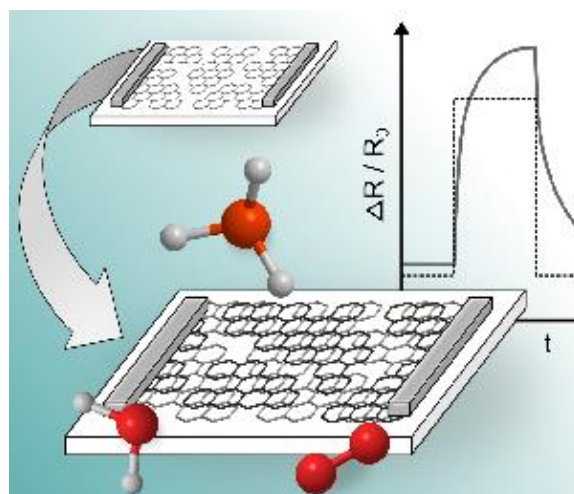


Figure 1: Schematic setup of discontinuous bilayer graphene chemiresistors. A modified transfer technique of CVD graphene by chemical etching allows the deposition of discontinuous but closely spaced graphene flakes from a single, continuous graphene layer. The chemiresistors gas sensing characteristics were analyzed towards NO₂, NH₃ and SO₂.

References:

1. Randeniya, L. K., Shi, H., Barnard, A. S., Fang, J., Martin, P. J., Ostrikov, K. (2013) Harnessing the influence of reactive edges and defects of graphene substrates for achieving complete cycle of room-temperature molecular sensing, *Small*, 9, 3993-3999.
2. Paul, R. K., Badhulika, S., Saucedo, N. M., Mulchandani, A. (2012), Graphene nanomesh as highly sensitive chemiresistor gas sensor, *Anal. Chem.*, 84, 8171-8178.
3. Babu, D. J., Yadav, S., Heinlein, T., Cherkashinin, G., Schneider, J. J., (2014), Carbon dioxide plasma as a versatile medium for purification and functionalization of vertically aligned carbon nanotubes, *J. Phys. Chem. C*, 118, 12028-12034.

Spin noise in graphene detected via cross-correlation

S. Omar¹, I.J. Vera-Marun^{1,2}, M.H.D. Guimarães³, A. Kaverzin¹, and B.J. van Wees¹

¹Physics of Nanodevices, Zernike Institute for Advanced Materials, University of Groningen, Groningen, The Netherlands

²School of Physics and Astronomy; The University of Manchester; Manchester M13 9PL; UK

³Kavli Institute at Cornell for Nanoscale Science Cornell University, Ithaca, NY – 14853, USA

Abstract:

Noise measurements on graphene can provide more understanding of electron as well as spin dynamics compared to the usual charge and spin transport measurements. In order to study the noise associated with the spin transport in graphene, we measure the fluctuations of the non-local spin signal with the ferromagnetic contacts, which are used to inject and detect a non-equilibrium spin-accumulation. We observe that the noise associated with the non-local signal has $1/f$ shape at low frequencies (0.01-10 Hz). The noise magnitude changes on modifying the spin accumulation underneath the detector contacts in both spin-valve and Hanle configuration, which indicates that the noise is produced by the spin accumulation. Further, we successfully demonstrate the use of spatial crosscorrelation method to separate out the spin accumulation/ injection noise from the polarization noise at the detector electrodes. The observed changes are only visible at very low frequencies, alluding to slow fluctuations in the contact polarization and possibly in the spin scattering cross-section of graphene lattice, which result in $1/f$ type of noise in the spin current. We also confirm our results by simulating the same noise level from a PSpice based 2-channel resistor model representing the spin transport properties of our actual device. This model also helps us to conclude that the Hooge parameter (γ_H) for the charge and spin transport are different by orders of magnitude and indicate that different processes governing the spin and charge transport.

Keywords: Spintronics, Graphene, electronic noise, magnetic noise, spin noise, Hanle analysis

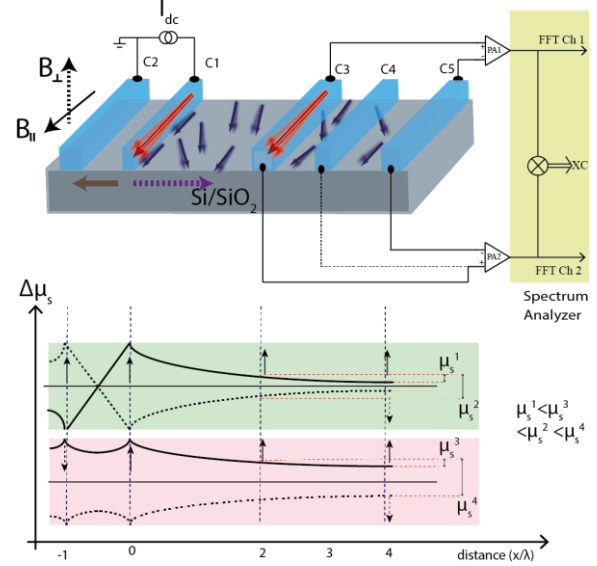


Figure 1: Figure illustrating the auto correlation and the cross correlation measurement scheme for measuring the noise associated with spin transport in graphene. Below the diagram the spin accumulation profile is demonstrated for the parallel and the anti-parallel magnetization directions of the injector electrodes.

References:

1. T. Arakawa, J. Shiogai, M. Ciorga, M. Utz, D. Schuh, M. Kohda, J. Nitta, D. Bougeard, D. Weiss, T. Ono, and K. Kobayashi, Phys. Rev. Lett. 114, 016601 (2015).
2. J. Foros, A. Brataas, G. E. W. Bauer, and Y. Tserkovnyak, Phys. Rev. B 79, 214407 (2009).
3. S. Omar *et al.*, (in preparation)

Graphene oxide framework membranes: Control the 2D interspacing toward strict molecular sieving

Gaofeng Zeng,^{*} Guihua Li, Benyu Qi, Xiaofan He, Yanfeng Zhang, Yuhan Sun
CAS Key Laboratory of Low-carbon Conversion Science and Engineering, Shanghai Advanced Research Institute, Chinese Academy of Sciences, Shanghai 201210, China

Abstract: Graphene oxide (GO) has generated a significant interest for water separation due to its hydrophilicity and regular interspacing [2]. However, the poor mechanical strength of GO membranes poses a critical challenge for any practical application. Graphene oxide frameworks (GOFs) [3], prepared by expanding the GO sheets with various linear pillaring units, are well meeting the requirements of stocking GO in short-range order because the interlamellar spacing of GO is well defined by the linking units. The chemical bonding between the GOF offers great mechanical stability compared with GO. In this work, we prepared ceramic supported 1, 4-phenyldiboronic acid (14PDBA) linked GOF/ polyvinyl alcohol (PVA) hybrid membranes by simple dip-coating method for the first time. The resulting membranes were characterized in detail. Excellent separation performance of selectivity and lifetime were achieved in the pervaporation of C3-C4 alcohols dehydration.

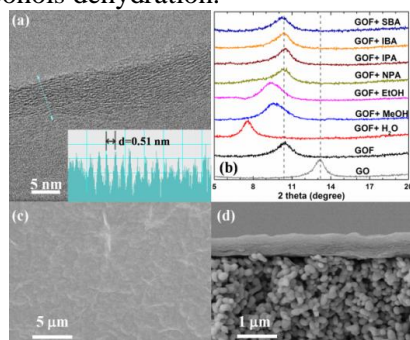


Fig. 1 (a) TEM cross-section view of GOF (inset d-value of GOF); (b) XRD patterns of GO and GOF in air and solvents; (c) SEM top view and (d) cross-section view of GOF/PVA membrane.

The cross-sectional view of mono-dispersed GOF delineates that the highly ordered and well packed GO precursors built the GOF mono-sheet with 6.5-9.1 nm thickness (Fig. 1a), which suggested that multilayer GO precursors were regularly fixed by 14PDBA linker. In XRD results (Fig. 1b), the dried GO exhibited a d-value of 6.8 Å. However, the d-value of GOF was increased to 8.4 Å, which is resulted in the insert of 14PDBA. The XRD determined interspace of GOF was 4.9 Å (=8.4 -3.5 Å), which is well agree with the carbon layers gap in GOF i.e ca. 5.1 Å measured by TEM (Fig. 1a, inset). The effects of water and alcohols on the GOF structure were evaluated by XRD (Fig. 2b). It indicated that small molecules can intercalated into the bulk of GOF since water (0.28 nm), methanol (0.36 nm) and ethanol (0.43 nm) are smaller than the interspace of GOF. While the propanols (ca. 0.47 nm) and butanol isomers (ca. 0.51 nm) cannot intercalate the GOF due

to the bulky size. The surface of GOF /PVA membrane exhibited dense coverage and no visible defects were observed (Fig. 1c). The cross-section of the GOF membrane shows a uniform thickness i.e. 590 nm with highly ordered and well-packed 2D lamellar structure (Fig. 1d).

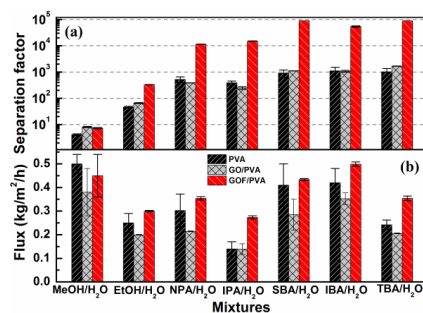


Fig. 2 Comparison of the separation performance of PVA, GO / PVA and GOF/PVA composite membranes for C1-C4 alcohol/ 10% water mixtures at 70 °C. a) separation factor (SF); b) flux.

The separation of the C1-C4 alcohols - 10 wt.% H₂O mixtures over GOF/PVA membrane was conducted at 70°C. The GOF/PVA membrane showed great performance for the dehydration of organic solvents. It exhibited a sharp molecular sieving effect with the cut-off diameter ca. 0.47 nm. The molecules larger than the cut-off point were sieved out e.g. C3 and C4 alcohols in this work, from which 11,300 - 89,000 separation factors were achieved. The separation factor of the GOF/PVA membrane for IPA and butanol isomers were much higher than that of literature results including polymeric membranes, inorganic membranes as well as GO based membranes. It demonstrates that GOF/PVA membrane has extraordinary separation properties even comparable with inorganic membranes, like zeolite membranes and silica membranes. On the other hand, choosing polymers with high capacity of water permeability as the blend phase is promising to improve the total flux of GOF based membranes.

Keywords: graphene oxide framework membrane; hybrid membrane; azeotropes separation; pervaporation

References:

- [1] G. Li, L. Shi, G. Zeng, M. Li, Y. Zhang, Y. Sun, *Chemical Communications*, 2015, 51, 7345-8.
- [2] Li, G., Shi, L., Zeng, G., Zhang, Y., Sun, Y., *RSC Adv.*, 4, 52012-52015.
- [3] Burrell, J. W., Gadipelli, S., Ford, J., Simmons, J., Zhou, W., Yildirim, T., *Angew. Chem. Int. Edit.*, 2010, 49, 8902-8904.

Hydrogen-decorated stabilization and thermal conductivity of penta-silicene: A first principles calculation

H. K. Liu^{1,2}, Y. Lin^{1,*}, M. Hu^{2,*}

¹State Key Laboratory of Electronic Thin Films and Integrated Devices, University of Electronic Science and Technology of China, Chengdu, Sichuan 610054, P. R. China

²Institute of Mineral Engineering, Division of Materials Science and Engineering, Faculty of Georesources and Materials Engineering, RWTH Aachen University, 52064 Aachen, Germany

Abstract:

The structural stability and thermal transport properties of penta-silicene monolayer was systematically investigated using first principles calculations, which are the Si analogues of recently proposed penta-graphene [1]. We find that the pristine penta-silicene sheet was unstable because of the stronger sp³ bonds between Si-Si than that for C-C bonds. However, the dynamic stability can be improved by hydrogen decoration, as well as the mechanical and thermal stability. The thermal conductivity of penta-SiH with increased biaxial strains was calculated to investigate its thermal behavior.

Unlike the graphene and penta-graphene, penta-SiH has a much lower thermal conductivity, which makes it promising for many potential applications in electronic nano-devices in future, such as thermoelectrics for energy conversion.

Keywords: thermal conductivity, penta-silicene, strain, first principles.

References:

S. Zhang et al., Proc. Natl. Acad. Sci. U.S.A., 2015, 112, 2372.

Enhancing the performance of dye-sensitized solar cells by incorporating various ratios of platinum and reduced graphene oxide thin film as a counter electrode

N. Ahmad-Ludin¹, A. Bolhan¹, M. Y. Sulaiman¹, M. S. Suait¹, M. A. Mat-Teridi¹, M. A. Ibrahim¹, S. Sepeai¹, K. Sopian¹, H. Arakawa²

¹Solar Energy Research Institute (SERI), Universiti Kebangsaan Malaysia, 43600 Bangi, Selangor, Malaysia

²Department of Industrial Chemistry, Faculty of Engineering, Tokyo University of Science, 162-0826, Japan

Abstract:

Counter electrode serve critical role to catalyst the reduction of redox process in dye sensitized solar cell (DSSC). Counter electrode collect the electron from external circuit and transfer into electrolyte. The redox process will occur in electrolyte where triiodide ion will reduce to iodide ion. Therefore, high catalytic activity of counter electrode results in high efficiency of DSSC. Platinum is conventional material for counter electrode thin film and have good catalytic activity. However, the problem occur when the DSSC are to be commercialized because the platinum is not cheap. Another promising material is graphene that has large surface area, low cost and good electrical conductivity. The consumption of platinum can be minimising by doping the graphene with platinum. A platinum/reduced graphene oxide (Pt-rGO) thin film was prepared and deposited on a fluorine-doped tin oxide (FTO) substrate using the doctor blade method and was annealed at 450 °C for 30 minutes. Thin films were used as counter electrode in a dye-sensitized solar cell (DSSC) with Pt-rGO ratios of 1:1, 1:2, and 2:1. Cyclic voltammetry showed that the Pt-rGO thin film with a ratio of 1:1 exhibits better electrocatalytic activity for I_3^-/I^- redox reaction. The current-voltage curve (I-V) revealed that DSSC using the Pt-rGO CE thin film with a ratio of 1:1 has a power conversion efficiency (PCE) of 6.3% under AM 1.5 illumination of 100 mW cm⁻² and this is higher than Pt (6.1%). The current density (J_{sc}) is 14.3 mA/cm⁻², open circuit voltage (V_{oc}) is 0.75 V, and fill factor (FF) is 58.98

Keywords: reduced graphene oxide, platinum, counter electrode, dye-sensitized solar cell

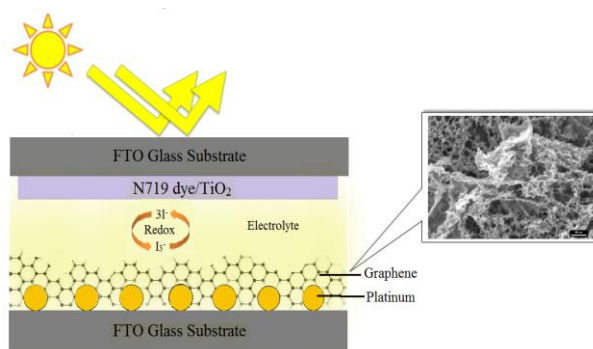


Figure 1: Figure illustrating the structure question that we are tempting to prepared experimentally: What is the optimum ratio of graphene doped with platinum that help increase electrocatalytic activity of the counter electrode that lead to higher efficiency of the dye sensitized solar cell

References:

1. Tsai, C.-H., Chen, C.-H., Hsiao, Y.-C., Chuang, P.-Y. (2015) Investigation of graphene nanosheets as counter electrodes for efficient dye-sensitized solar cells. *Organic electronics*, 17, 57-65.
2. Yue, G., Wu, J., Xiao, Y., Huang, M., Lin, J., Fan, L., Lan, Z. (2013) Platinum/graphene hybrid film as counter electrode for dye-sensitized solar cells, *Electrochimica Acta*, 92, 64-70.

EGF 2016 Session III
Graphene and 2D Materials
properties and applications

Platinum-Gold Alloy Nanoparticles Decorated Crumpled Graphene for Electrocatalyst

H.D. Jang,^{1,2} S.K. Kim,¹ Ji-Hyuk Choi and¹ H. Chang,^{1,2}

¹ Korea Institute of Geoscience and Mineral Resources, Rare Metals Research Center, Daejeon, Korea

²University of Science & Technology, Department of Nanomaterials Science and Engineering Daejeon, Korea

Abstract:

Enhanced performance of electrocatalysts for direct methanol fuel cells was developed by crumpled graphene (CGR) decorated with platinum (Pt)-gold (Au) alloy nanoparticles (CGR/PtAu). The CGR/PtAu composite looked like a crumpled paper ball was synthesized from a colloidal mixture of GR and Pt-Au alloy nanoparticles with aerosol spray drying. The CGR/PtAu had a high specific surface area and electrochemical surface area of up to 238 and 325 m²/g (Pt), respectively. The electrocatalytic applications of the CGR/PtAu were examined through methanol oxidation reactions. The CGR/PtAu prepared with a concentration of 0.1 wt% graphene oxide and a Pt/Au weight ratio of 3 had the highest electrocatalytic activity for methanol oxidation reactions compared with commercial Pt-carbon black and Pt-GR (Figure 1). The CGR/PtAu was also highly sensitive electrocatalytic activity in the methanol oxidation reaction compared with the flat-GR/Pt-Au. Furthermore, the electrocatalytic activity of the CGR/PtAu had the highest performance among the catalysts containing Pt, Au, and GR for the methanol oxidation reactions. The increased electrocatalytic activity is attributed to the high specific surface area of the CGR formation and the effective surface structure of the Pt-Au alloy nanoparticles. Thus, it is noted that the as-prepared 3D-GR/PtAu is a promising material for DMFC catalysts.

Keywords: electrocatalyst, crumpled graphene, platinum-gold alloy nanoparticles, direct methanol fuel cell, aerosol process..

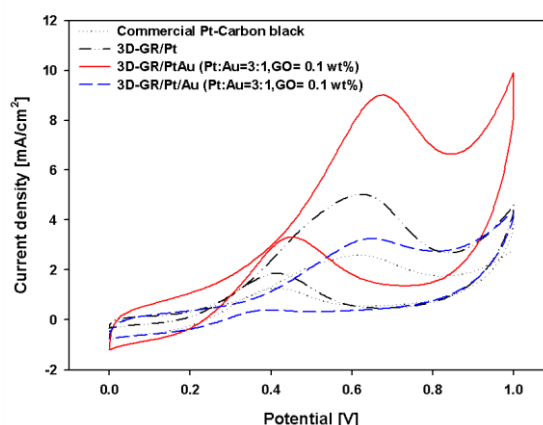


Figure 1: Figure illustrating cyclic voltammograms for methanol oxidation reaction catalyzed by CGR/PtAu and CGR/Pt/Au in the mixture solution of 0.05 M H₂SO₄ + 1 M CH₃OH within the potential range of 0 - 1.0 V.

References:

- Park, I., Lee, K., Cho, Y., Park, H., Sung, Y. (2008), Methanol electro-oxidation on carbon-supported and Pt-modified Au nanoparticles, *Catal. Today*, 132, 127-131.
- Zhang, S. Shao, Y., Liao, H., Liu, J. Aksay, I.A., Yin, G., Lin, Y. (2011), Graphene Decorated with PtAu Alloy Nanoparticles: Facile Synthesis and Promising Application for Formic Acid Oxidation, *Chem. Mater.*, 23, 1079-1081.
- Yang, G., Li, Y., Rana, R. K., Zhu, J., Pt-Au/nitrogen-doped graphene nanocomposites for enhanced electrochemical activities, *J. Mater. Chem. A*, 2013, 1, 1754-1762.

Graphene Transistor Monitoring Properties of Functional Oxides

Dongseok Suh,^{1,2,*}

¹ Center for Integrated Nanostructured Physics, Institute for Basic Science, Sungkyunkwan University, Suwon, Korea

² Department of Energy Science, Sungkyunkwan University, Suwon, Korea

Abstract:

By using the well-known charge transport phenomena of monolayer graphene in the field-effect transistor configuration, we have investigated the properties of various gate-oxide layers in contact with graphene, which include a defective silicon oxide, a ferroelectric single-crystal, and an ultra-high-k epitaxial thin-film.

For the graphene on a defective silicon oxide layer, two-terminal quantum Hall conductance and charge-trap memory behaviors were combined together without degrading each phenomena, resulting in the hysteretic quantum Hall conductance. In the case of $[\text{Pb}(\text{Mg}_{1/3}\text{Nb}_{2/3})\text{O}_3]_{1-x}[\text{PbTiO}_3]_x$ (PMN-PT) ferroelectric single-crystal, the direct variation of graphene's carrier density at the ferroelectric switching point, the systematic change from normal hysteresis to antihysteresis depending on the gate-voltage sweep range, and the polarization-induced charge-trapping behavior were simultaneously monitored from the graphene's conductance change. For the SrTiO_3 (STO) epitaxial-thin-film, the voltage-scaling due to its ultra-high-k properties was clearly observed in the graphene transistor, and the non-hysteretic quantum Hall transport phenomena enabled the estimation of STO's effective dielectric constant at low-temperatures. From these results, we proved that the graphene transistor can be used as a good probe monitoring the properties of functional oxides.

Keywords: graphene transistor, ferroelectric single-crystal, PMN-PT, ultra-high-k, epitaxial thin-film, SrTiO_3 , quantum Hall conductance

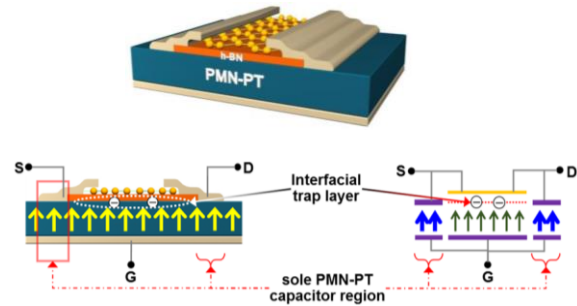


Figure 1: (Top) Illustration showing the shape of device, graphene/hexagonal-BN/ferroelectric single-crystal (PMN-PT) field-effect transistor. (Bottom) Schematic cross-sectional view and the corresponding symbolic expression including the interfacial trap layer and the sole PMN-PT capacitor region.

References:

1. Park, J., Kang, H., Kang, K. T., Yun, Y., Lee, Y. H., Choi, W. S., Suh, D. (2016), Voltage scaling of graphene device on SrTiO_3 epitaxial thin film, *Nano Lett.*, 16, 1754–1759.
2. Park, N., Kang, H., Park, J., Lee, Y., Yun, Y., Lee, J.-H., Lee, S.-G., Lee, Y. H., Suh, D. (2015), Ferroelectric single-crystal gated graphene/hexagonal-BN/ferroelectric field-effect transistor, *ACS Nano*, 9, 10729–10736.
3. Kang, H., Yun, Y., Park, J., Kim, J., Truong, T. K., Kim, J.-G., Park, N., Yun, H., Lee, S. W., Lee Y. H., Suh, D. (2015), Quantum Hall conductance of graphene combined with charge-trap memory operation", *Nanotechnology*, 26, 345202.

Infrared spectroscopy of closely aligned heterostructures of graphene and hexagonal boron nitride

D.S.L. Abergel,¹ and M. Mucha-Kruczyński.²

¹Nordita, KTH Royal Institute of Technology and Stockholm University, Roslagstullsbacken 23, SE-106 91 Stockholm, Sweden.

² Department of Physics, University of Bath, Claverton Down, BA2 3FL, United Kingdom.

Abstract: Graphene and hexagonal boron nitride (hBN) are both two-dimensional crystals with hexagonal lattice structure. Their lattice constants are very closely matched, so that when graphene is placed on top of hBN, a moiré pattern can form if the relative rotation angle between the two layers is small. An example of this is shown in Fig. 1. The moiré pattern can be described by an effective theory [1], but this theory contains parameters which are unknown *a priori*. We propose that optical absorption spectroscopy may be used as an experimental technique to determine the value of these parameters, and thus distinguish between various theoretical proposals that exist in the literature.

We compute the absorption spectra and describe the general features which are induced by the moiré potential [2]. Then, we show the dependence of the spectra on the doping for an almost completely full first valence miniband and extract meaningful information about the moiré characteristics which differentiates between the theoretical proposals [3]. An example is shown in Fig 2, where two different models produce qualitatively different behavior as the hole density is swept through n_0 , the density of a filled first hole band. Finally, we show that for bilayer graphene on hBN, comparing spectra for opposite signs of electric-field-induced interlayer asymmetry may provide additional information about the moiré parameters.

Keywords: Graphene, boron nitride, vertical heterostructures, optical spectroscopy, theory.

References:

- [1] J.R. Wallbank, A.A. Patel, M. Mucha-Kruczyński, A.K. Geim, and V.I. Fal'ko, Phys. Rev. B **87**, 245408 (2013).
- [2] D.S.L. Abergel, J.R. Wallbank, X. Chen, M. Mucha-Kruczyński, and V.I. Fal'ko, New J. Phys. **15**, 123009 (2013).
- [3] D. S. L. Abergel and M. Mucha-Kruczyński, Phys. Rev. B **92**, 115430 (2015).

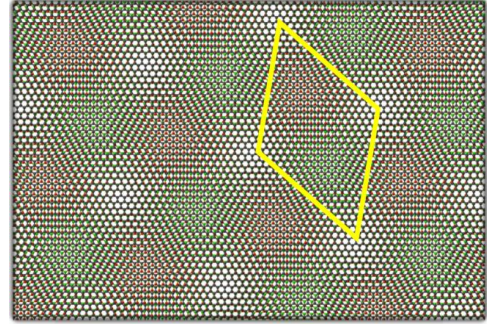


Figure 1: Example moiré pattern of graphene on top of hexagonal boron nitride. The yellow rhombus shows the moiré unit cell.

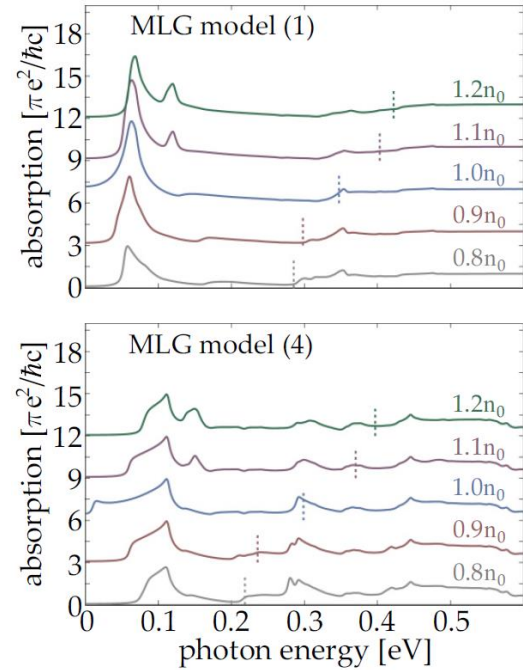


Figure 2: Absorption spectra for monolayer graphene on top of hexagonal boron nitride as a function of incident photon energy as the hole density in the graphene is swept through the first miniband. Two different models from the literature are compared.

Anisotropy of Unstrained Pristine Graphene

G. Shpenkov

Abstract:

In result of a profound analysis of the three-dimensional particular solutions of the general (“classical”) wave equation in spherical polar coordinates it was found that they contain information about the structure of matter and about such regularities in nature which were unknown earlier. In particular, from the solutions it follows that atoms are the wave formations. They have a quasi-spherical shell-nodal structure coincident with the nodal structure of standing waves formed in local volumes of the three-dimensional wave space-field. Each atom with $Z \geq 2$ represents one of the elementary molecules of the hydrogen atoms, to which we refer *proton*, *neutron* and *protium* (^1H). The wave shell-nodal atomic structure was verified by different ways. All they completely confirmed the reality of the found structure. Graphene gave us a unique possibility for the direct verification of the discovery. According to the modern data, the hexagonal lattice of graphene, a two-dimensional crystal (a giant macromolecule), has a six-fold axis of symmetry. Hence, the physical properties of graphene, in particular, electrical conductivity, must be isotropic in a plane perpendicular to this axis, in full agreement with the basic symmetry theory. It is considered as taken for granted. However, in accord with the shell-nodal structure, graphene is an anisotropic crystal having a two-fold axis of symmetry. Along the major axis of anisotropy there are empty polar nodes, which form the specific channel responsible for the so-called “ballistic” motion of charges. In this direction, graphene behaves like a metal; in the perpendicular direction graphene exhibits semiconducting properties. The fact that we do not see empty polar nodes (on electron microscope images) forming the ballistic channel does not quite mean that these nodes do not exist. Modern technological means are too imperfect at present to observe all peculiarities of the shell-nodal structure of atoms.

Laboratory tests have confirmed our prediction. The polar diagrams of conductivity of one-atom thick graphene layers, measured along a plane in all directions (Figures 1, 2), have the characteristic elliptical form, at all test samples that is inherent in anisotropic materials.

Keywords: wave equation solutions, atomic structure, graphene structure, conductivity anisotropy, bonds nature, ballistic channel.

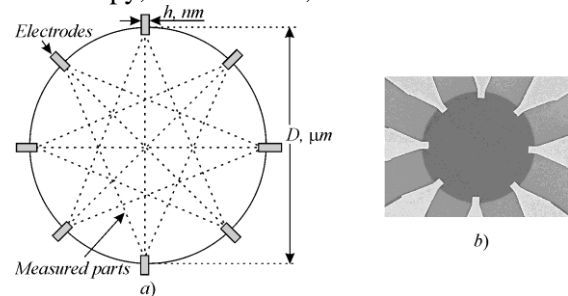


Figure 1: (a) A measurement scheme of one-atom-thick graphene plate of the round form. (b) An electron microscope image of one of the test samples.

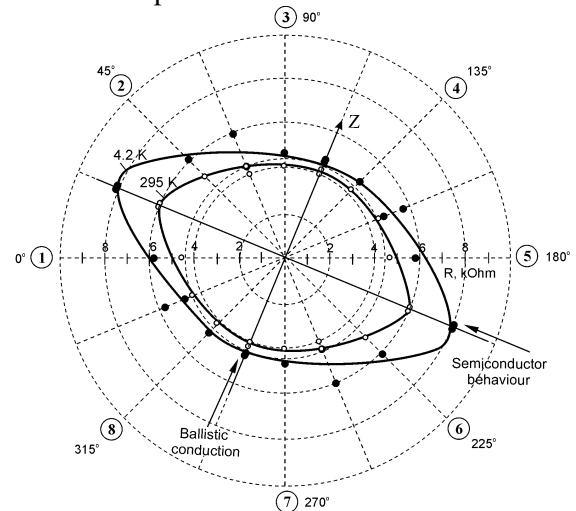


Figure 2: Anisotropy of resistance in a plane of unstrained pristine graphene at the two temperatures; $D=10 \mu\text{m}$, $h=580 \text{ nm}$.

Reference:

Shpenkov, G., Three-dimensional solutions of the Helmholtz equation, Gottingen, 23DGK, (2015); <http://shpenkov.janmax.com/Talk-Gottingen2015.Eng.pdf>

Temperature dependent fracture of defected graphene sheets: a Molecular Dynamics study

S. Nasiri,^{1,*} M. Zaiser,¹

¹Friedrich-Alexander Universität Erlangen-Nürnberg, Department of Materials Science, Chair of Materials Simulation, Fürth, Germany

Abstract:

Pristine graphene is known as the strongest material in terms of its in-plane tensile strength – a property which makes it a candidate for novel structural applications on the nano scale. However defects are unavoidable during the synthesis and fabrication of graphene-based devices. In this Paper we investigate the effect of defects on the temperature-dependent rupture strength of graphene sheets, for two different types of defects, namely randomly distributed point defects (vacancies) and single extended defects (cracks). We first study the effect of different vacancy concentrations and crack sizes on the fracture strength of graphene sheets at various temperatures and interpret our results with reference to continuum fracture mechanics concepts which we generalize to account for discreteness of the atomic and defect structure.

Keywords: Graphene, Vacancies, Cracks, Temperature, Molecular Dynamics, Fracture Mechanics.

References:

1. Zdenek P., Bazant, B. H. Oh, (1983), Crack band theory for fracture of concrete, J Materials and structures, 16, 155-177
2. Alessandro Luigi Sellerio, Alessandro Taloni, Stefano Zapperi, (2015), Fracture size effects in nanoscale materials: the case of graphene, J Physic. Review. Applied 4, 024011.
3. M.A.N. Dewapriya, R.K.N.D Rajapakse, and A.S. Phani (2014), Atomistic and continuum modeling of temperature dependent fracture of graphene. Int .J. Fracture ., 18, 199–212.

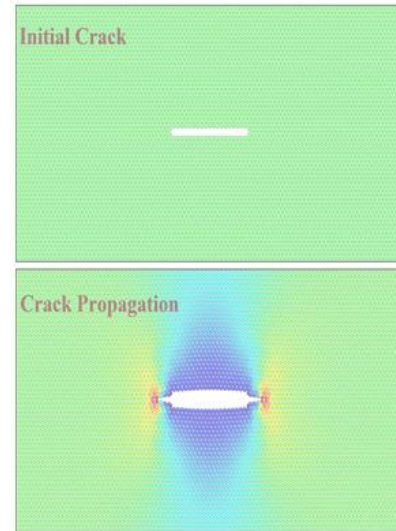


Figure 1: Crack Propagation of a central crack in a graphene sheet under tensile load from Molecular dynamic simulation. The simulated system consists of single layer, monocrystalline graphene sheets, composed of a variable number N of atoms: N varies from approximately 10×10^3 to 40×10^3 atoms. The sheets have an almost square shape lying on the XY coordinate plane and the crack length is one fifth the specimen width. Crack propagates perpendicular to loading direction along the crack tip because of intensive stress concentration on a nano-size tip.

Graphene: A Tunable Kerr Nonlinear Medium

Behrooz Semnani,^{1,2,*} Amir Hamed Majedi,^{1,2} Safieddin Safavi-Naeini,¹

¹Department of Electrical & Computer Engineering, University of Waterloo, Waterloo, ON, Canada

²Waterloo Institute for Nanotechnology, University of Waterloo, Waterloo, ON, Canada

Abstract:

Graphene is a monolayer of carbon atoms sitting in a hexagonal lattice. Owing to the special symmetries of the crystalline structure, the band structure of graphene differs substantially from the other condensed matter systems. The effective Hamiltonian describes quasirelativistic massless Dirac fermions. The Dirac fermions introduced by the low energy Hamiltonian are dominantly chiral [1]. Moreover, the band structure of graphene is scale-invariant in the low energy limit [2]. It has been shown that the chirality of the charged carrier leads to several unconventional transport properties such as minimum conductivity, Klein paradox and Zitterbewegung [1]. The impact of the chirality on the optical response of graphene has not been investigated so far.

We have shown that the chiral nature of the charged carriers in conjunction with the scale invariance of the band structure results in a strong nonlinear optical response. The time evolution of the quasiparticles in the presence of the electromagnetic field can be decomposed into the quasiclassical intraband transport and interband time evolution. Employing Semiconductor Bloch Equations (SBEs) [3] for graphene, we have decoupled the quasiclassical and quantum dynamics. Based on SBEs, the dynamics is governed by a classical theory with quantum fluctuations superimposed. The principle advantage of SBEs is twofold: first they provide a convenient mathematical scheme leading to analytical expressions for arbitrary order of interaction. Secondly, SBEs encode the topological properties of band structure in an effective dipole appearing in the equations. As a matter of fact, the geometrical properties of the band structures affect the intraband contribution of the optical response and interband transitions are influenced by the special topological aspects of the band.

We exploit the band renormalizations such as spin-orbit coupling to calculate the nonlinear optical response. We have shown that the nonlinear response function can be expressed as the summation of three different contributions: pure-intraband, pure-interband and combination of the both.

It has been demonstrated that the Kerr nonlinearity of graphene can be tuned and enhanced by applying a gate voltage. A strong Kerr nonlinearity much higher than the other known semiconductors can be achieved in monolayer and chiral multilayer graphene.

Keywords: graphene, nonlinear optics, Kerr nonlinearity, chiral symmetry.

References:

1. A. H. Castro Neto, F. Guinea and N. M. R. Peres, K. S. Novoselov and A. K. Geim, The electronic properties of graphene, *Rev. Mod. Phys.*, Vol 81, pp.109-162 (2009).
2. Bácsi, Ádám and A. Virosztek, Low-frequency optical conductivity in graphene and in other scale-invariant two-band systems, in *Phys. Rev. B*, pp.125425 (2013).
3. C. Aversa, and J.E. Sipe, Nonlinear optical susceptibilities of semiconductors: Results with a length-gauge analysis, in *Phys. Rev. B*, pp.14636–14645 (1995).

Substantial improvement of graphene-enhanced raman scattering through strain engineering of graphene

G. Dobrik, P. Nemes-Incze, L.P. Biró, L. Tapasztó*

Hugarian Academy of Sciences, Centre For Energy Research, Institute for Technical Physics and Materials Science, Budapest, Hungary

Abstract:

Surface Enhanced Raman Scattering (SERS) is a technique of high practical relevance for the detection of various molecules in small concentrations. However, our understanding of the underlying mechanism is far from complete. Two main processes are thought to contribute to the enhancement effect, the electromagnetic mechanism mediated by surface plasmons, and the chemical mechanism enabled by charge transfer. Metallic substrates with nanometer scale roughness have proven the most efficient SERS surfaces so far, mainly attributed to the electromagnetic enhancement. However, there are clear advantages in using other, more inert substrates, such as graphene, to replace the metal nanoparticles that display a low biocompatibility and can induce a substantial fluorescent background. It has been demonstrated earlier¹ that graphene can enhance the Raman signal of various molecules deposited on its surface. However, the enhancement factors observed were much lower than typical for rough metallic SERS substrates, that limits its applicability. Here we show that by strain engineering graphene, one can substantially enhance the efficiency of graphene as SERS substrate, allowing the detection of molecules at much lower concentrations as compared to as-exfoliated graphene flakes. The possible mechanism of the increased Raman scattering enhancement will be discussed, shedding more light on the origin of graphene-enhanced Raman scattering process.

Keywords: graphene, Raman spectroscopy, Surface Enhanced Raman Scattering, strain-engineering.

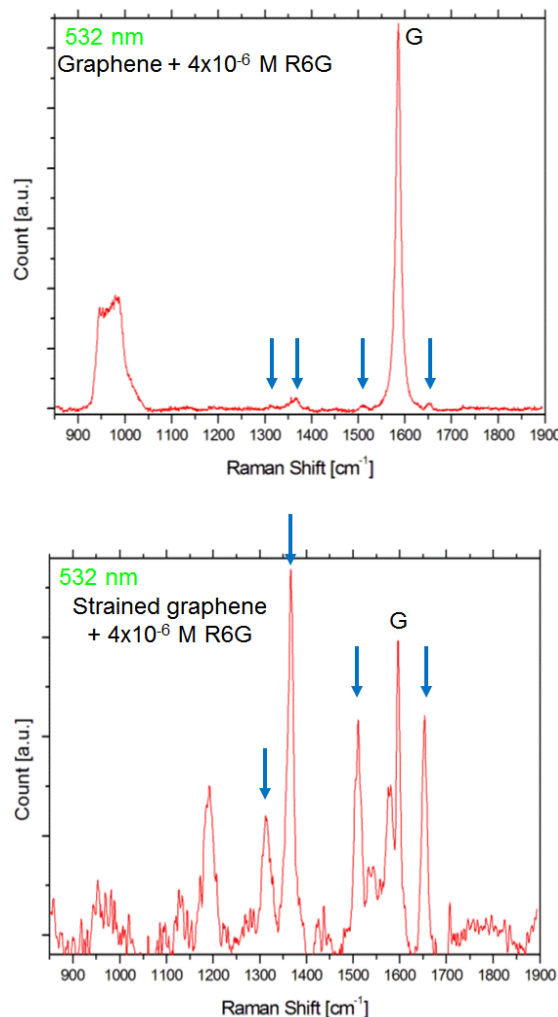


Figure 1: Raman spectra of Rhodamine 6G molecules on as-exfoliated (top) and strained (bottom) graphene flakes displaying a substantial enhancement of the SERS efficiency on the strained graphene substrates.

References:

- ¹ Huang, S. et al. (2015) Molecular selectivity of Graphene-enhanced Raman Scattering, *Nano Lett.*, 15, 2892-2901.

Evaluation of Graphene Suspensions

T. J. Nacken,¹ C. E. Halbig,² C. Damm,¹ J. Walter,¹ S. Eigler,² W. Peukert¹

¹University Erlangen-Nürnberg, Institute of Particle Technology, Germany.

²University Erlangen-Nürnberg, Department of Chemistry and Pharmacy, Joint Institute of Advanced Materials and Processes, Germany.

Abstract:

Graphene is one of the most desired materials to be taken to mass production in the new century. One promising production method is liquid phase exfoliation of graphite. Fast and careful product characterization methods are necessary for production process parameter studies. Well established methods for Graphene analytics, e.g. transmission electron microscope (TEM), Raman spectroscopy, atomic force microscopy (AFM) require deposition of the particles from the suspension to a substrate. Suitable methods for analyzing delaminated sheets directly in suspension are rare. Due to their anisotropic shape standard diagnostics as dynamic light scattering yield large deviations for lateral dimension and height (~40%). (Lotya et al.; 2013) Thus, to gain precise information on height and diameter of the flakes, very time consuming measurements, e.g. flakes counting in TEM or AFM is used. Though this combination leaves a third critical information unaddressed, potential in-plane defects that are created while the graphite feed is processed.

Within our work we can demonstrate, how statistical Raman spectroscopy (sRs) in combination with AFM is able to address both dimensions of the obtained flakes, while giving representative information of potential defects. (Nacken et al.; 2015) Further we report how graphene oxide can be used as reference material for individualized flakes in suspensions to be quantitatively evaluated for their lateral dimension by Analytical Ultracentrifugation (AUC). (Walter et al.; 2015; Halbig et al.; 2015) The combination of these techniques enables time efficient and/or highly accurate feedback cycles to further improve existing and design new production methods for high yield/quality graphene production.

Keywords: Graphene, Graphene oxide, statistical Raman spectroscopy, Analytical Ultracentrifugation.

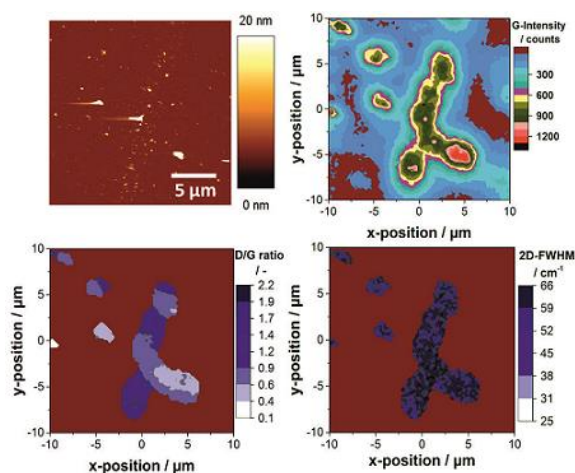


Figure 1: A representative AFM and Raman - Colocalization of a delaminated and coated graphene suspension. Upper left AFM image, upper right and bottom statistical Raman evaluation of the identical position.

References:

1. Lotya, M., Rakovich, A., Donegan, J. F., Coleman, J. N. (2013) Measuring the lateral size of liquid-exfoliated nanosheets with dynamic light scattering, *Nanotechn.*, 24, 265703 (6).
2. Nacken, T. J., Damm, C., Xing, H., Rüger, A., Peukert, W. (2015) Determination of quantitative structure-property and structure-process relationships for graphene production in water, *Nano Res.*, 8, 1865-1881.
3. Walter, J., Nacken, T. J., Damm, C., Thaseem, T., Eigler, S., Peukert, W. (2015) Determination of the Lateral Dimension of Graphene Oxide Nanosheets Using Analytical Ultracentrifugation, *Small*, 11, 814-825.
4. Halbig, C. E., Nacken, T. J., Walter, J., Damm, C., Peukert, W., Eigler, S. (2015) Quantitative investigation of the fragmentation process and defect density evolution of oxo-functionalized graphene due to ultrasonication and milling, *Carbon*, 96, 897-903.

Pt nanoparticles supported on rGO/SiC hybrid material as a cathode catalyst in DMFC

B. Ozdincer,^{1*} K. K. Maniam,¹ S. M. Holmes¹

¹School of Chemical Engineering & Analytical Science, The University of Manchester, Manchester, UK

Abstract:

Direct methanol fuel cells (DMFCs) have been considered as promising power sources for applications in portable devices. However, several challenging issues still prevent the commercialization of DMFCs such as methanol crossover, sluggish reaction kinetics and high manufacturing costs (Huang & Wang 2014). At present, platinum (Pt) based electrocatalysts are still the most commonly used electrocatalysts in DMFCs with their good catalytic properties. But the high cost and easy-poisoning of Pt catalysts limit their practical application in DMFCs. The use of supporting materials with high surface area, good stability and high electrical conductivity not only maximize the catalytic activity but also minimize the amount of catalyst (Q. Liu et al. 2014). In recent years, graphene has attracted significant attention as a catalyst support due to its large specific surface area, ultra high electrical conductivity and strong metal interaction. However, graphene nanosheets tend to aggregate because of the van der Waals force and π - π interactions. Attaching some other support materials between the sheets is an approach in order to decrease the aggregation of graphene sheets. In this context, hybrid support materials are being explored as alternative support for catalysts in DMFCs (M. Liu et al. 2014). Silicon carbide (SiC), a non-carbonaceous material, has been studied as an alternative support material due to its good mechanical properties, excellent thermal stability, low specific weight and high resistance towards oxidation (Jiang et al. 2014). The present study aims at the synthesis of Pt catalyst on reduced graphene oxide/silicon carbide (rGO/SiC) hybrid support and its application as a cathode catalyst in DMFCs. Pt/rGO-SiC catalysts will be prepared by chemical co-reduction method and characterized physically using SEM, XRD, BET and Raman spectroscopy. The electrochemically active surface area (ECSA) of the catalysts will be characterized by cyclic voltammetry (CV) studies.

The synthesized catalysts will be tested as a cathode catalyst in a single DMFC and the effect of the hybrid support on the fuel cell performance will be discussed in details.

Keywords: catalyst support, reduced graphene oxide, silicon carbide, fuel cell, DMFC, scanning electron microscopy (SEM), x-ray diffraction (XRD) and Brunauer – Emmett- Teller (BET)

References:

1. Huang, H. & Wang, X., 2014. Recent progress on carbon-based support materials for electrocatalysts of direct methanol fuel cells. *Journal of Materials Chemistry A*, 2, pp.6266–6291.
2. Jiang, L. et al., 2014. Pt loaded onto silicon carbide/porous carbon hybrids as an electrocatalyst in the methanol oxidation reaction. *RSC Adv.*, 4, pp.51272–51279.
3. Liu, M., Zhang, R. & Chen, W., 2014. Graphene-Supported Nanoelectrocatalysts for Fuel Cells: Synthesis, Properties, and Applications. *Chemical reviews*, 114(10), pp.5117–60.
4. Liu, Q. et al., 2014. A Review of Graphene Supported Electrocatalysts for Direct Methanol Fuel Cells. *Advanced Materials Research*, 1070-1072, pp.492–496.

Graphene based coatings against corrosion

Karanveer. S. Aneja^{1*}, Siva Bohm¹, A.S. Khanna¹, Mark Thompson²

¹Department of Metallurgical Engineering and Materials Science, Indian Institute of Technology Bombay, Powai, Mumbai 400076, India

²Talga Resources Ltd, Level 1, 2 Richardson Street, West Perth 6005 Australia

Abstract:

Corrosion has been a perennial issue of concern for the industrial sector. Commonly used anti-corrosive coatings suffer from high environmental impact, low availability, low performance or cost factors. Graphene, a two-dimensional hexagonally arranged array of carbon atoms, has been shown to be an effective alternative to traditional coating systems [1]. Graphene, with its superlative properties, upon functionalisation, can provide a conductive and near impermeable barrier coating. The current bottleneck in using graphene is the poor availability of low cost high quality graphene and its effective incorporation into coating systems. On overcoming these factors, protective coatings can prove to be a significant application for graphene in terms of volume consumption.

In this talk, various aspects involved in graphene based coatings for anticorrosion applications will be discussed. Graphene, produced from industrially scalable and cost effective routes, is functionalised to make it easily dispersible in resin matrix and to form a strong three-dimensional coating network with the substrate. The performance of functionalized graphene, both as a pretreatment primer and as an additive in polymer resins is evaluated using electrochemical techniques and ASTM tests. Further, studies conducted to establish the corrosion protection mechanism shall also be discussed.

Keywords: graphene, corrosion, functionalisation, electrochemical techniques, mechanistic studies



References:

K.S. Aneja, et.al. Graphene based anticorrosive coatings for Cr (VI) replacement. *Nanoscale*, 2015,7, 17879-17888

Impact of reduction degree of graphene oxide on the photocatalytic activity of graphene oxide/TiO₂ nanotubes

M. Hamandi¹, G. Berhault², C. Guillard², H. Kochkar^{1,3}

¹Université de Tunis El Manar, Faculté des Sciences de Tunis, Laboratoire de Chimie des Matériaux et Catalyse, 2092 El Manar Tunisia.

²Institut de Recherches sur la Catalyse et l'Environnement (IRCELYON) du CNRS- University of Lyon, Villeurbanne, 69100, France.

³Centre National de Recherches en Sciences des Matériaux (CNRSM), Laboratoire de Valorisation des Matériaux Utiles, BorjCedriaTechnopark, BP73, Soliman 8027 Tunisia.

Abstract:

Reduced graphene oxide–TiO₂ nanotubes (RGO–TiO₂) nanocomposites have been successfully synthesized in two steps: (i) TiO₂ nanotubes were obtained through a facile hydrothermal reaction with minor modification using commercial P25 as starting material, followed by calcining temperature at 400 °C for 2 h in air, (ii) GO was introduced onto TiO₂ nanotubes by wet impregnation. The reduction of graphene–TiO₂ nanotubes was performed under H₂ at different temperatures (200 and 300 °C). These nanocomposites prepared with different ratios of graphene oxide (GO) and reduction temperature, were characterized by means of transmission electron microscopy, X-ray diffraction (XRD), Raman spectroscopy, Fourier transform infrared spectroscopy (FTIR), X-ray photoelectron spectroscopy (XPS) and ultraviolet photoelectron spectroscopy (UPS). The photocatalytic activity of these nanocomposites was investigated in the photodegradation of formic acid under UV/A light irradiation. The influence of two important parameters namely: (i) the percentage of GO and (ii) the ratio RGO/Graphene on their photoactivity is highlighted. We demonstrated that the photocatalytic activity increases with GO loading with an optimum of 1 wt%. A partial reduction of 1 wt% GO–TiO₂ nanocomposites (200 °C) enhances the photocatalytic activity. However, a fully reduced GO to graphene (300 °C) has surprisingly no effect. This might be related to the surface properties of reduced graphene oxide arising from different reduction degree and its interaction with titanium dioxide as demonstrated by UPS and XPS analysis. Therefore, a higher charge carrier mobility in partially reduced graphene oxide is observed with respect to fully reduced one. During the test the RGO acts as an electron trap until it is totally reduced into graphene (Figure 1). The photocatalytic activity enhancement of RGO–TiO₂ nanocomposites is due to the transfer of electron-hole pairs between TiO₂ and

RGO, hence improving their separation and inhibiting the electron-hole recombination.

Keywords: graphene oxide, reduction, TiO₂ nanotube, photocatalysis

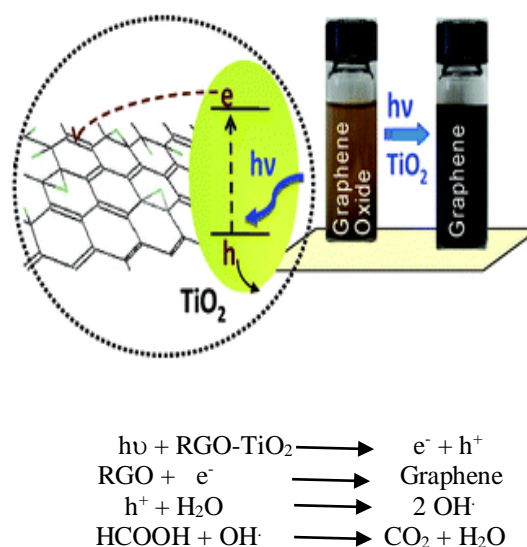


Figure 1: Figure illustrating the photocatalytic mechanism of degradation of organic pollutants by graphene oxide/TiO₂ nanotubes under UV light before and after reduction of the nanocomposite.

References:

1. Wang, J., Wang, M., Xiong, J., Lu, C. (2015) Enhanced photocatalytic activity of a TiO₂/graphene composite by improving the reduction degree of graphene, *New Carbon Materials*, 30, 357-363.
2. Williams, G., Seger, B., Kamat, P. (2008) TiO₂-Graphene Nanocomposites. UV-Assisted Photocatalytic Reduction of Graphene Oxide, *ACS NANO*, 2, 1487-1491.

Fabrication of Graphen oxides (GO) based rGO-TiO₂/Fe₃O₄ nanocomposites for the removal of Methylene Blue and Arsenic(III) from Wastewater

Poonam Benjwal^{1*}, Manish Kumar², Pankaj Chamoli¹ and Kamal K. Kar^{1,2}

¹Advanced Nanoengineering Materials laboratory, Materials Science Programme,
Indian Institute of Technology Kanpur, Kanpur-208016, India

²Advanced Nanoengineering Materials laboratory, Department of Mechanical Engineering,
Indian Institute of Technology Kanpur, Kanpur-208016, India

Abstract:

Graphene and graphene based materials have shown a lot of potential in the field of environmental pollutant remediation application, as they exhibit peculiar properties such as large surface area, high adsorption capacity and excellent electron transfer rate. Recently, graphene oxide (GO) has investigated extensively as it consists of various functional groups, which make it highly hydrophilic and water soluble. Due to this, GO can support or attach metal oxides particles. The incorporation of metal oxides on GO improves its properties by utilizing the advantage of graphene and it has also become a proficient way to prepare the environment friendly composite. In this work, metal oxide (TiO₂/Fe₃O₄) based binary/ternary composite of GO are synthesized for the removal of toxic methylene blue (MB) and As(III) from wastewater. The synthesized nanocomposites sustain the properties of each constituent like, TiO₂ nanoparticles degrades the pollutant, rGO provides the pathway to increase the surface area as well as suppress the recombination of charge carriers in TiO₂, and Fe₃O₄, being a magnetic material, increases the adsorption capabilities of rGO towards the heavy metal impurities. In addition incorporation of Fe₃O₄ also helps in magnetic separation of nanocomposite after the purification process. Here, a systematic study is provided for investigating the photocatalytic activity under UV and visible light irradiation for MB and adsorption of As(III) metal ions by analyzing their adsorption isotherm and adsorption kinetics models, respectively. The observed results demonstrate that GO based metal oxide nanocomposite can be effectively used in the removal of wastewater treatment.

Keywords: •, graphene oxide, adsorption, water pollution, photocatalysis, nanocomposite,

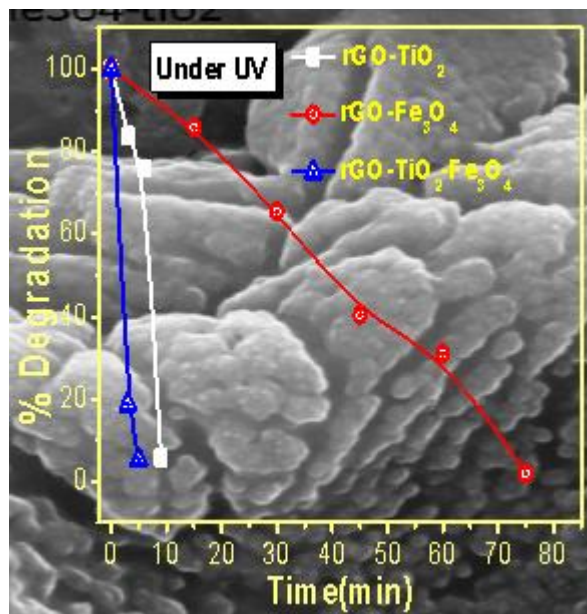


Figure 1: Figure showing the SEM image of ternary nanocomposite (rGO-TiO₂-Fe₃O₄) where the graph display the degradation of of methylene blue dye under UV. The observed result shows that ternary nanocomposite exhibits very high degradation efficiency towards the MB pollutant.

Graphene nanoplatelets biocompatibility is improved by surface adsorption of polymers

A. Pinto^{1,2,3}, A. Moreira⁴, F. Magalhães^{1,#}, I. Gonçalves^{2,3,#}

¹LEPABE, Faculty of Engineering of University of Porto, Porto, Portugal

²INEB - Instituto de Engenharia Biomédica, Universidade do Porto, Porto, Portugal

³i3S - Instituto de Investigação e Inovação em Saúde, Universidade do Porto, Portugal

⁴IFIMUP and IN – Institute of Nanoscience and Nanotechnology, Faculty of Sciences of University of Porto, Porto, Portugal

[#]authors contributed equally

Abstract

In view of the growing interest in using graphene-based materials (GBMs) in medical applications, it is relevant to evaluate their biocompatibility, which depends on their intrinsic physical-chemical properties [1]. This work studies graphene nanoplatelets (GNP), which have a reduced cost comparing with single layer graphene. Covalent and non-covalent surface modification with polymers is a strategy to overcome possible toxicity of GBMs. Covalent functionalization often implies using toxic solvents, while the procedures for non-covalent surface modification are simple and easily up-scalable. This work aims to study the effect of GNP non-covalent surface modification with biocompatible polymers.

Polymers and GNP-C (XG Sciences) were dispersed in water (1:1 ratio) by sonication, then centrifuged and supernatant discarded, removing excess polymer. Polymers tested were: PVA (poly(vinyl alcohol)), HEC (hydroxyethyl cellulose), PEG (poly(ethylene glycol)), PVP (poly(vinyl pyrrolidone)), chondroitin, glucosamine, and hyaluronic acid. SEM (Scanning electron microscopy), DLS (Dynamic Light Scattering), XPS (X-ray photoelectron spectroscopy), Raman spectroscopy, and TGA (Thermogravimetric analysis) were used for physico-chemical characterization and Hemolysis, Resazurin and LIVE/DEAD, TEM, and CM-H₂DCFH-DA to evaluate biocompatibility.

All materials were characterized, but results for GNP-C modified with PVA and HEC are highlighted, since they unveiled the best hemolysis results. DLS shows that surface adsorption of PVA and HEC increases GNP-C particle size from 0.5-2 to 25 and 8 μm , respectively. Agglomeration for GNP-C-PVA and HEC was observed by SEM (images not shown). XPS, Raman and TGA confirm the presence of 21 wt.% PVA and 15 wt.% HEC at GNP-C surface. Hemolysis induced by all GNP-polymers is below 1.7%, in concentrations up to 500 $\mu\text{g/mL}$ (3h). Resazurin assay shows that GNP-C is toxic at 24 h for concentrations above 20 $\mu\text{g mL}^{-1}$, however,

the cell metabolic activity recovers along time until 72 h. For GNP-C-HEC no improvements in biocompatibility are observed comparing to pristine GNP-C. GNP-C-PVA is non-toxic up to a concentration of 100 $\mu\text{g/mL}$ until 72h. LIVE/DEAD assay show that at concentrations of 72h, 20 and 50 $\mu\text{g/mL}$, GNP-C-PVA induce lower cell death than GNP-C. For GNP-C-HEC no differences were observed comparing with GNP-C. For a concentration of 50 $\mu\text{g/mL}$, ROS production is increased by 4.4 fold when GNP-C contacts cells, while only by 3.3 fold for GNP-C-PVA. For GNP-C-HEC, ROS production is increased by 5.2 fold. TEM images (not shown) show that GNP-C was almost completely exfoliated interacting with plasma membrane, being internalized without membrane damages, and in some cases is found interacting with mitochondria. GNP-C-PVA was more agglomerated, being found more often outside plasma membrane. Internalized GNP-C-HEC particles presented smaller length (0.5 - 1.5 μm) than GNP-C-PVA and GNP-C (0.5 - 3 μm), being often found spread in cytoplasm. GNP-C-HEC was also observed in contact in mitochondria.

Polymer adsorption decreases hemolysis of GNP-C. Small sized GNP-C enter cells inducing ROS production, and therefore, toxicity. The best result was obtained with PVA encapsulation of GNP-C, which increases particle size, decreasing internalization and avoiding ROS production. Thus, GNP-C-PVA has potential to be used safely for bioapplications at concentrations up to 50 $\mu\text{g/mL}$, while GNP-C can only be used at a maximum concentration of 20 $\mu\text{g/mL}$.

Keywords: Graphene; Polymers; Surface modification; Biocompatibility; Fibroblast.

References: 1. Pinto, A. *et al.*, (2013) “Graphene-based materials biocompatibility: a review”, *Colloids Surf B Biointerfaces*, 111, 188-202.

Functionalization of graphene field-effect transistor channel for ischemic stroke biomarker detection

P. D. Cabral,¹ E. Fernandes,¹ F. Cerqueira,² G. Machado Jr.,¹ J. Borme,¹ P. Alpuim^{1,2,*}

¹INL - International Iberian Nanotechnology Laboratory, 4715-330, Braga, Portugal.

²CFUM - Center of Physics of the University of Minho, 4710-057, Braga, Portugal.

Abstract:

Graphene extreme sensitivity to electric charges and fields in its vicinity, together with its high chemical stability, make it a strong candidate for biosensing applications. The electrolyte-gated field-effect transistor (EGFET) architecture provides the ideal sensing platform to explore those qualities, simultaneously providing the ability for integration and upscaling. However, graphene high sensitivity and chemical stability comes at the cost of a poor analyte selectivity. To overcome this drawback graphene needs to be functionalized for specific biomarkers. In this work we address that issue, using a linker to bind the biospecific recognition structure to the graphene surface.

Stroke is one major cause of death and long term disability. Recently a panel of biomarkers have been associated to the haemorrhagic transformation development in thrombolytic treatment. Two of those biomarkers are Matrix metalloproteinase-9 (MMP-9) and Neuroserpin (NS). In this work we study the detection of MMP-9 and NS on single layer graphene (SLG) surfaces obtained by transferring CVD graphene onto Si/SiO₂ substrates as a preliminary step for GFET channel functionalization. Our detection strategy, based on a sandwich assay, was performed on pyrene-functionalized graphene surfaces, where specific antibodies were immobilized to detect the respective targets captured by antibody-functionalized nanoparticles in solution (Fig.1a)). On the same substrate unspecific antibodies were also immobilized and worked as a negative control. Raman spectra and optical images were acquired to confirm the target binding. The results clearly show the difference between positive and negative control samples. Whereas in the positive sample (Fig.1b)) the Raman spectrum shows a double peak located at ~2900-3000 cm⁻¹ superimposed to the typical SLG spectrum, attributable to the captured target, the spectrum of the negative control sample only displays the SLG Raman spectrum (with prominent D, G and 2D peaks). A semi quantitative analysis of the optical image allows to estimate the surface coverage density over the graphene surface: 99.4% of coverage using the positive sample against 15.0% when using the

negative sample (inset images b) and c) respectively).

Keywords: graphene, field-effect transistor, functionalization, biomarkers, stroke.

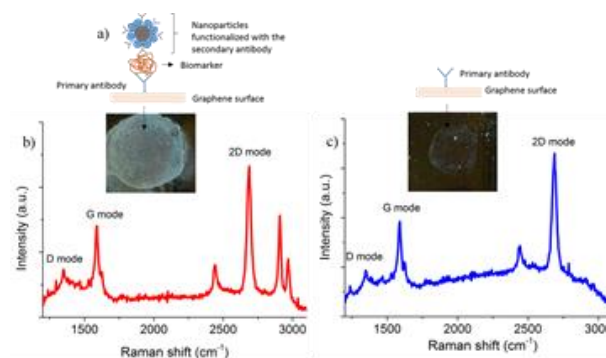


Figure 1: (a) Scheme of the detection strategy; Raman spectra and optical images of (b) specific detection and (c) negative control

References:

- Vieira, N.C.S., et al. (2016) Graphene field-effect transistor array with integrated electrolytic gates scaled to 200 mm, J. Phys.: Condens. Matter, in press (<http://arxiv.org/abs/1601.01491>)
- Yepes, M. et al. (2000) Neuroserpin reduces cerebral infarct volume and protects neurons from ischemia-induced apoptosis, Blood 96(2), 569-576
- Rodríguez-González, R. et al (2011) Association between neuroserpin and molecular markers of brain damage in patients with acute ischemic stroke, J. Transl. Med. 9:58

A Novel SPR biosensor chip with GrapheneOxide Linking Layer

Yu.V. Stebunov^{1,*}, O.A. Aftenieva¹, A.V. Arsenin¹, V.S. Volkov^{1,2}

¹ Moscow Institute of Physics and Technology, Laboratory of Nanooptics and Plasmonics, Dolgoprudny, Russian Federation

² University of Southern Denmark, Institute of Technology and Innovation, Odense, Denmark

Abstract:

Graphene and graphene oxide are opening up many new opportunities for biosensing applications. The hexagonal lattice structure of graphene and its derivatives allows its interaction with a wide range of biological substances via pi-stacking. In addition, graphene oxide possesses different oxygen-containing functional groups for the covalent immobilization of biomolecules. Moreover, reduction of graphene oxide can finely tune chemical, electrical and optical properties of carbon material for specific biosensing applications. The major advantage of graphene and its derivatives for biosensing applications is the extremely high surface area of different structures made from these materials, which provides high immobilization efficiency for a wide range of biologically significant substances such as DNAs, RNAs, proteins, including antibodies and membrane proteins, viruses, and bacteria. Here, we describe a novel type of graphene oxide linking layer for highly sensitive biosensing based on surface plasmon resonance (SPR), which has become an indispensable tool for scientific research and drug development [1]. During the last three decades, researchers have used only two technologies of linking layers for SPR biosensors, which are based on self-assembled monolayers of thiol molecules and on hydrogel layers. Using graphene and its derivatives, we developed biosensor chips for existing commercial biosensors, whose sensitivity is higher than for commercial sensor chips available on the market [2] (Fig. 1). Modification of carboxyl groups to N-hydroxysuccinimide esters in the flow cell of SPR biosensor demonstrated that the number of carboxyl groups, which can be used for molecule immobilization, is more than 20 times higher in the graphene oxide linking layer than in the linking layer of commercial hydrogel-based sensor chip. In addition, the graphene oxide sensor chip was demonstrated to be 3 times more sensitive comparing to the commercial hydrogel chips when using in the standard biosensing protocol based on streptavidin-biotin interaction with streptavidin immobilized on the GO surface via

pi-stacking. In conclusion, SPR biosensor chips based on graphene and its derivatives have higher sensitivity comparing to commercially available chips based on hydrogels. This will enable us to investigate interactions of protein targets with small ligands and will broaden and accelerate academic and pharmaceutical research.

Keywords: graphene, graphene oxide, biosensing, surface plasmon resonance, biosensor chips.



Figure 1: Biosensor chips based on monolayer graphene, graphene oxide, and carboxyl graphene linking layers designed for use with a commercial SPR instrument.

References:

1. Stebunov, Yu.V., Aftenieva, O.A., Arsenin, A.V., and Volkov, V.S. (2015), Highly sensitive and selective sensor chips with graphene-oxide linking layer. *ACS Applied Materials and Interfaces.*, 7(39): 21727–21734.
2. A.V. Arsenin, Yu.V. Stebunov. RU Patent Application No. 2527699 (Feb 2013); US Patent Application No. 20150301039 (Oct 2015).

Heartbeat resistive sensor based on graphene nanobelt thin films

A. Alaferdov^{a,b}, R. Savu^a, S. Rackauskas^a, T. Rackauskas^a, E. Joanni^c, S. A. Moshkalev^{a*}

^a UNICAMP, Center for Semiconductor Components, Campinas, 13083-870, Brazil

^b Lobachevsky State University of Nizhni Novgorod, Nizhni Novgorod, 603950, Russia

^c Center for Information Technology Renato Archer, Campinas, 13069-901, Brazil

e-mail: stanisla@unicamp.br

Abstract:

Multilayer graphene (MLG) has found numerous applications in different areas, including bio-medical technologies and nano-electronics. In these applications, individual MLG platelets or different kinds of networks or films based on MLG can be employed. To monitor activities of the human body such as muscle contraction, breathing and heart beating, the skin-inspired devices based on graphene or graphene like materials are increasingly being used [1,2].

In this work we demonstrate a new highly sensitive flexible heartbeat sensor based on a specific type of MLG – graphene nanobelts (GNBs), arranged in a form of thin conductive films. The principal difference between conventional MLG flakes and GNB is the aspect ratio (length/width). In the GNB case it can reach 50, whereas for MLG its typical value is 5 -10. Nanobelts, obtained from Nacional de Grafite Ltd, Brazil, are 3-30nm thick, 1-5 μ m wide and up to 50-100 μ m long (Fig. 1a).

GNB-films were fabricated from GNB suspensions in N-methylpyrrolidone using modified Langmuir-Blodgett (LB) technique [3]. Pludimethylsilaxane (PDMS) with thickness of 250 μ m was used as a flexible substrate for this sensor (with lateral dimensions of 25 mm x 15 mm). For GNB film deposition the surface of a PDMS-substrate was activated by capacitively coupled O₂-plasma (300W, 50 mTorr, 10 min) to make the surface hydrophilic that is required for LB-deposition. Further, metallic Ti/Au electrodes (50nm/200nm thick, respectively and 5 mm wide) were sputter deposited onto the ends of the film using a shadow mask. High electrical conductivity (down to a $\sim 10\Omega/\text{sq.}$) of the films was obtained, due to high degree of percolation between nanobelts. Then, the sensitive area of GNB-sensor was covered by a top PDMS layer. Next, macrocontact wires were fixed on Ti/Au-electrodes using silver paste. For tests, the fabricated sensors were fixed at different places on carotid artery on the neck or wrist. Clearly distinguishable heartbeat signals were obtained, being possible to determine the shape and frequency of the pulses (Fig. 1b).

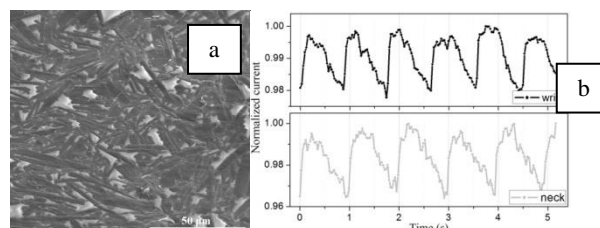


Figure 1: a) SEM image of GNB-film on PDMS substrate; b) Response characteristics of GNB-heartbeat sensor performed on different parts of a human body (top: wrist, bottom: neck).

The response of the sensor, determined as $(\Delta I/I_0) \cdot 100\%$, where ΔI – the current changes due the blood vessel pulsations, I_0 – the initial current passing through the sensor, is in the range of 3-6 %. Low energy consumption of the sensor (about 10 μ W at 0.5 V operating voltage) and good sensitivity makes this sensor very promising compared with similar devices based on other principles [1,2].

Finally, the mechanism responsible for sensing of blood pressure variation in the sensor is likely to be related to changes in resistance of contacts between individual nanobelts in the film during bending (or strain) of the sensor substrate as the skin surface curvature changes during blood vessels pulsation.

Keywords: graphene nanobelts, thin films, heartbeat sensor

References:

- [1] S.M. Lee, H.J. Byeon, J.H. Lee, D.H. Baek, K.H. Lee, J.S. Hong, S.-H. Lee, Scientific Reports 4 (2014) 6074.
- [2] S. Jung, J.H. Kim, J. Kim, S. Choi, J. Lee, I. Park, T. Hyeon, D. Kim, Advanced Materials 26 (2014) 4825
- [3] A.V. Alaferdov, S.M. Balashov, M.A. Canesqui, S. Parada, Y.A. Danilov, S.A. Moshkalev, Bulletin of the Russian Academy of Sciences: Physics 78 (2014) 1357.

Title:

The potential of graphene based active components in silicon photonic systems

Daniel Schall, and Daniel Neumaier

Affiliation:

AMO GmbH, Otto-Blumenthal-Strasse 25, 52074 Aachen, Germany

The on-chip integration of different optical components is expected to become the next paradigm shift needed for increasing the performance of optical communication systems. As for electronic devices also for photonic devices silicon will be an excellent platform, providing well-developed high volume production capabilities. Especially for guiding and routing infrared light, silicon is already a perfect material because of its low light interaction and high refractive index. However, because of this low light-interaction the heterointegration of other materials is needed to realize key active components like modulators, phase shifters and photodetectors. Graphene offers high carrier mobility, broadband and electrical tune-able light interaction in combination with the possibility to transfer graphene on nearly any substrate. This offers an excellent opportunity for graphene to enter silicon technology by adding the missing active functionalities on a silicon photonic platform.

In this talk I will discuss our latest results on graphene based photodetectors, electro-optical modulators and phase shifters integrated on silicon waveguides and I will provide an outline on future challenges. The key parameters of these devices will be assessed and compared with competing technologies.

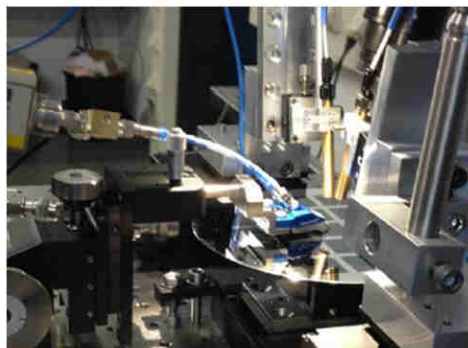


Figure 1. On-wafer high-frequency electro-optical characterisation of graphene based electro-optical devices on a silicon photonic platform.

References

- [1] D. Schall, et al. 50 GBit/s photodetectors based on wafer-scale graphene for integrated silicon photonic communication systems *ACS Photonics* 1, 781 (2014).
- [2] M. Mohsin, D. Schall, M. Otto, A. Noculak, D. Neumaier, and H. Kurz, Graphene based low insertion loss electro-absorption modulator on SOI waveguide. *Optics Express*. 22, 15292 (2014).
- [3] D. Schall, M. Mohsin, A. A. Sagade, M. Otto, B. Chmielak, S. Suckow, A. L. Giesecke, D. Neumaier, and H. Kurz, Infrared transparent graphene heater for silicon photonic integrated circuits. *Optics Express* 24, 7871-7878 (2016)

Few-Layer Graphene Langmuir Nanofilm Decorated by Palladium Nanoparticles for NO₂ and H₂ Gas Sensing

D. Kostiuk¹, S. Luby¹, M. Demydenko¹, Y. Halahovets¹, P. Siffalovic¹, K. Vegso¹, J. Ivanco¹,
M. Jergel¹, M. Kotlar², R. Redhammer², E. Majkova^{1*}

¹Institute of Physics, Slovak Academy of Sciences, Bratislava, Slovakia

²Slovak University of Technology, Bratislava, Slovakia

Abstract:

The high surface-to-volume ratio of graphene stimulated its application in high sensitive chemical gas sensors. It was demonstrated that their sensitivity could be enhanced with graphene decorated by metallic nanoparticles, e.g. Pd or Pt. In this work we present the NO₂ and H₂ gas sensing properties of the few-layer graphene (FLG) Langmuir nanofilm decorated by Pd nanoparticles. The graphene nanosheets were deposited onto SiO₂(500 nm)/Si substrates by a modified Langmuir-Schaeffer technique allowing to cover uniformly large area substrates. A solution of FLG in 1-methyl-2-pyrrolidone was obtained by a mild sonication of the expanded milled graphite followed by centrifugation at 10⁴ g. The FLG films were characterized by AFM, XRD, and Raman spectroscopy. Average FLG nanosheet thickness and lateral dimension are 5 nm and 300 nm, respectively. From the intensity of D vs. G Raman band relatively low density of defects in our samples is assumed. During the subsequent vacuum annealing of the FLG nanofilm the initial resistance of FLG dropped from 2 M Ω to the final value of 10 k Ω at room temperature. Repeated heating cycles of FLG nanofilm revealed its semiconducting character. The FLG nanofilm was decorated by colloidal Pd nanoparticles (6–7 nm) by spin-coating. SEM analysis confirmed uniform distribution of Pd nanoparticles over the FLG nanofilm, the nanoparticles are preferentially located at the edges of individual nanosheets. The gas sensing properties were tested in the mixtures of dry air with 6 ppm NO₂, 10000 and 1000 ppm H₂ from room temperature up to 250 °C. The response of FLG with Pd decoration is of p-type for all mixtures. The gas response of 22% ($\Delta R/R_a$ sensor resistance change over resistance in air) was observed for the exposition to 6 ppm NO₂ at room temperature (Fig. 1). The Pd decoration increased the NO₂ sensitivity approximately twice. With increasing temperature the sensitivity of the gas sensor decreased significantly. For 10000 ppm and 1000 ppm of

H₂ the gas response at room temperature of 13 and 10% response was found. The maximum sensitivity of 27% was achieved at 70° C. After 6 months storage of the device in air the best response towards NO₂ decreased only from 22 % to 20 %.

The sensing properties of our device are comparable with those of other types of graphene sensors and nanoparticle based sensors of transition metal oxides (Capone *et al.* 2014).

Keywords: few-layered graphene, Langmuir-Schaeffer technique, palladium decoration, NO₂ and H₂ gas sensing, long-term stability.

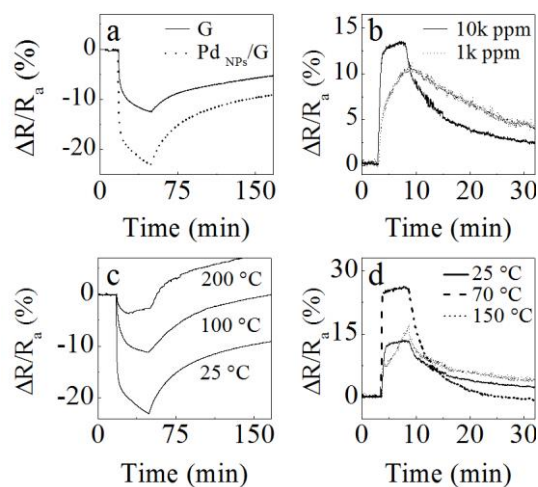


Figure 1: Response to NO₂ (a) and H₂ (b) gas mixture for Pd decorated FLG sensors at room temperature and voltage of 2 V. Effect of the temperature on the NO₂ and H₂ sensitivity is shown in (c) and (d), respectively.

References:

Capone, S., et. al, (2014), Fe₃O₄/γ-Fe₂O₃ nanoparticle multilayers deposited by Langmuir-Blodgett technique for gas sensing, *Langmuir*, 30, 1190 – 1197.

EGF 2016 Session IV
Graphene and 2D Materials
applications

Radionuclide Therapy with Neutron-Activated Graphen Oxide Nanoplatelets

J Kim,¹ M. Jay,^{1*}

¹Division of Molecular Pharmaceutics, UNC Eshelman School of Pharmacy
University of North Carolina, Chapel Hill, NC USA

Abstract:

Radiation therapy is a standard of care for 60-70% of cancer patients. For the purpose of achieving targeted systemic radionuclide delivery with minimum handling of radioactive materials, we investigated the use of nanocarriers for delivering radionuclides to targeted tumors. Utilizing a neutron-activation strategy, a stable isotope (^{165}Ho) was loaded into a nanocarrier and subsequently irradiated in a nuclear reactor to produce a nanocarrier with a radioactive isotope (^{166}Ho). Some limitations of this strategy are that heat is generated during the neutron-activation process and the most resistant nanocarriers are dense materials that negatively impact their biodistribution. To overcome these issues, we are investigating the use of graphene oxide nanoplatelets (GONs) as carriers of neutron-activatable isotopes due to their low density, high metal adsorption capacity, heat resistance and low toxicity profile. GONs were successfully synthesized from pure graphite which confirmed by AFM and FTIR. GONs were PEGylated for improving colloidal stability and biocompatibility. The PEGylated GONs were 62.09 nm in diameter, 12.98 nm in thickness and monodisperse. 8.38% holmium (w/w) were loaded into GONs by simple physical adsorption. As a preliminary test of stability under the neutron-activation, GONs were irradiated for one hour in a nuclear reactor (thermal neutron flux: 5.5×10^{12} neutrons/cm²*s). These particles retained their structural integrity and did not leach any holmium following neutron irradiation. Non-radioactive holmium-loaded GONs did not exhibit cytotoxicity in a human ovarian cancer cell.

Keywords: neutron activation, nanocarriers, graphine oxide nanoplatelets, systemic radiation therapy, holmium

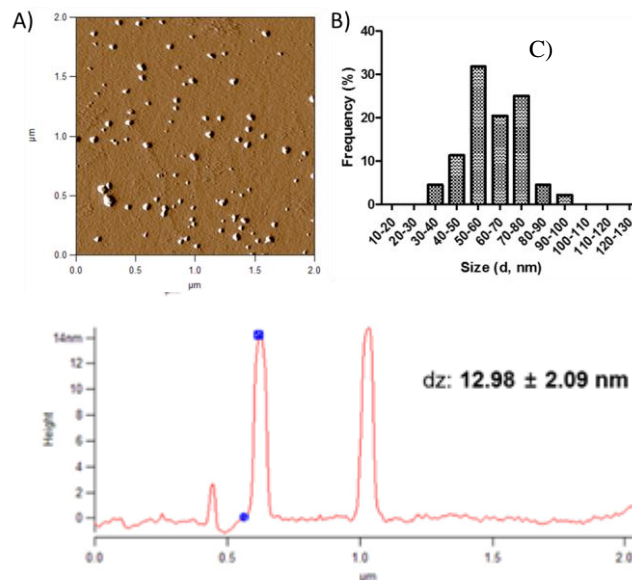


Figure 1: A) Atomic force microscopy (AFM) topological image, B) size distribution and C) thickness measurement of GONs-PEG containing stable ^{165}Ho .

References:

1. Georgakilas, A. G. (2013). Role of oxidatively-induced DNA damage and inflammation in radiation long term effects and carcinogenesis. *J Solid Tumors*, 3, 1-4.
2. Di Pasqua, A. J., Yuan H., Chung Y., Kim J.K., Huckle J.E., Li C., Sadgrove M., Tran T.H., Jay M., Lu X. (2013). Neutron-activatable holmium-containing mesoporous silica nanoparticles as a potential radionuclide therapeutic agent for ovarian cancer. *J Nucl Med.*, 54, 111-116.

Thixotropic Properties of Graphene Oxide/Hydrogel for 3D Bioprinting

H. Li and L. Li*

Nanyang Technological University, School of Mechanical and Aerospace Engineering, Singapore

Abstract:

Hydrogels have attracted great attention as biomaterials for printing three dimensional scaffolds, tissues, or even organs. However the relations between rheological properties of hydrogels and 3D printability have not been systematically studied. In this study, alginate-based hydrogels were used as a printing material for an extrusion-based printer and graphene oxide (GO) was added in order to improve thixotropic properties and mechanical strength of the hydrogel. The effect of graphene oxide on viscosity, shear thinning, viscosity recovery, quality of printing was studied and discussed. We proposed the measurable parameters that quantify the quality of printing.

As shown in the figure below, the alginate/Ca²⁺ hydrogels exhibited the thixotropic behavior and the viscosity could recover upto 75%. With adding a small amount of GO, viscosity of the hydrogel increased and could recover more than 90% after the high shear rate was removed.

Keywords: hydrogel, printability, rheology, 3D printing, graphene oxide, thixotropy

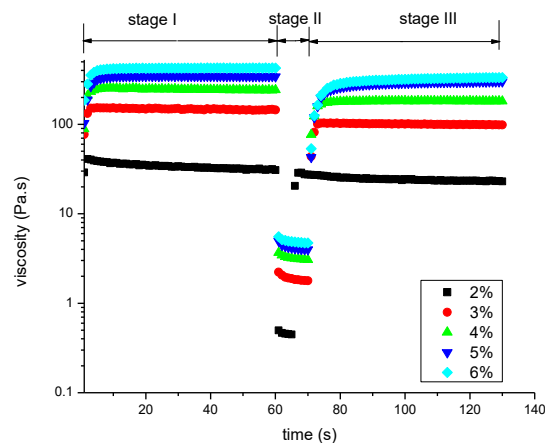


Figure 1: Recovery of viscosity for alginate/Ca²⁺ hydrogels over a range of alginate concentrations (2 wt% to 6 wt%).

References:

1. S. Liu, H. Li, B. Tang, S. Bi, L. Li, Scaling Law and Microstructure of Alginate Hydrogels, *Carbohydrate Polymers*, 135, 101–109 (2016).
2. H. A. Barnes, Thixotropy—a Review, *Journal of Non-Newtonian Fluid Mechanics*, 70, 1-33 (1997).
3. M. Ionita, M. A. Pandeale, H. Iovu, Sodium alginate/graphene oxide composite films with enhanced thermal and mechanical properties, *Carbohydrate Polymers* 94, 339-44 (2013).

Graphene for transparent electrodes and optical sensing

V.Pruneri^{1,2}

¹ ICFO-Institut de Ciències Fotoniques, The Barcelona Institute of Science and Technology, 08860 Castelldefels, Spain

² ICREA-Institució Catalana de Recerca i Estudis Avançats, 0810 Barcelona, Spain

Abstract:

It is known that Cu and Ni foils chemical vapor deposition (CVD) of graphene. After the deposition, transfer is needed to obtain the graphene layer on the chosen substrate. Direct deposition of graphene on substrates would thus avoid costly, time consuming and defective transfer techniques.

We used ultrathin films of Ni, with thickness ranging from 5 to 50 nm, as a catalytic surface on glass to seed and promote CVD of graphene. When a critical temperature (>700 °C) was reached, Ni films retracted and holes formed that are open to the glass surface, where graphene deposited. As the temperature raised, dewetting continued leading to formation of metal nanoparticles and large graphene surface coverage. After CVD, the residual Ni could be etched away and the glass substrate with graphene regained maximum transparency ($>90\%$).

Such deposition approach is very valuable to scale graphene covered substrates for optoelectronic applications. In the talk we will present results on transparent electrodes and photodetectors. More specifically, first we will show how graphene can be combined with silver nanowires to obtain a transparent electrode which has performances similar to widely used indium tin oxide (ITO). Second, how the combination with materials possessing spontaneous polarizations can lead to a platform for light sensing.

Keywords: graphene deposition, transparent electrodes, optical sensing.

Ballistic regimes in hBN-encapsulated graphene devices

John Wallbank and **Vladimir Falko**

National Graphene Institute, the University of Manchester

Abstract:

The talk will review the extremes electronic properties of graphene (G) encapsulated between layers of hexagonal boron nitride (hBN) and device concepts enabled by the high quality of this material. Encapsulation in hBN enables us to achieve a micron-length collision-less propagation of electrons in graphene, whereas technology of making low-resistance edge-contacts with normal and superconducting opens ways to manufacture ballistic electronic devices: electronic lenses and focusing beam splitters, as well as superconducting proximity effect transistors and interferometers. Moreover, electrostatic gating of hBN-G-hBN structures permits to open a large and spatially modulated band gap in bilayer graphene, hence offering new routes towards creating quantum wires, dots, and their various circuits. We shall discuss vertical tunnelling in hBN-G-hBN-G-hBN tunnelling field effect transistors with highly aligned graphene electrodes, where we were able to show resonance tunnelling of ballistic electrons.

We shall also discuss extreme physics realised in the highly aligned G-hBN heterostructures, where the long mean free path of carriers enables one to observe the formation of minibands due moiré superlattice determined by the incommensurability of G and hBN crystals, which in strong magnetic field takes the extreme form of a fractal spectrum of Brown-Zak magnetic minibands (also known as Hofstadter's butterfly).

Optoelectronics with atomically thin materials

Thomas Mueller

Vienna University of Technology, Institute of Photonics, Vienna, Austria

Abstract:

Two-dimensional (2D) atomic crystals are currently receiving a lot of attention for applications in (opto-)electronics. In this talk I will review our research activities on photovoltaic energy conversion, photon detection and light emission in these materials. In particular, I will present monolayer p-n junctions, formed by electrostatic doping using a pair of split gate electrodes and MoS₂/WSe₂ van der Waals heterojunctions. Upon optical illumination, conversion of light into electrical energy occurs in both types of devices.

I will present measurements of the electrical characteristics, the photovoltaic properties, and ultrafast measurements of the carrier dynamics.

In atomically thin field effect transistors, we identify photovoltaic and photoconductive effects, which both show strong photoconductive gain. In the second part of my talk, I will discuss studies of ultrafast photocurrent generation in graphene and applications in optical communications. We envision that the efficient photon conversion, combined with the advantages of 2D materials, such as flexibility, high mechanical stability and low costs of production, could lead to new optoelectronic technologies.

Keywords: graphene, transition metal dichalcogenides, optoelectronics

Nonlinear Electrodynamics and Optics of Graphene

S. A. Mikhailov

Institute of Physics, University of Augsburg, Augsburg, Germany

Abstract:

The nonlinear electrodynamic and optical properties of graphene currently attract much attention and continuously growing interest. It was theoretically predicted [1] that the linear energy dispersion of graphene electrons should lead to a strongly nonlinear electrodynamic response of this material. This prediction was experimentally confirmed, both at microwave and optical frequencies. The nonlinear parameters of graphene, such as the effective third-order nonlinear susceptibility $\chi^{(3)}$, were found to be orders of magnitude larger than in many nonlinear materials.

In this talk our recent results on the theory of nonlinear electrodynamic and optical effects in graphene will be presented. Among them:

1. Development of a quantum theory of the third-order nonlinear effects in graphene [2]. A third-order non-linear response of an isolated graphene layer to a normally incident electromagnetic radiation with an arbitrary time dependence is considered. An analytical solution for the third-order conductivity $\sigma_{\alpha\beta\gamma\delta}^{(3)}(\omega_1, \omega_2, \omega_3)$, as a function of the input-wave frequencies, electron density and the effective scattering rate is found within the third-order perturbation theory. A large number of nonlinear physical effects, including harmonics generation, frequency mixing, saturable absorption, etc., are described by the theory.

2. Prediction of a giant enhancement of the third harmonic in graphene integrated in a layered structure [3]. A third harmonic generation from graphene laying on a dielectric substrate with a metalized back side is investigated. It is shown that, properly choosing the dielectric thickness one can get more than two orders of magnitude larger intensity of the third harmonic as compared to the isolated graphene layer [2]. On the other hand, if the dielectric thickness does not satisfy the optimal condition, the output third-harmonic intensity can be suppressed by many orders of magnitude. A correct choice of parameters is thus shown to be crucially important for the design of successfully operating graphene-based frequency multipliers.

3. Experimental discovery and theoretical explanation of a new method of detecting electromagnetic radiation [4]. The method makes use of the photo-conductance of a MOSFET-type struc-

ture with a quantum point contact (QPC). It is shown that replacing a traditional split-gate QPC by the invented in this work bridged-gate QPC leads to the enhancement of the detector photoresponse by about three orders of magnitude. The effect was experimentally demonstrated [4] in a semiconductor quantum-well structure at microwave frequencies, but the underlying physical mechanism is able to work at up to near-infrared frequencies and in graphene related materials.

The work was supported by the European Union under the Program Graphene Flagship (No. CNECT-ICT-604391) and the FET-open grant GOSFEL.

Keywords: graphene, nonlinear electrodynamics, nonlinear optics, frequency multiplication, saturable absorption, Kerr effect, four-wave mixing.

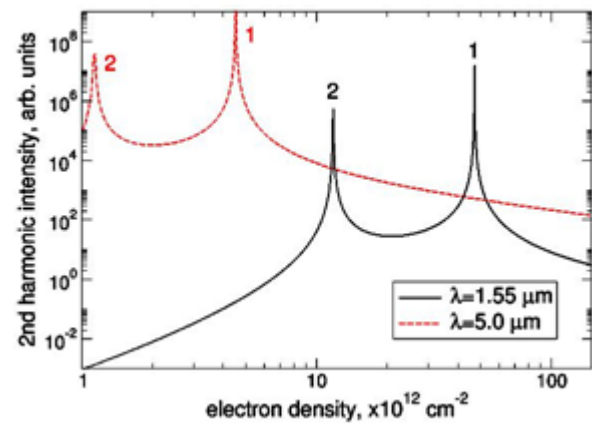


Figure. Theoretically predicted [2] intensity of the dc current induced second harmonic from a single isolated graphene layer. The resonances correspond to the conditions $\hbar\omega=2E_F$ and E_F .

References:

1. S.A.Mikhailov, Europhys.Lett. **79**, 27002 (2007).
2. S.A.Mikhailov, Phys. Rev. B **93**, 085403 (2016).
3. N.A.Savostianova and S.A.Mikhailov, Appl. Phys. Lett. **107**, 181104 (2015).
4. A.D.Levin, G.M.Gusev, Z.D.Kvon, A.K.Bakarov, N.A.Savostianova, S.A.Mikhailov, E.E.Rodyakina, and A.V.Latyshev, Appl. Phys. Lett. **107**, 072112 (2015).

Graphene membranes and their use as pressure sensors

Herre S.J. van der Zant

Kavli Institute of Nanoscience, Delft University of Technology, Lorentzweg 1, 2628
CJ, Delft, The Netherlands

Abstract:

Nano-electromechanical systems (NEMS) make use of electrically induced mechanical motion and vice versa. Atomically thin membranes are ideal building blocks of NEMS because of their unique mechanical properties and their low mass. It puts them in an unexplored regime of motion which approaches the detection limit set by quantum mechanics and which may open the route to new applications.

We make suspended membranes by transferring atomically thin layers from materials such as graphene or MoS₂ on top of silicon oxide substrates prepatterned with (circular) holes, thereby forming thin drums with (sub)micron diameters. The suspended parts form the membranes that are characterized by atomic force microscopy to determine their static mechanical properties (Young's modulus, pre-stress); the method is automated as to gain statistics over large areas. Complimentary to this scanning force microscopy (AFM) technique, we have built a laser interferometer set-up that gives access to the information on the dynamics in the frequency- and time-domain. In addition, the interferometer set-up has also been equipped with a moveable x-y stage so that the membrane motion can be visualized with a lateral resolution of 140 nm and a displacement resolution of 11 fm/ $\sqrt{\text{Hz}}$ [1]. We observe a distortion of the mode shapes with increasing mode number, which can be attributed to structural imperfections in the membrane not seen by other imaging methods such as AFM.

As an application of these thin membranes, we have built a graphene-based pressure sensor. Most pressure sensors operate by measuring the pressure difference. When the absolute pressure is measured, for example in a barometer, a hermetically sealed cavity provides a well-known reference pressure. Even though graphene is impermeable in theory, typically our graphene drums show leakage over the timescale of a couple of hours, therefore no longer maintaining the reference pressure. For industrial applications, the timescale of leakage has to be increased considerably. Since at this point it is unclear whether long enough timescales can be reached, we explore other pressure sensing concepts such as the

squeeze-film pressure sensor. Its operating principle is based on the pressure dependence of a membrane's resonance frequency, caused by the compression of the surrounding gas which changes the resonator stiffness. We have demonstrated the use of a few-layer graphene membrane as a squeeze-film pressure sensor [2]: The measured responsivity of the device is 9000 Hz/mbar, which is a factor 45 higher than state-of-the-art MEMS-based squeeze-film pressure sensors while using a 25 times smaller membrane area.

Keywords: atomically thin membranes, mechanical properties, nanomechanics, graphene-based sensors.

Acknowledgement: Work done in collaboration with Peter Steeneken, Robin Dolleman, Santiago Cartamil Bueno, Dejan Davidovikj, Warner Venstra and Samer Hourri. Financial support is obtained from the Dutch Technology Foundation (STW), the European Union's Horizon 2020 research and innovation programme under grant agreement No 649953 (Graphene Flagship) and NOW/OCW as part of the Frontiers of Nanoscience program.

References:

1. D. Davidovikj, S.J. Cartamil-Bueno, H.S.J. van der Zant, P.G. Steeneken and W. Venstra, Visualizing the Motion of Graphene Nanodrums, *Nano Letters* **16** (2016) 2768-2773.
2. R.J. Dolleman, D. Davidovikj, S.J. Cartamil-Bueno, H.S.J. van der Zant and P.G. Steeneken, Graphene squeeze-film pressure sensors, *Nano Letters* **16** (2016) 568-571.

Functionalized graphene for flexible light-emitting devices

Elias Torres Alonso, George Karkera, Gareth F. Jones, Saverio Russo, Monica F. Craciun*
Centre for Graphene Science, College of Engineering, Mathematics and Physical Sciences, University of Exeter, UK

Abstract:

The development of future flexible and transparent electronics relies on novel materials which combine high electrical conductivity, transparency and bendability. Currently, indium tin oxide (ITO) is the widest spread transparent conductor in consumer electronics. However due to its stiffness, this material does not qualify for bendable electronic applications. The leading candidates to substitute ITO are graphene based materials. Monolayer graphene only absorbs 2% of visible light and it is highly flexible. However, its sheet resistance exceeds $1\text{k}\Omega/\text{sq}$, making it unsuitable for large-area devices. Functionalization of graphene offers a simple way to improve the electrical properties of these materials. Recently, we showed that functionalization with FeCl_3 of few-layer graphene ($\text{FeCl}_3\text{-FLG}$) results in the best flexible transparent conductor with a sheet resistance lower than $10\Omega/\text{sq}$ [1,2], highly stable against 100% humidity and temperature up to 150°C [3], and a promising material for work function matched transparent electrodes in photovoltaic and organic light emitting devices [4] and transparent photo-detectors [5]

In this talk we present the use of this recently discovered transparent conductor $\text{FeCl}_3\text{-FLG}$, for highly uniform, flexible and foldable alternating current electroluminescent (ACEL) devices. We compare the performance of this emerging material against the widely-used conductive polymer PEDOT:PSS and other graphene electrodes such as single-layer graphene (SLG) and FLG. Our experimental findings demonstrate that $\text{FeCl}_3\text{-FLG}$ -based ACEL devices display up to 46% higher electroluminescent intensity at low operational voltage compared to devices embedding pristine SLG or FLG. Contrary to ACEL devices employing alternative electrode materials, the use of $\text{FeCl}_3\text{-FLG}$ transparent electrodes does not show any measurable gradient of the intensity of the emitted light in flat panels 4cm long and 1cm wide, owing to the low sheet resistance of $\text{FeCl}_3\text{-FLG}$. This finding is in stark contrast to the experimentally measured 70% reduction in the intensity of the emitted light measured in ACEL devices embedding SLG electrodes. Finally, we demonstrate the performance of this outstanding transparent electrode

in flexible and foldable lighting devices fabricated on polyethylene terephthalate (PET). These flexible ACEL devices are both highly flexible and durable, showing no degradation in performance under flexural strains beyond the common requirements of wearable electronics applications and over more than 1000 bending cycles. Our results pave the way for the next generation of energy efficient, flexible, high performance and large-area optoelectronics based on highly transparent and conductive electrodes.

Keywords: functionalized graphene, transparent electrodes, optoelectronics, electroluminescent devices, flexible lights, foldable devices

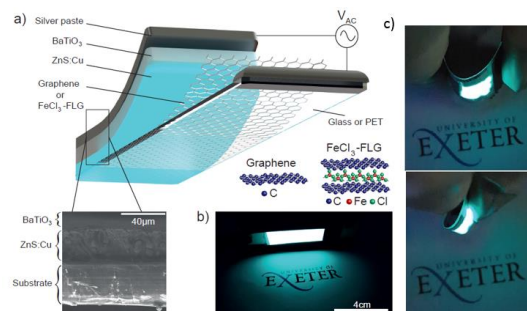


Figure 1: a) schematic of an ACEL device with a zoom on the cross section showing a scanning electron microscope image of the sequence of materials. The atomic structure of the transparent electrodes based on graphene and $\text{FeCl}_3\text{-FLG}$ is shown in the inset. b) ACEL device with $\text{FeCl}_3\text{-FLG}$ electrode. c) flexible ACEL device undergoing increasing bending

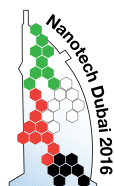
Reference

1. Advanced Materials 24, 2844 (2012)
2. Nano Lett., 14, 1751 (2014)
3. Scientific Reports 5, 7609 (2015)
4. Scientific Reports 5, 16464 (2015)
5. ACS Nano 7, 5052 (2013)

Allied Events



**nano tech
2016**
International Nanotechnology
Exhibition & Conference



NANO KOREA 2016

July 13 (Wed.) ~ 15 (Fri.), **KINTEX**, Gyeonggi-do, Korea

With the support of



Media Partners



www.nanopro.biz
PROMOTING NANOTECHNOLOGIES



www.setcor.org